Synthesis and Pharmacological Characterization of Subtype-Selective Ligands, Including Radio- and Fluorescence Labeled Ligands, for the Histamine H_2 Receptor

Dissertation

zur Erlangung des Doktorgrades der Naturwissenschaften
(Dr. rer. nat.)
an der Fakultät für Chemie und Pharmazie der Universität Regensburg

vorgelegt von
Sabrina Biselli
aus Friedrichshafen

im Jahr 2019

Die vorliegende Arbeit entstand in der Zeit von Dezember 2013 bis Juli 2019 unter der Leitung von Prof. Dr. Günther Bernhardt (ehemals Prof. Dr. Armin Buschauer († 18.07.2017)) am Institut für Pharmazie der Fakultät für Chemie und Pharmazie der Universität Regensburg.

Das Promotionsgesuch wurde eingereicht am:	26.07.2019
Tag der mündlichen Prüfung:	30.08.2019
Vorsitzender des Prüfungsausschusses:	Prof. Dr. Dominik Horinek
Erstgutachter:	Prof. Dr. Günther Bernhardt
Zweitgutachter:	Prof. Dr. Sigurd Elz
Drittprüfer:	Prof. Dr. Joachim Wegener

PUBLICATIONS, POSTERS, ORAL PRESENTATIONS AND PROFESSIONAL TRAINING

Publications (published results prior to the submission of this thesis):

Keller, M.; Kuhn, K. K.; Einsiedel, J.; Hubner, H.; Biselli, S.; Mollereau, C.; Wifling, D.; Svobodova, J.; Bernhardt, G.; Cabrele, C.; Vanderheyden, P. M.; Gmeiner, P.; Buschauer, A. Mimicking of Arginine by Functionalized N(omega)-Carbamoylated Arginine as a New Broadly Applicable Approach to Labeled Bioactive Peptides: High Affinity Angiotensin, Neuropeptide Y, Neuropeptide FF, and Neurotensin Receptor Ligands As Examples. *Journal of medicinal chemistry* **2016**, 59, 1925-1945.

Baumeister, P.; Erdmann, D.; Biselli, S.; Kagermeier, N.; Elz, S.; Bernhardt, G.; Buschauer, A. [^{3}H]UR-DE257: Development of a Tritium-Labeled Squaramide-Type Selective Histamine H_2 Receptor Antagonist. *ChemMedChem* **2015**, 10, 83-93.

Poster Presentations:

Biselli, S.; Alencastre, I.; Erdmann, D.; Maia, A.; Chen, M.; Lazaro, M.; Keller, M.; Bernhardt, G.; Lamghari, M.; Buschauer, A.
Squaramide-type H_2R Ligands as Molecular Tools. *Emil Fischer School Research Day* **2017**, Erlangen, Germany.

Biselli, S.; Alencastre, I.; Erdmann, D.; Maia, A.; Chen, M.; Lazaro, M.; Keller, M.; Bernhardt, G.; Lamghari, M.; Buschauer, A.
Histamine H_2 Receptor Binding of Fluorescence Labeled Piperidinomethylphenoxypropyl Squaramide-type Ligands. *8th International Summerschool „Medicinal Chemistry“* **2016**, Regensburg, Germany.

Biselli, S.; Honisch, C.; Plank, N.; Bernhardt, G.; Buschauer, A.
N^G-Carbamoylated Hetarylalkylguanidines: Bioisosteric Replacement in Histamine H_2 Receptor Agonists. *GLISTEN Working Group Meeting* **2016**, Erlangen, Germany.

Biselli, S.; Baumeister, P.; Erdmann, D.; Bernhardt, G.; Buschauer, A.
Towards High Affinity Subtype-selective Antagonists as Radioligands for the Histamine H_2 Receptor. *7th International Summerschool „Medicinal Chemistry“* **2014**, Regensburg, Germany.

Biselli, S.; Baumeister, P.; Erdmann, D.; Bernhardt, G.; Buschauer, A.
Towards High Affinity Subtype-selective Antagonists as Radioligands for the Histamine H_2 Receptor. *EFMC-ISMC 2014 XXIII International Symposium on Medicinal Chemistry* **2014**, Lisbon, Portugal.

Oral Presentations:

Squaramide-type Histamine H_2 Receptor Ligands as Fluorescent Molecular Tools. *Emil Fischer School Research Day* **2017**, Erlangen, Germany.

Squaramide-type Histamine H_2 Receptor Ligands as Fluorescent Molecular Tools. *ChemPharm Colloquium* **2017**, Regensburg, Germany.

Professional Training:

12/2013 – 07/2019	Member of the Research Training Group (Graduiertenkolleg 1910) *"Medicinal Chemistry of selective GPCR Ligands"*. Regensburg, Germany
12/2013 – 07/2019	Member of the Emil Fischer Graduate School of Pharmaceutical Sciences and Molecular Medicine. Erlangen, Germany
03/2017	Gentechnikrecht: Staatlich anerkannte Fortbildungsveranstaltung zur Erlangung der Sachkunde für Projektleiter gentechnischer Arbeiten und Beauftragte für Biologische Sicherheit nach §§15 und 17 der Gentechniksicherheitsverordnung. Regensburg, Germany

ACKNOWLEDGEMENTS AND DECLARATION OF COLLABORATIONS

An dieser Stelle möchte ich mich bedanken bei:

Herrn Prof. Dr. Armin Buschauer († 18.07.2017) für die Möglichkeit der Mitarbeit an diesem interessanten Projekt, seine wissenschaftlichen Anregungen und seine Förderung,

Herrn Prof. Dr. Günther Bernhardt für seine wissenschaftlichen Ratschläge, die gute Betreuung und die konstruktive Kritik bei der Durchsicht meiner Arbeit,

Herrn Dr. Max Keller für die fachliche Unterstützung , die Durchführung der Radiosynthese von [^{3}H]UR-SB69, seine Hilfe bei der Radiosynthese von [^{3}H]UR-DE257, seine Hilfe bei den Synthesen sowie der Charakterisierung der Fluoreszenzliganden und die Organisation des Syntheseseminars,

Frau Prof. Dr. Meriem Lamghari für die Möglichkeit in ihrem Labor Fluoreszenzligand-Bindungsstudien mit dem ImageStream X und dem IN Cell Analyzer 2000 durchzuführen,

Frau Dr. Inês Alencastre für die geduldige Einarbeitung in Porto, sowie die interessanten Diskussionen, Ratschläge und Ideen, insbesondere bei Zellkultur und ImageStream X,

Herrn Dr. Andre Maia und Frau Dr. Maria Gomez Lazaro für die geduldige Einarbeitung am IN Cell Analyzer 2000 und ImageStream X und die Hilfe bei der Auswertung der Ergebnisse,

Frau Mengya Chen für die Synthese der Vorstufe **5.3**, des Farbstoffes Py-5 und der Fluoreszenzliganden **5.12** und **5.13** im Rahmen ihrer Masterarbeit,

Frau Claudia Honisch für die Synthese der Vorstufen **6.13-6.18**, der Carbamoylguanidine **6.47-6.52** und die Durchführung der Stabilitätstests von **6.49**, **6.50**, **6.52**, **UR-Bit22**, **UR-Bit23** und **UR-Bit29** im Rahmen ihrer Masterarbeit,

Frau Lisa Forster für die Durchführung der Radioligand-Bindungsexperimente an Dopamin Rezeptoren im Rahmen ihrer Doktorarbeit,

Herrn Timo Littmann für seine Hilfe bei der Durchführung der Konfokalmikroskopie-Experimente,

Frau Edith Bartole für die Durchführung der Stabilitätsmessung von [^{3}H]UR-SB69 nach 15 Monaten,

Herrn Dr. Paul Baumeister für die geduldige Einarbeitung am Lehrstuhl und vielen fachlichen Tipps,

Frau Maria Beer-Krön für die Herstellung von Membranpräparationen, sowie die tatkräftige Unterstützung bei der Durchführung von Radioligand-Bindungsexperimenten, funktionellen GTPγS Assays und Kultivierung der verschiedenen Zelllinien,

Frau Dita Fritsch und Frau Elvira Schreiber für die tatkräftige Unterstützung bei der Durchführung verschiedener Assays,

Frau Sieglinde Dechant für die Unterstützung bei der Synthese verschiedener Zwischenstufen,

Meinen Forschungspraktikanten David Konieczny, Julia Mändl, Oliver Sarosi, Josef Hartl und Niklas Rosier für die Unterstützung bei diversen Synthesen,

meiner langjährigen Laborkollegin und Freundin Edith Bartole für die unzähligen (nicht nur) wissenschaftlichen Diskussionen und ihre stete Hilfsbereitschaft und Geduld,

den Synthesechemikern Jianfei Wan, Coco (Xueke She) ,Edith Bartole, Frauke Antoni, Andrea Pegoli und Jonas Buschmann für die zahlreichen wissenschaftlichen Diskussionen und die tatkräftige Unterstützung bei Syntheseproblemen,

allen Mitgliedern des Lehrstuhls für ihre Kollegialität und das sehr gute Arbeitsklima. Mein besonderer Dank gilt Edith Bartole, Coco (Xueke She), Frauke Antoni, Jonas Buschmann, Jianfei Wan und Timo Littmann für die persönliche Unterstützung und die vielen aufmunternden Gespräche,

der Deutschen Forschungsgemeinschaft für die finanzielle Unterstützung im Rahmen des Graduiertenkollegs 1910,

und natürlich meinen Eltern, meiner Schwester Franziska und meinem Mann Attila für ihre stete Unterstützung, Liebe und unendliche Geduld, ohne die diese Arbeit niemals fertig geworden wäre.

CONTENTS

CHAPTER 1

GENERAL INTRODUCTION

1.1 THE HISTAMINE H_2 RECEPTOR AS A PROTOTYPIC AMINERGIC GPCR

The histamine H_2 receptor (H_2R) belongs to the superfamily of G-protein coupled receptors (GPCRs).[1] GPCRs are integral membrane receptors and are characterized by seven hydrophobic transmembrane (TM) domains with an extracellular amino terminus and an intracellular carboxyl terminus. The extracellular regions combined with the transmembrane regions are important for ligand binding.[2] The intracellular regions are substantially involved in signaling and feedback mechanisms.[2] With around 30% of the most prominent approved drugs targeting these membrane receptors, GPCRs are the most important drug targets.[3,4] GPCRs are mediated by numerous endogenous ligands e.g. biogenic amines (aminergic GPCRs), amino acids, peptides, proteins, purins and lipids, to name only a few.[1,5,6]

The H_2R is one of currently four histamine receptor subtypes (H_1R, H_3R and H_4R), which are all activated by binding the endogenous ligand histamine and therefore are aminergic GPCRs.[7-10] All histamine receptors belong to the rhodopsin family of GPCRs.[1] The H_2R is primarily located on parietal cells in the stomach,[11] in mammalian brain,[12,13] on neutrophiles and eosinophiles[14] as well as on smooth muscle cells[15] (e.g. in the heart, airways and uterus). An essential physiological function of the H_2R is the control of the gastric acid secretion.[8,11] Furthermore, activation of H_2R results in smooth muscle relaxation and positive inotropic and chronotropic effects.[16]

The H_2R species isoforms (e.g. human (hH_2R), guinea pig (gpH_2R), rat (rH_2R), mouse (mH_2R) and dog (cH_2R)), like many GPCRs, interact similarily with their endogenous ligand, but quite differently with most synthetic ligands.[17,18] The pharmacological differences between the hH_2R and the gpH_2R mainly concern agonists and not antagonists, which was very fortunate as the first potent antagonists for the treatment of gastroduodenal ulcers were developed relying on animal models.[17] The cH_2R exhibits an increased constitutive activity compared to hH_2R and rH_2R.[18] These findings show that for the development of highly potent and selective agonists it is crucial to study hH_2R and not the orthologs.

1.2 G-PROTEIN ACTIVATION AND SIGNALING PATHWAYS

In the classical model the active receptor conformation (either stabilized by agonist binding or constitutively active) is functioning as a guanosine nucleotide exchange factor (GEF) on the Gα subunit of the heterotrimeric G-protein (Figure 1.1).[5] The binding of the G-protein complex to the active receptor leads to conformational changes which result in the release of GDP from its binding site at the Gα subunit and the formation of the ternary complex.[19] Subsequently, GTP is bound and the ternary complex dissociates into the Gα–GTP subunit, the Gβγ complex and the free receptor.[19] Both subunits can interact with effector proteins resulting, through an increase or a decrease in the concentration of second messangers, in various cellular responses.[19] After a certain period of time, the intrinsic GTPase activity of the Gα subunit converts GTP to GDP and phosphate.[19] The Gα–GDP subunit re-associates with the Gβγ complex to the inactive heterotrimeric G-protein.[19]

Based on their structures and signaling pathways, G-proteins are grouped in four families according to their Gα subunit: $G\alpha_{i/o}$, $G\alpha_{s}$, $G\alpha_{q/11}$, $G\alpha_{12/13}$.[20,21] The H_2R predominantly couples to

$G\alpha_s$ proteins, resulting in an increase of the second messenger cAMP by stimulation of the isoforms of the effector protein adenylyl cyclase (Figure 1.1).[22,23] By contrast, the H_3R and the H_4R signal mainly via $G\alpha_{i/o}$ proteins, which inhibit the adenylyl cyclase.[24] The H_1R preferentially couples to $G\alpha_{q/11}$ leading to the activation of phospholipase C (PLC) and subsequent release of IP_3 and DAG.[24,25]

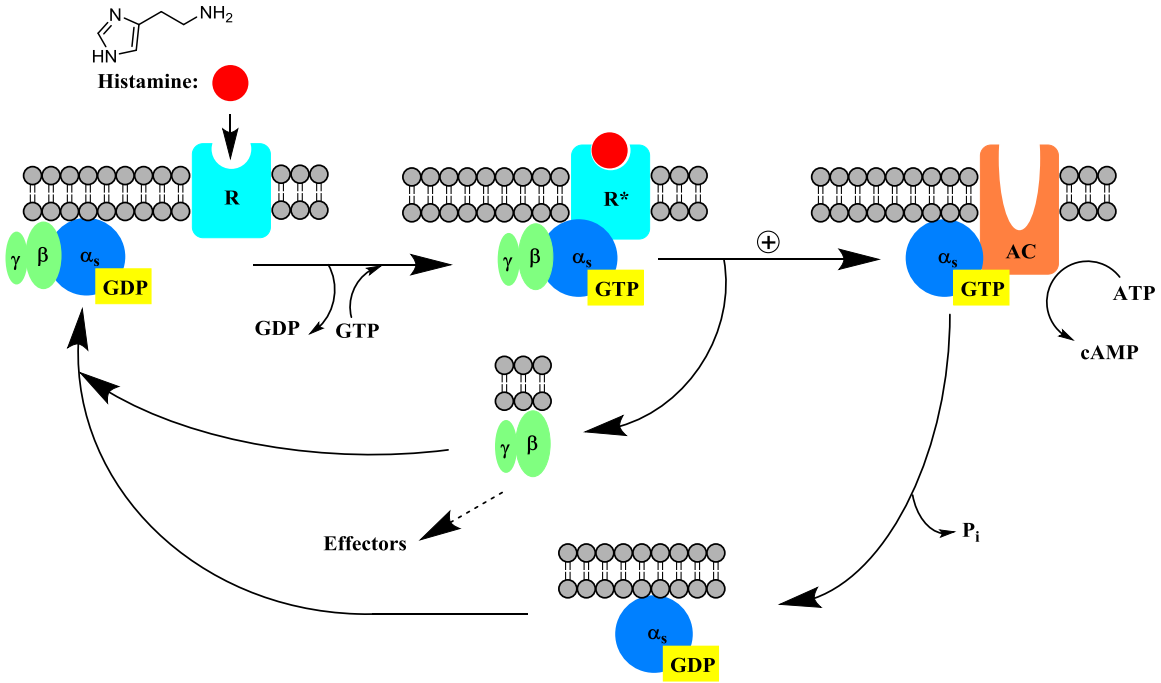

Figure 1.1. Activation of the heterotrimeric G-protein by the agonist occupied receptor using the H_2R as an example. R represents the inactive receptor conformation and R* the active receptor conformation. The dissociated subunits ($G\alpha_s$ and Gβγ complex) regulate effector proteins such adenylyl cyclase (AC), which is activated by $G\alpha_s$. Modified from Rasmussen et al.[26]

For analyzing GPCR-mediated guanine nucleotide exchange at G-proteins, a widely employed method is the [^{35}S]GTPγS binding assay.[27] This assay utilizes, like the closely related steady-state GTPase assay, the intrinsic GTPase activity of the Gα subunit. An advantage of the GTPγS binding assay (and GTPase assay) is that it assesses coupling at a proximal level, avoiding potential bias introduced by downstream events.[27] For the H_2R the usage of membranes of Sf9 insect cells, which are expressing mammalian H_2R-$G_{s\alpha}$ fusion proteins is well established.[17,28,29] GPCR-$G_{s\alpha}$ fusion proteins ensure a defined 1:1 stoichiometry of the signaling partners and efficient coupling.[17,29,30] Therefore, the ternary complex formation is more efficient compared to the coexpression of H_2R plus $G_{s\alpha}$.[28] In our workgroup, the H_2R-$G_{s\alpha}$ fusion protein system is routinely employed for analyzing new ligands for the H_2R in radioligand binding and functional studies (GTPγS binding assay and GTPase assay).[31-36]

1.3 G-Protein Independent Signaling, Ligand Classification and Functional Selectivity

Besides the signal transduction cascades mediated by G-proteins, GPCRs are reported to participate in numerous other protein-protein-interactions which initiate signaling pathways independent from G-protein activation.[19,37,38] Most intriguing is the interaction with β-arrestins, which are mainly involved in receptor desensitization and internalization, but also act as alternative signal transducers.[19,37] β-Arrestin recruitment is initiated by phosphorylation of the active conformation of the GPCR by G-protein coupled receptor kinases (GRK).[38,39] The β-arrestin binds to the cytosolic surface of the phosphorylated receptor and sterically hinders an interaction with the G-proteins.[40] Furthermore, β-arrestins were reported to be involved in the degradation of second messengers.[41,42] These two effects effectively lead to the deactivation of the G-protein mediated signal transduction. Beyond desensitization, the bound β-arrestin also mediates internalization via clathrin-coated pits.[38]

A classical "two state" model, which is often suitable for explaining the pharmacodynamic activity of ligands is the cubic ternary complex model.[43-45] This model distinguishes between an active (R*) and inactive (R) receptor state, which are in equilibrium and are able to isomerize without agonist binding. This spontaneous activation of the receptor in the absence of an agonist is referred to as constitutive activity.[46] The G-protein is able to bind to both states, albeit only the G-protein-active-receptor-complex (R*G) activates intra cellular signaling via a GDP-GTP exchange. Ligand binding can shift the equilibrium of the receptor state. Agonists bind with high affinitiy to R* and stabilize the active conformation. Inverse agonists prefer to bind to R and stabilize the inactive conformation. Neutral antagonists bind with the same affinity to both conformations and therefore do not alter the equilibrium. With regard to β-arrestin mediated signaling, along site with other mechanism such as phosphorylisation, internalization and oligomerisation, there is growing evidence that there are multiple active and inactive receptor conformations.[47,48] Structurally different ligands stabilize distinct receptor conformations leading to an activation of only a subset of cellular effectors [48] This selective activation of only some of all possible signaling pathways has been referred to as ´functional selectivity´,[49] ´biased agonism´[50] or ´differential receptor-linked effector actions´[51].

Recently, several monomeric and dimeric H_2R ligands were investigated for biased agonism regarding G-protein activation and β-arrestin recruitment.[52] The β-arrestin recruitment was measured by an enzyme fragment complementation assay using split luciferase fragments from *P. termitilluminans,* developed by Misawa *et al*.[53] While all antagonists were unbiased, the investigated acyl- and carbamoyl guanidine agonists revealed varying degrees of G-Protein bias.[52]

1.4 H_2R Antagonists

The classical H_2R antagonists can be devided into two groups depicted in Figure 1.2: compounds comprising a flexible chain (group I) and compounds containing diaryl moiety (goup II).[54] The antagonists consist of an aromatic system, which is linked to a polar, planar group (urea equivalent) by either a flexible chain (group I) or by a second aromatic system (group II). The

classification of the antagonists is made according to the aromatic system. Most H_2R antagonists belong to one of four major structural classes: imidazole-, guanidinothiazole-, aminomethylfurane- and piperidinomethylphenoxy-containing compounds.

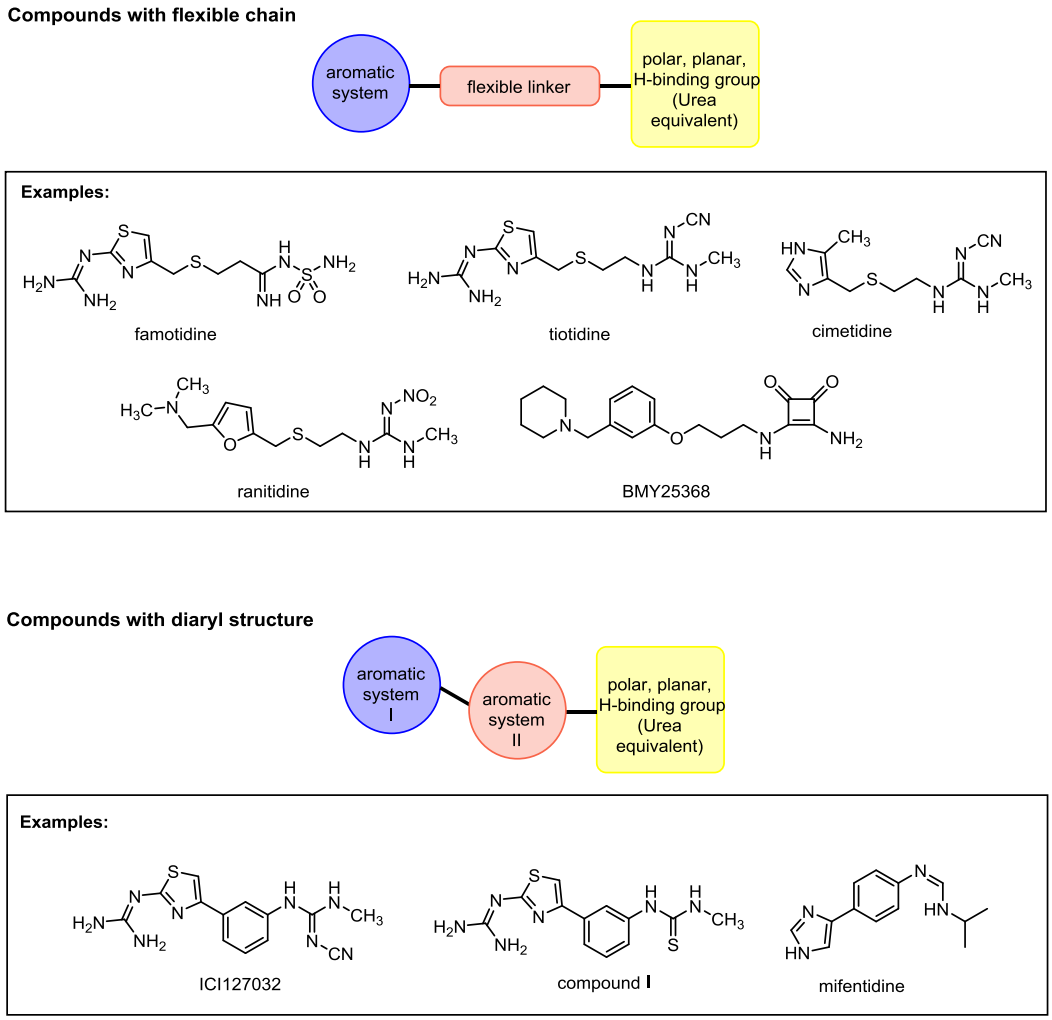

Figure 1.2. Selected H_2R antagonists and their classification into two groups: compounds with a flexible chain and compounds with a diaryl moiety.[54]

The aminopotentidine derivatives as well as fluorescent ligands (e.g. compound **II**) showed that within the piperidinomethylphenoxy-containing compounds additional substituents at the urea equivalent are well tolerated or provided additional H_2R binding affinity (Figure 1.3).[55-57] Up to date, iodoaminopotentidine, a piperidinomethylphenoxy-containing cyanoguanidine (Figure 1.3), which was also synthesized in a radiolabeled form ([^{125}I]iodoaminopotentidine), showed the highest affinity.[13] This radioligand was used to map the H_2R densities in human and mammalian brain.[12,13] Recently, a series of piperidinomethylphenoxyalkylamine-containing ligands, coupled with various polar groups ("urea equivalents") such as cyanoguanidine, nitroethenediamine, amide or squaric amide moieties, and a terminal amino group, connected via a linker of different length, was developed by our group.[35] The squaramides, which also tolerated propionylation at the terminal amino-group showed the highest affinities. UR-DE257, which showed a high affinity (pK_i value: 7.55), was also synthesized in radiolabeled form ([^{3}H]UR-DE257) and is frequently used in competition binding experiments.[35,36]

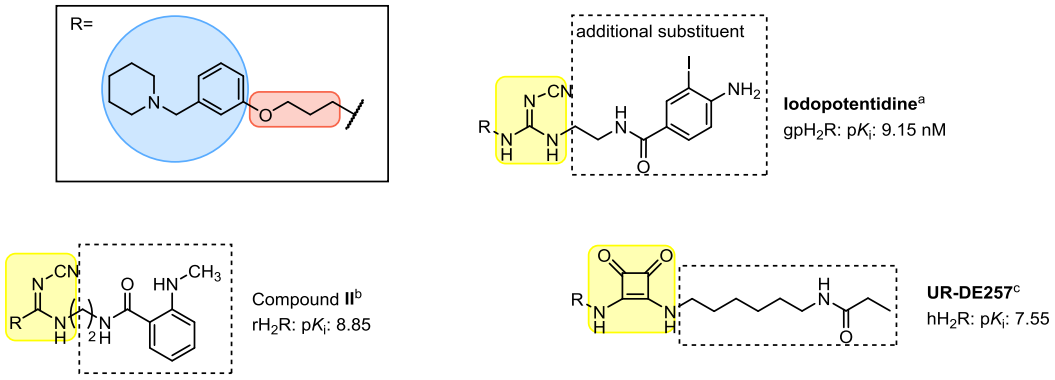

Figure 1.3. Structures of exemplary piperidinomethylphenoxy-containing ligands. a: Hirschfeld et al and Ruat et al[13,57]; b: Malan et al[58]; c: Baumeister et al[35].

Whereas in the late 1970s to 1980s, the H_2R antagonists (H_2 blockers) revolutionized the treatment of peptic ulcers, former blockbuster drugs like cimetidine, ranitidine or famotidine are outdated. They were largely superseded by the more effective proton pump inhibitors (e.g. omeprazole). Nevertheless, H_2R antagonists are valuable molecular tools to study the H_2R, especially it´s role in the brain, which is still far from being completely understood.

1.5 H_2R Agonists

The early agonists for the H_2R were derived from histamine and consististed of an imidazole pharmakophore coupled to a guanidine by a flexible linker (e.g. impromidine and arpromidine, see Figure 1.4).[59,60] Arpromidine and related compounds showed up to 400 times potency of histamine at the spontaneously beating guinea pig right atrium, but the strongly basic guanidine moiety led to poor oral bioavailability and CNS penetration.[59] The bioisosteric replacement of the guanidine (pK_a ~13) with an acylguanidine (pK_a ~8) resulted in ligands with either retained or even increased agonistic potency (e.g. UR-PG80 and UR-AK24, see Figure 1.4).[31,32] Modification of these N^G-acylated imidazolylpropylguanidines, which lacked subtype selectivity (H_3R and H_4R), to N^G-acylated aminothiazolylpropylguanidines led to highly potent and selective H_2R agonists.[34] Surprisingly, the H_2R potency was increased up to 4000-fold the potency of histamine by linking two acylguanidine moieties (e.g. UR-AK381, see Figure 1.4).[33] The aminothiazole dimeric ligands are the most potent and selective H_2R agonists known so far. Traditionally, dimeric (bivalent) ligands consist of two pharmacophoric moieties linked through a spacer and are designed to bridge two neighboring receptor protomers.[61] Porthogese *et al* suggested a distance of about 22-27 Å between the two orthosteric binding sites of a receptor dimer.[62] Interestingly, the most active dimeric ligands have spacer of lengths insufficient to bridge the protomers of putative H_2R dimers.[33] The enormous gain in potency is speculated to result from an interaction with the orthosteric and an accessory binding site at the same protomer.[33] Recently, it was shown that bioisosteric replacement of the acylguanidines with the more stable carbamoylguanidine led to dimeric ligands with retained potency and intrinsic activity (e.g. UR-NK22, see Figure 1.4).[36]

So far, there is no H_2R agonist for therapeutic use on the market, but H_2R agonists are valuable molecular tools to study the H_2R. Nonetheless, there are numerous possible indications e.g. as positive inotropic vasodilators for the treatment of congestive heart failure or as differentiation-introducing agents for treatment of acute myeloid leukemia (AML). For the later, the endogenous

agonist histamine is used as an orphan drug in combination with interleukin 2. Histamine promotes the activation of T cells and natural killer cells by interleukin 2, which results in the killing of cancer cells.[63] Given the effect of histamine is mediated via H_2R, the application of highly selective H_2R agonists might be beneficial in regard to potency and a reduction of adverse effects. Recently, investigation of the dimeric N^G-carbamoylated aminothiazolylpropylguanidines on human monocytes revealed a high H_2R agonist potency, suggesting that this class of compounds is a promising starting point for the development of H_2R agonists for the treatment of AML.[36]

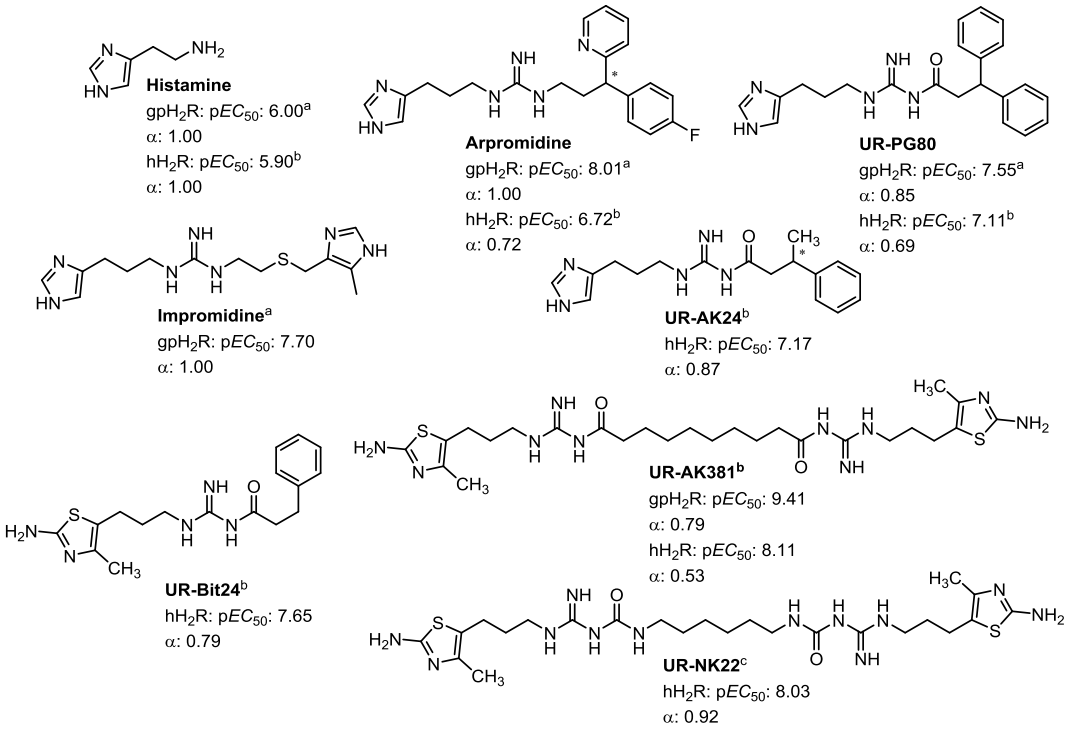

Figure 1.4. Structures of selected H_2R agonists. Agonism measured on [a]guinea pig right atrium[32], [b]steady-state GTPase assay[31,33,34] or [c]GTPγS binding assay[36].

1.6 Receptor Ligand Binding Assays and Labeled Molecular Tools for GPCRs

The initial step in every signaling cascade, that causes a receptor-mediated biological response, is the binding of a ligand to the receptor. There are multiple ways to utilize receptor-ligand-interactions in research, e.g. as a tool for determining receptor distribution, for identification of receptor subtypes and for screening of new compounds.[64]

The classical approach for the determination of ligand affinity is the radioligand binding assay, which has been unchallenged for a long time regarding sensity and reproducibility.[64,65] Radioligand binding experiments can be divided in three basic types: Saturation binding experiments are used to determine the affinity of the radioligand and the number of specific binding sites. In kinetic experiments, the rate constants of association and dissoviation of a radioligand can be determined. Competition binding experiments are widely used to identify unlabeled compounds, which bind to the receptor in question by displacement of a radioligand. The major disadvantages include that radioligands are potentially hazardous to human health,

produce high costs in production and waste disposal, require special licences and laboratory equippment, and separation of bound from unbound ligand is necessary.

Today, new highly sensitive fluorescence and bioluminescence methods such as fluorescence polarization (FP),[66] total internal reflection fluorescence (TIRF),[67] fluorescence/bioluminescence resonance energy transfer (FRET/BRET),[68] fluorescence recovery after photobleaching (FRAP),[69] high content imaging[70] and flow cytometry[71] became promising alternatives. Like radioligands, fluorescent ligands can be used in the basic types of binding experiments. Several peptidic and non-peptidic fluorescent ligands were identified for GPCRs, including NPY,[72,73] muscarinic[74] and histamine[55,56,75] receptors. In general, a fluorescent ligand comprises of a pharmacophore, a linker and the fluorophore. A major challenge in the development of small-molecule fluorescent ligands is to retain affinity, when a, compared to the ligand, bulky fluorophore is attached. In comparison, a radiolabel, especially tritium, does not alter the affinity of the ligand.

When selecting a radio- or fluorescent labeled ligand for binding experiments, several aspects have to be considered.[65,76,77] Firstly, the ligand should be selective and bind with high affinity to the respective receptor. Secondly, high (radiochemical) purity and high specific activity (radioligand) or quantum yield (fluorescent ligand) is required. Thirdly, the labeled ligand should be chemically stable under assay conditions for at least the duration of the experiment performed. Furthermore, unspecific binding has to be considered, the choice of radio- or fluorescent label and, whether an agonist or an antagonist is desired as labeled ligand. Under unspecific binding all binding sites other than the receptor of interest are summarized. A competition binding assay, were only 50% of total radioligand binding is specific is considered adequate, 70% is good and 90% is excellent.[76] Tritium is often considered as the radioisotope of choice. Compared to ^{125}I or the occasionally used $^{32/33}$P or ^{35}S, tritium has a longer half-life (14-87 days vs. 12.3 years) and the tritiated compounds are more convenient in handeling with respect to safety precautions.[76] When choosing a fluorophore, excitation and emission wavelengths, stoke shifts and quantum yields have to be considered. Generally, red-emitting (λ_{em}: > 600 nm) fluorophores with a long stoke shift and a high quantum yield are preferred. [77] Agonists label only an active conformation of the receptor and therefore, only a fraction of the total active receptor population.[78] By contrast, antagonists bind to all receptor states with the same affinity according to the classical model described above.[78]

1.7 REFERENCES

1. Fredriksson, R.; Lagerstrom, M. C.; Lundin, L. G.; Schioth, H. B. The G-protein-coupled receptors in the human genome form five main families. Phylogenetic analysis, paralogon groups, and fingerprints. *Molecular pharmacology* **2003**, 63, 1256-1272.
2. Luttrell, L. M. Reviews in molecular biology and biotechnology: transmembrane signaling by G protein-coupled receptors. *Mol Biotechnol* **2008**, 39, 239-264.
3. Wise, A.; Gearing, K.; Rees, S. Target validation of G-protein coupled receptors. *Drug Discov Today* **2002**, 7, 235-246.
4. Stevens, R. C.; Cherezov, V.; Katritch, V.; Abagyan, R.; Kuhn, P.; Rosen, H.; Wuthrich, K. The GPCR Network: a large-scale collaboration to determine human GPCR structure and function. *Nat Rev Drug Discov* **2013**, 12, 25-34.
5. Pierce, K. L.; Premont, R. T.; Lefkowitz, R. J. Seven-transmembrane receptors. *Nat Rev Mol Cell Biol* **2002**, 3, 639-650.
6. Vassilatis, D. K.; Hohmann, J. G.; Zeng, H.; Li, F.; Ranchalis, J. E.; Mortrud, M. T.; Brown, A.; Rodriguez, S. S.; Weller, J. R.; Wright, A. C.; Bergmann, J. E.; Gaitanaris, G. A. The G protein-coupled receptor repertoires of human and mouse. *Proc Natl Acad Sci U S A* **2003**, 100, 4903-4908.
7. Ash, A. S.; Schild, H. O. Receptors mediating some actions of histamine. *Br J Pharmacol Chemother* **1966**, 27, 427-439.
8. Black, J. W.; Duncan, W. A.; Durant, C. J.; Ganellin, C. R.; Parsons, E. M. Definition and antagonism of histamine H 2 -receptors. *Nature* **1972**, 236, 385-390.
9. Arrang, J. M.; Garbarg, M.; Schwartz, J. C. Auto-inhibition of brain histamine release mediated by a novel class (H3) of histamine receptor. *Nature* **1983**, 302, 832-837.
10. Oda, T.; Morikawa, N.; Saito, Y.; Masuho, Y.; Matsumoto, S. Molecular cloning and characterization of a novel type of histamine receptor preferentially expressed in leukocytes. *J Biol Chem* **2000**, 275, 36781-36786.
11. Domschke, W.; Domschke, S.; Classen, M.; Demling, L. Histamine and cyclic 3',5'-AMP in gastric acid secretion. *Nature* **1973**, 241, 454-455.
12. Traiffort, E.; Pollard, H.; Moreau, J.; Ruat, M.; Schwartz, J. C.; Martinez-Mir, M. I.; Palacios, J. M. Pharmacological characterization and autoradiographic localization of histamine H2 receptors in human brain identified with [125I]iodoaminopotentidine. *Journal of neurochemistry* **1992**, 59, 290-299.
13. Ruat, M.; Traiffort, E.; Bouthenet, M. L.; Schwartz, J. C.; Hirschfeld, J.; Buschauer, A.; Schunack, W. Reversible and Irreversible Labeling and Autoradiographic Localization of the Cerebral Histamine H-2-Receptor Using [I-125] Iodinated Probes. *P Natl Acad Sci USA* **1990**, 87, 1658-1662.
14. Reher, T. M.; Brunskole, I.; Neumann, D.; Seifert, R. Evidence for ligand-specific conformations of the histamine H(2)-receptor in human eosinophils and neutrophils. *Biochem Pharmacol* **2012**, 84, 1174-1185.
15. Mitznegg, P.; Schubert, E.; Fuchs, W. Relations between the effects of histamine, pheniramin and metiamide on spontaneous motility and the formation of cyclic AMP in the isolated rat uterus. *Naunyn Schmiedebergs Arch Pharmacol* **1975**, 287, 321-327.
16. Reinhardt, D.; Schmidt, U.; Brodde, O. E.; Schumann, H. J. H1 - and H2-receptor mediated responses to histamine on contractility and cyclic AMP of atrial and papillary muscles from guinea-pig hearts. *Agents Actions* **1977**, 7, 1-12.
17. Kelley, M. T.; Burckstummer, T.; Wenzel-Seifert, K.; Dove, S.; Buschauer, A.; Seifert, R. Distinct interaction of human and guinea pig histamine H2-receptor with guanidine-type agonists. *Molecular pharmacology* **2001**, 60, 1210-1225.

18. Preuss, H.; Ghorai, P.; Kraus, A.; Dove, S.; Buschauer, A.; Seifert, R. Constitutive activity and ligand selectivity of human, guinea pig, rat, and canine histamine H2 receptors. *The Journal of pharmacology and experimental therapeutics* **2007**, 321, 983-995.
19. Hilger, D.; Masureel, M.; Kobilka, B. K. Structure and dynamics of GPCR signaling complexes. *Nat Struct Mol Biol* **2018**, 25, 4-12.
20. Downes, G. B.; Gautam, N. The G protein subunit gene families. *Genomics* **1999**, 62, 544-552.
21. Simon, M. I.; Strathmann, M. P.; Gautam, N. Diversity of G proteins in signal transduction. *Science* **1991**, 252, 802-808.
22. Bristow, M. R.; Cubicciotti, R.; Ginsburg, R.; Stinson, E. B.; Johnson, C. Histamine-mediated adenylate cyclase stimulation in human myocardium. *Molecular pharmacology* **1982**, 21, 671-679.
23. Leurs, R.; Smit, M. J.; Menge, W. M.; Timmerman, H. Pharmacological characterization of the human histamine H2 receptor stably expressed in Chinese hamster ovary cells. *British journal of pharmacology* **1994**, 112, 847-854.
24. Hamm, H. E. The many faces of G protein signaling. *J Biol Chem* **1998**, 273, 669-672.
25. Lieb, S.; Littmann, T.; Plank, N.; Felixberger, J.; Tanaka, M.; Schafer, T.; Krief, S.; Elz, S.; Friedland, K.; Bernhardt, G.; Wegener, J.; Ozawa, T.; Buschauer, A. Label-free versus conventional cellular assays: Functional investigations on the human histamine H1 receptor. *Pharmacological research* **2016**, 114, 13-26.
26. Rasmussen, S. G.; DeVree, B. T.; Zou, Y.; Kruse, A. C.; Chung, K. Y.; Kobilka, T. S.; Thian, F. S.; Chae, P. S.; Pardon, E.; Calinski, D.; Mathiesen, J. M.; Shah, S. T.; Lyons, J. A.; Caffrey, M.; Gellman, S. H.; Steyaert, J.; Skiniotis, G.; Weis, W. I.; Sunahara, R. K.; Kobilka, B. K. Crystal structure of the beta2 adrenergic receptor-Gs protein complex. *Nature* **2011**, 477, 549-555.
27. Harrison, C.; Traynor, J. R. The [35S]GTPgammaS binding assay: approaches and applications in pharmacology. *Life sciences* **2003**, 74, 489-508.
28. Houston, C.; Wenzel-Seifert, K.; Burckstummer, T.; Seifert, R. The human histamine H2-receptor couples more efficiently to Sf9 insect cell Gs-proteins than to insect cell Gq-proteins: limitations of Sf9 cells for the analysis of receptor/Gq-protein coupling. *Journal of neurochemistry* **2002**, 80, 678-696.
29. Milligan, G. Insights into ligand pharmacology using receptor-G-protein fusion proteins. *Trends in pharmacological sciences* **2000**, 21, 24-28.
30. Seifert, R.; Wenzel-Seifert, K.; Kobilka, B. K. GPCR-Galpha fusion proteins: molecular analysis of receptor-G-protein coupling. *Trends in pharmacological sciences* **1999**, 20, 383-389.
31. Xie, S. X.; Ghorai, P.; Ye, Q. Z.; Buschauer, A.; Seifert, R. Probing ligand-specific histamine H1- and H2-receptor conformations with NG-acylated Imidazolylpropylguanidines. *The Journal of pharmacology and experimental therapeutics* **2006**, 317, 139-146.
32. Ghorai, P.; Kraus, A.; Keller, M.; Gotte, C.; Igel, P.; Schneider, E.; Schnell, D.; Bernhardt, G.; Dove, S.; Zabel, M.; Elz, S.; Seifert, R.; Buschauer, A. Acylguanidines as bioisosteres of guanidines: NG-acylated imidazolylpropylguanidines, a new class of histamine H2 receptor agonists. *Journal of medicinal chemistry* **2008**, 51, 7193-7204.
33. Birnkammer, T.; Spickenreither, A.; Brunskole, I.; Lopuch, M.; Kagermeier, N.; Bernhardt, G.; Dove, S.; Seifert, R.; Elz, S.; Buschauer, A. The Bivalent Ligand Approach Leads to Highly Potent and Selective Acylguanidine-Type Histamine H-2 Receptor Agonists. *Journal of medicinal chemistry* **2012**, 55, 1147-1160.
34. Kraus, A.; Ghorai, P.; Birnkammer, T.; Schnell, D.; Elz, S.; Seifert, R.; Dove, S.; Bernhardt, G.; Buschauer, A. N-G-Acylated Aminothiazolylpropylguanidines as Potent and Selective Histamine H-2 Receptor Agonists. *ChemMedChem* **2009**, 4, 232-240.
35. Baumeister, P.; Erdmann, D.; Biselli, S.; Kagermeier, N.; Elz, S.; Bernhardt, G.; Buschauer, A. [3H]UR-DE257: Development of a Tritium-Labeled Squaramide-Type Selective Histamine H2 Receptor Antagonist. *ChemMedChem* **2015**, 10, 83-93.

36. Kagermeier, N.; Werner, K.; Keller, M.; Baumeister, P.; Bernhardt, G.; Seifert, R.; Buschauer, A. Dimeric carbamoylguanidine-type histamine H receptor ligands: A new class of potent and selective agonists. *Bioorganic & medicinal chemistry* **2015**.
37. Gurevich, V. V.; Gurevich, E. V. Overview of different mechanisms of arrestin-mediated signaling. *Curr Protoc Pharmacol* **2014**, 67, Unit 2 10 11-19.
38. Peterson, Y. K.; Luttrell, L. M. The Diverse Roles of Arrestin Scaffolds in G Protein-Coupled Receptor Signaling. *Pharmacological reviews* **2017**, 69, 256-297.
39. Gurevich, V. V.; Gurevich, E. V. Extensive shape shifting underlies functional versatility of arrestins. *Curr Opin Cell Biol* **2014**, 27, 1-9.
40. Shenoy, S. K.; Lefkowitz, R. J. beta-Arrestin-mediated receptor trafficking and signal transduction. *Trends in pharmacological sciences* **2011**, 32, 521-533.
41. Perry, S. J.; Baillie, G. S.; Kohout, T. A.; McPhee, I.; Magiera, M. M.; Ang, K. L.; Miller, W. E.; McLean, A. J.; Conti, M.; Houslay, M. D.; Lefkowitz, R. J. Targeting of cyclic AMP degradation to beta 2-adrenergic receptors by beta-arrestins. *Science* **2002**, 298, 834-836.
42. Nelson, C. D.; Perry, S. J.; Regier, D. S.; Prescott, S. M.; Topham, M. K.; Lefkowitz, R. J. Targeting of diacylglycerol degradation to M1 muscarinic receptors by beta-arrestins. *Science* **2007**, 315, 663-666.
43. Weiss, J. M.; Morgan, P. H.; Lutz, M. W.; Kenakin, T. P. The cubic ternary complex receptor-occupancy model. III. resurrecting efficacy. *J Theor Biol* **1996**, 181, 381-397.
44. Weiss, J. M.; Morgan, P. H.; Lutz, M. W.; Kenakin, T. P. The Cubic Ternary Complex Receptor–Occupancy Model I. Model Description. *Journal of Theoretical Biology* **1996**, 178, 151-167.
45. Weiss, J. M.; Morgan, P. H.; Lutz, M. W.; Kenakin, T. P. The Cubic Ternary Complex Receptor–Occupancy Model II. Understanding Apparent Affinity. *Journal of Theoretical Biology* **1996**, 178, 169-182.
46. Seifert, R.; Wenzel-Seifert, K. Constitutive activity of G-protein-coupled receptors: cause of disease and common property of wild-type receptors. *Naunyn Schmiedebergs Arch Pharmacol* **2002**, 366, 381-416.
47. Perez, D. M.; Karnik, S. S. Multiple signaling states of G-protein-coupled receptors. *Pharmacological reviews* **2005**, 57, 147-161.
48. Kenakin, T. Ligand-selective receptor conformations revisited: the promise and the problem. *Trends in pharmacological sciences* **2003**, 24, 346-354.
49. Urban, J. D.; Clarke, W. P.; von Zastrow, M.; Nichols, D. E.; Kobilka, B.; Weinstein, H.; Javitch, J. A.; Roth, B. L.; Christopoulos, A.; Sexton, P. M.; Miller, K. J.; Spedding, M.; Mailman, R. B. Functional selectivity and classical concepts of quantitative pharmacology. *The Journal of pharmacology and experimental therapeutics* **2007**, 320, 1-13.
50. Jarpe, M. B.; Knall, C.; Mitchell, F. M.; Buhl, A. M.; Duzic, E.; Johnson, G. L. [D-Arg(1),D-Phe(5),D-Trp(7,9),Leu(11)]substance P acts as a biased agonist toward neuropeptide and chemokine receptors. *Journal of Biological Chemistry* **1998**, 273, 3097-3104.
51. Roth, B. L. Modulation of phosphatidylinositol-4,5-bisphosphate hydrolysis in rat aorta by guanine nucleotides, calcium and magnesium. *Life sciences* **1987**, 41, 629-634.
52. Felixberger, J. Luciferase complementation for the determination of arrestin recruitment: Investigations at histamine and NPY receptors. University of Regensburg, Regensburg, 2014. https://epub.uni-regensburg.de/31292/.
53. Misawa, N.; Kafi, A. K.; Hattori, M.; Miura, K.; Masuda, K.; Ozawa, T. Rapid and high-sensitivity cell-based assays of protein-protein interactions using split click beetle luciferase complementation: an approach to the study of G-protein-coupled receptors. *Anal Chem* **2010**, 82, 2552-2560.
54. Williams, M.; Glennon, R. A.; Timmermans, P. B. M. W. M. (ed.). *Receptor Pharmacology and Function*. Marcel Dekker Inc: 1989; Vol. 13, p 808.

55. Li, L.; Kracht, J.; Peng, S.; Bernhardt, G.; Elz, S.; Buschauer, A. Synthesis and pharmacological activity of fluorescent histamine H2 receptor antagonists related to potentidine. *Bioorganic & medicinal chemistry letters* **2003**, 13, 1717-1720.
56. Xie, S. X.; Petrache, G.; Schneider, E.; Ye, Q. Z.; Bernhardt, G.; Seifert, R.; Buschauer, A. Synthesis and pharmacological characterization of novel fluorescent histamine H2-receptor ligands derived from aminopotentidine. *Bioorganic & medicinal chemistry letters* **2006**, 16, 3886-3890.
57. Hirschfeld, J.; Buschauer, A.; Elz, S.; Schunack, W.; Ruat, M.; Traiffort, E.; Schwartz, J. C. Iodoaminopotentidine and Related-Compounds - a New Class of Ligands with High-Affinity and Selectivity for the Histamine-H2-Receptor. *Journal of medicinal chemistry* **1992**, 35, 2231-2238.
58. Malan, S. F.; van Marle, A.; Menge, W. M.; Zuliani, V.; Hoffman, M.; Timmerman, H.; Leurs, R. Fluorescent ligands for the histamine H2 receptor: synthesis and preliminary characterization. *Bioorganic & medicinal chemistry* **2004**, 12, 6495-6503.
59. Buschauer, A. Synthesis and in vitro pharmacology of arpromidine and related phenyl(pyridylalkyl)guanidines, a potential new class of positive inotropic drugs. *Journal of medicinal chemistry* **1989**, 32, 1963-1970.
60. Durant, G. J.; Duncan, W. A.; Ganellin, C. R.; Parsons, M. E.; Blakemore, R. C.; Rasmussen, A. C. Impromidine (SK&F 92676) is a very potent and specific agonist for histamine H2 receptors. *Nature* **1978**, 276, 403-405.
61. Portoghese, P. S. Bivalent Ligands and the Message-Address Concept in the Design of Selective Opioid Receptor Antagonists. *Trends in pharmacological sciences* **1989**, 10, 230-235.
62. Portoghese, P. S. From models to molecules: opioid receptor dimers, bivalent ligands, and selective opioid receptor probes. *Journal of medicinal chemistry* **2001**, 44, 2259-2269.
63. Yang, L. P.; Perry, C. M. Spotlight on histamine dihydrochloride in acute myeloid leukaemia. *Drugs Aging* **2011**, 28, 325-329.
64. Kenakin, T. *A Pharmacology Primer*. 3 ed.; Elsevier Academic Press: Burlington, 2009; p 389.
65. Crevat-Pisano, P.; Hariton, C.; Rolland, P. H.; Cano, J. P. Fundamental aspects of radioreceptor assays. *J Pharm Biomed Anal* **1986**, 4, 697-716.
66. Jameson, D. M.; Ross, J. A. Fluorescence polarization/anisotropy in diagnostics and imaging. *Chem Rev* **2010**, 110, 2685-2708.
67. Fish, K. N. Total internal reflection fluorescence (TIRF) microscopy. *Curr Protoc Cytom* **2009**, Chapter 12, Unit12 18.
68. Lohse, M. J.; Nuber, S.; Hoffmann, C. Fluorescence/bioluminescence resonance energy transfer techniques to study G-protein-coupled receptor activation and signaling. *Pharmacological reviews* **2012**, 64, 299-336.
69. Deschout, H.; Raemdonck, K.; Demeester, J.; De Smedt, S. C.; Braeckmans, K. FRAP in pharmaceutical research: practical guidelines and applications in drug delivery. *Pharm Res* **2014**, 31, 255-270.
70. Zanella, F.; Lorens, J. B.; Link, W. High content screening: seeing is believing. *Trends Biotechnol* **2010**, 28, 237-245.
71. Black, C. B.; Duensing, T. D.; Trinkle, L. S.; Dunlay, R. T. Cell-based screening using high-throughput flow cytometry. *Assay Drug Dev Technol* **2011**, 9, 13-20.
72. Keller, M.; Erdmann, D.; Pop, N.; Pluym, N.; Teng, S.; Bernhardt, G.; Buschauer, A. Red-fluorescent argininamide-type NPY Y1 receptor antagonists as pharmacological tools. *Bioorganic & medicinal chemistry* **2011**, 19, 2859-2878.
73. Dukorn, S.; Littmann, T.; Keller, M.; Kuhn, K.; Cabrele, C.; Baumeister, P.; Bernhardt, G.; Buschauer, A. Fluorescence- and Radiolabeling of [Lys4,Nle17,30]hPP Yields Molecular Tools for the NPY Y4 Receptor. *Bioconjugate chemistry* **2017**, 28, 1291-1304.
74. Bonnet, D.; Ilien, B.; Galzi, J. L.; Riche, S.; Antheaune, C.; Hibert, M. A rapid and versatile method to label receptor ligands using "click" chemistry: Validation with the muscarinic M1 antagonist pirenzepine. *Bioconjugate chemistry* **2006**, 17, 1618-1623.

75. Li, L.; Kracht, J.; Peng, S.; Bernhardt, G.; Buschauer, A. Synthesis and pharmacological activity of fluorescent histamine H1 receptor antagonists related to mepyramine. *Bioorganic & medicinal chemistry letters* **2003**, 13, 1245-1248.
76. Keen, M. The problems and pitfalls of radioligand binding. *Methods in molecular biology* **1995**, 41, 1-16.
77. Kuder, K. J.; Kiec-Kononowicz, K. Fluorescent GPCR Ligands as New Tools in Pharmacology-Update, Years 2008-Early 2014. *Curr Med Chem* **2014**, 21, 3962-3975.
78. Leff, P. The two-state model of receptor activation. *Trends in pharmacological sciences* **1995**, 16, 89-97.

Chapter 2

SCOPE AND OBJECTIVES

The Histamine H_2 receptor, an aminergic GPCR, is primarily known for its physiological role in the control of gastric acid secretion.[1,2] Additionally, activation of H_2R results in positive inotropic and chronotropic effects and smooth muscle relaxation.[3] The H_2R is primarily located on parietal cells in the stomach,[2] in mammalian brain,[4,5] on human neutrophiles and eosinophiles[6] as well as on smooth muscle cells[7]. Antagonists, which were intensively studied as antiulcer therapeutics in the 1960s to 80s, play only a minor role today, but are still important. Although, there is no H_2R agonist for therapeutic usage on the market, H_2R agonists are valuable molecular tools to study the pharmacology of the H_2R. Nonetheless, there are numerous possible indications e.g. as positive inotropic vasodilators for the treatment of congestive heart failure or as differentiation-introducing agents for treatment of acute myeloid leukemia. The development of selective high affinity molecular tools for the H_2R, including agonists as well as labeled molecules like radioligands and fluorescent ligands, is very important to identifiy new ligands, investigate receptor distribution and further unravel its (patho-)physiological role.

The number of suitable high affinity radioligands for the H_2R is very limited. [^{3}H]Histamine, as well as several reported tritiated antagonists (e.g. [^{3}H]cimetidine,[8,9] [^{3}H]ranitidine[10] and [^{3}H]tiotidine[11]) are less than ideal molecular tools to study the H_2R. As [^{3}H]cimetidine is reported to label an imidazole recognition site rather than the H_2R[8] and ranitidine as well as histamine suffer from low H_2R affinity and potency.[5,11] [^{3}H]Tiotidine is frequently used as a radioligand, although it shows very high unspecific binding and is reported to address only a subpopulation of the H_2R.[11] [^{125}I]Iodoaminopotentidine suffers from a short half-life of only 60 days, but shows the highest affinity to the H_2R reported so far (gpH_2R: K_d value: 0.34 nM).[5,12] An tritated alternative presents the recently published high-affinity tritium-labeled H_2R antagonist [^{3}H]UR-DE257[13] (hH_2R: K_d value: 31 nM), which is structurally related with the squaramide BMY25368[14]. This radioligand proved to be useful for the determination of pK_i values, but turned out as an insurmountable antagonist in functional assays.[13] One objective of this thesis was to design new ligands with a free terminal amino group and exploration of the applicability of them as precursors for the attachment of a radioactive (tritiated) moiety. Two reported classical antagonistic structures were used as scaffolds: the guanidinothiazoles and the aminopotentidines.

The guanidinothiazole-moiety is a privileged structure for H_2R antagonism. Previous functional studies identified guanidinothiazole-containing ligands, e.g. famotidine and ICI127032, as surmountable H_2R antagonists.[15,16] In this thesis, two different guanidinothiazole-precursors derived from famotidine and ICI127032 had to be combined with an “urea” equivalent. As a strategy to enable radiolabeling, the introduction of diaminoalkyl-linkers varying in length at the “urea” equivalent was envisaged. The resulting terminal amino group could be propionylated by succinimidyl propionate, to obtain ”cold forms” of the potential radioligands.

Aminopotentidine and its derivatives are reported as high affinity H_2R antagonists.[12] Interestingly, iodination in the 3-position of the 4-aminobenzoic acid amide moiety resulted in an enormous gain in affinity (iodoaminopotentidine).[4,12] Aminopotentidine and its analogs containing different substituents (e.g. iodine, bromine, chlorine, trifluoromethyl) in position 3 were synthesized as precursors for radiolabeling. The derivatization of the anilinic amino group of these precursors was performed with various reagents (e.g. N-succinimidyl propionate, propionic acid chloride, methyl iodide or acetyl chloride), which are also commercially available in tritiated form. Anilinic

amines show a reduced nucleophilicity which resulted in a reduced reactivity in the (radio-)labeling reaction. To overcome this challenge, the synthesis and characterization of a series of aminopotentidine derivatives, containing a functionalized (propionylated, acetylated or methylated) aminomethyl substituent in position 4 of the aromatic ring was considered.

The availability of high affinity red-emitting H_2R fluorescent ligands is very limited. Recently, a series of fluorescent ligands with a piperidinomethylphenoxypropylamino (potentidine) pharmacophore was reported.[17] The most promising ligands within this series are the squaramide-type ligands UR-DE229 and UR-DE56.[17] Both ligands consist of a BMY 2536[14] pharmacophore, which is linked to a fluorescent label (pyridinium or cyanine) by a n-alkyl linker. Another objective of this thesis was the synthesis and biological characterisation of fluorescent high affinity H_2R antagonists with improved optical and physicochemical properties to gain access to a wide range of potential applications, in particular to confocal microscopy and to high throughput or/and high content imaging. Therefore, the fluorescent labeled antagonists UR-DE229 and UR-DE56 were investigated in different assay/imaging systems. For the exploration of the impact of alkyl linker length and different net charges of fluorophores, a series of derivatives of UR-DE229 and UR-DE56 was considered.

N^G-acylated amino(methyl)thiazolepropylguanidines represent a class of potent and selective histamine H_2R agonists.[18-20] As it was reported that N^G-acylguanidines undergo hydrolytic cleavage upon storage in aqueous solution, more stable analogues are needed.[21,22] A bioisosteric approach, replacing the N^G-acylguanidine structure with a N^G-carbamoylguanidine, was planned in the final part of this thesis, aiming at N^G-carbamoylated aminothiazole-containing compounds with high affinity and improved long term stability. Furthermore, structure-activity (H_2R) and the structure-selectivity relationships (H_2R versus H_1R, H_3R and H_4R) of this class of compounds were considerd.

REFERENCES

1. Black, J. W.; Duncan, W. A.; Durant, C. J.; Ganellin, C. R.; Parsons, E. M. Definition and antagonism of histamine H 2 -receptors. *Nature* **1972**, 236, 385-390.
2. Domschke, W.; Domschke, S.; Classen, M.; Demling, L. Histamine and cyclic 3',5'-AMP in gastric acid secretion. *Nature* **1973**, 241, 454-455.
3. Reinhardt, D.; Schmidt, U.; Brodde, O. E.; Schumann, H. J. H1 - and H2-receptor mediated responses to histamine on contractility and cyclic AMP of atrial and papillary muscles from guinea-pig hearts. *Agents Actions* **1977**, 7, 1-12.
4. Traiffort, E.; Pollard, H.; Moreau, J.; Ruat, M.; Schwartz, J. C.; Martinez-Mir, M. I.; Palacios, J. M. Pharmacological characterization and autoradiographic localization of histamine H2 receptors in human brain identified with [125I]iodoaminopotentidine. *J. Neurochem.* **1992**, 59, 290-299.
5. Ruat, M.; Traiffort, E.; Bouthenet, M. L.; Schwartz, J. C.; Hirschfeld, J.; Buschauer, A.; Schunack, W. Reversible and Irreversible Labeling and Autoradiographic Localization of the Cerebral Histamine H-2-Receptor Using [I-125] Iodinated Probes. *P. Natl. Acad. Sci. USA* **1990**, 87, 1658-1662.
6. Reher, T. M.; Brunskole, I.; Neumann, D.; Seifert, R. Evidence for ligand-specific conformations of the histamine H(2)-receptor in human eosinophils and neutrophils. *Biochem. Pharmacol.* **2012**, 84, 1174-1185.
7. Mitznegg, P.; Schubert, E.; Fuchs, W. Relations between the effects of histamine, pheniramin and metiamide on spontaneous motility and the formation of cyclic AMP in the isolated rat uterus. *Naunyn Schmiedeberg´s Arch. Pharmacol.* **1975**, 287, 321-327.
8. Rising, T. J.; Norris, D. B.; Warrander, S. E.; Wood, T. P. High affinity 3H-cimetidine binding in guinea-pig tissues. *Life. Sci.* **1980**, 27, 199-206.
9. Warrander, S. E.; Norris, D. B.; Rising, T. J.; Wood, T. P. 3H-cimetidine and the H2-receptor. *Life. Sci.* **1983**, 33, 1119-1126.
10. Bristow, D. R.; Hare, J. R.; Hearn, J. R.; Martin, L. E. Radioligand binding studies using [^{3}H]-cimetidine and [^{3}H]-ranitidine. *Br. J. Pharmacol.* **1981**, 72, 487–590.
11. Kelley, M. T.; Bürckstümmer, T.; Wenzel-Seifert, K.; Dove, S.; Buschauer, A.; Seifert, R. Distinct interaction of human and guinea pig histamine H2-receptor with guanidine-type agonists. *Mol. Pharmacol.* **2001**, 60, 1210-1225.
12. Hirschfeld, J.; Buschauer, A.; Elz, S.; Schunack, W.; Ruat, M.; Traiffort, E.; Schwartz, J. C. Iodoaminopotentidine and Related-Compounds - a New Class of Ligands with High-Affinity and Selectivity for the Histamine-H2-Receptor. *J. Med. Chem.* **1992**, 35, 2231-2238.
13. Baumeister, P.; Erdmann, D.; Biselli, S.; Kagermeier, N.; Elz, S.; Bernhardt, G.; Buschauer, A. [3H]UR-DE257: Development of a Tritium-Labeled Squaramide-Type Selective Histamine H2 Receptor Antagonist. *ChemMedChem* **2015**, 10, 83-93.
14. Algieri, A. A.; Crenshaw, R. R. 1,2-Diaminocyclobutene-3,4-diones and a pharmaceutical composition containing them. FR 2505835, 1982. Chem. Abstr. 99:22320.
15. Yellin, T. O.; Buck, S. H.; Gilman, D. J.; Jones, D. F.; Wardleworth, J. M. ICI 125,211: a new gastric antisecretory agent acting on histamine H2-receptors. *Life. Sci.* **1979**, 25, 2001-2009.
16. Black, J. W.; Leff, P.; Shankley, N. P. Further Analysis of Anomalous Pkb Values for Histamine H-2-Receptor Antagonists on the Mouse Isolated Stomach Assay. *Br. J. Pharmacol.* **1985**, 86, 581-587.
17. Erdmann, D. Histamine H2- and H3-receptor antagonists : synthesis and characterization of radiolabelled and fluorescent pharmacological tools. Dissertation, Universität Regensburg, Regensburg, 2010. https://epub.uni-regensburg.de/19062/.
18. Kraus, A.; Ghorai, P.; Birnkammer, T.; Schnell, D.; Elz, S.; Seifert, R.; Dove, S.; Bernhardt, G.; Buschauer, A. N-G-Acylated Aminothiazolylpropylguanidines as Potent and Selective Histamine H-2 Receptor Agonists. *ChemMedChem* **2009**, 4, 232-240.

19. Birnkammer, T.; Spickenreither, A.; Brunskole, I.; Lopuch, M.; Kagermeier, N.; Bernhardt, G.; Dove, S.; Seifert, R.; Elz, S.; Buschauer, A. The Bivalent Ligand Approach Leads to Highly Potent and Selective Acylguanidine-Type Histamine H-2 Receptor Agonists. *J. Med. Chem.* **2012**, 55, 1147-1160.
20. Ghorai, P.; Kraus, A.; Birnkammer, T.; Geyer, R.; Bernhardt, G.; Dove, S.; Seifert, R.; Elz, S.; Buschauer, A. Chiral NG-acylated hetarylpropylguanidine-type histamine H2 receptor agonists do not show significant stereoselectivity. *Bioorg. Med. Chem. Lett.* **2010**, 20, 3173-3176.
21. Brennauer, A.; Keller, M.; Freund, M.; Bernhardt, G.; Buschauer, A. Decomposition of 1-(ω-aminoalkanoyl)guanidines under alkaline conditions. *Tetrahedron Letters* **2007**, 48, 6996-6999.
22. Kagermeier, N.; Werner, K.; Keller, M.; Baumeister, P.; Bernhardt, G.; Seifert, R.; Buschauer, A. Dimeric carbamoylguanidine-type histamine H receptor ligands: A new class of potent and selective agonists. *Bioorg. Med. Chem.* **2015**.

Chapter 3

Guanidinothiazoles: Towards the Squaramide- Type H_2R Radioligand [^{3}H]UR-SB69

Note: The synthesis and purification of [^{3}H]**3.25** was performed by Max Keller.

3.1 INTRODUCTION

Over the years, the endogenous agonist histamine and several H_2R antagonists were synthesized in a radiolabeled form (Figure 3.1). Nevertheless, [^{3}H]histamine,[1] [^{3}H]cimetidine,[2,3] [^{3}H]ranitidine[4] and [^{3}H]tiotidine[5] are less than ideal molecular tools to study the H_2R. As [^{3}H]cimetidine is reported to label an imidazole recognition site rather than the H_2R[2] and ranitidine as well as histamine suffer from low H_2R affinity and potency,[5,6] [^{3}H]tiotidine is frequently used as a radioligand, although it shows very high unspecific binding and is reported to address only a subpopulation of the H_2R.[5] By contrast, the labeling of aminopotentidine with ^{125}iodine resulted in a high affinity radioligand ([^{125}I]iodoaminopotentidine, gpH_2R: K_d value: 0.34 nM) which was used e.g. for autoradiography of the H_2R in human and rodent brain and heart as well as for saturation and kinetic binding studies.[6,7] Although ^{125}iodine labeled ligands have, compared to tritium labeled ligands, the advantage of a higher specific activity, their preparation and usage require higher safety precautions and the ligands can only be used for 4-5 weeks after preparation.[8]

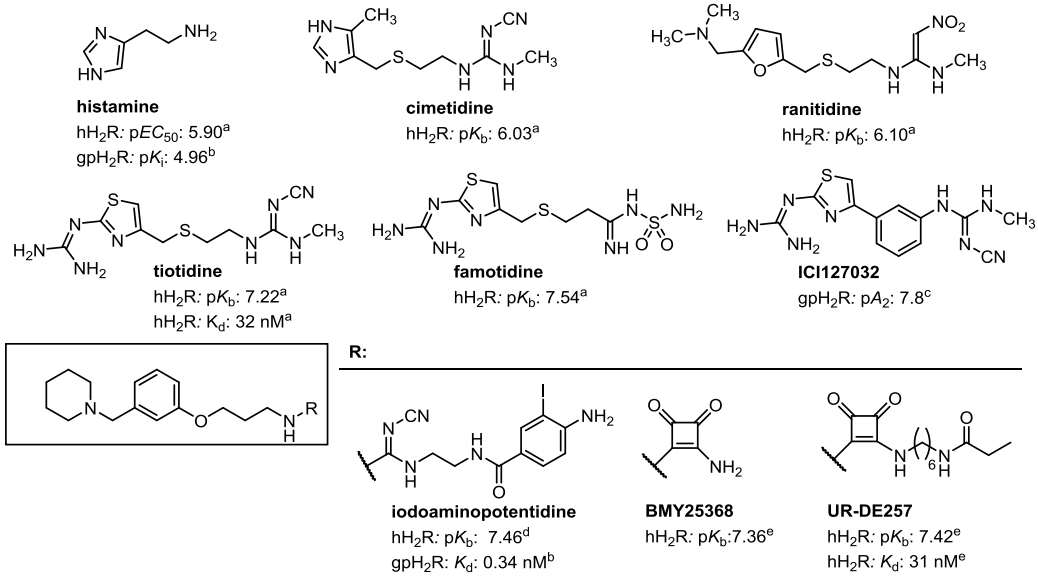

Figure 3.1. Structures of the endogenous ligand histamine and selected standard H_2R antagonists. [a]Kelley et al[5], [b]Ruat et al[6], [c]Yellin et al[9], [d]Preuss et al[10], [e]Baumeister et al[11].

An alternative to [^{125}I]iodoaminopotentidine is the recently published high-affinity tritium-labeled H_2R antagonist [^{3}H]UR-DE257 (K_d value: 31 nM)[11], which is structurally related to the squaramide BMY25368.[11,12] Although UR-DE257 was an insurmountable antagonist in functional assays, this radioligand proved to be very useful for the determination of pK_i values.[11]

Aiming at the development of high affinity tritium-labeled surmountable H_2R antagonists, guanidinothiazole-containing amines were considerd promising precursors. In previous functional studies, the antagonists with guanidinothiazole sub-structure, namely famotidine and ICI127032 were identified as surmountable H_2R antagonists.[9,13]

The 2-guanidino-4-[(2-aminoethyl)thiomethyl]thiazole precursor derived from famotidine and the 2-guanidino-4-(3-aminophenyl)thiazole precursor derived from ICI127032 were combined with the squaramide moiety (“urea” equivalent) of BMY25368 (general structure: Figure 3.2). In

order to enable radiolabeling, a terminal amino group connected to the squaramide via *n*-alkyl linker of different length, was introduced following the same strategy as in case of UR-DE257. The terminal amino group was propionylated using N-succinimidyl propionate to obtain ”cold forms” of the potential radioligands. Furthermore, the squaramide moiety was replaced by a cyanoguanidine moiety resulting in tiotidine-like compounds.

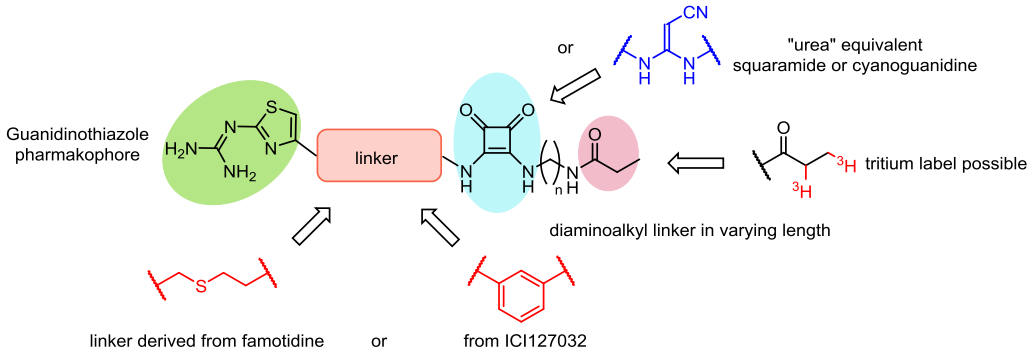

Figure 3.2. General structure of the guanidinothiazoles as potential new radioligands.

Interestingly, linking two amino(methyl)thiazolepropyl containing acyl or carbamoyl guanidines resulted in high affinity H_2R agonists (e.g. UR-NK22).[14,15] Therefore, this strategy was also adapted to the guanidinothiazoles: The replacement of the amino(methyl)thiazolepropyl moiety of UR-NK22 with either 2-guanidino-4-[(2-aminoethyl)thiomethyl]thiazole or 2-guanidino-4-(3-aminophenyl)thiazole resulted in two bivalent ligands (Figure 3.3).

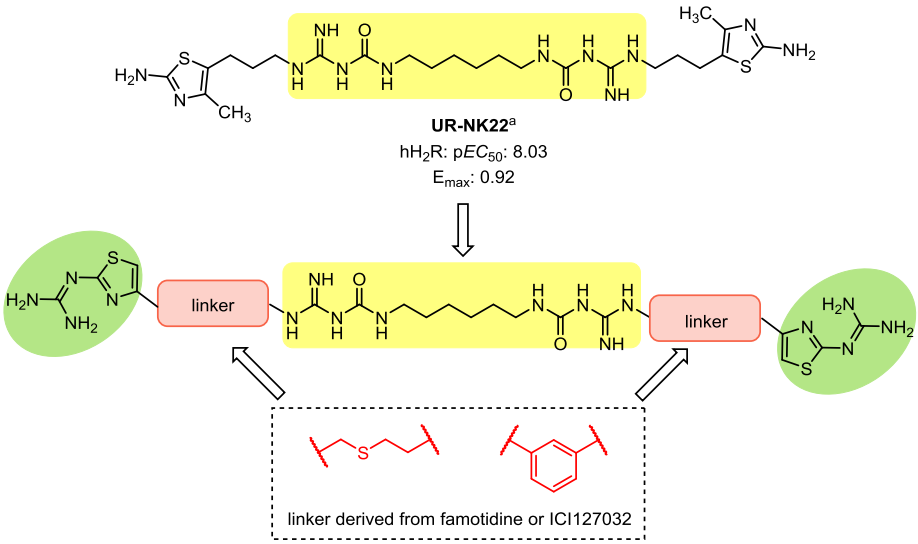

Figure 3.3. General structure of the dimeric guanidinothiazoles. [a]Kagermeier et al[14].

The amine precursors and the “cold forms” of the potentional radioligands as well as the two bivalent ligands were characterized in binding and functional (GTPγS binding assay) studies on recombinant histamine receptors (preferentially hH_2R and hH_3R). Radiolabeling is accessible by coupling of the commercially available N-succinimidyl [2,3-^{3}H]propionate with the respective amine precursor.

3.2 RESULTS AND DISCUSSION

3.2.1 Chemistry

The synthesis of the amine building block 2-guanidino-4-[(2-aminoethyl)thiomethyl]thiazole (**3.3**) according to published procedures is outlined in Scheme 3.1.[16] Firstly, 2-guanidino-4-chloromethylthiazole hydrochloride (**3.2**) was synthesized from amidinothiourea and 1,3-dichloroacetone. Secondly, **3.2** was coupled with 2-aminoethanthiole in a substitution reaction in the presence of sodium ethanolate to obtain **3.3** in excellent yield.

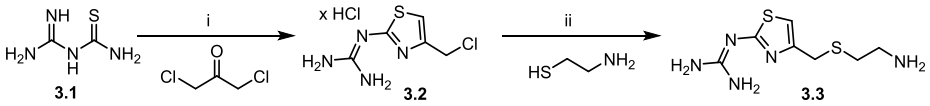

Scheme 3.1. Synthesis of 2-guanidino-4-[(2-aminoethyl)thiomethyl]thiazole **3.3**. Reagents and conditions: i) acetone, RT, 24 h, 56%; ii) EtONa, EtOH, 0 °C to RT, 24 h, 84%.

The conformationally constrained amine building block **3.7** was synthesized from 1-(3-aminophenyl)ethan-1-one and amidinothiourea according to literature procedures (Scheme 3.2).[17] After phthalimide protection **3.4** was brominated in alpha position and subsequently treated with amidinothiourea in order to form the protected building block **3.6** in a good yield of 70% (over two steps). Deprotection of the phthalimide group in a mixture of HCl and acetic acid afforded the conformationally constrained amine building block **3.7**.

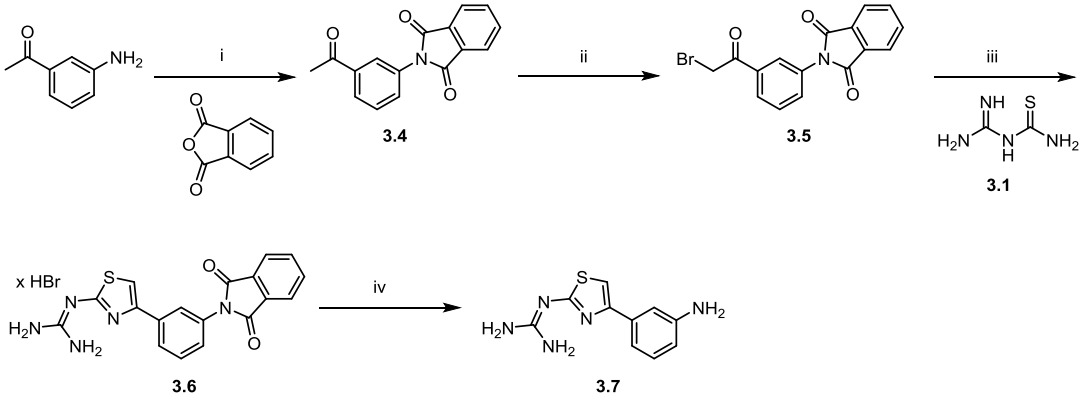

Scheme 3.2. Synthesis of 2-guanidino-4-(3-aminophenyl)thiazole **3.7**. Reagents and conditions: i) Acetic acid, reflux, 2.5 h, 96%; ii) Br_2, HBr, CH_2Cl_2, $CHCl_3$, RT, 0.5 h, no purification; iii) CH_3CN, EtOH, reflux, 5 h, 70%; iv) HCl, acetic acid, reflux, 24 h, 52%.

The synthetic route leading to the H_2R antagonists **3.8** and ICI127032 (**3.10**) is depicted in Scheme 3.3 as described in literature[17] with minor modifications. The formation of the thiourea **3.8** resulted from treatment of building block **3.7** with methylisothiocyanate. ICI127032 (**3.10**) was synthesized in two steps: Diphenylcyanocarbonimidate was first coupled with **3.7** and the resulting intermediate **3.9** was than treated with methylamine.

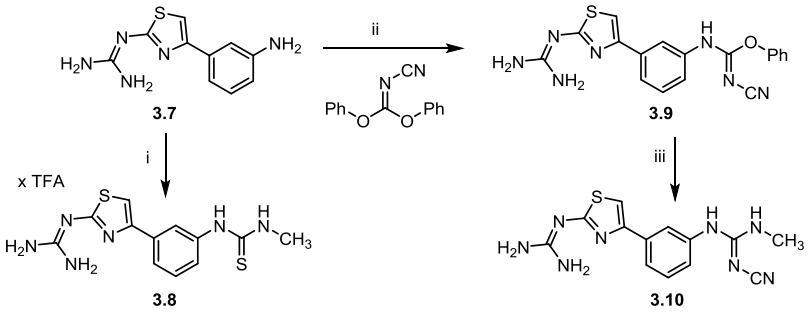

Scheme 3.3. Synthesis of the H_2R antagonists **3.8** and ICI127032 (**3.10**).[17] Reagents and conditions: i) methylisothiocyanate, acetone, RT, ON, 53%; ii) 2-propanol, RT, ON, no purification; iii) aq. methylamine solution, RT, ON, 55%.

The synthesis of the cyanoguanidine-type guanidinothiazole **3.13** followed a three step route (Scheme 3.4). The building block **3.3** was treated with the cyanoguanidinylating reagent diphenylcyanocarbonimidate[18] by analogy to published protocols.[7,11] The resulting intermediate **3.11** was treated with an excess of 1,8-diaminooctane in order to preferably form the monovalent ligand **3.12**. The propionamide **3.13** were synthesized from **3.12** and N-succinimidyl propionate.

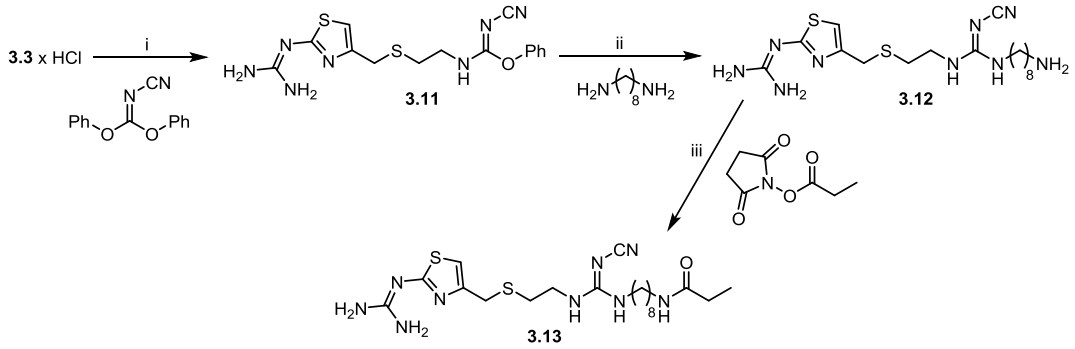

Scheme 3.4. Synthesis of the cyanoguanidine-type guanidinothiazole **3.13**. Reagents and conditions: i) TEA, MeOH, RT, ON, no purification; ii) MeCN, 50 °C, 3 h, 62%; iii) TEA, CH_2Cl_2, DMF, RT, 3 h, 22%.

The synthesis of the squaramide-type guanidinothiazoles **3.24**-**3.26** was adopted from known procedures (Scheme 3.5).[11,16] The reaction of precursor **3.3** and 3,4-diethoxycyclobut-3-ene-1,2-dione gave the squaric acid ester amide **3.14** as an intermediate, which was treated with the respective mono-Boc protected diamine **3.15**-**3.17** to yield the *tert*-butyl carbamates **3.18**-**3.20**. The mono-Boc protected amines were synthesized by treating an excess of the diamine with Di-*tert*-butyl dicarbonate. Final cleavage of the protecting group with TFA afforded the amines **3.21**-**3.23**. The propionylated ligands **3.24**-**3.26** were accessible through acylation of the respective amine precursor **3.21**-**3.23** with N-succinimidyl propionate.

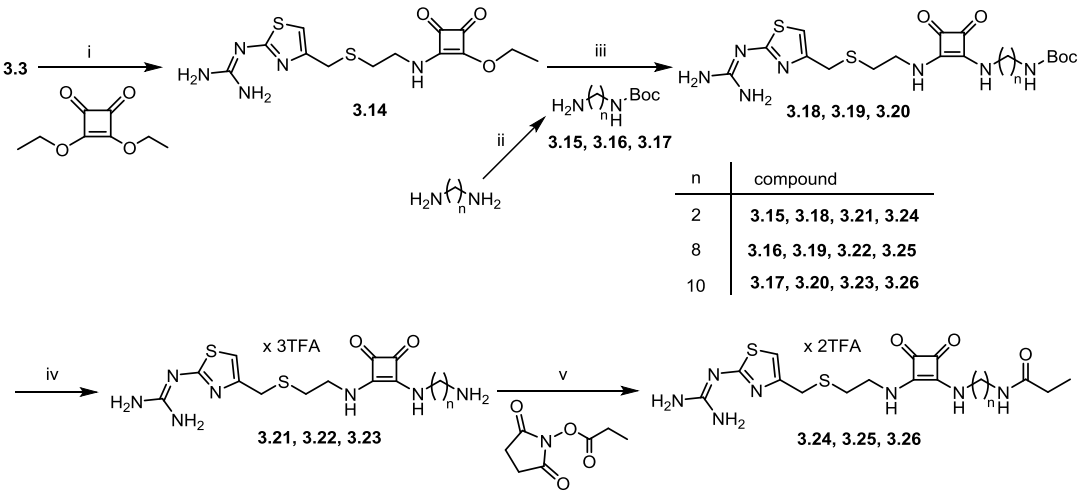

Scheme 3.5 Synthesis of the squaramide-type guanidinothiazoles **3.24**-**3.26**. Reagents and conditions: i) TEA, EtOH, RT, ON, 87%; ii) Di-*tert*-butyl dicarbonate, $CHCl_3$, 0 °C to RT, ON, 41-63%; iii) TEA, EtOH, 60-70 °C to RT, 6 h - 2 days, 63-88%; iv) TFA, CH_2Cl_2, RT, 1.5 h, 57-97%; v) TEA, CH_2Cl_2, RT, ON, 33-72%.

The conformationally constrained squaramide-type guanidinothiazole **3.30** was synthesized by following the same protocol as in case of the compounds **3.24**-**3.26** (Scheme 3.6). Starting from precursor **3.9**, treatment with 3,4-diethoxycyclobut-3-ene-1,2-dione gave the squaric acid ester amide intermediate **3.27**, which was reacted with *tert*-butyl N-(8-aminooctyl)carbamate (**3.16**) to obtain the *tert*-butyl carbamate **3.28**. Deprotection led to the amine precursor **3.29** which was propionylated with N-succinimidyl propionate.

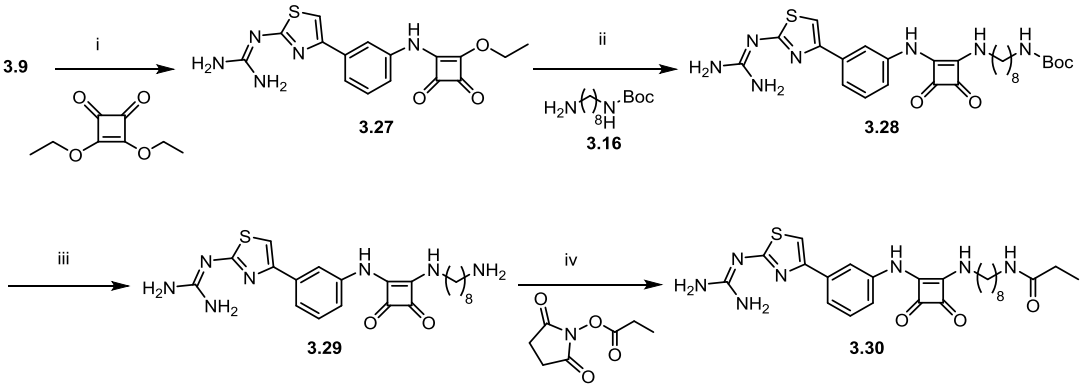

Scheme 3.6 Synthesis of the conformationally constrained squaramide-type guanidinothiazole **3.30**. Reagents and conditions: i) EtOH, RT, ON, no purification; ii) TEA, EtOH, 80 °C, ON, 34%; iii) TFA, CH_2Cl_2, RT, 5 h, 61%; iv) TEA, DMF, CH_2Cl_2, RT, ON, 12%.

The synthetic route leading to the bivalent guanidinothiazole containing ligands **3.34** and **3.35** was adopted from published protocols[14] and is depicted in Scheme 3.7. Thiourea was methylated with methyl iodine and subsequently mono-Boc protected, resulting in the well-established guanidinylating reagent **3.32**. Treatment of **3.32** with 1,6-diisocyanohexane afforded the bivalent guanidinylating reagent **3.33**. The bivalent ligands **3.34** and **3.35** were prepared by reaction of **3.33** with the respective guanidinothiazole building block (**3.3** or **3.7**) in the presence of a base, followed by preparative HPLC purification of the Boc-protected intermediates. The protecting group remained stable over the course of the purification, and deprotection was achieved by storage in the TFA consisting eluate for several hours, followed by a second preparative HPLC

purification. The addition of Hg(II) ions in guanidinylation reaction, as described in many published protocols[14,19], led to many by-products and only traces of the desired product.

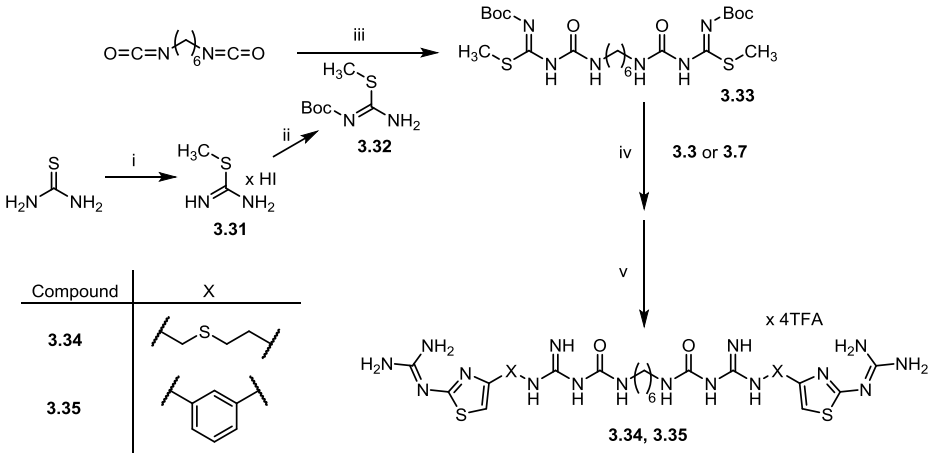

Scheme 3.7. Synthesis of the bivalent guanidinothiazole containing ligands **3.34** and **3.35**. Reagents and conditions: i) Methyliodide, MeOH, reflux, 1.5 h, 100%; ii) Di-*tert*-butyl dicarbonate, TEA, CH_2Cl_2, 0 °C to RT, ON, 73%; iii) TEA, CH_2Cl_2, Ar-atmosphere, RT, ON, 88%; iv)/v) DIPEA, MeOH, reflux, 5-48 h, deprotection after preparative HPLC in eluate consisting of H_2O, MeCN and TFA, 3-11% over two steps.

3.2.2 Biological Evaluation

H_2R affinity, selectivity and antagonism

The monovalent guanidinothiazole containing ligands **3.8, 3.10, 3.12, 3.13, 3.21-3.26, 3.29, 3.30**, the bivalent guanidinothiazole containing ligands **3.34**, **3.35** and exemplary published H_2R ligands were investigated in equilibrium competition binding experiments on membrane preparations from Sf9 insect cells, expressing the hH_2R-$G_{s\alpha S}$ fusion protein, using either the antagonist [^{3}H]UR-DE257[11] or [^{3}H]tiotidine as radioligands. The selectivity of these compounds for the hH_2R compared to hH_3R was investigated by competition binding experiments using Sf9 insect cell membranes co-expressing the hH_3R and $G_{\alpha i2}$ and $G_{\beta 1\gamma 2}$ proteins using [^{3}H]N^{α}-methylhistamine as radioligand. The "cold" form of the radioligand **3.25**, its precursor **3.22** and the bivalent ligands **3.34** and **3.35** were additionally investigated on membrane preparations of Sf9 insect cells, co-expressing either the hH_1R-$G_{s\alpha S}$ fusion protein (radioligand: [^{3}H]mepyramine) and RGS4 or hH_4R and $G_{\alpha i2}$ and $G_{\beta 1\gamma 2}$ proteins (radioligand: [^{3}H]histamine or [^{3}H]UR-PI294 [20]) in order to determine a "selectivity profile" at all four H_2R subtypes. Selected displacement curves are shown in Figure 3.4 and the results are summarized in Table 3.1.

The cyanoguanidine-type guanidinothiazole containing amine precursor **3.12** showed lower hH_2R affinity with a pK_i value of 6.5 than the structurally related H_2R antagonist famotidine (pK_i value: 7.26). Propionylation was tolerated without any decrease of affinity (ligand **3.13**). The hH_2R affinity of the squaramide-type guanidinothiazole containing amine precursors **3.21-3.23** increased with the chain length of the n-alkandiyl linker (pK_i values: 5.94-8.42). The propionylated squaramide-type ligands **3.24-3.26** showed a high affinity at the hH_2R (pK_i values: 7.07-7.65). Interestingly, the affinities of **3.25** and **3.26** decreased and the affinity of **3.24** increased compared to the respective amine precursor. The conformationally constrained squaramide-type guanidinothiazole containing ligand **3.30** showed a decreased hH_2R affinity (pK_i value: 6.8) compared to the closely related, more flexible ligand **3.25** (pK_i value: 7.65) and the cyanoguanidine-type analog ICI127032 (**3.10**) (pK_i value: 7.70). The amine precursor **3.29** showed compared to **3.30** a clearly increased pK_i value of 7.31. Within the series of propionylated ligands ("cold" forms of potential radioligands) **3.25** showed the highest hH_2R affinity (pK_i value: 7.65) which was comparable to the affinity of UR-DE257 (pK_i value: 7.55).

The ligands **3.8**, **3.21-3.26**, **3.29** and **3.30** showed a low affinity at the hH_3R with pK_i values of 4.28-5.5 and **3.10** showed a very low affinity (pK_i value <4). The precursor **3.22** and the "cold" form of the radioligand **3.25** showed a low affinity to the hH_4R with pK_i values of 4.3 and 4.4. **3.22** bound with moderate affinity to the hH_1R (pK_i value: 6.12), whereas binding of the propionylated **3.25** was not detectable up to a concentration of 100 µM.

The replacement of the amino(methyl)thiazolyl propyl head group of the bivalent ligand UR-NK22 with either a 2-guanidino-4-[(2-aminoethyl)thiomethyl]thiazole residue (**3.34**) or a 2-guanidino-4-(3 aminophenyl)thiazole residue (**3.35**) resulted in high affinity hH_2R ligands with pK_i values of 7.3 and 7.14. Compared to the bivalent agonist UR-NK22 the hH_2R affinity (pK_i value: 8.07)[14] and subtype selectivity was decreased.

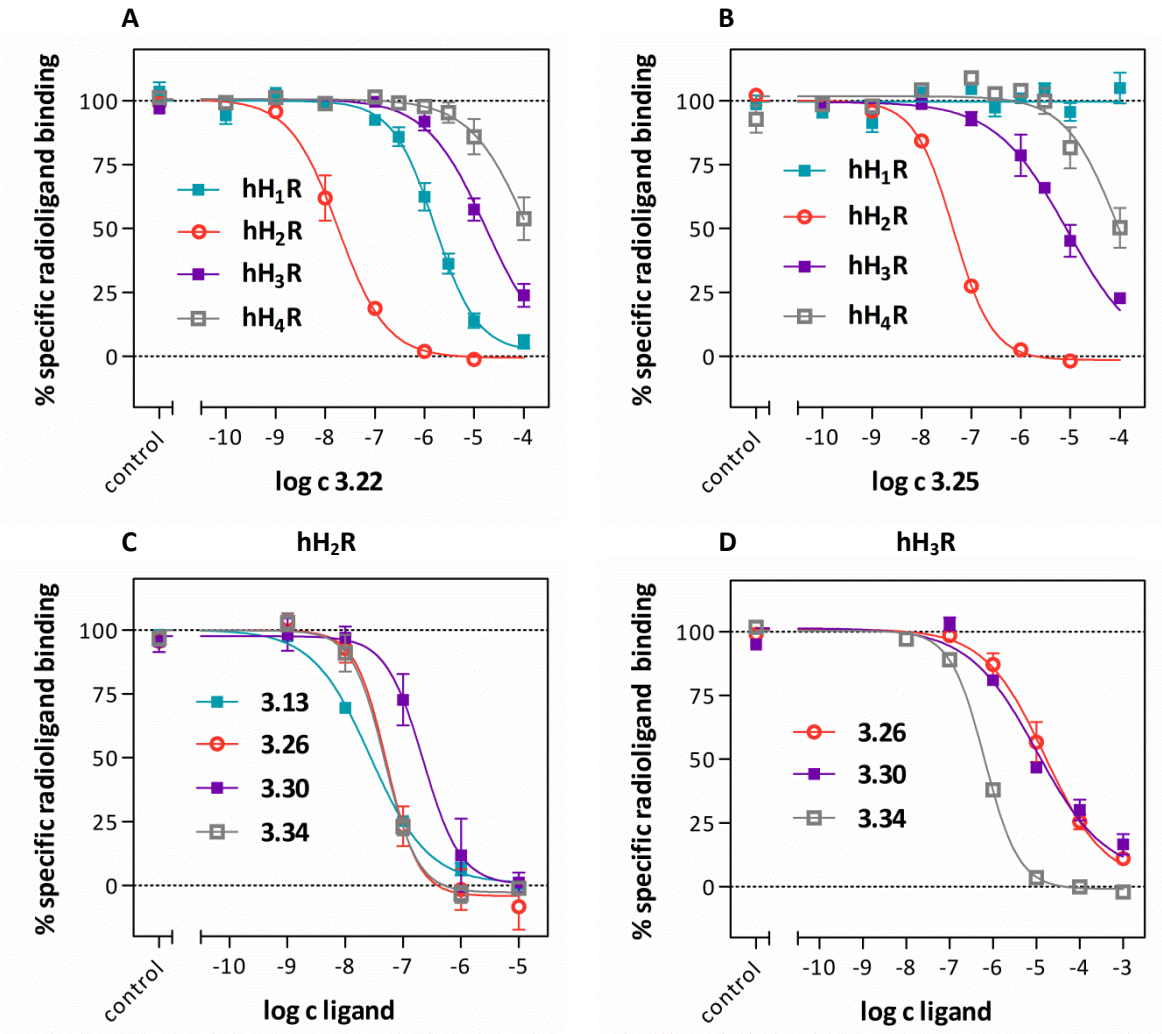

Figure 3.4. Displacement of the respective radioligand by amine precursor **3.22 (A)** or ligand **3.25** (B) from membrane preparations of Sf9 insect cells co-expressing the hH_1R-$G_{s\alpha S}$ fusion protein and RGS4 (radioligand: [^{3}H]mepyramine, c = 5 nM, K_d = 4.5 nM), expressing the hH_2R-$G_{s\alpha S}$ fusion protein (radioligand: [^{3}H]UR-DE257, c = 20 nM, K_d = 12.2 nM), co-expressing the hH_3R and $G_{\alpha i2}$ plus $G_{\beta 1\gamma 2}$ proteins (radioligand: [^{3}H]N^{α}-methylhistamine, c = 3 nM, K_d = 3 nM) or co-expressing the hH_4R and $G_{\alpha i2}$ plus $G_{\beta 1\gamma 2}$ proteins (radioligand: [^{3}H]UR-PI294, c = 5 nM, K_d = 5.1 nM). Displacement of the respective radioligand from membrane preparations of Sf9 insect cells (C) expressing the hH_2R-$G_{s\alpha S}$ fusion protein (radioligand: [^{3}H]UR-DE257, c = 20 nM, K_d = 12.2 nM or [^{3}H]tiotidine, c = 10 nM, K_d = 12.75 nM) or co-expressing the hH_3R and $G_{\alpha i2}$ plus $G_{\beta 1\gamma 2}$ proteins (radioligand: [^{3}H]N^{α}-methylhistamine, c = 3 nM, K_d = 3 nM) by exemplary guanidinothiazoles. Data represent mean values ± SEM of 2-3 experiments performed in triplicate.

Table 3.1. Affinities of standard H_2R ligands, UR-DE257, UR-NK22, the monovalent guanidinothiazole containing ligands **3.8**, **3.10**, **3.12**, **3.13**, **3.21-3.26**, **3.29**, **3.30** and the bivalent guanidinothiazole containing ligands **3.34**, **3.35** to $hH_{1\text{-}4}R$, obtained from equilibrium competition binding studies on membrane preparations from Sf9 insect cells, expressing the respective histamine receptor subtype.

	hH_1R[a]		**hH_2R[b]**		**hH_3R[d]**		**hH_4R[e]**	
No.	**pK_i**	**N**	**pK_i**	**N**	**pK_i**	**N**	**pK_i**	**N**
His	-	-	6.53 ± 0.04	3	7.8 ± 0.1	3	7.65 ± 0.03	3
UR-DE257	> 5.0[11]	-	7.55[11]	-	5.42[11]	-	> 5.0[11]	-
famotidine	-	-	7.26 ± 0.03	2	-	-	-	-
UR-NK22	6.06[14]	-	8.07[14]	-	5.94[14]		5.69[14]	-
3.8	n.d.	-	6.5 ± 0.1	3	4.28 ± 0.02	2	n.d.	-
3.10	n.d.	-	7.70 ± 0.07	3	> 4.0	2	n.d.	-
3.12	n.d.		6.5 ± 0.3	3	n.d.	-	n.d.	-
3.13	n.d.		6.4 ± 0.2	3	n.d.	-	n.d.	-
3.21	n.d.		5.94 ± 0.05	3	4.95 ± 0.03	2	n.d.	-
3.22	6.12 ± 0.08	3	8.0 ± 0.2	3	4.87 ± 0.09	3	4.3 ± 0.1[f]	3
3.23	n.d.	-	8.42 ± 0.09[c]	4	5.5 ± 0.1	2	n.d.	-
3.24	n.d.	-	7.07 ± 0.09	3	5.2 ± 0.1	2	n.d.	-
3.25	**> 4.0**	**3**	**7.65 ± 0.02**	**3**	**5.3 ± 0.1**	**3**	**4.4 ± 0.1[f]**	**3**
3.26	n.d.	-	7.43 ± 0.02[c]	3	5.08 ± 0.09	3	n.d.	-
3.29	n.d.	-	7.31 ± 0.07[c]	3	5.3 ± 0.2	2	n.d.	-
3.30	n.d.	-	6.8 ± 0.1[c]	3	5.44 ± 0.07	3	n.d.	-
3.34	n.d.	-	7.3 ± 0.1[c]	3	6.32 ± 0.02	4	6.21 ± 0.04	3
3.35	n.d.	-	7.14 ± 0.05	3	5.8 ± 0.1	3	6.09 ± 0.06	3

Competition binding assay on membrane preparations of Sf9 insect cells: [a]co-expression of the hH_1R-$G_{s\alpha S}$ fusion protein and RGS4 (radioligand: [^{3}H]mepyramine, c = 5 nM, K_d = 4.5 nM), [b]expression of the hH_2R-$G_{s\alpha S}$ fusion protein (radioligand: [^{3}H]UR-DE257, c = 20 nM, K_d = 12.2 nM or [c][^{3}H]tiotidine, c = 10 nM, K_d = 12.75 nM), [d]co-expression of the hH_3R and $G_{\alpha i2}$ and $G_{\beta 1\gamma 2}$ proteins (radioligand: [^{3}H]N^{α}-methylhistamine, c = 3 nM, K_d = 3 nM) or [e]co-expression of the hH_4R and $G_{\alpha i2}$ plus $G_{\beta 1\gamma 2}$ proteins (radioligand: [^{3}H]histamine c = 10 nM, K_d = 15.9 nM or [f][^{3}H]UR-PI294, c = 5 nM, K_d = 5.1 nM). The incubation period was 60 min. Data were analyzed by nonlinear regression and were best fitted to four-parameter sigmoidal concentration-response curves. Data shown are means ± SEM of N independent experiments, each performed in triplicate. The appreviation n.d. stands for not determined.

The monovalent guanidinothiazole containing ligands **3.8**, **3.10**, **3.12**, **3.13**, **3.21-3.26**, **3.29**, **3.30** and the bivalent guanidinothiazole containing ligands **3.34**, **3.35** were investigated for hH_2R agonism in the GTPγS binding assay on membrane preparations from Sf9 insect cells expressing the hH_2R-$G_{s\alpha S}$ fusion protein. Ligands which exhibited no agonism were also investigated in the antagonistic mode versus histamine as agonist. Selected curves are shown in Figure 3.5 and the results are summarized in Table 3.2.

The investigated monovalent and bivalent guanidinothiazole containing ligands were identified as antagonists or inverse agonists in the GTPγS assay. All ligands were able to completely displace histamine, but only the pK_b values of the ligands **3.8**, **3.30** and **3.35** were in good agreement with the pK_i values. The pK_b values of the ligands **3.10**, **3.22-3.26**, **3.29** and **3.34** were considerably lower compared to the corresponding pK_i values. Interestingly, propionylation of the amine precursors **3.22** and **3.29** (pK_b value: 6.95 and 6.68) was tolerated with nearly no change of the pK_b values. Nonetheless, ligand **3.25** also showed the highest pK_b value (7.04) within the series of propionylated ligands ("cold" forms of potential radioligands), which was only slightly decreased compared to UR-DE257 (pK_b value: 7.42)[11].

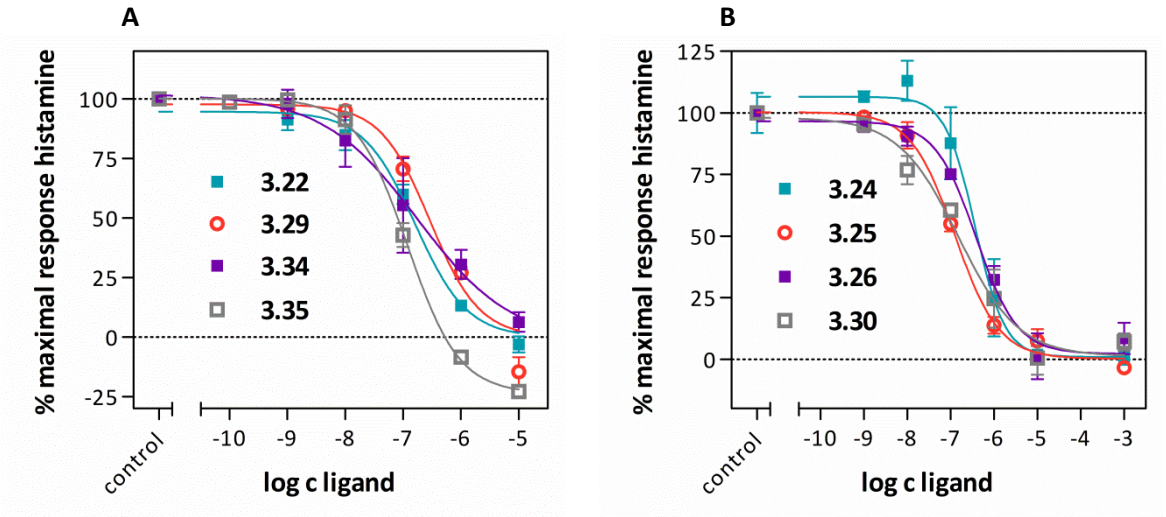

Figure 3.5. Antagonism of the guanidinothiazole containing ligands (A) **3.22**, **3.29**, **3.34**, **3.35** and (B) **3.24-3.26**, **3.30** on hH_2R determined in a GTPγS assay (antagonistic mode) on membrane preparations of Sf9 insect cells expressing the hH_2R-$G_{s\alpha S}$ fusion protein. Histamine (1 µM) was used for stimulation. Data represent mean values ± SEM of 2-4 experiments performed in triplicate.

Table 3.2. hH_2R antagonism and the calculated pK_b values of UR-DE257, the monovalent guanidinothiazole containing ligands **3.8**, **3.10**, **3.12**, **3.13**, **3.21-3.26**, **3.29**, **3.30** and the bivalent guanidinothiazole containing ligands **3.34**, **3.35** determined by a GTPγS assay.

	hH_2R (GTPγS)				hH_2R (GTPγS)		
No.	**pEC_{50} (pK_b)**	**N**	**α**	**No.**	**pEC_{50} (pK_b)**	**N**	**α**
His	5.80 ± 0.06	9	1.0	**3.24**	(6.6 ± 0.2)	3	-0.16
UR-NK22	8.03[14]	-	0.92[14]	**3.25**	(7.06 ± 0.03)	3	-0.30
UR-DE257	(7.42)[11]	-	0.08[11]	**3.26**	(6.5 ± 0.1)	3	-0.11
3.8	(6.9 ± 0.1)	4	-0.23	**3.29**	(6.68 ± 0.03)	2	-0.25
3.10	(7.0 ± 0.2)	3	-0.33	**3.30**	(6.9 ± 0.2)	2	-0.18
3.22	(6.95 ± 0.03)	3	-0.06	**3.34**	(7.0 ± 0.5)	2	-0.53
3.23	(7.5 ± 0.2)	4	-0.07	**3.35**	(7.09 ± 0.08)	3	-0.21

[^{35}S]GTPγS assay performed with membrane preparations of Sf9 insect cells expressing the hH_2R-$G_{s\alpha S}$ fusion protein. The intrinsic activity (α) of histamine was set to 1.00, and α values of investigated compounds were referred to this value. The pK_B values of neutral antagonists were determined in the antagonist mode versus histamine (c = 1 µM) as agonist. Data represent mean values ± SEM of N experiments, each performed in triplicate.

Discrepancies between pK_i and pK_b value of antagonists were observed by several groups.[7,21] Possible explanation are different experimental setups which led to varying access to the H_2R (e.g. guinea pig striatal membranes vs. intact isolated guinea pig heart)[7] or, when a very similar setup was used (e.g. membrane preparations in both binding and functional studies), the use of different competitors (histamine vs. radiolabeled antagonist).[21] Agonists and antagonists may stabilize different receptor conformations that exhibit different affinities for the investigated agonists/antagonists/inverse agonists.[21] The antagonistic radioligand [^{3}H]tiotidine was reported to bind only to a fraction of the functionally active H_2Rs.[5]

3.2.3 Chemical stability of 3.25

The ligand **3.25** showed the highest hH_2R affinity and subtype selectivity and was a good candidate for radiolabeling. Therefore the chemical stability of the "cold" radioligand **3.25** was investigated under radioligand storage conditions ($EtOH/H_2O$; 80:20; v/v) at a concentration of 15 µM at room temperature in the dark (Figure 3.6). After 7 days RP-HPLC analysis showed no decomposition.

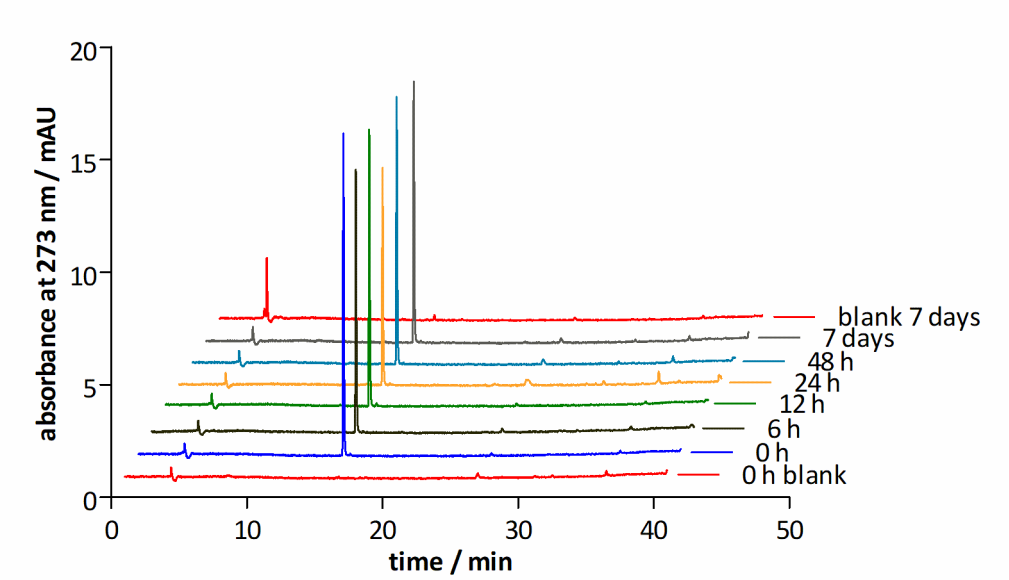

Figure 3.6. RP-HPLC analysis (λ: 273 nm) of **3.25** stock solution (t_R= 15.0 min) in EtOH/H_2O (80:20, v/v) after different times of incubation.

3.2.4 Radiosynthesis

Based on the pharmacological and chemical stability data presented, squaramide-type guanidinothiazole **3.25** was also synthesized with a tritium label ([^{3}H]**3.25**/ [^{3}H]UR-SB69) (Scheme 3.8). For this purpuse, an excess of the amine precursor **3.22** was acylated with the commercially available N-succinimidyl [2,3-^{3}H]propionate in the presence of DIPEA. After purification by HPLC, the radioligand [^{3}H]**3.25** was obtained in a radiochemical purity of 87% (Figure 3.7) with one impurity present. As the second peak (t_R = 14.3 min, Figure 3.7B) is amounting to ca. 13% of the total peak area, determination of the specific activity of [^{3}H]**3.25** was not feasible. Therefore, the specific activity of [^{3}H]**3.25** was estimated based on the specific activity (2.41 TBq/mmol, 65.03 Ci/mmol) of [^{3}H]UR-MK300[19] prepared on the same day from the same lot of N-succinimidyl [2,3-^{3}H]propionate. In order to prevent oxidation of the radioligand, the antioxidant ascorbinic acid was added to the radioligand stock solution (final concentration: 6.69 µmol/L [^{3}H]**3.25** and 76.9 µmol/L ascorbinic acid in EtOH/ H_2O 80:20).

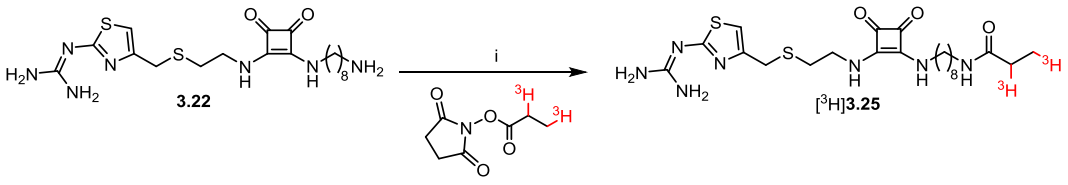

Scheme 3.8. Synthesis of the tritium-labeled squaramide-type guanidinothiazole [^{3}H]**3.25** ([^{3}H]UR-SB69). Reagents and conditions: i) DIPEA, anhydrous DMF, RT, 80 min, radiochemical yield: 64%.

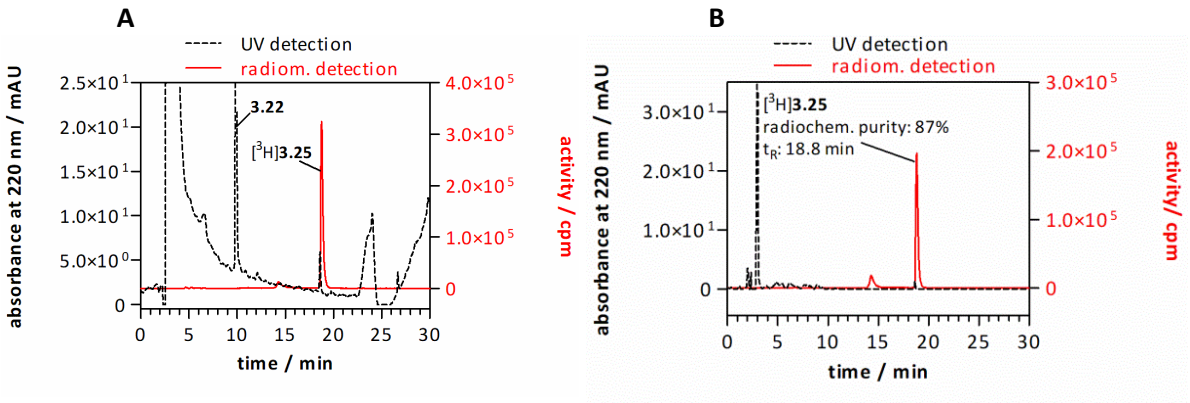

Figure 3.7. RP-HPLC analysis of the radioligand [^{3}H]**3.25** (A) before and (B) after purification by RP-HPLC (conditions, see Experimental Section). UV chromatogram of [^{3}H]**3.25** at 220 nm (black dashed line) and radiochromatogram of [^{3}H]**3.25** (red line).

3.2.5 Biological Evaluation of [^{3}H]3.25

Determination of binding constants of [^{3}H]3.25

The radioligand [^{3}H]**3.25** was characterized by saturation binding experiments on membrane preparations from Sf9 insect cells expressing the hH_2R-$G_{s\alpha S}$ fusion protein as well as on HEK293T-hH_2R-qs5 and HEK293T-hH_2R-βArr2 cells in suspension, both stably expressing the hH_2R. Additionally, kinetic binding experiments were performed on membrane preparations from Sf9 insect cells expressing the hH_2R-$G_{s\alpha S}$ fusion protein. The results are summarized in Table 3.3. [^{3}H]UR-SB69 bound in a saturable manner to both membranes and HEK cells (Figure 3.8).

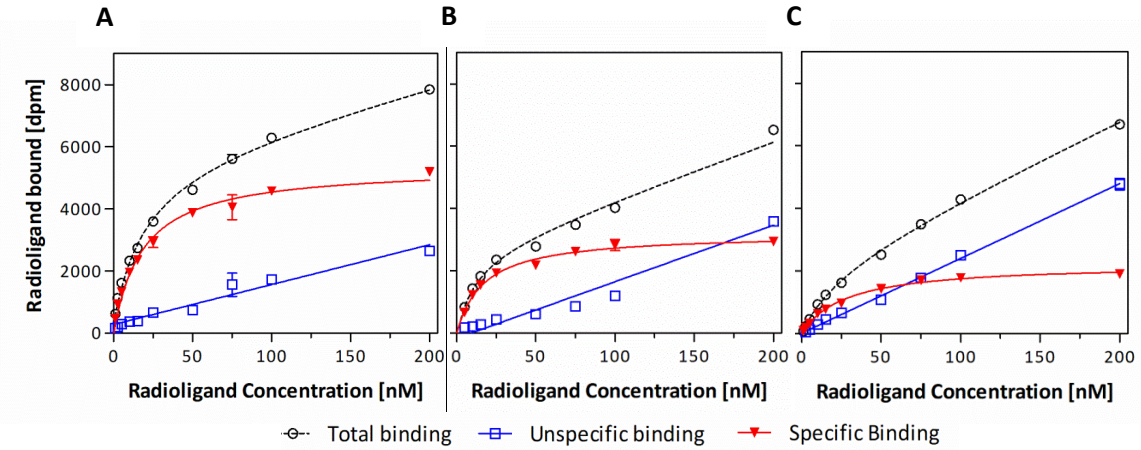

Figure 3.8. Representative saturation isotherms (red line) of specific hH_2R binding of [^{3}H]**3.25** on (A) membrane preparations from Sf9 insect cells expressing the hH_2R-$G_{s\alpha S}$ fusion protein, (B) cell suspension of HEK293T-hH_2R-qs5 cells and (C) cell suspension of HEK293T-hH_2R-βArr2 cells. Unspecific binding was determined in the presence of a 300 fold excess of famotidine. Specific binding was analyzed by a one-site binding equation. Error bars of specific binding and error bars of the Scatchard plot represent propagated errors calculated according to the Gaussian law. Error bars of total and unspecific binding represent the SEM. Experiments were performed in triplicate.

Unspecific binding was low when either membrane preparations or intact HEK293T-hH_2R-qs5 cells were used (<17% at the K_d value). Saturation binding studies performed with intact HEK293T-hH_2R-βArr2 cells resulted in considerably higher unspecific binding (<42% at the K_d

value). The specific binding versus [^{3}H]**3.25** concentration was best fitted by nonlinear regression to a one-site binding model and the unspecific binding to a linear curve. The determined K_d values (15-22 nM) were similar to the K_i value of 23 nM determined with [^{3}H]UR-DE257 on membrane preparations of Sf9 cells.

Table 3.3. hH_2R binding characteristics of [^{3}H]**3.25** determined on membrane preparations from Sf9 insect cells expressing the hH_2R-$G_{s\alpha S}$ fusion protein, HEK293T-hH_2R-qs5 or HEK293T-hH_2R-βArr2 cells at 25 °C.

		[^{3}H]3.25 ([^{3}H]UR-SB69)			
Receptor	K_i[d]	$K_{d\ (sat)}$[e]	$K_{d\ (kin)}$[f]	k_{on}[g]	k_{off}[h]
	[nM]	[nM]	[nM]	[min^{-1}·nM^{-1}]	[min^{-1}]
hH_2R	23 ± 1[a]	15 ± 1[a]/ 22 ± 4[b]/ 19 ± 4[c]	26.0 ± 0.3 [a]	0.00108 ± 0.00001[a]	0.028 ± 0.002[a]

Radioligand binding assay determined on [a]membrane preparations from Sf9 insect cells expressing the hH_2R-$G_{s\alpha S}$ fusion protein or cell suspension of [b]HEK293T-hH_2R-qs5 or [c]HEK293T-hH_2R-βArr2 cells. [d]Derived from competition binding with [^{3}H]UR-DE257, c = 20 nM, K_d = 12.2 nM (cf. Table 3.1). [e]Equilibrium dissociation constant determined by saturation binding. [f]Kinetically determined dissociation constant $K_{d\ (kin)}$= k_{off}/k_{on}. [g]Association rate constant derived from nonlinear regression; calculated from k_{obs}, k_{off} and the radioligand concentration (c= 20 nM). [h]Dissociation rate constant derived from nonlinear regression. Data represent means ± SEM from two to four independent experiments each performed in duplicate (association) or triplicate.

The association and dissociation curves of [^{3}H]**3.25** determined on membrane preparations of Sf9 insect cells expressing the hH_2R-$G_{s\alpha S}$ fusion protein are depicted in Figure 3.9. The association of the radioligand to the hH_2R was complete after 80 min and could be described by a monophasic fit with a k_{on} value of 0.00108 min^{-1}·nM^{-1}. Also linearization of the association curve revealed a straight line (k_{ob} value of 0.055 min^{-1}). The dissociation of [^{3}H]**3.25** (c = 20 nM, 90 min pre-incubation) in the presence of famotidine was incomplete, reaching a plateau at 23% of the initially bound radioligand. These data suggested a (pseudo)irreversible binding.[22,23]

Several GPCR ligands were reported to show a similar behavior in kinetic and functional experiments[22-25] and several explanations were provided such as irreversible (covalent) binding to the receptor,[26] a slow rate of dissociation from the receptor,[22] a slow rate of interconversion between inactive and active receptor conformations,[27] stabilization of an inactive ligand-specific receptor conformation,[28,29] binding to a site distinct from the agonist binding site,[30] internalization of the ligand-receptor-complex[25]. Nevertheless, the equilibrium dissociation constant $K_{d(kin)}$= 26.0 nM, calculated from kinetics (nonlinear regression, K_d = k_{off}/k_{on}), were consistent with the K_d value obtained from saturation binding experiments (Table 3.3) and the pseudo-irreversible binding to the hH_2R was far less pronounced compared to the radioligand [^{3}H]UR-DE257 (plateau at 60-70%).[11]

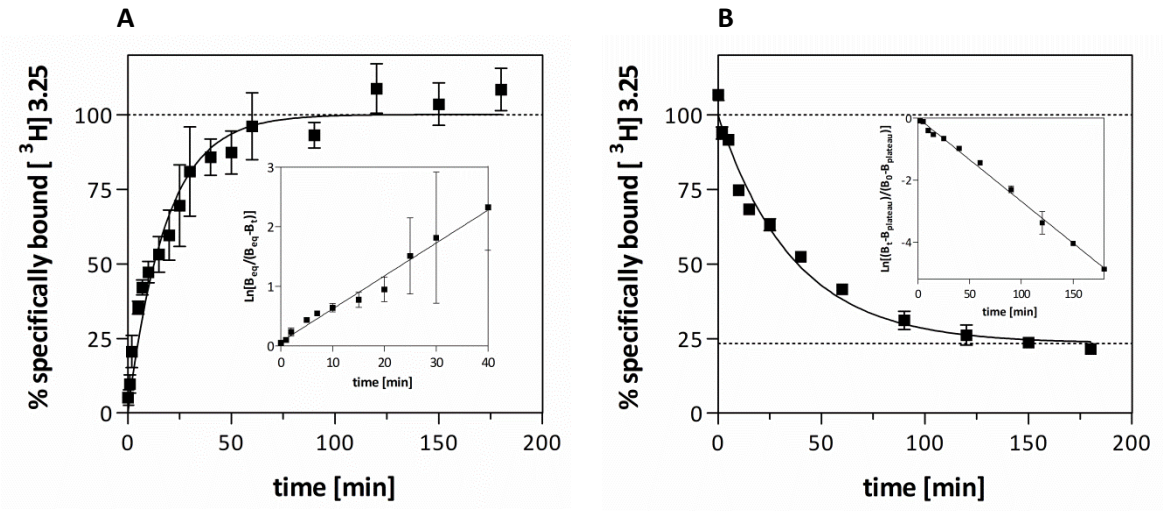

Figure 3.9. Association (A) and dissociation (B) kinetics of [^{3}H]**3.25** determined at membrane preparations from Sf9 insect cells expressing the hH_2R-$G_{s\alpha S}$ fusion protein at room temperature. Association (c = 20 nM) to the hH_2R as a function of time (nonlinear regression: k_{obs} = 0.049 min^{-1}). Inset: $\ln[B_{eq}/(B_{eq} - B_t)]$ versus time, k_{obs} = slope = 0.055 min^{-1}. Dissociation (preincubation: 90 min, c = 20 nM) in the presence of famotidine (c = 3 µM) from the hH_2R as a function of time, showing incomplete monophasic decline (nonlinear regression: k_{off} = 0.028 min^{-1}, $t_{1/2}$ = 25 min, plateau = 23%), Inset: $\ln[(B_t\text{-}B_{plateau})/(B_0\text{-}B_{plateau})]$ versus time, slope·(-1) = k_{off} = 0.027 min^{-1}. Data represent means ± SEM from two independent experiments each performed either in duplicate (association) or triplicate (dissociation).

Equilibrium competition binding experiments of [^{3}H]3.25

[^{3}H]**3.25** was used in equilibrium competition binding experiments with membrane preparations of Sf9 cells (Table 3.4). [^{3}H]**3.25** was completely displaceable by histamine and the standard H_2R antagonists famotidine and ICI127032 (Figure 3.10). Interestingly, lamtidine could only displace 75% of [^{3}H]**3.25**, but completely displace the radioligand [^{3}H]UR-DE257. The pK_i values were consistently lower but the order remained the same compared to the ones determined with [^{3}H]UR-DE257.

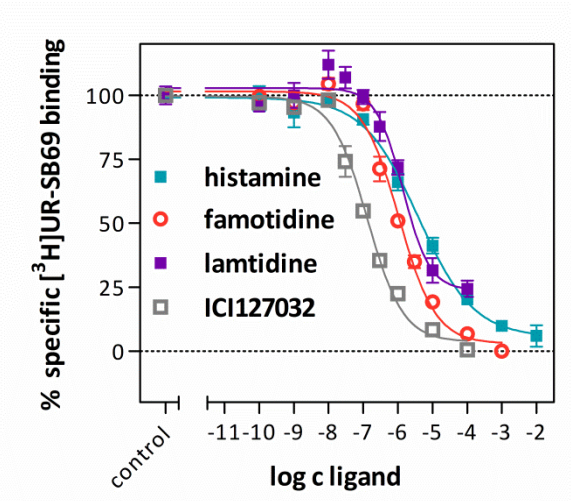

Figure 3.10. Displacement of the radioligand [^{3}H]UR-SB69 ([^{3}H]**3.25**, c = 20 nM, K_d = 15 nM) from membrane preparations of Sf9 insect cells expressing the hH_2R-$G_{s\alpha S}$ fusion protein by standard H_2R ligands. Data represent mean values ± SEM of 3 experiments performed in triplicate.

Table 3.4. Affinities of the standard H_2R ligands to hH_2R, obtained from equilibrium competition binding studies on membrane preparations from Sf9 insect cells, expressing the hH_2R with the radioligands [^{3}H]UR-DE257 and [^{3}H]**3.25**.

	pK_i values			
	[^{3}H]UR-DE257[a]	N	[^{3}H]UR-SB69 ([^{3}H]3.25)[b]	N
Histamine	6.53 ± 0.04	3	5.77 ± 0.08	3
Famotidine	6.87 [11]	-	6.36 ± 0.03	3
Lamtidine	6.8 ± 0.2	3	6.22 ± 0.07	3
ICI127032 (**3.10**)	7.70 ± 0.07	3	7.26 ± 0.03	3

Competition binding assay performed on membrane preparations of Sf9 insect cells expressing the hH_2R-$G_{s\alpha S}$ fusion protein. Radioligand: [a][^{3}H]UR-DE257, c = 20 nM, K_d = 12.2 nM or [b][^{3}H]**3.25**, c = 20 nM, K_d = 15 nM). The incubation period was 60 min. Data were analyzed by nonlinear regression and were best fitted to four-parameter sigmoidal concentration-response curves. Data shown are means ± SEM of N independent experiments, each performed in triplicate.

3.2.6 Chemical stability of [^{3}H]3.25

The long-term stability of [^{3}H]**3.25** in stock solution was investigated by RP-HPLC (conditions, see experimental section). The radiochemical purity of [^{3}H]**3.25** after 15 month still amounted to 45% (Figure 3.11) with one major impurity present (t_R= 12.6 min).

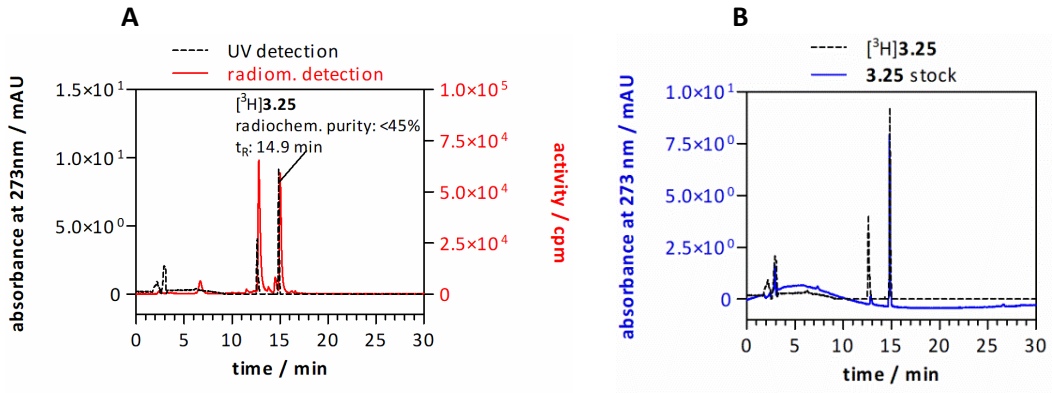

Figure 3.11. RP-HPLC analysis of the (A) radioligand stock solution [^{3}H]**3.25** 15 month after purification (UV chromatogram at 273 nm (black dashed line) and radiochromatogram (red line)) and (B) radioligand stock solution [^{3}H]**3.25** 15 month after purification (black dashed line) and stock solution of "cold" **3.25** in DMSO (blue line) (UV-chromatograms at 273 nm).

3.3 EXPERIMENTAL SECTION

3.3.1 General procedures

Chemicals and solvents were purchased from the following suppliers: Merck (Darmstadt, Germany), Acros Organics (Geel, Belgium), Sigma Aldrich (Munich, Germany) and TCI (Tokyo, Japan). All solvents were of analytical grade or distilled prior to use. Anhydrous solvents were stored over molecular sieve under protective gas. Deuterated solvents for NMR spectroscopy were purchased from Deutero (Kastellaun, Germany). For the preparation of buffers and HPLC eluents Millipore water was used throughout. Column chromatography was carried out using Merck silica gel 60 (0.040-0.063 mm). Reactions were monitored by thin layer chromatography (TLC) on Merck silica gel 60 F254 aluminium sheets, and compounds were detected with UV light at 254 nm and ninhydrin solution (0.8 g ninhydrin, 200 mL n-butanol, 6 mL acetic acid). Melting points were determined with a B-540 apparatus (BÜCHI GmbH, Essen, Germany) and are uncorrected. IR spectra were measured on a NICOLET 380 FT-IR spectrophotometer (Thermo Electron Corporation, USA). Nuclear Magnetic Resonance (^{1}H NMR and ^{13}C NMR) spectra were recorded on a Bruker Avance-300 (7.05 T, ^{1}H: 300 MHz, ^{13}C: 75.5 MHz), Avance-400 (9.40 T, ^{1}H: 400 MHz, ^{13}C: 100.6 MHz), or Avance-600 (14.1 T; ^{1}H: 600 MHz, ^{13}C: 150.9 MHz; cryogenic probe) NMR spectrometer (Bruker BioSpin, Karlsruhe, Germany). Chemical shifts are given in δ (ppm) relative to external standards. Multiplicities are specified with the following abbreviations: s (singlet), d (doublet), t (triplet), q (quartet), qui (quintet), m (multiplet), br s (broad signal), as well as combinations thereof. In certain cases 2D-NMR techniques (COSY, HSQC, HMBC and NOESY) were used to assign ^{1}H and ^{13}C chemical shifts. High-resolution mass spectrometry (HRMS) was performed on an Agilent 6540 UHD Accurate-Mass Q-TOF LC/MS system (Agilent Technologies, Santa Clara, USA) using an ESI source. Preparative HPLC was performed with a system from Knauer (Berlin, Germany) consisting of two K-1800 pumps and a K-2001 detector. A Nucleodur 100-5 C18 (250 x 21 mm, 5 µm, Macherey-Nagel, Dueren, Germany), a Kinetex XB-C18 100A (250 x 21.2 mm, 5 µm, Phenomenex, Aschaffenburg, Germany) and a YMC Triart C18 (150 x 20 mm, 5 µm, YMC Europe GmbH, Dinslacken, Germany) served as RP-columns at a flow rate of 15 ml/min at room temperature. In case of the cyanoguanidines **3.10**, **3.12** and **3.13** the mobile phase consisted of mixtures of CH_3CN and 0.1% aq. NH_3. Mixtures of CH_3CN and 0.05-0.1% aq. TFA were used as mobile phase for compounds **3.8**, **3.21-3.26**, **3.29**, **3.30**, **3.34**, **3.35**. A detection wavelength of 220 nm was used throughout. CH_3CN was removed from the eluates under reduced pressure (final pressure: 80 mbar) at 45 °C prior to lyophilisation (Christ alpha 2-4 LD lyophilisation apparatus equipped with a vacuubrand RZ 6 rotary vane vacuum pump). Analytical HPLC analysis was performed on a system from Meck Hitachi, composed of a D-6000 interface, a L-6200A pump, a AS2000A auto sampler and a L-4000 UV-VIS detector. A Kinetex XB-C18 100A (250 x 4.6 mm, 5 µm, Phenomenex, Aschaffenburg, Germany) served as RP-column. Mixtures of 0.05% TFA in CH_3CN (A) and 0.05% aq. TFA (B) were used as mobile phase. Helium degassing, room temperature, a flow rate of 0.8 mL/min and a detection wavelength of 220 nm were used throughout. Solutions for injection (concentration: 100-500 µM) were either prepared from stock solution (10 mM in DMSO) in a mixture of CH_3CN and H_2O corresponding to the initial eluent composition, or as a one to one mixture of the eluate (preparative HPLC) with Millipore water. The following linear gradients were applied for analytical HPLC analysis: gradient 1: 0-30 min: A/B 5:95-80:20, 30-32 min: 80:20-95:5, 32-42 min: 95:5 or gradient 2: 0-30 min: A/B 10:90-80:20, 30-

32 min: 80:20-95:5, 32-42 min: 95:5 or gradient 3: 0-30 min: A/B 15:85-90:10, 30-35 min: 90:10. Microanalysis was performed on a Vario micro cube (Elementar, Langenselbold, Germany).

3.3.2 Experimental protocols and analytical data

The synthesis of amidinothiourea[31] (**3.1**) and N-succinimidyl propionate[32] were described elsewhere.

2-Guanidino-4-chloromethylthiazole hydrochloride (3.2)[33]

1,3-Dichloroacetone (1.08 g, 8.46 mmol, 1 eq) dissolved in acetone (4 mL) was added to a suspension of **3.1** (1.0 g, 8.46 mmol, 1 eq) in acetone (5 mL). After approximately 10 min most of the solid dissolved and the supernatant turned yellow. The reaction mixture was stirred over night at room temperature. The product precipitated as the HCl salt. Separation by filtration and washing with acetone (5 mL) afforded the product as a yellow solid (1.07 g, 56%). Mp: 176.9-181.7 °C decomposition (Lit.[33] mp: 191-193 °C). R_f = 0.58 (CH_2Cl_2/NH_3in MeOH 9:1). ^{1}H-NMR (300 MHz, [D_6]DMSO): δ (ppm) 4.74 (s, 2H), 7.41 (s, 1H), 8.39 (s, 4H), 12.83 (s, 1H). ^{13}C-NMR (75.5 MHz, [D_6]DMSO): δ (ppm) 40.7, 113.4, 147.2, 154.2, 160.3. HRMS: (ESI): *m/z* [*M*+H]$^+$ calcd. for $C_5H_8ClN_4S^+$: 191.0153, found: 191.0151. $C_5H_7ClN_4S \cdot HCl$ (190.65 + 36.46).

2-Guanidino-4-[(2-aminoethyl)thiomethyl]thiazole (3.3)[33]

2-Aminoethanthiole hydrochloride (500 mg, 4.41 mmol, 2 eq) dissolved in EtOH (5 mL) were added dropwise to a sodium ethanolate solution (prepared from 250 mg Na in 8 mL EtOH) at 0 °C. The reaction mixture was stirred for 1.5 h at 0 °C. **3.2** (500 mg, 2.20 mmol, 1 eq) was added portion wise over 15 min at 0 °C. After stirring for overnight at room temperature, the solvent was evaporated under reduced pressure and the crude product was purified by column chromatography (eluent: CH_2Cl_2 / 3.5 M NH_3 in MeOH 90:10 isocratic). Removal of the solvent *in vacuo* afforded the product as yellow oil (430 mg, 84%). R_f = 0.2 (CH_2Cl_2 / 7 N NH_3 in MeOH 9:1). ^{1}H-NMR (400 MHz, [D_6]DMSO): δ (ppm) 2.63-2.78 (m, 4H), 3.56 (s, 2H), 6.47 (s, 1H), 6.85 (br s, 4H). ^{13}C-NMR (100 MHz, [D_4]MeOH): δ (ppm) 32.6, 35.2, 41.3, 106.8, 149.6, 159.0, 175.8. HRMS: (ESI) *m/z* [*M*+H]$^+$ calcd. for $C_7H_{14}N_5S_2^+$: 232.0685, found: 232.0689. $C_7H_{13}N_5S_2$ (231.34).

2-(3-Acetylphenyl)isoindoline-1,3-dione (3.4)[17]

1-(3-Aminophenyl)ethan-1-one (1 g, 7.40 mmol, 1 eq) and phthalic anhydride (1.2 g, 8.14 mmol, 1.1 eq) were suspended in acetic acid (20 mL). The reaction mixture was stirred under reflux for 2.5 h and part of the solvent was evaporated under reduced pressure. Water (10 mL) was added and the resulting precipitate was filtered through a Buchner funnel. Removal of residual solvent *in vacuo* afforded the product as beige fine crystals (1.9 g, 96%). Mp: 180-184.5°C. R_f = 0.24 (PE/EtOAc 3:1). ^{1}H-NMR (300 MHz, $CDCl_3$): δ (ppm) 2.62 (s, 3H), 7.58-7.68 (m, 2H), 7.77-7.83 (m,

2H), 7.92-8.00 (m, 3H), 8.03-8.05 (m, 1H). ^{13}C-NMR (75.5 MHz, $CDCl_3$): δ (ppm) 26.8, 124.0, 126.6, 127.8, 129.5, 131.1, 131.6, 132.3, 134.7, 138.1, 167.1, 197.1. HRMS: (ESI): *m/z* $[M+H]^+$ calcd. for $C_{16}H_{12}NO_3^+$: 266.0812, found: 266.0814. $C_{16}H_{11}NO_3$ (265.27).

2-Guanidino-4-(3-phthalimidophenyl)thiazole hydrobromide (3.6)[17]

To a solution of **3.4** (4.36 g, 16.44 mmol, 1 eq) in $CHCl_3$ (50 mL) was added HBr solution in acetic acid (45 % w/v, 110 µL) under stirring. Bromine (5.52 g, 34.52 mmol, 2.1 eq) was added drop wise. The reaction mixture was stirred for 30 min at room temperature. Removal of the solvent *in vacuo* afforded the **3.5** as a white solid, which was applied to the next step without further purification. The crude **3.5** was dissolved in hot CH_3CN (100 mL) and poured in a hot solution of **3.1** (1.94 g, 16.44 mmol, 1 eq) in EtOH (100 mL). The reaction mixture was stirred under reflux for 5 h. Removal of the solvent *in vacuo* afforded a beige solid, which was suspended in EtOAc and filtered through a Buchner funnel. **3.6** was afforded as a beige solid (5.12 g, 70%). Mp: 311.9-315.4 °C decomposition (Lit.[17] mp: >300 °C). R_f = 0.7 (CH_2Cl_2 / 7 N NH_3 in MeOH 6:1). ^{1}H-NMR (400 MHz, [D_6]DMSO): δ (ppm) 7.43-7.45 (m, 1H), 7.60 (t, 1H, *J* 7.83 Hz), 7.84 (s, 1H), 7.92-7.95 (m, 2H), 7.97-8.00 (m, 2H), 8.03-8.05 (m, 2H), 8.25 (br s, 4H), 12.04 (br s, 1H). ^{13}C-NMR (100 MHz, [D_6]DMSO): δ (ppm) 109.3, 123.5, 125.2, 125.7, 127.5, 129.4, 131.5, 132.5, 133.8, 134.8, 148.9, 153.8, 160.0, 167.0. HRMS: (ESI): *m/z* $[M+H]^+$ calcd. for $C_{18}H_{14}N_5O_2S^+$: 364.0863, found: 364.0866. $C_{18}H_{13}N_5O_2S \cdot HBr$ (363.40 + 80.91).

2-Guanidino-4-(3-aminophenyl)thiazole (3.7)[17]

3.6 (5.09 g, 11.46 mmol, 1eq) was suspended in a mixture of concentrated hydrochloric acid (75 mL) and acetic acid (75mL) and the reaction mixture was stirred under reflux overnight. The solvent was removed under reduced pressure and the residue was suspended in aqueous NaOH solution (2.5 % w/w, 200 mL). The resulting precipitate was filtered through a Buchner funnel and washed with H_2O (50 mL). Recrystallisation from CH_3CN and removal of residual solvent *in vacuo* afforded the product as a brown solid (1.40 g, 52%). Mp: 219.3-223.1 °C decomposition (Lit.[17] mp: 223-224 °C). R_f = 0.4 (CH_2Cl_2 / 7 N NH_3 in MeOH 9:1). ^{1}H-NMR (400 MHz, [D_6]DMSO): δ (ppm) 5.04 (s, 2H), 6.47-6.50 (m, 1H), 6.92 (s, 1H), 6.95-6.97 (m, 1H), 7.00-7.02 (m, 1H), 7.03-7.04 (m, 1H). ^{13}C-NMR (100 MHz, [D_6]DMSO): δ (ppm) 102.1, 111.2, 113.1, 113.4, 128.8, 135.4, 148.6, 150.0, 156.9, 174.7. HRMS: (ESI): *m/z* $[M+H]^+$ calcd. for $C_{10}H_{12}N_5S^+$: 234.0808, found: 234.0807. $C_{10}H_{11}N_5S$ (233.29).

2-Guanidino-4-[3-(3-methylthioureido)phenyl]thiazole hydrotrifluoracetate (3.8)[17]

Methylisothiocyanate (32 mg, 0.43 mmol, 1 eq) was added to a stirring solution of **3.7** (100 mg, 0.43 mmol, 1 eq) in acetone (2 mL). The reaction mixture was stirred overnight at room temperature. The solvent was removed *in vacuo* and the residue was purified by preparative HPLC (column: Nucleodur, gradient: 0-30 min: MeCN/0.05% aq. TFA 10:90-55:45, t_R = 14.93 min). The TFA-salt was obtained as a white solid (70 mg; 53%). Mp: 204.2 °C decomposition (Lit.[17]

oxalate mp: 219-222°C, decomposition). R_f = 0.25 (CH_2Cl_2/7M NH_3 in MeOH 9:1). RP-HPLC (gradient 2, 220 nm) (TFA-Salz): 95.8% (t_R = 13.67 min, k = 3.7). ^{1}H-NMR (600 MHz, [D_6]DMSO): δ (ppm) 2.92-2.93 (m, 3H), 7.32-7.33 (m, 1H), 7.36-7.39 (m, 1H), 7.65-7.66 (m, 1H), 7.69 (s, 1H), 7.81 (br s, 1H), 7.98 (s, 1H), 8.36 (br s, 4H), 9.65 (br s, 1H), 12.30 (br s, 1H). ^{13}C-NMR (150 MHz, [D_6]DMSO): δ (ppm) 31.3, 108.3, 120.6, 121.7, 123.1, 129.1, 133.5, 139.7, 149.5, 154.2, 158.6 (q, J 34 Hz, TFA), 160.6, 181.3. HRMS: (ESI): *m/z* [M+H]$^+$ calcd. for $C_{12}H_{15}N_6S_2^+$: 307.0794, found: 307.0797. $C_{12}H_{14}N_6S_2 \cdot C_2HF_3O_2$ (306.41 + 114.02).

4-[3-(2-Cyano-3-methylguanidino)phenyl]thiazole / ICI127032 (3.10)[17]

Diphenylcyanocarbonimidate (112 mg, 0.47 mmol, 1.1 eq) was dissolved in 2-propanol (10 mL). **3.7** (100 mg, 0.43 mmol, 1 eq) was added and the reaction mixture was stirred overnight at room temperature. The solvent was removed under reduced pressure, diethylether was added and solvent was again removed under reduced pressure. The solid (crude **3.9**) was dissolved in aqueous methylamine solution (40% w/w, 5mL) and the reaction mixture was stirred overnight at room temperature. The solvent was removed *in vacuo* and the residue was purified by preparative HPLC (column: YMC Triart C_{18}, gradient: 0-30 min: MeCN/0.1% aq. NH_3 10:90-40:60, t_R = 20.51 min). **3.10** was obtained as a white solid (74.5 mg; 55%). Mp: 167.4-192.4 °C. R_f = 0.25 (CH_2Cl_2/7M NH_3 in MeOH 9:1). RP-HPLC (gradient 3, 220 nm: 96.7% (t_R = 10.32 min, k = 3.1). ^{1}H-NMR (300 MHz, [D_6]DMSO): δ (ppm) 2.78 (d, 3H, J 4.48 Hz), 6.93 (br s, 4H), 7.16-7.21 (m, 3H), 7.35 (t, 1H, J 7.97 Hz), 7.60-7.63 (m, 1H), 7.71 (s, 1H), 8.94 (br s, 1H). ^{13}C-NMR (150 MHz, [D_6]DMSO): δ (ppm) 28.8, 103.6, 117.5, 121.1, 122.0 122.8, 129.0, 135.6, 138.0, 148.8, 157.1, 158.9, 175.2. HRMS: (ESI): *m/z* [M+H]$^+$ calcd. for $C_{13}H_{15}N_8S^+$: 315.1135, found: 315.1139. $C_{13}H_{14}N_8S$ (314.37).

1-(8-Aminooctyl)-2-cyano-3-(2-[2-(diaminomethyleneamino)thiazol-4-ylmethylthio]ethyl)guanidine (3.12)

Triethylamine (200 mg, 1.97 mmol, 4 eq) was added to a suspension of **3.3** as hydrochloride (150 mg, 0.49 mmol, 1 eq) in methanol (45 mL). Diphenyl-*N*-cyanocarbonimidate (118 mg, 0.49 mmol, 1 eq) was added and the reaction mixture was stirred overnight at room temperature. The solvent was partially removed under reduced pressure and H_2O (10 mL) was added. The product was extracted with EtOAc (3 x 15 mL), the organic layers were combined and dried over sodium sulfate. Removal of the solvent *in vacuo* afforded **3.11** as yellow oil which was directly used for the next step. The crude **3.11** and octan-1,8-diamine (285 mg, 1.97 mmol, 3 eq) were suspended in MeCN (1 mL) and the reaction mixture was stirred for 3 h at 50 °C. The solvent was removed *in vacuo* and the residue was purified by preparative HPLC (column: YMC Triart C_{18}, gradient: 0-30 min: MeCN/1% aq. NH_3 15:85-65:35, t_R = 16.7 min). **3.12** was obtained as white, highly hygroscopic solid (130 mg, 62.0%). R_f = 0.3 (CH_2Cl_2/7M NH_3 in MeOH 6:1). RP-HPLC (gradient 2, 220 nm): 95.7% (t_R = 12.74min, k = 4.1). ^{1}H-NMR (600 MHz, CD_3OD): δ (ppm) 1.35 (br s, 8H), 1.51-1.57 (m, 4H), 2.66-2.74 (m, 4H) 3.18 (t, 2H, J 7.1 Hz), 3.39 (t, 2H, J 6.97 Hz), 3.68 (s, 2H), 6.54 (s, 1H). ^{13}C-NMR (150 MHz, CD_3OD): δ (ppm) 22.1, 27.6, 27.7, 30.2, 30.28, 30.33, 31.8, 32.7, 41.9,

42.0, 42.7, 107.0, 120.1, 149.5, 159.1, 161.1, 175.9. HRMS: (ESI): *m/z* $[M+H]^+$ calcd. for $C_{17}H_{32}N_9S_2^+$: 426.2217, found: 426.2215. $C_{17}H_{31}N_9S_2$ (425.21).

N-(8-[2-Cyano-3-(2-[2-(diaminomethylenamino)thiazol-4-ylmethylthio]ethyl)guanidine]-octyl)propionamide (3.13)

Triethylamine (79 mg, 0.78 mmol, 3 eq) and N-succinimidyl propionate (34 mg, 0.29 mmol, 1.1 eq) were added to a suspension of **3.12** (111 mg, 0.26 mmol, 1eq) in CH_2Cl_2 (1 mL) and DMF (1 mL).The reaction mixture was stirred for 3 h at room temperature. The solvent was partially removed *in vacuo* and the residue was purified by preparative HPLC (column: YMC Triart C_{18}, gradient: 0-30 min: MeCN/1% aq. NH_3 15:85-80:20, t_R = 19.0 min). **3.13** was obtained as white, hygroscopic solid (28 mg, 22.3%). R_f = 0.4 (CH_2Cl_2/7M NH_3 in MeOH 6:1). IR (KBr): 3355, 3330, 3180, 2930, 2850, 2160, 1635, 1585, 1555, 1460, 1355, 1250, 1170, 1000, 850, 640, 605 cm^{-1}. RP-HPLC (gradient 2, 220 nm): 95.9% (t_R = 16.82 min, k = 5.7). ^{1}H-NMR (400 MHz, CD_3OD): δ (ppm) 1.12 (t, 3H, *J* 7.6 Hz), 1.34 (br s, 8H), 1.47-1.57 (m, 4H), 2.15-2.21 (q, 2H, *J* 7.7 Hz), 2.68 (t, 2H, *J* 6.9 Hz), 3.13-3.19 (m, 4H), 3.38 (t, 2H, *J* 6.8 Hz), 3.68 (s, 2H), 6.54 (s, 1H). ^{13}C-NMR (150 MHz, [D_6]DMSO, COSY, HSQC, HMBC): δ (ppm) 10.6, 27.7, 27.9, 30.2, 30.26 (2C), 30.29, 30.4, 31.8, 32.7, 40.4, 42.0, 42.8, 107.0, 120.1, 149.5, 159.1, 161.1, 175.9, 177.0. HRMS: (ESI): *m/z* $[M+H]^+$, calcd. for $C_{20}H_{36}N_9S_2O^+$: 482.2479, found: 482.2484. Anal. calcd. for $C_{20}H_{35}N_9S_2O$: C 49.87, H 7.32, N 26.17, S 13.31, found: C 49.56, H 7.19, N 26.24, S 12.88. $C_{20}H_{35}N_9S_2O$ (481.58).

2-(4-[2-(2-Ethoxy-3,4-dioxocyclobut-1-ene-1-ylamino)ethylthiomethyl]thiazol-2-yl)guanidine (3.14)[34]

3,4-Diethoxycyclobut-3-ene-1,2-dione (246 mg, 1.45 mmol, 1.1 eq) was dissolved in EtOH (15 mL). **3.3** as hydrochloride (400 mg, 1.32 mmol, 1 eq) and triethylamine (533 mg, 5.26 mmol, 4 eq) dissolved in EtOH (15 mL) were added drop wise under stirring. The reaction mixture was stirred over night at room temperature. The precipitated product was filtered off and washed with EtOH. Some product was still contained in the supernatant. EtOH was removed *in vacuo* and the residue was purified by column chromatography (eluent: CH_2Cl_2 / 7 M NH_3 in MeOH 95:5 isocratic). The precipitated product and the column purified product were combined and the solvent was removed *in vacuo*. **3.14** was obtained as beige solid (408 mg, 87%). Mp: 187.5-189.9 °C decomposition (Lit.[34] mp >135 °C decomposition). R_f = 0.5 (CH_2Cl_2/7M NH_3 in MeOH 6:1).^{1}H-NMR (400 MHz, [D_6]DMSO, COSY, HSQC, HMBC): δ (ppm) 1.34-1.39 (m, 3H), 2.63-2.68 (m, 2H), 3.46-3.48 (m, 1H), 3.61 (s, 2H), 3.67-3.68 (m, 1H), 4.63-4.68 (q, 2H, *J* 7.0 Hz), 6.47 (s, 1H), 6.83 (br s, 3.7H), 8.66-8.85 (d, 1H, *J* 75.8 Hz). ^{13}C-NMR (100 MHz, CD_3OD): δ (ppm) 15.5 (-$OCH_2C\mathbf{H_3}$), 31.0 (d, *J* 20 Hz, thiazolyl-$\mathbf{C}H_2$), 31.4 (d, *J* 34 Hz, -S$\mathbf{C}H_2CH_2NH$-), 43.0 (d, *J* 68 Hz, -$SCH_2\mathbf{C}H_2NH$-), 68.8 (d, *J* 9 Hz, -O$\mathbf{C}H_2CH_3$), 104.4 (d, *J* 10 Hz, $\mathbf{C^5}$ thiazolyl), 147.4 (d, *J* 11 Hz, $\mathbf{C^4}$ thiazolyl), 156.8 ($(NH_2)_2\mathbf{C}$=N-), 172.4 (d, *J* 32 Hz, cyclobutendion), 175.4 ($\mathbf{C^2}$ thiazolyl), 176.7 (d, *J* 21 Hz, cyclobutendion), 182.0 (d, *J* 19 Hz, **C**=O cyclobutendion), 189.2 (d, *J* 31 Hz, **C**=O cyclobutendion). HRMS: (ESI): *m/z* $[M+H]^+$, calcd. for $C_{13}H_{18}N_5S_2O_3^+$: 356.0846, found: 356.0847. $C_{13}H_{17}N_5S_2O_3$ (355.43).

General procedure for the synthesis of the Mono-Boc-protected diamines (3.15-3.17)

The corresponding alkane diamine (2 eq) was dissolved in chloroform (30 mL). Di-*tert*-butyl dicarbonate (1 eq) was dissolved in chloroform (25 mL) and added drop wise over a period of 3 h under ice-cooling. The reaction mixture was allowed to warm up to room temperature while stirring overnight. Potentially precipitated alkane diamine was filtered off. The organic layer was washed with alkaline saturated NaCl solution (45 mL sat. aq. NaCl and 1 mL 1 M aq. NaOH), saturated NaCl solution (45 mL) and H_2O (45 mL). The organic layer was dried over sodium sulphate and concentrated by evaporation under reduced pressure. The residue was purified by column chromatography (eluent: CH_2Cl_2 / 2 M NH_3 in MeOH 97.5:2.5-90:10).

***tert*-Butyl *N*-(2-aminoethyl)carbamate (3.15)[35-38]**

Ethylendiamine (1.5 g, 25.0 mmol, 2 eq) was treated with di-*tert*-butyldicarbonate (2.72 g, 12.5 mmol, 1 eq) according to the general procedure. Removal of the solvent *in vacuo* afforded the product as slightly yellow oil (1.25 g, 62.5%). R_f = 0.5 (CH_2Cl_2/3 M NH_3 in MeOH 5:1). ^{1}H-NMR (400 MHz, $CDCl_3$): δ (ppm) 1.34 (s, 2H), 1.38 (s, 9H), 2.73 (t, 2H, *J* 5.6 Hz), 3.10 (m, 2H), 5.11 (br s, 1H,). HRMS (ESI): *m/z* $[M+H]^+$ calcd. for $C_7H_{17}N_2O_2^+$: 161.1285, found: 161.1284. $C_7H_{16}N_2O_2$ (160.22).

***tert*-Butyl *N*-(8-aminooctyl)carbamate (3.16)[38,39]**

Octane-1,8-diamine (2.0 g, 13.9 mmol, 2 eq) was treated with di-*tert*-butyldicarbonate (1.5 g, 7.0 mmol, 1 eq) according to the general procedure. Removal of the solvent *in vacuo* afforded the product as colorless oil (700 mg, 41.2%). R_f = 0.3 (CH_2Cl_2/3.5 M NH_3 in MeOH 9:1). ^{1}H-NMR (400 MHz, $CDCl_3$): δ (ppm) 1.26 (br s, 8H), 1.30 (br s, 2H), 1.38-1.41 (m, 13H), 2.62-2.66 (t, 2H; *J* 7.0 Hz), 3.04-3.09 (m, 2H), 4.58 (br s, 1H). ^{13}C-NMR (100 MHz, $CDCl_3$): δ (ppm) 26.8, 26.9, 28.5, 29.3, 29.5, 30.1, 33.9, 40.7, 42.3, 79.0, 156.1. HRMS (ESI): *m/z* $[M+H]^+$ calcd. for $C_{13}H_{29}N_2O_2^+$: 245.2224, found: 245.2225. $C_{13}H_{28}N_2O_2$ (244.38).

***tert*-Butyl *N*-(10-aminodecyl)carbamate (3.17)[38]**

Decane-1,10-diamine (2.0 g, 11.6 mmol, 2 eq) was treated with di-*tert*-butyldicarbonate (1.3 g, 5.8 mmol, 1 eq) according to the general procedure. Removal of the solvent *in vacuo* afforded the product as colorless oil (820 mg, 51.2%). R_f = 0.6 (CH_2Cl_2/7 M NH_3 in MeOH 7: 1). ^{1}H-NMR (400 MHz, $CDCl_3$): δ (ppm) 1.26 (br s, 12H), 1.42-1.46 (m, 13H), 1.67 (br s, 2H), 2.67 (t, 2H, *J* 7.1 Hz), 3.06-3.10 (m, 2H), 4.53 (br s, 1H). ^{13}C-NMR (100 MHz, $CDCl_3$): δ (ppm) 26.9, 27.0, 28.6, 29.4, 29.55, 29.60, 29.62, 30.2, 33.7, 40.8, 42.3, 79.1, 156.1. HRMS (ESI): *m/z* $[M+H]^+$ calcd. for $C_{15}H_{33}N_2O_2^+$: 273.2537, found: 273.2537. $C_{15}H_{32}N_2O_2$ (272.43).

tert-Butyl [2-(2-[2-(2-guanidinothiazol-4-ylmethylthio)ethylamino]-3,4-dioxocyclobut-1-ene-1-ylamino)ethyl]carbamate (3.18)

Compound **3.14** (150 mg, 0.42 mmol, 1 eq) was dissolved in EtOH (10 mL) and a solution of **3.15** (74 mg, 0.46 mmol, 1.1 eq) in EtOH (10 mL) was added under stirring. The reaction mixture was stirred over night at room temperature. Due to incomplete conversion triethylamine (214 mg, 2.11 mmol, 5 eq) was added and the reaction mixture was stirred at 70 °C for 6 h. The solution was allowed to cool to room temperature and stirred at this temperature over night. Removal of the solvent *in vacuo* and purification by column chromatography (eluent: CH_2Cl_2 / 7 M NH_3 in MeOH 95:5- 80:20) afforded the product as white solid (158 mg, 79.2%). Mp: 187.7-195.6 °C decomposition. R_f = 0.2 (CH_2Cl_2/7 M NH_3 in MeOH 9:1). ^{1}H-NMR (400 MHz, [D_6]-DMSO): δ (ppm) 1.36 (s, 9H), 2.64-2.67 (t, 2H, *J* 6.7 Hz), 3.07-3.11 (q, 2H, *J* 5.9 Hz), 3.50 (br s, 2H), 3.66-3.70 (m, 4H), 6.62 (s, 1H), 6.88-7.09 (br s, 5H), 7.58 (br s, 2H). HRMS: (ESI): *m/z* [*M*+H]$^+$, calcd. for $C_{18}H_{28}N_7O_4S_2^+$: 470.1639, found: 470.1643. $C_{18}H_{27}N_7O_4S_2$ (469.58).

tert-Butyl [8-(2-[2-(2-guanidinothiazol-4-ylmethylthio)ethylamino]-3,4-dioxocyclobut-1-ene-1-ylamino)octyl]carbamate (3.19)

3.14 (163 mg, 0.46 mmol, 1 eq), **3.16** (124 mg, 0.50 mmol, 1.1 eq) and triethylamine (232 mg, 2.29 mmol, 5 eq) were dissolved in EtOH (20 mL). The reaction mixture was stirred for 6 h at 70 °C. Removal of the solvent *in vacuo* and purification by column chromatography (eluent: CH_2Cl_2 / 7 M NH_3 in MeOH 95:5- 90:10) afforded the product as white solid (224 mg, 88.1%). Mp: 174.6-177.9 °C decomposition. R_f = 0.5 (CH_2Cl_2/3 M NH_3 in MeOH 9:1). ^{1}H-NMR (400 MHz, [D_6]-DMSO, COSY, HSQC, HMBC, NOESY): δ (ppm) 1.23-1.26 (m, 8H), 1.33-1.36 (m, 11H), 1.48-1.52 (m, 2H), 2.65-2.68 (t, 2H, *J* 6.6 Hz), 2.85-2.90 (q, 2H, *J* 6.6 Hz), 3.48 (br s, 2H), 3.63 (s, 2H), 3.69-3.71 (m, 2H), 6.50 (s, 1H), 6.72-6.75 (m, 1H), 6.84 (br s, 4H), 7.45 (br s, 2H). ^{13}C-NMR (100 MHz, [D_6]-DMSO, COSY, HSQC, HMBC, NOESY): δ (ppm) 25.8, 26.2, 28.3, 28.6, 28.7, 29.4, 30.7, 31.1, 32.3, 40.2, 42.6, 43.3, 77.3, 104.5, 147.5, 155.6, 156.9, 167.5, 167.8, 175.3, 182.3, 182.5. HRMS: (ESI): *m/z* [*M*+H]$^+$, calcd. for $C_{24}H_{40}N_7O_4S_2^+$: 554.2578, found: 554.2584. $C_{24}H_{39}N_7O_4S_2$ (553.74).

tert-Butyl [10-(2-[2-(2-guanidinothiazol-4-ylmethylthio)ethylamino]-3,4-dioxocyclobut-1-ene-1-ylamino)decyl]carbamate (3.20)

3.14 (155 mg, 0.41 mmol, 1 eq), **3.17** (124 mg, 0.45 mmol, 1.1 eq) and triethylamine (209 mg, 2.06 mmol, 5 eq) were suspended in EtOH (20 mL). The reaction mixture was stirred overnight at 60 °C. Removal of the solvent *in vacuo* and purification by column chromatography (eluent: CH_2Cl_2/3.5 M NH_3 in MeOH 95:5 isocratic) afforded the product as white solid (150 mg, 63%). Mp: 178.7-182.1 °C decomposition. R_f = 0.45 (CH_2Cl_2/7 M NH_3 in MeOH 6: 1). ^{1}H-NMR (300 MHz, [D_6]DMSO): δ (ppm) 1.23-1.25 (m, 14H), 1.36 (s, 9H), 1.48-1.52 (m, 2H), 2.65 (t, 2H, *J* 6.26 Hz), 2.84-2.91 (m, 2H), 3.48 (br s, 2H), 3.63 (s, 2H), 3.69-3.71 (m, 2H), 6.49 (s, 1H), 6.74-6.84 (m, 5H), 7.47 (br s, 2H). ^{13}C-NMR (300 MHz, [D_6]DMSO): δ (ppm) 25.9, 26.3, 28.3, 28.67, 28.74, 28.96, 29.00, 29.5, 30.8, 31.1 32.3, 1C under solvent peak (38.7-40.3), 42.6, 43.3, 77.3, 104.5, 147.5,

155.6, 156.9, 167.5, 167.9, 175.5, 182.3, 182.5. HRMS: (ESI): *m/z* $[M+H]^+$, calcd. for $C_{26}H_{44}N_7O_4S_2^+$: 582.2891, found: 582.2895. $C_{26}H_{43}N_7O_4S_2$ (581.80).

General procedure for the Boc-deprotection of 3.18-3.20 to the free amines 3.21-3.23

The Boc-protected amine **3.18, 3.19** or **3.20** (1 eq) was dissolved in a mixture of CH_2Cl_2 (2 mL) and TFA (0.3 mL) and stirred for 1.5 h at room temperature. The solvent was removed *in vacuo*, CH_2Cl_2 was added and then again removed. This process was repeated several times in order to remove residual TFA. Part of the product was directly used in the next step of the synthesis and a part was purified by preparative HPLC.

1-[4-(2-[2-(2-Aminoethylamino)-3,4-dioxocyclobut-1-ene-1-ylamino]–ethylthiomethyl)thiazol-2-yl]guanidine-tri(hydrotrifluoracetate) (3.21)

3.18 (150 mg, 0.32 mmol, 1 eq) was treated according to the general procedure. The crude product was obtained as white hygroscopic solid (212 mg). Further purification of 100 mg by preparative HPLC (column: Nucleodur, gradient: 0-30 min: MeCN/0.1% aq. TFA 10:90-30:70, t_R = 10.6 min) afforded the product as white hygroscopic solid (54 mg, 50.4%). R_f = 0.3 (CH_2Cl_2/7 M NH_3 in MeOH 7:1). RP-HPLC (gradient 2, 220 nm): 91.0% (t_R = 8.67 min, k = 2.4). ^{1}H-NMR (400 MHz, [D_6]-DMSO, COSY, HSQC, HMBC): δ (ppm) 2.67 (t, 2H, *J* 6.8 Hz), 3.02 (br s, 2H), 3.69-3.71 (m, 4H), 3.79 (s, 2H), 7.12 (s, 1H), 7.78-7.90 (br s, 5H), 8.40 (br s, 4H), 12.42 (br s, 1H). ^{13}C-NMR (150 MHz, [D_6]-DMSO, COSY, HSQC, HMBC): δ (ppm) 30.0, 32.1, 39.6, 40.9, 42.6, 110.0, 148.5, 154.3, 158.7 (q, *J* 32 Hz, TFA), 160.7, 167.9, 168.2, 182.4, 182.9. HRMS: (ESI): *m/z* $[M+H]^+$, calcd. for $C_{13}H_{20}N_7O_2S_2^+$: 370.1114, found: 370.1114. $C_{13}H_{19}N_7O_2S_2 \cdot C_6H_3F_9O_6$ (369.46 + 342.07).

1-[4-(2-[2-(8-Aminooctylamino)-3,4-dioxocyclobut-1-ene-1-ylamino]ethylthiomethyl)thiazol-2-yl]guanidine-tri(hydrotrifluoracetate) (3.22)

3.19 (190 mg, 0.34 mmol, 1 eq) was treated according to the general procedure. The crude product was obtained as white hygroscopic solid (255 mg). Further purification of 148 mg by preparative HPLC (column: Nucleodur, gradient: 0-30 min: MeCN/0.1% aq. TFA 15:85-40:60, t_R = 11.0 min) afforded the product as white hygroscopic solid (91 mg, 57.3%). R_f = 0.2 (CH_2Cl_2/7 M NH_3 in MeOH 7:1). RP-HPLC (gradient 1, 220 nm): 95.4% (t_R = 13.22 min, k = 4.3). ^{1}H-NMR (600 MHz, [D_6]-DMSO, COSY, HSQC, HMBC): δ (ppm) 1.23-1.27 (br s, 8H), 1.49-1.52 (m, 4H), 2.66-2.68 (t, 2H, *J* 6.8 Hz), 2.74-2.79 (m, 2H), 3.50 (br s, 2H), 3.70 (br s, 2H), 3.79 (s, 2H), 7.14 (s, 1H), 7.69 (br s, 5H), 8.46 (br s, 4H), 12.44 (br s, 1H). ^{13}C-NMR (150 MHz, [D_6]-DMSO, COSY, HSQC, HMBC): δ (ppm) 25.7, 26.9, 27.0, 28.37, 28.41, 30.0, 30.7, 32.2, 38.7, 42.5, 43.2, 110.2, 116.7 (q, *J* 297 Hz, TFA), 148.6, 154.2, 158.6 (q, *J* 33 Hz, TFA), 160.2, 167.6, 167.7, 182.3, 182.4. HRMS: (ESI): *m/z* $[M+H]^+$, calcd. for $C_{19}H_{32}N_7O_2S_2^+$: 454.2053, found: 454.2049. $C_{19}H_{31}N_7O_2S_2 \cdot C_6H_3F_9O_6$ (453.62 + 342.07).

1-[4-(2-[2-(10-Aminodecylamino)-3,4-dioxocyclobut-1-ene-1-ylamino]ethylthiomethyl)thiazol-2-yl]guanidine-tri(hydrotrifluoracetate) (3.23)

3.20 (50 mg, 0.086 mmol, 1 eq) was treated according to the general procedure. Purification by preparative HPLC (column: Nucleodur, gradient: 0-30 min: MeCN/0.1% aq. TFA 15:85-70:30, t_R = 11.5 min) afforded the product as white solid (60.4 mg, 85.4%). Mp: 98.1-100.8 °C. R_f = 0.2 (CH_2Cl_2/7 M NH_3 in MeOH 6:1). RP-HPLC (gradient 2, 220 nm): 96.8% (t_R = 13.82 min, k = 4.5). ^{1}H-NMR (300 MHz, [D_6]-DMSO, COSY, HSQC, HMBC): δ (ppm) 1.24 (br s, 12H), 1.46-1.53 (m, 4H), 2.64-2.68 (m, 2H), 2.72-2.79 (m, 2H), 3.48 (br s, 2H), 3.69-3.71 (m, 2H), 3.79 (s, 2H), 7.13 (s, 1H), 7.76 (br s, 5H), 8.59 (s, 4H), 12.73 (br s, 1H). ^{13}C-NMR (150 MHz, [D_6]-DMSO, COSY, HSQC, HMBC): δ (ppm) 25.77, 25.84, 27.0, 28.5, 28.6, 28.77, 28.83, 30.0, 30.7, 32.2, 38.8, 42.5, 43.3, 110.1, 116.4 (q, J 296Hz, TFA), 148.5, 154.4, 159.1 (q, J 34 Hz, TFA), 160.3, 167.6, 167.9, 182.3, 182.5. HRMS: (ESI): m/z [M+H]$^+$, calcd. for $C_{21}H_{36}N_7O_2S_2^+$: 482.2366, found: 482.2364. Anal. calcd. for $C_{21}H_{35}N_7O_2S_2 \cdot C_6H_3F_9O_6$: C 39.37, H 4.68, N 11.90, S 7.78, found: C 39.16, H 4.86, N 11.86, S 7.76. $C_{21}H_{35}N_7O_2S_2 \cdot C_6H_3F_9O_6$ (481.68+ 342.07).

***N*-[2-(2-[2-(2-Guanidinothiazol-4-ylmethylthio)ethylamino]-3,4-dioxocyclobut-1-ene-1-ylamino)ethyl]propionamide bis(hydrotrifluoracetate) (3.24)**

3.21 (100 mg, 0.17 mmol, 1 eq) and triethylamine (68 mg, 0.67 mmol, 4 eq) were suspended in CH_2Cl_2 (2.5 mL). After stirring for 5 min N-succinimidyl propionate (32 mg, 0.18 mmol, 1.1 eq) was added and the reaction mixture was stirred over night at room temperature. The conversion was incomplete due to the poor solubility of the educts in the solvent. DMF (2 mL) was added and the mixture was stirred for 10 min at 50°C to dissolve the educts. The reaction mixture was allowed to cool to room temperature while stirring for additional 2 h. Removal of the solvent *in vacuo* and purification by preparative HPLC (column: Nucleodur, gradient: 0-30 min: MeCN/0.1% aq. TFA 10:90-45:55, t_R = 9.5 min) afforded the product as white hygroscopic solid (48 mg, 52.8%). R_f = 0.3 (CH_2Cl_2/7 M NH_3 in MeOH 9:1). RP-HPLC (gradient 2, 220 nm): 97.3% (t_R = 10.80 min, k = 3.3). ^{1}H-NMR (400 MHz, [D_6]-DMSO): δ (ppm) 0.97 (t, 3H, J 7.5 Hz), 2.03-2.09 (q, 2H, J 7.6 Hz), 2.67 (t, 2H, J 6.7 Hz), 3.19-3.21 (m, 2H), 3.52 (br s, 2H, interfering with the water signal), 3.69-3.70 (m, 2H, interfering with the water signal), 3.79 (s, 2H), 7.14 (s, 1H), 7.59 (br s, 2H), 7.92 (br s, 1H), 8.38 (br s, 4H), 12.29 (br s, 1H). ^{13}C-NMR (150 MHz, [D_6]-DMSO): δ (ppm) 9.8, 28.4, 30.0, 32.1, 39.7, 42.5, 42.9, 110.2, 116.8 (q, J 298 Hz, TFA), 148.6, 154.1, 158.8(q, J 33 Hz,TFA), 160.2, 167.6, 168.1, 173.3, 182.4, 182.6. HRMS: (ESI): m/z [M+H]$^+$, calcd. for $C_{16}H_{24}N_7O_3S_2^+$: 426.1377, found: 426.1377. $C_{16}H_{23}N_7O_3S_2 \cdot C_4H_2F_6O_4$ (425.53 + 228.04).

***N*-[8-(2-[2-(2-Guanidinothiazol-4-ylmethylthio)ethylamino]-3,4-dioxocyclobut-1-ene-1-ylamino)octyl]propionamide bis(hydrotrifluoracetate) (3.25)**

3.22 (100 mg, 0.15 mmol, 1 eq) and triethylamine (59 mg, 0.59 mmol, 4 eq) were suspended in CH_2Cl_2 (2.5 mL). After stirring for 5 min N-succinimidyl propionate (19 mg, 0.16 mmol, 1.1 eq) was added and the reaction mixture was stirred over night at room temperature. Removal of the solvent *in vacuo* and purification by preparative HPLC (column: Nucleodur, gradient: 0-30 min:

MeCN/0.1% aq. TFA 15:85-40:60, t_R = 14.6 min) afforded the product as white hygroscopic solid (66 mg, 72%). R_f = 0.6 (CH_2Cl_2/7 M NH_3 in MeOH 7:1). RP-HPLC (gradient 2, 220 nm): 98.8% (t_R = 15.21 min, k = 5.1). ^{1}H-NMR (400 MHz, [D_6]-DMSO): δ (ppm) 0.97 (t, 3H, J 7.6 Hz), 1.19-1.31 (m, 8H), 1.32-1.39 (m, 2H), 1.45-1.55 (m, 2H), 2.04 (q, 2H, J 7.6 Hz), 2.67 (t, 2H, J 6.7 Hz), 2.97-3.02 (m, 2H), 3.49 (br s, 2H, interfering with the water signal), 3.70 (br s, 2H), 3.79 (s, 2H), 7.14 (br s, 1H), 7.53 (br s, 2H), 7.68 (br s, 1H), 8.36 (br s, 4H), 12.24 (br s, 1H). ^{13}C-NMR (150 MHz, [D_6]-DMSO, COSY, HSQC, HMBC): δ (ppm) 10.0, 25.8, 26.4, 28.5, 28.6, 28.7, 29.1, 30.0, 30.7, 32.2, 38.4, 42.5, 43.3, 110.3, 116.6 (q, J 296 Hz, TFA), 148.6, 154.1, 158.7 (q, J 33 Hz, TFA), 160.2, 167.5, 167.9, 172.6, 182.3, 182.4. HRMS: (ESI): m/z [M+H]$^+$, calcd. for $C_{22}H_{36}N_7O_3S_2^+$: 510.2316, found: 510.2322. $C_{22}H_{35}N_7O_3S_2 \cdot C_4H_2F_6O_4$ (509.69 + 228.04).

N-[10-(2-[2-(2-Guanidinothiazol-4-ylmethylthio)ethylamino]-3,4-dioxocyclobut-1-ene-1-ylamino)decyl]propionamide-bis(hydrotrifluoracetate) (3.26)

3.23 (144 mg, 0.20 mmol, 1 eq), N-succinimidyl propionate (26 mg, 0.22 mmol, 1.1 eq) and triethylamine (82 mg, 0.81 mmol, 4 eq) were dissolved in a mixture of CH_2Cl_2 (3.5 mL) and DMF (2 mL). The reaction mixture was stirred for 2 h at room temperature. The conversion was incomplete due to the poor solubility of the educts in the solvent. The mixture was stirred for 1 h at 60°C to dissolve the educts. The reaction mixture was allowed to cool to room temperature while stirring for additional 48 h. Removal of the solvent *in vacuo* and purification by preparative HPLC (column: Nucleodur, gradient: 0-30 min: MeCN/0.1% aq. TFA 25:75-75:25, t_R = 12.08 min) afforded the product as white fluffy solid (43 mg, 32.5%). Mp: 149.2-153.0 °C. R_f = 0.52 (CH_2Cl_2/7 M NH_3 in MeOH 6:1). RP-HPLC (gradient 2, 220 nm): 98.8% (t_R = 18.05 min, k = 6.2). ^{1}H-NMR (400 MHz, [D_6]-DMSO): δ (ppm) 0.96 (t, 3H, J 7.60 Hz), 1.22-1.25 (m, 12H), 1.33-1.36 (m, 2H), 1.48-1.49 (m, 2H), 2.02 (q, 2H, J 7.60 Hz), 2.65-2.67 (m, 2H), 2.97-3.00 (m, 2H), 3.48 (br s, 2H), 3.69 (br s, 2H), 3.78(s, 2H), 7.11 (s, 1H), 7.59-7.67 (m, 3H), 8.39 (br s, 4H), 12.42 (br s, 1H). ^{13}C-NMR (150 MHz, [D_6]-DMSO): δ (ppm) 10.0, 25.8, 26.4, 28.5, 28.6, 28.7, 28.90, 28.91, 29.1, 30.0, 30.7, 32.2, 38.4, 42.5, 43.2, 110.0, 116.9 (q, J 298 Hz, TFA), 148.5, 154.2, 159.2 (q, J 32Hz, TFA), 160.6, 167.5, 167.9, 172.6, 182.3, 182.4. HRMS: (ESI): m/z [M+H]$^+$, calcd. for $C_{24}H_{40}N_7O_3S_2^+$: 538.2629, found: 538.2636. $C_{24}H_{39}N_7O_3S_2 \cdot C_4H_2F_6O_4$ (537.74 + 228.04).

tert-Butyl [8-(2-[3-(2-guanidinothiazol-4-yl)phenylamino]-3,4-dioxocyclobut-1-ene-1-ylamino)octyl]carbamate (3.28)

3.7 (200 mg, 0.86 mmol, 1 eq) was dissolved in EtOH (7 mL) and poured into a solution of 3,4-diethoxy-3-cyclobutene-1,2-dione in EtOH (7 mL). The reaction mixture was stirred over night at room temperature. The precipitated **3.27** was filtered off, washed with EtOH (2 mL) and dried *under vacuo*.

3.27 (160 mg, 0.45 mmol, 1 eq), **3.16** (120 mg, 0.49 mmol, 1.1 eq) and triethylamine (227 mg, 2.24 mmol, 5 eq) were suspended in EtOH (15 mL). The reaction mixture was stirred over night at 80 °C and subsequently cooled to room temperature. The precipitated product was filtered off and residual solvent was removed *in vacuo*. **3.28** was afforded as a beige solid (160 mg, 33.6 %

over two steps). Mp: 262 °C decomposition. R_f = 0.5 (CH_2Cl_2/7 M NH_3 in MeOH 6:1). ^{1}H-NMR (300 MHz, [D_6]-DMSO): δ (ppm) 1.25-1.57 (m, 19H), 1.55-1.57 (m, 2H), 2.85-2.91 (m, 2H), 3.60-3.62 (m, 2H), 6.76-6.79 (m, 1H), 6.9 (br s, 3.5H), 7.08-7.15 (m, 2H), 7.32 (t, 1H, *J* 7.84 Hz), 7.46-7.48 (m, 1H), 7.70 (br s, 1H), 8.30 (s, 1H), 9.67 (s, 1H). ^{13}C-NMR (150 MHz, [D_6]-DMSO): δ (ppm) 25.8, 26.2, 28.3, 28.6, 28.7, 29.5, 30.6, 30.7, 43.7, 77.3, 103.5, 115.2, 116.3, 119.2, 129.4, 136.1, 139.5, 148.9, 155.6, 157.1, 163.4, 169.3, 174.9, 180.1, 183.9. HRMS: (ESI): *m/z* [*M*+H]$^+$, calcd. for $C_{27}H_{38}N_7O_4S^+$: 556.2700, found: 556.2706. $C_{27}H_{37}N_7O_4S$ (555.70).

1-[4-(3-[2-(8-Aminooctylamino)-3,4-dioxocyclobut-1-ene-1-ylamino]phenyl)thiazol-2-yl]guanidine- hydrotrifluoracetate (3.29)

3.28 (140 mg, 0.25 mmol, 1eq) was suspended in CH_2Cl_2 (20 mL). TFA (689 mg, 6.05 mmol, 24 eq) was added and the reaction mixture was stirred for 5 h at room temperature. Removal of the solvent *in vacuo* afforded the crude product as an off-white solid (140 mg, 99%). 50 mg were further purified by preparative HPLC (column: Nucleodur, gradient: 0-30 min: MeCN/0.05% aq. TFA 15:85-65:35, t_R = 12.5 min). **3.29** was obtained as a white fluffy solid (31 mg, 61.3%). Mp: 210.0-217.6 °C decomposition. R_f = 0.2 (CH_2Cl_2/7 M NH_3 in MeOH 6:1). RP-HPLC (gradient 2, 220 nm): 97.6% (t_R = 14.76 min, *k* = 4.9). ^{1}H-NMR (400 MHz, [D_6]-DMSO, COSY, HSQC, HMBC): δ (ppm) 1.23-1.32 (m, 8H), 1.48-1.52 (m, 2H), 1.55-1.60 (m, 2H), 2.74-2.77 (m, 2H), 3.59-3.63 (m, 2H), 7.20-7.21 (m, 1H), 7.37 (t, 1H, *J* 7.86 Hz), 7.54-7.55 (m, 1H), 7.68 (br s, 3H), 7.74 (s, 1H), 8.12 (br s, 1H), 8.46 (br s, 4H), 8.55 (s, 1H), 10.08 (s, 1H), 12.53 (br s, 1H). ^{13}C-NMR (150 MHz, [D_6]-DMSO, COSY, HSQC, HMBC): δ (ppm) 25.7, 27.0, 28.40, 28.41, 30.5, 30.7, 38.8, 43.7, 108.4, 115.5, 116.9 (q, *J* 298 Hz, TFA), 117.2, 119.4, 129.8, 134.2, 139.9, 149.4, 154.2, 158.7 (q, *J* 32 Hz, TFA),160.2, 163.2, 169.6, 180.2, 183.7. HRMS: (ESI): *m/z* [*M*+H]$^+$, calcd. for $C_{22}H_{30}N_7O_2S^+$: 456.2176, found: 456.2175. $C_{22}H_{29}N_7O_2S \cdot C_2HF_3O_2$ (455.58 + 114.02).

***N*-[8-(2-[3-(2-Guanidinothiazol-4-yl)phenylamino]-3,4-dioxocyclobut-1-ene-1-ylamino)octyl]propionamide-hydrotrifluoracetate (3.30)**

3.29 (110 mg, 0.16 mmol, 1 eq) was dissolved in a mixture of triethylamine (65 mg, 0.64 mmol, 4 eq), DMF (1 mL) and CH_2Cl_2 (1 mL). N-Succinimidyl propionate (21mg, 0.18 mmol, 1.1 eq) was added and the reaction mixture was stirred over night at room temperature. Removal of the solvent *in vacuo* and purification by preparative HPLC (column: Nucleodur, gradient: 0-30 min: MeCN/0.05% aq. TFA 25:75-70:30, t_R = 13.1 min) afforded the product as white fluffy solid (12 mg, 11.6%). Mp: 224-236.4 °C. R_f = 0.67 (CH_2Cl_2/7 M NH_3 in MeOH 6:1). RP-HPLC (gradient 2, 220 nm): 98.5% (t_R = 18.85 min, *k* = 6.5). ^{1}H-NMR (400 MHz, [D_6]-DMSO, COSY, HSQC, HMBC): δ (ppm) 0.96 (t, 3H, *J* 7.62 Hz), 1.22-1.58 (m, 10H), 1.55-1.58 (m, 2H), 2.02 (q, 2H, *J* 7.62 Hz), 2.97-3.01 (m, 2H), 3.60-3.61 (m, 2H), 7.13-7.15 (m, 1H), 7.37 (t, 1H, *J* 7.92 Hz), 7.54-7.55(m, 1H), 7.67-7.71(m, 2H), 7.91 (br s, 1H), 8.29 (br s, 4H), 8.56 (s, 1H), 9.87 (s, 1H), 12.26 (br s, 1H). ^{13}C-NMR (150 MHz, [D_6]-DMSO, COSY, HSQC, HMBC): δ (ppm) 10.0, 25.8, 26.3, 28.48, 28.54, 28.6, 29.1, 30.5, 38.3, 43.7, 108.3, 115.4, 117.1, 119.4, 129.8, 134.4, 139.8, 149.3, 154.2, 162.8, 163.1,169.5, 172.6, 180.2, 183.8. HRMS: (ESI): *m/z* [*M*+H]$^+$, calcd. for $C_{25}H_{34}N_7O_3S^+$: 512.2438, found: 512.2443. $C_{25}H_{33}N_7O_3S \cdot C_2HF_3O_2$ (511.65 + 114.02).

S-Methylthiouronium iodide (3.31)[40]

Methyliodide (9.30 g, 65.50 mmol, 1 eq) was added to a stirring solution of thiourea (5 g, 65.50 mmol, 1 eq) in MeOH (50 mL). The reaction mixture was stirred under reflux for 1.5 h. The solvent was removed *in vacuo* and the residue was washed two times with diethyl ether (50 mL). **3.31** was afforded as white solid (14.30 g, 99.9%). Mp: 117.2-118.1°C. R_f = 0.1 (PE/EtOAc 3:1). ^{1}H-NMR (300 MHz, [D_6]-DMSO): δ (ppm) 2.56 (s, 3H), 8.89 (br s, 4H). ^{13}C-NMR (75 MHz, [D_6]-DMSO): δ (ppm) 13.2, 171.0. HRMS: (ESI): *m/z* $[M+H]^+$, calcd. for $C_2H_7N_2S^+$: 91.0324, found: 91.0327. $C_2H_6N_2S \cdot HI$ (90.14 + 127.91).

***N*-*tert*-Butoxycarbonyl-S-methylisothiourea (3.32)**[40]

3.31 (13.65 g, 62.45 mmol, 1 eq) and triethylamine (6.32 g, 62.45 mmol, 1 eq) were dissolved in CH_2Cl_2 (110 mL) and cooled to 0 °C. Di-*tert*-butyl dicarbonate (13.63 g, 62.45 mmol, 1 eq) dissolved in CH_2Cl_2 (30 mL) was added drop wise at 0 °C. The reaction mixture was allowed to warm to room temperature and was stirred over night. The organic layer was washed two times with water (200 mL). Product which passed in the aqueous layer was extracted two times with CH_2Cl_2 (100 mL). The combined organic layers were dried over sodium sulfate. Removal of the solvent *in vacuo* and purification by column chromatography (eluent: PE/EtOAc 6:1- 3:1) afforded the product as white solid (8.64 g, 72.6%). Mp: 88.4-90.3 °C. R_f = 0.45 (PE/EtOAc 3:1). ^{1}H-NMR (300 MHz, $CDCl_3$): δ (ppm) 1.44 (s, 9H), 2.38 (s, 3H), 7.50 (br s, 2H). ^{13}C-NMR (75 MHz, $CDCl_3$): δ (ppm) 13.4, 28.1, 79.9, 172.9. HRMS: (ESI): *m/z* $[M+H]^+$, calcd. for $C_7H_{15}N_2O_2S^+$: 191.0849, found: 191.0847. $C_7H_{14}N_2O_2S$ (190.26).

***N*^{1},*N*^{6}-Bis([(*tert*-butoxycarbonylamino)(methylsulfanyl)methylene]aminocarbonyl)hexane-1,6-diamine (3.33)**[14]

3.32 (4.03 g, 21.1 mmol, 2.2 eq) and triethylamine (0.97 g, 9.62 mmol, 1) were dissolved in anhydrous CH_2Cl_2 (17 mL). 1,6-Diisocyanohexane (1.62 g, 9.6 mmol, 1 eq) was added under Ar-atmosphere. The reaction mixture was stirred over night at room temperature. Removal of the solvent *in vacuo* and purification by column chromatography (eluent: PE/EtOAc 3:1- 1:3) afforded the product as white solid (4.65 g, 88.0%). Mp: 128.8-133.6 °C. R_f = 0.14 (PE/EtOAc 3:1). ^{1}H-NMR (400 MHz, $CDCl_3$): δ (ppm) 1.36-1.40 (m, 4H), 1.48 (s, 18H), 1.51-1.57 (m, 4H), 2.30 (s, 6H), 3.19-3.24 (m, 4H), 5.53 (m, 2H), 12.30 (s, 2H). ^{13}C-NMR (100 MHz, $CDCl_3$): δ (ppm) 14.4, 26.7, 28.1, 29.7, 40.1, 82.7, 151.2, 162.1, 167.4. HRMS: (ESI): *m/z* $[M+H]^+$, calcd. for $C_{22}H_{41}N_6O_6S_2^+$: 549.2524, found: 549.2526. $C_{22}H_{40}N_6O_6S_2$ (548.72).

1-(Amino[2-(2-guanidinothiazol-4-ylmethylthio)ethylamino]methylene)-3-(6-[3-(amino[2-(2-guanidinothiazol-4-ylmethylthio)ethylamino]methylene)ureido]hexyl)urea tetra(hydrotrifluoracetate) (3.34)

The HCl salt of **3.3** (244 mg, 0.80 mmol, 2.2 eq), **3.33** (200mg, 0.36 mmol, 1 eq) and diisopropylethylamine (233 mg, 1.80 mmol, 5 eq) were suspended in MeOH (7 mL). The reaction mixture was stirred under reflux for 5 h. The solvent was removed under reduced pressure and the residue was purified by preparative HPLC (column: Nucleodur, gradient: 0-30 min: MeCN/0.05% aq. TFA 15:85-80:20, t_R = 15.2 min). Removal of the MeCN *in vacuo* and lyophilisation afforded the Boc-deprotected **3.34** as a white solid. The residue was again purified by preparative HPLC (column: Nucleodur, gradient: 0-30 min: MeCN/0.05% aq. TFA 10:90-65:35, t_R = 12.7 min). **3.34** was obtained as a white solid (45 mg, 10.7%). Mp: 59.1-61.9 °C. RP-HPLC (gradient 2, 220 nm): 96.2% (t_R = 12.95 min, k = 4.2). ^{1}H-NMR (600 MHz, [D$_6$]-DMSO, COSY, HSQC, HMBC): δ (ppm) 1.25-1.26 (m, 4H), 1.41-1.43 (m, 4H), 2.66 (t, 4H, J 6.78 Hz), 3.06-3.09 (m, 4H), 3.44-3.47 (m, 4H, interfering with the water signal), 3.79 (s, 4H), 7.13 (s, 2H), 7.56(br s, 2H), 8.49 (br s, 2H), 9.13 (br s, 2H), 10.34 (br s, 2H), 12.54 (br s, 2H). ^{13}C-NMR (150 MHz, [D$_6$]-DMSO, COSY, HSQC, HMBC): δ (ppm) 25.9, 28.8, 29.4, 30.0, 40.2, 53.5, 110.1, 116.9 (q, J 299 Hz, TFA), 148.5, 153.7, 153.8, 154.3, 159.2 (q, J 32 Hz, TFA), 160.5. HRMS: (ESI): *m/z* [M+H]$^+$, calcd. for $C_{24}H_{43}N_{16}O_2S_4^+$: 715.2632, found: 715.2627. $C_{24}H_{42}N_{16}O_2S_4 \cdot C_8H_4F_{12}O_8$ (714.95 + 456.09).

1-(Amino[3-(2-guanidinothiazol-4-yl)phenylamino]methylene)-3-(6-[3-(amino[3-(2-guanidinothiazol-4-yl)phenylamino]methylene)ureido]hexyl)urea tetra(hydrotrifluoracetate) (3.35)

3.7 (280 mg, 1.21 mmol,2.2 eq) and **3.33** (300 mg, 0.55 mmol, 1 eq) were suspended in MeOH (15 mL). The reaction mixture was stirred under reflux for 48h. The solvent was removed under reduced pressure and the residue was purified by preparative HPLC (column: Nucleodur, gradient: 0-30 min: MeCN/0.05% aq. TFA 15:85-80:20, t_R = 19.1 min). Removal of the MeCN *in vacuo* and lyophilisation afforded the Boc-deprotected **3.35** as a white solid. The residue was again purified by preparative HPLC (column: Nucleodur, gradient: 0-30 min: MeCN/0.05% aq. TFA 15:85-45:55, t_R = 15.3 min). **3.35** was obtained as a white solid (22 mg, 3.4%). Mp: 201.1 °C. RP-HPLC (gradient 2, 220 nm): 98.5% (t_R = 14.54 min, k = 4.8). ^{1}H-NMR (600 MHz, [D$_6$]-DMSO, COSY, HSQC, HMBC): δ (ppm) 1.26-1.29 (m, 4H), 1.42-1.45 (m, 4H), 3.10-3.13 (m, 4H), 7.30-7.32 (m, 2H), 7.53-7.55 (t, 2H, J 7.85 Hz), 7.65 (br s, 2H), 7.82 (s, 2H), 7.92 (s, 2H), 7.96-7.97 (m, 2H), 8.47-8.93 (m, 12H), 10.36 (br s, 2H), 10.81 (br s, 2H), 12.63 (br s, 2H). ^{13}C-NMR (150 MHz, [D$_6$]-DMSO, COSY, HSQC, HMBC): δ (ppm) 25.9, 28.8, 1C under solvent peak (38.7-40.3), 109.1, 115.9, 116.9 (q, J 297 Hz, TFA), 123.4, 125.3, 125.7, 130.3, 134.3, 134.8, 148.9, 153.6, 154.2, 159.3 (q, J 31 Hz, TFA), 161.0. HRMS: (ESI): *m/z* [M+H]$^+$, calcd. for $C_{30}H_{39}N_{16}O_2S_2^+$: 719.2878, found: 719.2880. $C_{30}H_{38}N_{16}O_2S_2 \cdot C_8H_4F_{12}O_8$ (718.86 + 456.09).

_N_-[8-(2-[2-(2-Guanidinothiazol-4-ylmethylthio)ethylamino]-3,4-dioxocyclobut-1-ene-1-ylamino)octyl]-[2,3-^{3}H]propionamide-hydrotrifluoracetate ([^{3}H]3.25)

The radioligand [^{3}H]**3.25** was prepared by [^{3}H]propionylation of the amine precursor **3.22** using reported protocols with minor modifications.[11,19,24] A solution of N-succinimidyl [2,3-^{3}H]propionate (specific activity: 88 Ci/mmol, 1.5 mCi, 3.0 µg, 17.05 nmol, from American Radiolabeled Chemicals Inc., St. Louis, MO via Biotrend, Köln, Germany) in hexane/EtOAc 9:1 was transferred into a 1.5 mL reaction vessel with a screw cap. The solvent was evaporated in a vacuum concentrator at approx. 30 °C in 30 min. A solution of **3.22** (0.35 mg, 0.38 µmol, 22 eq) in a mixture of anhydrous DMF (50 µL) and DIPEA (0.8 µL) was added and the mixture was shaken at room temperature for 80 min. The analysis of the reaction mixture was performed with an RP-HPLC system (*cf.* Figure 3.7) (Waters, Eschborn, Germany) consisting of two 510 pumps, a pump control module, a 486 UV/vis detector and a Flow-one Beta series A-500 radiodetector (Packard, Meriden; CT). A Luna C18 (3 µm, 150 mm x 4.6 mm) was used RP-column at a flow rate of 0.8 mL/min. Mixtures of 0.04% TFA in CH_3CN (A) and 0.05% aq. TFA (B) were used as mobile phase. The following linear gradient was applied: 0-20 min, A/B 14:86-32:68; 20-22min, 32:68-95:5; 22-32min, 95:5 isocratic), (UV detection: 220 nm).

For the isolation of [^{3}H]**3.25** (peak at t_R = 18.8 min, *cf.* Figure 3.7) by analytical RP-HPLC (conditions as for the analysis of the reaction mixture, no radiometric detection), a H_2O/TFA (96:4, v/v, 11.5 µL) was added to the reaction mixture. The eluates (three injections), containing [^{3}H]**3.25**, were combined in a 2 mL reaction vessel with a screw cap and the volume was reduced in a vacuum concentrator to 200 µL. EtOH (800 µL) was added and the solution was transferred into a 3 mL borosilicate glass vial with conical bottom (Wheaton NextGen 3 mL V-vials). The 2 mL reaction vessel was rinsed twice with EtOH/H2O 80:20 (v/v, 2 x 200µL) and the wash solutions were transferred to the 3 mL glass vials yielding the tentative stock solution with a volume of 1200 µL.

As analysis of the tentative stock solution by radio-HPLC (4 µL dissolved in 126 µL of 0.05% aq TFA/MeCN 90:10; same conditions as for the isolation) revealed a second peak (t_R = 14.3 min, *cf*. Figure 3.7B), amounting to ca. 13% of the total peak area, determination of the specific activity of [^{3}H]**3.25** was not feasible. Therefore, the specific activity of [^{3}H]**3.25** was estimated based on the specific activity (2.41 TBq/mmol, 65.03 Ci/mmol) of [^{3}H]UR-MK300[19] prepared on the same day from the same lot of N-succinimidyl [2,3-^{3}H]propionate. The molarity of the tentative stock solution was calculated from the specific activity of [^{3}H]UR-MK300 (2.41 TBq/mmol) and the activity concentration (determined with a LS 6500 liquid scintillation counter (Beckmann-Coulter, Munich, Germany)) of the tentative stock solution with respect to [^{3}H]**3.25** ($2.47 \cdot 10^{-5}$ TBq/mL, 87% of the total activity concentration). The final total activity concentration was adjusted to 18.5 MBq/mL (0.5 mCi/mL) by the addition of EtOH/H_2O (80:20 v/v) containing 0.22 mM ascorbinic acid (625 µL) resulting in the final stock solution with 6.69 µmol/L [^{3}H]**3.25** and 76.9 µmol/L ascorbinic acid (radiochemical yield for [^{3}H]**3.25**: 28.9 MBq, 64.3%).

Investigation of the chemical stability of 3.25

The chemical stability of the "cold form" of the radioligand (**3.25**) was investigated in a mixture of EtOH/H_2O (80:20, v/v) at room temperature. Initially, a solution of **3.25** (100 µM) in EtOH/H_2O (80:20, v/v) was prepared. The incubation was started by dilution of this 100 µM solution of **3.25** with a mixture of EtOH/H_2O (80/20, v/v) resulting in a 15 µM solution of **3.25**. After 0 h, 6 h, 12 h, 24 h, 48 h, 72 h and 7 days a 8 µL aliquot was added to 192 µL of a mixture of CH_3CN/ 0.05% aq. TFA (10:90, v/v). A sample (80 µL) was immediately analyzed by analytical HPLC (Gradient 2, detection wavelength of 273 nm).

3.3.3 Pharmacological Methods

Radioligand competition binding assay on Sf9 insect cell membranes

Preparation of the membranes of Sf9 insect cells, expressing the hH_2R-$G_{s\alpha S}$ fusion protein or co-expressing the hH_1R + RGS4, the hH_3R + $G_{i\alpha 2}$ + $\beta_1\gamma_2$ or hH_4R + $G_{i\alpha 2}$ + $\beta_1\gamma_2$ proteins was described elsewhere.[41]

Radioligand competition binding assays were performed as described previously with minor modifications, using the following radioligands: [^{3}H]mepyramine (Hartmann Analytic, Braunschweig, Germany; hH_1R, specific activity = 20 Ci/mmol, K_d = 4.5 nM, c_{final} = 5 nM), [^{3}H]UR-DE257[11] batch 04/2015 (hH_2R, specific activity = 32.89 Ci/mmol, K_d = 12.2 nM, c_{final} = 20 nM), [^{3}H]tiotidine (Hartmann Analytic, Braunschweig, Germany; hH_2R, specific activity = 78.42 Ci/mmol, K_d = 12.75 nM, c_{final} = 10 nM), [^{3}H]N^{α}-methylhistamine (Hartmann Analytic, Braunschweig, Germany; hH_3R, specific activity = 80 Ci/mmol, K_d = 3 nM, c_{final} = 3 nM), [^{3}H]histamine (Hartmann Analytic, Braunschweig, Germany; hH_4R, specific activity = 25 Ci/mmol, K_d = 15.9 nM, c_{final} = 10 nM).and [^{3}H]UR-PI294[20] (hH_4R, specific activity = 93.3 Ci/mmol, K_d = 5.1 nM, c_{final} = 5 nM).

On the day of the experiment, Sf9 membranes were thawed and sedimented by centrifugation at 13,000 rpm at 4 °C for 10 min. The membranes were resuspended in ice cold binding buffer (12.5 mM $MgCl_2$, 1mM EDTA and 75 mM Tris/HCl, pH 7.4; in the following referred to as BB) and adjusted to a protein concentration of 2-4 µg/µL. 80 µL BB containing 0.2% BSA and the respective radioligand, followed by 10 µL of the investigated ligands at various concentrations (dissolved in H_2O), were added to every well of a 96-well plate (PP microplates 96 well, Greiner Bio-One, Frickenhausen, Germany). Incubation was started by addition of the membrane suspension (10 µL). The plates were shaken for 60 min at room temperature in the dark. Subsequently, bound radioligand was separated from free radioligand by filtration through glass microfiber filters (Whatman GF/C, Maidstone, UK), treated with 0.3% polyethylenimine, using a 96-well Brandel harvester (Brandel Inc., Unterföhring, Germany). The punched out filter pieces were transferred into clear, flexible 96-well PET microplate (round bottom, 1450-401, Perkin Elmer, Rodgau, Germany). Each well was supplemented with 200 µL scintillation cocktail (Rotiscint Eco plus, Roth, Karlsruhe, Germany) and incubated in the dark for at least 4 h. The radioactivity was measured with a MicroBeta2 1450 scintillation counter (Perkin Elmer, Rodgau, Germany).

Functional GTPγS assay on Sf9 insect cell membranes

GTPγS assays were performed as described previously[14] with minor modifications. [^{35}S]GTPγS (specific activity = 1000 Ci/mmol) was purchased from Hartmann Analytic (Braunschweig, Germany). Sf9 membranes were prepared in the same manner as for radioligand competition binding and the protein concentration was adjusted to 0.5-1.5 µg/µL.

Agonist mode: 80 µL of BB containing BSA (0.05% final), GDP (1 µM final) and [^{35}S]GTPγS (20 nCi final), followed by 10 µL of the investigated ligands at various concentrations (dissolved in H_2O) were added to every well of a 96-well plate (PP microplates 96 well, Greiner Bio-One, Frickenhausen, Germany). Incubation was started by addition of the membrane suspension (10 µL). The plates were shaken for 60 min at room temperature in the dark. Subsequently, bound radioligand was separated from free radioligand by filtration through glass microfiber filters (Whatman GF/C, Maidstone, UK) using a 96-well Brandel harvester (Brandel Inc., Unterföhring, Germany).

Antagonist mode of the GTPγS assay was performed in the same way as the agonist mode, but in the presence of the agonist histamine (1 µM final).

Radioligand binding assays with [^{3}H]UR-SB69 on Sf9 insect cell membranes

The radioligand binding experiments were performed as described for competition binding assays on Sf9 insect cell membranes with minor adjustments.

Saturation binding: For the determination of total binding 10 µL of H_2O, followed by 70 µL BB containing 0.2% BSA, were added to every well of a 96-well plate (Primaria clear flat bottom microplates, Corning, New York, USA). For the determination of unspecific binding 10 µL famotidine (300 fold excess compared to the radioligand concentration, 3-600 µM) in H_2O was added. 10 µL of [^{3}H]**3.25** in concentrations of 1-200 nM in H_2O (for economic reasons the radioligand was mixed 1:4 with the cold form) were added to every well and the incubation was started by addition of the membrane suspension (10 µL). The plates were shaken for 90 min at room temperature in the dark.

Competition binding: [^{3}H]**3.25** (specific activity = 65.03 Ci/mmol, K_D = 15 nM) was used in a final concentration of 20 nM. The incubation time was 90 min.

Association: 70 µL BB containing 0.2% BSA, followed by 10 µL of membrane suspension, were added to every well of a 96-well plate (Primaria clear flat bottom microplates, Corning, New York, USA). 10 µL [^{3}H]**3.25** (final concentration: 20 nM) in H_2O and either 10 µL H_2O (total binding) or 10 µL famotidine (300-fold excess, unspecific binding) in H_2O were added at different time points (0-180 min) at 25 °C. After the last addition the bound radioligand was separated from the free radioligand. The last time point (last addition of the radioligand) represented the shortest incubation time (0 min) and the first time point the longest incubation time (180 min).

Dissociation: 70 µL BB containing 0.2% BSA, followed by 10 µL of membrane suspension, were added to every well of a 96-well plate (Primaria clear flat bottom microplates, Corning, New York,

USA). 10 µL [^{3}H]**3.25** (final concentration: 20 nM) in H_2O and either 10 µL H_2O (total binding) or 10 µL famotidine (300-fold excess, unspecific binding) in H_2O were added at different time points (0-180 min). Every time point was preincubated for 60 min at 25 °C. After the incubation time was over 100 µL famotidine (final concentration: 3 µM) in BB was added. After the last addition the bound radioligand was separated from the free radioligand. The last time point (last addition of the radioligand) represented the shortest dissociation time (0 min) and the first time point the longest dissociation time (180 min).

Cell culture

The preparation of stably transfected HEK cells (HEK293T-hH_2R-qs5[42] and HEK293T-hH_2R-βArr2[43,44]) was described elsewhere.

Cells were cultivated at 37 °C in a water saturated atmosphere containing 5% CO_2. Dulbecco´s Modified Eagle Medium, containing 4.5 g/L glucose, 3.7 g/L $NaHCO_3$, 110 mg/L sodium pyruvate (DMEM, Sigma-Aldrich Munich, Germany) and supplemented with 0.584 g/L L-glutamine (L-glutamine solution, Sigma-Aldrich Munich, Germany), 1% (v/v) Penicillin-Streptomycin (P/S, 10,000 U/mL, Sigma-Aldrich Munich, Germany), 10% (v/v) fetal calf serum (FCS, Biochrom GmbH, Merck, Berlin, Germany) were used as a culture medium. Additionally, 100 µg/mL hygromycin B (A.G. Scientific, Inc., San Diego, CA) and 400 µg/mL G418 (Biochrom GmbH, Merck, Berlin, Germany) were added to the culture medium of HEK293T-hH_2R-qs5 cells, and 400 µg/mL zeocin (InvivoGen, San Diego,USA) and 600 µg/mL G418 were added to the culture medium of HEK293T-hH_2R-βArr2 cells.

Radioligand saturation binding assays with [^{3}H]UR-SB69 on intact HEK293T-hH_2R-qs5 and HEK293T-hH_2R-βArr2 cells

HEK293T cells were seeded in a 175-cm^2 culture flask 5-7 days prior to the experiment. On the day of the experiment, cells were trypsinized and detached with fresh culture medium (5 mL). After centrifugation (250 *g*, 10 min) the cell pellet was resuspended in Leibovitz´s L-15 culture medium (L-15 medium, Gibco/Life Technologies, Carlsbad, USA) and the concentration was adjusted to 0.25-0.5 · 10^6 cells/mL. 80 µL cell suspension was added to every well of a 96-well plate (Primaria clear flat bottom microplates, Corning, New York, USA). 10 µL of [^{3}H]**3.25** in concentrations of 1-200 nM in H_2O (for economic reasons the radioligand was mixed 1:4 with the cold form) and either 10 µL H_2O (total binding) or 10 µL famotidine (300 fold excess, unspecific binding) in H_2O were added to every well. The plates were shaken for 90 min at room temperature in the dark. The separation of bound from free radioligand was performed as described for membranes.

3.3.4 Data analysis

Retention factors *k* were calculated according to $k = (t_R - t_0)/ t_0$ (t_0 = dead time). Corrected counts per minute (ccpm) from the GTPγS assay (agonist mode) were plotted against the log(concentration of the test compound), and data were analyzed by a four parameter logistic equation (GraphPad Prism Software 5.0, GraphPad Software, San Diego, CA), followed by normalization (0% = water value (basal activity), 100% = "top" histamine equation) and analysis by four-parameter logistic equation (log(agonist) vs. response – variable slope, GraphPad Prism). Data of the GTPγS assay (antagonist mode) were analysed by a four parameter logistic equation (GraphPad Prism), followed by normalization (100% = "top" of the four-parameter logistic fit, 0% = unspecifically bound radioligand (ccpm) determined in the presence of famotidine at 100 µM) and analysis by four-parameter logistic equation (log(inhibitor) vs response – variable slope, GraphPad Prism). pIC_{50} values were converted into pK_B values according to the Cheng-Prusoff equation[45]. Specific binding data from saturation binding experiments were plotted against the total radio labeled ligand concentration (approximately equivalent to the "free" ligand concentration) and analyzed by a two-parameter equation describing hyperbolic binding (one site – specific binding, GraphPad Prism) and unspecific binding data was analyzed by linear regression. Specific binding data from association binding experiments were analyzed by a two parameter equation describing an exponential rise to a maximum (one-phase association, GraphPad Prism) to obtain the observed association constant k_{obs}. Specific binding data from dissociation binding experiments were analyzed by a three parameter equation (one phase decay, GraphPad Prism) to obtain the dissociation rate constant k_{off}. Kinetic dissociation constants $K_{d\,(kin)}$ were calculated from k_{on} and k_{off} ($k_{on} = (k_{obs} - k_{off})/[L]$; $K_{d\,(kin)} = k_{off}/ k_{on}$). Specific binding data from association and dissociation binding experiments were normalized (100% = Y_{max} (association) or Y_0 (dissociation)). Total binding data from radioligand competition binding experiments were plotted against log(concentration competitor) and analyzed by a four-parameter logistic equation (log(inhibitor) vs response – variable slope, GraphPad Prism), followed by normalization (100% = "top" of the four-parameter logistic fit, 0% = unspecifically bound radioligand ligand determined in the presence of famotidine at 100 µM). Normalized data from competition binding experiments were again analyzed by a four-parameter logistic equation and obtained pIC_{50} values were converted into pK_i values according to the Cheng-Prusoff equation[45].

3.4 SUMMARY AND CONCLUSION

The combination of the 2-guanidino-4-[(2-aminoethyl)thiomethyl]thiazole structure derived from famotidine or the guanidino-4-(3-aminophenyl)thiazole structure derived from ICI127032 with the derivatized squaramide moiety of BMY25368 led to propionylated H_2R high affinity antagonists (**3.24**-**3.26** and **3.30**, pK_i values: 6.8-7.65). The linking of two guanidinothiazole pharmacophores by a carbamoyl guanidine linker resulted in the high affinity bivalent antagonists **3.34** and **3.35** (pK_i values: 7.3 and 7.14). The ligand **3.25** showed a high affinity to the hH_2R (pK_i value: 7.65) and selectivity over the other subtypes (no affinity to the hH_1R, hH_3R: pK_i value of 5.3 and hH_4R: pK_i value of 4.4). The radiolabeled form [^{3}H]**3.25** (radiochemical purity of 87%) bound in a saturable manner to membrane preparations of Sf9 cells and intact HEK293T cells, both expressing recombinant hH_2Rs and the specific binding was best fitted by nonlinear regression to a one-site binding model. The determined K_d values (15-22 nM) were similar to the K_i value of 23 nM determined with [^{3}H]UR-DE257 on membrane preparations of Sf9 cells. Although a part of [^{3}H]**3.25** bound in (pseudo)irreversible manner (plateau at 23%), the kinetic K_d value of 26 nM was comparable to the equilibrium one and the radioligand was completely displacable by histamine, famotidine and ICI127032. Lamtidine, by contrast, could only displace 75% of [^{3}H]**3.25**.

However, the results of the biological evaluation of [^{3}H]**3.25** should be looked at critically, as the radiochemical puritiy of the radioligand was only moderate to begin with (87%) and stability studies showed that the radiochemical purity was further decreasing over a period of 15 month to 45%. Furthermore, only one major impurity, with unknown H_2R affinity and potency, was formed. This was all very surprising, as the squaramide radioligand [^{3}H]UR-DE257 was stable in EtOH for at least 24 month.[11] As such one can well assume that the 2-guanidino-4-[(2-aminoethyl)thiomethyl]thiazole structure is the part vulnerable for decomposition. Most propably the impurity was formed by oxidation of the sulfide linker to either the sulfoxide or sulfone. For unequivocal identification of the impurity, a solution of the radioligand containing the impurity should be spiked with either the sulfoxide or the sulfone compound and be analyzed by RP-HPLC. For this purpose both compounds have to be specifically synthesized. Depending on the structure of the impurity, this results may also question the stability of previously described H_2R radioligands like [^{3}H]ranitidine, [^{3}H]cimetidine and [^{3}H]tiotidine which contain the same sulfide linker.

Nevertheless, [^{3}H]**3.25** could be a valuable molecular tool provided that purity and stability under storage conditions are improvable. Alternatively, it should also be considered to further optimize the derivatives of ICI127032 (e.g. **3.30**) in order to obtain more stable ligands suitable for radiolabelling with high affinity.

3.5 REFERENCES

1. Sinkins, W. G.; Kandel, M.; Kandel, S. I.; Schunack, W.; Wells, J. W. G protein-linked receptors labeled by [3H]histamine in guinea pig cerebral cortex. I. Pharmacological characterization [corrected]. *Mol. Pharmacol.* **1993**, 43, 569-582.
2. Rising, T. J.; Norris, D. B.; Warrander, S. E.; Wood, T. P. High affinity 3H-cimetidine binding in guinea-pig tissues. *Life. Sci.* **1980**, 27, 199-206.
3. Warrander, S. E.; Norris, D. B.; Rising, T. J.; Wood, T. P. 3H-cimetidine and the H2-receptor. *Life. Sci.* **1983**, 33, 1119-1126.
4. Bristow, D. R.; Hare, J. R.; Hearn, J. R.; Martin, L. E. Radioligand binding studies using [^{3}H]-cimetidine and [^{3}H]-ranitidine. *Br. J. Pharmacol.* **1981**, 72, 487–590.
5. Kelley, M. T.; Bürckstümmer, T.; Wenzel-Seifert, K.; Dove, S.; Buschauer, A.; Seifert, R. Distinct interaction of human and guinea pig histamine H2-receptor with guanidine-type agonists. *Mol. Pharmacol.* **2001**, 60, 1210-1225.
6. Ruat, M.; Traiffort, E.; Bouthenet, M. L.; Schwartz, J. C.; Hirschfeld, J.; Buschauer, A.; Schunack, W. Reversible and Irreversible Labeling and Autoradiographic Localization of the Cerebral Histamine H-2-Receptor Using [I-125] Iodinated Probes. *P. Natl. Acad. Sci. USA* **1990**, 87, 1658-1662.
7. Hirschfeld, J.; Buschauer, A.; Elz, S.; Schunack, W.; Ruat, M.; Traiffort, E.; Schwartz, J. C. Iodoaminopotentidine and Related-Compounds - a New Class of Ligands with High-Affinity and Selectivity for the Histamine-H2-Receptor. *J. Med. Chem.* **1992**, 35, 2231-2238.
8. Crevat-Pisano, P.; Hariton, C.; Rolland, P. H.; Cano, J. P. Fundamental aspects of radioreceptor assays. *Journal of Pharmaceutical and Biomedical Analysis* **1986**, 4, 697-716.
9. Yellin, T. O.; Buck, S. H.; Gilman, D. J.; Jones, D. F.; Wardleworth, J. M. ICI 125,211: a new gastric antisecretory agent acting on histamine H2-receptors. *Life. Sci.* **1979**, 25, 2001-2009.
10. Preuss, H.; Ghorai, P.; Kraus, A.; Dove, S.; Buschauer, A.; Seifert, R. Constitutive activity and ligand selectivity of human, guinea pig, rat, and canine histamine H2 receptors. *J. Pharmacol. Exp. Ther.* **2007**, 321, 983-995.
11. Baumeister, P.; Erdmann, D.; Biselli, S.; Kagermeier, N.; Elz, S.; Bernhardt, G.; Buschauer, A. [3H]UR-DE257: Development of a Tritium-Labeled Squaramide-Type Selective Histamine H2 Receptor Antagonist. *ChemMedChem* **2015**, 10, 83-93.
12. Algieri, A. A.; Crenshaw, R. R. 1,2-Diaminocyclobutene-3,4-diones and a pharmaceutical composition containing them. FR 2505835, 1982. Chem. Abstr. 99:22320.
13. Black, J. W.; Leff, P.; Shankley, N. P. Further Analysis of Anomalous Pkb Values for Histamine H-2-Receptor Antagonists on the Mouse Isolated Stomach Assay. *Br. J. Pharmacol.* **1985**, 86, 581-587.
14. Kagermeier, N.; Werner, K.; Keller, M.; Baumeister, P.; Bernhardt, G.; Seifert, R.; Buschauer, A. Dimeric carbamoylguanidine-type histamine H receptor ligands: A new class of potent and selective agonists. *Bioorg. Med. Chem.* **2015**.
15. Birnkammer, T.; Spickenreither, A.; Brunskole, I.; Lopuch, M.; Kagermeier, N.; Bernhardt, G.; Dove, S.; Seifert, R.; Elz, S.; Buschauer, A. The Bivalent Ligand Approach Leads to Highly Potent and Selective Acylguanidine-Type Histamine H-2 Receptor Agonists. *J. Med. Chem.* **2012**, 55, 1147-1160.
16. Gilman, D. J.; Wardleworth, J. M.; Yellin, T. O. Guanidine derivatives of imidazoles and thiazoles. US 4165378, 1979. Chem. Abstr. 91:193297.
17. Jones, D. F.; Oldham, K. Antisecretory guanidine derivatives and pharmaceutical compositions containing them. EP 0003640A2, 1979. Chem. Abstr. 92:94405.
18. Webb, R. L.; Labaw, C. S. Diphenyl cyanocarbonimidate. A versatile synthon for the construction of heterocyclic systems. *Journal of Heterocyclic Chemistry* **1982**, 19, 1205-1206.
19. Keller, M.; Kuhn, K. K.; Einsiedel, J.; Hubner, H.; Biselli, S.; Mollereau, C.; Wifling, D.; Svobodova, J.; Bernhardt, G.; Cabrele, C.; Vanderheyden, P. M.; Gmeiner, P.; Buschauer, A.

Mimicking of Arginine by Functionalized N(omega)-Carbamoylated Arginine As a New Broadly Applicable Approach to Labeled Bioactive Peptides: High Affinity Angiotensin, Neuropeptide Y, Neuropeptide FF, and Neurotensin Receptor Ligands As Examples. *J. Med. Chem.* **2016**, 59, 1925-1945.

20. Igel, P.; Schnell, D.; Bernhardt, G.; Seifert, R.; Buschauer, A. Tritium-labeled N(1)-[3-(1H-imidazol-4-yl)propyl]-N(2)-propionylguanidine ([(3)H]UR-PI294), a high-affinity histamine H(3) and H(4) receptor radioligand. *ChemMedChem* **2009**, 4, 225-231.
21. Appl, H.; Holzammer, T.; Dove, S.; Haen, E.; Strasser, A.; Seifert, R. Interactions of recombinant human histamine H(1)R, H(2)R, H(3)R, and H(4)R receptors with 34 antidepressants and antipsychotics. *Naunyn Schmiedeberg´s Arch. Pharmacol.* **2012**, 385, 145-170.
22. Mullins, D.; Adham, N.; Hesk, D.; Wu, Y.; Kelly, J.; Huang, Y.; Guzzi, M.; Zhang, X.; McCombie, S.; Stamford, A.; Parker, E. Identification and characterization of pseudoirreversible nonpeptide antagonists of the neuropeptide Y Y5 receptor and development of a novel Y5-selective radioligand. *Eur. J. Pharmacol.* **2008**, 601, 1-7.
23. Pluym, N.; Baumeister, P.; Keller, M.; Bernhardt, G.; Buschauer, A. [(3)H]UR-PLN196: a selective nonpeptide radioligand and insurmountable antagonist for the neuropeptide Y Y(2) receptor. *ChemMedChem* **2013**, 8, 587-593.
24. Pegoli, A.; She, X.; Wifling, D.; Hubner, H.; Bernhardt, G.; Gmeiner, P.; Keller, M. Radiolabeled Dibenzodiazepinone-Type Antagonists Give Evidence of Dualsteric Binding at the M2 Muscarinic Acetylcholine Receptor. *J. Med. Chem.* **2017**, 60, 3314-3334.
25. Dukorn, S.; Littmann, T.; Keller, M.; Kuhn, K.; Cabrele, C.; Baumeister, P.; Bernhardt, G.; Buschauer, A. Fluorescence- and Radiolabeling of [Lys4,Nle17,30]hPP Yields Molecular Tools for the NPY Y4 Receptor. *Bioconjug. Chem.* **2017**, 28, 1291-1304.
26. Doughty, M. B.; Li, K.; Hu, L.; Chu, S. S.; Tessel, R. Benextramine-neuropeptide Y (NPY) binding site interactions: characterization of 3H-NPY binding site heterogeneity in rat brain. *Neuropeptides* **1992**, 23, 169-180.
27. Meini, S.; Patacchini, R.; Lecci, A.; Quartara, L.; Maggi, C. A. Peptide and non-peptide bradykinin B2 receptor agonists and antagonists: a reappraisal of their pharmacology in the guinea-pig ileum. *Eur. J. Pharmacol.* **2000**, 409, 185-194.
28. Seifert, R.; Schneider, E. H.; Dove, S.; Brunskole, I.; Neumann, D.; Strasser, A.; Buschauer, A. Paradoxical stimulatory effects of the "standard" histamine H4-receptor antagonist JNJ7777120: the H4 receptor joins the club of 7 transmembrane domain receptors exhibiting functional selectivity. *Mol. Pharmacol.* **2011**, 79, 631-638.
29. Vauquelin, G.; Morsing, P.; Fierens, F. L.; De Backer, J. P.; Vanderheyden, P. M. A two-state receptor model for the interaction between angiotensin II type 1 receptors and non-peptide antagonists. *Biochem. Pharmacol.* **2001**, 61, 277-284.
30. Lazareno, S.; Birdsall, N. J. Detection, quantitation, and verification of allosteric interactions of agents with labeled and unlabeled ligands at G protein-coupled receptors: interactions of strychnine and acetylcholine at muscarinic receptors. *Mol. Pharmacol.* **1995**, 48, 362-378.
31. Kretzschmar, E.; Laban, G.; Menzer, M.; Kazmirowski, H. G.; Meisel, P. Amidinothiourea. DD 298638, 1992. Chem. Abstr. 116:255205.
32. Keller, M.; Pop, N.; Hutzler, C.; Beck-Sickinger, A. G.; Bernhardt, G.; Buschauer, A. Guanidine-acylguanidine bioisosteric approach in the design of radioligands: synthesis of a tritium-labeled N(G)-propionylargininamide ([3H]-UR-MK114) as a highly potent and selective neuropeptide Y Y1 receptor antagonist. *J Med Chem* **2008**, 51, 8168-8172.
33. David J. Gilman, M.; James M. Wardleworth, W.; Tobias O. Yellin, W. P. A. Guanidine derivatives of imidazoles and thiazoles. US 4165378, 1979. Chem. Abstr. 91:193297.
34. Erdmann, D. Histamine H2- and H3-receptor antagonists : synthesis and characterization of radiolabelled and fluorescent pharmacological tools. Dissertation, Universität Regensburg, Regensburg, 2010. https://epub.uni-regensburg.de/19062/.

35. Callahan, J. F.; Ashton-Shue, D.; Bryan, H. G.; Bryan, W. M.; Heckman, G. D.; Kinter, L. B.; McDonald, J. E.; Moore, M. L.; Schmidt, D. B.; Silvestri, J. S.; et al. Structure-activity relationships of novel vasopressin antagonists containing C-terminal diaminoalkanes and (aminoalkyl)guanidines. *J. Med. Chem.* **1989**, 32, 391-396.
36. Saari, W. S.; Schwering, J. E.; Lyle, P. A.; Smith, S. J.; Engelhardt, E. L. Cyclization-activated prodrugs. Basic carbamates of 4-hydroxyanisole. *J. Med. Chem.* **1990**, 33, 97-101.
37. Keller, M. Guanidine-acylguanidine bioisosteric approach to address peptidergic receptors: pharmacological and diagnostic tools for the NPY Y1 receptor and versatile building blocks based on arginine substitutes. Dissertation, Universität Regensburg, Regensburg, 2009. https://epub.uni-regensburg.de/12092/.
38. Cinelli, M. A.; Cordero, B.; Dexheimer, T. S.; Pommier, Y.; Cushman, M. Synthesis and biological evaluation of 14-(aminoalkyl-aminomethyl)aromathecins as topoisomerase I inhibitors: investigating the hypothesis of shared structure-activity relationships. *Bioorg. Med. Chem.* **2009**, 17, 7145-7155.
39. Huang, G.; Pemp, D.; Stadtmuller, P.; Nimczick, M.; Heilmann, J.; Decker, M. Design, synthesis and in vitro evaluation of novel uni- and bivalent ligands for the cannabinoid receptor type 1 with variation of spacer length and structure. *Bioorg. Med. Chem. Lett.* **2014**, 24, 4209-4214.
40. Kraus, A.; Ghorai, P.; Birnkammer, T.; Schnell, D.; Elz, S.; Seifert, R.; Dove, S.; Bernhardt, G.; Buschauer, A. N-G-Acylated Aminothiazolylpropylguanidines as Potent and Selective Histamine H-2 Receptor Agonists. *ChemMedChem* **2009**, 4, 232-240.
41. Pop, N.; Igel, P.; Brennauer, A.; Cabrele, C.; Bernhardt, G. N.; Seifert, R.; Buschauer, A. Functional reconstitution of human neuropeptide Y (NPY) Y(2) and Y(4) receptors in Sf9 insect cells. *J. Recept. Signal. Transduct. Res.* **2011**, 31, 271-285.
42. Mosandl, J. Radiochemical and luminescence-based binding and functional assays for human histamine receptors using genetically engineered cells. University of Regensburg, Regensburg, 2009. https://epub.uni-regensburg.de/12335/.
43. Felixberger, J. Luciferase complementation for the determination of arrestin recruitment: Investigations at histamine and NPY receptors. University of Regensburg, Regensburg, 2014. https://epub.uni-regensburg.de/31292/.
44. Lieb, S.; Littmann, T.; Plank, N.; Felixberger, J.; Tanaka, M.; Schafer, T.; Krief, S.; Elz, S.; Friedland, K.; Bernhardt, G.; Wegener, J.; Ozawa, T.; Buschauer, A. Label-free versus conventional cellular assays: Functional investigations on the human histamine H1 receptor. *Pharm. Res.* **2016**, 114, 13-26.
45. Cheng, Y.; Prusoff, W. H. Relationship between the inhibition constant (K1) and the concentration of inhibitor which causes 50 per cent inhibition (I50) of an enzymatic reaction. *Biochem. Pharmacol.* **1973**, 22, 3099-3108.

Chapter 4

Aminopotentidine Derivatives as Highly Potent H_2R Antagonists: Synthesis and Pharmacological Characterization of Amine Precursors and "Cold" Forms of Potential Radioligands

Note: Prior to the submission of this thesis, parts of this chapter (the synthesis of **4.1**, **4.2** and **4.3**) were published in cooperation with partners:

Baumeister, P.; Erdmann, D.; Biselli, S.; Kagermeier, N.; Elz, S.; Bernhardt, G.; Buschauer, A. [^{3}H]UR-DE257: Development of a Tritium-Labeled Squaramide-Type Selective Histamine H_2 Receptor Antagonist. *ChemMedChem* **2015**, 10, 83-93.

4.1 INTRODUCTION

The piperidinomethylphenoxypropylamine (potentidine) moiety is a privileged structure for H_2R antagonism and part of many high affinity ligands. Some of the most important representatives are aminopotentidine and its derivatives (Figure 4.1).[1,2] It was reported that aminopotentidine shows a high antagonistic activity (pK_b value: 7.28) and a second or even a third substituent at the aromatic ring of the residue is well tolerated (e.g. iodoaminopotentidine: pK_b value: 7.52 and diiodoaminopotentidine: pK_b value: 7.79).[1] Also compounds with only one substituent in 3-position (e.g. Compound **I**) or even compounds with an aromatic heterocycle as aromatic ring (e.g. Compound **II**) showed a similar or slightly lower activity.[1] Interestingly, the ^{125}Iodine labeled iodoaminopotentidine was a very high affinity ligand at the hH_2R (K_d value of 0.32 nM) and the pK_i values of aminopotentidine, iodoaminopotentidine and iodoazidopotentidine obtained with the afore mentioned radioligand were considerably higher than the corresponding pK_b values.[1,3] [^{125}I]Iodoaminopotentidine was used to map the H_2R densities in human and mammalian brain.[3,4]

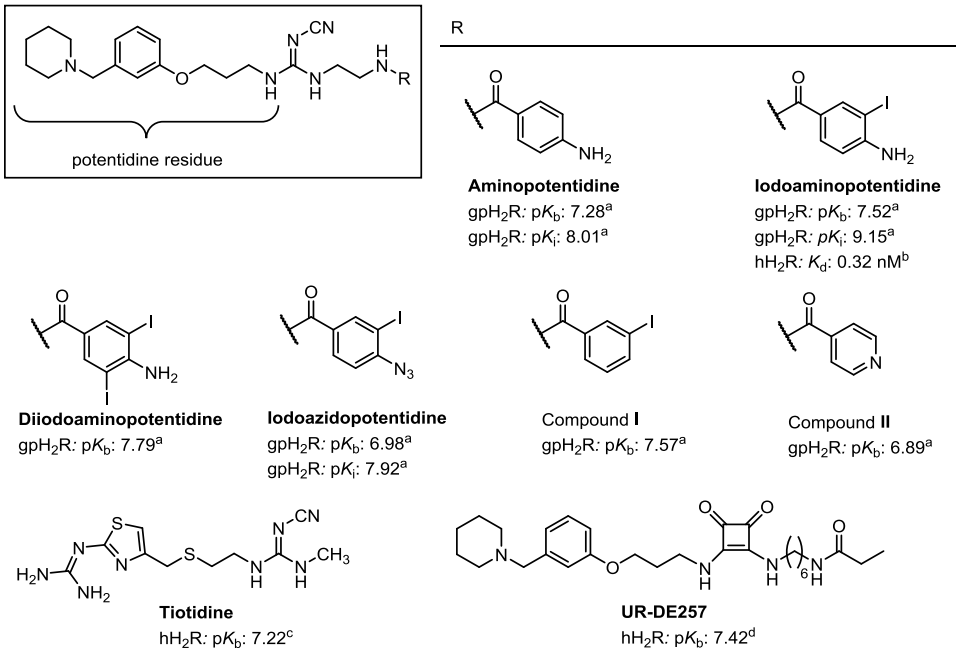

Figure 4.1. Structures of aminopotentidine, selected aminopotentidine derivatives, tiotidine and UR-DE257. [a]Hirschfeld et al.[1] [b]Traiffort et al.[4] [c]Kelley et al.[5] [d]Baumeister et al.[6]

Although ^{125}iodine labeled ligands have, compared to tritium labeled ligands, the advantage of a higher specific activity, their preparation and usage require higher safety precautions and the ligands can only be used for 4-5 weeks after preparation.[7] In our workgroup tritiated compounds are highly preferred due to their longer half-life. The published tritiated radioligands showed a 100-fold lower H_2R affinity (e.g. [^{3}H]tiotidine and [^{3}H]UR-DE257) compared to [^{125}I]iodoaminopotentidine.[5,6]

Here, the synthesis and pharmacological characterization of aminopotentidine and its analogs with different substituents (e.g. iodine, bromine, chlorine, trifluoromethyl) in the 3-position as precursors for potential tritiated ligands and synthesis of the “cold” form of potential radioligands are reported. The derivatisation of the terminal anilinic amino group of these

precursors was performed with different acylating reagents e.g. N-hydroxy succinimidyl propionate or propionic acid chloride, which are also available in tritiated form. Furthermore, a series of aminopotentidine derivatives containing a functionalized (propionylated, acetylated or methylated) aminomethyl substituent in 4-position of the aromatic ring was synthesized and characterized. In order to enable radiolabeling, the substituents of the amino-group were chosen with regard to commercially available labeling reagents such as tritiated N-hydroxy succinimidyl propionate, propionic acid chloride, acetyl chloride or methyl iodide.

4.2 Results And Discussion

4.2.1 Chemistry

The intermediate 1-(2-aminoethyl)-2-cyano-3-(3-[3-(1-piperidinylmethyl)phenoxy]-propyl)guanidine **4.5** was prepared in a five step synthesis as described before[1,2,8] with minor modifications (Scheme 4.1). Starting from 3-hydroxybenzaldehyde a reductive amination with piperidine in the presence of formic acid (Leuckart-Wallach reaction) led to **4.1**. Addition of acrylonitrile to intermediate **4.1** led to **4.2** (variation of the Michael-addition reaction). The resulting cyanine **4.2** was reduced to the amine **4.3** by $LiAlH_4$. Coupling of diphenyl-*N*-cyanocarbonimidate with **4.3** and subsequently with ethylene diamine resulted in the cyanoguanidine **4.5**.

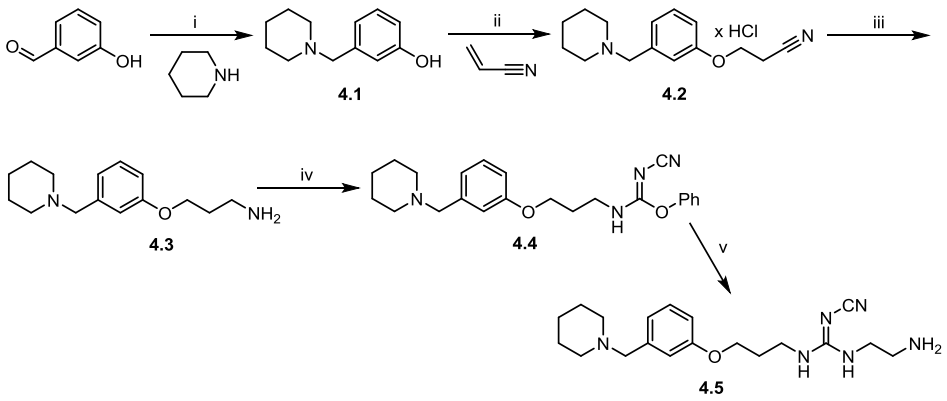

Scheme 4.1. Synthesis of 1-(2-Aminoethyl)-2-cyano-3-(3-[3-(1-piperidinylmethyl)phenoxy]propyl)guanidine **4.5**. Reagents and conditions: i) formic acid, 110° C, 3 h, 87%; ii) benzyltrimethylammonium hydroxide, reflux, 24 h, 55%; iii) $LiAlH_4$, anhydrous diethyl ether, RT, 4 h, 99.6%; iv) diphenyl-*N*-cyanocarbonimidate, 2-propanol, RT, 3 h, no purification; v) ethylene diamine, CH_3CN, 150° C, 15 min under microwave radiation, 60% over two steps.

The initial step of the synthesis of the aminopotentidine derivatives was the amide coupling of **4.5** and the respective benzoic acid derivatives, resulting in either the amine-precursors (**4.30-4.34**), amine-protected precursors (**4.39**, **4.45**) or directly in the final products (**4.42-4.44**, **4.49** and **4.50**).

The benzoic acid derivatives **4.15-4.17** were prepared in a four step synthesis (Scheme 4.2). Starting from 4-methyl benzoic acid derivatives, substituted with trifluoromethyl, chlorine, or bromine in 3-position, a side chain bromination using N-bromosuccinimide and AIBN were performed. The 4-bromomethyl benzoic acid derivatives **4.6-4.8** were transferred to the corresponding ethyl esters **4.9-4.11** using thionyl chloride and ethanol. A substitution reaction with sodium azide converted the ethyl esters **4.9-4.11** into the corresponding azides **4.12-4.14**. The 4-aminomethyl benzoic acid ethylesters **4.15-4.17** were synthesized from **4.12-4.14** by a Staudinger Reaction using triphenylphosphine.

The phthalimide protected (4-Aminomethyl)benzoic acid (**4.19**) was synthesized from **4.18** and phthalic anhydride in the presence of acetic acid according to published protocols (Scheme 4.2).[9,10] 4-(Aminomethyl)-3-bromobenzoic acid (**4.21**) was synthesized from **4.14** by first

saponification of the ester and second Staudinger reaction of the azide with triphenylphosphine to the amine (Scheme 4.2). The phthalimide protection of **4.21** under the same conditions as of **4.19** failed. This could be due to steric hindrance of the substituent in 3-position.

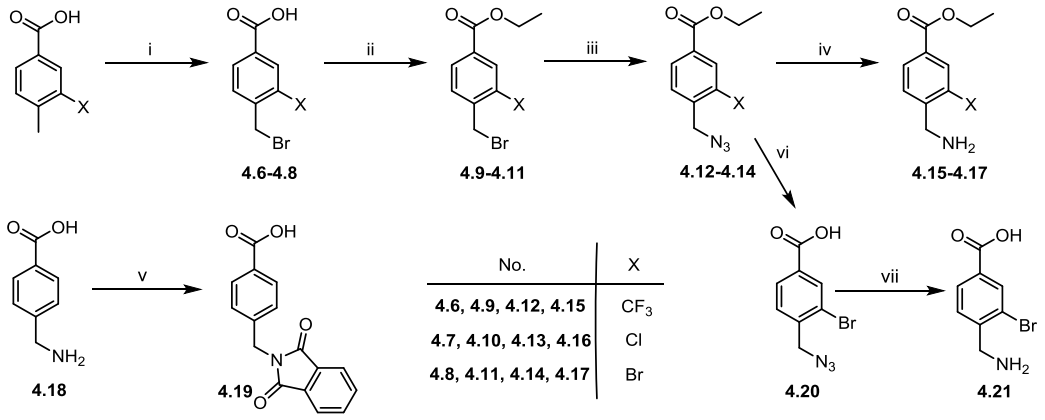

Scheme 4.2. Synthesis of benzoic acid derivatives **4.15-4.17** and **4.19-4.21**. Reagents and conditions: i) N-Bromosuccinimide, AIBN, $CHCl_3$, 75° C, 3-5 h, no purification; ii) thionyl chloride, EtOH, 65° C, 2-24 h, 43-52% over two steps; iii) NaN_3, anhydrous DMF, RT, 24 h, 49-91%; iv) PPh_3, THF/H_2O (1:2, v/v), RT, 24 h, 66-80%; v) phthalic anhydride, AcOH, reflux, 3.5 h, 84%; vi) NaOH, THF, RT, 24 h, 93%; vii) PPh_3, THF and H_2O, RT, 24 h, 27%.

The 4-(Propionamidomethyl)benzoic acids **4.25-4.27** were synthesized from **4.15-4.17** by amide coupling with succinimidyl propionate followed by saponification of the ethyl ester (Scheme 4.3).

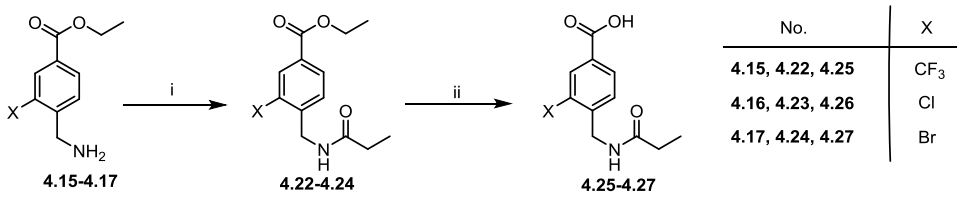

Scheme 4.3. Synthesis of benzoic acid derivatives **4.25-4.27**. Reagents and conditions: i) TEA, succinimidyl propionate, CH_2Cl_2, RT, ON, no purification; ii) Aq. NaOH, THF, RT, ON, 49-84% over two steps.

4-[(Dimethylamino)methyl]benzoic acid (**4.28**) and 3-bromo-4-[(dimethylamino)methyl]benzoic acid (**4.29**) were synthesized by Eschweiler-Clarke-Methylation of the corresponding amino acid **4.18** or **4.21** with formaldehyde in the presence of formic acid (Scheme 4.4).[11]

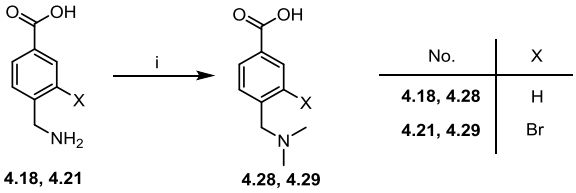

Scheme 4.4. Synthesis of benzoic acid derivatives **4.28** and **4.29**. Reagents and conditions: i) Aqueous formaldehyde, formic acid, reflux, ON, 94-100%.

In scheme 4.5 the synthesis of the propionylated aminopotentidine derivatives **4.35-4.38** is depicted. Aminopotentidine[1] (**4.30**), iodoaminopotentidine[1,3] (**4.34**) and its derivatives **4.31-4.33** were synthesized from **4.5** by amide coupling with the corresponding 4-amino benzoic acid using TBTU as coupling reagent and DIPEA as base. The anilinic amino group of **4.30-4.34** showed a reduced nucleophilicity which made the labeling by amide coupling a challenge. The classical

reaction with succinimidyl propionate in the presence of triethylamine (see synthesis of **4.22-4.24,** Scheme 4.3) failed. The propionylation by an excess of propionyl chloride in the presence of DMAP and TEA resulted in the desired products **4.35-4.38** in very low yields 11-23%.

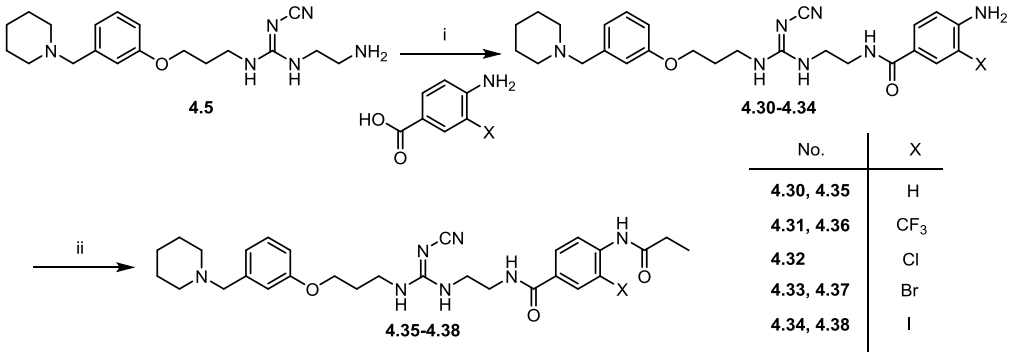

No.	X
4.30, 4.35	H
4.31, 4.36	CF_3
4.32	Cl
4.33, 4.37	Br
4.34, 4.38	I

Scheme 4.5. Synthesis of the aminopotentidine derivatives **4.35-4.38**. Reagents and conditions: i) TBTU, DIPEA, CH_2Cl_2, RT, ON, 34-68%; ii) propionyl chloride, DMAP, TEA, CH_2Cl_2, RT, ON, 11-23%.

The aminopotentidine derivative **4.41** was synthesized in three steps starting by amide coupling of **4.5** and **4.19** using same conditions by analogy with **4.30-4.34** (Scheme 4.6). The resulting **4.39** was first phthalimide deprotected by hydrazine and then propionylated using succinimidyl propionate.

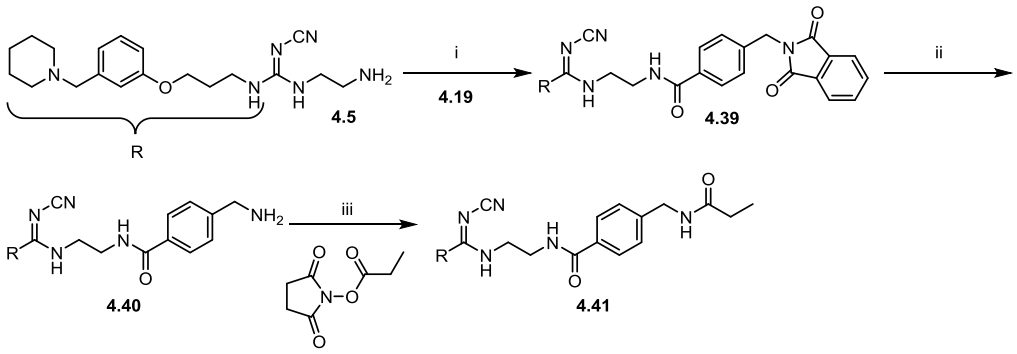

Scheme 4.6. Synthesis of the aminopotentidine derivative **4.41**. Reagents and conditions: i) TBTU, DIPEA, CH_2Cl_2, RT, ON, 74%; ii) Hydrazinium hydroxide, EtOH, RT, 4 h, 68%; iii) TEA, CH_2Cl_2, RT, ON, 81%.

In case of the aminopotentidine derivatives **4.42-4.44** the final step was the amide coupling of the amine precursor **4.5** with the respective benzoic acids **4.25-4.27** using the same conditions as for the preparation of **4.30-4.34** (Scheme 4.7).

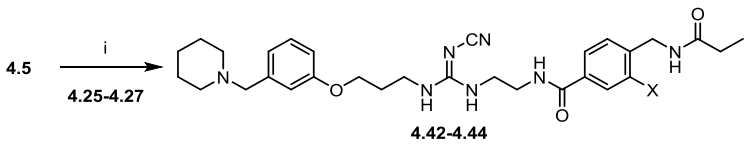

No.	X
4.42	CF_3
4.43	Cl
4.44	Br

Scheme 4.7. Synthesis of the aminopotentidine derivatives **4.42-4.44**. Reagents and conditions: i) TBTU, DIPEA, CH_2Cl_2, RT, ON, 6-44%.

The synthesis of the acetylated aminopotentidine derivatives **4.47** and **4.48** is depicted in Scheme 4.8. The amide coupling of **4.5** and **4.20**, followed by a Staudinger Reaction and

acetylation of the resulting amine **4.46** with acetyl chloride resulted in the product **4.48**. The acetylation of **4.40** under similar conditions led to **4.48**.

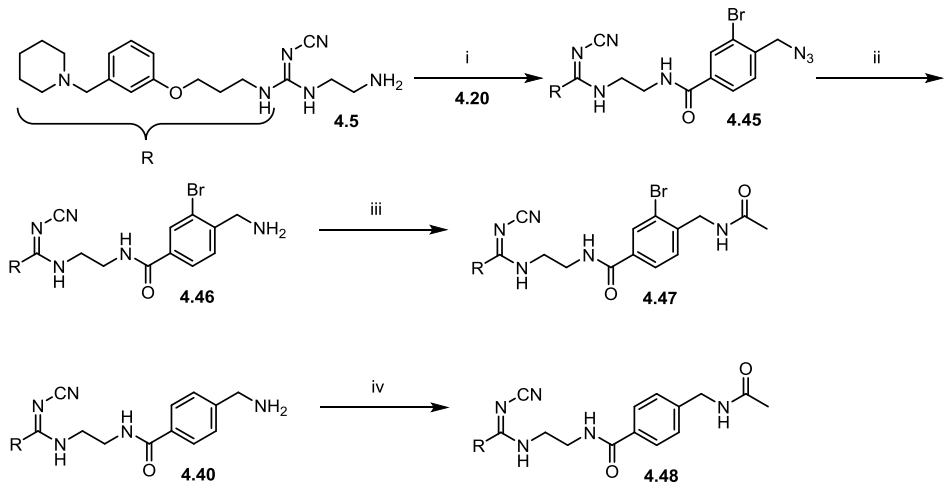

Scheme 4.8. Synthesis of the aminopotentidine derivatives **4.47** and **4.48**. Reagents and conditions: i) HBTU, DIPEA, CH_2Cl_2, RT, ON, 44%; ii) PPh_3, THF/H_2O (1:2, v/v), RT, ON, 19%; iii) acetyl chloride, DIPEA, CH_2Cl_2, RT, ON, 20%; iv) acetyl chloride, DMAP, DIPEA, CH_2Cl_2, RT, 2 days, 25%.

The dimethylated aminopotentidine derivatives **4.49** and **4.50** were synthesized by coupling of **4.5** with the respective benzoic acid using HBTU as coupling reagent and DIPEA as base (Scheme 4.9).

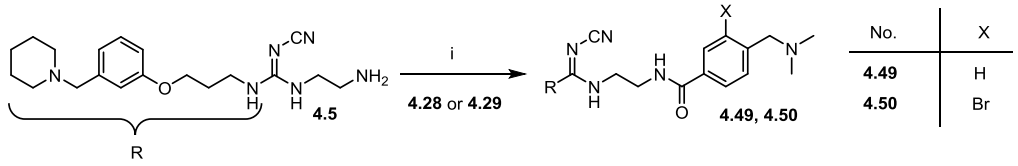

Scheme 4.9. Synthesis of the aminopotentidine derivatives **4.49** and **4.50**. Reagents and conditions: i) HBTU, DIPEA, CH_2Cl_2, RT, ON, 28-32%.

Adaptation of the synthetic route to radiosynthetic requirements

Radiosynthesis makes special demands on synthesis planning and reaction conditions. The labeling reaction is the key-step of the synthesis and should be the last step. In general, for radiosynthesis an excess of precursor compared to radioactive labeling reagent is used. This facilitates handling with respect of safety precautions and reduces the costs of the overall synthesis. Within the series of the "cold" forms of potential radioligands the propionylated ligands **4.37** and **4.38** showed the highest hH_2R affinity (see biological evaluation) and were therefore considered for radiolabeling.

However, the reaction conditions for the synthesis of **4.37** and **4.38** were not suitable for radiosynthesis due to the necessary high excess of the "cold" labeling reagent propionic chloride and the low yields. In order to adjust the reaction conditions to radiosynthesis standards, a test reaction was carried out in small scale and with an excess of **4.33** (6.98 µg, 10 eq). HRMS analysis of the reaction mixture showed no **4.37** was formed. This preliminary test showed that the

radiosynthesis of **4.37** (and **4.38**) will be a challenge. An alternative could be the synthesis of radiolabeled **4.50**. Comound **4.50** showed high hH_2R affinity in the range of UR-DE257 and tiotidine (see Biological evaluation). Dimethylation of **4.46** with methyliodide should be easily adaptable to radiosynthetic requirements. The main challenge will be to minimize formation of monomethylated and/or trimethylated by-product and the separation of **4.50** from the amine precursor and these by-products.

4.2.2 Biological Evaluation

H_2R affinity, selectivity compared to H_3R and antagonism

The aminopotentidine derivatives **4.30-4.38**, **4.40-4.44** and **4.46-4.50** were investigated in equilibrium competition binding experiments on membrane preparations from Sf9 insect cells expressing the hH_2R-$G_{s\alpha S}$ fusion protein using the antagonist [^{3}H]UR-DE257[6] as radioligand. The selectivity of several compounds for the hH_2R over the hH_3R was investigated by competition binding experiments using membranes of Sf9 insect cells co-expressing the hH_3R and $G_{\alpha i2}$ and $G_{\beta 1\gamma 2}$ proteins using [^{3}H]N^{α}-methylhistamine as radioligand. Additionally, representative compounds were examined for hH_2R agonism in the GTPγS binding assay on membrane preparations from Sf9 insect cells expressing the hH_2R-$G_{s\alpha S}$ fusion protein. Ligands which exhibited no agonism were also investigated in antagonist mode versus histamine as agonist. Selected curves are depicted in Figure 4.1 and the results are summarized in Table 4.1.

Within the aminopotentidine derivatives iodoaminopotentidine (**4.34**) showed the highest hH_2R affinity. The pK_i value of 9.51 was in good agreement with the literature (gpH_2R: pK_i value of 9.15[1] and hH_2R: K_d value of 0.32 nM[4]). Also the 3-brominated aminopotentidine **4.33** showed a high hH_2R affinity with a pK_i value of 8.58. While the introduction of a bromine or iodine substituent in 3-position of the benzoic acid moiety (**4.33** or **4.34**) led to an increase in affinity compared to aminopotentidine (**4.30**, pK_i value of 7.7), a trifluoromethyl or chlorine substituent (**4.31** or **4.32**) retained the hH_2R affinity (pK_i value of 7.57-7.7). Likewise, the exchange of the anilinic amino group in 4-position with an aminomethyl group (**4.40**) was tolerated with almost no change in affinity (pK_i value of 7.6) compared to **4.30**. The 4-(propionamidomethyl)-3-bromobenzamide containing ligand **4.46** showed with a pK_i value of 7.71 a decreased affinity compared to the 3-brominated aminopotentidine **4.33**.

Within the target compounds ("cold" forms of potential radioligands) the propionylated iodoaminopotentidine **4.38** and the propionylated 3-bromo aminopotentidine **4.37** showed the highest hH_2R affinities with pK_i values of 8.18 and 8.5. The propionylation of the 3-halogenated aminopotentidines **4.35**, **4.36** and **4.38** resulted in a decrease of hH_2R affinity by one order of magnitude. By contrast, in case of **4.37**, the propionylated analog of **4.33,** the hH_2R affinity was retained (pK_i value of 8.5). The 4-(propionamidomethyl)benzamide containing ligands **4.41-4.44** showed only moderate affinity to hH_2R with pK_i values of 6.58-7.2. The acetylation (**4.48**: pK_i value of 6.4 and **4.47**: pK_i value of 7.09) as well as the propionylation (**4.41**: pK_i value of 6.58 and **4.44**: pK_i value of 6.9) of the 4-aminomethyl benzamide-containing amine precursors **4.40** and **4.46** resulted in a decrease of hH_2R affinity. The dimethylated analog of **4.40** (**4.49**) showed a low hH_2R affinity with a pK_i value of 5.61. In contrast, **4.50**, the dimethylated **4.46**, showed a high hH_2R affinity with a pK_i value of 7.54.

The ligands **4.30**, **4.31**, **4.33-4.38**, **4.40**, **4.41**, **4.43** and **4.44** showed a low hH_3R affinity with pK_i values of 4.5-5.22. Iodoaminopotentidine (**4.34**) showed with a 32000-fold higher affinity for the hH_2R compared to hH_3R the highest selectivity. Also the propionylated ligands **4.37** and **4.38** showed a lower but still excellent selectivity (6900- or 2500-fold).

All investigated ligands (**4.30**, **4.31**, **4.33-4.35**, **4.37**, **4.38**, **4.40**, **4.41** and **4.44)** were antagonists or inverse agonists in the GTPγS binding assay. Except for the pK_b values of **4.40** and **4.44** (pK_b value:

7.5 and 6.5), the calculated pK_b values, obtained in the antagonistic mode, were considerably lower compared to the pK_i values. Especially bromoaminopotentidine (**4.33**) and iodoaminopotentidine (**4.34**), which were high affinity hH_2R antagonists in binding experiments (pK_i values of 8.58 and 9.51), showed only low activities in the GTPγS binding assay (pK_b values of 6.5 and 6.7). With a pK_b value of 7.6, the propionylated 3-bromo aminopotentidine **4.37** showed the highest activity among the investigated ligands.

Antagonism of aminopotentidine (**4.30**) and iodoaminopotentidine (**4.34**) (pK_b values of 6.0 and 6.7) measured with a GTPγS binding assay on membrane preparations from Sf9 insect cells expressing the hH_2R-$G_{s\alpha S}$ fusion protein were lower than described in literature (pK_b values of 6.63 and 7.46, obtained by steady-state GTPase assay).[5,12] Discrepancies between pK_i values of aminopotentidine (**4.30**) and iodoaminopotentidine (**4.34**) from radioligand binding and pK_b values from functional experiments were also described for the gpH_2R by Hirschfeld et al (gpH_2R: pK_i values of 8.01 and 9.15 vs. pK_b values of 7.28 and 7.52)[1]. Hirschfeld et al gave as possible explanation the different experimental setups which led to varying access to the H_2R (e.g. guinea pig striatal membranes vs. intact isolated guinea pig right atrium). When a very similar experimental setup was used (in our study membrane preparations in both binding and functional studies), the use of different competitors (histamine vs. radiolabeled antagonist) could lead to the different results[13]. Agonists and antagonists may stabilize different receptor conformations that exhibit different affinities for the investigated agonists/antagonists/inverse agonists.[13] For the antagonistic radioligand [^{3}H]tiotidine it was already shown that it binds only to a fraction of the functionally active H_2Rs.[5]

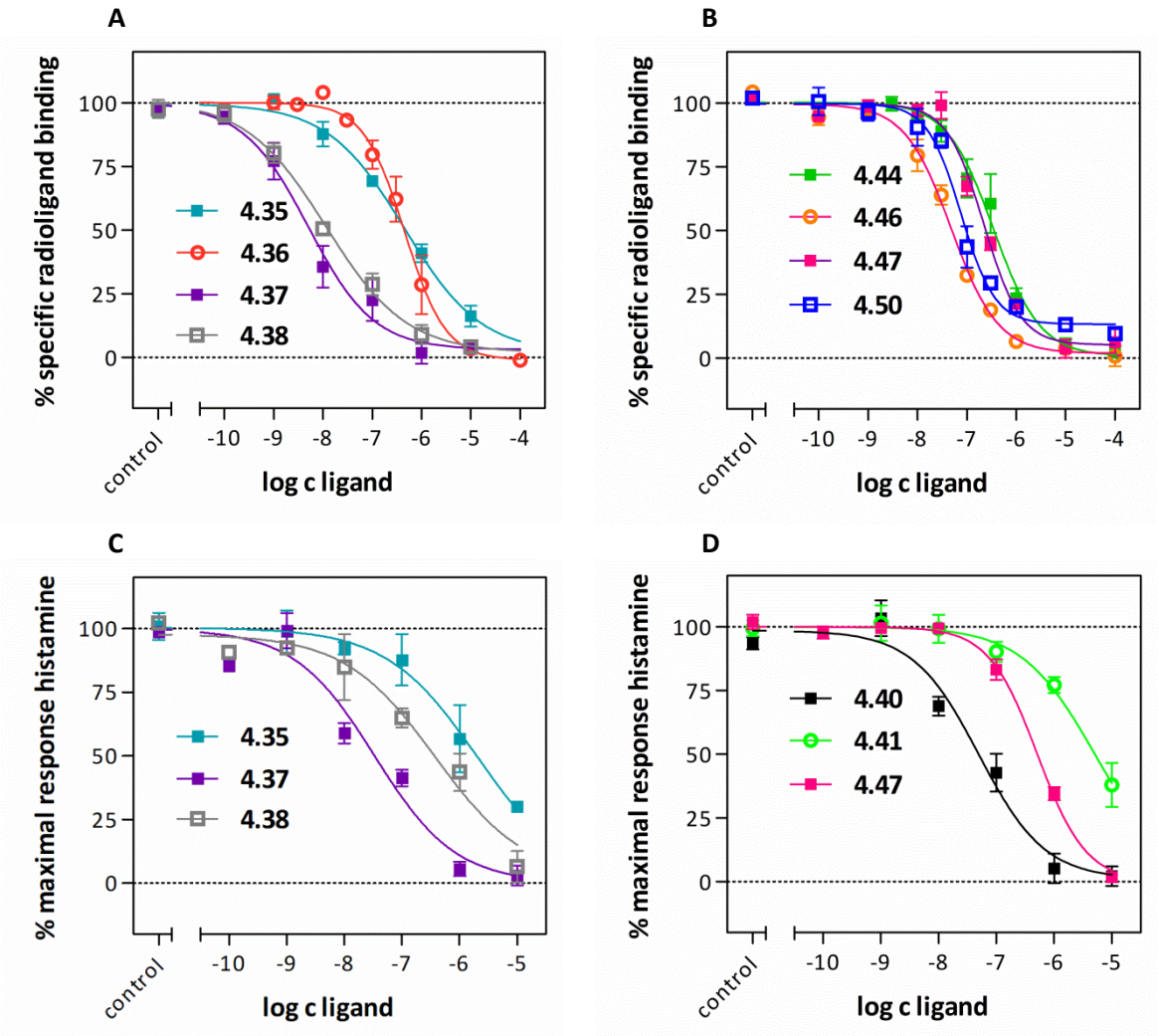

Figure 4.1. Displacement of the radioligand [^{3}H]UR-DE257 (c = 20 nM, K_d = 12.2 nM) by (A) compounds **3.35-3.38** and (B) compounds **4.44**, **4.46**, **4.47**, **4.50** and antagonism of (C) compounds **4.35**, **4.37**, **4.38** and (D) compounds **4.40**, **4.41**,**4.47** on hH_2R determined in a GTPγS assay (antagonistic mode). Histamine (1 µM) was used for stimulation. Both determined on membrane preparations of Sf9 insect cells expressing the hH_2R-$G_{s\alpha S}$ fusion protein. Data represent mean values ± SEM of 2-4 experiments performed in triplicate.

Table 4.1. Affinities of the aminopotentidine derivatives **4.30-4.38**, **4.40-4.44** and **4.46-4.50** to $hH_{2,3}R$, obtained from equilibrium competition binding studies and hH_2R antagonism expressed in the calculated pK_b values determined by a GTPγS assay.

	hH_2R				hH_3R		
	Binding[a]		**GTPγS**[c]		**Binding**[d]		**Selectivity**[e]
Compound	**pK_i**	**N**	**pEC_{50} (pK_B)**	**N**	**pK_i**	**N**	**hH_2R:hH_3R**
His	6.53 ± 0.04	3	5.80 ± 0.06	9	7.8 ± 0.1	3	19:1
4.30 (APT)	7.7 ± 0.1/ gpH_2R: 8.01[1]	3	(6.0 ± 0.4)/ (6.63)[5]	3	4.92 ± 0.08	3	1:600
4.31	7.7 ± 0.2[b]	3	(6.6 ± 0.4)	4	5.03 ± 0.07	3	1:470
4.32	7.57 ± 0.01	3	n.d.	-	n.d.	-	n.d.
4.33	8.58 ± 0.05	2	(6.5 ± 0.4)	4	4.8 ± 0.1	3	1:6000
4.34 (IAPT)	9.51 ± 0.06/ gpH_2R: 9.15[1]	3	(6.7 ± 0.1)/ (7.46)[12]	3	5.0 ± 0.1	4	1:32000
4.35	6.60 ± 0.08	3	(5.9 ± 0.2)	2	4.50 ± 0.09	4	1:130
4.36	6.7 ± 0.1	3	n.d.	-	4.7 ± 0.1	3	1:100
4.37	8.5 ± 0.3	3	(7.6 ± 0.1)	3	4.66 ± 0.07	4	1:6900
4.38	8.18 ± 0.07	3	(6.6 ± 0.4)	3	4.82 ± 0.09	4	1:2500
4.40	7.6 ± 0.2[b]	2	(7.5 ± 0.2)	4	5.22 ± 0.09	2	1:240
4.41	6.58 ± 0.04	3	(5.4 ± 0.3)	3	4.75 ± 0.06	3	1:68
4.42	6.98 ± 0.08	3	n.d.	-	n.d.	-	n.d.
4.43	7.2 ± 0.1	3	n.d.	-	4.96 ± 0.03	2	1:170
4.44	6.9 ± 0.1	3	(6.5 ± 0.1)	4	5.04 ± 0.08	2	1:72
4.46	7.71 ± 0.07	3	n.d.	-	n.d.	-	n.d.
4.47	7.09 ± 0.09	3	n.d.	-	n.d.	-	n.d.
4.48	6.4 ± 0.1	4	n.d.	-	n.d.	-	n.d.
4.49	5.61 ± 0.07	3	n.d.	-	n.d.	-	n.d.
4.50	7.54 ± 0.09	3	n.d.	-	n.d.	-	n.d.

Competition binding assay on membrane preparations of Sf9 insect cells: [a]expression of the hH_2R-$G_{s\alpha S}$ fusion protein (radioligand: [^{3}H]UR-DE257, c = 20 nM, K_d = 12.2 nM or [b][^{3}H]tiotidine, c = 10 nM, K_d = 12.75 nM), [d]co-expression of the hH_3R and $G_{\alpha i2}$ and $G_{\beta 1\gamma 2}$ proteins (radioligand: [^{3}H]N^{α}-methylhistamine, c = 3 nM, K_d = 3 nM). [c][^{35}S]GTPγS assay determined on membrane preparations of Sf9 insect cells expressing the hH_2R-$G_{s\alpha S}$ fusion protein. The intrinsic activity (α) of histamine was set to 1.00, and α values of investigated compounds were referred to this value. The pK_B values were determined in the antagonist mode versus histamine (c = 1 µM) as agonist. [e]Selectivity represents the ratio of the corresponding K_i values. Data represent mean values ± SEM of N experiments performed in triplicate. Data were analyzed by nonlinear regression and were best fitted to four-parameter sigmoidal concentration-response curves. Data shown are means ± SEM of N independent experiments, each performed in triplicate.

4.3 EXPERIMENTAL SECTION

4.3.1 General procedures

Chemicals and solvents were purchased from the following suppliers: Merck (Darmstadt, Germany), Acros Organics (Geel, Belgium), Fluka (Buchs, Swiss), Alfa Aesar (Karlsruhe, Germany), Sigma Aldrich (Munich, Germany) and TCI (Tokyo, Japan). All solvents were of analytical grade or distilled prior to use. Anhydrous solvents were stored over molecular sieve under protective gas. Deuterated solvents for NMR spectroscopy were purchased from Deutero (Kastellaun, Germany). For the preparation of buffers and HPLC eluents Millipore water was used throughout. Column chromatography was carried out using Merck silica gel 60 (0.040-0.063 mm). Microwave assisted synthesis was performed with an Initiator 2.0 (Biotage, Uppsala, Sweden) using microwave reaction vials (Biotage, Uppsala, Sweden) combined with caps and septa. Automated flash chromatography was performed with a 971-FP flash-purification system (Agilent Technologies, Santa Clara, CA). Pre-packed columns (SuperFlash SF10-4 g, SF12-8 g, SF 15-12 g und SF15-24 g, Agilent Technologies, Santa Clara, CA) were used throughout. Reactions were monitored by thin layer chromatography (TLC) on Merck silica gel 60 F254 aluminium sheets, and compounds were detected with UV light at 254 nm and ninhydrin solution (0.8 g ninhydrin, 200 mL n-buthanol, 6 mL acetic acid). Melting points were determined with a B-540 apparatus (BÜCHI GmbH, Essen, Germany) and are uncorrected. IR spectra were measured on a NICOLET 380 FT-IR spectrophotometer (Thermo Electron Corporation, USA). Nuclear Magnetic Resonance (^{1}H NMR, ^{13}C NMR and ^{19}F NMR) spectra were recorded on a Bruker Avance-300 (7.05 T, ^{1}H: 300 MHz, ^{13}C: 75.5 MHz, ^{19}F: 282 MHz), Avance-400 (9.40 T, ^{1}H: 400 MHz, ^{13}C: 100.6 MHz), or Avance-600 (14.1 T; ^{1}H: 600 MHz, ^{13}C: 150.9 MHz; cryogenic probe) NMR spectrometer (Bruker BioSpin, Karlsruhe, Germany). Chemical shifts are given in δ (ppm) relative to external standards. Multiplicities are specified with the following abbreviations: s (singlet), d (doublet), t (triplet), q (quartet), qui (quintet), m (multiplet), br s (broad signal), as well as combinations thereof. In certain cases 2D-NMR techniques (COSY, HSQC, HMBC and NOESY) were used to assign ^{1}H and ^{13}C chemical shifts. Low-resolution mass spectrometry (MS) was performed on a Finnigan ThermoQuest TSQ 7000 instrument using an electrospray ionization (ESI) source or on a Finnigan SSQ 710A instrument (EI-MS, 70 eV). High-resolution mass spectrometry (HRMS) was performed on an Agilent 6540 UHD Accurate-Mass Q-TOF LC/MS system (Agilent Technologies, Santa Clara, USA) using an ESI source. Preparative HPLC was performed with a system from Knauer (Berlin, Germany) consisting of two K-1800 pumps and a K-2001 detector. A YMC Triart C18 (150 x 20 mm, 5 µm, YMC Europe GmbH, Dinslacken, Germany) served as RP-column at a flow rate of 15 mL/min at room temperature. A detection wavelength of 220 nm and mixtures of CH_3CN and 0.1% aq. NH_3 as mobile phase were used throughout. CH_3CN was removed from the eluates under reduced pressure (final pressure: 80 mbar) at 45 °C prior to lyophilisation (Christ alpha 2-4 LD lyophilisation apparatus equipped with a Vacuubrand RZ 6 rotary vane vacuum pump). Analytical HPLC analysis was performed on a system from Meck Hitachi, composed of a D-6000 interface, a L-6200A pump, a AS2000A auto sampler and a L-4000 UV-VIS detector. A Kinetex XB-C18 100A (250 x 4.6 mm, 5 µm, t_0 = 2.9 min, Phenomenex, Aschaffenburg, Germany) served as RP-column for acidic runs (flow rate of 0.8 mL/min) and mixtures of 0.05% TFA in CH_3CN (A) and 0.05% aq. TFA (B) were used as mobile phase. A YMC Triart C18 (150 x 2 mm, 5 µm, t_0 = 1.63 min; YMC, Japan) served as RP-column for basic runs (flow rate of 0.35 mL/min) and mixtures of 0.1% NH_3 in

CH_3CN (A) and 0.1% aq. NH_3 (B) were used as mobile phase. Helium degassing, room temperature and a detection wavelength of 220 nm were used throughout. Solutions for injection (concentration: 100-500 µM) were either prepared from stock solution (10 mM in DMSO) in a mixture of CH_3CN and H_2O corresponding to the initial eluent composition, or as a one to one mixture of the eluate (preparative HPLC) with Millipore water. The following linear gradients were applied for analytical HPLC analysis: gradient 1: 0-30 min: A/B 5:95-80:20, 30-32 min: 80:20-95:5, 32-42 min: 95:5 or gradient 2: 0-30 min: A/B 10:90-80:20, 30-32 min: 80:20-95:5, 32-42 min: 95:5 or gradient 3 (basic conditions, YMC Triat): 0-30 min: A/B 10:90-90:10, 30-32 min: 90:10-95:5, 32-42 min: 95:5. Microanalysis was performed on a Vario micro cube (Elementar, Langenselbold, Germany).

4.3.2 Experimental protocols and analytical data

3-(Piperidin-1-ylmethyl)phenol (4.1)[2,6]

Piperidine (4.18 g, 49.1 mmol, 2 eq) and formic acid (98%, 3,3 g, 71,3 mmol, 2,6 eq) were added under ice cooling to 3-hydroxybenzaldehyde (3.00 g, 24.6 mmol, 1 eq) and the reaction mixture was stirred at 110 °C for 3 h. After cooling to room temperature, the reaction mixture was poured in H_2O (15 mL). The aqueous solution was alkalized using ammonia solution (25%, w/w). The precipitated white solid product was filtered off and dried *in vacuo* (4.06 g, 87%). Mp: 134-138 °C (Lit.[2] mp. 136-137 °C). R_f = 0.2 (EtOAc/PE 85:15). ^{1}H-NMR (400 MHz, [D_6]DMSO, COSY): δ (ppm) 1.37-1.40 (m, 2H), 1.45-1.50 (m, 4H), 2.29 (br s, 4H), 3.31 (s, 2H), 6.59-6.62 (m, 1H), 6.67-6.68 (d, 1H, *J* 7.4 Hz), 6.70-6.71 (m, 1H), 7.05-7.09 (t, 1H, *J* 7.7 Hz), 9.23 (s, 1H). ^{13}C-NMR (100 MHz, [D_6]DMSO, COSY): δ (ppm) 24.0, 25.6, 53.9, 62.9, 113.7, 115.4, 119.3, 128.9, 140.1, 157.2. MS (LC-MS, CI, NH_3, t_R = 11.7 min): *m/z* (%) 192.1 (100) $[M+H]^+$. $C_{12}H_{17}NO$ (191.13).

3-[3-(Piperidin-1-ylmethyl)phenoxy]propanenitrile hydrochloride (4.2)[2,6]

4.1 (4.00 g, 20.9 mmol, 1 eq) was suspended in acrylonitrile (14 mL, 210 mmol, 10 eq) and a catalytic amount of benzyltrimethylammonium hydroxide (40% in MeOH, 0.2 mL) was added. The reaction mixture was stirred over night under reflux. The excess of acrylonitrile was removed under reduced pressure and the oily residue was dissolved in diethyl ether (25 mL). The organic layer was washed with sodium hydroxide solution (5%, w/w, 20 mL) and H_2O (20 mL). The combined aqueous layers were extracted with diethyl ether (20 mL). The organic layers were combined and dried over Na_2SO_4. The product was precipitated as HCl salt with HCl in 2-propanol (5-6 M). Removal of the solvent *in vacuo* afforded the product as white solid (3.25 g, 55%). Mp: 163.5-165.7 °C (Lit. [2] Mp: 161-162 °C). R_f = 0.2 (EtOAc/PE 85:15). ^{1}H-NMR (400 MHz, [D_6]DMSO, HSQC, NOESY): δ (ppm) 1.28-1.39 (m, 1H), 1.66-1.88 (m, 5H), 2.76-2.85 (m, 2H), 3.03-3.06 (t, 2H, *J* 5.9 Hz), 3.22-3.25 (d, 2H, *J* 11.8 Hz), 4.20-4.24 (m, 4H), 7.02-7.05 (dd, 1H, ^4J 2.0 Hz, ^3J 8.3 Hz), 7.18-7.20 (d,1H, *J* 7.7 Hz), 7.35-7.39 (m, 2H), 10.92 (br s, 1H). ^{13}C-NMR (100 MHz, [D_6]DMSO, HSQC, NOESY): δ (ppm) 17.9, 21.4, 22.0, 51.5, 58.6, 62.8, 115.6, 117.3, 118.8, 124.1, 129.9, 131.4, 157.7. MS (LC-MS, CI, NH_3, t_R= 13.5 min): *m/z* (%) 245.2 (100) $[M+H]^+$. $C_{15}H_{20}N_2O \cdot HCl$ (244.34 + 36.46).

3-[3-(Piperidin-1-ylmethyl)phenoxy]propan-1-amine (4.3) [2,6]

4.2 (3.00 g, 10.71 mmol, 1 eq) was slowly added to a suspension of lithium aluminium hydride (609 mg, 16.90 mmol, 1.6 eq) in anhydrous diethyl ether (30 mL) and the reaction mixture was stirred for 4 h at room temperature. After the remaining lithium aluminium hydride was hydrolyzed with sodium hydroxide solution (5%, w/w, 35 mL), diethyl ether (50 mL) was added and the insoluble material was filtered off. The two layers were separated and the organic layer was dried over Na_2SO_4. Removal of the solvent *in vacuo* afforded the product as colorless oil (2.59 g, 99.6%). R_f = 0.1 (EtOAc/MeOH + 1-3 drops TEA 80:20). ^{1}H-NMR (400 MHz, $CDCl_3$): δ (ppm) 1.36 (br s, 2H), 1.39-1.45 (m, 2H), 1.54-1.59 (m, 4H), 1.88-1.95 (qui, 2H, *J* 6.5 Hz), 2.36 (m, 4H), 2.90 (t, 2H, *J* 6.7 Hz), 3.43 (s, 2H), 4.04 (t, 2H, *J* 6.2 Hz), 6.76-6.78 (m, 1H), 6.87-6.89 (m, 2H), 7.19 (m, 1H). ^{13}C-NMR (100 MHz, $CDCl_3$): δ (ppm) 24.5, 26.1, 33.3, 39.4, 54.6, 63.9, 65.9, 113.0, 115.3, 121.6, 129.1, 140.5, 159.1. HRMS (ESI): *m/z* $[M+H]^+$ calcd. for $C_{15}H_{25}N_2O^+$: 249.1961, found: 249.1961. $C_{15}H_{24}N_2O$ (248.37).

Phenyl-*N'*-cyano-*N*-(3-[3-(piperidin-1-ylmethyl)phenoxy]propyl)carbamimidate (4.4) [8]

4.3 (600 mg, 2.42 mmol, 1 eq) was added to a solution of diphenyl-N-cyanocarbonimidate (633 mg, 2,66 mmol, 1,1 eq) in 2-propanol (90 mL) and the reaction mixture was stirred for 3 h at room temperature. The solvent was removed under reduced pressure and the product was recristallized in diethylether. **4.4** obtained as a white solid (877 mg, 93%) which still contained the by-product phenol and was directly used for the next step. R_f = 0.9 (CH_2Cl_2 / 7 N NH_3 in MeOH 90:10). MS: (LC-MS, ESI, t_R = 5.2 min): *m/z* (%) 393,1 (100) $[M+H]^+$. $C_{23}H_{28}N_4O_2$ (392.22).

1-(2-Aminoethyl)-2-cyano-3-(3-[3-(1-piperidinylmethyl)phenoxy]propyl)guanidine (4.5)[1]

Ethylendiamine (307 mg, 5.10 mmol, 20 eq) was added to a stirring solution of **4.4** (100 mg, 0.26 mmol, 1 eq) in CH_3CN (5 mL). The reaction mixture was stirred for 15 min at 150 °C under microwave radiation. The solvent was removed under reduced pressure and the residue was dissolved in CH_2Cl_2 (7 mL). The organic layer was washed three times with H_2O (7 mL) and three times with aqueous sodium hydroxide solution (5 M, 7 mL). The organic layer was dried over Na_2SO_4. Removal of the solvent *in vacuo* afforded the product as colorless oil (55 mg, 60%). R_f = 0.3 (CH_2Cl_2 / 7 N NH_3 in MeOH 90:10).^{1}H-NMR (400 MHz, $CDCl_3$, COSY, HSQC, HMBC): δ (ppm) 1.39-1.41 (m, 2H), 1.50-1.56 (m, 4H), 1.97-2.03 (qui, 2H, *J* 6.2 Hz), 2.33 (br s, 4H), 2.80 (t, 2H, *J* 5.2 Hz), 3.18 (t, 2H, *J* 5.2 Hz), 3.39 (m, 4H), 4.00 (t, 2H, *J* 5.8 Hz), 6.20 (br s, 0.8H), 6.74-6.76 (m, 1H), 6.85-6.88 (m, 2H), 7.17 (t, 1H, *J* 7.7 Hz). ^{1}H-NMR (400 MHz, CD_3OD): δ (ppm) 1.46-1.48 (m, 2H), 1.57-1.63 (m, 4H), 2.02-2.08 (m, 2H), 2.42 (br s, 4H), 2.72-2.75 (t, 2H, *J* 6.3 Hz), 3.23-3.26 (t, 2H, *J* 6.3 Hz), 3.41-3.44 (t, 2H, *J* 6.7 Hz), 3.47 (s, 2H), 4.05-4.08 (t, 2H, *J* 5.8 Hz), 6.86-6.90 (m, 2H), 6.95-6.96 (m, 1H), 7.20-7.25 (t, 1H, *J* 7.8 Hz). ^{13}C-NMR (100 MHz, $CDCl_3$, COSY, HSQC, HMBC): δ (ppm) 24.4, 26.0, 28.9, 39.1, 41.8, 45.3, 54.6, 63.8, 65.4, 112.9, 115.1, 119.2, 122.0, 129.2, 140.5, 158.6, 161.3. HRMS: (ESI): *m/z* $[M+H]^+$, calcd. for $C_{19}H_{31}N_6O^+$: 359.2554, found: 359.2552. $C_{19}H_{30}N_6O$ (358.49).

General procedure for the synthesis of the ester protected benzoic acid derivatives 4.9-4.11

In order to remove residual water and the stabilisator from the $CHCl_3$, the solvent was filtered through extra dry AlO_3 (50 g for 100 mL). The 4-methyl benzoic acid derivative (1 eq) and AIBN (0.1 eq) were suspended in $CHCl_3$ (15-20 mL). N-bromosuccinimide (1.5 eq) was added portion wise and under stirring to the hot (75 °C) suspension. The reaction mixture was stirred for 3-5 h at 75 °C. Removal of the solvent under reduced pressure afforded the 4-(bromomethyl)benzoic acid derivatives **4.6**-**4.8** which were used for the next step without further purification. The crude **4.6**, **4.7** or **4.8** was suspended in EtOH (10 mL) and thionyl chloride (2-3 eq) was added drop wise. The reaction mixture was stirred for 2-24 h at 65 °C. The product was purified by automated flash chromatography. Varying amounts of the respective ethyl 4-(chloromethyl) benzoate derivative were formed as by-product and couldn´t be separated by flash chromatography.

Ethyl 4-(bromomethyl)-3-(trifluoromethyl)benzoate (4.9)[14]

4.9 was prepared from 4-methyl 3-(trifluoromethyl) benzoic acid (500 mg, 2.45 mmol, 1 eq), AIBN (40 mg, 0.24 mmol, 0.1 eq), N-bromosuccinimide (654 mg, 3.67 mmol, 1.5 eq) in $CHCl_3$ (20 mL) and ester formation with thionyl chloride (583 mg, 4.90 mmol, 2 eq) in EtOH (10 mL) according to the general procedure. Purification by automated flash chromatography (PE/EtOAc 100:0-97:3 in 20 min) and removal of the solvent *in vacuo* afforded the product as colourless oil (280 mg, 43%). R_f = 0.45 (PE/EtOAc 95:5).^{1}H-NMR (300 MHz, $CDCl_3$, COSY, HSQC, HMBC): δ (ppm) 1.41 (t, 3H, *J* 7.14 Hz), 4.38-4.45 (q, 2H, *J* 7.14 Hz), 4.78 (s, 2H), 7.74-7.77 (m, 1H), 8.22-8.25 (m, 1H), 8.33 (m, 1H). ^{13}C-NMR (100 MHz, $CDCl_3$, COSY, HSQC, HMBC): δ (ppm) 14.3, 41.4, 61.7, 123.6 (q, 1C, $J_{C,F}$ 275.25 Hz), 127.35 (q, 1C, $J_{C,F}$ 5.85 Hz), 128.5 (q, 1C, $J_{C,F}$ 31.52 Hz), 130.8, 131.9, 133.2, 140.13 (q, 1C, $J_{C,F}$ 1.40 Hz), 164.9. ^{19}F-NMR (282 MHz, $CDCl_3$): δ (ppm) -60.24. HRMS: (ESI): *m/z* $[M+H]^+$, calcd. for $C_{11}H_{11}BrF_3O_2^+$: 310.9889, found: 310.9892. HRMS: (ESI): *m/z* $[M+H]^+$, calcd. for $C_{11}H_{11}ClF_3O_2^+$: 267.0394, found: 267.0395. $C_{11}H_{10}BrF_3O_2$ (311.10).

Ethyl 4-(bromomethyl)-3-chlorobenzoate (4.10)[15]

4.10 was prepared from 3-chloro 4-methyl benzoic acid (380 mg, 2.23 mmol, 1 eq), AIBN (37 mg, 0.22 mmol, 0.1 eq), N-bromosuccinimide (595 mg, 3.34 mmol, 1.5 eq) in $CHCl_3$ (15 mL) and ester formation with thionyl chloride (691 mg, 6.69 mmol, 3 eq) in EtOH (10 mL) according to the general procedure. Purification by automated flash chromatography (PE/EtOAc 100:0-97.5:2.5 in 25 min) and removal of the solvent *in vacuo* afforded the product as colourless oil (320 mg, 52%). R_f = 0.74 (PE/EtOAc 6:1).^{1}H-NMR (300 MHz, $CDCl_3$): δ (ppm) 1.40 (t, 3H, *J* 7.14 Hz), 4.35-4.42 (q, 2H, *J* 7.14 Hz), 4.72 (s, 2H), 7.56 (d, 1H, *J* 8.14 Hz), 7.92-7.95 (m, 1H), 8.06-8.07 (m, 1H). ^{13}C-NMR (100 MHz, $CDCl_3$): δ (ppm) 14.3, 43.0, 61.6, 128.2 130.6, 130.8, 132.1, 134.1, 139.5, 165.0. HRMS: (ABCI): *m/z* $[M+H]^+$, calcd. for $C_{10}H_{11}BrClO_2^+$: 276.9625, found: 276.9626. HRMS: (ABCI): m/z $[M+H]^+$, calcd. for $C_{10}H_{11}Cl_2O_2^+$: 233.0131, found: 233.0131. $C_{10}H_{10}BrClO_2$ (277.54).

Ethyl 4-(bromomethyl)-3-bromobenzoate (4.11)[16,17]

4.11 was prepared from 3-bromo 4-methyl benzoic acid (2.00 g, 9.30 mmol, 1 eq), AIBN (153 mg, 0.93 mmol, 0.1 eq), N-bromosuccinimide (2.48 g, 13.95 mmol, 1.5 eq) in $CHCl_3$ (150 mL) and ester formation with thionyl chloride (2.21 g, 18.60 mmol, 2 eq) in EtOH (50 mL) according to the general procedure. The crude product was purified first by column chromatography (PE/EtOAc 100:0-90:10) and then by automated flash chromatography (PE/EtOAc 100:0-85:15 in 40 min). Removal of the solvent *in vacuo* afforded the product as a slightly yellow oil (1.39 g, 46%). R_f = 0.60 (PE/EtOAc 5:1).^{1}H-NMR (400 MHz, $CDCl_3$): δ (ppm) 1.40 (t, 3H, *J* 7.19 Hz), 4.36-4.42 (q, 2H, *J* 7.19 Hz), 4.72 (s, 2H), 7.57 (d, 1H, *J* 8.01 Hz), 7.98-8.00 (m, 1H), 8.25 (m, 1H). ^{13}C-NMR (100 MHz, $CDCl_3$): δ (ppm) 14.3, 45.5, 61.5, 123.8, 128.9, 130.6, 132.1, 134.1, 141.1, 164.8. HRMS: (ESI): *m/z* $[M+H]^+$, calcd. for $C_{10}H_{11}Br_2O_2^+$: 320.9120, found: 320.9114. HRMS: (ESI): *m/z* $[M+H]^+$, calcd. for $C_{10}H_{11}BrClO_2^+$: 276.9626, found: 276.9624. $C_{10}H_{10}Br_2O_2$ (322.00).

General procedure for the synthesis of the azide derivatives 4.12-4.14

Sodium azide (4 eq) was added to a solution of **4.9-4.11** (1 eq) in anhydrous DMF (5-10mL). The reaction mixture was stirred for 24 h at room temperature. H_2O (80 mL) was added and the product was extracted three times with CH_2Cl_2 (60 mL). The organic layers were combined and the solvent was removed under reduced pressure. The residue was dissolved in EtOAc (80 mL) and the organic layer was washed three times saturated $CaCl_2$ solution (50 mL), one time with brine (50 mL) and was then dried over Na_2SO_4. Removal of the solvent afforded the desired product.

Ethyl 4-(azidomethyl)-3-(trifluoromethyl)benzoate (4.12)

4.12 was prepared from **4.9** (490 mg, 1.84 mmol, 1 eq) and sodium azide (1478 mg, 7.35 mmol, 4 eq) according to general procedure. Removal of the solvent *in vacuo* afforded the product as a slightly yellow oil (430 mg, 83%). R_f = 0.5 (PE/EtOAc 95:5).^{1}H-NMR (300 MHz, [D_6]DMSO): δ (ppm) 1.34 (t, 3H, *J* 7.10 Hz), 4.32-4.39 (q, 2H, *J* 7.10 Hz), 4.76 (s, 2H), 7.85-7.88 (m, 1H), 8.20 (m, 1H), 8.26-8.29 (m, 1H). ^{13}C-NMR (75 MHz, [D_6]DMSO): δ (ppm) 13.9, 49.86 (q, 1C, $J_{C,F}$ 2.08 Hz), 61.4, 123.4 (q, 1C, $J_{C,F}$ 274.04 Hz), 126.35 (q, 1C, $J_{C,F}$ 5.81 Hz), 127.2 (q, 1C, $J_{C,F}$ 30.85 Hz), 130.1, 131.7, 133.3, 138.70 (q, 1C, $J_{C,F}$ 1.46 Hz), 164.1. ^{19}F-NMR (282 MHz, [D_6]DMSO): δ (ppm) -58.39. HRMS: (ESI): *m/z* $[M+H]^+$, calcd. for $C_{11}H_{11}F_3N_3O_2^+$: 274.0798, found: 274.0797. $C_{11}H_{10}F_3N_3O_2$ (273.22).

Ethyl 4-(azidomethyl)-3-chlorobenzoate (4.13)

4.13 was prepared from **4.10** (260 mg, 1.12 mmol, 1 eq) and sodium azide (290 mg, 4.46 mmol, 4 eq) according to general procedure. Removal of the solvent *in vacuo* afforded the product as colorless oil (130 mg, 49%). R_f = 0.44 (PE/EtOAc 95:5).^{1}H-NMR (300 MHz, $CDCl_3$): δ (ppm) 1.40 (t, 3H, *J* 7.12 Hz), 4.35-4.42 (q, 2H, *J* 7.13 Hz), 4.68 (s, 2H), 7.54-7.57 (d, 1H, *J* 8.00 Hz), 8.00-8.03 (m, 1H), 8.50-8.51 (m, 1H). ^{13}C-NMR (75 MHz, $CDCl_3$): δ (ppm) 14.4, 50.5, 61.7, 98.87, 129.91, 129.95,

132.02, 140.9, 144.4, 164.7. HRMS: (ESI): *m/z* [*M*+H]$^+$, calcd. for $C_{10}H_{11}ClN_3O_2^+$: 240.0534, found: 240.0538. $C_{10}H_{10}ClN_3O_2$ (239.66).

Ethyl 4-(azidomethyl)-3-bromobenzoate (4.14)

4.14 was prepared from **4.11** (290 mg, 1.05 mmol, 1 eq) and sodium azide (272mg, 4.18 mmol, 4 eq) according to general procedure. Removal of the solvent *in vacuo* afforded the product as yellow oil (270 mg, 91%). R_f = 0.33 (PE/EtOAc 95:5).^{1}H-NMR (400 MHz, $CDCl_3$): δ (ppm) 1.40 (t, 3H, *J* 7.12 Hz), 4.36-4.42 (q, 2H, *J* 7.12 Hz), 4.55 (s, 2H), 7.48-7.50 (d, 1H, *J* 7.96 Hz), 8.00-8.02 (m, 1H), 8.26 (m, 1H). HRMS: (ESI): *m/z* [*M*+H]$^+$, calcd. for $C_{10}H_{11}BrN_3O_2^+$: 284.0029, found: 284.0032. $C_{10}H_{10}BrN_3O_2$ (284.11).

General procedure for the synthesis of the amine derivatives 4.15-4.17

4.12, 4.13 or **4.14** (1 eq) and triphenylphosphine (1.12 eq) were dissolved in a mixture of THF and H_2O (5/1, v/v, 4 mL). The reaction mixture was stirred over night at room temperature. The THF was removed under reduced pressure and the residue was diluted with H_2O (1-7 mL). The pH value was adjusted to two by adding aqueous HCl solution (0.5 M). The aqueous layer was washed three times with EtOAc (10-20 mL). Removal of the H_2O afforded the desired product as HCl salt.

Ethyl 4-(aminomethyl)-3-(trifluoromethyl)benzoate (4.15)

4.15 was prepared from **4.12** (170 mg, 0.62 mmol, 1 eq) and triphenylphosphine (183 mg, 0.70 mmol, 1.12 eq) dissolved in a mixture of THF and H_2O (5/1, v/v, 4 mL) according to general procedure. Removal of the solvent *in vacuo* afforded the product as yellow solid (140 mg, 80%). R_f = 0.36 (CH_2Cl_2 / 2 N NH_3 in MeOH 95:5).^{1}H-NMR (300 MHz, [D_6]DMSO): δ (ppm) 1.34 (t, 3H, *J* 7.11 Hz), 4.24 (br s, 2H), 4.33-4.40 (q, 2H, *J* 7.12 Hz), 8.02-8.05 (d, 1H, *J* 8.17 Hz), 8.21 (m, 1H), 8.29-8.32 (m, 1H), 8.99 (br s, 3H). ^{13}C-NMR (75 MHz, [D_6]DMSO): δ (ppm) 13.9, 38.3(q, 1C, $J_{C\text{-}F}$ 3.40 Hz), 61.4, 123.4 (q, 1C, $J_{C\text{-}F}$ 274.35 Hz), 126.06 (q, 1C, $J_{C\text{-}F}$ 5.56 Hz), 127.3 (q, 1C, $J_{C\text{-}F}$ 30.57 Hz), 130.1, 131.0, 133.0, 137.1 (q, 1C, $J_{C\text{-}F}$ 1.41 Hz), 164.0. ^{19}F-NMR (282 MHz, [D_6]DMSO): δ (ppm) -58.24. HRMS: (ESI): *m/z* [*M*+H]$^+$, calcd. for $C_{11}H_{13}F_3NO_2^+$: 248.0893, found: 248.0895. $C_{11}H_{12}F_3NO_2$ (247.22).

Ethyl 4-(aminomethyl)-3-chlorobenzoate (4.16)

4.16 was prepared from **4.13** (920 mg, 3.84 mmol, 1 eq) and triphenylphosphine (1128 mg, 4.30 mmol, 1.12 eq) dissolved in a mixture of THF and H_2O (5/1, v/v, 20 mL) according to general procedure. Removal of the solvent *in vacuo* afforded the product as white solid (630 mg, 66%). R_f = 0.5 (CH_2Cl_2 / 2 N NH_3 in MeOH 95:5). ^{1}H-NMR (400 MHz, [D_6]DMSO): δ (ppm) 1.33 (t, 3H, *J* 7.08 Hz), 4.19 (br s, 2H), 4.31-4.37 (q, 2H, *J* 7.10 Hz), 7.81-7.83 (m, 1H), 7.96-7.98 (m, 2H), 8.85 (br s,

3H). ^{13}C-NMR (100 MHz, [D$_6$]DMSO): δ (ppm) 14.0, 39.7, 61.3, 127.7, 129.4, 130.6, 131.4, 133.0, 136.7, 164.1. HRMS: (ESI): *m/z* [*M*+H]$^+$, calcd. for $C_{10}H_{13}ClNO_2^+$: 214.0629, found: 214.0631. $C_{10}H_{12}ClNO_2$ (213.66).

Ethyl 4-(aminomethyl)-3-bromobenzoate (4.17)

4.17 was prepared from **4.14** (730 mg, 2.51 mmol, 1 eq) and triphenylphosphine (755 mg, 2.88 mmol, 1.12 eq) dissolved in a mixture of THF and H_2O (5/1, v/v, 15 mL) according to general procedure. Removal of the solvent *in vacuo* afforded the product as white solid (550 mg, 73%). Mp: 212-213 °C. R_f = 0.5 (CH_2Cl_2 / 3.5 N NH_3 in MeOH 95:5). ^{1}H-NMR (400 MHz, [D$_6$]DMSO): δ (ppm) 1.34 (t, 3H, *J* 7.12 Hz), 4.18 (br s, 2H), 4.31-4.37 (q, 2H, *J* 7.11 Hz), 7.77-7.79 (d, 1H, *J* 8.11 Hz), 8.01-8.03 (m, 1H), 8.15 (m, 1H), 8.78 (br s, 3H). ^{13}C-NMR (100 MHz, [D$_6$]DMSO): δ (ppm) 14.0, 41.8, 61.3, 123.1, 128.2, 130.3, 131.4, 132.6, 138.3, 164.0. HRMS: (ESI): *m/z* [*M*+H]$^+$, calcd. for $C_{10}H_{13}BrNO_2^+$: 258.0124, found: 258.0127. $C_{10}H_{12}BrNO_2$ (258.12).

4-((1,3-Dioxoisoindolin-2-yl)methyl)benzoic acid (4.19)[9,10]

(4-Aminomethyl)benzoic acid (**4.18**) (200 mg, 1.32 mmol, 1 eq) and phthalic anhydride (212 mg, 1.46 mmol, 1.1 eq) were suspended in acetic acid (1 mL) and the reaction mixture was stirred under reflux for 3.5 h. The solvent was removed under reduced pressure and the residue was suspended in H_2O (2 mL). The product was filtered off and dried *in vacuo*. **4.19** was obtained as white solid (312 mg, 84%). Mp: 262-266 °C (Lit. mp[9]: 267-270 °C). R_f = 0.8 (CH_2Cl_2 / MeOH + 2 drops TFA 95:5). ^{1}H-NMR (300 MHz, [D$_6$]DMSO): δ (ppm) 4.84 (s, 2H), 7.42 (d, 2H, *J* 8.22 Hz), 7.85-7.94 (m, 6H), 12.95 (br s, 1H). ^{13}C-NMR (100 MHz, [D$_6$]DMSO): δ (ppm) 40.6, 123.3, 127.4, 129.6, 129.9, 131.6, 134.6, 141.5, 167.0, 167.7. HRMS: (ESI): *m/z* [*M*+H]$^+$, calcd. for $C_{16}H_{12}NO_4^+$: 282.0761, found: 282.0764. $C_{16}H_{11}NO_4$ (281.27).

4-(Azidomethyl)-3-bromobenzoic acid (4.20)

4.14 (1.29 g, 4.54 mmol, 1 eq) was suspended in THF (50 mL). Aqueous NaOH solution (1 mol/L, 23 mL, 5 eq) was added and the reaction mixture was stirred over night at room temperature. The pH value was adjusted with aqueous HCl solution (0.5 mol/L) to two. The THF was removed under reduced pressure and the product was extracted with EtOAc (3 x 40 mL). The organic layers were combined, washed with brine (40 mL) and dried over Na_2SO_4. Removal of the solvent *in vacuo* afforded the product as beige solid (1.08 g, 93%). Mp: 124 °C. R_f = 0.1 (PE / EtOAc 95:5). ^{1}H-NMR (400 MHz, [D$_6$]DMSO): δ (ppm) 4.64 (s, 2H), 7.64 (d, 1H, J 7.92 Hz), 7.95-7.98 (m, 1H), 8.12 (m, 1H). ^{13}C-NMR (100 MHz, [D$_6$]DMSO): δ (ppm) 53.8, 123.6, 129.3, 131.2, 133.1, 133.7, 140.0, 166.2. HRMS: (ESI): *m/z* [*M*+H]$^+$, calcd. for $C_8H_7BrN_3O_2^+$: 255.9716, found: 255.9719. $C_8H_6BrN_3O_2$ (256.06).

4-(Aminomethyl)-3-bromobenzoic acid (4.21)[18]

4.20 (280 mg, 1.09 mmol, 1 eq) and triphenylphosphine (321 mg, 1.22 mmol, 1.12 eq) were dissolved in a mixture of THF and H_2O (5/1, v/v, 6 mL). The reaction mixture was stirred over night at room temperature. The yellow precipitate was filtered off and washed with CH_2Cl_2 (1 mL). Removal of residual solvent *in vacuo* afforded the product as yellow solid (67 mg, 27%). ^{1}H-NMR (400 MHz, [D_6]DMSO + 3 drops of TFA): δ (ppm) 4.20-4.22 (m, 2H), 7.66 (d, 1H, *J* 8.06 Hz), 8.00-8.03 (m, 1H), 8.15 (m, 1H), 8.44 (br s, 3H). ^{13}C-NMR (100 MHz, [D_6]DMSO + 3 drops of TFA): δ (ppm) 42.6, 123.6, 129.1, 130.5, 133.2, 133.6, 138.3, 166.1. HRMS: (ESI): *m/z* [*M*+H]$^+$, calcd. for $C_8H_9BrNO_2^+$: 229.9811, found: 229.9811. $C_8H_8BrNO_2$ (230.06).

General procedure for the synthesis of the benzoic acid derivatives 4.25-4.27

4.15, **4.16** or **4.17** (1 eq) and TEA (3 eq) were dissolved in CH_2Cl_2 (3 mL). Succinimidyl propionate (1.5 eq) was added and the reaction mixture was stirred over night at room temperature. The mixture was diluted with CH_2Cl_2 (5 mL) and the organic layer was washed three times with aqueous HCl solution (0.5 mol/L, 10 mL), two times with H_2O (10 mL) and with brine (10 mL). The organic layer was dried over Na_2SO_4 and the solvent was removed under reduced pressure to afford the intermediates **4.22**-**4.24**. These intermediates were ester deprotected subsequently. **4.22**, **4.23** or **4.24** was suspended in THF (3-5 mL). Aqueous NaOH solution (1 mol/L, 5 eq) was added and the reaction mixture was stirred over night at room temperature. The pH value was adjusted with aqueous HCl solution (0.5 mol/L) to 2-7. The THF was removed under reduced pressure and the product was extracted with EtOAc (3 x 5-20 mL). The organic layers were combined and dried over Na_2SO_4. Removal of the solvent under reduced pressure afforded the desired product.

4-(Propionamidomethyl)-3-(trifluoromethyl)benzoic acid (4.25)

4.25 was prepared from **4.15** (80 mg, 0.28 mmol, 1 eq), TEA (86 mg, 0.84 mmol, 3 eq) and succinimidyl propionate (72 mg, 0.42 mmol, 1.5 eq) dissolved in CH_2Cl_2 (3 mL) according to general procedure. **4.22** was obtained as a yellow oily solid (90mg, 99.9%). Removal of the ester protecting group by aqueous NaOH solution (1 mol/L, 1.4 mL) afforded **4.25** as slightly pink solid (50 mg, 66%). R_f = 0.2 (PE / EtOAc +2 drops TFA 1:2). ^{1}H-NMR (400 MHz, [D_6]DMSO): δ (ppm) 1.10 (t, 3H, *J* 7.59 Hz), 2.27 (q, 2H, *J* 7.58 Hz), 4.53-4.54 (m, 2H), 7.66 (d, 1H, *J* 8.28 Hz), 8.21-8.24 (m, 2H), 8.49 (t, 1H, *J* 5.70 Hz). ^{13}C-NMR (100 MHz, [D_6]DMSO): δ (ppm) 9.7, 28.3, 38.5 (q,1C, $J_{C\text{-}F}$ 2.89 Hz), 123.9 (q, 1C, $J_{C\text{-}F}$ 273.79 Hz), 126.1 (q. 1C, $J_{C\text{-}F}$ 5.68 Hz), 126.3 (q, 1C, $J_{C\text{-}F}$ 30.78 Hz), 128.9, 130.1, 133.1, 142.6 (q,1C, $J_{C\text{-}F}$ 1.46 Hz), 165.9, 173.2. ^{19}F-NMR (282 MHz, [D_6]DMSO): δ (ppm) -59.5. HRMS: (ESI): *m/z* [*M*+H]$^+$, calcd. for $C_{12}H_{13}F_3NO_3^+$: 276.0842, found: 276.0843. $C_{12}H_{12}F_3NO_3$ (275.23).

3-Chloro-4-(propionamidomethyl)benzoic acid (4.26)

4.26 was prepared from **4.16** (200 mg, 0.80 mmol, 1 eq), TEA (243 mg, 2.40 mmol, 3 eq) and succinimidyl propionate (205 mg, 1.20 mmol, 1.5 eq) dissolved in CH_2Cl_2 (8 mL) according to general procedure. **4.23** was obtained as a white oily solid (230 mg). Removal of the ester protecting group by aqueous NaOH solution (1 mol/L, 4.1 mL) afforded **4.26** as white solid (150 mg, 84%). R_f = 0.2 (PE / EtOAc +2 drops TFA 1:2). ^{1}H-NMR (300 MHz, [D_6]DMSO): δ (ppm) 1.04 (t, 3H, *J* 7.58 Hz), 2.21 (q, 2H, *J* 7.58 Hz), 4.35-4.37 (m, 2H), 7.42 (d, 1H, *J* 7.85 Hz), 7.86-7.89 (m, 2H), 8.40 (t, 1H, *J* 5.72 Hz), 13.26 (s, 1H). ^{13}C-NMR (75 MHz, [D_6]DMSO): δ (ppm) 9.8, 28.2, 39.9, 127.9, 128.6, 129.5, 131.0, 132.0, 141.4, 165.9, 173.2. HRMS: (ESI): *m/z* [*M*+H]$^+$, calcd. for $C_{11}H_{13}ClNO_3^+$: 242.0579, found: 242.0581. $C_{11}H_{12}ClNO_3$ (241.67).

3-Bromo-4-(propionamidomethyl)benzoic acid (4.27)

4.27 was prepared from **4.17** (260 mg, 1.01 mmol, 1 eq), TEA (204 mg, 2.02 mmol, 2 eq) and succinimidyl propionate (258 mg, 1.51 mmol, 1.5 eq) dissolved in CH_2Cl_2 (5 mL) according to general procedure. **4.24** was obtained as a white oily solid (220 mg, 70%). Removal of the ester protecting group by aqueous NaOH solution (1 mol/L, 3.2 mL) afforded **4.27** as white solid (90 mg, 49%). R_f = 0.2 (PE / EtOAc +2 drops TFA 1:2). ^{1}H-NMR (400 MHz, [D_6]DMSO): δ (ppm) 1.05 (t, 3H, *J* 7.58 Hz), 2.22 (q, 2H, *J* 7.58 Hz), 4.33 (d, 2H, *J* 5.87 Hz), 7.39-7.41 (m, 1H), 7.90-7.93 (m, 1H), 8.06-8.07 (m, 1H), 8.39 (t, 1H, *J* 5.86 Hz), 13.23 (br s, 1H). ^{13}C-NMR (100 MHz, [D_6]DMSO): δ (ppm) 9.8, 28.3, 42.4, 122.0, 128.4, 128.5, 131.2, 132.8, 143.0, 165.8, 173.2. HRMS: (ESI): *m/z* [*M*+H]$^+$, calcd. for $C_{11}H_{13}BrNO_3^+$: 288.0052, found: 288.0055. $C_{11}H_{12}BrNO_3$ (286.13).

General procedure for the methylation of 4.19 and 4.21 (synthesis of 4.28 and 4.29)

4.19 or **4.21** was dissolved in formic acid (1 mL) under heating. Aqueous formaldehyde solution (37%, 1 mL) was added and the reaction mixture was stirred over night under reflux. The mixture was cooled to room temperature and aqueous HCl solution (20%, 1mL) was added. Removal of the solvent *in vacuo* afforded the desired product.

4-[(Dimethylamino)methyl]benzoic acid hydrochloride(4.28) [11]

4.28 was prepared from **4.19** (400 mg, 2.65 mmol, 1 eq) according to general procedure. The product was obtained as white solid (570 mg, 100%). ^{1}H-NMR (400 MHz, MeOD + 3 drops of TFA): δ (ppm) 2.88 (s, 6H), 4.42 (s, 2H), 7.65-7.67 (m, 2H), 8.11-8.13 (m, 2H). ^{13}C-NMR (100 MHz, MeOD + 3 drops of TFA): δ (ppm) 41.8, 60.1, 130.2, 130.8, 132.3, 134.3, 167.4. HRMS: (ESI): *m/z* [*M*+H]$^+$, calcd. for $C_{10}H_{14}NO_2^+$: 180.1019, found: 180.1022. $C_{10}H_{13}NO_2 \cdot HCl$ (179.22 + 36.46).

3-Bromo-4-[(dimethylamino)methyl]benzoic acid hydrochloride (4.29)

4.29 was prepared from **4.21** (50 mg, 0.22 mmol, 1 eq) according to general procedure. The product was obtained as yellow hygroscopic solid (60 mg, 94%). ^{1}H-NMR (400 MHz, MeOD + 3 drops of TFA): δ (ppm) 2.96 (s, 6H), 4.60 (s, 2H), 7.81 (d, 1H, *J* 7.99 Hz), 8.07-8.09 (m, 1H), 8.30-8.31 (m, 1H). ^{13}C-NMR (100 MHz, MeOD + 3 drops of TFA): δ (ppm) 42.4, 59.8, 125.3, 129.1, 133.1, 133.8, 134.28, 134.30, 165.9. HRMS: (ESI): *m/z* $[M+H]^+$, calcd. for $C_{10}H_{13}BrNO_2^+$: 258.0124, found: 258.0145. $C_{10}H_{12}BrNO_2 \cdot HCl$ (258.12 + 36.46).

General procedure for the synthesis of the aminopotentidine derivatives 4.30-4.34

4-Aminobenzoic acid, 4-amino-3-(trifluoromethyl)benzoic acid, 4-amino-3-chlorobenzoic acid, 4-amino-3-bromobenzoic acid or 4-amino-3-iodobenzoic acid (1-1.5 eq) and DIPEA (3 eq) were dissolved in CH_2Cl_2 (5-100 mL). *O*-(Benzotriazol-1-yl)-*N,N,N',N*'-tetramethyluronium-tetrafluoroborate (TBTU, 1.2-1.5 eq) was added and the mixture was stirred for 10-30 min. Subsequently, **4.5** (1eq) was added and the reaction mixture was stirred over night at room temperature. The organic layer was further diluted with CH_2Cl_2 (10-100 mL) and washed three times with H_2O (10-100 mL) and three times with aqueous NaOH solution (5%, w/w, 10-100 mL). The organic layer was dried over Na_2SO_4 and the solvent was removed *in vacuo*. The resulting crude product was either directly used in the next synthesis step or purified by preparative HPLC.

4-Amino-N-(2-(2-cyano-3-(3-(3-(piperidin-1-ylmethyl)phenoxy)propyl)guanidino)ethyl)benzamide (Aminopotentidine, 4.30)[1,3]

4.30 was prepared from 4-aminobenzoic acid (29 mg, 0.21 mmol, 1.5 eq), DIPEA (54 mg, 0.42 mmol, 3 eq), TBTU (67 mg, 0.21 mmol, 1.5 eq) and **4.5** (50 mg, 0.14 mmol, 1 eq) according to general procedure. Purification by preparative HPLC (column: YMC Triart C_{18}, gradient: 0-30 min: MeCN/0.1% aq. NH_3 33:67-70:30, t_R = 10.6 min) afforded the product as white solid (23 mg, 34%). Mp: 66-80 °C (Lit.[1,3] Mp: 92-95 °C). R_f = 0.5 (CH_2Cl_2/3 M NH_3 in MeOH 7:2). RP-HPLC (gradient 2, 220 nm): 98% (t_R = 13.61 min, *k* = 3.7). ^{1}H-NMR (400 MHz, $CDCl_3$): δ (ppm) 1.47-1.49 (m, 2H), 1.63-1.71 (m, 4H), 2.02-2.09 (qui, 2H, *J* 6.1 Hz), 2.59 (br s, 4H), 3.38-3.55 (m, 6H), 3.63 (br s, 2H), 4.03-4.07 (m, 4H), 6.59-6.64 (d, 2H, *J* 8.7 Hz), 6.84-6.92 (m, 2H), 7.01 (br s, 1H), 7.07 (br s, 1H), 7.22 (t, 1H, *J* 7.9 Hz), 7.57-7.60 (d, 2H, *J* 8.6 Hz). ^{1}H-NMR (600 MHz, CD_3OD, COSY, HSQC, HMBC): δ (ppm) 1.50 (br s, 2H), 1.62-1.66 (m, 4H), 2.02-2.06 (qui, 2H, *J* 6.2 Hz), 2.61 (br s, 4H), 3.37-3.39 (m, 2H), 3.42-3.47 (m, 4H), 3.65 (br s, 2H), 4.06 (t, 2H, *J* 5.8 Hz), 6.63-6.65 (d, 2H, *J* 8.6 Hz), 6.90-6.93 (m, 2H), 6.98 (br s, 1H), 7.25 (t, 1H, *J* 7.9 Hz), 7.56-7.59 (d, 2H, *J* 8.9 Hz). ^{13}C-NMR (150 MHz, CD_3OD, COSY, HSQC, HMBC): δ (ppm) 24.5, 25.8, 29.9, 40.4, 40.5, 42.7, 55.0, 63.9, 66.8, 114.7, 115.3, 117.5, 119.9, 122.7, 123.7, 130.0, 130.6, 137.6, 153.4, 160.4, 161.5, 171.1. HRMS: (ESI): *m/z* $[M+H]^+$, calcd. for $C_{26}H_{36}N_7O_2^+$: 478.2925, found: 478.2927. $C_{26}H_{35}N_7O_2$ (477.61).

4-Amino-3-trifluoromethyl-*N*-(2-(2-cyano-3-(3-(3-(piperidin-1-ylmethyl)phenoxy)propyl)-guanidino)ethyl)benzamide (Trifluoromethylaminopotentidine, 4.31)

4.31 was prepared from 4-amino-3-trifluoromethylbenzoic acid (172 mg, 0.84 mmol, 1 eq), DIPEA (325 mg, 2.51 mmol, 3 eq), TBTU (323 mg, 1.00 mmol, 1.2 eq) and **4.5** (300 mg, 0.84 mmol, 1 eq) according to general procedure. The solvent was removed under reduced pressure and the residue was purified by column chromatography (CH_2Cl_2/3.5 M NH_3 in MeOH 97.5:2.5-95:5). Removal of the solvent *in vacuo* afforded the product as yellow solid (267 mg, 68%). 70 mg was further purified by preparative HPLC (column: YMC Triart C_{18}, gradient: 0-30 min: MeCN/0.1% aq. NH_3 30:70-60:40, t_R = 14.4 min). **4.31** was obtained as white solid (49 mg, 66%). Mp: 62-88 °C. R_f = 0.4 (CH_2Cl_2/7 M NH_3 in MeOH 97:3). RP-HPLC (gradient 2, 220 nm): 96% (t_R = 17.83 min, k = 5.2). ^{1}H-NMR (400 MHz, CD_3OD): δ (ppm) 1.43-1.44 (m, 2H), 1.54-1.60 (m, 4H), 2.00-2.06 (m, 2H), 2.39 (br s, 4H), 3.38-3.48 (m, 8H), 4.04 (t, 2H, *J* 5.87 Hz), 6.81-6.88 (m, 3H), 6.92 (m, 1H), 7.19 (t, 1H, *J* 7.88 Hz), 7.72-7.74 (m, 1H), 7.93-7.94 (m, 1H). ^{13}C-NMR (100 MHz, CD_3OD): δ (ppm) 25.2, 26.5, 30.0, 40.4, 40.6, 42.6, 55.4, 64.7, 66.7, 112.7 (q, 1C, $J_{C\text{-}F}$ 30.35 Hz), 114.7, 117.0, 117.4, 120.0, 122.1, 123.5, 126.4 (q, 1C, $J_{C\text{-}F}$ 271.34 Hz), 127.6 (q, 1C, $J_{C\text{-}F}$ 5.39 Hz), 130.3, 133.0, 139.8, 150.5 (q, 1C, $J_{C\text{-}F}$ 1.63 Hz), 160.3, 161.6, 169.7. HRMS: (ESI): *m/z* $[M+H]^+$, calcd. for $C_{27}H_{35}F_3N_7O_2^+$: 546.2799, found: 546.2802. $C_{27}H_{34}F_3N_7O_2$ (545.61).

4-Amino-3-chloro-*N*-(2-(2-cyano-3-(3-(3-(piperidin-1-ylmethyl)phenoxy)propyl)-guanidino)ethyl)benzamide (Chloroaminopotentidine, 4.32)

4.32 was prepared from 4-amino-3-chlorobenzoic acid (96 mg, 0.56 mmol, 1 eq), DIPEA (216 mg, 1.67 mmol, 3 eq), TBTU (215 mg, 0.67 mmol, 1.2 eq) and **4.5** (200 mg, 0.56 mmol, 1 eq) according to general procedure. The solvent was removed under reduced pressure and the residue was purified by automated flash chromatography (CH_2Cl_2/MeOH 100:0-75:25 in 53 min). Removal of the solvent *in vacuo* afforded the product as white solid (140 mg, 49%). 90 mg was further purified by preparative HPLC (column: YMC Triart C_{18}, gradient: 0-30 min: MeCN/0.1% aq. NH_3 30:70-70:30, t_R = 20.6 min). **4.32** was obtained as white solid (60 mg, 33%). Mp: 100-103 °C. R_f = 0.4 (CH_2Cl_2/1.7 M NH_3 in MeOH 90:10). RP-HPLC (gradient 1, 220 nm): 97.2% (t_R = 17.74 min, k = 5.1). ^{1}H-NMR (600 MHz, [D_6]DMSO, COSY, HSQC, HMBC): δ (ppm) 1.35 (br s, 2H), 1.45-1.47 (m, 4H), 1.89-1.93 (m, 2H), 2.27 (br s, 4H), 3.23-3.35 (m, 8H, interfering with the water signal), 3.95 (t, 2H, *J* 6.13 Hz), 5.88 (s, 2H), 6.76-6.77 (m, 2H), 6.82-6.83 (m, 2H), 7.07-7.19 (m, 3H), 7.53-7.55 (m, 1H), 7.73 (m, 1H), 8.30 (m, 1H). ^{13}C-NMR (150 MHz, [D_6]DMSO, COSY, HSQC, HMBC): δ (ppm) 24.0, 25.5, 28.6, 38.4, 38.8, 41.0, 53.9, 62.8, 65.0, 112.7, 114.1, 114.6, 116.1, 118.0, 120.9, 122.2, 127.2, 128.4, 129.0, 140.3, 147.4, 158.5, 159.5, 165.7. HRMS: (ESI): *m/z* $[M+H]^+$, calcd. for $C_{26}H_{35}ClN_7O_2^+$: 512.2535, found: 512.2544. $C_{26}H_{34}ClN_7O_2$ (512.06).

4-Amino-3-bromo-*N*-(2-(2-cyano-3-(3-(3-(piperidin-1-ylmethyl)phenoxy)propyl)-guanidino)ethyl)benzamide (Bromoaminopotentidine, 4.33)

4.33 was prepared from 4-amino-3-bromobenzoic acid (121 mg, 0.56 mmol, 1 eq), DIPEA (216 mg, 1.67 mmol, 3 eq), TBTU (215 mg, 0.67 mmol, 1.2 eq) and **4.5** (200 mg, 0.57 mmol, 1 eq)

according to general procedure. The crude product was obtained as sticky yellow solid (315 mg). 215 mg was purified by preparative HPLC (column: YMC Triart C_{18}, gradient: 0-30 min: MeCN/0.1% aq. NH_3 40:60-80:20, t_R = 13.1 min). **4.33** was obtained as white solid (115 mg, 54%). Mp: 94 °C. R_f = 0.5 (CH_2Cl_2/3 M NH_3 in MeOH 90:10). IR (KBr): 3325, 2935, 2165, 1585, 1500, 1300,1255, 1160, 755 cm^{-1}. RP-HPLC (gradient 2, 220 nm): 98.7% (t_R = 16.76 min, k = 4.8). ^{1}H-NMR (400 MHz, $CDCl_3$): δ (ppm) 1.42-1.43 (m, 2H), 1.54-1.60 (m, 4H), 2.00-2.07 (qui, 2H, J 6.1 Hz), 2.41 (br s, 4H), 3.38-3.52 (m, 8H), 4.02 (t, 2H, J 5.7 Hz), 4.53 (s, 2H), 6.35 (br s, 1H), 6.64 (br s, 1H), 6.68 (d, 1H, J 8.4 Hz), 6.79-6.82 (dd, 1H, J 8.1 Hz, J 2.1 Hz), 6.88 (d, 1H, J 7.6 Hz), 6.92 (br s, 1H), 7.19 (t, 1H, J 7.8 Hz), 7.44 (br s, 0.9H), 7.51-7.54 (dd, 1H, J 8.4 Hz, J 2.0 Hz), 7.91 (d, 1H, J 2.0 Hz). ^{1}H-NMR (400 MHz, CD_3OD): δ (ppm) 1.42-1.44 (m, 2H), 1.53-1.59 (m, 4H), 1.99-2.05 (qui, 2H, J 6.4 Hz), 2.37 (br s, 4H), 3.35-3.46 (m, 8H), 4.03 (t, 2H, J 5.8 Hz), 6.78 (d, 1H, J 8.6 Hz), 6.81-6.87 (m 2H), 6.90-6.91 (m, 1H), 7.19 (t, 1H, J 7.9 Hz), 7.54-7.56 (dd, 1H, J 8.5 Hz, J 2.1 Hz), 7.89 (d, 1H, J 2.1 Hz). ^{13}C-NMR (100 MHz, CD_3OD): δ (ppm) 25.1, 26.4, 30.0, 40.3, 40.5, 42.6, 55.4, 64.7, 66.6, 108.3, 114.6, 115.3, 116.9, 119.9, 123.4, 124.1, 128.8, 130.2, 133.3, 139.8, 150.3, 160.2, 161.5, 169.5. HRMS: (ESI): *m/z* $[M+H]^+$, calcd. for $C_{26}H_{35}BrN_7O_2^+$: 556.2030, found: 556.2032. $C_{26}H_{34}BrN_7O_2$ (556.51).

4-Amino-*N*-(2-(2-cyano-3-(3-(3-(piperidin-1-ylmethyl)phenoxy)propyl)guanidino)ethyl)-3-iodobenzamide (Iodoaminopotentidine, 4.34)[1]

4.34 was prepared from 4-amino-3-iodobenzoic acid (147 mg, 0.56 mmol, 1 eq), DIPEA (216 mg, 1.67 mmol, 3 eq), TBTU (215 mg, 0.67 mmol, 1.2 eq) and **4.5** (200 mg, 0.57 mmol, 1 eq) according to general procedure. The crude product was obtained as yellow oil (419 mg). 319 mg was purified by preparative HPLC (column: YMC Triart C_{18}, gradient: 0-30 min: MeCN/0.1% aq. NH_3 40:60-80:20, t_R = 14.0 min). **4.34** was obtained as white solid (166 mg, 65%). Mp: 94 °C (Lit.[1] Mp: 114-117 °C decomposition). R_f = 0.5 (CH_2Cl_2/7 M NH_3 in MeOH 90:10). IR (KBr) 3320, 2935, 2165, 1590, 1490, 1300, 1260, 1150 cm^{-1}. RP-HPLC (gradient 2, 220 nm): 98.3% (t_R = 17.46 min, k = 5.0).^{1}H-NMR (400 MHz, CD_3OD): δ (ppm) 1.43-1.44 (m, 2H), 1.54-1.60 (m, 4H), 2.00-2.06 (qui, 2H, J 6.3 Hz), 2.39 (br s, 4H), 3.35-3.46 (m, 8H), 4.03 (t, 2H, J 5.8 Hz), 6.74 (d, 1H, J 8.5 Hz), 6.82-6.88 (m, 2H), 6.91 (m, 1H), 7.20 (t, 1H, J 7.9 Hz), 7.56-7.59 (dd, 1H, J 8.5 Hz, J 2.1 Hz), 8.11 (d, 1H, J 2.1 Hz). ^{13}C-NMR (100 MHz, CD_3OD): δ (ppm) 25.2, 26.5, 30.1, 40.4, 40.6, 42.6, 55.4, 64.8, 66.7, 82.3, 114.2, 114.7, 117.0, 120.0, 123.5, 124.7, 129.8, 130.3, 139.8, 139.9, 153.0, 160.3, 161.6, 169.4. HRMS: (ESI): *m/z* $[M+H]^+$, calcd. for $C_{26}H_{35}IN_7O_2^+$: 604.1891, found: 604.1896. Anal. calcd. for $C_{26}H_{34}IN_7O_2$: C 51.75, H 5.68, N 16.25, found: C 51.25, H 5.66, N 16.19. $C_{26}H_{34}IN_7O_2$ (603.51).

General procedure for the propionylation of the aminopotentidine derivatives

The respective aminopotentidine derivative **4.30-4.34**, 4-(dimetylamino)pyridine (DMAP, 0.1-1.1 eq) and triethylamine (2-5 eq) were dissolved in CH_2Cl_2 (2-3 mL). The mixture was stirred for several minutes and propionyl chloride (3 eq) was added. The reaction mixture was stirred over night at room temperature. The organic layer was further diluted with CH_2Cl_2 (3 mL), washed three times with aqueous NaOH solution (5%, w/w, 5 mL) and then dried over Na_2SO_4. The product was purified by preparative HPLC.

N-(2-[2-Cyano-3-(3-[3-(piperidin-1-ylmethyl)phenoxy]propyl)guanidino]ethyl)-4-(propionamido)benzamide (4.35)

4.35 was prepared from **4.30** (100 mg, 0.21 mmol, 1 eq), 4-(dimethylamino)pyridine (28 mg, 0.23 mmol, 1.1 eq), triethylamine (106 mg, 1.05 mmol, 5 eq) and propionyl chloride (58 mg, 0.63 mmol, 3 eq) according to general procedure. Due to incomplete conversion additional propionyl chloride (116 mg, 1.26 mmol, 6 eq) and triethylamine (212 mg, 2.1 mmol, 10 eq) were added. The reaction mixture was stirred for 17 h at room temperature. Purification by preparative HPLC (column: YMC Triart C_{18}, gradient: 0-30 min: MeCN/0.1% aq. NH_3 40:60-70:30, t_R = 11.3 min) afforded the product as white solid (26 mg, 23%). Mp: 171-176 °C. R_f = 0.3 (CH_2Cl_2/7 M NH_3 in MeOH 95:5). IR (KBr): 3295, 2935, 2160, 1665, 1590, 1525, 1440, 1375, 1345, 1310, 1260, 1205, 845, 770, 690, 580 cm^{-1}. RP-HPLC (gradient 2, 220 nm): 97.9% (t_R = 15,71 min, k = 4.4). ^{1}H-NMR (400 MHz, CD_3OD): δ (ppm) 1.18-1.22 (t, 3H, J 7.6 Hz), 1.45-1.46 (m, 2H), 1.56-1.61 (m, 4H), 2.01-2.07 (qui, 2H, J 6.2 Hz), 2.38-2.44 (m, 6H), 3.40-3.44 (m, 4H), 3.48-3.51 (m, 4H), 4.04 (t, 2H, J 5.9 Hz), 6.84-6.90 (m, 2H), 6.93 (br s, 1H), 7.21 (t, 1H, J 7.8 Hz), 7.65 (d, 2H, J 8.7 Hz), 7.77 (d, 2H, J 8.7 Hz). ^{13}C-NMR (100 MHz, CD_3OD): δ (ppm) 10.1, 25.1, 26.4, 30.0, 31.2, 40.4, 40.7, 42.5, 55.3, 64.6, 66.7, 114.8, 117.1, 120.3, 123.5, 129.3, 130.2, 130.3, 139.4, 139.5, 143.5, 160.3, 161.6, 170.3, 175.6. HRMS: (ESI): *m/z* $[M+H]^+$, calcd. for $C_{29}H_{40}N_7O_3^+$: 534.3187, found: 534.3189. $C_{29}H_{39}N_7O_3$ (533.68).

N-(2-[2-Cyano-3-(3-[3-(piperidin-1-ylmethyl)phenoxy]propyl)guanidino]ethyl)-3-(trifluoromethyl)-4-(propionamido)benzamide (4.36)

4.36 was prepared from **4.31** (183 mg, 0.34 mmol, 1 eq), 4-(dimethylamino)pyridine (45 mg, 0.37 mmol, 1.1 eq), triethylamine (172 mg, 1.70 mmol, 5 eq) and propionyl chloride (94 mg, 1.02 mmol, 3 eq) according to general procedure. Due to incomplete conversion additional propionyl chloride (94 mg, 1.02 mmol, 3 eq) were added after stirring over night. The reaction mixture was stirred overnight at room temperature. Purification by preparative HPLC (column: YMC Triart C_{18}, gradient: 0-30 min: MeCN/0.1% aq. NH_3 35:65-55:45, t_R = 24.2 min) afforded the product as white solid (31 mg, 15%). Mp: 137-138 °C. R_f = 0.3 (CH_2Cl_2/7 M NH_3 in MeOH 97:3). RP-HPLC (gradient 2, 220 nm): 96.4% (t_R = 17.86 min, k = 5.2). ^{1}H-NMR (600 MHz, CD_3OD, COSY, HSQC, HMBC, NOESY): δ (ppm) 1.22 (t, 3H, J 7.57 Hz), 1.45 (br s, 2H), 1.56-1.60 (m, 4H), 2.02-2.06 (m, 2H), 2.41-2.48 (m, 6H), 3.41-3.45 (m, 6H), 3.51-3.53 (m, 2H), 4.04-4.06 (m, 2H), 6.84-6.88 (m, 2H), 6.94 (s, 1H), 7.20 (t, 1H, J 7.84 Hz), 7.72-7.73 (m, 1H), 8.03-8.05 (m, 1H), 8.18 (s, 1H). ^{13}C-NMR (150 MHz, CD_3OD, COSY, HSQC, HMBC, NOESY): δ (ppm) 10.0, 25.1, 26.4, 30.0, 30.4, 40.3, 40.7,42.3,55.3, 64.7, 66.6, 114.7, 116.9, 119.8, 123.4, 124.8 (q, 1C, $J_{C\text{-}F}$ 272.45 Hz), 126.0 (q, 1C, $J_{C\text{-}F}$ 30.42 Hz), 126.8 (q, 1C, $J_{C\text{-}F}$ 5.27 Hz), 130.2, 130.4, 132.5, 133.4, 139.4, 139.8, 160.2, 161.5, 168.5, 176.3. HRMS: (ESI): *m/z* $[M+H]^+$, calcd. for $C_{30}H_{39}F_3N_7O_3^+$: 602.3061, found: 602.3065. Anal. calcd. for $C_{30}H_{38}F_3N_7O_3 \cdot H_2O$: C 58.15, H 6.51, N 15.82, found: C 57.82, H 6.21, N 15.30. $C_{30}H_{38}F_3N_7O_3$ (601.68).

_N_-(2-[2-Cyano-3-(3-[3-(piperidin-1-ylmethyl)phenoxy]propyl)guanidino]ethyl)-3-bromo-4-(propionamido)benzamide (4.37)

4.37 was prepared from **4.33** (100 mg, 0.18 mmol, 1 eq), 4-(dimethylamino)pyridine (2.2 mg, 0.02 mmol, 0.1 eq), triethylamine (36 mg, 0.36 mmol, 2 eq) and propionyl chloride (25 mg, 0.27 mmol, 1.5 eq) according to general procedure. Due to incomplete conversion additional propionyl chloride (25 mg, 0.27 mmol, 1.5 eq), 4-(dimethylamino)-pyridine (2.2 mg, 0.018 mmol, 0.1 eq) and triethylamine (36 mg, 0.36 mmol, 2 eq) were added after 3 h of stirring. The reaction mixture was stirred over night at room temperature. Purification by preparative HPLC (column: YMC Triart C_{18}, gradient: 0-30 min: MeCN/0.1% aq. NH_3 40:60-60:40, t_R = 17.6 min) afforded the product as white solid (12 mg, 11%). Mp: 155-159 °C decomposition. R_f = 0.6 (CH_2Cl_2/7 M NH_3 in MeOH 95:5). IR (KBr): 3310, 2935, 2165, 1600, 1540, 1510, 1465, 1275, 1195, 700, 565 cm^{-1}. RP-HPLC (gradient 2, 220 nm): 95.1% (t_R = 17.34 min, k = 5.0). ^{1}H-NMR (400 MHz, CD_3OD): δ (ppm) 1.22 (t, 3H, J 7.6 Hz), 1.44 (m, 2H), 1.55-1.59 (qui, 4H, J 5.6 Hz), 2.01-2.05 (qui, 2H, J 6.2 Hz), 2.40 (br s, 4H), 2.47-2.51 (q, 2H, J 7.6 Hz), 3.40-3.42 (m, 4H), 3.45 (br s, 2H), 3.47-3.49 (m, 2H), 4.03-4.05 (t, 2H, J 5.9 Hz), 6.83-6.85 (dd, 1H, J 8.1 Hz, J 2.0 Hz), 6.87 (d, 1H, J 7.6 Hz), 6.92 (m, 1H), 7.19 (t, 1H, J 7.8 Hz), 7.75-7.77 (dd, 1H, J 8.5 Hz, J 2.0 Hz), 7.90 (d, 1H, J 8.5 Hz), 8.08 (d, 1H, J 2.0 Hz). ^{13}C-NMR (100 MHz, CD_3OD): δ (ppm) 10.0, 25.1, 26.4, 30.0, 30.7, 40.3, 40.7, 42.3, 55.3, 64.7, 66.6, 114.7, 116.9, 117.5, 119.8, 123.4, 126.2, 128.0, 130.2, 133.1, 133.2, 139.7, 140.4, 160.2, 161.5, 168.6, 175.5. HRMS: (ESI): m/z $[M+H]^+$, calcd. for $C_{29}H_{39}BrN_7O_3^+$: 612.2292, found: 612.2295. $C_{29}H_{38}BrN_7O_3$ (612.57).

_N_-[2-(2-Cyano-3-(3-[3-(piperidin-1-ylmethyl)phenoxy]propyl)guanidino)ethyl]-3-iodo-4-(propionamido)benzamide (4.38)

4.38 was prepared from **4.34** (100 mg, 0.17 mmol, 1 eq), 4-(dimethylamino)pyridine (22 mg, 0.18 mmol, 1.1 eq), triethylamine (84 mg, 0.83 mmol, 5 eq) and propionyl chloride (46 mg, 0.5 mmol, 3 eq) according to general procedure. Due to incomplete conversion additional propionyl chloride (46 mg, 0.50 mmol, 3 eq) was added after 5 hours of stirring. The reaction mixture was stirred over night at room temperature. Purification by preparative HPLC (column: YMC Triart C_{18}, gradient: 0-30 min: MeCN/1% aq. NH_3 40:60-80:20, t_R = 13.7 min) afforded the product as white solid (24 mg, 22%). Mp: 148-150 °C. R_f = 0.3 (CH_2Cl_2/7 M NH_3 in MeOH 95:5). IR (KBr): 3310, 2935, 2160, 1645, 1595, 1540, 1510, 1315, 1275, 1200, 1155, 1120, 785, 695, 570 cm^{-1}. RP-HPLC (gradient 2, 220 nm): 97.2% (t_R = 17.50 min, k = 5.0). ^{1}H-NMR (400 MHz, CD_3OD): δ (ppm) 1.25 (t, 3H, J 7.6 Hz), 1.44-1.45 (m, 2H), 1.55-1.60 (m, 4H), 2.01-2.07 (qui, 2H, J 6.2 Hz), 2.40 (br s, 4H), 2.45-2.50 (q, 2H, J 7.6 Hz), 3.39-3.44 (m, 6H), 3.47-3.50 (m, 2H), 4.05 (t, 2H, J 5.9 Hz), 6.83-6.88 (m, 2H), 6.93 (m, 1H), 7.20 (t, 1H, J 7.8 Hz), 7.68 (d, 1H, J 8.4 Hz), 7.78-7.81 (dd, 1H, J 8.4 Hz, J 2.0 Hz), 8.33 (d, 1H, J 2.0 Hz). ^{13}C-NMR (100 MHz, CD_3OD): δ (ppm) 10.2, 25.2, 26.5, 30.0, 30.8, 40.4, 40.7, 42.4, 55.4, 64.7, 66.7, 114.7, 117.0, 119.9, 123.5, 126.7, 128.9, 130.3, 132.3, 134.0, 139.7, 139.9, 143.5, 160.3, 161.6, 168.5, 175.5. HRMS: (ESI): m/z $[M+H]^+$, calcd. for $C_{29}H_{39}IN_7O_3^+$: 660.2154, found: 660.2160. $C_{29}H_{38}IN_7O_3$ (659.57).

N-(2-(2-Cyano-3-(3-(3-(piperidin-1-ylmethyl)phenoxy)propyl)guanidino)ethyl)-4-((1,3-dioxoisoindolin-2-yl)methyl)benzamide (4.39)

4.19 (390 mg, 1.39 mmol, 1 eq) and DIPEA (538 mg, 4.16 mmol, 3 eq) were dissolved in CH_2Cl_2 (120 mL) and TBTU (534 mg, 1.66, 1.2 eq) was added. The mixture was stirred for 10 min at room temperature. **4.5** (497 mg, 1.39 mmol, 1 eq) dissolved in CH_2Cl_2 (2 mL) was added and the reaction mixture was stirred over night at room temperature. The organic layer was washed two times with H_2O (100 mL), aqueous NaOH solution (5%, w/w, 100 mL) and brine (100 mL). The organic layer was dried over Na_2SO_4. The solvent was removed under reduced pressure and the residue was purified by column chromatography (CH_2Cl_2/3.5 M NH_3 in MeOH 97.5:2.5-95:5). Removal of the solvent *in vacuo* afforded the product as light yellow solid (640 mg, 74%). Mp: 70-72 °C. R_f = 0.3 (CH_2Cl_2/7 M NH_3 in MeOH 90:10). ^{1}H-NMR (400 MHz, [D$_6$]DMSO): δ (ppm) 1.35-1.37 (m, 2H), 1.46-1.47 (m, 4H), 1.87-1.94 (m, 2H), 2.28 (br s, 4H), 3.26-3.36 (m, 8H), 3.94-3.97 (m, 2H), 4.82 (s, 2H), 6.77-6.84 (m, 3H), 7.08-7.20 (m, 3H), 7.38 (d, 2H, *J* 8.27 Hz), 7.79 (d, 2H, *J* 8.30 Hz), 7.86-7.92 (m, 2H), 8.57 (t, 1H, *J* 5.36 Hz). ^{13}C-NMR (100 MHz, $CDCl_3$): δ (ppm) 19.6, 24.3, 25.8, 28.9, 39.85, 39.94, 41.3, 54.5, 63.7, 65.7, 113.3, 115.3, 119.0, 122.1, 123.6, 127.8, 128.6, 129.3, 132.1, 133.2, 134.3, 139.8, 140.1, 158.6, 160.3, 168.0, 168.6. HRMS: (ESI): *m/z* [*M*+H]$^+$, calcd. for $C_{35}H_{40}N_7O_4^+$: 622.3136, found: 622.3149. $C_{35}H_{39}N_7O_4$ (621.74).

4-(Aminomethyl)-*N*-(2-(2-cyano-3-(3-(3-(piperidin-1-ylmethyl)phenoxy)propyl)guanidino)-ethyl)benzamide (4.40)

4.39 (360 mg, 0.58 mmol, 1 eq) and hydrazinium hydroxide (145 mg, 2.9 mmol, 5 eq) were dissolved in EtOH (20 mL). The reaction mixture was stirred for 4 h at room temperature and subsequently cooled down in the freezer for 30 min. The precipitated by-product 2,3-dihydrophthalazine-1,4-dione was filtered off and washed with EtOH (5 mL). The organic layers were combined and the solvent was removed under reduced pressure. Purification by column chromatography (CH_2Cl_2/3.5 M NH_3 in MeOH 95:5 isocratic) afforded the product as white solid (193 mg, 68%). 70 mg of **4.40** were further purified by preparative HPLC (column: YMC Triart C_{18}, gradient: 0-30 min: MeCN/0.1% aq. NH_3 30:70-60:40, t_R = 14.4 min). The product was obtained as white solid (49 mg, 47%). Mp: 62-88 °C. R_f = 0.75 (CH_2Cl_2/6 M NH_3 in MeOH 80:20). RP-HPLC (gradient 2, 220 nm): 98.9% (t_R = 11.84 min, *k* = 3.1). ^{1}H-NMR (600 MHz, [D$_6$]DMSO, COSY, HSQC, HMBC): δ (ppm) 1.35 (br s, 2H), 1.44-1.48 (m, 4H), 1.91 (qui, 2H, *J* 6.49 Hz), 2.28 (br s, 4 H), 3.25-3.29 (m, 4H, interfering with the water signal), 3.34-3.37 (m, 4H, interfering with the water signal), 3.76 (s, 2H), 3.95 (t, 2H, *J* 6.20 Hz), 6.77-6.78 (m, 1H), 6.83-6.84 (m, 2H), 7.08-7.12 (m, 2H), 7.18 (t, 1H, *J* 7.98 Hz), 7.39 (d, 2H, *J* 8.16 Hz), 7.77 (d, 2H, *J* 8.18 Hz), 8.52 (t, 1H, *J* 5.45 Hz). ^{13}C-NMR (150 MHz, [D$_6$]DMSO, COSY, HSQC, HMBC): δ (ppm) 24.0, 25.6, 28.6, 38.4, 38.9, 40.8, 45.1, 53.9, 62.8, 65.0, 112.7, 114.6, 118.0, 120.9, 126.8, 127.1, 129.0, 132.3, 140.3, 147.0, 158.5, 159.5, 166.7. HRMS: (ESI): *m/z* [*M*+H]$^+$, calcd. for $C_{27}H_{38}N_7O_2^+$: 492.3081, found: 492.3085. $C_{27}H_{37}N_7O_2$ (491.64).

_N_-(2-(2-Cyano-3-(3-(3-(piperidin-1-ylmethyl)phenoxy)propyl)guanidino)ethyl)-4-(propionamidomethyl)benzamide (4.41)

4.40 (118 mg, 0.24 mmol, 1 eq), triethylamine (49 mg, 0.48 mmol, 2 eq) and succinimidyl propionate (62 mg, 0.36 mmol, 1.5 eq) were dissolved CH_2Cl_2 (5 mL). The reaction mixture was stirred over night at room temperature. Removal of the solvent *in vacuo* and purification by preparative HPLC (column: YMC Triart C_{18}, gradient: 0-30 min: MeCN/0.1% aq. NH_3 35:65-70:30, t_R = 11.8 min) afforded the product as white solid (106 mg, 81%). Mp: 166-170 °C. R_f = 0.5 (CH_2Cl_2/7 M NH_3 in MeOH 90:10). RP-HPLC (gradient 2, 220 nm): 96.6% (t_R = 14.87 min, k = 4.1). ^{1}H-NMR (600 MHz, [D_6]DMSO, COSY, HSQC, HMBC): δ (ppm) 1.02 (t, 3H, *J* 7.59 Hz), 1.36 (br s, 2H), 1.46-1.47 (m, 4H), 1.91 (qui, 2H, *J* 6.47 Hz), 2.14 (q, 2H, *J* 7.60 Hz), 2.29 (br s, 4H), 3.25-3.29 (m, 2H, interfering with the water signal), 3.33-3.36 (m,4H, interfering with the water signal), 3.95 (t, 2H, *J* 6.15 Hz), 4.28 (d, 2H, *J* 5.94 Hz), 6.78-6.79 (m, 1H), 6.83-6.84 (m, 2H), 7.07-7.12 (m, 2H), 7.17-7.20 (m, 1H), 7.29 (d, 2H, *J* 8.07 Hz), 7.77 (d, 2H, *J* 8.22 Hz), 8.30 (t, 1H, *J* 5.88 Hz), 8.53 (t, 1H, *J* 5.46 Hz). ^{13}C-NMR (150 MHz, [D_6]DMSO, COSY, HSQC, HMBC): δ (ppm) 10.0, 24.0, 25.5, 28.5, 28.6, 38.4, 38.9, 40.8, 41.7, 53.9, 62.7, 65.0, 112.7, 114.7, 118.0, 121.0, 126.9, 127.2, 129.1, 132.7, 140.3, 143.1, 158.5, 159.5, 166.6, 173.0. HRMS: (ESI): *m/z* $[M+H]^+$, calcd. for $C_{30}H_{42}N_7O_3^+$: 548.3344, found: 548.3349. Anal. calcd. for $C_{30}H_{41}N_7O_3$: C 65.79, H 7.55, N 17.90, found: C 65.50, H 7.43, N 17.84. $C_{30}H_{41}N_7O_3$ (547.70).

General procedure for the synthesis of the aminopotentidine derivatives 4.42-4.44

4.25, **4.26** or **4.27** (1 eq) and DIPEA (3 eq) were dissolved in CH_2Cl_2 (15-35 mL). O-(Benzotriazol-1-yl)-N,N,N',N'-tetramethyluronium-tetrafluoroborate (TBTU, 1.2 eq) was added and the mixture was stirred for 10-15 min. Subsequently, **4.5** (1 eq) was added and the reaction mixture was stirred over night at room temperature. The organic layer was washed three times with H_2O (30 mL), two times with aqueous NaOH solution (5%, w/w, 15-30 mL) and 1-2 times with brine (15-30 mL). The organic layer was dried over Na_2SO_4 and the solvent was removed in vacuo. The resulting crude product was purified by preparative HPLC.

_N_-(2-(2-Cyano-3-(3-(3-(piperidin-1-ylmethyl)phenoxy)propyl)guanidino)ethyl)-4-(propionamidomethyl)-3-(trifluoromethyl)benzamide (4.42)

4.42 was prepared from **4.25** (80 mg, 0.29 mmol, 1 eq), DIPEA (109 mg, 0.84 mmol, 3 eq), TBTU (105 mg, 0.34 mmol, 1.2 eq) and **4.5** (104 mg, 0.29 mmol, 1 eq) according to general procedure. Removal of the solvent *in vacuo* and purification by preparative HPLC (column: YMC Triart C_{18}, gradient: 0-30 min: MeCN/0.1% aq. NH_3 25:75-65:35, t_R = 24.2 min) afforded the product as white solid (10 mg, 6%). Mp: 94-96 °C. R_f = 0.3 (CH_2Cl_2/MeOH 90:10). RP-HPLC (gradient 2, 220 nm): 95.0% (t_R = 17.77 min, k = 5.1). ^{1}H-NMR (600 MHz, [D_6]DMSO, COSY, HSQC, HMBC): δ (ppm) 1.03 (t, 3H, *J* 7.45 Hz), 1.37 (br s, 2H), 1.48 (br s, 4H), 1.88-1.92 (m, 2H), 2.20 (q, 2H, *J* 7.59 Hz), 2.33 (br s, 3H), 2.88 (br s, 1H), 3.24-3.44 (8H, interfering with the water signal), 3.95 (t, 2H, *J* 6.20 Hz), 4.45 (d, 2H, *J* 5.72 Hz), 6.80-6.85 (m, 3H), 7.09-7.10 (m, 2H), 7.18-7.21 (m, 1H), 7.55 (d, 1H, *J* 8.17 Hz), 8.07 (d, 1H, *J* 8.19 Hz), 8.14 (s, 1H), 8.40 (t, 1H; *J* 5.87 Hz), 8.80 (t, 1H, *J* 5.59 Hz). ^{13}C-NMR (150

MHz, [D_6]DMSO, COSY, HSQC, HMBC): δ (ppm) 9.8, 23.8, 25.4, 28.3, 28.5, 38.4, 38.5, 38.9, 40.6, 53.7, 62.6, 65.0, 112.9, 114.8, 118.0, 121.0, 124.1 (q, 1C, $J_{C\text{-}F}$ 274.40 Hz), 124.6 (q, 1C, $J_{C\text{-}F}$ 5.95 Hz), 125.0, 126.1 (q, 1C, $J_{C\text{-}F}$ 30.83 Hz), 128.7, 129.1, 131.2, 133.2, 141.0, 158.5, 159.4, 165.1, 173.3. HRMS: (ESI): *m/z* [*M*+H]$^+$, calcd. for $C_{31}H_{41}F_3N_7O_3^+$: 616.3217, found: 616.3223. $C_{31}H_{40}F_3N_7O_3$ (615.70).

3-Chloro-*N*-(2-(2-cyano-3-(3-(3-(piperidin-1-ylmethyl)phenoxy)propyl)guanidino)ethyl)-4-(propionamidomethyl)benzamide (4.43)

4.43 was prepared from **4.26** (120 mg, 0.50 mmol, 1 eq), DIPEA (193 mg, 1.49 mmol, 3 eq), TBTU (191 mg, 0.60 mmol, 1.2 eq) and **4.5** (178 mg, 0.50 mmol, 1 eq) according to general procedure. Removal of the solvent *in vacuo* and purification by preparative HPLC (column: YMC Triart C_{18}, gradient: 0-30 min: MeCN/0.1% aq. NH_3 25:75-70:30, t_R = 20.9 min) afforded the product as white solid (138 mg, 48%). R_f = 0.7 (CH_2Cl_2/2 M NH_3 in MeOH 90:10). RP-HPLC (gradient 2, 220 nm): 99.3% (t_R = 16.61 min, *k* = 4.7). ^{1}H-NMR (600 MHz, [D_6]DMSO, COSY, HSQC, HMBC): δ (ppm) 1.02 (t, 3H, *J* 7.61 Hz), 1.36 (br s, 2H), 1.48 (br s, 4H), 1.91 (qui, 2H, *J* 6.55 Hz), 2.23 (q, 2H, *J* 7.56 Hz), 2.32 (br s, 4H), 3.24-3.39 (m, 8H, interfering with the water signal), 3.95 (t, 2H, *J* 6.12 Hz), 4.33 (d, 2H, *J* 5.82 Hz), 6.78-6.80 (m, 1H), 6.84-6.85 (m, 2H), 7.07-7.11 (m, 2H), 7.20 (t, 1H, *J* 7.75 Hz), 7.37 (d, 1H, *J* 7.99 Hz), 7.75-7.76 (m, 1H), 7.87 (m, 1H), 8.33 (t, 1H; *J* 5.94 Hz), 8.65 (t, 1H, *J* 5.53 Hz). ^{13}C-NMR (150 MHz, [D_6]DMSO, COSY, HSQC, HMBC): δ (ppm) 9.9, 23.8, 25.4, 28.4, 28.6, 30.7, 38.4, 39.9 (1C under solvent peak (38.7-40.3)), 40.6, 53.7, 62.6, 65.0, 112.8, 114.8, 118.0, 121.1, 126.0, 127.7, 128.5, 129.1, 131.9, 134.6, 139.7, 140.2, 158.5, 159.4, 165.1, 173.2. HRMS: (ESI): *m/z* [*M*+H]$^+$, calcd. for $C_{30}H_{41}ClN_7O_3^+$: 582.2954, found: 582.2960. $C_{30}H_{40}ClN_7O_3$ (582.15).

3-Bromo-*N*-(2-(2-cyano-3-(3-(3-(piperidin-1-ylmethyl)phenoxy)propyl)guanidino)ethyl)-4-(propionamidomethyl)benzamide (4.44)

4.44 was prepared from **4.27** (62 mg, 0.22 mmol, 1 eq), DIPEA (84 mg, 0.65 mmol, 3 eq), TBTU (84 mg, 0.26 mmol, 1.2 eq) and **4.5** (78 mg, 0.22 mmol, 1 eq) according to general procedure. Removal of the solvent *in vacuo* and purification by preparative HPLC (column: YMC Triart C_{18}, gradient: 0-30 min: MeCN/0.1% aq. NH_3 35:65-70:30, t_R = 16.2 min) afforded the product as white solid (60 mg, 44%). Mp: 165 °C decomposition. R_f = 0.7 (CH_2Cl_2/3.5 M NH_3 in MeOH 90:10). RP-HPLC (gradient 2, 220 nm): 99.5% (t_R = 16.51min, *k* = 4.7). ^{1}H-NMR (600 MHz, [D_6]DMSO, COSY, HSQC, HMBC): δ (ppm) 1.03 (t, 3H, *J* 7.63 Hz), 1.35 (br s, 2H), 1.44-1.48 (m, 4H), 1.90 (qui, 2H, *J* 6.48 Hz), 2.20 (q, 2H, *J* 7.63 Hz), 2.27 (br s, 4H), 3.24-3.29 (m, 4H), 3.33-3.36 (m, 4H, interfering with the water signal), 3.95 (t, 2H, *J* 6.11 Hz), 4.30 (d, 2H, *J* 5.82 Hz), 6.76-6.78 (m, 1H), 6.82-6.83 (m, 2H), 7.07-7.11 (m, 2H), 7.17-7.20 (m, 1H), 7.34 (d, 1H, *J* 8.11 Hz), 7.79-7.81 (m, 1H), 8.04-8.05 (m, 1H), 8.34 (t, 1H; *J* 5.89 Hz), 8.65 (t, 1H, *J* 5.56 Hz). ^{13}C-NMR (150 MHz, [D_6]DMSO, COSY, HSQC, HMBC): δ (ppm) 9.9, 24.0, 25.5, 28.4, 28.6, 38.4, 38.9, 40.6, 42.4, 53.9, 62.8, 65.0, 112.7, 114.6, 118.0, 120.9, 122.0, 126.5, 128.3, 129.0, 130.9, 134.7, 140.3, 141.2, 158.4, 159.4, 165.0, 173.2. HRMS: (ESI): *m/z* [*M*+H]$^+$, calcd. for $C_{30}H_{41}BrN_7O_3^+$: 626.2449, found: 626.2454. $C_{30}H_{40}BrN_7O_3$ (626.60).

4-(Azidomethyl)-3-bromo-N-(2-(2-cyano-3-(3-(3-(piperidin-1-ylmethyl)phenoxy)propyl)guanidino)ethyl)benzamide (4.45)

4.20 (400 mg, 1.56 mmol, 1.4 eq) and DIPEA (433 mg, 3.35 mmol, 3 eq) were dissolved in CH_2Cl_2 (100 mL). *O*-(Benzotriazol-1-yl)-N,N,N',N'-tetramethyluronium-hexafluorophosphate (HBTU, 508 mg, 1.56 mmol, 1.4 eq) was added and the mixture was stirred for 30 min. Subsequently, **4.5** (400 mg, 1.12 mmol, 1 eq) was added and the reaction mixture was stirred over night at room temperature. The organic layer was washed two times with saturated aqueous $NaHCO_3$ solution (100 mL) and with brine (100 mL). Purification by column chromatography (CH_2Cl_2/MeOH 95:5-90:10) and removal of the solvent *in vacuo* afforded the product as yellow oil (290 mg, 44%). R_f = 0.2 (CH_2Cl_2/2 M NH_3 in MeOH 90:10). ^{1}H-NMR (400 MHz, CD_3OD): δ (ppm) 1.57-1.59 (m, 2H),1.72-1.78 (m, 4H), 2.01-2.07 (m, 2H), 2.94 (br s, 4H), 3.40-3.45 (m, 4H), 3.49-3.52 (m, 2H), 3.99 (s, 2H), 4.07 (t, 2H, *J* 5.78 Hz), 4.54 (s, 2H), 6.96-7.00 (m, 2H), 7.09-7.10 (m, 1H), 7.30 (t, 1H, *J* 7.94 Hz), 7.51 (d, 1H, *J* 7.94 Hz), 7.80-7.82 (m, 1H), 8.07-8.08 (m, 1H). ^{13}C-NMR (100 MHz, CD_3OD): δ (ppm) 22.1, 23.4, 28.4, 39.2, 39.3, 40.9, 53.0, 53.7, 61.2, 65.7, 114.9, 116.7, 122.8, 123.3, 126.4, 128.3, 129.7, 130.0, 131.6, 132.8, 135.6, 138.7, 159.1, 160.1, 167.2. HRMS: (ESI): *m/z* $[M+H]^+$, calcd. for $C_{27}H_{35}BrN_9O_2^+$: 596.2092, found: 596.2114. $C_{27}H_{34}BrN_9O_2$ (596.53).

4-(Aminomethyl)-3-bromo-N-(2-(2-cyano-3-(3-(3-(piperidin-1-ylmethyl)phenoxy)propyl)guanidino)ethyl)benzamide (4.46)

4.45 (390 mg, 0.65 mmol, 1 eq) was dissolved in a mixture of THF and H_2O (1/2, v/v, 7.5 mL). Triphenylphosphine (427 mg, 1.63 mmol, 2.5 eq) dissolved in mixture of THF and H_2O (5/2, v/v, 7 mL) was added dropwise and the reaction mixture was stirred over night at room temperature. The solvent was partially removed under reduced pressure and the residue was purified by column chromatography (CH_2Cl_2/MeOH 90:10 - CH_2Cl_2/0.1% NH_3 in MeOH 90:10). The product was obtained as yellow oil (200 mg, 54%). Further purification by preparative HPLC (column: YMC Triart C_{18}, gradient: 0-30 min: MeCN/1% aq. NH_3 10:90-91:9, t_R = 19.9 min) afforded the product as white fluffy solid (70 mg, 19%). Mp: 73-77 °C. R_f = 0.4 (CH_2Cl_2/0.2% NH_3 in MeOH 95:5). RP-HPLC (gradient 3, 220 nm): 98.4% (t_R = 28.19 min, *k* = 16.3). ^{1}H-NMR (600 MHz, CD_3OD, COSY, HSQC, HMBC): δ (ppm) 1.46 (br s, 2H), 1.57-1.61 (m, 4H), 2.02-2.06 (m, 2H), 2.44 (br s, 4H), 3.41-3.43 (m, 4H), 3.48-3.50 (m, 4H), 3.90 (s, 2H), 4.05 (t, 2H, *J* 5.82 Hz), 6.85-6.89 (m, 2H), 6.94 (s, 1H), 7.21 (t, 1H, *J* 7.92 Hz), 7.53 (d, 1H, *J* 7.99 Hz), 7.78-7.80 (m, 1H), 8.04 (m, 1H). ^{13}C-NMR (150 MHz, CD_3OD, COSY, HSQC, HMBC): δ (ppm) 25.0, 26.3, 30.0, 40.4, 40.7, 42.3, 46.7, 55.3, 64.6, 66.6, 114.7, 117.0, 119.8, 123.5, 124.3, 127.7, 130.1, 130.3, 132.7, 135.8, 139.5, 146.1, 160.3, 161.5, 168.9. HRMS: (ESI): *m/z* $[M+H]^+$, calcd. for $C_{27}H_{37}BrN_7O_2^+$: 570.2187, found: 570.2183. $C_{27}H_{36}BrN_7O_2$ (570.54).

4-(Acetamidomethyl)-3-bromo-N-(2-(2-cyano-3-(3-(3-(piperidin-1-ylmethyl)phenoxy)propyl)guanidino)ethyl)benzamide (4.47)

4.46 (70 mg, 0.12 mmol, 1 eq) and DIPEA (32 mg, 0.25 mmol, 2 eq) were dissolved in CH_2Cl_2 (5 mL). Acetyl chloride (14 mg, 0.18 mmol, 1.5 eq) dissolved in CH_2Cl_2 (5 mL) was added drop wise

over a period of 2 h and the reaction mixture was stirred over night at room temperature. The organic layer was further diluted with CH_2Cl_2 (10 mL) and washed two times with aqueous NaOH solution (5%, w/w, 20 mL) and with brine (20 mL). Removal of the solvent *in vacuo* and purification by preparative HPLC (column: YMC Triart C_{18}, gradient: 0-30 min: MeCN/0.1% aq. NH_3 20:80-91:9, t_R = 16.05 min) afforded the product as white fluffy solid (30 mg, 40%). The purity determined by analytical HPLC was under 95% and therefore the product was again purified by preparative HPLC (column: YMC Triart C_{18}, gradient: 0-30 min: MeCN/0.1% aq. NH_3 10:90-70:30, t_R = 23.7 min). The product was obtained as white fluffy solid (15 mg, 20%). Mp: 89-95 °C. R_f = 0.3 (CH_2Cl_2/0.2% NH_3 in MeOH 90:10). RP-HPLC (gradient 3, 220 nm): 99.0% (t_R = 28.01 min, k = 16.2). ^{1}H-NMR (600 MHz, CD_3OD, COSY, HSQC, HMBC): δ (ppm) 1.45 (br s, 2H), 1.56-1.60 (m, 4H), 2.01-2.05 (m, 5H), 2.43 (br s, 4H), 3.40-3.42 (m, 4H), 3.47-3.49 (m, 4H), 4.04 (t, 2H, *J* 5.81 Hz), 4.44 (s, 2H), 6.84-6.88 (m, 2H), 6.93 (m, 1H), 7.20 (t, 1H, *J* 7.90 Hz), 7.39 (d, 1H, *J* 8.04 Hz), 7.74-7.76 (m, 1H), 8.03 (m, 1H). ^{13}C-NMR (150 MHz, CD_3OD, COSY, HSQC, HMBC): δ (ppm) 22.5, 25.0, 26.3, 30.0, 40.3, 40.7, 42.3, 44.5, 55.3, 64.6, 66.6, 114.8, 117.0, 119.8, 123.5, 124.1, 127.5, 130.1, 130.3, 132.8, 136.1, 142.4 (2C), 160.3, 161.5, 168.8, 173.4. HRMS: (ESI): *m/z* $[M+H]^+$, calcd. for $C_{29}H_{39}BrN_7O_3^+$: 612.2292, found: 612.2298. $C_{29}H_{38}BrN_7O_3$ (612.57).

4-(Acetamidomethyl)-N-(2-(2-cyano-3-(3-(3-(piperidin-1-ylmethyl)phenoxy)propyl)guanidino)ethyl)benzamide (4.48)

4.40 (70 mg, 0.14 mmol, 1 eq), 4-(dimethylamino)-pyridine (17 mg, 0.14 mmol,1 eq) and DIPEA (28 mg, 0.21 mmol, 1.5 eq) were dissolved in CH_2Cl_2 (5 mL). Acetyl chloride (12 mg, 0.16 mmol, 1.1 eq) dissolved in CH_2Cl_2 (2 mL) was added drop wise and the reaction mixture was stirred over night at room temperature. Additional acetyl chloride (12 mg, 0.16 mmol, 1.1 eq) and DIPEA (28 mg, 0.21 mmol, 1.5 eq) were added and mixture was again stirred over night at room temperature. The organic layer was further diluted with CH_2Cl_2 (40 mL) and washed with H_2O (50 mL), aqueous NaOH solution (1 M, 50 mL) and brine (50 mL). The solvent was removed under reduced pressure and the residue was purified by column chromatography (CH_2Cl_2/MeOH 100:0-90:10). The product was obtained as colourless oil (40 mg, 53%). Further purification by preparative HPLC (column: YMC Triart C_{18}, gradient: 0-30 min: MeCN/0.1% aq. NH_3 20:80-91:9, t_R = 14.02 min) afforded the product as white fluffy solid (19 mg, 25%). Mp: 75-85 °C. R_f = 0.2 (CH_2Cl_2/1.5 N NH_3 in MeOH 90:10). RP-HPLC (gradient 3, 220 nm): 99.8% (t_R = 25.91 min, k = 14.9). ^{1}H-NMR (600 MHz, CD_3OD, COSY, HSQC, HMBC): δ (ppm) 1.45 (br s, 2H), 1.56-1.60 (m, 4H), 2.00 (s, 3H), 2.02-2.06 (qui, 2H, *J* 6.22 Hz), 2.41 (br s, 4H), 3.41-3.43 (m, 4H), 3.46 (s, 2H), 3.49-3.51 (m, 2H), 4.05 (t, 2H, *J* 5.87 Hz), 4.40 (s, 2H), 6.84-6.89 (m, 2H), 6.94 (m, 1H), 7.21 (t, 1H, *J* 7.87 Hz), 7.35 (d, 2H, *J* 8.40 Hz), 7.77 (m, 2H). ^{13}C-NMR (150 MHz, CD_3OD, COSY, HSQC, HMBC): δ (ppm) 22.5, 25.1, 26.4, 30.0, 40.3, 40.7, 42.4, 43.8, 55.3, 64.7, 66.6, 114.7, 116.9, 119.9, 123.4, 128.58, 128.60, 130.2, 134.2, 139.8, 144.1, 160.3, 161.6, 170.5, 173.2. HRMS: (ESI): *m/z* $[M+H]^+$, calcd. for $C_{29}H_{40}N_7O_3^+$: 534.3187, found: 534.3191. $C_{29}H_{39}N_7O_3$ (533.68).

_N_-(2-(2-Cyano-3-(3-(3-(piperidin-1-ylmethyl)phenoxy)propyl)guanidino)ethyl)-4-((dimethylamino)methyl)benzamide (4.49)

4.28 (33 mg, 0.15 mmol, 1.1 eq) and DIPEA (90 mg, 0.70 mmol, 5 eq) were dissolved in CH_2Cl_2 (10 mL). *O*-(Benzotriazol-1-yl)-N,N,N',N'-tetramethyluronium-hexafluorophosphate (HBTU, 74 mg, 0.20 mmol, 1.4 eq) was added and the mixture was stirred for 30 min. Subsequently, **4.5** (50 mg, 0.14 mmol, 1 eq) was added and the reaction mixture was stirred over night at room temperature. The organic layer was diluted with CH_2Cl_2 (40 mL) and washed with H_2O (50 mL), aqueous NaOH solution (1 M, 50 mL) and brine (50 mL). Purification by automated flash chromatography (CH_2Cl_2/MeOH 100:0-80:20 in 20 min) and removal of the solvent *in vacuo* afforded the product as colourless oil (40 mg, 56%). Further purification by preparative HPLC (column: YMC Triart C_{18}, gradient: 0-30 min: MeCN/0.1% aq. NH_3 10:90-91:9, t_R = 21.50 min) afforded the product as white fluffy solid (20 mg, 28%). Mp: 62-68 °C. R_f = 0.2 (CH_2Cl_2/2 M NH_3 in MeOH 95:5). RP-HPLC (gradient 3, 220 nm): 99.0% (t_R = 30.29 min, k = 17.6). ^{1}H-NMR (600 MHz, CD_3OD, COSY, HSQC, HMBC): δ (ppm) 1.45 (br s, 2H), 1.57-1.61 (m, 4H), 2.02-2.06 (qui, 2H, J 6.20 Hz), 2.24 (s, 6H), 2.43 (br s, 4H), 3.41-3.43 (m, 4H), 3.48-3.51 (m, 6H), 4.05 (t, 2H, J 5.87 Hz), 6.85-6.89 (m, 2H), 6.94-6.95 (m, 1H), 7.21 (t, 1H, J 7.85 Hz), 7.40 (d, 2H, J 8.22 Hz), 7.78-7.79 (m, 2H). ^{13}C-NMR (150 MHz, CD_3OD, COSY, HSQC, HMBC): δ (ppm) 25.1, 26.4, 30.0, 40.3, 40.6, 42.4, 45.3, 55.3, 64.5, 64.6, 66.6, 114.7, 117.0, 119.9, 123.4, 128.4, 130.3, 130.7, 134.5, 139.6, 142.9, 160.3, 161.6, 170.5. HRMS: (ESI): *m/z* $[M+H]^+$, calcd. for $C_{29}H_{42}N_7O_2^+$: 520.3395, found: 520.3394. $C_{29}H_{41}N_7O_2$ (519.69).

3-Bromo-_N_-(2-(2-cyano-3-(3-(3-(piperidin-1-ylmethyl)phenoxy)propyl)guanidino)ethyl)-4-((dimethylamino)methyl)benzamide (4.50)

4.29 (60 mg, 0.20 mmol, 1.1 eq) and DIPEA (120 mg, 0.93 mmol, 5 eq) were dissolved in CH_2Cl_2 (10 mL). *O*-(Benzotriazol-1-yl)-N,N,N',N'-tetramethyluronium-hexafluorophosphate (98 mg, 0.26 mmol, 1.4 eq) was added and the mixture was stirred for 30 min. Subsequently, **4.5** (66 mg, 0.19 mmol, 1 eq) was added and the reaction mixture was stirred over night at room temperature. The organic layer was diluted with CH_2Cl_2 (40 mL) and washed with H_2O (50 mL), aqueous NaOH solution (1 M, 50 mL) and brine (50 mL). Purification by column chromatography (CH_2Cl_2 100% - CH_2Cl_2/1 M NH_3 in MeOH 90:10) and removal of the solvent *in vacuo* afforded the product as colourless oil (50 mg, 45%). Further purification by preparative HPLC (column: YMC Triart C_{18}, gradient: 0-30 min: MeCN/0.1% aq. NH_3 10:90-91:9, t_R = 22.38 min) afforded the product as white fluffy solid (36 mg, 32%). Mp: 105-115 °C. R_f = 0.3 (CH_2Cl_2/1.5 M NH_3 in MeOH 90:10). RP-HPLC (gradient 3, 220 nm): 99.6% (t_R = 33.11 min, k = 19.3). ^{1}H-NMR (600 MHz, CD_3OD, COSY, HSQC, HMBC): δ (ppm) 2.06 (br s, 2H), 1.56-1.60 (m, 4H), 2.02-2.06 (qui, 2H, J 6.21 Hz), 2.29 (s, 6H), 2.41 (br s, 4H), 3.41-3.45 (m, 6H), 3.49-3.51 (m, 2H), 3.61 (s, 2H), 4.05 (t, 2H, J 5.87 Hz), 6.84-6.89 (m, 2H), 6.93 (m, 1H), 7.20 (t, 1H, J 7.85 Hz), 7.53 (d, 1H, J 8.04 Hz), 7.76-7.78 (m, 1H), 8.05 (d, 1H, J 1.80 Hz). ^{13}C-NMR (150 MHz, CD_3OD, COSY, HSQC, HMBC): δ (ppm) 25.1, 26.4, 30.0, 40.3, 40.7, 42.3, 45.6, 55.3, 63.6, 64.7, 66.6, 114.7, 116.9, 119.8, 123.4, 125.9, 127.3, 130.2, 132.4, 132.9, 136.1, 139.8, 142.4, 160.2, 161.5, 168.9. HRMS: (ESI): *m/z* $[M+H]^+$, calcd. for $C_{29}H_{41}BrN_7O_2^+$: 598.2500, found: 598.2502. $C_{29}H_{40}BrN_7O_2$ (598.59).

4.3.3 Pharmacological Methods

Radioligand competition binding assay on Sf9 insect cell membranes

Preparation of the membranes of Sf9 insect cells expressing the hH_2R-$G_{s\alpha S}$ fusion protein or co-expressing the hH_3R + $G_{i\alpha 2}$ + $\beta_1\gamma_2$ proteins was described elsewhere.[19]

Radioligand competition binding assays were performed as described previously with minor adjustments using the following radioligands: [^{3}H]UR-DE257[6] (hH_2R: specific activity = 32.89 Ci/mmol, K_d = 12.2 nM, c_{final} = 20 nM) or [^{3}H]N^{α}-methylhistamine (Hartmann Analytic, Braunschweig, Germany; hH_3R: specific activity = 80 Ci/mmol, K_d = 3 nM, c_{final} = 3 nM).

On the day of the experiment Sf9 membranes were thawed and sedimented by centrifugation at 13,000 rpm at 4 °C for 10 min. The membranes were resuspended in ice cold binding buffer (75 mM Tris/HCl, pH 7.4 containing 12.5 mM $MgCl_2$, 1mM EDTA and; in the following referred to as BB) and adjusted to a protein concentration of 2-4 µg/µL. 80 µL BB containing 0.2% BSA and the respective radioligand, followed by 10 µL of the investigated ligands at various concentrations (dissolved in H_2O or 10 mM HCl, prepared less than 10 min prior), were added to every well of a 96-well plate (Primaria clear flat bottom microplates, Corning, New York, USA). Incubation was started by addition of the membrane suspension (10 µL). The plates were shaken for 60 min at room temperature in the dark. Subsequently, bound radioligand was separated from free radioligand by filtration through glass microfiber filters (Whatman GF/C, Maidstone, UK), treated with 0.3% polyethylenimine (PEI), using a 96-well Brandel harvester (Brandel Inc., Unterföhring, Germany). The punched out filter pieces were transferred into clear, flexible 96-well PET microplate (round bottom, 1450-401, Perkin Elmer, Rodgau, Germany). Each well was supplemented with 200 µL scintillation cocktail (Rotiscint Eco plus, Roth, Karlsruhe, Germany) and incubated in the dark for at least 4 h. The radioactivity was measured with a MicroBeta2 1450 scintillation counter (Perkin Elmer, Rodgau, Germany).

Functional GTPγS assay on Sf9 insect cell membranes

GTPγS assays were performed as described previously[20] with minor modifications. [^{35}S]GTPγS (specific activity = 1000 Ci/mmol) was purchased from Hartmann Analytic (Braunschweig, Germany). Sf9 membranes were prepared in the same manner as for radioligand competition binding and the protein concentration was adjusted to 0.5-1.5 µg/µL.

Agonist mode: 80 µL of BB containing BSA (0.05% final), GDP (1 µM final) and [^{35}S]GTPγS (20 nCi final), followed by 10 µL of the investigated ligands at various concentrations (dissolved in H_2O) were added to every well of a 96-well plate (Primaria clear flat bottom microplates, Corning, New York, USA). Incubation was started by addition of the membrane suspension (10 µL). The plates were shaken for 60 min at room temperature in the dark. Subsequently, bound radioligand was separated from free radioligand by filtration through glass microfiber filters (Whatman GF/C, Maidstone, UK) using a 96-well Brandel harvester (Brandel Inc., Unterföhring, Germany).

Antagonist mode of the GTPγS assay was performed in the same way as the agonist mode, but in the presence of the agonist histamine (1 µM final).

4.3.4 Data analysis

Retention factors *k* were calculated according to $k = (t_R - t_0)/ t_0$ (t_0 = dead time; t_R = retention time). Corrected counts per minute (ccpm) from the GTPγS assay (agonist mode) were plotted against the log(concentration of the test compound), and data were analyzed by a four parameter logistic equation (GraphPad Prism Software 5.0, GraphPad Software, San Diego, CA), followed by normalization (0% = water value (basal activity), 100% = "top" histamine equation) and analysis by four-parameter logistic equation (log(agonist) vs. response – variable slope, GraphPad Prism). Data of the GTPγS assay (antagonist mode) were analysed by a four parameter logistic equation (GraphPad Prism), followed by normalization (100% = "top" of the four-parameter logistic fit, 0% = unspecifically bound radioligand (ccpm) determined in the presence of famotidine at 100 µM) and analysis by four-parameter logistic equation (log(inhibitor) vs response – variable slope, GraphPad Prism). pIC_{50} values were converted into pK_B values according to the Cheng-Prusoff equation[21]. Total binding data from radioligand competition binding experiments were plotted against log(concentration competitor) and analyzed by a four-parameter logistic equation (log(inhibitor) vs response – variable slope, GraphPad Prism), followed by normalization (100% = "top" of the four-parameter logistic fit, 0% = unspecifically bound radioligand ligand determined in the presence of famotidine at 100 µM). Normalized data from competition binding experiments were again analyzed by a four-parameter logistic equation and obtained pIC_{50} values were converted into pK_i values according to the Cheng-Prusoff equation[21].

4.4 References

1. Hirschfeld, J.; Buschauer, A.; Elz, S.; Schunack, W.; Ruat, M.; Traiffort, E.; Schwartz, J. C. Iodoaminopotentidine and Related-Compounds - a New Class of Ligands with High-Affinity and Selectivity for the Histamine-H2-Receptor. *J. Med. Chem.* **1992**, 35, 2231-2238.
2. Buschauer, A.; Postius, S.; Szelenyi, I.; Schunack, W. Isohistamine and homologs as components of H2-antagonists. 22. H2-antihistaminics. *Arzneimittelforschung* **1985**, 35, 1025-1029.
3. Ruat, M.; Traiffort, E.; Bouthenet, M. L.; Schwartz, J. C.; Hirschfeld, J.; Buschauer, A.; Schunack, W. Reversible and Irreversible Labeling and Autoradiographic Localization of the Cerebral Histamine H-2-Receptor Using [I-125] Iodinated Probes. *P. Natl. Acad. Sci. USA* **1990**, 87, 1658-1662.
4. Traiffort, E.; Pollard, H.; Moreau, J.; Ruat, M.; Schwartz, J. C.; Martinez-Mir, M. I.; Palacios, J. M. Pharmacological characterization and autoradiographic localization of histamine H2 receptors in human brain identified with [125I]iodoaminopotentidine. *J. Neurochem.* **1992**, 59, 290-299.
5. Kelley, M. T.; Bürckstümmer, T.; Wenzel-Seifert, K.; Dove, S.; Buschauer, A.; Seifert, R. Distinct interaction of human and guinea pig histamine H2-receptor with guanidine-type agonists. *Mol. Pharmacol.* **2001**, 60, 1210-1225.
6. Baumeister, P.; Erdmann, D.; Biselli, S.; Kagermeier, N.; Elz, S.; Bernhardt, G.; Buschauer, A. [3H]UR-DE257: Development of a Tritium-Labeled Squaramide-Type Selective Histamine H2 Receptor Antagonist. *ChemMedChem* **2015**, 10, 83-93.
7. Crevat-Pisano, P.; Hariton, C.; Rolland, P. H.; Cano, J. P. Fundamental aspects of radioreceptor assays. *Journal of Pharmaceutical and Biomedical Analysis* **1986**, 4, 697-716.
8. Schickaneder, H.; Herter, R.; Postius, S.; Moersdorf, P.; Szelenyi, I.; Ahrens, K. H. Sulfenamide derivatives and a pharmaceutical containing these compounds. 1985. Chem. Abstr. 103:123485.
9. Chorell, E.; Chorell, E. Efficient Synthesis of 2-Substituted Phthalimides from Phthalic Acids in One Step. *Eur. J. Org. Chem.* **2013**, 2013, 7512-7516.
10. Delorme, D.; Zhou, Z. Preparation of aminophenylbenzamides as inhibitors of histone deacetylase. 2004. Chem. Abstr. 141:140470.
11. Wischnewski, G.; Hesse, K.; Lorch, B.; Grupe, R.; Ziska, T.; Weiher, B.; Goeres, E.; Kossowicz, J. Preparation of phenyl 4-(aminomethyl)benzoates as drugs. 1991. Chem. Abstr. 116:58983.
12. Preuss, H.; Ghorai, P.; Kraus, A.; Dove, S.; Buschauer, A.; Seifert, R. Constitutive activity and ligand selectivity of human, guinea pig, rat, and canine histamine H2 receptors. *J. Pharmacol. Exp. Ther.* **2007**, 321, 983-995.
13. Appl, H.; Holzammer, T.; Dove, S.; Haen, E.; Strasser, A.; Seifert, R. Interactions of recombinant human histamine H(1)R, H(2)R, H(3)R, and H(4)R receptors with 34 antidepressants and antipsychotics. *Naunyn Schmiedeberg´s Arch. Pharmacol.* **2012**, 385, 145-170.
14. Allen, D. G.; Coe, D. M.; Cooper, A. W. J.; Gore, P. M.; House, D.; Senger, S.; Sollis, S. L.; Vile, S.; Wilson, C. Preparation of N-pyrazolyl carboxamides as CRAC channel inhibitors. 2010. Chem. Abstr. 153:555155.
15. Terentjeva, S.; Muceniece, D.; Petushkova, J.; Lusis, V. Synthesis of novel 3-substituted benzamides related to imatinib. *J. Chem. Res.* **2016**, 224-227.
16. Sekine, M.; Aoyagi, M.; Ushioda, M.; Ohkubo, A.; Seio, K. Chemically stabilized phenylboranylidene groups having a dimethoxytrityl group as a colorimetrically detectable protecting group designed for cis-1,2-diol functions of ribonucleosides in the solid-phase synthesis of m(2)(2,2)G5 ' ppT. *J. Org. Chem.* **2005**, 70, 8400-8408.

17. Zhang, R.; Lei, L.; Xu, Y. G.; Hua, W. Y.; Gong, G. Q. Benzimidazol-2-yl or benzimidazol-2-ylthiomethyl benzoylgunnidines as novel Na+/H+ exchanger inhibitors, synthesis and protection against ischemic-reperfusion injury. *Bioorg. Med. Chem. Lett.* **2007**, 17, 2430-2433.
18. Swinnen, D.; Bombrun, A.; Gonzalez, J.; Gerber, P.; Pittet, P. Methylene amides, particularly [(arylmethyl)amino](oxo)acetic acids, useful as modulators, and especially inhibitors, of protein tyrosine phosphatases (PTPs), and their preparation, uses, e.g., as antidiabetics, and pharmaceutical compositions. 2003. Chem. Abstr. 139:179889.
19. Pop, N.; Igel, P.; Brennauer, A.; Cabrele, C.; Bernhardt, G. N.; Seifert, R.; Buschauer, A. Functional reconstitution of human neuropeptide Y (NPY) Y(2) and Y(4) receptors in Sf9 insect cells. *J. Recept. Signal. Transduct. Res.* **2011**, 31, 271-285.
20. Kagermeier, N.; Werner, K.; Keller, M.; Baumeister, P.; Bernhardt, G.; Seifert, R.; Buschauer, A. Dimeric carbamoylguanidine-type histamine H receptor ligands: A new class of potent and selective agonists. *Bioorg. Med. Chem.* **2015**.
21. Cheng, Y.; Prusoff, W. H. Relationship between the inhibition constant (K1) and the concentration of inhibitor which causes 50 per cent inhibition (I50) of an enzymatic reaction. *Biochem. Pharmacol.* **1973**, 22, 3099-3108.

Chapter 5

Fluorescence Labeled H_2R Ligands with BMY25368 Core Structure: Synthesis, Characterization and Application in Flow Cytometry, Confocal Microscopy and High Content Imaging

Note: Prior to the submission of this thesis, parts of this chapter (the synthesis of **5.2**, **5.7** and **5.10**) were published in cooperation with partners:

Baumeister, P.; Erdmann, D.; Biselli, S.; Kagermeier, N.; Elz, S.; Bernhardt, G.; Buschauer, A. [^{3}H]UR-DE257: Development of a Tritium-Labeled Squaramide-Type Selective Histamine H_2 Receptor Antagonist. *ChemMedChem* **2015**, 10, 83-93.

The synthesis of **5.3**, **5.12**, **5.13** and Py-5 were performed by Mengya Chen during her Master Thesis 2015.

5.1 INTRODUCTION

Fluorescence labeled GPCR ligands have become an attractive alternative to radiotracers for the investigation of ligand-receptor interactions. Besides advantages with respect to safety issues and waste disposal, fluorescent ligands are a prerequisite for the application of a plethora of optical techniques (confocal microscopy, FRET,[1] FRAP,[2] TIRF,[3] high content imaging,[4] fluorescence polarization[5]). In general, a fluorescent ligand consists of a pharmacophore, a linker and the fluorophore. A major challenge in the development of fluorescent ligands for aminergic GPCRs is to retain affinity, when a bulky fluorophore is attached to a relatively small ligand. It is important to consider that the attachment site, the type and length of the linker as well as the nature of the fluorophore (size, net charge and lipophilicity) might affect receptor affinity as well as selectivity and can lead to unfavorable physicochemical properties (high unspecific binding, aggregation, internalization, etc.).[6] Nonetheless, various fluorescent ligands for aminergic GPCRs have been reported, for example for muscarinic,[7-9] α and β adrenergic,[10-12] dopamine,[13] histamine H_1[14,15] and H_3[16-18] receptors. In the H_2R field, most of the reported fluorescent ligands are emitting at wavelengths below 550 nm (common fluorophores: fluorescein, acridine, 5-(dimethylamino)naphthalin-1-sulfonic acid amide (dansyl), N-methylanthranilic acid amide and 1-cyanoisoindol-2-yl).[19,20] The majority of the fluorescent ligands consist of a piperidinomethylphenoxypropylamino (potentidine) pharmacophore, derived either from roxatidine or iodoaminopotentidine, which is linked to the fluorophore by an alkyl chain (Figure 5.1).

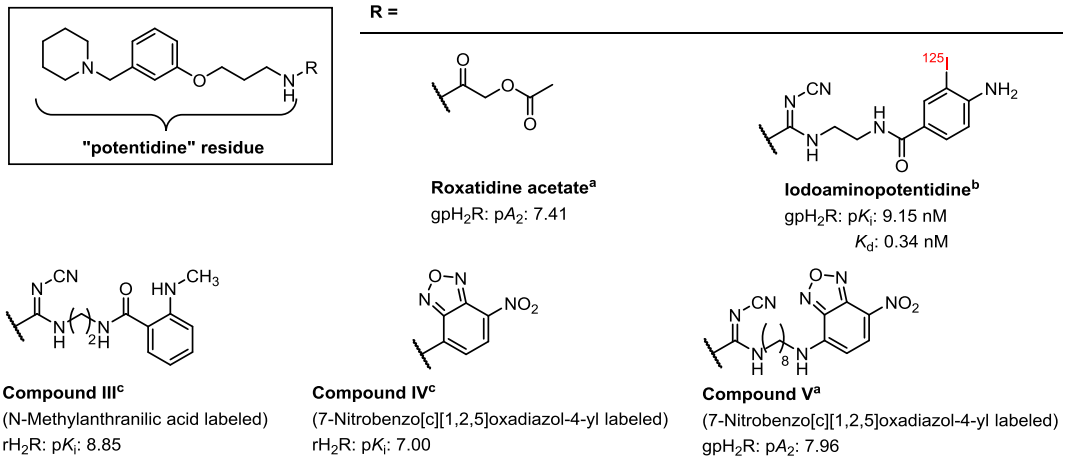

Figure 5.1. Structures of the standard H_2R antagonists roxatidine acetate and iodoaminopotentidine[21] as well as fluorescently labeled derivatives[19,20]. pA_2 values were [a]determined on the isolated guinea pig right atrium[19] and pK_i values and the pK_d value were [b]determined on membranes of guinea pig striatum[21,22] and [c]determined on homogenates of COS-7 cells transiently expressing the rH_2R[20].

Labeling with relatively small chromophores such as the N-methylanthranilic acid amide or a 7-nitrobenzo[c][1,2,5]oxadiazol-4-yl moiety resulted in fluorescent ligands (Compound III-V) with high H_2R affinity (pA_2 or pK_i values: >7.0) (Figure 5.1).[19,20] However, the reported ligands were inapplicable for cell-based methods like confocal microscopy and flow cytometry due to the high cellular autofluorescence at the emission wavelength which resulted in low signal-to-noise ratios. In order to expand the range of applications and avoid the high cellular autofluorescence,

fluorescent ligands labeled with red-emitting fluorophores (emission wavelength > 600 nm) are required.

Recently, with the squaramide-type radioligand [^{3}H]UR-DE257 our group developed a high-affinity and highly subtype selective hH_2R antagonist (K_d value: 31 nM)[23] (Figure 5.2) consisting of the pharmacophore of BMY 2536[24], which is linked to the tritium labeled propionic acid amide by a hexyl linker. Replacing the radiolabeled propionic acid amide by red-emitting fluorophores was the starting point for the development of high affinity hH_2R fluorescent ligands.[25] The most promising results were achieved by the pyridinium (Py-5) labeled ligand UR-DE229 and the cyanine labeled ligand (S0536) UR-DE56 (Figure 5.2).[25,26] Both ligands were antagonists in the GTPase assay with pK_b values of 7.06-7.66 and showed a low unspecific binding in flow cytometric binding assays and confocal microscopy.

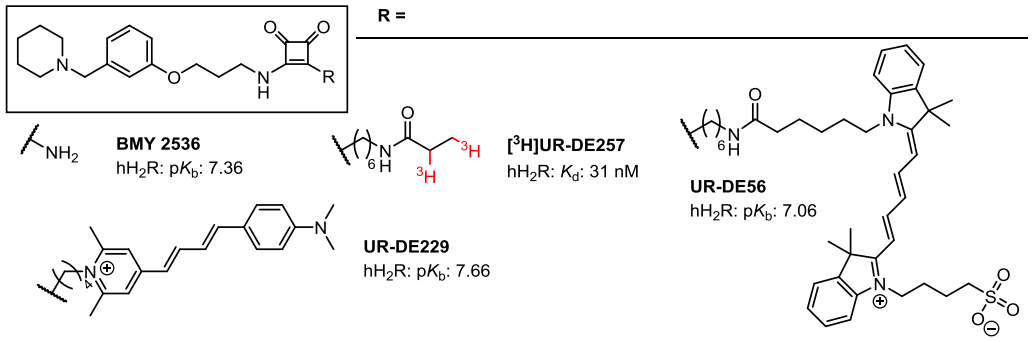

Figure 5.2. Chemical structures of the H_2R radioligand [^{3}H]UR-DE257, the parent compound BMY 2536, as well as of the pyridinium labeled H_2R antagonist UR-DE229 and the cyanine labeled H_2R antagonist UR-DE56. Binding affinities (radioligand binding assay, K_d value)[23] and antagonism (steady-state GTPase assay, pK_b value)[23,25] were determined on membranes of Sf9 insect cells expressing the hH_2R-$G_{s\alpha S}$ fusion protein.

The present study is aiming at fluorescent high affinity H_2R antagonists with improved optical and physicochemical properties to gain access to a wide range of potential applications, in particular to confocal microscopy and to high throughput or/and high content imaging systems. Therefore, the fluorescent labeled antagonists UR-DE229 and UR-DE56 were investigated in different assay systems. Furthermore, a small library of fluorescent ligands were synthesized for the exploration of the impact of length of the alkyl linker and the variation of the net charge of the fluorophores by coupling the positively charged pyrilium dye (Py-5) or differently charged cyanine dyes (positive: S2197, neutral: S0536 or negative: S0586, succinimidyl esters) with various amine precursors (Figure 5.3).

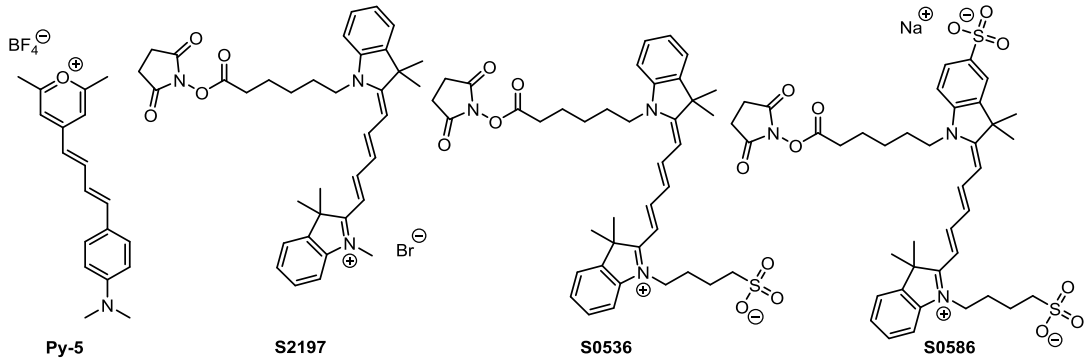

Figure 5.3. Chemical structures of the fluorescent dyes used for the preparation of the fluorescent H_2R ligands.

5.2 Results and Discussion

5.2.1 Chemistry

Starting from 3-[3-(piperidin-1-ylmethyl)phenoxy]propan-1-amine (**4.3**) the amine precursors were prepared in a three step synthesis (Scheme 5.1) as described before.[27] **4.3** was treated with 3,4-diethoxycyclobut-3-ene-1,2-dione (**5.1**) to form the corresponding squaric acid ester amide **5.2**, before a second amidation with mono-boc protected alkanediamines (**5.3**-**5.5**) was performed. The intermediates **5.3**-**5.5** were accessible by reaction of di-*tert*-butyl dicarbonate (Boc_2O) with an excess of the alkanediamines. The resulting *tert*-butyl carbamates **5.6**-**5.8** were cleaved with either TFA or HCl and the products were purified by preparative HPLC to afford the amine precursors **5.9**-**5.11** as TFA-salts.

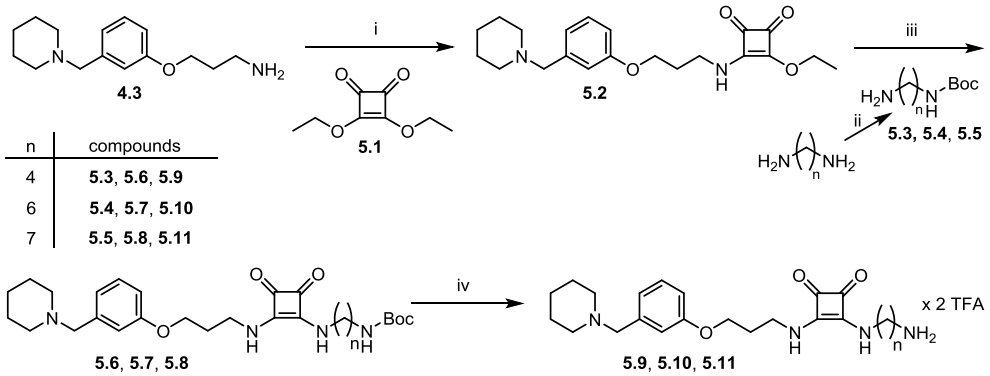

Scheme 5.1. Synthesis of the amine precursors **5.9**, **5.10**, **5.11**. Reagents and conditions: i) EtOH, RT, 2 h, 78%; ii) Boc_2O, $CHCl_3$, 0 °C to RT, ON, 44-92%; iii) EtOH, RT, ON, 42-83%; iv) TFA or HCl, CH_2Cl_2, RT, ON, 65-93%.

BMY 25368 was synthesized from **5.2** by treatment with ammonia in MeOH (Scheme 5.2) according to published protocols.[24,28]

The pyridinium labeled fluorescent ligands **5.12**-**5.14** were synthesized by direct coupling of the pyrilium dye Py-5 (chameleon label) with the respective amine precursor **5.9**-**5.11** under basic conditions (Scheme 5.3).[29] The reaction progresses rapidly accompanied by a change in color from blue to red. The cyanine labeled fluorescent ligands **5.15**-**5.20** were derived from the amine precursors **5.9**-**5.11** by amide coupling with the succinimidyl ester of the fluorescent dyes (S2197, S0536, S0586).

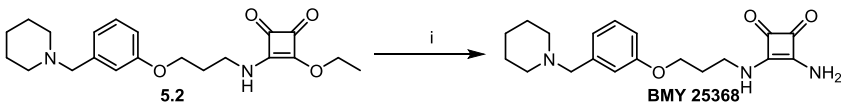

Scheme 5.2. Synthesis of the parent compound BMY 25368. Reagents and conditions: i) EtOH, RT, ON, 74%.

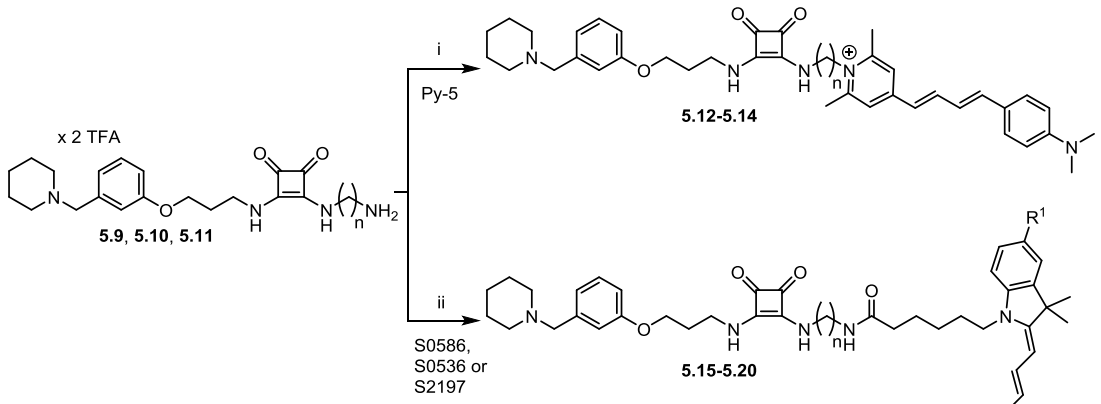

Compound	n	R^1	R^2	fluorophore net charge
5.12 (UR-DE229) **5.13** **5.14**	4 6 7	-	-	positive
5.15 **5.16**	4 6	H	H	positive
5.17 **5.18** (UR-DE56)	4 6	H	$(CH_2)_3$-SO_3^-	neutral
5.19 **5.20**	4 6	SO_3^-	$(CH_2)_3$-SO_3^-	negative

Scheme 5.3. Synthesis of the fluorescent compounds **5.12**-**5.20**. Reagents and conditions: i) DMF, TEA or DIPEA, RT, 90-120 min, 24-32%; ii) DMF, DIPEA, RT, 45-90 min, 18-44%.

5.2.2 Fluorescence properties of the labeled ligands

The fluorescence properties of representative compounds (**5.13**, **5.14**, **5.16**, **5.18**, **5.20**) were determined in PBS at pH 7.4 and PBS containing 1% (w/v) of BSA. The excitation and corrected emission spectra of the pyridinium labeled compound **5.14** and the cyanine labeled compounds (**5.16**, **5.18**, **5.20**) are depicted in Figure 5.4. The Stoke's shift was much more pronounced for the Py-5 labeled compounds (Figure 5.4, Table 5.1). These compounds (**5.12**-**5.14**) can be excited with the argon laser at 488 nm. The cyanine labeled compounds showed a considerably lower Stoke's shift, allowing excitation by the red diode laser at 635 nm.

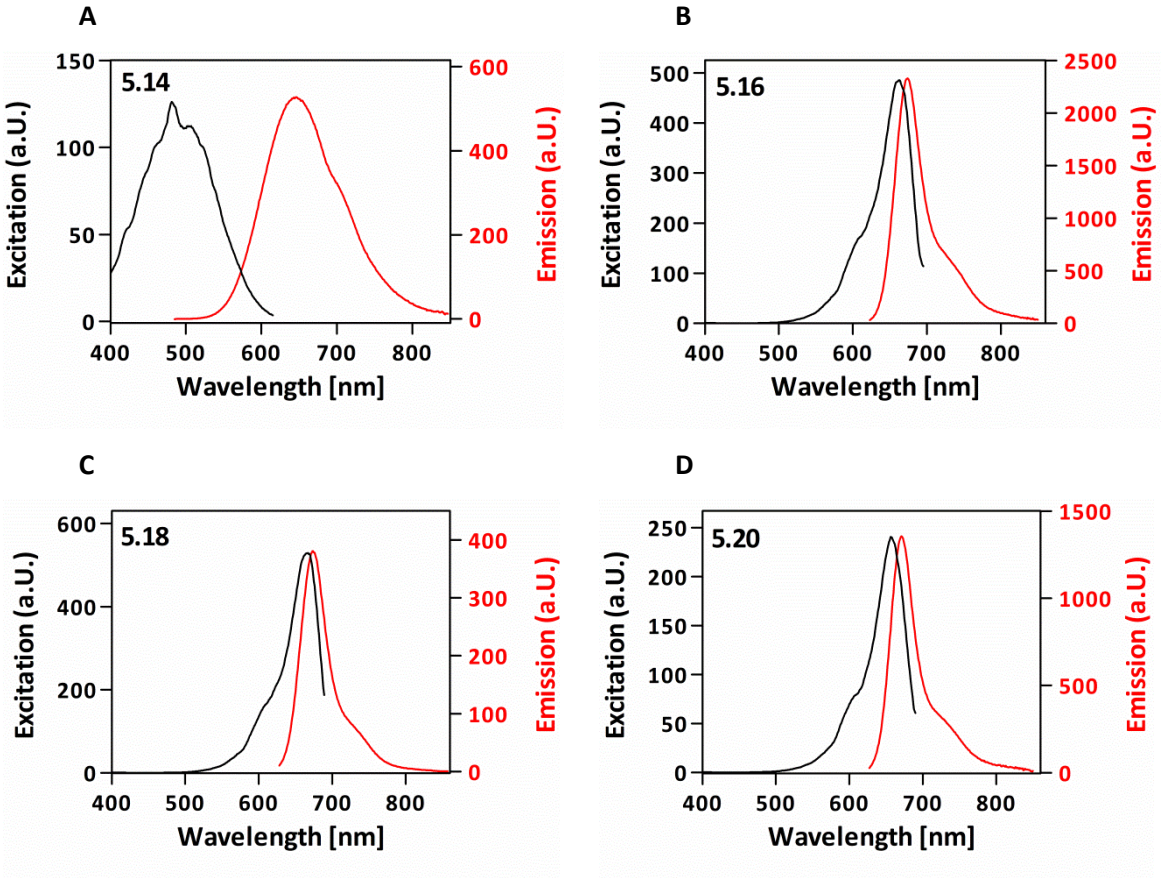

Figure 5.4. Excitation and corrected emission spectra of A: Py-5 (**5.14**), B: S0223 (**5.16**), C: S0436 (**5.18**) and D: S0387 (**5.20**) labeled compounds dissolved in PBS containing 1% BSA. Ligand concentration: 1.5-6 µM. Excitation and emission spectra were recorded with an excitation slit of 10 nm and an emission slit of 10 nm. The excitation wavelength was chosen as close to the absorption maximum as possible (**5.14**) or at an inflection point (**5.16**, **5.18** and **5.20**). The emission wavelength was chosen close to the emission maximum (**5.14**) or at an inflection point (**5.16**, **5.18** and **5.20**).

The quantum yields (Table 5.1) were determined in PBS and in PBS containing 1% (w/v) of BSA. For the pyridinium labeled compounds **5.13** and **5.14** the quantum yields were very low in PBS alone (less than 4%), whereas the addition of BSA increased the quantum yield up to 24% (7-fold). In case of the investigated cyanine labeled compounds **5.16**, **5.18**, **5.20** the quantum yields were significantly higher in PBS (19-27%) and increased (38-45%) in the presence of BSA. This effect was described for several cyanine and pyridinium labeld ligands primarily resulting from intermolecular hydrophobic and electrostatic interactions of the fluorophores with the protein.[30,31]

Table 5.1. Fluorescence properties of compounds **5.13**, **5.14**, **5.16**, **5.18** and **5.20** in PBS (pH 7.4) and PBS containing 1% BSA: excitation/emission maxima and fluorescent quantum yields ϕ (reference: cresyl violet perchlorate).

Compound	**Dye**[a]	**PBS**		**PBS + 1% BSA**	
		$\lambda_{ex}/\lambda_{em}$	ϕ (%)	$\lambda_{ex}/\lambda_{em}$	ϕ (%)
5.13	Py-5	457/706	3.2	481/646	22.9
5.14	Py-5	458/705	3.7	481/646	24.4
5.16	S0223	646/663	26.5	663/672	44.6
5.18	S0436	648/669	19.3	667/676	41.7
5.20	S0387	649/669	24.2	656/670	38.3

[a]Fluorescent dye used for the preparation of the fluorescent ligand.

5.2.3 Biological Evaluation

H_2R affinity, selectivity and antagonism

The fluorescent H_2R antagonists **5.12**-**5.20** as well as the parent compound BMY2536 and the amine precursors **5.9**-**5.11** were investigated in equilibrium competition binding experiments on membrane preparations from Sf9 insect cells expressing the hH_2R-$G_{s\alpha S}$ fusion protein using the antagonist [^{3}H]UR-DE257[23] as radioligand. The selectivity of the compounds for the hH_2R compared to hH_3R and, for selected ligands, to hH_4R was investigated by competition binding experiments using Sf9 insect cell membranes co-expressing either the hH_3R or the hH_4R and $G_{\alpha i2}$ and $G_{\beta 1\gamma 2}$ proteins with [^{3}H]histamine as radioligand. Representative radioligand binding curves are depicted in Figure 5.5 and the results are shown in Table 5.2.

Radioligand competition binding experiments revealed that most of the fluorescent labels were tolerated with no or a slight decrease in affinity (Table 5.2). Exceptions were the cyanine labeled ligands **5.19** and **5.20** in which the introduction of the S0387 fluorophore with a negative net charge resulted in a decrease in hH_2R affinity (**5.19**: pK_i value: 5.69, **5.20**: pK_i value: 5.88) compared to the corresponding amine-precursors (**5.9**: pK_i value: 6.52, **5.10**: pK_i value: 7.87). The pyridinium labeled ligands **5.12**-**5.14** showed, independent of linker length, high hH_2R affinities (pK_i values: 7.71-7.76) in the same range as the parent compound BMY 25368 (pK_i value: 7.80). In case of **5.12**, the hH_2R affinity even increased with the labeling (amine precursor **5.9**: pK_i value: 6.52 compared with **5.12**: pK_i value: 7.75). In the cyanine series, ligand **5.16**, labeled with fluorophore S0223 (positive net charge), and ligand **5.18**, labeled with fluorophore S0436 (neutral net charge), showed the highest hH_2R affinity (**5.16**: pK_i value: 7.67 and **5.18**: pK_i value: 7.11).

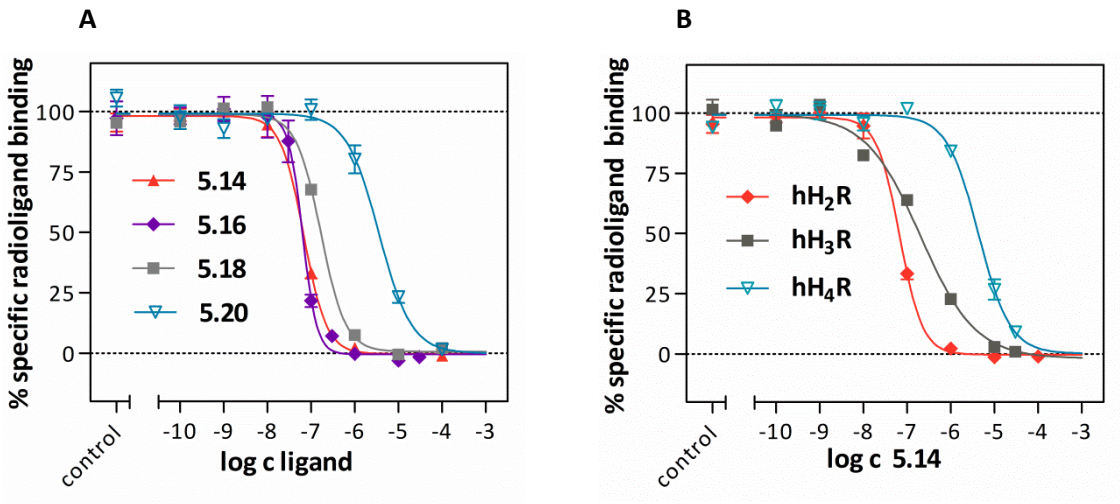

Figure 5.5. Displacement of the radioligand [^{3}H]UR-DE257 (c = 20 nM, K_d = 12.2 nM) by the fluorescent ligands **5.14**, **5.16**, **5.18** and **5.20** determined on membrane preparations of Sf9 insect cells expressing the hH_2R-$G_{s\alpha S}$ fusion protein (A). Displacement of the respective radioligand from membrane preparations of Sf9 insect cells expressing the hH_2R-$G_{s\alpha S}$ fusion protein (radioligand: [^{3}H]UR-DE257, c = 20 nM, K_d = 12.2 nM), co-expressing the hH_3R and $G_{\alpha i2}$ plus $G_{\beta 1\gamma 2}$ proteins (radioligand: [^{3}H]histamine c = 15 nM, K_d = 12.1 nM) or co-expressing the hH_4R and $G_{\alpha i2}$ plus $G_{\beta 1\gamma 2}$ proteins (radioligand: [^{3}H]histamine c = 10 nM, K_d = 15.9 nM) by the fluorescent ligand **5.14** (B). Data represent mean values ± SEM of 2-3 experiments performed in triplicate.

Interestingly, labeling with Py-5, S0223 and S0436 led to an increase in hH_3R receptor affinity up to two orders of magnitude compared to the corresponding amine precursors (Table 5.2). The pyridinium labeled ligands **5.12**-**5.14** and the cyanine labeled ligands **5.16** and **5.18** showed slight selectivity for the hH_2R over hH_3R (pK_i values: 6.4 - 7.18). In case of the cyanine labeled ligands **5.15** and **5.17**, the selectivity even changed in favour of the hH_3R (pK_i value: 7.0 and 6.8).

Table 5.2. Affinities of the parent compound BMY2536, the amine precursors **5.9**-**5.11** and fluorescent ligands **5.12**-**5.20** to $hH_{2-4}R$, obtained from equilibrium competition binding studies on membrane preparations from Sf9 insect cells, expressing the respective histamine receptor subtype.

			hH_2R[c]		**hH_3R[d]**		**hH_4R[e]**	
Compound	**Dye[a]**	**n[b]**	**pK_i**	**N**	**pK_i**	**N**	**pK_i**	**N**
His	-	-	6.53 ± 0.04	3	7.8 ± 0.1	3	7.65 ± 0.03	3
BMY 25368	-	-	7.80 ± 0.01[23]	3	4.66 ± 0.01	3	n.d.	-
5.9	-	4	6.52 ± 0.04	4	4.96 ± 0.07	3	n.d.	-
5.10	-	6	7.87 ± 0.02	3	5.08 ± 0.03	3	n.d.	-
5.11	-	7	7.86 ± 0.02	3	5.12 ± 0.05	3	n.d.	-
5.12	Py-5	4	7.75 ± 0.02	3	6.4 ± 0.1	3	n.d.	-
5.13	Py-5	6	7.71 ± 0.04	3	7.11 ± 0.08	4	5.64 ± 0.06	3
5.14	Py-5	7	7.763 ± 0.008	3	7.01 ± 0.04	3	5.57 ± 0.07	3
5.15	S0223	4	6.57 ± 0.02	3	7.0 ± 0.1	3	n.d.	-
5.16	S0223	6	7.67 ± 0.07	3	7.18 ± 0.03	2	n.d.	-
5.17	S0436	4	6.49 ± 0.04	3	6.8 ± 0.1	3	n.d.	-
5.18	S0436	6	7.105 ± 0.003	3	6.59 ± 0.03	2	n.d.	-
5.19	S0387	4	5.69 ± 0.08	3	5.45 ± 0.04	3	n.d.	-
5.20	S0387	6	5.88 ± 0.09	3	n.d.	-	n.d.	-

[a]Dye used for the preparation of the fluorescent ligand. [b]Length of the linker between the squaric acid amide and the fluorescent dye given as the number of carbon atoms. Competition binding assay on membrane preparations of Sf9 insect cells: [c]expression of the hH_2R-$G_{s\alpha S}$ fusion protein (radioligand: [^{3}H]UR-DE257, c = 20 nM, K_d = 12.2 nM), [d]co-expression of the hH_3R and $G_{\alpha i2}$ and $G_{\beta 1\gamma 2}$ proteins (radioligand: [^{3}H]histamine c = 15 nM, K_d = 12.1 nM) or [e]co-expresson of the hH_4R and $G_{\alpha i2}$ plus $G_{\beta 1\gamma 2}$ proteins (radioligand: [^{3}H]histamine c = 10 nM, K_d = 15.9 nM). The incubation period was 60 min. Data were analyzed by nonlinear regression and were best fitted to four-parameter sigmoidal concentration-response curves. Data shown are means ± SEM of N independent experiments, each performed in triplicate.

Compounds **5.13** and **5.14** were also investigated for hH_4R affinity. These ligands showed a high preference for the hH_2R over hH_4R. The impaired hH_2R selectivity with respect to the hH_3R limited the application of the fluorescent ligands to recombinant systems in which the hH_2R was expressed.

The amine precursors **5.9**, **5.10**, **5.11** as well as representative fluorescent ligands (**5.13**, **5.14**, **5.16**, **5.18**) were investigated for hH_2R antagonism in a GTPγS assay on membrane preparations of Sf9 insect cells expressing the hH_2R-$G_{s\alpha S}$ fusion protein.[32] The results are summarized in Table 5.3 and representative concentration-response curves derived from GTPγS assays performed in antagonist mode are depicted in Figure 5.6A.

The parent compound BMY 25368, the amine precursors **5.9**-**5.11** as well as the investigated fluorescent ligands **5.13**, **5.14**, **5.16** and **5.18** were antagonists at hH_2R in a GTPγS assay. In general, the pK_b values were in good agreement with the pK_i values from radioligand competition binding. Only the amine intermediates **5.9** and **5.10** as well as the cyanine labeled ligand **5.18** showed significally lower pK_b values compared to the pK_i values (difference up to one order of magnitude). Furthermore, representative fluorescent ligands (**5.13**, **5.14**, **5.16** and **5.19**) were investigated for hH_2R agonism in a β-arrestin2 recruitment assay (split luciferase complementation) on HEK293T-hH_2R-βArr2 cells.[33] All investigated ligands were antagonists in the β-arrestin2 recruitment assay, indicating that no β-arrestin2 mediated internalization of the receptor-ligand-complex took place (Figure 5.6B).

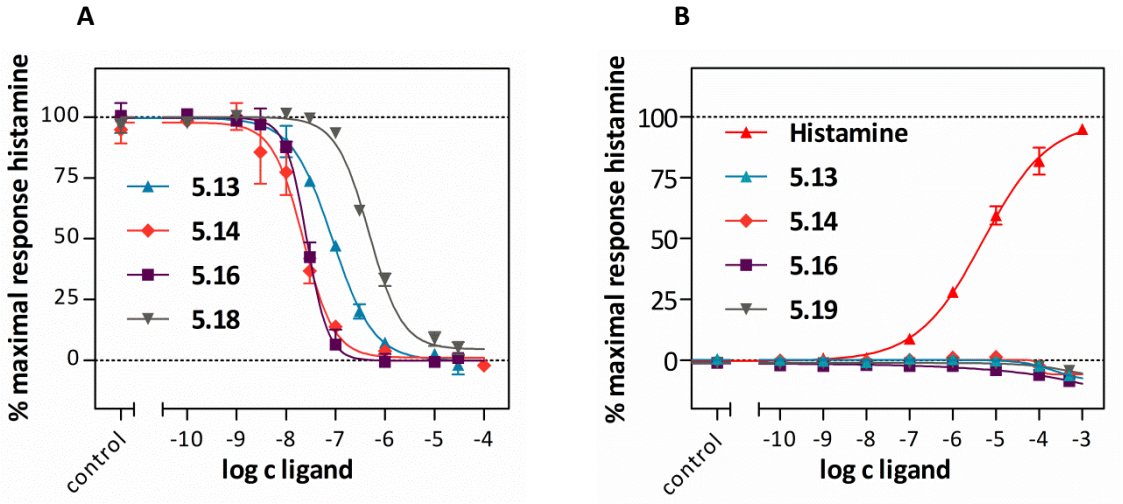

Figure 5.6. Antagonism of the fluorescent ligands **5.13**, **5.14**, **5.16** and **5.18** on hH_2R determined in a GTPγS assay (antagonistic mode) on membrane preparations of Sf9 insect cells expressing the hH_2R-$G_{s\alpha S}$ fusion protein (A). In the antagonist mode histamine (1 µM) was used for stimulation. Concentration-response curves of histamine, the fluorescent ligands **5.13**, **5.14**, **5.16** and **5.19** on hH_2R determined by a luciferase complementation assay measuring β-arrestin2 recruitment on HEK293T-hH_2R-βArr2 cells (B). Data represent mean values ± SEM of 2-3 experiments performed in duplicate (β-arrestin2) or triplicate (GTPγS).

Table 5.3. hH_2R antagonism and the calculated pK_b values of histamine, BMY 25368, the amine-precursors **5.9**-**5.11** and the fluorescent ligands **5.13**, **5.14**, **5.16** and **5.18** determined by a GTPγS assay.

			hH_2R (GTPγS)[c]		
No.	**Dye**[a]	**n**[b]	**pK_b (pEC_{50})**	**N**	**α**
His	-	-	(5.80 ± 0.06)	9	1.0
BMY 25368	-	-	7.03 ± 0.02	2	-0.011 ± 0.007
5.9	-	4	5.8 ± 0.2	2	-0.040 ± 0.003
5.10	-	6	6.73 ± 0.08	3	-0.025 ± 0.005
5.11	-	7	7.1 ± 0.1	3	-0.011 ± 0.006
5.13	Py-5	6	7.21 ± 0.04	3	-0.016 ± 0.002
5.14	Py-5	7	7.9 ± 0.1	3	-0.038 ± 0.006
5.16	S0223	6	7.73 ± 0.04	3	-0.026 ± 0.003
5.18	S0436	6	6.49 ± 0.03	3	-0.015 ± 0.005

[a]Dye used for the preparation of the fluorescent ligand. [b]Length of the linker between the squaric acid amide and fluorescent dye given as the number of carbon atoms. [c][^{35}S]GTPγS assay determined on membrane preparations of Sf9 insect cells expressing the hH_2R-$G_{s\alpha S}$ fusion protein. The intrinsic activity (α) of histamine was set to 1.00, and α values of investigated compounds were referred to this value. The pK_B values of neutral antagonists were determined in the antagonist mode versus histamine (c = 1 μM) as agonist. Data represent mean values ± SEM of 2-3 experiments performed in triplicate.

Confocal microscopy

The hH_2R binding of the fluorescently labeled ligands **5.14**, **5.16** and **5.18** was also investigated by confocal microscopy (Figure 5.7). All investigated ligands were localized at the cell membrane of HEK293T-hH_2R-qs5 cells. The ligands **5.14** and **5.18** showed a low unspecific binding at a concentration of 100 nM in the presence of a 300-fold excess of famotidine, whereas **5.16** showed a higher unspecific binding.

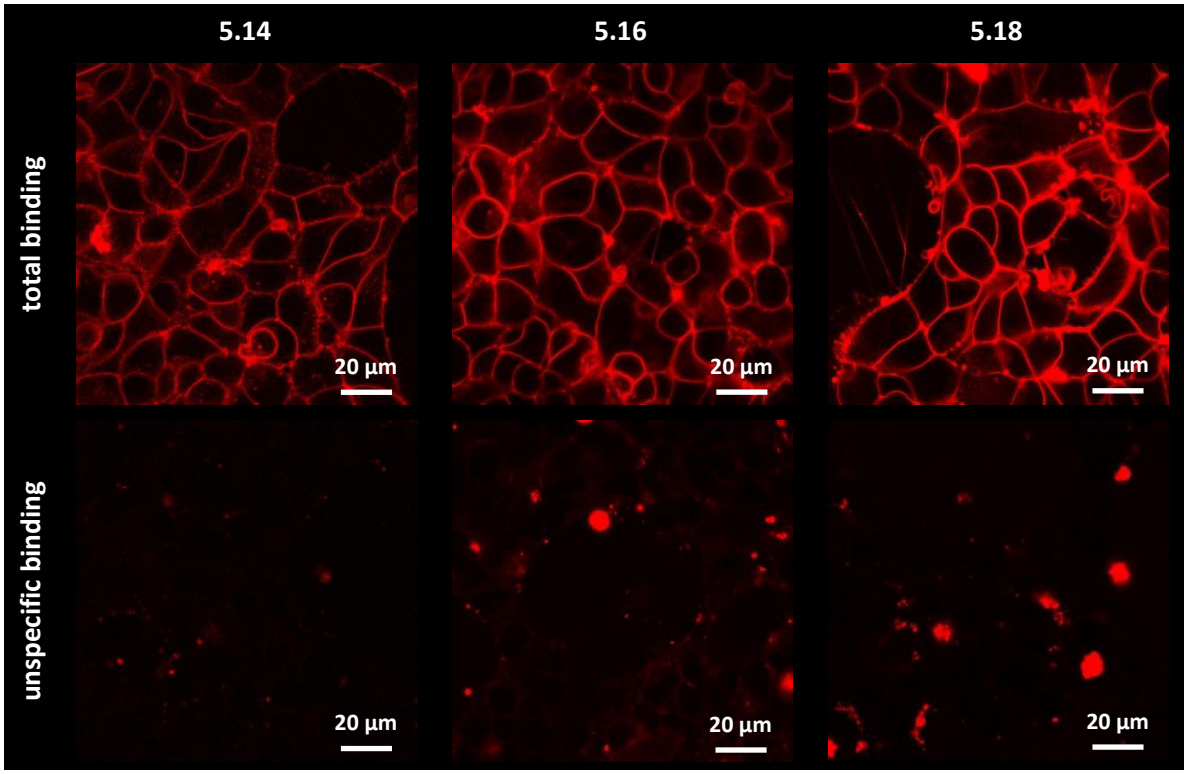

Figure 5.7. Localization of the fluorescent H_2R ligands **5.14** (100 nM), **5.16** (100 nM) and **5.18** (100 nM) at the membrane of HEK293T-hH_2R-qs5 cells determined by confocal microscopy after 20 min of incubation (25 °C). Unspecific binding was determined in the presence of famotidine (300-fold excess). All images were acquired with a Zeiss Axiovert 200 M microscope equipped with the LSM 510 Laser scanner. A 63x/1.40 oil immersion objective was used.

Flow cytometric hH_2R binding studies on HEK293T-hH_2R-qs5 cells

Fluorescent ligands **5.12**-**5.18**, which showed moderate to high hH_2R affinity (pK_i values > 6.0) were used for binding studies by flow cytometry on HEK293T-hH_2R-qs5 cells[26]. Representative saturation binding curves are depicted in Figure 5.8 and the results are summarized in Table 5.4. All investigated ligands afforded K_d values which were in good agreement with the K_i values obtained from competition binding experiments with [^{3}H]UR-DE257 on membranes of Sf9 insect cells. Within the pyridinium labeled ligands **5.12**-**5.14** the carbon linker length (n = 4-7) had no significant influence on affinity (K_d value: 14.9 – 27.9 nM), and unspecific binding was low (under 10% relative to total binding around the K_d).

The cyanine labeled ligand **5.16** (positive charge of the fluorophore) showed the highest affinity (K_d value: 13.9 nM) within the cyanine series, but a higher unspecific binding (20% relative to

total binding around the K_d value). The introduction of a sulfonic acid group into the cyanine moiety and the associated change of fluorophore charge to neutrality (compound **5.18**) resulted in a slight decrease in affinity (K_d value: 48.2 nM), but had a positive effect regarding unspecific binding (around 10% relative to total binding around the K_d value).

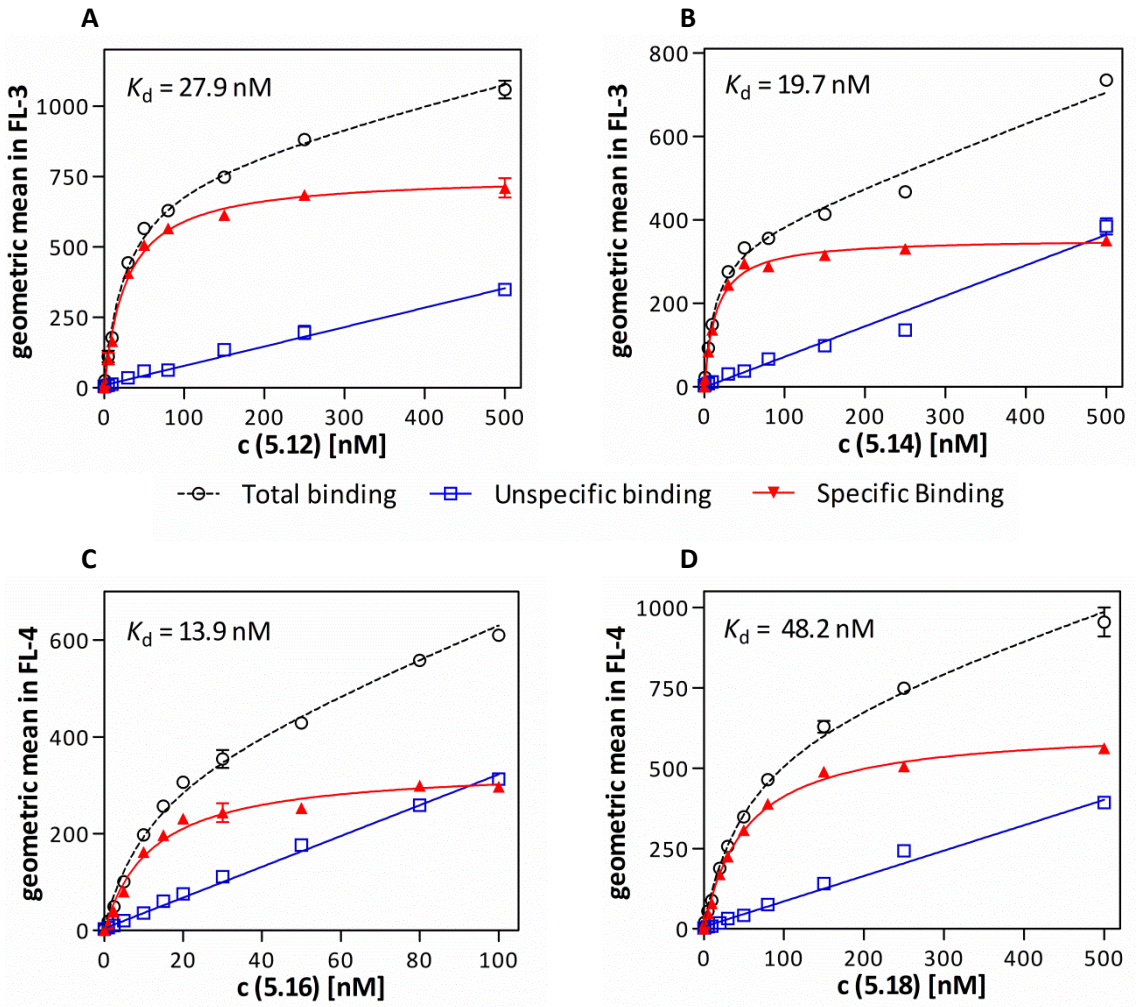

Figure 5.8. Representative flow cytometric saturation binding experiments on HEK293T-hH_2R-qs5 cells with the fluorescent ligands (A) **5.12**, (B) **5.14**, (C) **5.16** and (D) **5.18**. Unspecific binding was determined in the presence of famotidine (300-fold excess). Cells were incubated with the fluorescent ligands at RT in the dark for 90 min. Error bars of specific binding represent propagated errors calculated according to the Gaussian law. Error bars of total and unspecific binding represent the SEM. Experiments were performed in dublicate.

Table 5.3. hH_2R saturation binding data of fluorescent ligands **5.12**-**5.18** determined by flow cytometry on HEK293-hH_2R-qs5 cells in comparison with competition binding data determined on membrane preparations from Sf9 insect cells, expressing the hH_2R.

No	Dye[a]	n[b]	K_d (nM)[c]	K_i (nM)[d]
5.12	Py-5	4	27.9 ± 2.0	18 ± 1
5.13	Py-5	6	14.9 ± 2.3	20 ± 2
5.14	Py-5	7	19.7 ± 4.4	23.6 ± 0.4
5.15	S0223	4	289 ± 29	270 ± 14
5.16	S0223	6	13.9 ± 2.2	22 ± 4
5.17	S0436	4	684 ± 95	328 ± 28
5.18	S0436	6	48.2 ± 2.3	78.5 ± 0.5

[a]Dye used for the preparation of the fluorescent ligand. [b]Length of the linker between the squaric acid amide and fluorescent dye given as the number of carbon atoms. [c]Flow cytometric saturation binding experiments on HEK293T-hH_2R-qs5 cells. Unspecific binding was determined in the presence of famotidine (300-fold excess). Cells were incubated with the fluorescent ligands at RT in the dark for 90 min. Data represent mean ± SEM from three independent experiments (each performed in duplicate). Specific binding data were analyzed by an equation describing one-site (monophasic) binding. [d]Competition binding assay on membrane preparations of Sf9 insect cells hH_2R-$G_{s\alpha S}$ fusion protein (radioligand: [^{3}H]UR-DE257, c = 20 nM, K_d = 12.2 nM), *cf*. results from Table 5.2 here shown as K_i values to facilitate comparison.

The association and dissociation kinetics of **5.14**, **5.16** and **5.18** were determined on HEK293T-hH_2R-qs5 cells at 37 °C using flow cytometry (*cf.* Figure 5.9). The Py-5 labeled ligand **5.14** (c = 50 nM) showed a fast association i. e. the plateau was reached after approx. 20 min. The dissociation of **5.14** (c = 50 nM, 90 min pre-incubation) in the presence of famotidine was incomplete. After 150 min, the residual specific binding of the fluorescent ligand amounted to approximately 60% (curve plateau at 57%). The investigated cyanine dyes **5.16** and **5.18** (c = 15 nM and 25 nM) showed much slower association, i. e. the plateau was reached after 140 min. The association is strongly concentration dependent which resulted in the differences in association rate between **5.14** (c = 50 nM) and **5.16** (c = 15 nM) or **5.18** (c = 25 nM). A comparison of the association rate constants (k_{on}) which are concentration independent, revealed that Py-5 ligand **5.14** (k_{on} value: 0.0043 min^{-1} nM^{-1}) associated two times faster than **5.16** (k_{on} value: 0.002 min^{-1} nM^{-1}) and 4 times faster **5.18** (k_{on} value: 0.00093 min^{-1} nM^{-1}) (Table 5.5). The dissociation of the ligands **5.16** and **5.18** (90 min pre-incubation) was incomplete after 150 min, reaching a plateau at 22% (**5.16**) and 67% (**5.18**) of initially bound ligand. These data suggested a (pseudo)irreversible binding[34,35] of **5.14**, **5.16** and **5.18**.

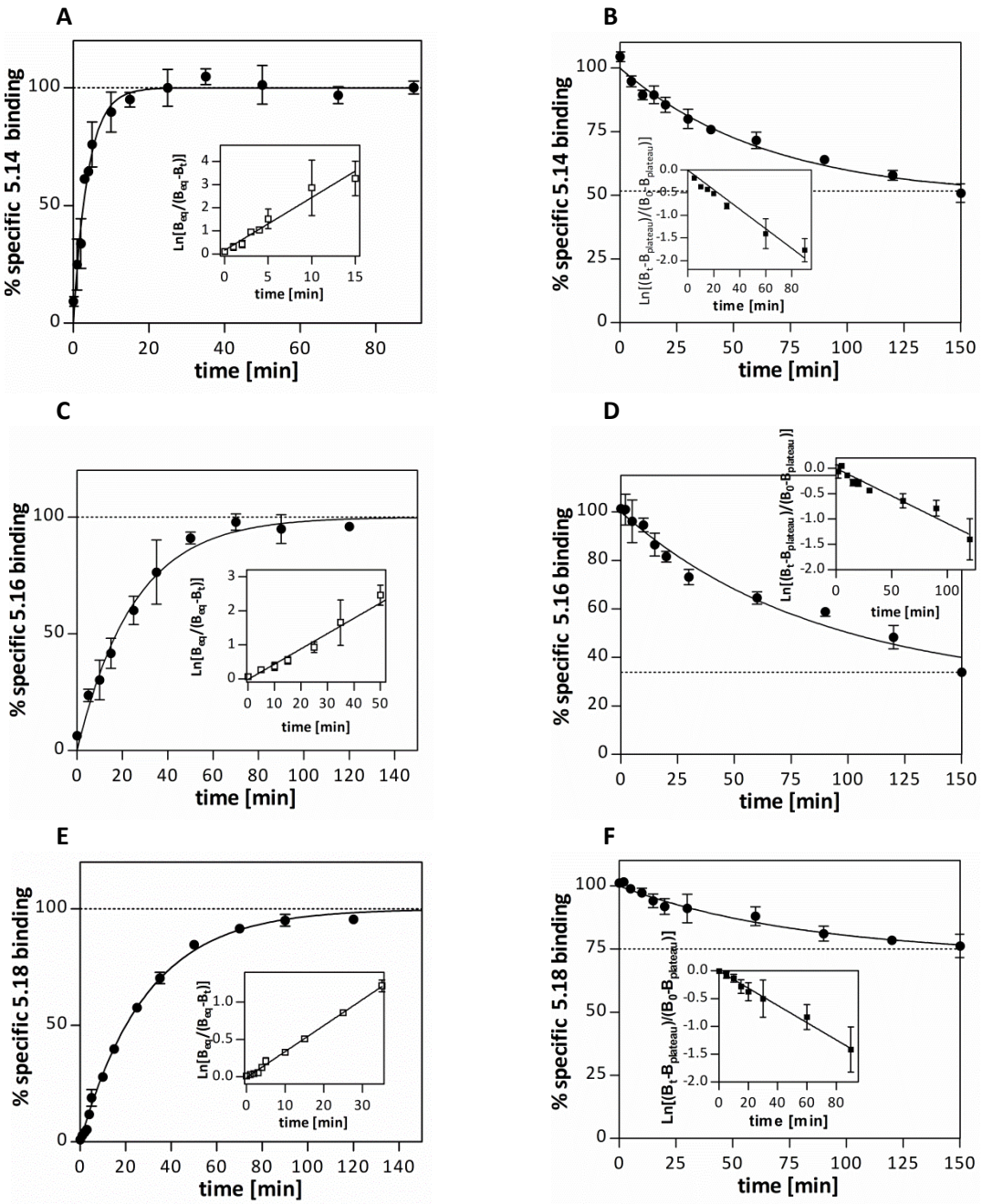

Figure 5.9. Association and dissociation kinetics of **5.14** (A, B), **5.16** (C, D) and **5.18** (E, F) determined at intact HEK293T-hH_2R-qs5 cells at 37 °C by flow cytometry. (A) Association of **5.14** (c = 50 nM) to the hH_2R as a function of time (nonlinear regression: k_{obs} = 0.24 min^{-1}). Inset: $ln[B_{eq}/(B_{eq} - B_t)]$ versus time, k_{obs} = slope = 0.23 min^{-1}. (B) Dissociation of **5.14** (preincubation: 90 min, c = 50 nM) in the presence of famotidine (c = 15 µM) from the hH_2R as a function of time, showing incomplete monophasic decline (nonlinear regression: k_{off} = 0.027 min^{-1}, $t_{1/2}$ = 26 min, plateau = 57%), Inset: $ln[(B_t-B_{plateau})/(B_0-B_{plateau})]$ versus time, slope·(-1) = k_{off} = 0.023 min^{-1}. (C) Association of **5.16** (c = 15 nM) to the hH_2R as a function of time (nonlinear regression: k_{obs} = 0,061 min^{-1}). Inset: $ln[B_{eq}/(B_{eq} - B_t)]$ versus time, k_{obs} = slope = 0.045 min^{-1}. (D) Dissociation of **5.16** (preincubation: 90 min, c = 15 nM) in the presence of famotidine (c = 4.5 µM) from the hH_2R as a function of time, showing incomplete monophasic decline (nonlinear regression: k_{off} = 0.011 min^{-1}, $t_{1/2}$ = 64 min, plateau = 22%), Inset: $ln[(B_t-B_{plateau})/(B_0-B_{plateau})]$ versus time, slope·(-1) = k_{off} = = 0.012 min^{-1}. (E) Association of **5.18** (c = 25 nM) to the hH_2R as a function of time (nonlinear regression: k_{obs} = 0,038 min^{-1}). Inset: $ln[B_{eq}/(B_{eq} - B_t)]$ versus time, k_{obs} = slope = 0,035 min^{-1}. (D) Dissociation of **5.18** (preincubation: 90 min, c = 25 nM) in the presence of famotidine (c = 7.5 µM) from the hH_2R as a function of time, showing incomplete monophasic decline (nonlinear regression: k_{off} = 0.015 min^{-1}, $t_{1/2}$ = 75 min, plateau = 67%), Inset: $ln[(B_t-B_{plateau})/(B_0-B_{plateau})]$ versus time, slope·(-1) = k_{off} = 0.012 min^{-1}. Data represent means ± SEM from two to three independent experiments (each performed in duplicate).

Nevertheless, the equilibrium dissociation constants of **5.14** ($K_{d(kin)}$ value: 6.7 nM), **5.16** ($K_{d(kin)}$ value: 6.3 nM) and **5.18** ($K_{d(kin)}$ value: 16.7 nM), calculated from kinetics (nonlinear regression, $K_{d(kin)} = k_{off}/k_{on}$), were consistent with the K_d values obtained from saturation binding experiments (Table 5.5).

Pseudo-irreversible binding to the human, rat and mouse H_2R was also observed in case of the closely related radioligand [^{3}H]UR-DE257 using either Sf9 insect cell membranes or HEK293T-hH_2R-CreLuc cells.[23] Squaramides, such as BMY25368 and the amine precursor **5.10,** were described as insurmountable H_2R antagonists.[23] Unlike standard the antagonist famotidine, both compounds caused a concentration-dependent depression of the maximal agonist response of the guinea pig right atrium.

Several GPCR ligands were reported to show a similar behavior in kinetic and functional experiments[34-37] and several explanations were provided such as irreversible (covalent) binding to the receptor,[38] a slow rate of dissociation from the receptor,[34] a slow rate of interconversion between inactive and active receptor conformations,[39] stabilization of an inactive ligand-specific receptor conformation,[40,41] binding to a site distinct from the agonist binding site[42] or internalization of the ligand-receptor-complex[37].

Table 5.4. hH_2R binding characteristics of **5.14**, **5.16** and **5.18** determined by flow cytometry on HEK293T-hH_2R-qs5 cells at 37 °C.

	Binding Kinetics			**Saturation Binding**
	k_{off}[a]	k_{on}[b]	k_{off}/k_{on}[c]	$K_{d\,(sat)}$[d]
No	**(min^{-1})**	**(min^{-1} nM^{-1})**	**$K_{d\,(kin.)}$ (nM)**	**(nM)**
5.14	0.027 ± 0.002	0.0043 ± 0.001	6.7 ± 1.7	19.7 ± 4.4
5.16	0.011 ± 0.003	0.0020 ± 0.0009	6.3 ± 2.7	13.9 ± 2.2
5.18	0.015 ± 0.013	0.00093 ± 0.00021	16.70 ± 3.3	48.2 ± 2.3

[a]Dissociation rate constant derived from nonlinear regression. [b]Association rate constant derived from nonlinear regression; calculated from k_{obs}, k_{off} and the fluorescent ligand concentration (cf. Figure 5.9 and experimental section). [c]Kinetically determined dissociation constant. [d]Equilibrium dissociation constant determined by saturation binding. Data represent means ± SEM from two to three independent experiments (each performed in duplicate).

Regardless of the slow dissociation, the pyridinium labeled ligand **5.14** and the cyanine labeled ligand **5.18** were selected for equilibrium competition binding experiments with HEK293T-hH_2R-qs5 cells. The results are summarized in Table 5.6 and the competition binding curves are depicted in Figure 5.10. Both ligands were completely displaceable by histamine and standard H_2R antagonists like famotidine and ICI127032.

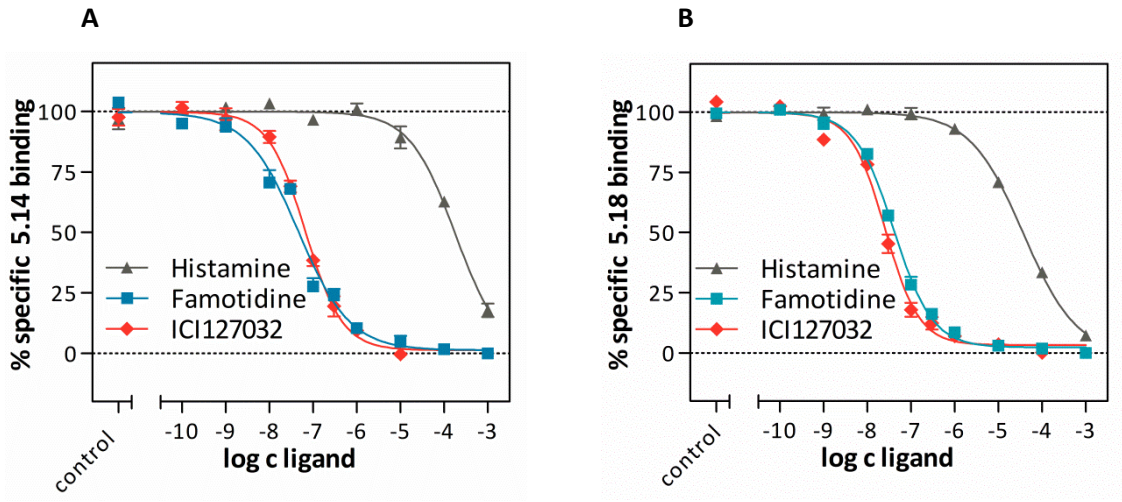

Figure 5.10. Displacement of (A) the fluorescent ligand **5.14** (c = 50 nM, K_d = 19.7nM) or [B) the fluorescent ligand **5.18** (c = 25 nM, K_d = 48.2 nM) by histamine, famotidine and ICI 127032 determined on HEK293T-hH_2R-qs5 cell by flow cytometry. Cells were incubated with the fluorescent ligands and the test compounds at RT in the dark for 90 min. Data represent means ± SEM from three independent experiments (each performed in duplicate).

The pK_i values of the standard H_2R antagonists famotidine and ICI127032 determined by flow cytometric equilibrium competition binding with the fluorescently labeled ligand **5.14** or **5.18** were in good agreement with data derived from radioligand equilibrium binding experiments with [^{3}H]UR-DE257 at sf9 insect cell membranes. However, the pK_i value of the endogenous ligand histamine determined by flow cytometry with either **5.14** or **5.18** was considerably lower compared to radioligand binding at sf9 insect cell membranes. This could be explained by the different receptor-G-protein-complexes used. In the Sf9-system a hH_2R-$G_{s\alpha S}$ fusion protein was utilized, which was reported to have a high affinity (pK_{ih} value: 7.10) and a low affinity binding site (pk_{il} value: 5.08) for histamine when [^{3}H]tiotidine was used as a radioligand (shallow biphasic competition binding curve).[43] In case [^{3}H]UR-DE257 was used as radioligand, the resulting dose-response curve of histamine was best fitted by a four-parameter logistic fit (shallow monophasic competition binding curve). The corresponding pK_i value of 6.53 was between the ones of the high affinity and low affinity binding site, which indicates, together with the shallow curve slope, that the high affinity and low affinity binding site are also available but not resolved in this experimental set up. In the HEK293T-hH_2R-qs5 cells the hH_2R was stably co-expressed with the chimeric G_α protein qs5-HA. It was reported, that these cells showed no high affinity binding site for histamine in radioligand equilibrium competition binding experiments with [^{3}H]tiotidine which resulted in monophasic competition binding curves and a pK_i value of 3.95.[26] This pK_i value was in good agreement with the results determined by flow cytometry using fluorescent ligand **5.14** or **5.18** as competitor and the same cell type (Table 5.5).

Table 5.5. hH_2R binding (pK_i values) of histamine, famotidine and ICI127032 determined by radioligand competition binding ([^{3}H]UR-DE257[a] or [^{3}H]tiotidine[b]) and by displacement of fluorescent ligands **5.14**[c] and **5.18**[d], respectively.

No	Radioligand Binding pK_i	Flow Cytometry (5.14)[c] pK_i	Flow Cytometry (5.18)[d] pK_i
Histamine	6.53 ± 0.04[a] (3.93[b])[26]	4.30 ± 0.04	4.61 ± 0.05
Famotidine	7.25 ± 0.03[a]	7.90 ± 0.02	7.58 ± 0.04
ICI127032	7.70 ± 0.07[a]	7.73 ± 0.02	7.73 ± 0.03

[a,b]Determined by competition binding with [a][^{3}H]UR-DE257 (c = 20 nM) at membrane preparations of sf9 insect cells expressing hH_2R-$G_{s\alpha s}$ or with [b][^{3}H]tiotidine (c = 5 nM) at intact HEK293T-hH_2R-qs5 cells. [c,d]Determined by competition binding with [c]**5.14** (c = 50 nM) or [d]**5.18** (c = 25 nM) at intact HEK293T-hH_2R-qs5 cells. Data were analyzed by nonlinear regression and were best fitted to four-parameter sigmoidal concentration-response curves. Data shown are means ± SEM of 3 independent experiments, each performed in [a,b]triplicate or [c,d]duplicate.

High content imaging on adherent and suspended HEK293T-hH_2R-qs5 cells

The fluorescent ligands **5.12**, **5.14**-**5.18** and **5.20** were also applied to high content imaging hH_2R binding assays enabling measurement on live and adherent HEK293T-hH_2R-qs5 cells in the 96-well plate format. The fluorescent ligands were incubated with the cells for 60 min at room temperature, washed with PBS, and images were obtained by an IN Cell Analyzer 2000 plate reader. Figure 5.11 shows representative images after incubation with the fluorescent ligands **5.14** (250 nM), **5.16** (75 nM), **5.18** (75 nM) and **5.20** (500 nM) for 60 min, followed by a washing step. All fluorescent ligands were localized at the cell membrane and there was a clear difference between total and unspecific binding.

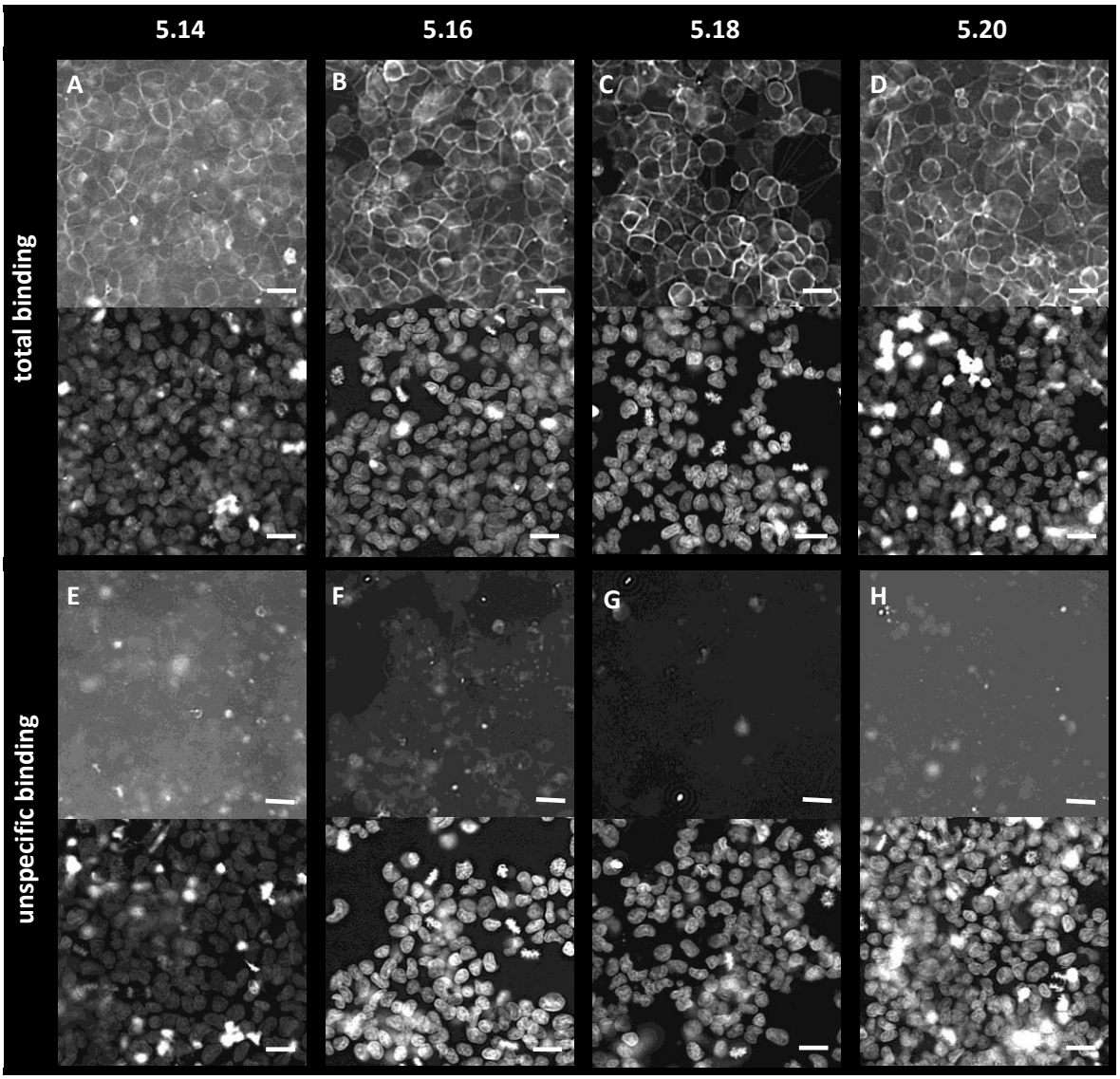

Figure 5.11. Localization of the fluorescent H_2R ligands A) **5.14** (250 nM), B) **5.16** (75 nM), C) **5.18** (75 nM) and D) **5.20** (500 nM) at the membrane of HEK293T-hH_2R-qs5 cells determined by high content imaging after 60 min of incubation (RT). Hoechst 33342 was used as a nuclear stain. Unspecific binding of **5.14** (E), **5.16** (F), **5.18** (G) and **5.20** (H) were determined in the presence of famotidine (300-fold excess). All images were acquired with a INCell Analyzer 2000. Scale bar: 20 µm.

The acquired images were transformed into saturation binding curves (representative curves are shown in Figure 5.12). The K_d values determined by high content imaging at adherent HEK cells (Table 5.7) were generally in good agreement with the ones obtained by flow cytometry

(Table 5.4). The pyridinium labeled ligands **5.12** and **5.14** showed a slightly lower affinity for the hH_2R (K_d values: 74.6 nM and 90.9 nM) compared to flow cytometry and radioligand competition binding. In contrast the cyanine labeled ligands **5.15**-**5.18** and **5.20** showed a similar or slightly higher affinity for the hH_2R. Within the series the ligands **5.16** and **5.18** showed the highest affinity with K_d values of 16.2 nM and 17.9 nM.

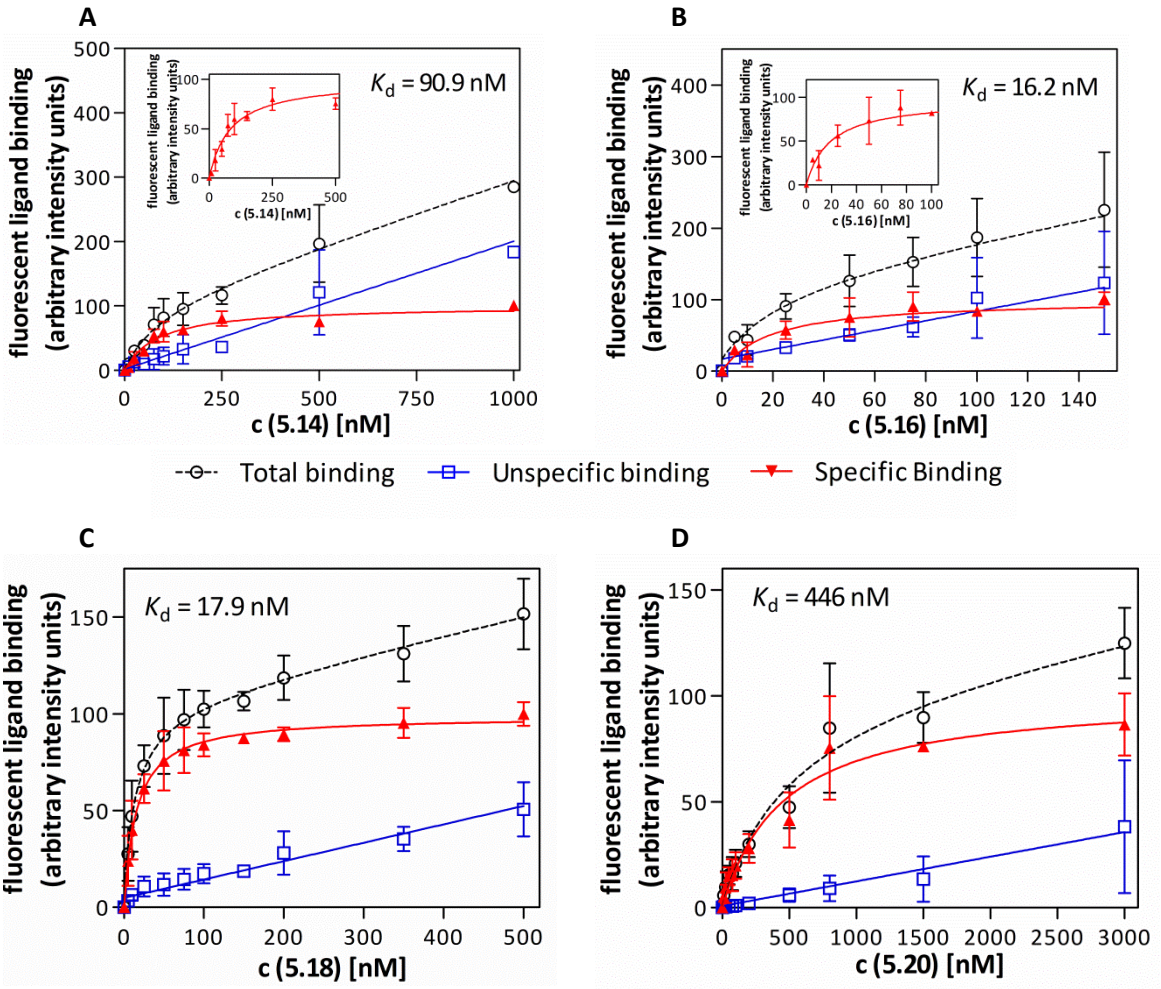

Figure 5.12. High content imaging: saturation binding experiments on adherent HEK293T-hH_2R-qs5 cells with fluorescent ligands (A) **5.14**, (B) **5.16**, (C) **5.18** and (D) **5.20**. Unspecific binding was determined in the presence of famotidine (300-fold excess). Cells were incubated with the fluorescent ligands at RT in the dark for 60 min. Error bars represent mean ± SEM from at least two independent experiments (each performed in duplicate).

Table 5.6. hH_2R saturation binding data of fluorescent ligands **5.12**, **5.14**-**5.18** and **5.20** determined by high content imaging on adherent HEK293-hH_2R-qs5 cells.

			Adherent Cells	
No	**Dye**[a]	**n**[b]	K_d **(nM)**	**N**
5.12	Py-5	4	74.6 ± 0.5	2
5.14	Py-5	7	90.9 ± 8.0	3
5.15	S0223	4	105 ± 21	5
5.16	S0223	6	16.2 ± 4.1	2
5.17	S0436	4	179 ± 44	3
5.18	S0436	6	17.9 ± 5.6	3
5.20	S0387	6	446 ± 41	2

[a]Dye used for the preparation of the fluorescent ligand. [b]Length of the linker between the squaric acid amide and the fluorescent dye given as the number of carbon atoms. [c]Saturation binding experiments on adherent cells determined by high content imaging. Unspecific binding was determined in the presence of famotidine (300-fold excess). Cells were incubated with the fluorescent ligands at RT in the dark for 60 min. Error bars represent mean ± SEM from N independent experiments (each performed in duplicate). Specific binding data were analyzed by an equation describing one-site (monophasic) binding.

Additionally, the association and dissociation kinetics of **5.18** were determined on adherent HEK293T-hH_2R-qs5 cells at 37 °C using high content imaging. The fluorescent ligand (50 nM) was added to the cells and the images of the same well were acquired at different time points (no washing step necessary). Figure 5.13 (A-D) shows the binding of **5.18** after increasing perids of incubation. The dissociation of **5.18** (50 nM) was determined in the presence of famotidine (300-fold excess) after 60 min pre-incubation with the fluorescent ligand. Sample images at different time points are shown in Figure 5.13 (E-H). The resulting association and dissociation binding curves are depicted in Figure 5.14. Association and dissociation rate of **5.18** (k_{on} value: 0.0098 min^{-1} nM^{-1} and k_{off} value: 0.091 min^{-1}, *cf*. Table 5.7) were ten times faster compared to flow cytometry. In high content imaging **5.18** (c = 50 nM) showed a fast association which was completed after approximately 10 min. The dissociation of **5.18** (c = 50 nM) in the presence of famotidine was incomplete. After 25 min, the residual specific binding of the fluorescent ligand reached a plateau at approximately 78%, suggesting (pseudo)irreversible binding, which was in good agreement with the results determined by flow cytometry. The images of the dissociation showed that the residual fluorescent ligand was preferentially located at the cell membrane and there was only low fluorescence in the cytoplasm. It is a matter of speculation why the association and dissociation kinetics were ten times faster compared to the kinetics determined by flow cytometry. Presumably, this was attributable to the different experimental conditions (adherent cells in monolayer vs cellsuspension, cell concentration: $3 \cdot 10^9$ cells/mL vs $0.5 - 1 \cdot 10^6$ cells/mL in assay, fluorescent ligand concentration: 50 nM vs 25 nM).

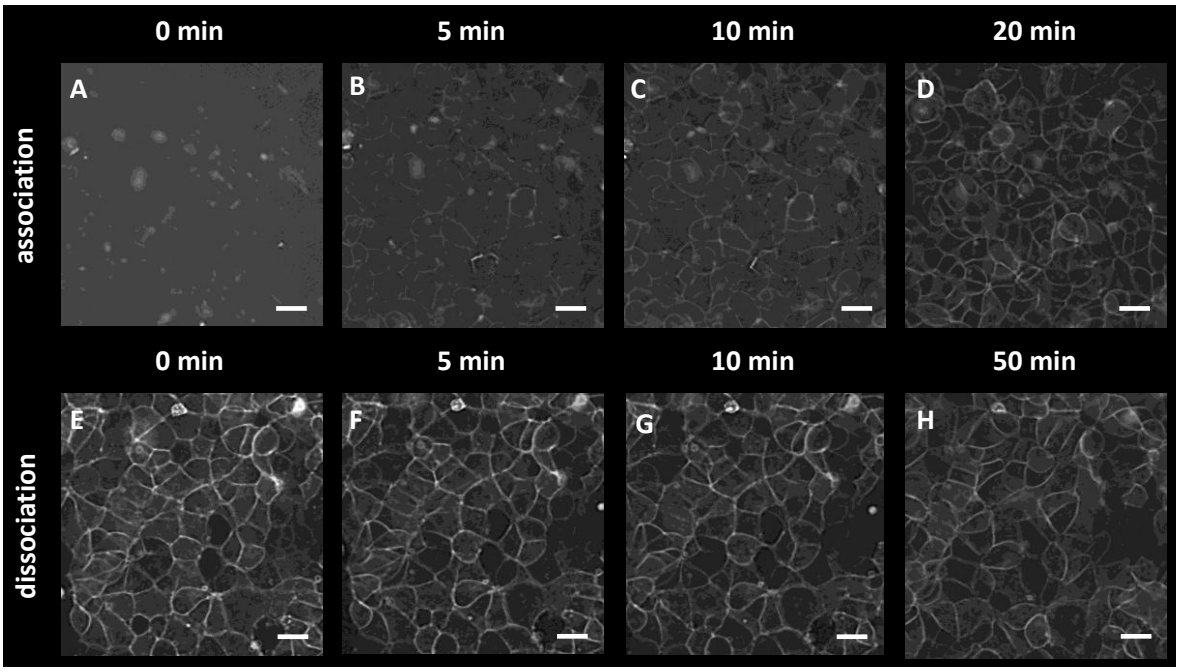

Figure 5.13.Time-dependent binding of fluorescent ligand **5.18** (50 nM) at HEK293T-hH_2R-qs5 cells measured after 0 min (A), 5 min (B), 10 min (C) and 20 min (D) and replacement of **5.18** (50 nM) with famotidine (300-fold excess) after pre-incubation for 60 min measured after 0 min (E), 5 min (F), 10 min (G) and 50 min (H). Cells were incubated with fluorescent ligand at 37 °C and images were acquired with high content imaging (INCell Analyzer 2000), scale bar: 20 µm.

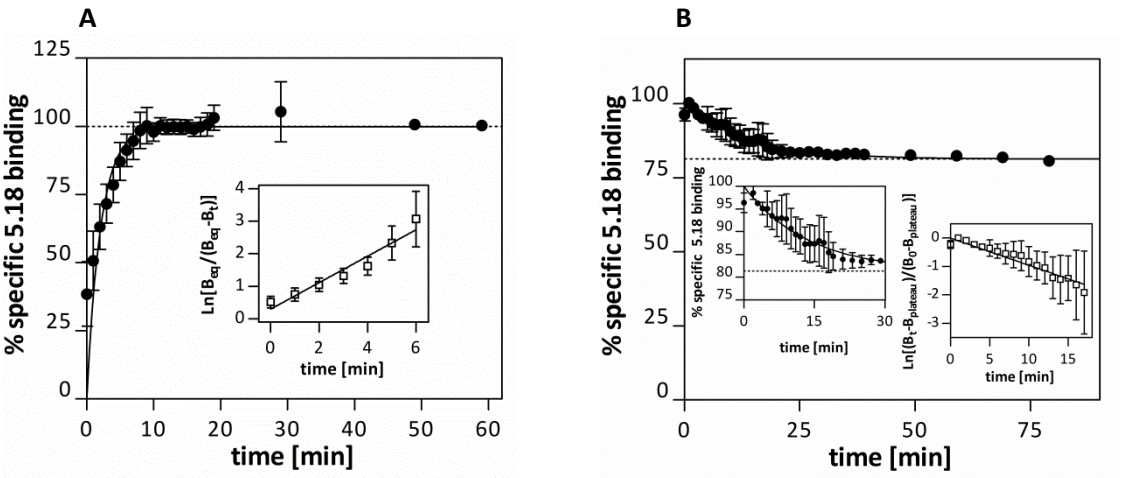

Figure 5.14. Association (A) and dissociation (B) kinetics of **5.18** at adherent HEK293T-hH_2R-qs5 cells at 37 °C determined by high content imaging. (A) Association of **5.18** (c = 50 nM) to the hH_2R as a function of time (nonlinear regression: k_{obs} = 0.40 min^{-1}). Inset: $ln[B_{eq}/(B_{eq} - B)]$ versus time, k_{obs} = slope = 0,41 min^{-1}. (B) Dissociation of 18 (preincubation: 60 min, c = 50 nM) in the presence of famotidine (c = 15 µM) from the hH_2R as a function of time, showing incomplete monophasic decline (nonlinear regression: k_{off} = 0.091 min^{-1}, $t_{1/2}$ = 13 min, plateau = 78%), inset left: magnification of the first 60 min, inset right: $ln[(B_t-B_{plateau})/(B_0-B_{plateau})]$ versus time, slope·(-1) = k_{off} = 0.099 min^{-1}. Data represent means ± SEM from two independent experiments (each performed in duplicate).

Nevertheless, the dissociation constant of **5.18** ($K_{d(kin)}$ value: 9.3 nM), calculated from kinetics (nonlinear regression, $K_d = k_{off}/k_{on}$), was consistent with the K_d value obtained from saturation binding experiments (Table 5.8).

Table 5.7. hH_2R binding characteristics of **5.18** determined by high content imaging on adherent HEK293T-hH_2R-qs5 cells (37 °C)

No	k_{off} [a] (min^{-1})	k_{on} [b] (min^{-1} nM^{-1})	k_{off}/k_{on} [c] $K_{d\ (kin.)}$ (nM)	$K_{d\ (sat)}$ [d] (nM)
5.18 (IN Cell)	0.091 ± 0.084	0.0098 ± 0.0004	9.3 ± 0.4	17.9 ± 5.6

[a]Dissociation rate constant derived from nonlinear regression. [b]Association rate constant derived from nonlinear regression; calculated from k_{obs}, k_{off} and the fluorescent ligand concentration (cf. Figure 5. and experimental section). [c]Kinetically determined dissociation constant. [d]Equilibrium dissociation constant determined by saturation binding. Data represent means ± SEM from two independent experiments (each performed in duplicate).

By high content imaging (96 well format) it was also possible to perform competition binding experiments with the cyanine labeled ligand **5.18** on HEK293T-hH_2R-qs5 cells. The results are summarized in Table 5.9 and the competition binding curves are depicted in Figure 5.15. Ligand **5.18** was completely displaceable by histamine and the standard H_2R antagonists lamtidine and ICI127032. The pK_i values of lamtidine and ICI127032 were in good agreement with the results from radioligand competition binding. The pK_i value of the endogenous ligand histamine determined by high content imaging with **5.18** was considerably lower compared to radioligand binding at sf9 insect cell membranes, but in good agreement with the results from flow cytometry, when using HEK293T-hH_2R-qs5 cells.

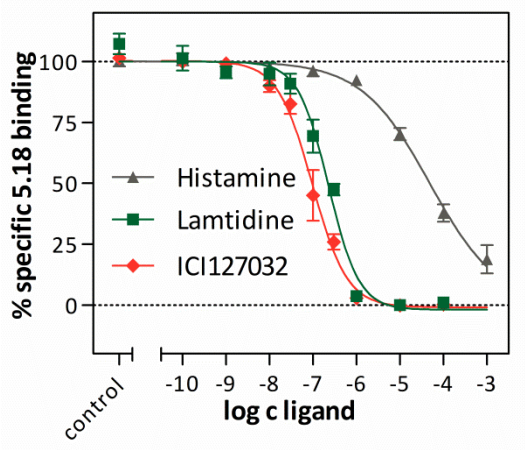

Figure 5.15. Displacement of the fluorescent ligand **5.18** (c = 50 nM, K_d = 17.9 nM) by histamine, lamtidine and ICI 127032 determined on adherent HEK293T-hH_2R-qs5 cells by high content imagig. Cells were incubated with the fluorescent ligands and the test compounds at RT in the dark for 60 min. Data represent means ± SEM from three independent experiments (each performed in duplicate or triplicate).

Table 5.8. hH_2R binding (pK_i values) of histamine, lamtidine and ICI127032 determined by radioligand binding ([^{3}H]UR-DE257) and by fluorescent ligand binding (**5.18**).

	Radioligand Binding[a]	**Fluorescent Ligand 5.18**[b]
No	**pK_i**	**pK_i**
Histamine	6.53 ± 0.04	4.54 ± 0.26
Lamtidine	6.8 ± 0.2	7.23 ± 0.03
ICI127032	7.70 ± 0.07	7.59 ± 0.09

[a]Determined by competition binding with [^{3}H]UR-DE257 (c = 20 nM) at membrane preparations of sf9 insect cells expressing hH_2R-$G_{s\alpha s}$. [b]Determined by competition binding with **5.18** (c = 50 nM) at adherent HEK293T-hH_2R-qs5 cells. Data were analyzed by nonlinear regression and were best fitted to four-parameter sigmoidal concentration-response curves. Data represent means ± SEM of 3 independent experiments, each performed in triplicate or duplicate.

The pyridinium labeled ligands **5.12** and **5.14** were also applied to binding studies on suspended HEK293T-hH_2R-qs5 cells using an imaging flow cytometer. This cytometer acquires multiple high-resolution images of every cell in the flow. The fluorescent ligands were incubated with the cells for 60 min at room temperature. The fluorescent ligands **5.12** and **5.14** were mainly localized at the cell membrane. Exemplary images of cells incubated with **5.12** (500 nM) are shown in Figure 5.16A. Only focused single cells were included in the data analysis and masks of the cell membrane and the whole cell were superimposed, enabling the determination of the fluorescent intensity in the region of interest.(Figure 5.16B and 5.16C).

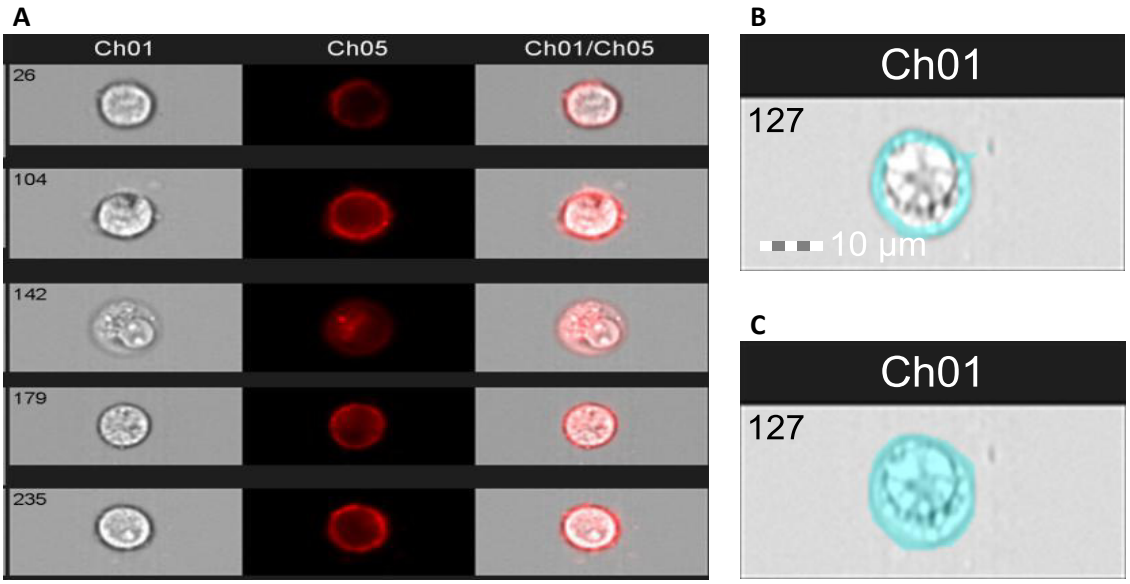

Figure 5.16. Typical images of focused single cells after 60 min of incubation with pyridinium labeled ligand **5.12** (c = 500 nM). Ch01: bright field, Ch05: emission at 702/85 nm, Ch01/Ch05: merged channels. Light blue coloring: (B) cell membrane mask and (C) cell mask.

The resulting saturation binding curves are shown in Figure 5.17 and the results are summarized in Table 5.10. The K_d values of **5.12** (88.3 nM) and **5.14** (64.9 nM) were by approx. a factor of 3 higher than the K_d values obtained by flow cytometry (Table 5.4). By contrast, the respective

dissociation constants were consistent with those (K_d values: 74.6 nM and 90.9 nM) determined by high content imaging (Table 6), irrespective of the data processing procedure.

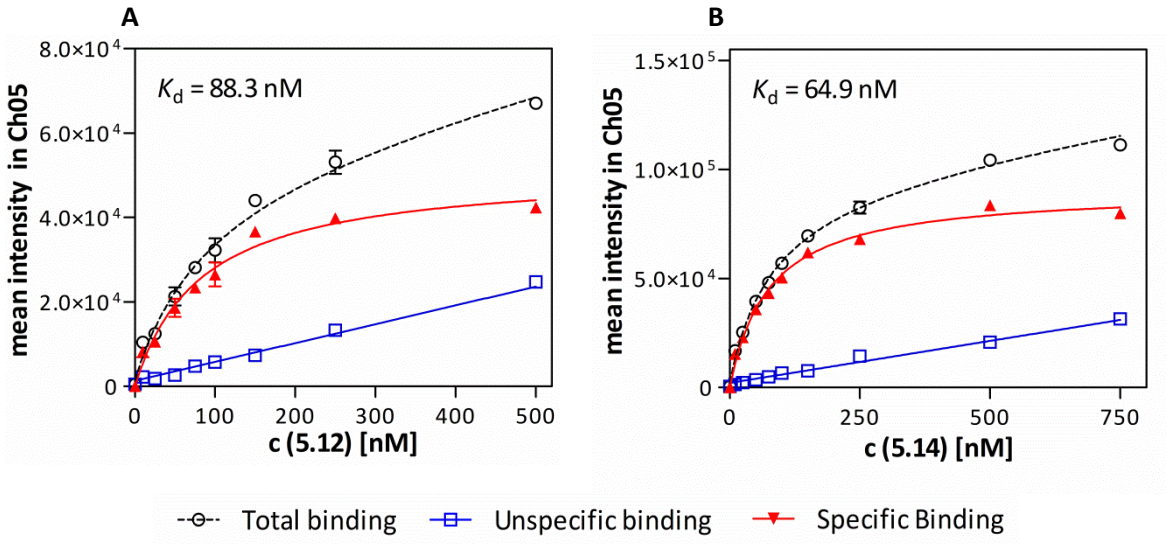

Figure 5.17. Imaging flow cytometric saturation binding experiments on adherent HEK293T-hH_2R-qs5 cells with pyridinium labeled ligands (A) **5.12** and (B) **5.14**. For the evaluation of the cell images the cell membrane mask was used. Unspecific binding was determined in the presence of famotidine (300-fold excess). Cells were incubated with the fluorescent ligands at RT in the dark for 60 min. Error bars represent mean ± SEM from at least two independent experiments (each performed in duplicate).

Table 5.9. hH_2R saturation binding data of fluorescent ligands **5.12** and **5.14** determined by imaging flow cytometry on HEK293T-hH_2R-qs5 cells.

	Imaging Flow Cytometry	
No	**K_d (nM) whole cell mask**[a]	**K_d (nM) cell membrane mask**[b]
5.12	87.9 ± 2.0	88.3 ± 5.5
5.14	62.1 ± 2.0	64.9 ± 4.6

For the evaluation of cell images either (A) the whole cell mask or (B) the cell membrane mask was used. Unspecific binding was determined in the presence of famotidine (300-fold excess). Cells were incubated with the fluorescent ligands at RT in the dark for 60 min. Error bars represent mean ± SEM from three independent experiments (each performed in duplicate). Specific binding data were analyzed by an equation describing one-site (monophasic) binding.

Additionally, histamine and ICI127032 were investigated by equilibrium competition binding experiments with fluorescent ligand **5.14** on HEK293T-hH_2R-qs5 cells using the imaging flow cytometer. The resulting pK_i values were in good agreement with the results from flow cytometry and high content image analysis (Table 5.11).

Table 5.10. hH_2R binding (pK_i values) of histamine and ICI127032 determined fluorimetrically on HEK293T-hH_2R-qs5 cells using different systems: flow cytometry (**5.14**), high content imaging on adherent cells (**5.18**) and imaging flow cytometry (**5.14**).

	Flow Cytometry (5.14)[a]	**IN Cell Analyzer (5.18)**[b]	**ImageStream X (5.14)**[c]
No	**pK_i**	**pK_i**	**pK_i**
Histamine	4.30 ± 0.04	4.54 ± 0.26	4.73 ± 0.08
ICI127032	7.73 ± 0.02	7.59 ± 0.09	7.81 ± 0.05

[a]Determined by displacement of **5.14** (c = 50 nM) in the presence of increasing concentrations of the respective H_2R ligand at intact cells by flow cytometry. [b]Determined by displacement of **5.18** (c = 50 nM) in the presence of increasing concentrations of the respective H_2R ligand at adherent cells. [c]Determined by competition binding of **5.14** (c = 70 nM) in the presence of increasing concentrations of the respective H_2R ligand at intact cells by imaging flow cytometry, for the evaluation of cell images the cell membrane mask was used. Data were analyzed by nonlinear regression and were best fitted to four-parameter sigmoidal concentration-response curves. Data represent means ± SEM of 3 independent experiments, each performed in triplicate or duplicate.

5.3 EXPERIMENTAL SECTION

5.3.1 General procedures

Chemicals and solvents were purchased from the following suppliers: Merck (Darmstadt, Germany), Acros Organics (Geel, Belgium), Sigma Aldrich (Munich, Germany) and TCI (Tokyo, Japan). The active esters of the cyanine dyes (S0586, S0536, S2197) were obtained from FEW Chemicals (Bitterfeld-Wolfen, Germany). All solvents were of analytical grade or distilled prior to use. Anhydrous solvents were stored over molecular sieve under protective gas. Deuterated solvents for NMR spectroscopy were purchased from Deutero (Kastellaun, Germany). For the preparation of buffers and HPLC eluents Millipore water was used throughout. Column chromatography was carried out using Merck silica gel 60 (0.040-0.063 mm). Reactions were monitored by thin layer chromatography (TLC) on Merck silica gel 60 F254 aluminium sheets, and compounds were detected with UV light at 254 nm and ninhydrin solution (0.8 g ninhydrin, 200 mL n-buthanol, 6 mL acetic acid). Melting points were determined with a B-540 apparatus (BÜCHI GmbH, Essen, Germany) and are uncorrected. IR spectra were measured on a NICOLET 380 FT-IR spectrophotometer (Thermo Electron Corporation, USA). Nuclear Magnetic Resonance (^{1}H NMR and ^{13}C NMR) spectra were recorded on a Bruker Avance-300 (7.05 T, ^{1}H: 300 MHz, ^{13}C: 75.5 MHz), Avance-400 (9.40 T, ^{1}H: 400 MHz, ^{13}C: 100.6 MHz), or Avance-600 (14.1 T; ^{1}H: 600 MHz, ^{13}C: 150.9 MHz; cryogenic probe) NMR spectrometer (Bruker BioSpin, Karlsruhe, Germany). Chemical shifts are given in δ (ppm) relative to external standards. Multiplicities are specified with the following abbreviations: s (singlet), d (doublet), t (triplet), q (quartet), qui (quintet), m (multiplet), br s (broad signal), as well as combinations thereof. In certain cases 2D-NMR techniques (COSY, HSQC and HMBC) were used to assign ^{1}H and ^{13}C chemical shifts. Low-resolution mass spectrometry (MS) was performed on a Finnigan ThermoQuest TSQ 7000 instrument using an electrospray ionization (ESI) source or on a Finnigan SSQ 710A instrument (EI-MS, 70 eV). High-resolution mass spectrometry (HRMS) was performed on an Agilent 6540 UHD Accurate-Mass Q-TOF LC/MS system (Agilent Technologies, Santa Clara, USA) using an ESI source. Preparative HPLC was performed with a system from Knauer (Berlin, Germany) consisting of two K-1800 pumps and a K-2001 detector. A Nucleodur 100-5 C18 (250 x21 mm, 5 µm, Macherey-Nagel, Dueren, Germany) and a Kinetex XB-C18 100A (250 x 21.2 mm, 5 µm, Phenomenex, Aschaffenburg, Germany) served as RP-columns at a flow rate of 15 ml/min at room temperature. Mixtures of CH_3CN and 0.1% aq. TFA were used as mobile phase and a detection wavelength of 220 nm was used throughout. CH_3CN was removed from the eluates containing BMY 25368, **5.9** and **5.10** under reduced pressure (final pressure: 80 mbar) at 45 °C prior to lyophilisation (Christ alpha 2-4 LD lyophilisation apparatus equipped with a vacuubrand RZ 6 rotary vane vacuum pump). In case of the fluorescently labeled ligands, the eluates were directly used for lyophilisation. Analytical HPLC analysis was performed on a system from Meck Hitachi, composed of a D-6000 interface, a L-6200A pump, a AS2000A auto sampler and a L-4000 UV-VIS detector. A Kinetex XB-C18 100A (250 x 4.6 mm, 5 µm, Phenomenex, Aschaffenburg, Germany) served as RP-column. Mixtures of 0.05% TFA in CH_3CN (A) and 0.05% aq. TFA (B) were use as mobile phase. Helium degassing, room temperature, a flow rate of 0.8 mL/min and a detection wavelength of 220 nm were used throughout. Solutions for injection (concentration: 100-500 µM) were either prepared from stock solution (5-10 mM in DMSO or DMSO/20 mM HCL 50:50) in a mixture of A and B corresponding to the initial eluent composition of the run, or as a one to one dilution of the eluate with

Millipore water. The following linear gradients were applied for analytical HPLC analysis: gradient 1: 0-30 min: A/B 5:95-80:20, 30-32 min: 80:20-95:5, 32-42 min: 95:5 or gradient 2: 0-30 min: A/B 10:90-80:20, 30-32 min: 80:20-95:5, 32-42 min: 95:5.

5.3.2 Experimental protocols and analytical data

The synthesis of the compound **4.3**[23,27] was described in chapter 4 and the tetrafluoroborate salt of Py-5[29,44] was synthesized by Mengya Chen during her master thesis.

3-Ethoxy-4-(3-[3-(piperidin-1-ylmethyl)phenoxy]propylamino)cyclobut-3-ene-1,2-dione (5.2)[23]

3,4-Diethoxycyclobut-3-ene-1,2-dione (226 mg, 1.33 mmol, 1.1 eq) was dissolved in EtOH (10 mL) and added to a solution of compound **4.3** (300 mg, 1.21 mmol, 1 eq) in EtOH (10 mL). The reaction mixture was stirred for 2 h at room temperature. After removal of the solvent under reduced pressure, the residue was dissolved in EtOAc (30 mL). The organic layer was washed with H_2O (3 x 20 mL) and dried over Na_2SO_4. The solvent was evaporated under reduced pressure and the crude product was purified by column chromatography (eluent: CH_2Cl_2 / 7 M NH_3 in MeOH 100:0-95:5). Removal of the solvent *in vacuo* afforded the product as yellow oil (350 mg, 78%). R_f = 0.5 (CH_2Cl_2 / 7 N NH_3 in MeOH 95:5). ^{1}H-NMR (400 MHz, $CDCl_3$, COSY, HSQC, HMBC): δ (ppm) 1.38-1.42 (m, 5H), 1.52-1.58 (m, 4H), 2.06-2.12 (m, 2H), 2.36 (br s, 4H), 3.42 (s, 2H), 3.66 (br s, 1.5H), 3.86 (br s, 0.6H), 4.00 (br s, 2H), 4.66-4.71 (q, 2H, *J* 7.3 Hz), 6.50 (br s, 0.2H), 6.72-6.75 (m, 1H), 6.86-6.89 (m, 2H), 7.16-7.20 (t, 1H, *J* 7.7 Hz), 7.27 (br, 0.7H); ^{13}C-NMR (100 MHz, $CDCl_3$, COSY, HSQC, HMBC): δ (ppm) 15.8, 24.3 , 25.9, 30.1, 42.4, 54.5, 63.7, 64.8, 69.7, 112.9, 115.1, 122.0, 129.1, 140.3, 158.5, 172.6, 177.5, 182.7, 189.6. HRMS: (ESI) *m/z* $[M+H]^+$ calcd. for $C_{21}H_{29}N_2O_4^+$: 373.2122, found: 373.2146. $C_{21}H_{28}N_2O_4$ (372.20).

3-Amino-4-[(3-[3-(piperidin-1-ylmethyl)phenoxy]propyl)amino]cyclo-but-3-ene-1,2-dione-hydrotrifluoracetate (BMY 25368)[24]

Compound **5.2** (180 mg, 0.48 mmol, 1 eq) was dissolved in EtOH (20 mL) and a solution of NH_3 in MeOH (7 N, 10 mL) was added. The reaction mixture was stirred over night at room temperature. The solvent was evaporated under reduced pressure and the residue was purified by column chromatography (eluent: CH_2Cl_2 / 7 M NH_3 in MeOH 95:5-90:10). Removal of the solvent *in vacuo* afforded the product as light yellow solid (123 mg, 74.1%). Mp: 199 °C decomposition (Lit.[24] mp HCl-salt: 254-257 °C). IR (KBr): 3295, 3135, 2930, 1805, 1645, 1570, 1530, 1260, 695 cm^{-1}. 50 mg of the product were further purified by preparative HPLC (column: Nucleodur, gradient: 0-30 min: MeCN/0.1% aq. TFA 15:85-75:25, t_R = 8.8 min). Removal of the solvent from eluate by evaporation and lyophilisation afforded the product as a hygroscopic white solid (53 mg). R_f = 0.4 (CH_2Cl_2 /7 N NH_3 in MeOH 7:1). RP-HPLC (gradient 2, 220 nm) (TFA-Salz): 99% (t_R = 11.38 min, *k* = 2.9). ^{1}H-NMR (400 MHz, [D_6]DMSO) (TFA-Salz): δ (ppm) 1.33-1.39 (m, 1H), 1.57-1.70 (m, 3H), 1.80-1.83 (m, 2H), 1.98-2.01 (m, 2H), 2.82-2.89 (m, 2H), 3.29-3.32 (m, 2H), 3.67 (br s, 2H, interfering with the water signal), 4.04-4.07 (t, 2H, *J* 6.0 Hz), 4.22-4.24 (d, 2H, *J* 4.9 Hz), 7.02-7.09

(m, 3H), 7.35-7.39 (t, 1H, *J* 7.9 Hz), 7.55 (br s, 1.8H), 7.68 (br s, 1H), 9.48 (br s, 1H). ^{1}H-NMR (400 MHz, $CDCl_3$, COSY, HSQC, HMBC) (TFA-Salz): *δ* (ppm) 1.46-1.56 (m, 1H), 1.70-1.83 (m, 3H), 1.91-1.95 (m, 2H), 2.07-2.17 (qui, 2H, *J* 6.2 Hz), 2.90-2.97 (m, 2H), 3.42-3.45 (m, 2H, *J* 12.6 Hz), 3.84 (br s, 2H), 4.11-4.14 (t, 2H, *J* 5.9 Hz), 4.23 (s, 2H), 7.01-7.04 (m, 3H), 7.34-7.38 (m, 1H). ^{13}C-NMR (100 MHz, $CDCl_3$, COSY, HSQC, HMBC) (TFA-Salz): *δ* (ppm) 22.7, 24.1, 31.6, 42.5, 54.1, 61.7, 66.3, 117.1, 118.3, 124.4, 131.4, 131.7, 160.7, 170.6, 170.8, 184.1, 184.4. HRMS (ESI) (TFA-Salz): *m/z* $[M+H]^+$, calcd. for $C_{19}H_{26}N_3O_3^+$: 344.1969, found: 344.1973. $C_{19}H_{25}N_3O_3 \cdot C_2HF_3O_2$ (343.19 + 114.02).

General procedure for the synthesis of the Mono-Boc-protected diamines

The corresponding alkane diamine (2 eq or 6 eq in case of butane-1,4-diamine) was dissolved in chloroform (30-35 mL). Di-*tert*-butyl dicarbonate (1 eq) was dissolved in chloroform (25-60 mL) and added dropwise over a period of 3 h under ice-cooling. The reaction mixture was allowed to warm up to room temperature while stirring overnight. Potentially precipitated alkane diamine was filtered off. The organic layer was washed with alkaline saturated NaCl solution (45 mL sat. aq. NaCl and 1 mL 1 M aq. NaOH), saturated NaCl solution (45 mL) and H_2O (45 mL). The organic layer was dried over sodium or magnesium sulphate and concentrated by evaporation under reduced pressure. The residue was purified by column chromatography on silica gel.

***tert*-Butyl *N*-(4-aminobutyl)carbamate (5.3)[45]** *Mengya Chen master thesis*

Butane-1,4-diamine (2.42 g, 27.4 mmol, 6 eq) was treated with di-*tert*-butyl dicarbonate (1 g, 4.57 mmol, 1 eq) according to the general procedure. The product was purified by column chromatography (eluent: CH_2Cl_2/1% aq.NH_3 in MeOH 25:1-7:1). Removal of the solvent *in vacuo* afforded the product as beige hygroscopic solid (790 mg, 92%). R_f = 0.2 (CH_2Cl_2/NH_3in MeOH 10:1) ^{1}H-NMR (400 MHz, $CDCl_3$): *δ* (ppm) 1.42 (s, 9H), 1.52 (m, 4H), 2.76 (br s, 2H), 3.11 (br s, 2H), 4.77 (br s, 0.8H). ^{13}C-NMR (100 MHz, $CDCl_3$): *δ* (ppm) 27.30, 28.44, 29.22, 40.28, 41.06, 79.08, 156.14. MS (LC-MS, ESI): *m/z* (%) 189 (100) $[M+H]^+$. $C_9H_{20}N_2O_2$ (188.15).

***tert*-Butyl *N*-(6-aminohexyl)carbamate (5.4)[45]**

Hexane-1,6-diamine (1.5 g, 12.9 mmol, 2 eq) was treated with di-*tert*-butyldicarbonate (1.4 g, 6.5 mmol, 1 eq) according to the general procedure. The product was purified by column chromatography (eluent: CH_2Cl_2 / 2 M NH_3 in MeOH 97.5:2.5-90:10). Removal of the solvent *in vacuo* afforded the product as colorless oil (620 mg, 44.3%). R_f = 0.8 (CH_2Cl_2/7M NH_3 in MeOH 5:1). ^{1}H-NMR (400 MHz, $CDCl_3$): *δ* (ppm) 1.29-1.33 (m, 4H), 1.40-1.48 (m, 13H), 1.53 (br s, 2H), 2.67 (t, 2H, *J* 6.9 Hz), 3.07-3.11 (t, 2H, *J* 6.5 Hz), 4.55 (br s, 1H). MS (LC-MS, ESI, t_R = 1.2 min): *m/z* (%) 217.2 (100) $[M+H]^+$, 161.1 (28) $[M-C_4H_8]^+$. HRMS (ESI): *m/z* $[M+H]^+$ calcd. for $C_{11}H_{25}N_2O_2^+$: 217.1911, found: 217.1931. $C_{11}H_{24}N_2O_2$ (216.33).

tert-Butyl _N_-(7-aminoheptyl)carbamate (5.5)[45]

Heptan-1,7-diamine (2.0 g, 15.4 mmol, 2 eq) was treated with di-*tert*-butyldicarbonate (1.7 g, 7.7 mmol, 1 eq) according to the general procedure. The product was purified by column chromatography (eluent: CH_2Cl_2 / 2 M NH_3 in MeOH 97.5:2.5-90:10) Removal of the solvent *in vacuo* afforded the product as colorless, oily solid (950 mg, 53.7%). R_f = 0.2 (CH_2Cl_2/2M NH_3 in MeOH 5:1). ^{1}H-NMR (400 MHz, $CDCl_3$): δ (ppm) 1.25 (br s, 6H), 1.31 (br s, 2H), 1.37-1.42 (m, 13H), 2.61 (t, 2H, *J* 6.9 Hz), 3.00-3.05 (m, 2H), 4.67 (br s, 1H). MS (LC-MS, ESI, t_R = 1.4 min): *m/z* (%) 231.2 (100), $[M+H]^+$, 175.1 (23) $[M-C_4H_8]^+$. HRMS (ESI): *m/z* $[M+H]^+$ calcd. for $C_{12}H_{27}N_2O_2^+$: 231.1067, found: 231.2066. $C_{12}H_{26}N_2O_2$ (230.35).

General procedure for the synthesis of Boc-protected squaramides with alkylamine spacers

Compound **5.2** (1 eq) was dissolved in EtOH (15-25 mL) and added to the respective mono-Boc-protected diamine (1.1 eq) in EtOH (15-25 mL). The reaction mixture was stirred over night at room temperature. The solvent was evaporated under reduced pressure and the product was crystallized from EtOAc (2 mL), NH_3 in MeOH (7 M, 50 µL) and n-hexane (3 mL). The precipitate was purified by column chromatography on silica gel.

tert-Butyl [4-([3,4-dioxo-2-[(3-[3-(piperidin-1-ylmethyl)phenoxy]propyl)amino]cyclobut-1-en-1-yl]amino)butyl]carbamate (5.6)

Compound **5.6** was synthesized from **5.2** (2.8 g, 7.63 mmol, 1 eq) and **3** (1.58 g, 8.39 mmol, 1.1 eq) according to the general procedure. The product was purified by column chromatography (eluent: CH_2Cl_2/1% aq. NH_3 in MeOH 40:1-20:1). Removal of the solvent *in vacuo* afforded the product as light yellow hygroscopic solid (1.66 g, 42%). R_f = 0.2 (CH_2Cl_2/2M NH_3 in MeOH 5:1). ^{1}H-NMR (400 MHz, $CDCl_3$): δ (ppm) 1.41 (s, 9H), 1.49-1.73 (m, 6H), 1.88 (br s, 4H), 2.00-2.19 (m, 2H), 2.95 (br s, 4H), 3.09-3.15 (m, 2H), 3.65 (q, *J* 6.3 Hz, 2H), 3.80 (q, *J* 6.2 Hz, 2H), 3.94 (s, 2H), 4.15 (t, *J* 6.3 Hz, 2H), 4.87 (br s, 1H), 6.85-6.91 (m, 2H), 7.22-7.26 (m, 2H), 7.99 (br s, 1.8H). ^{13}C-NMR (100 MHz, $CDCl_3$): δ (ppm) 22.6, 23.5, 26.9, 28.5, 30.4, 40.1, 41.1, 44.1, 53.4, 53.8, 62.2, 65.4, 79.1, 116.2, 116.7, 122.9, 129.9, 141.8, 156.2, 159.3, 168.0, 168.6, 182.4, 182.5. HRMS (ESI): *m/z* $[M+H]^+$ calcd. for $C_{28}H_{43}N_4O_5^+$: 515.3228, found: 515.3230. $C_{28}H_{42}N_4O_5$ (514.32).

tert-Butyl (6-[(3,4-dioxo-2-[(3-[3-(piperidin-1-ylmethyl)phenoxy]propyl)amino]cyclobut-1-en-1-yl)amino]hexyl)carbamate (5.7)[23]

Compound **5.7** was synthesized from **5.2** (160 mg, 0.43 mmol, 1 eq) and **5.4** (102 mg, 0.47 mmol, 1.1 eq) according to the general procedure. The product was purified by column chromatography (eluent: CH_2Cl_2 / 3.5 M NH_3 in MeOH 97.5:2.5-95:5). Removal of the solvent *in vacuo* afforded the product as light yellow solid (193 mg, 83%). Mp: 115.9-118.7 °C. R_f = 0.8 (CH_2Cl_2 / 7 M NH_3 in MeOH 90:10). ^{1}H-NMR (400 MHz, $CDCl_3$): δ (ppm) 1.30-1.47 (m, 17H), 1.59-1.62 (m, 6H), 2.08-2.14 (qui, 2H, *J* 6.3 Hz), 2.46 (br s, 4H), 3.03-3.08 (m, 2H), 3.48 (s, 2H), 3.60-3.65 (m, 2H), 3.79-

3.84 (m, 2H,), 4.02-4.05 (t, 2H, *J* 6.0 Hz), 5.13 (br s, 1H), 6.76-6.78 (dd, 1H, *J* 8.1 Hz, *J* 1.9 Hz), 6.84-6.89 (m, 2H), 7.16-7.20 (t, 1H, *J* 7.8 Hz), 7.36 (br s, 1.5 H). HRMS (ESI): *m/z* $[M+H]^+$ calcd. for $C_{30}H_{47}N_4O_5^+$: 543.3541, found: 543.3562. $C_{30}H_{46}N_4O_5$ (542.72).

tert-Butyl (7-[(3,4-dioxo-2-[(3-[3-(piperidin-1-ylmethyl)phenoxy]propyl)amino]cyclobut-1-en-1-yl)amino]heptyl)carbamate (5.8)

Compound **5.8** was synthesized from **5.2** (260 mg, 0.70 mmol, 1 eq) und **5.5** (177 mg, 0.77 mmol, 1.1 eq) according to the general procedure. The product was purified by column chromatography (eluent: CH_2Cl_2 / 3.5 M NH_3 in MeOH 97.5:2.5-95:5). Removal of the solvent *in vacuo* afforded the product as light yellow solid (204 mg, 48%). Mp: 109.8-112.9 °C. R_f = 0.9 (CH_2Cl_2 / 7 M NH_3 in MeOH 7:1). ^{1}H-NMR (400 MHz, $CDCl_3$): δ (ppm) 1.25-1.43 (m, 19H), 1.52-1.59 (m, 6H), 2.08-2.14 (qui, 2H, *J* 6.3 Hz), 2.37 (br s, 4H), 3.01-3.06 (m 2H), 3.40 (s, 2H), 3.60-3.64 (m, 2H), 3.82-3.84 (m, 2H), 4.01-4.04 (t, *J* 6.1 Hz, 2H), 5.15 (br s, 0.7H), 6.73-6.75 (m, 1H), 6.85-6.87 (m, 2H), 7.16 (t, 1H, *J* 7.8 Hz), 7.42 (br s, 0.7H), 7.50 (br s, 1H). ^{13}C-NMR (100 MHz, $CDCl_3$): δ (ppm) 24.4, 26.0, 26.5, 26.6, 28.6, 28.8, 30.0, 30.9, 31.0, 40.5, 41.7, 44.8, 54.7, 64.0, 64.9, 79.3, 113.4, 115.3, 122.1, 129.2, 140.1, 156.6, 158.8, 168.4, 182.6, 182.7. HRMS (ESI): *m/z* $[M+H]^+$ calcd. for $C_{31}H_{49}N_4O_5^+$: 557.3697, found: 557.3713. $C_{31}H_{48}N_4O_5$ (556.75).

3-((4-Aminobutyl)amino)-4-((3-(3-(piperidin-1-ylmethyl)phenoxy)propyl)amino)cyclobut-3-ene-1,2-dione bis(hydrotrifluoracetate) (5.9)[23]

Compound **5.6** (100 mg, 0.11 mmol, 1 eq) was stirred for 24 h at room temperature in a mixture of CH_2Cl_2 (25-30 mL) and TFA (1 mL). Removal of the solvent *in vacuo* afforded the product as a yellow hygroscopic solid (118 mg, 94%). For pharmacological characterization 57 mg of **9** were further purified by preparative HPLC (column: Kinetex, gradient: 0-30 min: MeCN/0.1% aq. TFA 5:95-60:40, t_R = 12.8 min). The TFA-salt was obtained as white sticky solid (40 mg; 65%).R_f = 0.1 (CH_2Cl_2/1.8M NH_3 in MeOH 90:10). RP-HPLC (gradient 2, 220 nm): 98% (t_R = 10.66 min, *k* = 2.7). ^{1}H-NMR (600 MHz, [D_4]MeOH): δ (ppm) 1.47-1.54 (1H, m), 1.70-1.83 (7H, m), 1,92-1.94 (2H, m), 2.10 (2H, qui, *J* 6.3 Hz), 2.91-2.97 (4H, m), 3.42-3.44 (2H, m), 3.62 (2H, br s), 3.83 (2H, br s), 4.12 (2H, t, *J* 6.0 Hz), 4.22 (2H, s), 7.02-7.04 (2H, m), 7.08 (1H, br s), 7.36 (1H, t, *J* 7.9 Hz). ^{13}C-NMR (150 MHz, [D_4]MeOH) (TFA-Salz): δ (ppm) 22.7, 24.1, 25.3, 29.1, 31.7, 40.2, 42.4, 44.3, 54.1, 61.7, 66.2, 118.4, 124.5, 131.4, 131.7, 160.8, 162.5 (q, *J* 40 Hz, TFA), 169.5, 169.7, 183.6 (2C). HRMS (ESI): *m*/z $[M+H]^+$ calcd. for $C_{23}H_{35}N_4O_3^+$: 415.2709, found: 415.2709. $C_{23}H_{34}N_4O_3 \cdot C_4H_2F_6O_4$ (414.26 + 228.05).

General procedure for the Boc-deprotection of the amine precursors

The corresponding Boc-protected squaramide derivative (**5.7** or **5.8**) was stirred for 4-24 h at room temperature in a mixture of CH_2Cl_2 (25-30 mL) and HCl in 2-propanol (5-6 M, 13-15 mL). Removal of the solvent *in vacuo* afforded the product as HCl salt. Part of the product was further purified by preparative HPLC.

3-((6-Aminohexyl)amino)-4-((3-(3-(piperidin-1-ylmethyl)phenoxy)propyl)amino)cyclobut-3-ene-1,2-dione bis(hydrotrifluoracetate) (5.10)[23]

Compound **5.10** was synthesized from **5.7** (185 mg, 0.34 mmol, 1 eq) according to the general procedure. Removal of the solvent *in vacuo* afforded the product as yellow hygroscopic solid (188 mg). For pharmacological characterization 40 mg of **5.10** were purified by preparative HPLC (column: Nucleodur, gradient: 0-30 min: MeCN/0.1% aq. TFA 15:85-75:25, t_R = 8.4 min). The TFA-salt was obtained as highly hygroscopic sticky solid (45 mg; 93%). R_f (TFA-Salz) = 0.1 (CH_2Cl_2/7M NH_3 in MeOH 7:1). RP-HPLC (gradient 2, 220 nm) (TFA-Salz): 98% (t_R = 12.17 min, k = 3.2). ^{1}H-NMR (400 MHz, [D_4]MeOH) (TFA-Salz): δ (ppm) 1.42-1.44 (m, 4H), 1.48-1.57 (m, 1H), 1.62-1.68 (m, 4H), 1.70-1.84 (m, 3H), 1.91-1.96 (m, 2H), 2.07-2.14 (qui, 2H, *J* 6.3 Hz), 2.90-2.98 (m, 4H), 3.43-3.46 (m, 2H), 3.60 (br s, 2H), 3.83 (br s, 2H), 4.13 (t, 2H, *J* 5.9 Hz), 4.23 (s, 2H), 7.02-7.07 (m, 3H), 7.37 (t, 1H, *J* 7.9 Hz). ^{13}C-NMR (100 MHz, [D_4]MeOH) (TFA-Salz): δ (ppm) 22.7, 24.1, 26.77, 26.85, 28.4, 31.6, 32.0, 40.6, 42.4, 45.0 , 54.1, 61.7, 66.3, 117.2, 118.3, 124.5, 131.4, 131.7, 160.8, 162.2 (q, *J* 41 Hz, TFA), 169.7 (2C), 183.6, 183.9. HRMS (TFA-Salz): (ESI): *m/z* [*M*+H]$^+$ calcd. for $C_{25}H_{39}N_4O_3^+$: 443.3017, found: 443.3019. $C_{25}H_{38}N_4O_3 \cdot C_4H_2F_6O_4$ (442.60 + 228.05).

3-((7-Aminoheptyl)amino)-4-((3-(3-(piperidin-1-ylmethyl)phenoxy)propyl)amino)cyclobut-3-ene-1,2-dione bis(hydrotrifluoracetate) (5.11)

Compound **5.11** was synthesized from **5.8** (187 mg, 0.33 mmol, 1 eq) according to the general procedure. Removal of the solvent *in vacuo* afforded the product as yellow hygroscopic solid (197 mg). For pharmacological characterization 85 mg of **5.11** were further purified by preparative HPLC (column: Nucleodur, gradient: 0-30 min: MeCN/0.1% aq. TFA 15:85-75:25, t_R = 9.1 min). The TFA-salt was obtained as white hygroscopic solid (84 mg, 76%). R_f (TFA-Salz) = 0.5 (CH_2Cl_2/7M NH_3 in MeOH 5:1). RP-HPLC (gradient 2, 220 nm) (TFA-Salz): 98% (t_R = 12.83 min, k = 3.4). ^{1}H-NMR (400 MHz, [D_6]DMSO) (TFA-Salz): δ (ppm) 1.28-1.39 (m, 7H), 1.51 (br s, 4H), 1.61-1.68 (m, 3H), 1.79-1.82 (m, 2H), 1.97-2.03 (qui, 2H, *J* 6.3 Hz), 2.72-2.89 (m, 4H), 3.29-3.32 (m, 2H), 3.48 (br s, 2H), 3.67-3.68 (br s, 2H), 4.05 (t, 2H, *J* 6.2 Hz), 4.23 (d, 2H, *J* 5.0 Hz), 7.00-7.05 (m, 2H), 7.09 (br s, 1H), 7.36 (t, 1H, *J* 7.9 Hz), 7.76-7.82 (br s, 5H), 9.68 (br s, 0.9H). ^{1}H-NMR (400 MHz, [D_4]MeOH, COSY, HSQC, HMBC) (TFA-Salz): δ (ppm) 1.39 (br s, 6H), 1.48-1.67 (m, 5H), 1.71-1.82 (m, 3H), 1.90-1.94 (m, 2H), 2.07-2.13 (qui, 2H, *J* 6.2 Hz), 2.89-2.98 (m, 4H), 3.42-3.45 (m, 2H), 3.59 (br s, 2H), 3.83 (br s, 2H), 4.12 (t, 2H, *J* 5.9 Hz), 4.23 (s, 2H), 7.01-7.07 (m, 3H), 7.35 (t, 1H, *J* 7.8 Hz). ^{13}C-NMR (100 MHz, [D_4]MeOH, COSY, HSQC, HMBC) (TFA-Salz): δ (ppm) 22.7, 24.0, 27.0, 27.2, 28.4, 29.6, 31.6, 32.0, 40.6, 42.4, 45.1, 54.0, 61.7, 66.2, 117.3, 117.8 (q, *J* 291 Hz, TFA), 118.2, 124.5, 131.3, 131.7, 160.7, 162.2 (q, *J* 37 Hz, TFA), 169.5 (2C), 183.3, 183.5. HRMS (TFA-Salz): (ESI): *m/z* [*M*+H]$^+$ calcd. for $C_{26}H_{41}N_4O_3^+$: 457.3173, found.: 457.3178. $C_{26}H_{40}N_4O_3 \cdot C_4H_2F_6O_4$ (456.63 + 228.05).

General procedure for the synthesis of pyridinium-labeled fluorescent ligands

The respective amine-precursor **5.9**, **5.10** or **5.11** (1 eq) was dissolved in anhydrous DMF (200-400 µL) and DIPEA (10 eq) or TEA (2-3 drops). The pyrylium dye Py-5 (3-8 eq) in anhydrous DMF

(180-200 µl) was added portion wise (50 µL) every 20-30 min. Subsequent to the last addition, the reaction mixture was incubated for additional 30 min at RT in the dark. The reaction was stopped by addition of TFA (10 % in H_2O_{milliQ}, 50-200 µL). After dilution with a mixture of H_2O_{milliQ} with 5% MeCN and 0.1% TFA (2 mL) the respective fluorescently labeled ligand was isolated as TFA-salt by preparative HPLC. After lyophilisation of the eluate the product was obtained as a red highly hygroscopic solid.

Compound 5.9 labeled with Py-5 (5.12)[25] *Mengya Chen master thesis*

5.9 (1.95 mg, 4 µmol, 1 eq), Py-5 (4.41 mg, 12 µmol, 3 eq) and TEA (2-3 drops) were applied according to the general procedure. Purification by preparative HPLC (column: Kinetex, gradient: 0-30 min: MeCN/0.1% aq. TFA 5:95-90:10, t_R = 15.5 min) and removal of the solvent by lyophilisation afforded **5.12** as a highly hygroscopic, red solid (1.17 mg, 32%). RP-HPLC (gradient 2, 220 nm): 96.9% (t_R = 16.4 min, k = 4.7). HRMS (ESI): *m/z* $[M]^+$ calcd. for $C_{42}H_{54}N_5O_3^+$: 676.4221, found: 676.4227. $C_{42}H_{54}N_5O_3^+ \cdot C_4HF_6O_4$ (676.42+ 227.04).

Compound 5.10 labeled with Py-5 (5.13) *Mengya Chen master thesis*

5.10 (2.21 mg, 5.00 µmol, 1 eq), Py-5 (11.02 mg, 30.00 µmol, 6 eq) and TEA (2-3 drops) were applied according to the general procedure. Purification by preparative HPLC (column: Kinetex, gradient: 0-30 min: MeCN/0.1% aq. TFA 10:90-90:10, t_R = 16.4 min) and removal of the solvent by lyophilisation afforded **5.13** as a highly hygroscopic, red solid (1.46 mg, 31%). RP-HPLC (gradient 2, 220 nm): 95.1% (t_R = 18.1 min, k = 5.2). ^{1}H-NMR (600 MHz, [D_4]MeOH): δ (ppm) 1.48-1.59 (m, 5H), 1.65-1.70 (m, 2H), 1.72-1.80 (m, 2H), 1.82-1.88 (m, 3H), 1.93-1.95 (m, 2H), 2.08-2.13 (qui, 2H, *J* 6.3 Hz), 2.80 (s, 6H), 2.92-2.97 (m, 2H), 3.03 (s, 6H), 3.42-3.45 (m, 2H), 3.62 (br s, 2H), 3.83 (br s, 2H), 4.13 (t, 2H, *J* 6.0 Hz), 4.23 (s, 2H), 4.36-4.38 (m, 2H), 6.58 (d, 1H, *J* 15.3 Hz), 6.77 (d, 2H, *J* 8.8 Hz), 6.93-6.97 (m, 1H), 7.00-7.07 (m, 4H), 7.37 (t, 1H, *J* 8.2 Hz), 7.44 (d, 2H, *J* 8.9 Hz), 7.63-7.68 (m, 1H), 7.71 (s, 2H). HRMS (ESI): *m/z* $[M]^+$ calcd. for $C_{44}H_{58}N_5O_3^+$: 704.4534, found: 704.4542. $C_{44}H_{58}N_5O_3^+ \cdot C_4HF_6O_4$ (704.45+ 227.04).

Compound 5.11 labeled with Py-5 (5.14)

5.11 (5 mg, 7.30 µmol, 1 eq), Py-5 (21.4 mg, 58.42 µmol, 8 eq) and DIPEA (12.8 µL, 73.03 µmol, 10 eq) were applied according to general procedure. Purification by preparative HPLC (column: Kinetex, gradient: 0-30 min: MeCN/0.1% aq. TFA 5:95-45:55, t_R = 28.9 min) and removal of the solvent by lyophilisation afforded **5.14** as a highly hygroscopic, red solid (1.59 mg, 24%). RP-HPLC (gradient 2, 220 nm): 96% (t_R = 18.4 min, k = 5.4). HRMS (ESI): *m/z* $[M]^+$ calcd. for $C_{45}H_{60}N_5O_3^+$: 718.4691, found: 718.4698. $C_{45}H_{60}N_5O_3^+ \cdot C_4HF_6O_4$ (718.47+ 227.04).

General procedure for the synthesis of cyanine-labeled fluorescent ligands

A solution of the activated fluorescent dye (1 eq) in anhydrous DMF (30-100 µl) was added to the respective amine-precursor **5.9** or **5.10** (2.0-3.3 eq) dissolved in anhydrous DMF (100 µL) and DIPEA (8-10 eq). The reaction mixture was incubated for 45-90 min at RT in the dark. The reaction was stopped by addition of TFA (10 % in H_2O_{milliQ}, 45-60 µL). After dilution with a mixture of H_2O_{milliQ} with 5% MeCN and 0.1% TFA (150-250 µL) the respective fluorescently labeled ligand was isolated as TFA-salt by preparative HPLC. After lyophilisation of the eluate the product was obtained as a blue fluffy solid.

Compound 5.9 labeled with S0223 (5.15)

5.9 (8.88 mg, 13.12 µmol, 2.5 eq), S2197 (3.65 mg, 4.84 µmol, 1 eq) and DIPEA (7.7 µL, 44.20 µmol, 8 eq) were applied according to the general procedure. Purification by preparative HPLC (column: Kinetex, gradient: 0-30 min: MeCN/0.1% aq. TFA 15:85-70:30, t_R = 24.1 min) and removal of the solvent by lyophilisation afforded **5.15** as a hygroscopic, blue fluffy solid (1.13 mg, 18%). RP-HPLC (gradient 1, 220 nm): 96% (t_R = 25.3 min, k = 7.7). HRMS (ESI): *m/z* $[M]^+$ calcd. for $C_{55}H_{71}N_6O_4^+$: 879.5531, found: 879.5533. $C_{55}H_{71}N_6O_4^+ \cdot C_4HF_6O_4^-$ (880.21 + 227.04).

Compound 5.10 labeled with S0223 (5.16)

5.10 (11.0 mg, 17.03 µmol, 3 eq), S2197 (3.75 mg, 5.68 µmol, 1 eq) and DIPEA (9.9 µL, 56.76 µmol, 10 eq) were applied according to the general procedure. Purification by preparative HPLC (column: Kinetex, gradient: 0-30 min: MeCN/0.1% aq. TFA 15:85-70:30, t_R = 24.9 min) and removal of the solvent by lyophilisation afforded **5.16** as a hygroscopic, blue fluffy solid (2.49 mg, 39%). RP-HPLC (gradient 2, 220 nm): 99% (t_R = 25.6 min, k = 7.8). HRMS (ESI): *m/z* $[M]^+$ calcd. for $C_{57}H_{75}N_6O_4^+$: 907.5844, found: 907.5839. $C_{57}H_{75}N_6O_4^+ \cdot C_4HF_6O_4^-$ (908.26 + 227.04).

Compound 5.9 labeled with S0436 (5.17)[25]

5.9 (7.78 mg, 12.11 µmol, 2.5 eq), S0536 (3.40 mg, 4.84 µmol, 1 eq) and DIPEA (6.8 µL, 38.75 µmol, 8 eq) were applied according to general procedure. Purification by preparative HPLC (column: Kinetex, gradient: 0-30 min: MeCN/0.1% aq. TFA 10:90-65:35, t_R = 22.6 min) and removal of the solvent by lyophilisation afforded **5.17** as a hygroscopic, blue fluffy solid (1.49 mg, 25%). RP-HPLC (gradient 1, 220 nm): 97% (t_R = 23.8 min, k = 7.2). HRMS (ESI): *m/z* $[M+H]^+$ calcd. for $C_{58}H_{77}N_6O_7S^+$: 1001.5569, found: 1001.5573. $C_{58}H_{76}N_6O_7S \cdot C_4H_2F_6O_4$ (1001.34 + 228.05).

Compound 5.10 labeled with S0436 (5.18)[25]

5.10 (8.0 mg, 11.93 µmol, 3.3 eq), S0536 (2.55 mg, 3.63 µmol, 1 eq) and DIPEA (5.1 µL, 29.01 µmol, 8 eq) were applied according to the general procedure. Purification by preparative HPLC (column: Kinetex, gradient: 0-30 min: MeCN/0.1% aq. TFA 5:95-65:35, t_R = 27.0 min) and removal

of the solvent by lyophilisation afforded **5.18** as a hygroscopic, blue fluffy solid (1.53 mg, 34%). RP-HPLC (gradient 2, 220 nm): 97% (t_R = 23.1 min, k = 7.0). ^{1}H-NMR (600 MHz, [D$_4$]MeOH): δ (ppm) 1.33-1.36 (5H, m), 1.43-1.52 (5H, m), 1.58-1.61 (2H, m), 1.67-1.84 (18H, m), 1.90-1.94 (4H, m), 1.96-2.02 (2H, m),2.04-2.08 (2H, m), 2.20 (2H, t, *J* 7.1 Hz), 2.87-2.95 (4H, m), 3.14 (2H, t, *J* 6.8 Hz), 3.40-3.42 (2H, m), 3.56 (2H, br s), 3.78 (2H, br s), 4.08-4.14 (6H, m), 4.20 (2H, s), 6.26 (1H, d, *J* 13.7 Hz), 6.32 (1H, d, *J* 13.7 Hz), 6.60 (1H, *J* 12.7 Hz), 6.98-7.01 (2H, m), 7.08 (1H, s), 7.23-7.34 (5H, m), 7.40 (2H, t, *J* 7.7 Hz), 7.47 (2H, t, *J* 7.0 Hz), 8.22 (2H, t, *J* 13.1 Hz). HRMS (ESI): *m/z* [*M*+H]$^+$ calcd. for $C_{60}H_{81}N_6O_7S^+$: 1029.5882, found: 1029.5883. $C_{60}H_{80}N_6O_7S \cdot C_4H_2F_6O_4$ (1029.40 + 228.05).

Compound 5.9 labeled with S0387 (5.19).

5.9 (5.1 mg, 7.93 µmol, 2.5 eq), S0586 (2.6 mg, 3.17 µmol, 1 eq) and DIPEA (4.4 µL, 25.38 µmol, 8 eq) were applied according to general procedure. Purification by preparative HPLC (column: Kinetex, gradient: 0-30 min: MeCN/0.1% aq. TFA 5:95-55:45, t_R = 22.6 min) and removal of the solvent by lyophilisation afforded **5.19** as a hygroscopic, blue fluffy solid (1.82 mg, 44%). RP-HPLC (gradient 1, 220 nm): 98% (t_R = 18.6 min, k = 5.4). HRMS (ESI): *m/z* [*M*+H]$^+$ calcd. for $C_{58}H_{77}N_6O_{10}S_2^+$: 1081.5137, found: 1081.5140. $C_{58}H_{76}N_6O_{10}S_2 \cdot C_4H_2F_6O_4$ (1081.40 + 228.05).

Compound 5.10 labeled with S0387 (5.20)

5.10 (4.76 mg, 7.09 µmol, 2 eq), S0586 (2.85 mg, 3.54 µmol, 1 eq) and DIPEA (4.8 µL, 27.61 µmol, 8 eq) were applied according to the general procedure. Purification by preparative HPLC (column: Kinetex, gradient: 0-30 min: MeCN/0.1% aq. TFA 5:95-55:45, t_R = 23.5 min) and removal of the solvent by lyophilisation afforded **5.20** as a hygroscopic, blue fluffy solid (0.91 mg, 19%). RP-HPLC (gradient 2, 220 nm): 99% (t_R = 17.6 min, k = 5.1). HRMS (ESI): *m/z* [*M*+H]$^+$ calcd. for $C_{60}H_{81}N_6O_{10}S_2^+$: 1109.5450, found: 1109.5447. $C_{60}H_{80}N_6O_{10}S_2 \cdot C_4H_2F_6O_4^-$ (1109.45 + 228.05).

Fluorescence spectroscopy and determination of quantum yields[30]

The recording of fluorescence spectra and the determination of quantum yields were performed with a Cary Eclipse spectrofluorometer (Varian Inc., Mulgrave, Victoria, Australia). The photomultiplier voltage of the spectrofluorimeter was set to 400 V throughout. Depicted excitation and emission spectra were recorded with an excitation slit of 10 nm and an emission slit of 10 nm. Appropriate concentrations of the fluorescent ligands, with absorbances between 0.1 and 0.2 at the respective excitation wavelength, were determined with a Cary 100 UV/VIS (Varian Inc., Mulgrave, Victoria, Australia) photometer. Absorption spectra were recorded within a concentration range of 1.5-6 µM. The excitation wavelength was chosen as close to the absorption maximum as possible (**5.13**, **5.14**) or at an inflection point (**5.20**, **5.18**, **5.16** and cresyl violet perchlorate). For the determination of quantum yields, cresyl violet perchlorate (Acros Organics, Geel, Belgium), with a reported quantum yield of 54% in EtOH[46], was used as a standard. All spectra were recorded in acryl cuvettes (10 x 10 mm, Ref. 67.755, Sarstedt, Nümbrecht, Germany).

Solutions of the fluorescent ligands in PBS and PBS containing 1% BSA (both pH 7.4) were prepared from 5 mM stock solutions in DMSO. Spectra of the cresyl violet standard were recorded in EtOH. The pure solvents with the same DMSO content were used as reference. The absorption spectra were immediately recorded at 22 °C. The emission spectra were recorded within 15-20 min after preparation of the solutions at a temperature of 22 °C using a 'medium scan rate'. The filter settings were 'auto' for the excitation and 'open' for the emission filter. Fluorescence spectra were recorded at two different slit adjustments (excitation/emission): 10/10 nm and 10/5 nm. The emission starting point was set 15 nm above the excitation wavelength. From every emission spectrum the corresponding reference spectrum was subtracted and the resulting net spectrum was multiplied with the corresponding lamp correction spectrum. These corrected net spectra were integrated up to 850 nm. From every raw absorption spectrum the corresponding reference spectrum was subtracted to afford the net absorption spectra. The absorbance at the excitation wavelength was obtained from the net absorption spectra. The quantum yield was calculated according to the following equation:

$$\phi_{F(X)} = (A_s/A_x)(F_x/F_s)(n_x/n_s)^2\phi_{F(S)}$$

A_s is the absorbance and F_s the integral of the corrected net emission spectrum of the cresyl violet standard solution. A_x and F_x are the absorbance and the integral of the corrected net emission spectrum of the fluorescent ligand. The refractive indices of the solvents for the fluorescent ligands and the cresyl violet standard are denoted n_x and n_s (fluorescent ligands: n_{PBS} = 1.33; BSA content was neglected and cresyl violet: n_{EtOH} = 1.36). The reported quantum yield of cresyl violet perchlorate (in this case 54%) is referred to as $\phi_{F(X)}$.

5.4.3 Pharmacological Methods

Radioligand competition binding assay on Sf9 insect cell membranes

Preparation of the membranes of Sf9 insect cells expressing the hH_2R-$G_{s\alpha S}$ fusion protein or co-expressing the $hH_3R + G_{i\alpha 2} + \beta_1\gamma_2$ or $hH_4R + G_{i\alpha 2} + \beta_1\gamma_2$ proteins was described elsewhere.[47]

Radioligand competition binding assays were performed as described previously with minor adjustments using the following radioligands: [^{3}H]UR-DE257[23] (specific activity = 32.89 Ci/mmol, hH_2R: K_d = 12.2 nM, c_{final} = 20 nM) and [^{3}H]histamine (Hartmann Analytic, Braunschweig, Germany; specific activity = 25 Ci/mmol; hH_3R: K_d = 12.1 nM, c_{final} = 15 nM, hH_4R: K_d = 15.9 nM, c_{final} = 10 nM).

On the day of the experiment Sf9 membranes were thawed and sedimented by centrifugation at 13,000 rpm at 4 °C for 10 min. The membranes were resuspended in ice cold binding buffer (12.5 mM $MgCl_2$, 1mM EDTA and 75 mM Tris/HCl, pH 7.4; in the following referred to as BB) and adjusted to a protein concentration of 2-4 µg/µL. 80 µL BB containing 0.2% BSA and the respective radioligand, followed by 10 µL of the investigated ligands at various concentrations (dissolved in H_2O), were added to every well of a 96-well plate (in case of fluorescent ligands: Primaria clear flat bottom microplates, Corning, New York, USA; for other ligands: PP microplates 96 well, Greiner Bio-One, Frickenhausen, Germany). Incubation was started by addition of the

membrane suspension (10 µL). The plates were shaken for 60 min at room temperature in the dark. Subsequently, bound radioligand was separated from free radioligand by filtration through glass microfiber filters (Whatman GF/C, Maidstone, UK), treated with 0.3% polyethylenimine (PEI), using a 96-well Brandel harvester (Brandel Inc., Unterföhring, Germany). The punched out filter pieces were transferred into clear, flexible 96-well PET microplate (round bottom, 1450-401, Perkin Elmer, Rodgau, Germany). Each well was supplemented with 200 µL scintillation cocktail (Rotiscint Eco plus, Roth, Karlsruhe, Germany) and incubated in the dark for at least 4 h. The radioactivity was measured with a MicroBeta2 1450 scintillation counter (Perkin Elmer, Rodgau, Germany).

Functional GTPγS assay on Sf9 insect cell membranes

GTPγS assays were performed as described previously[48] with minor modifications. [^{35}S]GTPγS (specific activity = 1000 Ci/mmol) was purchased from Hartmann Analytic (Braunschweig, Germany). Sf9 membranes were prepared in the same manner as for radioligand competition binding and the protein concentration was adjusted to 0.5-1.5 µg/µL.

Agonist mode: 80 µL of BB containing BSA (0.05% final), GDP (1 µM final) and [^{35}S]GTPγS (20 nCi final), followed by 10 µL of the investigated ligands at various concentrations (dissolved in H_2O) were added to every well of a 96-well plate (in case of fluorescent ligands: Primaria microplates; for other ligands: PP microplates). Incubation was started by addition of the membrane suspension (10 µL). The plates were shaken for 60 min at room temperature in the dark. Subsequently, bound radioligand was separated from free radioligand by filtration through glass microfiber filters (Whatman GF/C, Maidstone, UK) using a 96-well Brandel harvester (Brandel Inc., Unterföhring, Germany).

Antagonist mode of the GTPγS assay was performed in the same way as the agonist mode, but in the presence of the agonist histamine (1 µM final).

Cell culture

The preparation of stably transfected HEK cells (HEK293T-hH_2R-qs5[26] and HEK293T-hH_2R-βArr2[33,49]) was described elsewhere.

Cells were cultivated at 37 °C in a water saturated atmosphere containing 5% CO_2. Dulbecco´s Modified Eagle Medium, containing 4.5 g/L glucose, 3.7 g/L $NaHCO_3$, 110 mg/L sodium pyruvate (DMEM, Sigma-Aldrich Munich, Germany) and supplemented with 0.584 g/L L-glutamine (L-glutamine solution, Sigma-Aldrich Munich, Germany), 1% (v/v) Penicillin-Streptomycin (P/S, 10,000 U/mL, Sigma-Aldrich Munich, Germany), 10% (v/v) fetal calf serum (FCS, Biochrom GmbH, Merck, Berlin, Germany) were used as a culture medium. Additionally, 100 µg/mL hygromycin B (A.G. Scientific, Inc., San Diego, CA) and 400 µg/mL G418 (Biochrom GmbH, Merck, Berlin, Germany) were added to the culture medium of HEK293T-hH_2R-qs5 cells, and 400 µg/mL zeocin (InvivoGen, San Diego,USA) and 600 µg/mL G418 were added to the culture medium of HEK293T-hH_2R-βArr2 cells.

Flow cytometric binding assays

All flow cytometric binding studies were performed with a FACS Calibur™ flow cytomter (Becton Dickinson, Heidelberg, Germany), equipped with an argon laser (488 nm) and a red diode laser (635 nm) according to general protocols[26,50] with minor adjustments. The following instrument settings were used: FSC: E-1, SSC: 280 V, Fl-3: 600 V and Fl-4: 420-550 V. All samples were prepared in duplicate and recorded either in channel Fl-3 (pyridinium dyes, excitation: 488 nm, emission filter: >670 nm) or in Fl-4 (cyanine dyes, excitation: 635 nm, emission filter: 661 ± 18 nm). Sample measurement was complete after 30-45 s (this corresponds to approx. 20,000-90,000 gated events).

HEK293T-hH_2R-qs5 cells were seeded in a 175-cm^2 culture flask 5-7 days prior to the experiment. On the day of the experiment, cells were trypsinized and detached with fresh culture medium (5 mL). After centrifugation (250 *g*, 10 min) the cell pellet was resuspended in Leibovitz´s L-15 culture medium (L-15 medium, Gibco/Life Technologies, Carlsbad, USA) and the concentration was adjusted to 0.5-1.0 · 10^6 cells/mL.

Saturation binding: 500 µL of the cell suspension were either added to 5 µL of DMSO/H_2O (30/70, v/v, total binding) or to 5 µL of famotidine in DMSO/H_2O (30/70, v/v, unspecific binding, 300-fold excess to the fluorescent ligand). Incubation was started by the addition of 5 µL of fluorescent ligand in DMSO/H_2O (30/70, v/v, 100-fold concentrated) in intervals of 1 min (measuring time per sample = one concentration) starting with the lowest concentration of total binding. After 90 min of shaking in the dark at 25 °C, the samples were transferred to 5 mL polystyrol FACS tubes (Sarstedt, Nümbrecht,Germany) and immediately measured.

Competition binding: To 500 µL of cell suspension, 5 µL of competitor in DMSO/H_2O (30/70, v/v); 100-fold concentrated) were added at increasing concentrations and 5 µL of fluorescent ligand (concentration in the assay: 50 nM (**5.14**) or 25 nM (**5.18**)) in DMSO/H_2O (30/70, v/v, 100-fold concentrated) in intervals of 1 min (measuring time per sample). The incubation time was 90 min at 25 °C.

Association: 500 µL of the cell suspension were either added to 5 µL of DMSO/H_2O (30/70, v/v, total binding) or to 5 µL of famotidine in DMSO/H_2O (30/70, v/v, unspecific binding, 300-fold excess to the fluorescent ligand). Incubation started by addition of 5 µL of fluorescent ligand in DMSO/H_2O (30/70, v/v, 100-fold concentrated, final concentration: 50 nM (**5.14**), 15 nM (**5.16**) or 25 nM (**5.18**)). The incubation at 37 °C was stopped after different periods of time (0-120 min) by measuring the samples.

Dissociation: 500 µL of the cell suspension were either added to 5 µL DMSO/H_2O (30/70, v/v, total binding) or to 5 µL famotidine in DMSO/H_2O (30/70, v/v, unspecific binding, 300-fold excess to the fluorescent ligand). 5 µL of fluorescent ligand in DMSO/H_2O (30/70, v/v, 100-fold concentrated, final concentration of the fluorescent ligands: 50 nM (**5.14**), 15 nM (**5.16**) or 25 nM (**5.18**)) were added to every vessel and the samples were incubated at 25 °C for 90 min. The samples were centrifuged (250 *g*, 3.5 min,) and the supernatant, containing excess fluorescent ligand was aspirated. 500 µL pf L-15 medium containing famotidine (300-fold excess to the final fluorescent ligand concentration, 15 µM, 4.5 µM or 7.5 µM) were added to the cell pellet, before

the cells were resuspended. The incubation at 37 °C was stopped after different periods of time (0-150 min) by measuring the samples.

For data analysis the software FlowJo V10 (FlowJo, LLC, Ashland, USA) was used throughout. The geometrical mean values of Fl-3 or Fl-4 were obtained for a subpopulation of the gated cells which exhibited a high receptor density.

High content Imaging

Fluorescent ligand binding experiments with adherent HEK293T-hH_2R-qs5 cells (IN Cell Analyzer)

For high content imaging of adherent cells, a wide-field cell imaging system, the IN Cell Analyzer 2000 (GE Healthcare, Little Chalfont, UK), was used. An objective with a 20-fold magnification and a numerical aperture of 0.45, combined with a polychroic mirror (QUAD1), was used throughout. For imaging, two channels with different excitation/emission filters were applied: Cy5 channel (for cyanine dyes, excitation filter: 645/30 nm, emission filter: 705/72 nm, exposure time: 1,000 ms) or Cy3 channel (pyridinium dyes, excitation filter: 543/22 nm, emission filter: 605/64 nm, exposure time: 1,000 ms) and DAPI channel (H33342, excitation filter: 350/50 nm, emission filter: 455/50 nm, exposure time: 90 ms). 2.5-D images (imaging modality, the system uses the camera´s CCD/sCMOS chip to integrate the signal over the specified Z section and then deconvolves the result for a pseudo 3-D projection) were obtained throughout. In some cases a brightfield channel (excitation filter: 473/10 nm, emission filter: 455/50 nm, exposure time: 50 ms, imaging modality: 2-D images, the system acquires a standard two-dimensional image) was additionally applied. In every channel, 4 images were obtained per well. Binding experiments were performed in duplicate and were repeated at least twice.

One day prior to the experiment, HEK293T-hH_2R-qs5 cells were trypsinized and detached with DMEM medium (high glucose without phenol red (Gibco/Life Technologies, Carlsbad, USA) containing 1% (v/v) Penicillin-Streptomycin (P/S, 10,000 U/mL, Gibco/Life Technologies, Carlsbad, USA) and 10% (v/v) FCS (in the following referred to as DMEM w/o medium). The cell suspension was adjusted to 0.6-0.75 · 10^6 cells/mL and 200 µl (120,000 - 150,000 cells/well) were seeded in every well of a µ-slide-96-well plate (Ibidi, Martinsried, Germany) using an automated reagent dispenser (Multidrop, Thermo Fisher Scientific, Waltham, USA). The cells were cultivated at 37 °C overnight in a water saturated atmosphere containing 5% CO_2.

On the day of the experiment, the medium was removed and cells (concentration approximately 3 · 10^8 cells/well) were covered with 80 µl fresh DMEM w/o medium additionally containing 0.1% BSA (Albumin bovine fraction V, SERVA, Heidelberg, Germany) and H33342 (1 µg/mL in H_2O, Sigma Aldrich, Munich, Germany).

Saturation binding: For determination of total binding, DMEM w/o medium (10 µL) and for unspecific binding DMEM w/o medium (10 µL) and famotidine as competitor (300-fold referring to the fluorescent ligand) were added. Incubation was started by addition of DMEM w/o medium (10 µL) containing the respective concentrations of the fluorescent ligand (10-fold concentrated) to every well.

Competition binding: DMEM w/o medium (10 µL) containing the investigated ligands at various concentrations (10-fold concentrated) was added. For determination of unspecific binding famotidine (100 µM final) was used. Incubation time started by addition of DMEM w/o medium (10 µL) containing the fluorescent ligand **18** (10-fold concentrated, 50 nM final) to every well.

After incubation at room temperature in the dark for 60 min, the medium was removed and the cells were washed with PBS (100 µL) and covered with DMEM w/o medium (100 µL) followed by immediate acquisition of images at 37 °C.

For kinetic studies the cells were seeded in a 96-well plate one day prior to the experiment as described before. For one association or dissociation experiment only four wells of the plate (two wells for total binding and unspecific binding respectively) were required. The remaining wells were used for other experiments like saturation or competition binding experiments. On the day of the experiment the medium was removed and cells were incubated with 100 µl DMEM w/o medium containing 0.1% BSA and H33342 (1 µg/mL, Sigma Aldrich, Munich, Germany) for 1 h. The medium was carefully aspirated, the cells were washed with PBS (100 µL) and covered with 100 µl DMEM w/o medium. Either 10 µL (total binding) or 20 µL (unspecific binding) medium were removed from the wells. DMEM w/o medium (10 µL) containing famotidine (10-fold concentrated, 15 µM final) was added to the two wells of unspecific binding.

Association: DMEM w/o medium (10 µL) containing the fluorescent ligand **18** (10-fold concentrated, 50 nM final) was added to every well, and the plate was immediately transferred to the IN Cell Analyzer 2000. Images at different time points between 0 h and 1 h were acquired at 37 °C.

Dissociation: DMEM w/o medium (10 µL) containing the fluorescent ligand **18** (10-fold concentrated, 50 nM final) was added to every well, and the plate was incubated in the dark for 1 h. The medium was aspirated and DMEM w/o medium (100 µL) containing famotidine (15 µM) was added. Immediately, images at different time points between 0 h and 1 h were acquired at 37 °C.

For data analysis, the software Developer Toolbox 1.9.2 (IN Cell Investigator, GE Healthcare, Little Chalfont, UK) was used. For counting the nuclei per image a segmentation algorithm was applied to the images of the DAPI-channel (nuclei staining) to define the targets (nuclei) and the measure “count” (output: number of targets contained within the region of interest) was applied to the images. For the quantification of bound ligand an object segmentation algorithm was applied to the images of Cy3/Cy5 channel to define the targets (areas where the fluorescent ligand is bound). In case of the pyridinium labeled ligands, the density measure “density level” (measures the gray level intensity within the targets; uncalibrated intensity unit for IN Cell images, the higher the value, the brighter the pixel) was applied to the targets. As statistical function “sum” (output: sum of the density levels of all identified targets within one image) was chosen and the result was divided through the nuclei count. In case of the cyanine labeled ligands the density measure “Density x Area” (mean density within the target outline multiplied by its area, i.e. total density within the target outline) was applied to the targets. As statistical function “sum” (output: sum of the Density x Area of all identified targets within one image) was chosen and the result was divided through the nuclei count.

Imaging Flow Cytometry (ImageStreamX)

Imaging flow cytometry was performed with an ImageStreamX Imaging Cytometer (Amnis/Merck Millipore, Darmstadt, Germany), equipped with an objective with 40-fold magnification and a numerical aperture of 0.75. For imaging, an argon laser (488 nm, excitation wavelength) and a diode laser (785 nm, side scatter) were used, instrument settings were 488 nm laser: 75-85 mW, 785 nm laser: 13 mW and velocity 60 mm/s. Images were obtained in channel CH5 (emission filter: 702/85 nm). Measurement was completed after counting 1,000 to 1,500 cells within the defined area limits (bright field, upper limit: 250 and lower limit: 100, measuring time 1.5 to 2.0 min per sample). Binding experiments were performed in duplicate and were repeated at least twice.

HEK293T-hH_2R-qs5 cells were detached with DMEM w/o medium. After centrifugation (300 *g*, 5 min) the cell pellet was resuspended in fresh DMEM w/o medium. The cell suspension was adjusted to $2 \cdot 10^6$ cells/mL.

Saturation binding: For determination of total binding DMEM w/o medium (20 µL) containing 1% BSA (Albumin bovine fraction V, SERVA, Heidelberg, Germany) and for unspecific binding DMEM w/o medium (20 µL) containing 1% BSA and famotidine as competitor (300-fold referring to the fluorescent ligand) were added to 1.5 ml reaction vessels (Sarstedt, Nümbrecht, Germany). The cell suspension (160 µL) was transferred to the vessels and DMEM w/o medium (20 µL) containing 1% BSA and the fluorescent ligand in different concentrations (10-fold concentrated) was added. Samples were prepared at intervals of 2 min (measuring time per sample) starting with the highest concentration. After incubation for 60 min at room temperature in the dark, samples were filtered through a 70 µm nylon cell strainer (Falcon/Corning Inc., New York, USA) and images of the suspended cells were acquired with an ImageStreamX Imaging cytometer.

Competition binding: DMEM w/o medium (210 µL) containing the investigated ligands in various concentrations (10-fold concentrated) was added to 1.5 ml reaction vessels. For determination of unspecific binding, famotidine (100 µM final) was used. The cell suspension (160 µL) was transferred to the vessels and DMEM w/o medium (10 µL) containing the fluorescent ligand **14** (10-fold concentrated, 70 nM final) was added. All following steps were carried out as described for saturation binding.

For data analysis, the software IDEAS 6.0 (Amnis/Merck Millipore, Darmstadt, Germany) was used. From the gated cells only focused single cells were included in the data analysis. Furthermore, cells with high fluorescence intensity in the cytoplasm (dead or dying cells) were excluded. Then a mask for the cell membrane was created, allowing analysis of the fluorescent intensity in the area of the cell membrane. Additionally, the fluorescent intensity of the whole cell was analyzed.

Confocal Microscopy

Confocal microscopy was performed with a Zeiss Axiovert 200 M microscope equipped with the LSM 510 Laser scanner. A 63x/1.40 oil immersion objective was used.

Two days prior to the experiment, HEK293T-hH_2R-qs5 cells were trypsinized and seeded in a ibiTreat µ-slide 8-well chambered coverslip (Ibidi, Planegg, Germany) in DMEM ($0.6 \cdot 10^6$ cells/mL, 250 µL per well) containing 10% FCS and 1% P/S (10,000 U/mL, Sigma-Aldrich Munich, Germany). On the day of the experiment, the confluency of the cells was approximately 80-90%. The culture medium was replaced with L-15 containing 5% FCS and 1% P/S (120 µL). For the determination of total binding, blank L-15 medium (40 µL) and L-15 medium containing the respective fluorescent ligand (40 µL, 5-fold concentrated, 100 nM final) were added. Unspecific binding was determined by analogy; with the exception that blank medium was replaced with L-15 medium containing famotidine (40 µL, 5-fold concentrated, 30 µM final). Images of total and unspecific binding were acquired after an incubation period of 20 min at room temperature. Table 5.12 shows the settings for the detection of the investigated fluorescent ligands.

Table 5.11. Settings of the confocal microscope for the detection of the fluorescent ligands **5.14**, **5.16** and **5.18**.

Compounds	Excitation (laser intensity)	Filter	Pinhole (µm)
5.14	488 nm (10%)	LP 560	106
5.16	633 nm (10%)	LP 650	122
5.18	633 nm (10%)	LP 650	122

Beta-Arrestin2 recruitment assay

The β-Arrestin2 recruitment assays were performed as described previously for the H_1R using HEK293T-hH_2R-βArr2 cells, stably expressing the hH_2R-ElucC and βArr2-ElucNfusion constructs.[49]

One day prior to the experiment, HEK293T-hH_2R-βArr2 cells were trypsinized and detached with DMEM medium (high glucose without phenol red (Sigma Aldrich, Munich, Germany) containing 1% (v/v) P/S and 5% (v/v) FCS. The cell suspension was adjusted to $1.1 \cdot 10^6$ cells/mL and 90 µl (100,000 cells/well) were seeded in every well of a sterile, luciferase assay compatible, F-bottom 96-well plate (Cellstar®, Greiner Bio-One, Kremsmünster, Österreich). The cells were cultivated at 37 °C overnight in a water saturated atmosphere containing 5% CO_2. The investigated ligands were added at increasing concentrations (10 µL), and the plate was incubated at 25 °C for 60 min under shaking. 50 µL of the medium were removed, and 50 µL of Bright-Glo reagent (Promega, Madison, USA) were added. Bioluminescence was immediately measured for 1 s per well using a GENios Pro microplate reader (Tecan, Salzburg, Austria).

5.3.4 Data analysis

Retention factors k were calculated according to $k = (t_R - t_0)/ t_0$ (t_0 = dead time; t_R = retention time). Corrected counts per minute (ccpm) from the GTPγS assay (agonist mode) were plotted against the log(concentration of the test compound), and data were analyzed by a four parameter logistic equation (GraphPad Prism Software 5.0, GraphPad Software, San Diego, CA), followed by normalization (0% = water value (basal activity), 100% = "top" histamine equation) and analysis by four-parameter logistic equation (log(agonist) vs. response – variable slope, GraphPad Prism). Data of the GTPγS assay (antagonist mode) were analysed by a four parameter logistic equation (GraphPad Prism), followed by normalization (100% = "top" of the four-parameter logistic fit, 0% = unspecifically bound radioligand (ccpm) determined in the presence of famotidine at 100 µM) and analysis by four-parameter logistic equation (log(inhibitor) vs response – variable slope, GraphPad Prism). pIC_{50} values were converted into pK_B values according to the Cheng-Prusoff equation[51]. The luminescence (RLU) from the βArrestin2 recruitment assay (agonist mode) were plotted against log(concentration of the test compound) and analyzed by a four parameter logistic equation (GraphPad Prism) followed by normalization (0% = water value (basal activity), 100% = "top" histamine equation) and analysis by four-parameter logistic equation (log(agonist) vs. response – variable slope, GraphPad Prism). Specific binding data from saturation binding experiments were plotted against the "free" fluorescently labeled ligand concentration and analyzed by a two-parameter equation describing hyperbolic binding (one site – specific binding, GraphPad Prism). Specific binding data from association binding experiments were analyzed by a two parameter equation describing an exponential rise to a maximum (one-phase association, GraphPad Prism) to obtain the observed association constant k_{obs}. Specific binding data from dissociation binding experiments were analyzed by a three parameter equation (one phase decay, GraphPad Prism) to obtain the dissociation rate constant k_{off}. Kinetic dissociation constants $K_{d\,(kin)}$ were calculated from k_{on} and k_{off} ($k_{on} = (k_{obs} - k_{off})/[L]$; $K_{d\ (kin)} = k_{off}/ k_{on}$). Specific binding data from association and dissociation binding experiments were normalized (100% = Y_{max} (association) or Y_0 (dissociation)). Total binding data from radioligand and fluorescent ligand competition binding experiments were plotted against log(concentration competitor) and analyzed by a four-parameter logistic equation (log(inhibitor) vs response – variable slope, GraphPad Prism), followed by normalization (100% = "top" of the four-parameter logistic fit, 0% = unspecifically bound radioligand/ fluorescent ligand determined in the presence of famotidine at 100 µM). Normalized data from competition binding experiments was analyzed by a four-parameter logistic equation (log(inhibitor) vs response – variable slope, GraphPad Prism) and obtained pIC_{50} values were converted into pK_i values according to the Cheng-Prusoff equation.[51]

5.4 SUMMARY AND CONCLUSION

The introduction of different fluorophores by derivatization of amino-functionalized precursors, structurally related to BMY 2536, led to fluorescently labeled H_2R antagonists. The highest affinities on the hH_2R (pK_i values > 7.0) in radioligand competition assays were obtained by the pyridinium labeled ligands **5.12**-**5.14** and the cyanine labeled ligands **5.16** (positively charged fluorophore, net charge: 2^+) and **5.18** (electroneutral fluorophore, net charge: 1^+). Interestingly, labeling with S0387, the cyanine dye with the negative net charge, led to a decrease in hH_2R affinity (pK_i values < 6.0). While the linker length (4-7 carbon atoms) had no significant influence on the hH_2R affinity within the pyridinium ligands, the cyanine ligands with the hexyl linker (**5.16** and **5.18**) showed an increased hH_2R affinity compared to the butyl linker derivatives. Even though the low selectivity towards the hH_3R limited the application to recombinant systems, the investigated fluorescent ligands proved to be useful tools for binding studies using different techniques (flow cytometry and high content imaging). The ligands **5.12**-**5.18** and **5.20** bound in a saturable manner to the hH_2R (flow cytometry) and the determined K_d values (best results: **5.12**: 27.9 nM, **5.13**: 14.9 nM, **5.14**: 19.7 nM, **5.16**: 13.9 nM and **5.18**: 48.2 nM) were in good agreement with the corresponding K_i values. The $K_{d\,(kin)}$ values of **5.14**, **5.16** and **5.18**, calculated from kinetic experiments (nonlinear regression, flow cytometry) were consistent with the K_d values determined in saturation binding experiments. This indicates that the investigated fluorescent ligands follow in part the law of mass action even though they showed an incomplete dissociation (insurmountable antagonism). A similar behavior has been reported for several closely related ligands like the radioligand [^{3}H]UR-DE257. Its amine precursor **5.10** as well as related squaramide type derivatives were reported as insurmountable antagonists, which caused a concentration-dependent depression of the maximal response to the agonist relative to investigated standard ligands (guinea pig right atrium)[23]. Investigation of the association and dissociation kinetics of the cyanine labeled ligand **5.18** with high content imaging (INcCell Analyzer) revealed also incomplete dissociation and showed that the residual bound ligand is still located in the cell membrane. A possible explanation for the (pseudo-)irreversible binding of the fluorescent ligands **5.14**, **5.16** and **5.18** is a slow rate of dissociation from the receptor as also suggested for the radioligand [^{3}H]UR-DE257.[23] Nonetheless, the fluorescent ligands **5.14** and **5.18** can be used for the determination of binding affinities of unlabeled ligands in competition binding assays (shown for flow cytometry and two high content imaging systems: IN Cell Analyzer and imaging flow cytometry).

The high affinity fluorescent H_2R ligands **5.12**-**5.14**, **5.16** and **5.18** are an attractive nonradioactive alternative to the structurally related radioligand [^{3}H]UR-DE257[23] with similar pharmacological properties. Additionally these fluorescent ligands can be versatile molecular tools giving access to a plethora of optical techniques such as confocal microscopy, FRET, FRAP, TIRF, high content imaging and fluorescence polarization.

5.5 References

1. Lohse, M. J.; Nuber, S.; Hoffmann, C. Fluorescence/bioluminescence resonance energy transfer techniques to study G-protein-coupled receptor activation and signaling. *Pharmacol. Rev.* **2012**, 64, 299-336.
2. Deschout, H.; Raemdonck, K.; Demeester, J.; De Smedt, S. C.; Braeckmans, K. FRAP in pharmaceutical research: practical guidelines and applications in drug delivery. *Pharm. Res.* **2014**, 31, 255-270.
3. Fish, K. N. Total internal reflection fluorescence (TIRF) microscopy. *Current Protocols in Cytometry* **2009**, Chapter 12, Unit12 18.
4. Zanella, F.; Lorens, J. B.; Link, W. High content screening: seeing is believing. *Trends Biotechnol.* **2010**, 28, 237-245.
5. Jameson, D. M.; Ross, J. A. Fluorescence polarization/anisotropy in diagnostics and imaging. *Chem. Rev.* **2010**, 110, 2685-2708.
6. McGrath, J. C.; Arribas, S.; Daly, C. J. Fluorescent ligands for the study of receptors. *Trends Pharmacol. Sci.* **1996**, 17, 393-399.
7. Daval, S. B.; Valant, C.; Bonnet, D.; Kellenberger, E.; Hibert, M.; Galzi, J. L.; Ilien, B. Fluorescent derivatives of AC-42 to probe bitopic orthosteric/allosteric binding mechanisms on muscarinic M1 receptors. *J. Med. Chem.* **2012**, 55, 2125-2143.
8. Tahtaoui, C.; Parrot, I.; Klotz, P.; Guillier, F.; Galzi, J. L.; Hibert, M.; Ilien, B. Fluorescent pirenzepine derivatives as potential bitopic ligands of the human M1 muscarinic receptor. *J. Med. Chem.* **2004**, 47, 4300-4315.
9. Jones, L. H.; Randall, A.; Napier, C.; Trevethick, M.; Sreckovic, S.; Watson, J. Design and synthesis of a fluorescent muscarinic antagonist. *Bioorg. Med. Chem. Lett.* **2008**, 18, 825-827.
10. Baker, J. G.; Adams, L. A.; Salchow, K.; Mistry, S. N.; Middleton, R. J.; Hill, S. J.; Kellam, B. Synthesis and characterization of high-affinity 4,4-difluoro-4-bora-3a,4a-diaza-s-indacene-labeled fluorescent ligands for human beta-adrenoceptors. *J. Med. Chem.* **2011**, 54, 6874-6887.
11. Sugawara, T.; Hirasawa, A.; Hashimoto, K.; Tsujimoto, G. Differences in the subcellular localization of alpha1-adrenoceptor subtypes can affect the subtype selectivity of drugs in a study with the fluorescent ligand BODIPY FL-prazosin. *Life. Sci.* **2002**, 70, 2113-2124.
12. Baker, J. G.; Hall, I. P.; Hill, S. J. Pharmacology and direct visualisation of BODIPY-TMR-CGP: a long-acting fluorescent beta2-adrenoceptor agonist. *Br J Pharmacol* **2003**, 139, 232-242.
13. Leopoldo, M.; Lacivita, E.; Passafiume, E.; Contino, M.; Colabufo, N. A.; Berardi, F.; Perrone, R. 4-[omega-[4-arylpiperazin-1-yl]alkoxy]phenyl)imidazo[1,2-a]pyridine derivatives: fluorescent high-affinity dopamine D3 receptor ligands as potential probes for receptor visualization. *J. Med. Chem.* **2007**, 50, 5043-5047.
14. Li, L.; Kracht, J.; Peng, S.; Bernhardt, G.; Buschauer, A. Synthesis and pharmacological activity of fluorescent histamine H1 receptor antagonists related to mepyramine. *Bioorg. Med. Chem.* **2003**, 13, 1245-1248.
15. Rose, R. H.; Briddon, S. J.; Hill, S. J. A novel fluorescent histamine H(1) receptor antagonist demonstrates the advantage of using fluorescence correlation spectroscopy to study the binding of lipophilic ligands. *Br J Pharmacol* **2012**, 165, 1789-1800.
16. Isensee, K.; Amon, M.; Garlapati, A.; Ligneau, X.; Camelin, J. C.; Capet, M.; Schwartz, J. C.; Stark, H. Fluorinated non-imidazole histamine H3 receptor antagonists. *Bioorg. Med. Chem. Lett.* **2009**, 19, 2172-2175.
17. Amon, M.; Ligneau, X.; Schwartz, J. C.; Stark, H. Fluorescent non-imidazole histamine H3 receptor ligands with nanomolar affinities. *Bioorg. Med. Chem. Lett.* **2006**, 16, 1938-1940.
18. Amon, M.; Ligneau, X.; Camelin, J. C.; Berrebi-Bertrand, I.; Schwartz, J. C.; Stark, H. Highly potent fluorescence-tagged nonimidazole histamine H3 receptor ligands. *ChemMedChem* **2007**, 2, 708-716.

19. Li, L.; Kracht, J.; Peng, S.; Bernhardt, G.; Elz, S.; Buschauer, A. Synthesis and pharmacological activity of fluorescent histamine H2 receptor antagonists related to potentidine. *Bioorg. Med. Chem. Lett.* **2003**, 13, 1717-1720.
20. Malan, S. F.; van Marle, A.; Menge, W. M.; Zuliani, V.; Hoffman, M.; Timmerman, H.; Leurs, R. Fluorescent ligands for the histamine H2 receptor: synthesis and preliminary characterization. *Bioorg. Med. Chem.* **2004**, 12, 6495-6503.
21. Ruat, M.; Traiffort, E.; Bouthenet, M. L.; Schwartz, J. C.; Hirschfeld, J.; Buschauer, A.; Schunack, W. Reversible and Irreversible Labeling and Autoradiographic Localization of the Cerebral Histamine H-2-Receptor Using [I-125] Iodinated Probes. *P. Natl. Acad. Sci. USA* **1990**, 87, 1658-1662.
22. Hirschfeld, J.; Buschauer, A.; Elz, S.; Schunack, W.; Ruat, M.; Traiffort, E.; Schwartz, J. C. Iodoaminopotentidine and Related-Compounds - a New Class of Ligands with High-Affinity and Selectivity for the Histamine-H2-Receptor. *J. Med. Chem.* **1992**, 35, 2231-2238.
23. Baumeister, P.; Erdmann, D.; Biselli, S.; Kagermeier, N.; Elz, S.; Bernhardt, G.; Buschauer, A. [3H]UR-DE257: Development of a Tritium-Labeled Squaramide-Type Selective Histamine H2 Receptor Antagonist. *ChemMedChem* **2015**, 10, 83-93.
24. Algieri, A. A.; Crenshaw, R. R. 1,2-Diaminocyclobutene-3,4-diones and a pharmaceutical composition containing them. FR 2505835, 1982. Chem. Abstr. 99:22320.
25. Erdmann, D. Histamine H2- and H3-receptor antagonists : synthesis and characterization of radiolabelled and fluorescent pharmacological tools. Dissertation, Universität Regensburg, Regensburg, 2010. https://epub.uni-regensburg.de/19062/.
26. Mosandl, J. Radiochemical and luminescence-based binding and functional assays for human histamine receptors using genetically engineered cells. University of Regensburg, Regensburg, 2009. https://epub.uni-regensburg.de/12335/.
27. Buschauer, A.; Postius, S.; Szelenyi, I.; Schunack, W. Isohistamine and homologs as components of H2-antagonists. 22. H2-antihistaminics. *Arzneimittelforschung* **1985**, 35, 1025-1029.
28. Brown, T. H.; Young, R. C. Dioxocyclobutene compounds. EP 105702, 1986. Chem. Abstr. 101:130290
29. Wetzl, B. K.; Yarmoluk, S. M.; Craig, D. B.; Wolfbeis, O. S. Chameleon labels for staining and quantifying proteins. *Angew. Chem. Int. Ed. Eng.l* **2004**, 43, 5400-5402.
30. Keller, M.; Erdmann, D.; Pop, N.; Pluym, N.; Teng, S.; Bernhardt, G.; Buschauer, A. Red-fluorescent argininamide-type NPY Y1 receptor antagonists as pharmacological tools. *Bioorg. Med. Chem.* **2011**, 19, 2859-2878.
31. Schneider, E.; Keller, M.; Brennauer, A.; Hoefelschweiger, B. K.; Gross, D.; Wolfbeis, O. S.; Bernhardt, G.; Buschauer, A. Synthesis and characterization of the first fluorescent nonpeptide NPY Y1 receptor antagonist. *ChemBioChem* **2007**, 8, 1981-1988.
32. Kelley, M. T.; Bürckstümmer, T.; Wenzel-Seifert, K.; Dove, S.; Buschauer, A.; Seifert, R. Distinct interaction of human and guinea pig histamine H2-receptor with guanidine-type agonists. *Mol. Pharmacol.* **2001**, 60, 1210-1225.
33. Felixberger, J. Luciferase complementation for the determination of arrestin recruitment: Investigations at histamine and NPY receptors. University of Regensburg, Regensburg, 2014. https://epub.uni-regensburg.de/31292/.
34. Mullins, D.; Adham, N.; Hesk, D.; Wu, Y.; Kelly, J.; Huang, Y.; Guzzi, M.; Zhang, X.; McCombie, S.; Stamford, A.; Parker, E. Identification and characterization of pseudoirreversible nonpeptide antagonists of the neuropeptide Y Y5 receptor and development of a novel Y5-selective radioligand. *Eur. J. Pharmacol.* **2008**, 601, 1-7.
35. Pluym, N.; Baumeister, P.; Keller, M.; Bernhardt, G.; Buschauer, A. [(3)H]UR-PLN196: a selective nonpeptide radioligand and insurmountable antagonist for the neuropeptide Y Y(2) receptor. *ChemMedChem* **2013**, 8, 587-593.

36. Pegoli, A.; She, X.; Wifling, D.; Hubner, H.; Bernhardt, G.; Gmeiner, P.; Keller, M. Radiolabeled Dibenzodiazepinone-Type Antagonists Give Evidence of Dualsteric Binding at the M2 Muscarinic Acetylcholine Receptor. *J. Med. Chem.* **2017**, 60, 3314-3334.
37. Dukorn, S.; Littmann, T.; Keller, M.; Kuhn, K.; Cabrele, C.; Baumeister, P.; Bernhardt, G.; Buschauer, A. Fluorescence- and Radiolabeling of [Lys4,Nle17,30]hPP Yields Molecular Tools for the NPY Y4 Receptor. *Bioconjug. Chem.* **2017**, 28, 1291-1304.
38. Doughty, M. B.; Li, K.; Hu, L.; Chu, S. S.; Tessel, R. Benextramine-neuropeptide Y (NPY) binding site interactions: characterization of 3H-NPY binding site heterogeneity in rat brain. *Neuropeptides* **1992**, 23, 169-180.
39. Meini, S.; Patacchini, R.; Lecci, A.; Quartara, L.; Maggi, C. A. Peptide and non-peptide bradykinin B2 receptor agonists and antagonists: a reappraisal of their pharmacology in the guinea-pig ileum. *Eur. J. Pharmacol.* **2000**, 409, 185-194.
40. Seifert, R.; Schneider, E. H.; Dove, S.; Brunskole, I.; Neumann, D.; Strasser, A.; Buschauer, A. Paradoxical stimulatory effects of the "standard" histamine H4-receptor antagonist JNJ7777120: the H4 receptor joins the club of 7 transmembrane domain receptors exhibiting functional selectivity. *Mol. Pharmacol.* **2011**, 79, 631-638.
41. Vauquelin, G.; Morsing, P.; Fierens, F. L.; De Backer, J. P.; Vanderheyden, P. M. A two-state receptor model for the interaction between angiotensin II type 1 receptors and non-peptide antagonists. *Biochem. Pharmacol.* **2001**, 61, 277-284.
42. Lazareno, S.; Birdsall, N. J. Detection, quantitation, and verification of allosteric interactions of agents with labeled and unlabeled ligands at G protein-coupled receptors: interactions of strychnine and acetylcholine at muscarinic receptors. *Mol. Pharmacol.* **1995**, 48, 362-378.
43. Houston, C.; Wenzel-Seifert, K.; Burckstummer, T.; Seifert, R. The human histamine H2-receptor couples more efficiently to Sf9 insect cell Gs-proteins than to insect cell Gq-proteins: limitations of Sf9 cells for the analysis of receptor/Gq-protein coupling. *J. Neurochem.* **2002**, 80, 678-696.
44. Hoefelschweiger, B. K. The pyrylium dyes: A new class of biolabels. Synthesis, spectroscopy, and application as labels and in general protein assay. University Regensburg, Regensburg, 2005. https://epub.uni-regensburg.de/10331/.
45. Callahan, J. F.; Ashton-Shue, D.; Bryan, H. G.; Bryan, W. M.; Heckman, G. D.; Kinter, L. B.; McDonald, J. E.; Moore, M. L.; Schmidt, D. B.; Silvestri, J. S.; et al. Structure-activity relationships of novel vasopressin antagonists containing C-terminal diaminoalkanes and (aminoalkyl)guanidines. *J. Med. Chem.* **1989**, 32, 391-396.
46. Magde, D.; Brannon, J. H.; Cremers, T. L.; Olmsted, J. Absolute Luminescence Yield of Cresyl Violet - Standard for the Red. *J. Phys. Chem.* **1979**, 83, 696-699.
47. Pop, N.; Igel, P.; Brennauer, A.; Cabrele, C.; Bernhardt, G. N.; Seifert, R.; Buschauer, A. Functional reconstitution of human neuropeptide Y (NPY) Y(2) and Y(4) receptors in Sf9 insect cells. *J. Recept. Signal. Transduct. Res.* **2011**, 31, 271-285.
48. Kagermeier, N.; Werner, K.; Keller, M.; Baumeister, P.; Bernhardt, G.; Seifert, R.; Buschauer, A. Dimeric carbamoylguanidine-type histamine H receptor ligands: A new class of potent and selective agonists. *Bioorg. Med. Chem.* **2015**.
49. Lieb, S.; Littmann, T.; Plank, N.; Felixberger, J.; Tanaka, M.; Schafer, T.; Krief, S.; Elz, S.; Friedland, K.; Bernhardt, G.; Wegener, J.; Ozawa, T.; Buschauer, A. Label-free versus conventional cellular assays: Functional investigations on the human histamine H1 receptor. *Pharm. Res.* **2016**, 114, 13-26.
50. Schneider, E.; Mayer, M.; Ziemek, R.; Li, L.; Hutzler, C.; Bernhardt, G.; Buschauer, A. A simple and powerful flow cytometric method for the simultaneous determination of multiple parameters at G protein-coupled receptor subtypes. *ChemBioChem* **2006**, 7, 1400-1409.
51. Cheng, Y.; Prusoff, W. H. Relationship between the inhibition constant (K1) and the concentration of inhibitor which causes 50 per cent inhibition (I50) of an enzymatic reaction. *Biochem. Pharmacol.* **1973**, 22, 3099-3108.

6. CARBAMOYLGUANIDINE- TYPE H_2R LIGANDS: EXPLORATION OF STABILITY AND SELECTIVITY COMPARED TO THE ACYLGUANIDINE- ANALOGUES

Note: the synthesis of the intermediates **6.13-6.18** and the cabamoylguanidines **6.47-6.52** as well as the investigation of the chemical stability of **6.49**, **6.50**, **6.52**, **UR-Bit22**, **UR-Bit23** and **UR-Bit29** were performed by Claudia Honisch during her Master Thesis 2015.
The radioligand binding experiments at the dopamine receptors were performed by Lisa Forster during her doctoral thesis (ongoing).

6.1 INTRODUCTION

N^G-acylated hetarylpropylguanidines represent a class of potent histamine H_2R agonists.[1-3] The first generation N^G-acylguanidine ligands with an imidazole mojety lacked subtype selectivity, especially over the H_3R and H_4R (e.g. UR-AK24, Figure 6.1).[3] The bioisosteric replacement of the imidazole with a amino(methyl)thiazole moiety resulted in ligands with improved selectivity for the H_2R and retained H_2R potency (Figure 6.1 and Figure 6.2).[1,4] Investigation of optically active acylguanidine-type compounds (e.g. UR-AK24 and UR-PG267, Figure 6.1) in the GTPase assay revealed eudismic ratios from 1.1 to 3.2, indicating that stereochemistry plays only a minor role, if any.[4]

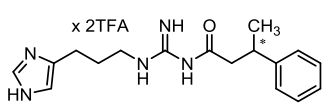

UR-AK24 (racemate)
hH_2R: pEC_{50}: 7.17, α: 0.87
hH_3R: pK_b: 7.71
hH_4R: pEC_{50}: 7.82, α: 0.89

eudismic ratio 1.5

(*R*)-UR-AK24
hH_2R: pEC_{50}: 6.92, α: 1.01

(*S*)-UR-AK24
hH_2R: pEC_{50}: 7.10, α: 1.07

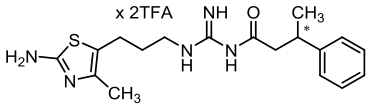

UR-PG267 (racemate)
hH_2R: pEC_{50}: 7.30, α: 0.82
hH_3R: pK_B: < 5
hH_4R: pK_B: < 5

eudismic ratio 1.9

(*R*)-UR-PG267
hH_2R: pEC_{50}: 7.27, α: 0.65

(*S*)-UR-PG267
hH_2R: pEC_{50}: 7.55, α: 0.87

Figure 6.1. Monovalent N^G-acylated 3-(imidazol-4-yl)propylguanidine UR-AK24 and the corresponding N^G-acylated 3-(2-amino-4-methylthiazol-5-yl)propylguanidine UR-PG267. Potencies were determined in a steady-state GTPase assay on membrane preparations of Sf9 insect cells expressing the respective receptor.

Interestingly, a broad variety of aliphatic and aromatic hydrocarbon residues was well tolerated in this class of H_2R agonists (Figure 6.2). An increase in H_2R potency was achieved by linking two acylguanidine pharmacophores together via alkyl spacer.[2] Bivalent ligands with an n-octyl linker (e.g. UR-AK381, Figure 6.2), showed the highest potency (pEC_{50}: 8.11, α: 0.53), although spacer length is too short to bridge the two orthosteric binding pockets of the individuals protomers of a putative receptor dimer.[2] The increased potency compared to that of the corresponding monovalent ligands seems to result from binding to an additional (allosteric) binding site of the same receptor.[2]

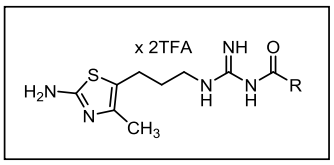

R =

UR-Bit22
hH_2R: pEC_{50}: 5.83
α: 0.56

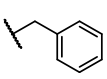

UR-Bit23
hH_2R: pEC_{50}: 7.02
α: 0.68

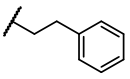

UR-Bit24
hH_2R: pEC_{50}: 7.65
α: 0.79

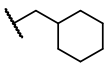

UR-Bit29
hH_2R: pEC_{50}: 7.30
α: 0.71

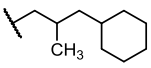

UR-AK421
hH_2R: pEC_{50}: 7.61
α: 0.42

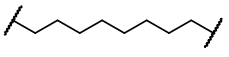

UR-AK381
hH_2R: pEC_{50}: 8.11
α: 0.53

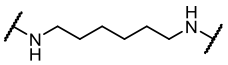

UR-NK22
hH_2R: pEC_{50}: 8.03
α: 0.92

Figure 6.2. Representative H_2R agonists: monomeric and bivalent N^G-acylated 3-(2-amino-4-methylthiazol-5-yl)propylguanidines and the bivalent carbamoylguainidine UR-NK22.[1,2,5] Potencies were determined in a steady-state GTPase assay on membrane preparations of Sf9 insect cells expressing the hH_2R-$G_{s\alpha S}$ fusion protein.

As it was reported that N^G-acylguanidines undergo hydrolytic cleavage upon storage in aqueous solution, more stable analogues are needed.[5,6] A bioisosteric approach replacing the N^G acylguanidine structure with a carbamoylguanidine has proven useful.[5,7,8] This was successfully

applied in case of the bivalent N^G-acylated hetarylpropylguanidine H_2R agonists leading to highly potent ligands with improved long term stability (e.g. UR-NK22 (Figure 6.2), no decomposition after 7 days in PBS, PH 7.4 at RT). [5]

The aminothiazole moiety is a privileged structure for dopamine receptors. The most prominent example is the nonselective $D_{2\text{-}4}R$ agonist pramipexole (Figure 6.3). But also bulkier pramipexole derivatives such as CJ-1639 with high $D_{2\text{-}4}R$ affinity were reported.[9] In preliminary binding studies on the $hD_{2long}R$ and hD_3R variants, UR-NK22 and other bivalent amino(methyl)thiazole containing ligands showed in part moderate to high affinity towards these receptors (*ongoing Dissertation Lisa Forster*).

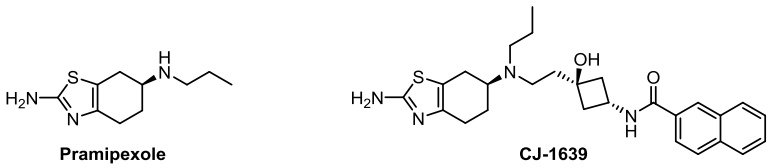

Figure 6.3. $D_{2\text{-}4}R$ ligands pramipexole and CJ-1639.

For exploration of the structure-activity relationship (H_2R) and the structure-selectivity relationships (H_2R versus H_1R, H_3R and H_4R) of this class of compounds, in addition to bivalent ligands, a series of carbamoylguanidines with various aminothiazole-based substructures, i.e., the 3-(2-amino-4-methylthiazol-5-yl)propyl moiety, a conformationally constrained (amino-thiazolyl)phenyl and a 2-amino-4,5,6,7-tetrahydrobenzothiazol-6-yl portion were synthesized (Figure 6.4) in this doctoral project. Additionally, two homobivalent ligands were prepared by replacement of the amino(methyl)thiazolepropyl moiety in UR-NK22 with either a (aminothiazolyl)phenyl or a pyrazolylpropyl moiety.

The synthesized monovalent and bivalent ligands were investigated in competition binding and functional assays (GTPγS binding and β-arrestin2 recruitment assay). In addition, selected compounds were investigated for $D_{2/3}R$ binding affinity on homogenates of HEK cells stably expressing the $hD_{2long}R$ or hD_3R.

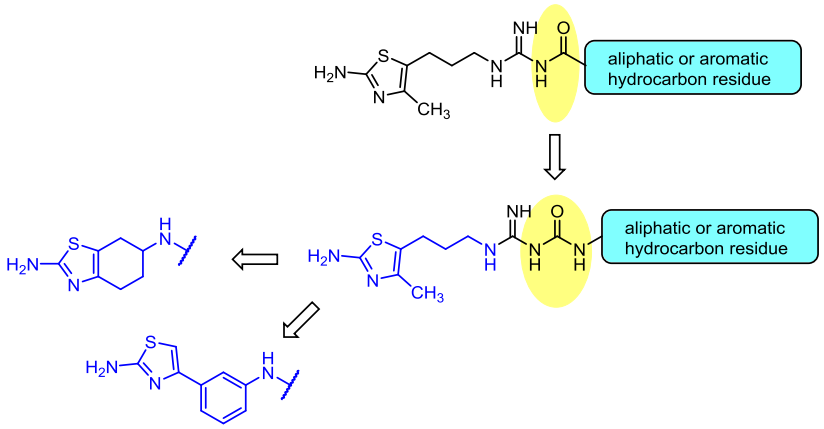

Figure 6.4. Bioisosteric replacement of the N^G-acylguanidine in H_2R agonists by a carbamoylguanidine and conformal restriction by replacement of the 3-(2-amino-4-methylthiazol-5-yl)propyl moiety by either an (aminothiazolyl)phenyl or an 2-amino-4,5,6,7-tetrahydrobenzothiazol-6-yl moiety.

6.2 Results and Discussion

6.2.1 Chemistry

The synthesis of the Boc-protected amine building block 3-(2-amino-4-methylthiazol-5-yl) propylamine (**6.5**) is outlined in Scheme 6.1 according to published procedures.[1] Starting from 6-chlorohexan-2-one, a Gabriel reaction led to the phthalimide **6.1**. Subsequent bromination at room temperature resulted in the thermodynamically more stable intermediate **6.2**. After evaporation of the solvent, the residue was treated with thiourea to give the 2-amino-4-methylthiazole derivative **6.3** in a substitution/ring closure reaction. Protection of the free amino group by a *tert*-butoxycarbonyl function and subsequent hydrazinolysis led to the amine intermediate 3-(2-amino-4-methylthiazol-5-yl) propylamine (**6.5**).

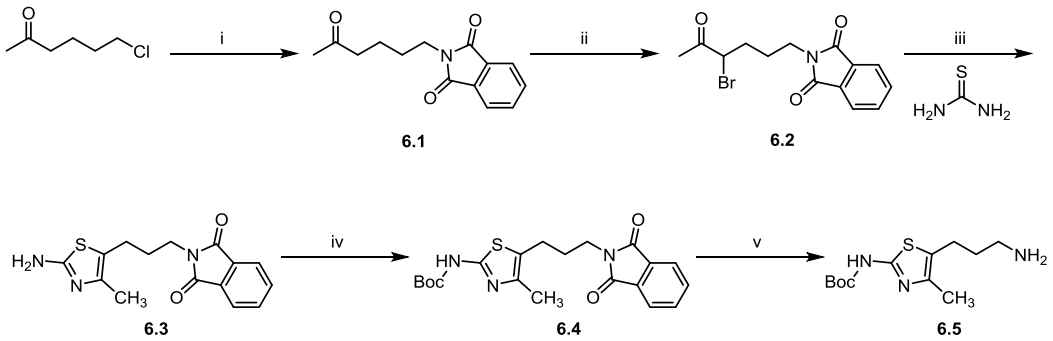

Scheme 6.1. Synthesis of the Boc-protected aminothiazole **6.5**. Reagents and conditions: i) phthalimide, K_2CO_3, DMF, 80 °C, 24 h, 70%; ii) Br_2, CH_2Cl_2, 1,6-dioxane, RT, 1 h, no purification; iii) DMF, 100 °C to RT, ON, 86%; iv) di-tert-butyldicarbonate, triethylamine, 4-(dimethylamino)-pyridine, $CHCl_3$, RT, ON, 20%; v) hydrazine-monohydrate, EtOH, RT, ON, 83%.

The synthesis of the second amine building block **6.7** was carried out by analogy with the synthesis of 2-guanidino-4-(3-phthalimidophenyl)thiazole hydrobromide (**3.6**) and is outlined in Scheme 6.2.[10] The ketone **3.4** was treated with bromine and subsequently with thiourea in order to form the protected aminothiazole building block **6.6** in a good yield of 78% over two steps. Deprotection of the phthalimide group in a mixture of HCl and acetic acid afforded the conformationally constrained amine building block **6.7**.

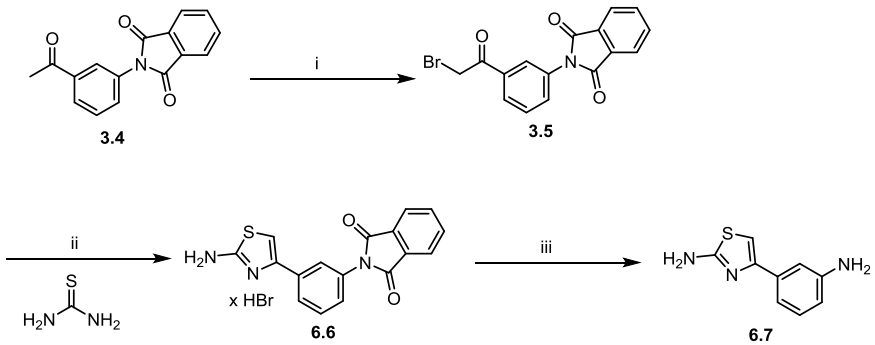

Scheme 6.2. Synthesis of 2-amino-4-(3-aminophenyl)thiazole (**6.7**). Reagents and conditions: i) Br_2, HBr in AcOH, $CHCl_3$, RT, 1h, no purification; ii) EtOH, MeCN, reflux, 3 h, 78%; iii) HCl, AcOH, reflux, ON, 60%.

The synthetic route of the third amine building block was adopted from the synthesis of pramipexole (Scheme 6.3).[11] 4-Amino cyclohexanol was amino protected using

N-(ethoxycarbonyl)phthalimide; then the hydroxy group was oxidized by pyridinium chlorochromate. The resulting ketone **6.9** was brominated in alpha position and subsequently treated with thiourea to afford the phthalimide protected aminothiazole building block **6.11**. 4,5,6,7-tetrahydrobenzo[d]thiazole-2,6-diamine (**6.12**) was obtained by refluxing **6.11** in a mixture of hydrochloric acid and acetic acid.

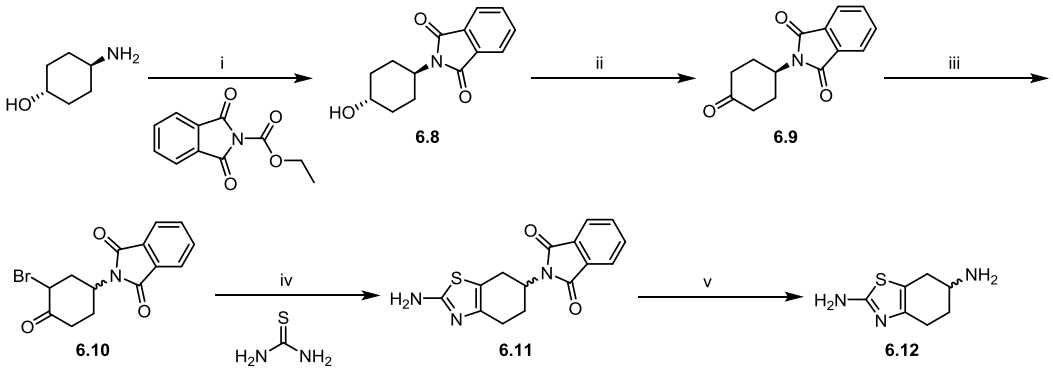

Scheme 6.3. Synthesis of the 4,5,6,7-tetrahydrobenzo[d]thiazole-2,6-diamine (**6.12**). Reagents and conditions: i) K_2CO_3, H_2O, RT, 30 min, 98%; ii) pyridinium chlorochromate, anhydrous CH_2Cl_2, RT, 3.5 h, 71%; iii) Br_2, 1,6-dioxane, CH_2Cl_2, RT, 1.5 h, no purification; iv) DMF, 100 °C, 2 h, 92%; v) HCl, AcOH, reflux, ON, 73%.

The N^G-carbamoylated guanidines were synthesized by guanidinylation of the amine building blocks **6.5**, **6.7** and **6.12**. S-methylcarbamoyl thiourea derivatives were used as guanidinylating reagents. These S-methylcarbamoyl thiourea derivatives (**6.13-6.25**) were synthesized by treatment of *N*-*tert*-butoxycarbonyl-S-methylisothiourea (**3.32,** synthesis in chapter 3) with the respective isocyanate (Scheme 6.4) in the presence of TEA at room temperature. The isocyanates were either commercially available (synthesis of **6.13-6.18**) or were prepared by Curtius rearrangement from the carboxylic acid (see synthesis of **6.19-6.25**). The branched carboxylic acids, which were previously synthesized in our group,[1,12] were treated with oxalyl chloride and the resulting acid chloride was converted into acyl azide by treatment with sodium azide. Thermal decomposition of the acyl azide led to the isocyanate, which was used for the synthesis of the corresponding S-methylcarbamoyl thiourea derivative (Scheme 6.4). The N^G-carbamoylated guanidines **6.47-6.67** were prepared by treating the amine building blocks **6.5**, **6.7** or **6.12** with the respective S-methylcarbamoyl thiourea derivative **6.13-6.25** in the presence of $HgCl_2$ and base. The resulting protected carbamoylguanidine-type intermediates **6.26-6.46** were treated with TFA to obtain the N^G-carbamoylated guanidines **6.47-6.67** in a yield of 16-75%. after purification by preparative HPLC.

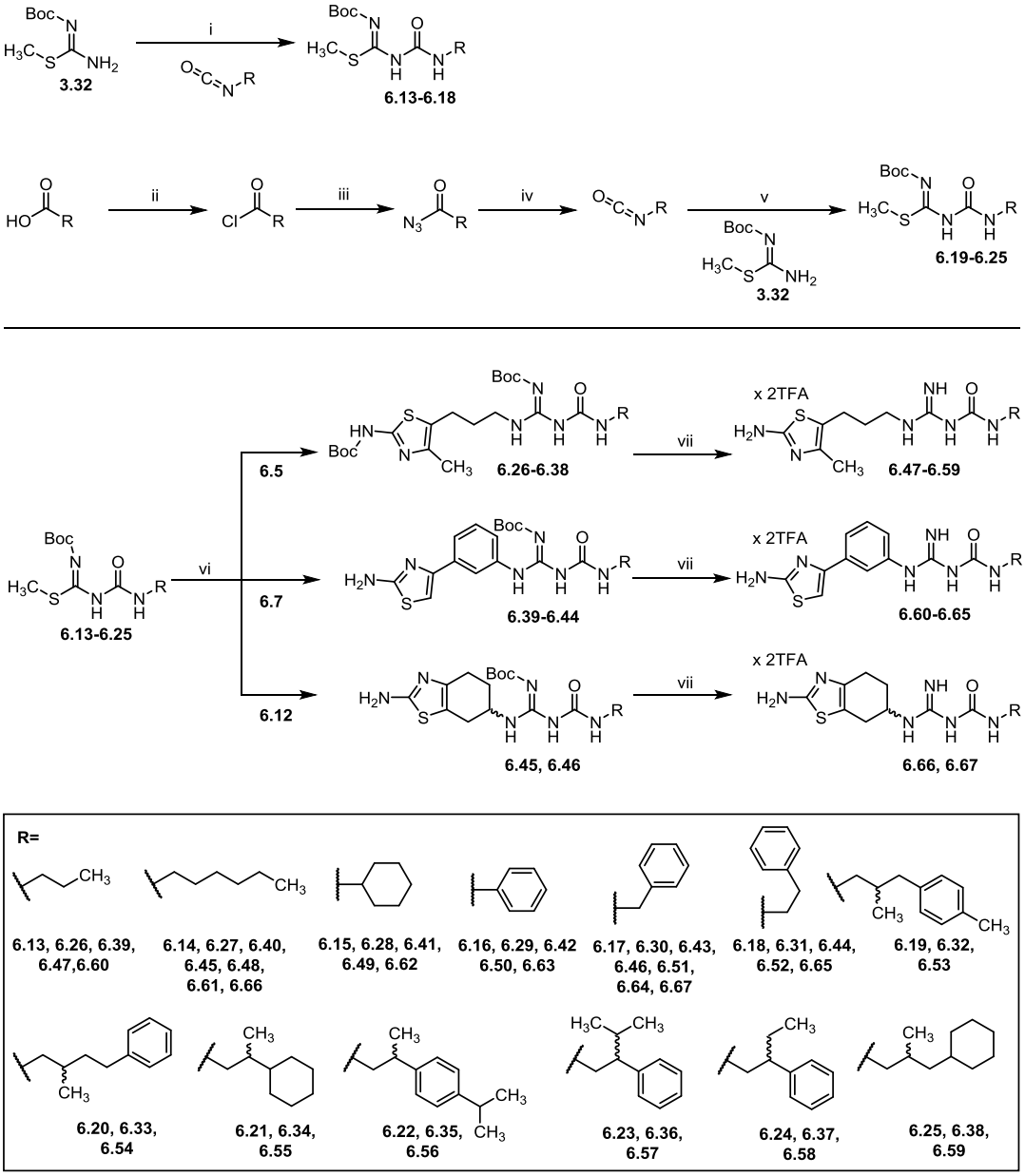

Scheme 6.4. Synthesis of the S-methylcarbamoyl thiourea derivatives **6.13**-**6.25** and the N^G-carbamoylated guanidines **6.47-6.67**. Reagents and conditions: i) TEA, CH_2Cl_2, RT, ON, 57-85%; ii) Oxalylchloride, DMF, CH_2Cl_2, 0 °C-RT, 25 min, no purification; iii) Sodium azide in H_2O, acetone, ice bath, 30 min, no purification; iv) CH_2Cl_2, reflux, 30 min, no purification; v) TEA, CH_2Cl_2, RT, ON, 38-77% over four steps; vi) $HgCl_2$, TEA, anhydrous CH_2Cl_2, Ar-atmosphere, RT, ON, 35-97%; vii) TFA, CH_2Cl_2, RT, ON, 16-75%

The bivalent carbamoylguanidine-type compounds **6.70** and **6.71** were synthesized using established protocols (Scheme 6.5).[5,13] The amine precursor **6.7** or 3-(1-trityl-1*H*-pyrazol-4-yl)prop-1-yl-amine was treated with guanidinylating reagent **3.33** in the presence of $HgCl_2$ and base. Subsequent treatment of the protected intermediates **6.68** and **6.69** with TFA afforded the bivalent N^G-carbamoylated guanidines **6.70** and **6.71**.

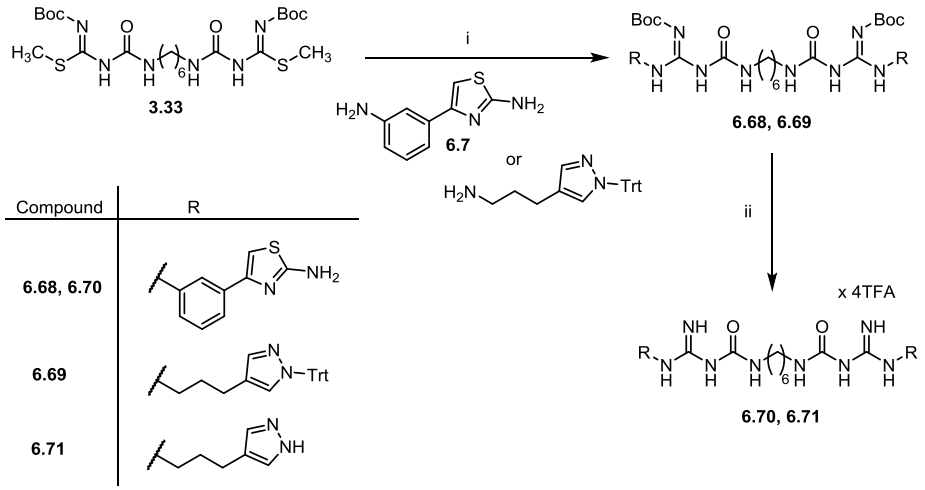

Scheme 6.5. Synthesis of the bivalent N^G-carbamoylated guanidines (**6.70**, **6.71**). Reagents and conditions: i) $HgCl_2$, TEA, anhydrous CH_2Cl_2, Ar-atmosphere, RT, ON, 81-91%; ii) TFA, CH_2Cl_2, RT, ON, 52-67%.

6.2.2 Chemical stability of monovalent carbamoylguanidines compared to acylguanidines

N^G-Carbamoylguanidines are reported to show higher stability in basic solution compared to the respective N^G-acylguanidines.[6] Previous investigations on stability (assay conditions: PBS pH 7.4) of bivalent aminothiazole-containing carbamoylguanidines compared to their acylguanidine counterparts showed that after 7 days 55% of the acylated guanidine decomposed while the carbamoylated guanidine remained intact.[5]

In order to compare the chemical stability of the monovalent thiazole containing carbamoylated guanidines with the corresponding acylated guanidines, and to investigate the influence of various hydrocarbon residues, the compounds **6.49**, **6.50** and **6.52** as well as the acylguanidines UR-Bit22, UR-Bit23 and UR-Bit29 were dissolved in PBS (pH 7.4), incubated at RT for 7 days and analysed by analytical HPLC (conditions see experimental section). Whereas the carbamoylated guanidines remained stable over this period of time (Figure 6.5), decomposition of the acylated guanidines was highly dependent on the nature of hydrocarbon residue (Figure 6.6). After 7 days approximately 62% of the acylguanidine UR-Bit23 was decomposed. However, only 51% of UR-Bit29 and only 33% of UR-Bit22 was decomposed after the same time. The formation of a decomposition product (t_R: 1.97 min) could be observed over a period 7 days (Figure 6.6).

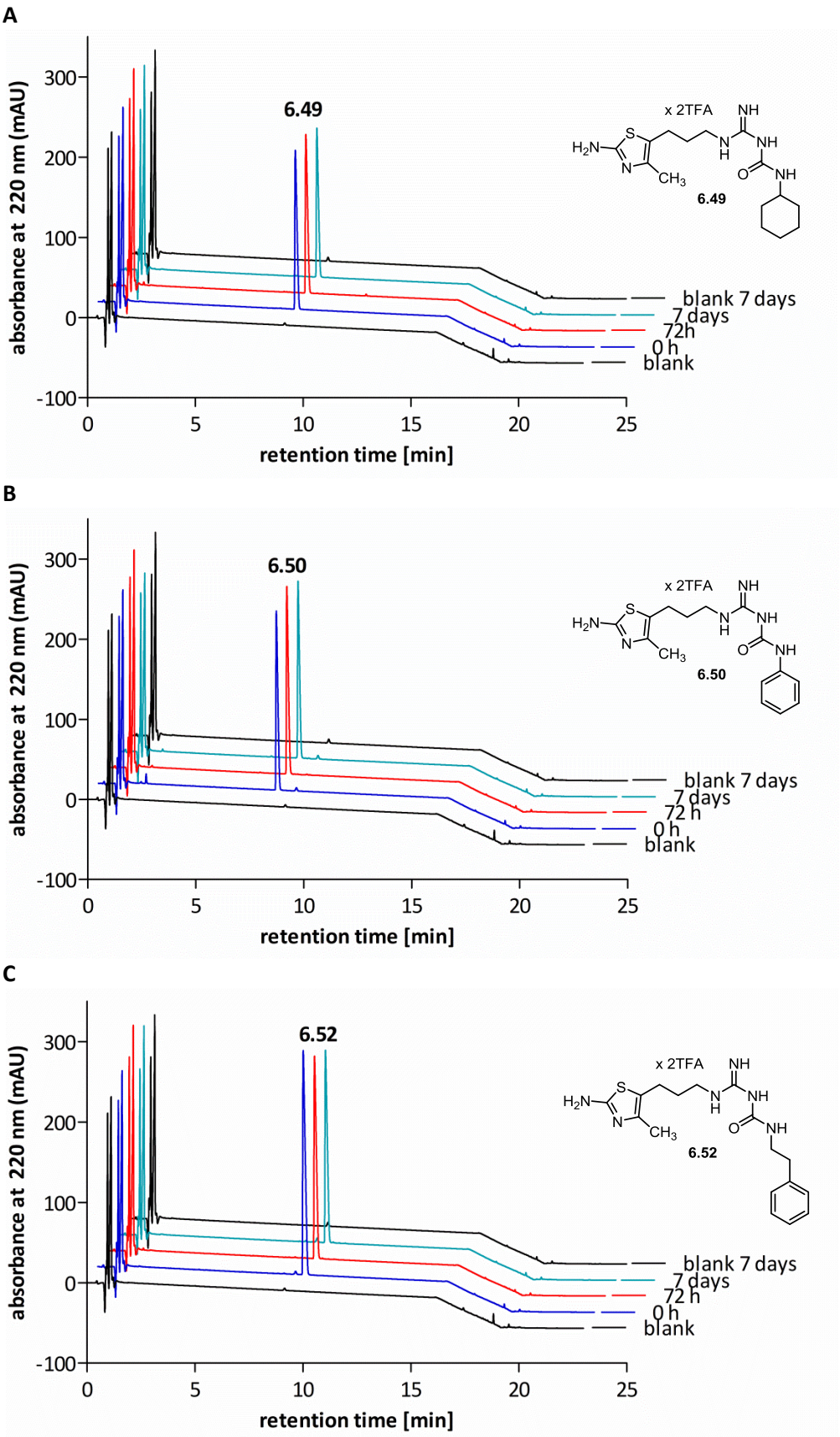

Figure 6.5. HPLC chromatograms (λ: 220 nm) of the N^G-carbamoylated guanidines after different time of incubation in PBS (pH 7.4): (A) **6.49**, t_R: 9.14min; (B) **6.50**, t_R: 8.23 min; and (C) **6.52**, t_R: 9.52 min.

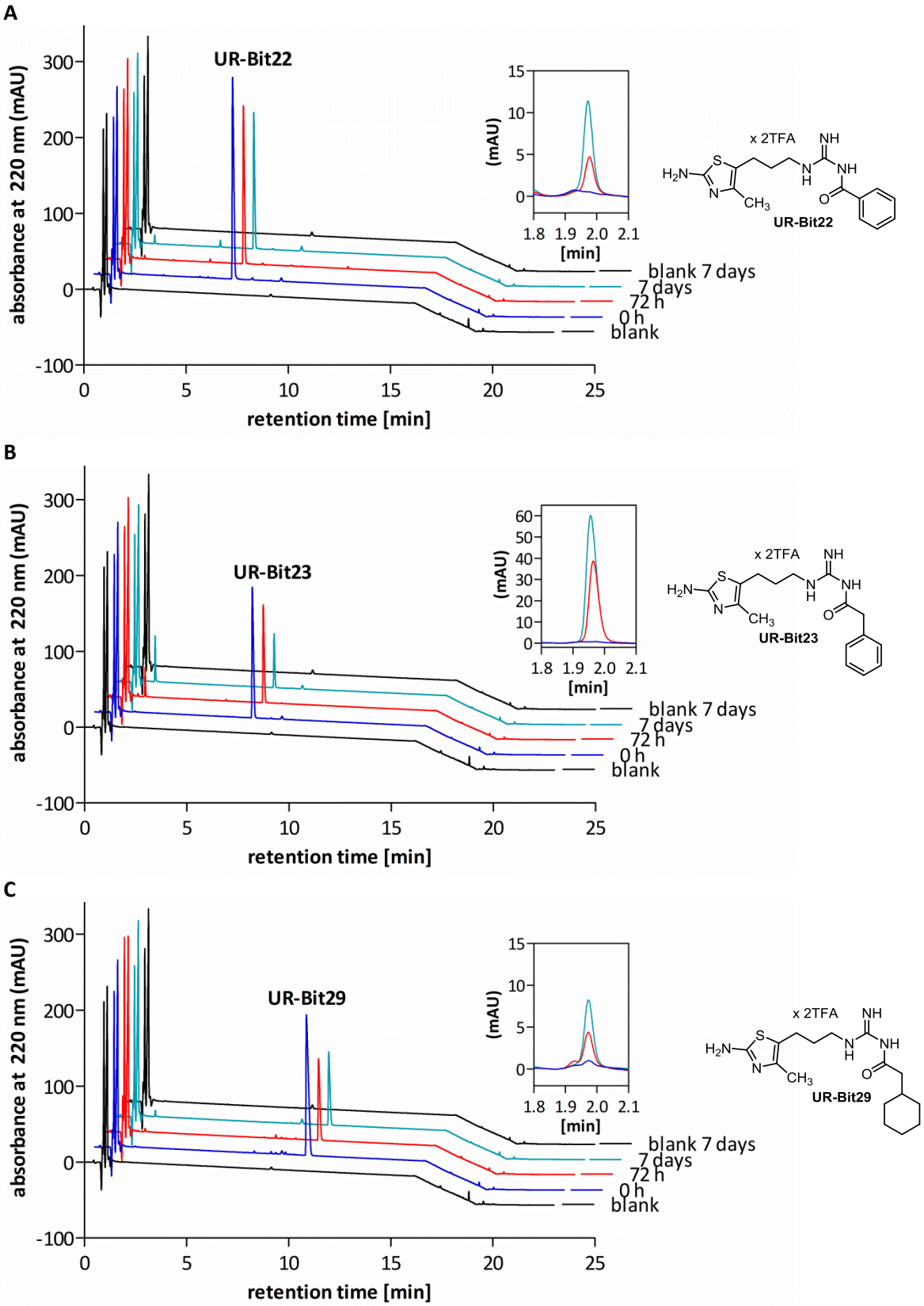

Figure 6.6. HPLC chromatograms (λ: 220 nm) of the N^G-acylated guanidines after different time of incubation in PBS (pH 7.4): (A) UR-Bit22 (t_R: 6.78min), Inset: reduced scaling, decomposition product (t_R: 1.97); (B) UR-Bit23, t_R: 7.71 min, Inset: reduced scaling, decomposition product (t_R: 1.96); and (C) UR-Bit29, t_R: 10.38 min, Inset: reduced scaling, decomposition product (t_R: 1.97).

6.2.3 Biological Evaluation

hH_2R affinities and subtype selectivities

The aminothiazole containing ligands **6.47-6.67**, the bivalent ligands **6.70** and **6.71**, histamine, UR-NK22, UR-Bit23 and pramipexole were investigated in equilibrium competition binding experiments on membrane preparations from Sf9 insect cells expressing the hH_2R-$G_{s\alpha S}$ fusion protein using the antagonist [^{3}H]UR-DE257[14] as radioligand. Selected displacement curves are shown in Figure 6.7 and the results are summarized in Table 6.1. The selectivity of representative compounds for the hH_2R compared to hH_1R, hH_3R and hH_4R was investigated by competition binding experiments using membrane preparations from Sf9 insect cells co-expressing either the hH_1R-$G_{s\alpha S}$ fusion protein and RGS4 ([^{3}H]Mepyramine as radioligand) or the $hH_{3/4}R$ and $G_{\alpha i2}$ and $G_{\beta 1\gamma 2}$ proteins ([^{3}H]histamine or [^{3}H]UR-PI294 as radioligand).

The monovalent N^G-carbamoylated amino(methyl)thiazolyl propylguanidines **6.47-6.59** showed moderate to high hH_2R affinity (Table 6.1). In general, aliphatic as well as aromatic residues were well tolerated, only ligand **6.50** which contains a phenyl residue showed a low affinity with a pK_i value of 5.50. The highest hH_2R affinities showed the compounds **6.55** (pK_i value: 7.40) and **6.48** (pK_i value: 7.54) which contain a branched cyclic or a linear aliphatic residue, respectively. In a similar manner as the bivalent N^G-acylated amino(methyl)thiazolylpropylguanidines, bivalent N^G-carbamoylated amino(methyl)thiazolyl propylguanidines (e.g. UR-NK22)[5] showed a higher affinity to the hH_2R (pK_i value: 8.02) compared to the monovalent ligands (**6.47-6.59**). In comparison, ligand **6.51** showed a considerably higher hH_2R affinity (pK_i value: 7.16) than the corresponding acylguanidine UR-Bit23 (pK_i value: 6.3). Incorporation of an aminothiazolylphenyl (compounds **6.60-6.65**) or a 2-amino-4,5,6,7-tetrahydrobenzothiazol-6-yl (compounds **6.66** and **6.67**) moiety resulted in a decrease in hH_2R affinity by one to two order(s) of magnitude. In comparison with the $D_{2/3}R$ ligand pramipexole (pK_i value: 4.86), which also contains a 2-amino-4,5,6,7-tetrahydrobenzothiazol-6-yl head group, the ligands **6.66** and **6.67** showed increased affinity for the hH_2R with pK_i values of 5.95 and 6.29. The replacement of the amino(methyl)thiazolyl propyl head group of the bivalent ligand UR-NK22 with either an aminothiazolylphenyl residue (**6.70**) or a pyrazolylpropyl residue (**6.71**) resulted in a strong decrease of hH_2R affinity (pK_i value: 5.98 and 6.75).

The monovalent N^G-carbamoylated amino(methyl)thiazolyl propylguanidines **6.47-6.59** showed a clear preference for the hH_2R over the other subtypes. In case of the aminothiazolylphenylguanidines **6.60-6.65** and the bivalent ligands (**6.70** and **6.71**) the affinity for the hH_4R was low (pK_i values 4-5) and, except for **6.63**, a slight preference for the hH_2R was obtained. While 2-amino-4,5,6,7-tetrahydrobenzothiazol-6-yl containing ligand **6.66** showed a similar affinity to hH_1R, hH_2R, hH_3R with pK_i values of 5.71-5.95 and a lower affinity to the hH_4R, ligand **6.67** showed a preference for hH_2R over the other subtypes of around one order of magnitude.

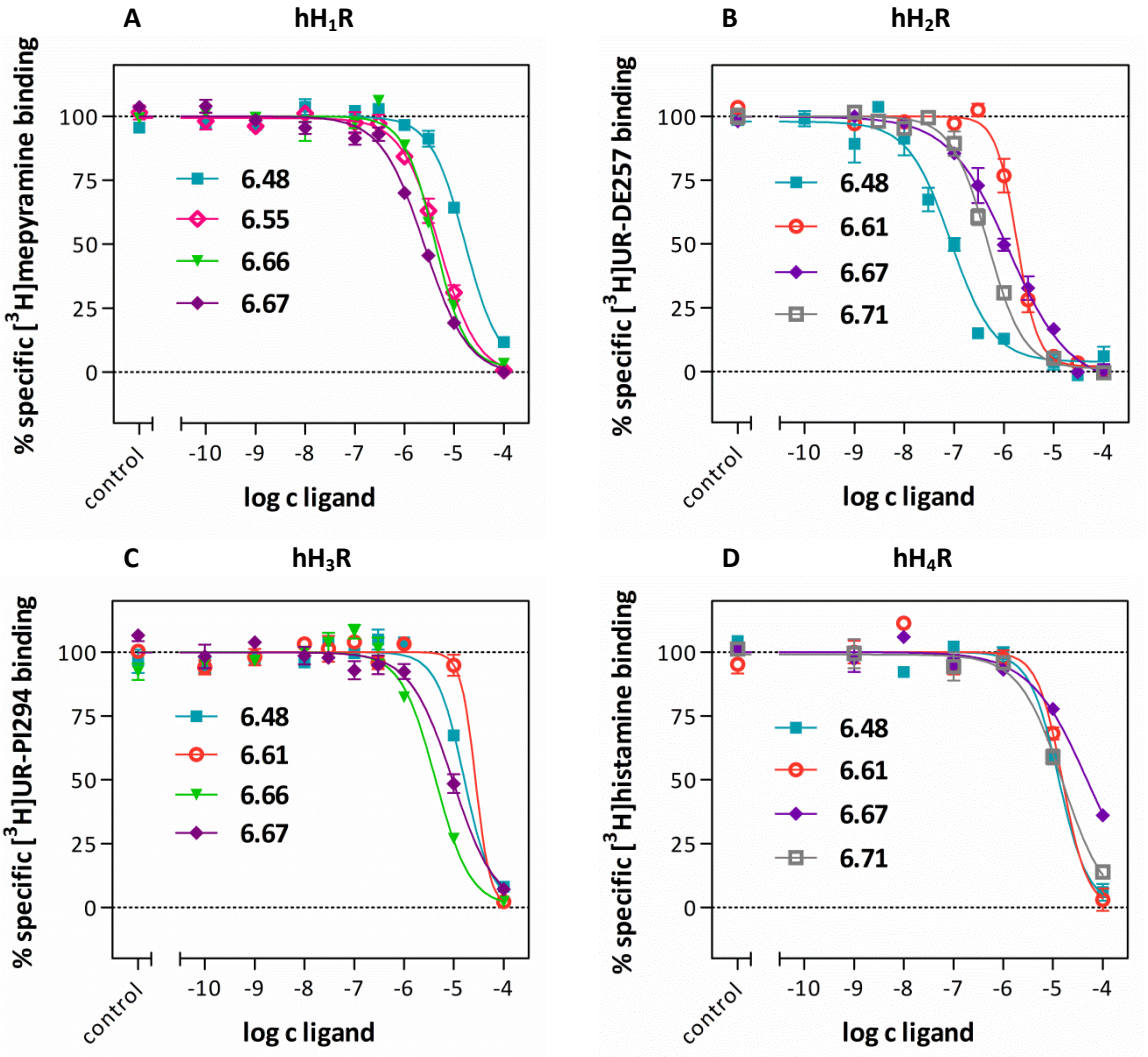

Figure 6.7. Displacement of the respective radioligand from membrane preparations of Sf9 insect cells (A) co-expressing the hH_1R-$G_{s\alpha S}$ fusion protein and RGS4 (radioligand: [^{3}H]mepyramine, c = 5 nM, K_d = 4.5 nM), (B) expressing the hH_2R-$G_{s\alpha S}$ fusion protein (radioligand: [^{3}H]UR-DE257, c = 20 nM, K_d = 12.2 nM), (C) co-expressing the hH_3R and $G_{\alpha i2}$ plus $G_{\beta 1\gamma 2}$ proteins (radioligand: [^{3}H]UR-PI294 c = 2 nM, K_d = 1.1 nM) or (D) co-expressing the hH_4R and $G_{\alpha i2}$ plus $G_{\beta 1\gamma 2}$ proteins (radioligand: [^{3}H]histamine c = 10 nM, K_d = 15.9 nM) by exemplary monovalent carbamoylated guanidines. Data represent mean values ± SEM of 2-3 experiments performed in triplicate.

Table 6.1. Affinities of histamine, pramipexole, UR-NK22, UR-Bit23, the monovalent carbamoylated guanidines **6.47**-**6.67** and the bivalent carbamoylated guanidines **6.70**-**6.71** to $hH_{1-4}R$, obtained from equilibrium competition binding studies on membrane preparations from Sf9 insect cells, expressing the respective histamine receptor subtype.

Compound	hH_1R[a]		hH_2R[b]		hH_3R[c]		hH_4R[e]	
	pK_i	N	pK_i	N	pK_i	N	pK_i	N
Histamine	n.d.	-	6.53 ± 0.04	3	7.8 ± 0.1	3	7.65 ± 0.03	3
Pramipexole	n.d.	-	4.86 ± 0.07	5	n.d.	-	n.d.	-
UR-NK22	6.06 ± 0.05[5]	2	8.07 ± 0.05[5]	3	5.94 ± 0.16[5]	4	5.69 ± 0.07[5]	3
UR-Bit23	n.d.	-	6.3 ± 0.4	2	n.d.	-	n.d.	-
6.47	4.54 ± 0.02	3	6.98 ± 0.11	3	4.35 ± 0.01[d]	3	4.06 ± 0.06	2
6.48	5.11 ± 0.03	3	7.54 ± 0.07	4	5.25 ± 0.02[d]	3	5.09 ± 0.02	2
6.49	4.61 ± 0.09	3	6.77 ± 0.27	3	n.d.	-	4.50 ± 0.06	2
6.50	n.d.	-	5.50 ± 0.08	3	n.d.	-	4.65 ± 0.05	2
6.51	5.21 ± 0.02	3	7.16 ± 0.05	3	n.d.	-	4.72 ± 0.09	2
6.52	n.d.	-	6.8 ± 0.2	4	n.d.	-	4.83 ± 0.06	2
6.53	5.8 ± 0.1	3	7.14 ± 0.08	2	5.49 ± 0.01[d]	3	5.44 ± 0.02[f]	3
6.54	5.87 ± 0.09	3	7.20 ± 0.04	3	5.04 ± 0.04	3	5.49 ± 0.08[f]	3
6.55	5.63 ± 0.06	3	7.40 ± 0.01	2	5.00 ± 0.08	3	5.72 ± 0.05[f]	3
6.56	5.31 ± 0.02	3	6.83 ± 0.08	3	5.10 ± 0.02	3	5.58 ± 0.01	3
6.57	5.23 ± 0.03	3	6.99 ± 0.05	3	4.93 ± 0.03	3	5.23 ± 0.03[f]	3
6.58	5.10 ± 0.08	3	7.11 ± 0.03	3	4.78 ± 0.03	3	5.17 ± 0.02[f]	3
6.59	5.42 ± 0.07	3	7.15 ± 0.02	4	5.13 ± 0.01	3	5.43 ± 0.01[f]	3
6.60	n.d.	-	5.28 ± 0.06	4	n.d.	-	<4.0	2
6.61	n.d.	-	6.16 ± 0.07	4	4.96 ± 0.07[d]	3	5.02 ± 0.06	2
6.62	n.d.	-	5.35 ± 0.02	3	n.d.	-	4.87 ± 0.03	2
6.63	n.d.	-	3.43 ± 0.07	3	n.d.	-	4.2 ± 0.1	2
6.64	n.d.	-	5.7 ± 0.1	3	n.d.	-	4.46 ± 0.01	2
6.65	n.d.	-	5.40 ± 0.05	3	n.d.	-	4.5 ± 0.1	2
6.66	5.71 ± 0.02	3	5.95 ± 0.06	4	5.82 ± 0.03[d]	3	4.78 ± 0.05	2
6.67	5.92 ± 0.02	3	6.29 ± 0.08	3	5.48 ± 0.06[d]	3	4.52 ± 0.01	2
6.70	n.d.	-	5.98 ± 0.06	3	n.d.	-	5.0 ± 0.2	2
6.71	n.d.	-	6.75 ± 0.04	3	n.d.	-	5.02 ± 0.07	3

Competition binding assay on membrane preparations of Sf9 insect cells [a]co-expression of the hH_1R-$G_{s\alpha S}$ fusion protein and RGS4 (radioligand: [^{3}H]mepyramine, c = 5 nM, K_d = 4.5 nM), [b]hH_2R-$G_{s\alpha S}$ fusion protein (radioligand: [^{3}H]UR-DE257, c = 20 nM, K_d = 12.2 nM), [c]co-expression of the hH_3R and $G_{\alpha i2}$ and $G_{\beta 1\gamma 2}$ proteins (radioligand: [^{3}H]histamine c = 15 nM, K_d = 12.1 nM or [d][^{3}H]UR-PI294 c = 2 nM, K_d = 1.1 nM) or [e]co-expresson of the hH_4R and$G_{\alpha i2}$ plus $G_{\beta 1\gamma 2}$ proteins (radioligand: [^{3}H]histamine c = 10 nM, K_d = 15.9 nM or [f][^{3}H]UR-PI294 c = 5 nM, K_d = 5.1 nM). The incubation period was 60 min. Data were analyzed by nonlinear regression and were best fitted to four-parameter sigmoidal concentration-response curves. Data shown are means ± SEM of N independent experiments, each performed in triplicate.

hH_2R agonism or antagonism in the GTPγS binding assay and βArrestin2 recruitment assay

The N^G-carbamoylated guanidines **6.47-6.71**, histamine, UR-NK22, UR-AK421, UR-Bit22, UR-Bit23, UR-Bit24, UR-Bit29 and pramipexole were examined for hH_2R agonism in the GTPγS binding assay on membrane preparations from Sf9 insect cells expressing the hH_2R-$G_{s\alpha S}$ fusion protein. Ligands which exhibited no agonism were also investigated in the antagonistic mode versus histamine as agonist. All identified agonists and selected antagonists were additionally investigated for agonism in the βArrestin2 recruitment assay on HEK293T-hH_2R-βArr2 cells, stably expressing the hH_2R-ElucC and βArr2-ElucNfusion constructs.[15] Prior studies suggested only minor differences between βArrestin1 and βArrestin2 recruitment[15] and therefore the βArrestin1 was not considered. Representative concentration response curves are depicted in Figure 6.8 (GTPγS binding assay) and Figure 6.9 (βArrestin2 recruitment assay). The results from these experiments are summarized in Table 6.2.

The monovalent N^G-carbamoylated amino(methyl)thiazolylpropylguanidines **6.47-6.59** were partial to full agonists in the GTPγS binding assay and showed moderate to high hH_2R potencies (up to 80 fold the potency of histamine; pEC_{50} values of 6.3-7.7) generally in good accordance to the acylguanidines (results from the GTPase assay)[1,16] (Table 6.2). At high concentrations (≥10-100 μM) the signal decreased again resulting in nearly bell-shaped concentration response curves (Figure 6.8). Compound **6.51** (α: 0.91, pEC_{50}: 7.5) showed the highest potency combined with full agonism, whereas the corresponding acylguanidine UR-Bit23 (α: 0.68, pEC_{50}: 6.59).was a partial agonist with only moderate potency.

Interestingly, the aminothiazolylphenyl containing monovalent ligands **6.60-6.65** and bivalent ligand **6.70** showed weak antagonism or inverse agonism at the hH_2R with pK_b values in good accordance to the pK_i values.

Incorporation of the less flexible 2-amino-4,5,6,7-tetrahydrobenzothiazol-6-yl (compounds **6.66** and **6.67**) moiety resulted in partial agonism (**6.67**, α: 0.57, pEC_{50}: 6.7) or in weak partial agonism (**6.66**, α: 0.16, pEC_{50}: 5.57) due to bell-shaped concentration response curves. In the antagonist mode of the GTPγS assay, **6.66** and **6.67** act as antagonists with pK_b values of 5.57 and 4.33. Also the structurally related dopamine receptor agonist pramipexole was a weak partial agonist at the hH_2R (α: 0.66, pEC_{50}: 5.07) with a sigmoidal curve. Although **6.67** was a racemic mixture, it was more potent than the enantiomerically pure pramipexole.

The pyrazole containing bivalent ligand **6.71** (α: 0.38, pEC_{50}: 7.0) was a partial agonist with low potency compared to the corresponding amino(methyl)thiazole containing full agonist UR-NK22 (α: 0.92, pEC_{50}: 8.03)[5].

All full or partial agonists identified in the GTPγS assay (**6.47**-**6.49**, **6.71**) showed a lower potency and efficacy in the βArrestin2 recruitment assay. The agonistic N^G-carbamoylated guanidine-type ligands exhibited some functional bias towards G-protein activation. This is in agreement with the findings for acylguanidines and bivalent carbamoylguanidines.[15] The bias was most pronounced in case of **6.53,** which was a full agonist in the GTPγS assay (α: 0.91) and a weak partial agonist in the βArrestin2 recruitment assay (α: 0.33). Nearly similar bias was determined for **6.53**, **6.57** and **6.58** which were partial agonists in the GTPγS assay (α: 0.52-0.68) and very weak partial agonists in the βArrestin2 recruitment assay (α: 0.10-0.16). Also in the βArrestin2 recruitment assay of the

ligands **6.53-6.59** the signal decreased again at high concentrations (≥30-100 µM) resulting in nearly bell-shaped concentration response curves. Interestingly, the 2-amino-4,5,6,7-tetrahydrobenzothiazole containing compounds **6.66** and **6.67**, which showed the most pronounced bell-shaped curves in the GTPγS assay, didn´t show a decreased signal at high concentrations in the βArrestin2 recruitment assay. Ligand **6.66** and two selected antagonists (**6.63** and **6.65**) identified in the GTPγS exhibited no βArrestin2 recruitment, too.

Bell shaped (or u-shaped) concentration response curves were described at several GPCRs such as muscarinic receptors,[17] β_2-adrenergic receptors[18] and serotonin receptors[19]. Some reasons for such a curve shape could be cytotoxicity,[20] binding to multiple binding sites,[21] multiple targets, receptor oligomers,[22] agonist-induced desensitization[18] or even due to physical properties like self-association of ligands into colloidal particals[23].

In case of the GTPγS assay plausible explanations would be binding to multiple binding sites or direct interaction with the $G_{s\alpha S}$ subunit of the fusion protein due to the use of membrane preparations from Sf9 insect cells expressing the hH_2R-$G_{s\alpha S}$ fusion protein instead of live cells. While in the GTPγS assay all agonists (**6.47-6.59**, **6.66** and **6.67**) showed more or less pronounced bell-shape curves, in the βArrestin2 recruitment assay only the agonists **6.53-6.59** showed a similar behavior. Interestingly, the ligands **6.48**, **6.50**, **6.52**, **6.66** and **6.67** with a distinguished bell-shaped curve in the GTPγS assay showed in the βArrestin2 recruitment assay a sigmoidal concentration response curve indicating that a different mechanism (e.g. cytotoxicity) is leading to the curve shape in the βArrestin2 recruitment assay. Moreover, it should be mentioned that all chiral compounds (**6.53-6.59**, **6.66** and **6.67**) were racemic mixtures. Therefore, the bell shaped curve could also be due to opposite effects of the enantiomers. However, investigation of enantiomeric pure acylguanidine-type compounds in the GTPase assay revealed only low eudismic ratios (1.1-3.2), indicating the stereochemistry of the acyl residue plays only a minor role.[4] However, according to the current state of knowledge this is all just speculation.

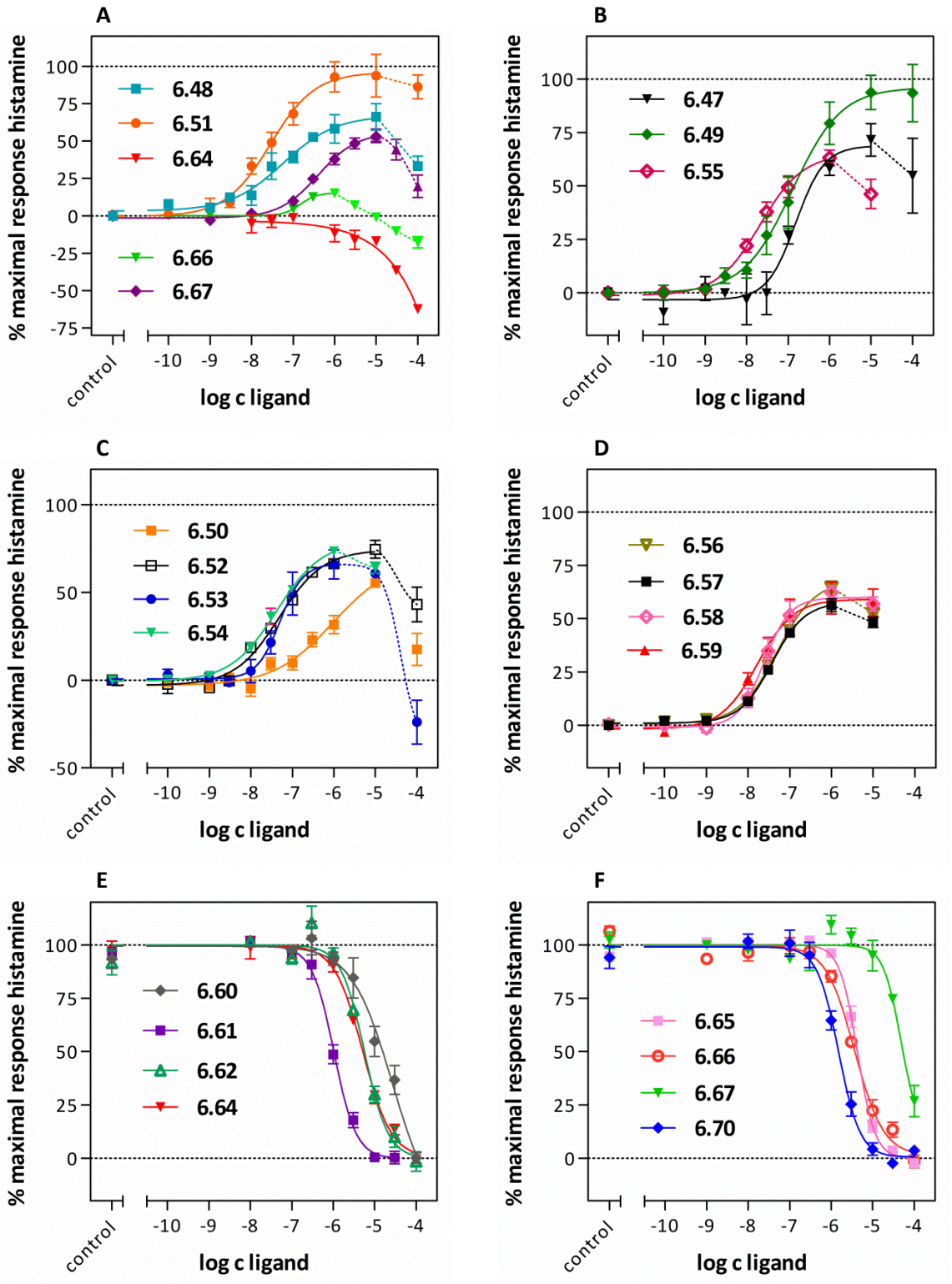

Figure 6.8. Concentration-response curves of representative monovalent carbamoylated guanidines on hH_2R determined by [^{35}S]GTPγS binding assay on membrane preparations of Sf9 insect cells expressing the hH_2R-$G_{s\alpha S}$ fusion protein. (A) Ligands **6.48**, **6.51**, **6.64**, **6.66** and **6.67**. (B) Ligands **6.47**, **6.49** and **6.55**. (C) Ligands **6.50**, **6.52-6.54**. (D) Ligands **6.56-6.59**. (E) and (F) Exemplary ligands measured in the antagonist mode; histamine (1 µM) was used for stimulation. Data represent mean values ± SEM of 2-5 experiments performed in triplicate.

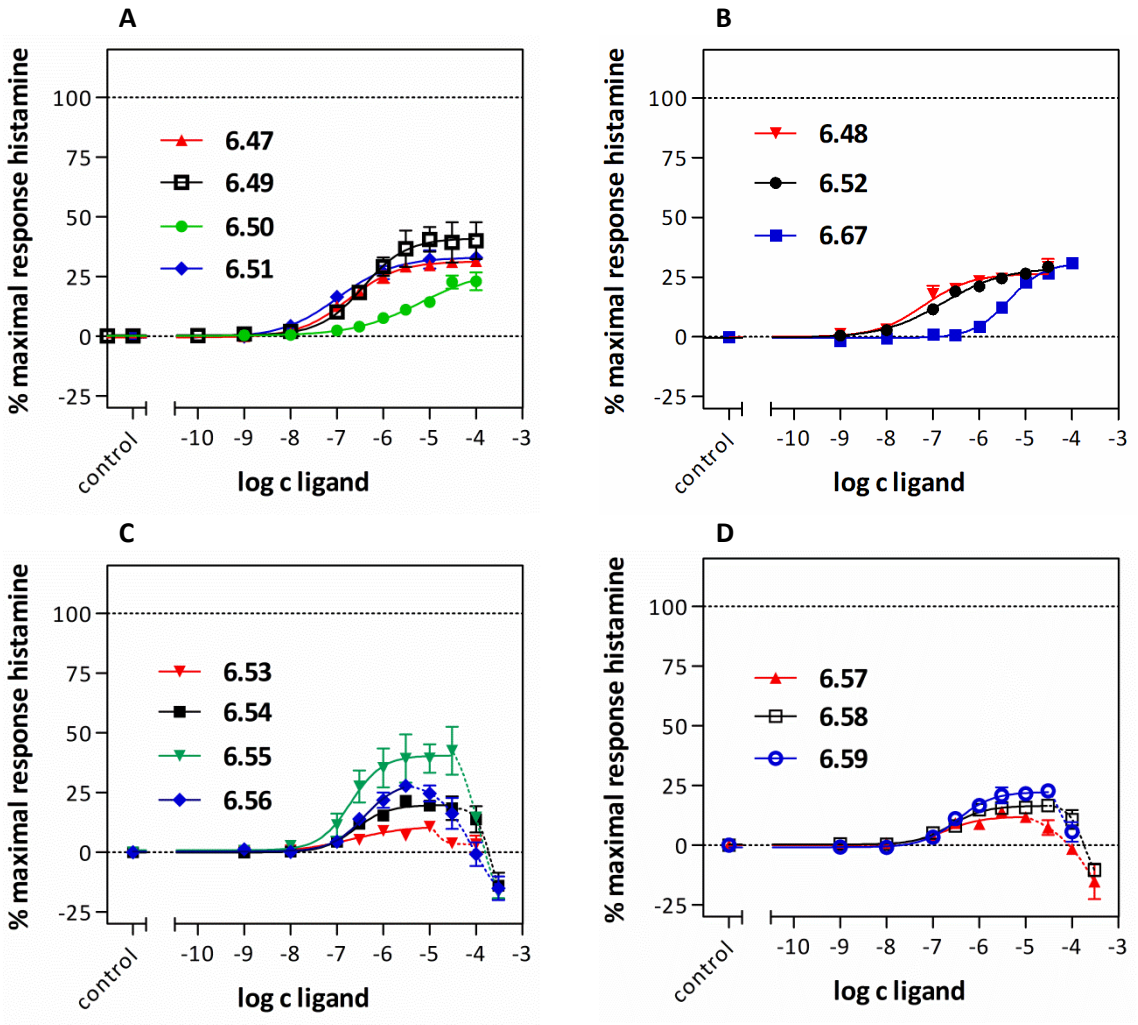

Figure 6.9. Concentration-response curves of representative monovalent carbamoylated guanidines on hH_2R determined by a luciferase complementation assay measuring β-arrestin2 recruitment on HEK293T-hH_2R-βArr2 cells. (A) and (B): Ligands with sigmoidal dose-response-curves. (C) and (D): Ligands with bell-shaped dose-response-curves. Data represent mean values ± SEM of 3 experiments performed in duplicate.

Table 6.2. hH_2R agonism or antagonism and the calculated pEC_{50} or pK_b values of histamine, pramipexole, UR-NK22, UR-AK421, UR-Bit22, UR-Bit23, UR-Bit24, UR-Bit29, the monovalent carbamoylated guanidines **6.47-6.67** and the bivalent carbamoylated guanidines **6.70-6.71** determined by a GTPγS assay and βArrestin2 recruitment assay.

Compound	hH_2R (GTPγS)[a]			hH_2R (βArrestin2 Recruitment)[b]		
	pEC_{50} (pK_b)	N	α	pEC_{50}	N	α
Histamine	5.80 ± 0.06	9	1.0	5.38 ± 0.04	19	1.0
Pramipexole	5.07 ± 0.06	5	0.66 ± 0.08	4.4 ± 0.1	4	0.35 ± 0.03
UR-NK22	8.03 ± 0.02[5]	2	0.92 ± 0.01[5]	7.19[15]	-	0.30[15]
UR-AK421	7.61[c 1]	-	0.42[c 1]	n.d.	-	n.d.
UR-Bit22	5.83[c 16]	-	0.56[c 16]	n.d.	-	n.d.
UR-Bit23	6.59 ± 0.06/ 7.02[c 1]	3 -	0.68 ± 0.13/ 0.68[c 1]	n.d.	-	n.d.
UR-Bit24	7.65[c 1]	-	0.79[c 1]	7.72[15]	-	0.14[15]
UR-Bit29	7.30[c 1]	-	0.71[c 1]	n.d.	-	n.d.
6.47	6.75 ± 0.06	3	0.79 ± 0.09	6.77 ± 0.04	3	0.32 ± 0.01
6.48	7.41 ± 0.07	3	0.60 ± 0.09	7.07 ± 0.02	3	0.28 ± 0.03
6.49	6.8 ± 0.2	3	0.96 ± 0.07	6.41 ± 0.03	3	0.43 ± 0.06
6.50	6.3 ± 0.2	2	0.59 ± 0.02	5.47 ± 0.06	3	0.25 ± 0.02
6.51	7.5 ± 0.1	4	0.91 ± 0.07	7.00 ± 0.08	3	0.33 ± 0.03
6.52	7.4 ± 0.2	3	0.72 ± 0.06	6.78 ± 0.03	3	0.29 ± 0.02
6.53	7.2 ± 0.1	5	0.68 ± 0.07	6.9 ± 0.1	3	0.10 ± 0.01
6.54	7.53 ± 0.06	3	0.69 ± 0.02	6.45 ± 0.06	3	0.20 ± 0.02
6.55	7.66 ± 0.08	3	0.65 ± 0.03	6.65 ± 0.09	3	0.40 ± 0.06
6.56	7.46 ±0.03	3	0.59 ± 0.02	6.55 ± 0.02	3	0.25 ± 0.03
6.57	7.51 ± 0.06	3	0.52 ± 0.03	6.8 ± 0.1	3	0.11 ± 0.01
6.58	7.5 ± 0.1	3	0.60 ± 0.04	6.57 ± 0.08	3	0.16 ± 0.02
6.59	7.76 ± 0.04	3	0.60 ±0.07	6.52 ± 0.07	3	0.22 ± 0.01
6.60	(4.91 ± 0.09)	3	-0.037	n.d.	-	n.d.
6.61	(6.14 ± 0.03)	3	-0.54	n.d.	-	n.d.
6.62	(5.40 ± 0.02)	3	-0.47	n.d.	-	n.d.
6.63	(4.8 ± 0.1)	3	-0.20 ± 0.02	-	-	0.018 ± 0.009
6.64	(5.44 ± 0.02)	3	-0.62	n.d.	-	n.d.
6.65	(5.52 ± 0.05)	3	-0.28 ± 0.04	-	-	0.043 ± 0.009
6.66	6.83 ± 0.06/ (5.57 ± 0.04)	3 3	0.16 ± 0.07	-	-	0.045 ± 0.005

Table 6.2 continued.

Compound	hH_2R (GTPγS)[a]			hH_2R (βArrestin2 Recruitment)[b]		
	pEC_{50} (pK_b)	N	α	pEC_{50} (pK_b)	N	α
6.67	6.7 ± 0.3/ (4.33 ± 0.09)	3 3	0.53 ± 0.05	5.36 ± 0.05	3	0.31 ± 0.03
6.70	(5.98 ± 0.06)	3	-0.46	n.d.	-	n.d.
6.71	7.0 ± 0.8	2	0.38 ± 0.03	5.75 ± 0.07	3	0.26 ± 0.08

[a][^{35}S]GTPγS assay determined on membrane preparations of Sf9 insect cells expressing the hH_2R-$G_{s\alpha S}$ fusion protein. [b]βArrestin2 recruitment assay determined on HEK293T-hH_2R-βArr2 cells, stably expressing the hH_2R-ElucC and βArr2-ElucNfusion constructs. The incubation period was 60 min. The intrinsic activity (α) of histamine was set to 1.00, and α values of investigated compounds were referred to this value. The pK_B values of neutral antagonists were determined in the antagonist mode versus histamine (c = 1 µM) as agonist. Data represent mean values ± SEM of N independent experiments performed in triplicate (GTPγS assay) or duplicate (βArrestin2 recruitment assay). [c]Steady-state GTPase assay determined on membrane preparations of Sf9 insect cells expressing the hH_2R-$G_{s\alpha S}$ fusion protein.

$hD_{2long}R$ and hD_3R affinities of carbamoylated guanidines

Aminothiazole containing ligands such as pramipexole and its derivatives are described as high affintiy dopamine receptor ligands (preferred D_2R, D_3R and D_4R).[24] Therefore, haloperidol, selected N^G-carbamoylated guanidines containing an aminothiazole moiety (**6.53**, **6.55**, **6.58**, **6.59**, **6.61**, **6.66**, **6.67**) and the bivalent ligand **6.71** were investigated in equilibrium competition binding experiments on homogenates of HEK293T-CRE-Luc-$hD_{2long}R$ and/or HEK293T-CRE-Luc-hD_3R cells using [^{3}H]N-methylspiperone as radioligand. The results are summarized in Table 6.3.

For the standard agonist pramipexole biphasic displacement curves were reported at $hD_{2long}R$ and hD_3R with pK_i values for high (pK_H value) and low affinity binding (pK_L value).[25] The standard antagonist haloperidol and the investigated ligands **6.53**, **6.55**, **6.58**, **6.59**, **6.61**, **6.66**, **6.67** and **6.71** showed monophasic displacement curves. The pK_i values of haloperidol at the $hD_{2long}R$ and hD_3R were in good accordance with literature results.[26]

The amino(methyl)thiazolylpropyl (**6.53, 6.55**, **6.58** and **6.59**), aminothiazolylphenyl (**6.61**) and 2-amino-4,5,6,7-tetrahydrobenzothiazol-6-yl (**6.66** and **6.67**) containing ligand(s) showed a weak to moderate affinity for the $hD_{2long}R$ (pK_i value 5.6-6.6). The bivalent ligand (**6.71**) showed a moderate affinity with a pK_i value of 6.97. The amino(methyl)thiazolylpropyl containing ligands **6.53, 6.55**, **6.58** and **6.59** clearly preferred the hH_2R over the $hD_{2long}R$. The 2-amino-4,5,6,7-tetrahydrobenzothiazol-6-yl containing ligands (**6.66** and **6.67**) and the bivalent ligand **6.71** showed a comparable affinity to the hH_2R and the $hD_{2long}R$.

The ligands **6.53**, **6.55, 6.58**, **6.59** and **6.71** showed a moderate affinity for the hD_3R with pK_i values between 6.9 and 7.6. The ligands **6.61**, **6.66** and **6.67** showed a low affinity for the hD_3R with pK_i values between 5.3 and 5.9. The N^G-carbamoylated amino(methyl)thiazolyl-propylguanidines **6.53**, **6.55**, **6.58** and **6.66** bound non-selectively to both the hH_2R and hD_3R receptors. The 2-amino-4,5,6,7-tetrahydrobenzothiazol-6-yl moiety containing ligand **6.67** showed a preference towards hH_2R and $hD_{2long}R$ over the hD_3R. In contrast, the bivalent ligand **6.71** showed a preference towards hD_3R over the $hD_{2long}R$ and hH_2R.

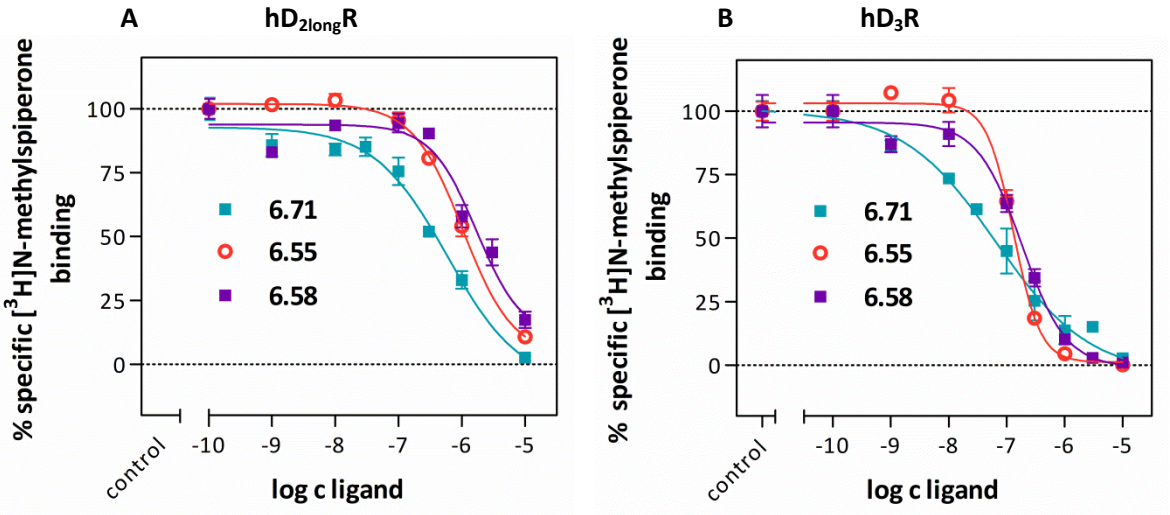

Figure 6.10. Displacement of [^{3}H]N-methylspiperone from homogenates of (A) HEK293T-CRE-Luc-$hD_{2long}R$ cells ([^{3}H]N-Methylspiperone: K_d = 0.014 nM, c = 0.05 nM) or (B) HEK293T-CRE-Luc-hD_3R cells ([^{3}H]N-methylspiperone: K_d = 0.026 nM, c = 0.05 nM) by selected monomeric carbamoylated guanidines. Data represent mean values ± SEM of 3 experiments performed in triplicate.

Table 6.3. Affinities of haloperidole, pramipexole and the monovalent carbamoylated guanidines **6.53**, **6.55**, **6.58**, **6.59**, **6.61**, **6.66**, **6.67** and **6.71** to the dopamine receptors $hD_{2long}R$ and hD_3R, obtained from equilibrium competition binding studies.

	$hD_{2long}R$[a]		**hD_3R[b]**	
Compound	**pK_i**	**N**	**pK_i**	**N**
Haloperidol	9.60[c 26]/	-	8.64[c 26]/	-
	9.3 ± 0.2	3	8.7 ± 0.1	3
Pramipexole	(pK_H: 7.40 / pK_L: 5.44)[d 25]	-	(pK_H: 9.06 / pK_L: 7.36)[d 25]	-
6.53	6.3 ± 0.1	3	7.07 ± 0.06	3
6.55	6.58 ± 0.03	3	7.36 ± 0.04	3
6.58	6.28 ± 0.08	3	7.19 ± 0.06	3
6.59	6.32 ± 0.08	3	6.88 ± 0.04	3
6.61	5.6 ± 0.2	3	5.89 ± 0.05	3
6.66	5.9 ± 0.1	3	5.9 ± 0.2	3
6.67	6.26 ±	1	5.3 ± 0.1	3
6.71	6.97 ± 0.06	3	7.6 ± 0.2	3

Determined by displacing [^{3}H]N-methylspiperone ([a]$hD_{2long}R$: K_d = 0.0149 nM, c = 0.05 nM or [b]hD_3R: K_d = 0.0258 nM, c = 0.05 nM) by increasing concentrations of the respective ligand at homogenates of [a]HEK293T-CRE-Luc-$hD_{2long}R$ or [b]HEK293T-CRE-Luc-hD_3R cells. [c]determined on CHO cells stably expressing the $hD_{2short}R$ or hD_3R. [d]High/low affinity binding determined on CHO cells stably expressing the $hD_{2short}R$ or hD_3R. Data were analyzed by nonlinear regression and were best fitted to four-parameter sigmoidal concentration-response curves. Data shown are means ± SEM of N independent experiments, each performed in triplicate.

6.3 EXPERIMENTAL SECTION

6.3.1 General procedures

Chemicals and solvents were purchased from the following suppliers: Merck (Darmstadt, Germany), Acros Organics (Geel, Belgium), Fluka (Buchs, Swiss), Alfa Aesar (Karlsruhe, Germany), Sigma Aldrich (Munich, Germany) and TCI (Tokyo, Japan). All solvents were of analytical grade or distilled prior to use. Anhydrous solvents were stored over molecular sieve under protective gas. Deuterated solvents for NMR spectroscopy were purchased from Deutero (Kastellaun, Germany). For the preparation of buffers and HPLC eluents Millipore water was used throughout. Column chromatography was carried out using Merck silica gel 60 (0.040-0.063 mm). Automated flash chromatography was performed with a 971-FP flash-purification system (Agilent Technologies, Santa Clara, CA). Pre-packed columns (SuperFlash SF10-4 g, SF12-8 g, SF 15-12 g und SF15-24 g, Agilent Technologies, Santa Clara, CA) were used throughout. Reactions were monitored by thin layer chromatography (TLC) on Merck silica gel 60 F254 aluminium sheets, and compounds were detected with UV light at 254 nm and ninhydrin solution (0.8 g ninhydrin, 200 mL n-buthanol, 6 mL acetic acid). Melting points were determined with a B-540 apparatus (BÜCHI GmbH, Essen, Germany) and are uncorrected. IR spectra were measured on a NICOLET 380 FT-IR spectrophotometer (Thermo Electron Corporation, USA) or on a FTS 3000 MX spectrometer (Excalibur Series, Bio-Rad, Hercules, CA) equipped with an ATR unit (Specac Golden Gate Diamond Single Reflection ATR system). Nuclear Magnetic Resonance (^{1}H NMR and ^{13}C NMR) spectra were recorded on a Bruker Avance-300 (7.05 T, ^{1}H: 300 MHz, ^{13}C: 75.5 MHz), Avance-400 (9.40 T, ^{1}H: 400 MHz, ^{13}C: 100.6 MHz), or Avance-600 (14.1 T; ^{1}H: 600 MHz, ^{13}C: 150.9 MHz; cryogenic probe) NMR spectrometer (Bruker BioSpin, Karlsruhe, Germany). Chemical shifts are given in δ (ppm) relative to external standards. Multiplicities are specified with the following abbreviations: s (singlet), d (doublet), t (triplet), q (quartet), qui (quintet), m (multiplet), br s (broad signal), as well as combinations thereof. In certain cases 2D-NMR techniques (COSY, HSQC, HMBC and NOESY) were used to assign ^{1}H and ^{13}C chemical shifts. High-resolution mass spectrometry (HRMS) was performed on an Agilent 6540 UHD Accurate-Mass Q-TOF LC/MS system (Agilent Technologies, Santa Clara, USA) using an ESI source. Preparative HPLC was performed with a system from Knauer (Berlin, Germany) consisting of two K-1800 pumps and a K-2001 detector. A Nucleodur 100-5 C18 (250 x 21 mm, 5 µm, Macherey-Nagel, Dueren, Germany), a Kinetex XB-C18 100A (250 x 21.2 mm, 5 µm, Phenomenex, Aschaffenburg, Germany) and a Interchim Puriflash PF15 C18 HQ (120 g, 15 µm, Interchim S. A., Montluçon, France) served as RP-columns at a flow rate of either 15 mL/min (Kinetex and Phenomenex column) or 30 mL/min (Interchim column) at room temperature. A detection wavelength of 220 nm and mixtures of CH_3CN and 0.05-0.1% aq. TFA as mobile phase were used throughout. CH_3CN was removed from the eluates under reduced pressure (final pressure: 80 mbar) at 45 °C prior to lyophilisation (Christ alpha 2-4 LD lyophilisation apparatus equipped with a vacuubrand RZ 6 rotary vane vacuum pump). Analytical HPLC analysis was performed on a system from Meck Hitachi, composed of a D-6000 interface, a L-6200A pump, a AS2000A auto sampler and a L-4000 UV-VIS detector. A Kinetex XB-C18 100A (250 x 4.6 mm, 5 µm, t_0 = 2.9 min, Phenomenex, Aschaffenburg, Germany) served as RP-column. Mixtures of 0.05% TFA in CH_3CN (A) and 0.05% aq. TFA (B) were used as mobile phase. Helium degassing, room temperature, a flow rate of 0.8 mL/min and a detection wavelength of 220 nm were used throughout. Solutions for injection (concentration:

100-500 µM) were either prepared from stock solution (10 mM in 20 mM aqueous HCl solution or 10 mM in a mixture of DMSO/ in 20 mM aqueous HCl solution 1:1) in a mixture of A and B corresponding to the initial eluent composition of the run, or as a one to one dilution of the eluate (preparative HPLC) with Millipore water. The following linear gradients were applied for analytical HPLC analysis: gradient 1: 0-30 min: A/B 5:95-80:20, 30-32 min: 80:20-95:5, 32-42 min: 95:5 or gradient 2: 0-30 min: A/B 10:90-80:20, 30-32 min: 80:20-95:5, 32-42 min: 95:5 or gradient 3: 0-30 min: A/B 15:85-90:10, 30-35 min: 90:10. Microanalysis was performed on a Vario micro cube (Elementar, Langenselbold, Germany).

6.3.2 Experimental protocols and analytical data

The branched carboxylic acids (3-methyl 4-(4-methylphenyl)butanoic acid, 3-methyl 5-phenyl pentanoic acid, 3-cyclohexyl butanoic acid, 3-(4-prop-2-yl phenyl) butanoic acid, 4-methyl 3-phenyl pentanoic acid, 3-phenyl pentanoic acid, 4-cyclohexyl 3-methyl butanoic acid) were synthesized by Anja Kraus [12]. The amine precursor 3-(1-trityl-1*H*-pyrazol-4-yl)prop-1-yl-amine was synthesized according to published protocols [13].

2-(5-Oxohexyl)isoindoline-1,3-dione (6.1)[1,16]

A solution of phthalimide (1.29 g, 8.74 mmol, 1 eq), 6-chlorohexan-2-one (2 g, 14.86 mmol, 1.7 eq) and K_2CO_3 (1.39 g, 10.05 mmol, 1.15 eq) in DMF (17 mL) were stirred at 80 °C for 24 h to obtain a white suspension. Ice cold water (60 mL) was added and the product was extracted with $CHCl_3$ (3 x 50 mL). The organic layers were combined and washed with brine (50 mL). The solvent was removed under reduced pressure. The crude product was dissolved in $CHCl_3$ (100 mL) and washed with water (2 x 50 mL) and brine (50 mL). The organic layer was dried over Na_2SO_4 and the solvent was removed under reduced pressure and the residue was purified by column chromatography (eluent: PE/EtOAc 90:10 - 70:30). Removal of the solvent *in vacuo* afforded the product as a white solid (1.5 g, 70%). Mp: 68.5 °C (Lit.[16] mp: 73-75 °C). R_f = 0.3 (PE/EtOAc 7:3). ^{1}H-NMR (400 MHz, $CDCl_3$): δ (ppm) 1.51-1.67 (m, 4H), 2.07 (s, 3H), 2.43 (t, 2H, *J* 7.15 Hz), 3.63 (t, 2H, *J* 6.94 Hz), 7.63-7.67 (m, 2H), 7.75-7.80 (m, 2H). ^{13}C-NMR (100 MHz, $CDCl_3$): δ (ppm) 20.8, 27.9, 29.9, 37.5, 42.9, 123.2, 132.1, 133.9, 168.4, 208.3. HRMS (ESI): *m/z* $[M+H]^+$ calcd. for $C_{14}H_{16}NO_3^+$: 246.1125, found: 246.1128. $C_{14}H_{15}NO_3$ (245.28).

2-[3-(2-Amino-4-methylthiazol-5-yl)propyl]-1,3-dihydro-2H-isoindol-1,3-dione hydrobromide (6.3)[1,16]

6.1 (5.00 g, 20.38 mmol, 1 eq) was dissolved in dioxane (100 mL). A solution of bromine (3.91 g, 24.46 mmol, 1.2 eq) in CH_2Cl_2 (60 mL) was added drop wise and the reaction mixture was stirred for 1 h at room temperature. Removal of the solvent *in vacuo* afforded **6.2** as a brown oil. The crude intermediate was dissolved in DMF (100 mL) and thiourea (1.55 g, 20.38 mmol, 1 eq) was added. The reaction mixture was stirred at 100 °C for 3 h and then over night at room temperature. The solvent was removed under reduced pressure and the residue was suspended

in EtOAc (100 mL). Subsequently, the precipitate was filtered off and washed with EtOAc (100 ml). Removal of residual solvent *in vacuo* afforded **6.3** as a beige solid (6.71 g, 86%). Mp: 211.0 °C (Lit.[16] mp: 242 °C). R_f= 0.30 (CH_2Cl_2 / 1.75 N NH_3 in MeOH 9:1). ^{1}H-NMR (400 MHz, [D_6]DMSO) δ (ppm): 1.78-1.91 (m, 2H), 2.08-2.14 (m, 3H), 2.61-2.73 (m, 2H), 3.59-3.63 (m, 2H), 7.81-7.88 (m, 4H). HRMS (ESI) *m/z* (*M*+H)$^+$ calcd. for $C_{15}H_{16}N_3O_2S^+$: 302.0958, found: 302.0963. $C_{15}H_{15}N_3O_2S$ · HBr (301.09 + 80.91).

tert-Butyl 4-methyl-5-[3-(1,3-dioxo-1,3-dihydro-2*H*-isoindol-2-yl)propyl]thiazol-2-ylcarbamate (6.4)[1,16]

6.3 (3.58 g, 9.40 mmol, 1 eq), di-*tert*-butyldicarbonate (2.46 g, 11.28 mmol, 1.2 eq), triethylamine (1.43 g, 14.09 mmol, 1.5 eq) and 4-(dimethylamino)-pyridine (105 mg, 0.94 mmol, 0.1 eq) were dissolved in $CHCl_3$ (40 ml). The mixture was stirred overnight at room temperature. The precipitate was filtered off. The product containing supernatant was washed with hydrochloric acid (0.25 M, 2 x 100 mL), brine (100 mL) and H_2O (100 mL). The organic layer was dried over Na_2SO_4 and the solvent was removed under reduced pressure. The residue was purified by automated flash chromatography (PE/EA 100:0 – 55:45 in 45 min). Removal of the solvent under reduced pressure afforded the product as yellow foam (750 mg, 20%). Mp: 81.5 °C (Lit.[16] mp: 70-72 °C). R_f= 0.3 (PE/EA 60:40). ^{1}H-NMR (400 MHz, $CDCl_3$): δ (ppm) 1.51 (s, 9H), 1.95-2.02 (m, 2H), 2.22 (s, 3H), 2.71 (t, 2H, *J* 7.80 Hz), 3.74 (t, 2H, *J* 7.15 Hz), 7.69-7.72 (m, 2H), 7.83-7.85 (m, 2H). ^{13}C-NMR (100 MHz, $CDCl_3$): δ (ppm) 14.4, 23.7, 28.3, 30.2, 37.5, 82.4, 123.1, 123.3, 132.1, 134.0, 141.5, 152.5, 157.6, 168.3. HRMS (ESI) *m/z* (*M*+H)$^+$ calcd. for $C_{20}H_{24}N_3O_4S^+$: 402.1482, found: 402.1489. $C_{20}H_{23}N_3O_4S$ (401.48).

tert-Butyl 5-(3-aminopropyl)-4-methylthiazol-2-ylcarbamate (6.5)[1,16]

To a suspension of **6.4** (710 mg, 1.77 mmol, 1 eq) in EtOH (7 ml) hydrazine-monohydrate (443 mg, 8.84 mmol, 5 eq) was added. The reaction mixture was stirred over night at room temperature. The precipitated phthalhydrazide (by-product) was filtered off. The product which was dissolved in the supernatant was purified by automated flash chromatography (CH_2Cl_2 / 1.75 N NH_3 in MeOH 100:0 – 90:10 in 35 min). Removal of the solvent *in vacuo* afforded the product as yellow oil (400 g, 83%). R_f= 0.56 (CH_2Cl_2 / 1.75 N NH_3 in MeOH 80:20). ^{1}H-NMR (400 MHz, [D_6]DMSO): δ (ppm) 1.46 (s, 9H), 1.54-1.61 (m, 2H), 2.11 (s, 3H), 2.55 (t, 2H, *J* 6.83 Hz), 2.63 (t, 2H, *J* 7.44 Hz). ^{13}C-NMR (75 MHz, $CDCl_3$): δ (ppm) 14.5, 23.3, 28.3, 34.9, 41.2, 82.1, 123.8, 141.6, 152.8, 157.5. HRMS (ESI) *m/z* (*M*+H)$^+$ calcd. for $C_{12}H_{22}N_3O_2S^+$: 272.1427, found: 272.1433. $C_{12}H_{21}N_3O_2S$ (271.38).

2-Amino-4-(3-phthalimidophenyl)thiazole hydrobromide (6.6)

To a solution of **3.4** (2 g, 7.54 mmol, 1 eq) in $CHCl_3$ (20 mL) was added HBr solution in acetic acid (45 % w/v, 1 mL) under stirring. Bromine (1.2 g, 7.54 mmol, 1 eq) in $CHCl_3$ (10 mL) was added drop wise. The reaction mixture was stirred for 1 h at room temperature. Removal of the solvent *in vacuo* afforded the **3.5** as a white solid, which was applied to the next step without further purification. The crude **3.5** was dissolved in hot CH_3CN (30 mL) and poured in a hot solution of

thiourea (574 mg, 7.54 mmol, 1 eq) in EtOH (30 mL). The reaction mixture was stirred under reflux for 3 h. Removal of the solvent *in vacuo* afforded a beige solid, which was recristallized in EtOAc (100 mL) and filtered through a Buchner funnel. **6.6** was afforded as a white solid (2.35 g, 78%). Mp: 269-279°C, decomposition. R_f = 0.7 (CH_2Cl_2/ 1.75 N NH_3 in MeOH 9:1). ^{1}H-NMR (400 MHz, [D_6]DMSO, COSY, HSQC, HMBC): δ (ppm) 7.26 (s, 1H), 7.51-7.54 (m, 1H), 7.66 (t, 1H, *J* 7.90 Hz), 7.81-7.85 (m, 2H), 7.93-7.96 (m, 2H), 7.98-8.01 (m, 2H), 8.94 (br s, 3H). ^{13}C-NMR (100 MHz, [D_6]DMSO): δ (ppm) 104.3, 124.0, 125.3, 125.9, 128.7, 130.1, 130.6, 131.9, 133.0, 135.4, 139.7, 167.3, 170.6. HRMS: (ESI): *m/z* [*M*+H]$^+$ calcd. for $C_{17}H_{12}N_3O_2S^+$: 322.0645, found: 322.0650. $C_{17}H_{11}N_3O_2S \cdot HBr$ (321.35 + 80.91).

2-Amino-4-(3-aminophenyl)thiazole (6.7)[27]

6.6 (1.69 g, 4.20 mmol, 1eq) was suspended in a mixture of concentrated hydrochloric acid (30 mL) and acetic acid (30 mL) and the reaction mixture was stirred under reflux overnight. The solvent was removed under reduced pressure and the residue was suspended in aqueous NaOH solution (0.03 M, 30 mL). The resulting precipitate (by-product: phthalic acid) was filtered through a Buchner funnel and washed with H_2O (20 mL). Aqueous layers were combined and part of the solvent was removed under reduced pressure. Aqueous NH_3 solution (25%, 5 mL) was added and the resulting precipitate was filtered off. The solid was washed with H_2O (40 mL) and the residual solvent was removed under reduced pressure. **6.7** was afforded as a yellow solid (560 mg, 60%). Mp: 177-178 °C. R_f = 0.6 (CH_2Cl_2/ 1.75 N NH_3 in MeOH 9:1). ^{1}H-NMR (300 MHz, [D_6]DMSO): δ (ppm) 5.05 (br s, 2H), 6.43-6.47 (m, 1H), 6.77 (s, 1H), 6.91-7.03 (m, 5H). ^{13}C-NMR (100 MHz, [D_6]DMSO): δ (ppm) 101.1, 111.9, 113.5, 114.0, 129.3, 136.0, 149.1, 151.2, 168.3. HRMS: (ESI): *m/z* [*M*+H]$^+$ calcd. for $C_9H_{10}N_3S^+$: 192.0590, found: 192.0590. $C_9H_9N_3S$ (191.25).

2-((*1r, 4r*)-4-hydroxycyclohexyl)isoindoline-1,3-dione (6.8)[28]

K_2CO_3 (10.50 g, 75.97 mmol, 1.75 eq) was added to a solution of trans-4-aminocyclohexanol (5.00 g, 43.41 mmol, 1 eq) in H_2O (50 mL). Under stirring N-(ethoxycarbonyl)phthalimide (10.24 g, 49.92 mmol, 1.15 eq) was added and the reaction mixture was stirred for 30 min at room temperature. The resulting precipitate was filtered off and washed with H_2O (50 mL). Removal of the residual solvent *in vacuo* afforded the product as a beige solid (4.94 mg, 98%). %). Mp: 183-185 °C (Lit.[28] mp: 177-178 °C). R_f = 0.2 (PE /EtOAc 3:1). ^{1}H-NMR (400 MHz, [D_6]DMSO): δ (ppm) 1.21-1.32 (m, 2H), 1.66-1.69 (m, 2H), 1.90-1.93 (m, 2H), 2.08-2.19 (m, 2H), 3.41-3.49 (m, 1H), 3.91-3.99 (m, 1H), 4.64 (d, 1H, *J* 4.26 Hz), 7.80-7.85 (m, 4H). ^{13}C-NMR (100 MHz, [D_6]DMSO): δ (ppm) 27.8, 35.1, 49.9, 68.5, 123.4, 131.9, 134.8, 168.3. HRMS: (ESI): *m/z* [*M*+H]$^+$ calcd. for $C_{14}H_{16}NO_3^+$: 246.1125, found: 246.1126. $C_{14}H_{15}NO_3$ (245.28).

2-(4-oxocyclohexyl)isoindoline-1,3-dione (6.9)[28,29]

6.8 (2.6 g, 10.61 mmol, 1 eq) was dissolved in anhydrous CH_2Cl_2 (70 mL). Under Ar-atmosphere first two spoons of Celite® were added followed by pyridinium chlorochromate (5.58 g, 25.88

mmol, 2.44 eq). The reaction mixture was stirred for 3.5 h at room temperature. 2-Propanol (2 mL) was added and after stirring for additional 30 min the solvent was removed under reduced pressure. The residue was purified by automated flash chromatography (EtOAc 100:0 isocratic for 10 min). Removal of the solvent afforded the product as light beige solid (1.82 g, 71%). Mp: 144-145 °C. R_f = 0.4 (PE /EtOAc 1:1). ^{1}H-NMR (300 MHz, $CDCl_3$): δ (ppm) 2.02-2.10 (m, 2H), 2.48-2.54 (m, 4H), 2.65-2.79 (m, 2H), 4.57-4.68 (m, 1H), 7.69-7.75 (m, 2H), 7.80-7.87 (m, 2H). ^{13}C-NMR (75 MHz, $CDCl_3$): δ (ppm) 28.6, 39.9, 48.3, 123.3, 131.8, 134.1, 168.1, 209.0. HRMS: (ESI): *m/z* [*M*+H]$^+$ calcd. for $C_{14}H_{14}NO_3^+$: 244.0968, found: 244.0973. $C_{14}H_{13}NO_3$ (243.26).

2-(2-Amino-4,5,6,7-tetrahydrobenzo[d]thiazol-6-yl)isoindoline-1,3-dione (6.11)[11,29]

6.9 (1.93 g, 7.93 mmol, 1 eq) was dissolved in a mixture of dioxane (22 mL) and CH_2Cl_2 (14 mL). Bromine (1.40 g, 8.73 mmol, 1.1 eq) dissolved in CH_2Cl_2 (24 mL) was added drop wise and the reaction mixture was stirred for 1.5 h at room temperature. The solvent was removed under reduced pressure and the residue (crude **6.10**) was dissolved in DMF (60 mL). After the addition of thiourea (0.60 g, 7.93 mmol, 1 eq) the reaction mixture was stirred for 2 h at 100 °C. The solvent was removed under reduced pressure and the residue was suspended in EtOAc (50 mL). The precipitate was filtered off and the residual solvent was removed *in vacuo* to afford the product as a beige solid (2.77 g, 92%). Mp: >300 °C decomposition (Lit.[11] mp: 244-246 °C decomposition). R_f= 0.90 (CH_2Cl_2 / 1.75 N NH_3 in MeOH 9:1). ^{1}H-NMR (400 MHz, [D_6]DMSO): δ (ppm) 1.99-2.05(m, 1H), 2.60-2.77 (m, 3H), 2.88-2.93 (m, 1H), 3.11-3.36 (m, 1H), 4.41-4.49 (m, 1H), 7.84.7.90 (m, 4H). HRMS: (ESI): *m/z* [*M*+H]$^+$ calcd. for $C_{15}H_{14}N_3O_2S^+$: 300.0801, found: 300.0817. $C_{15}H_{13}N_3O_2S$ (299.35).

4,5,6,7-Tetrahydrobenzo[d]thiazole-2,6-diamine (6.12)[29]

6.11 (200 mg, 0.53 mmol, 1 eq) was suspended in a mixture of hydrochloric acid (37%, w/v, 5 mL) and acetic acid (5mL). The reaction mixture was stirred over night at 100 °C. The solvent was removed under reduced pressure and the residue was dissolved in H_2O (5 mL). The pH value was adjusted to 6 by addition of NaOH solution (1 M, 2 mL). The aqueous layer was washed three times with CH_2Cl_2 in order to remove by-products. Then additional NaOH solution (5mL) was added until a pH value of 9 was reached. The aqueous layer was extracted with CH_2Cl_2 (10 mL) and six times with EtOAc (10 mL). In order to extract remaining product from the aqueous layer NaCl (1 spoon) was dissolved in the mixture and the layer was again extracted three times with EtOAc (10 mL). Water was partly removed under reduced pressure and the aqueous layer was again extracted five times with EtOAc (100 mL). All organic layers were combined and dried over Na_2SO_4. Removal of the solvent *in vacuo* afforded the product as a yellow hygroscopic solid (65 mg, 73%). R_f= 0.13 (CH_2Cl_2 / 1.75 N NH_3 in MeOH 9:1). ^{1}H-NMR (300 MHz, [D_6]DMSO): δ (ppm) 1.40-1.53 (m, 1H), 1.78-1.82 (m, 1H), 2.13-2.21 (m, 1H), 2.31-2.41 (m, 2H), 2.60-2.67 (m, 1H), 2.94-3.03 (m, 1H), 6.60 (br s, 2H). HRMS: (ESI): *m/z* [*M*+H]$^+$ calcd. for $C_7H_{12}N_3S^+$: 170.0746, found: 170.0747. $C_7H_{11}N_3S$ (169.25).

General procedure for the synthesis of S-methylcarbamoyl thiourea derivatives (6.13-6.18) from isocyanates

The respective isocyanate (1 eq) and triethylamine (2.25 eq) were added to a solution of **3.32** (1.5 eq) in CH_2Cl_2 (17-20 mL). The reaction mixture was stirred overnight at room temperature. The organic layer was washed with three times with water (30 mL) and subsequently with brine (30 mL). The organic layer was dried over Na_2SO_4 and the solvent was removed under reduced pressure. The crude product was purified by flash chromatography.

S-Methyl-(N-(tertbutoxycarbonyl))-(N'-propylcarbamoyl)thiourea (6.13) *Claudia Honisch master thesis*

6.13 was prepared from propylisocyanate (149 mg, 1.75 mmol), **3.32** (500 mg, 2.63 mmol) and triethylamine (400 mg, 3.94 mmol) according to the general procedure. Purification by automated flash chromatography (PE/EtOAc 100:0-85:15 in 30 min) and removal of the solvent *in vacuo* afforded the product as a white solid (0.31 g, 64%). Mp: 56.1-60.2 °C. R_f= 0.72 (PE/EtOAc 3:1). ^{1}H-NMR (400 MHz, $CDCl_3$): δ (ppm) 0.94 (t, 3H, *J* 7.4 Hz), 1.47 (s, 9H), 1.56 (m, 2H), 2.31 (s, 3H), 3.18 (q, 2H, *J* 6.9 Hz), 12.34 (s, 1H). ^{13}C-NMR (100 MHz, $CDCl_3$): δ (ppm) 11.4, 14.3, 22.9, 28.0, 41.9, 82.6, 151.1, 161.9, 167.5. HRMS (ESI) *m/z* $(M+H)^+$ calcd. for $C_{11}H_{22}N_3O_3S^+$: 276.1376, found: 276.1379. $C_{11}H_{21}N_3O_3S$ (275.37).

S-Methyl-(N-(tertbutoxycarbonyl))-(N'-hexylcarbamoyl)thiourea (6.14) *Claudia Honisch master thesis*

6.14 was prepared from hexylisocyanate (223 mg, 1.75 mmol), **3.32** (500 mg, 2.63 mmol) and triethylamine (400 mg, 3.94 mmol) according to general procedure. Purification by automated flash chromatography (PE/EtOAc 100:0-85:15 in 35 min) and removal of the solvent *in vacuo* afforded the product as a white solid (0.45 g, 81%). Mp: 56.4-59.2 °C. R_f=0.67 (PE/EtOAc 3:1). ^{1}H-NMR (400 MHz, $CDCl_3$): δ (ppm) 0.85-0.90 (m, 3H), 1.26-1.37 (m, 6H), 1.47 (s, 9H), 1.49-1.59 (m, 2H), 2.31 (s, 3H), 3.19-3.24 (m, 2H), 12.35 (br s, 1H). ^{13}C-NMR (100 MHz, $CDCl_3$): δ (ppm) 14.0, 14.3, 22.6, 26.6, 28.0, 29.7, 31.5, 40.2, 82.6, 151.1, 161.8, 167.7. HRMS (ESI) *m/z* $(M+H)^+$ calcd. for $C_{14}H_{28}N_3O_3S^+$: 318.1846, found: 318.1851. $C_{14}H_{27}N_3O_3S$ (317.45).

S-Methyl-(N-(tertbutoxycarbonyl))-(N'-cyclohexylcarbamoyl)thiourea (6.15) *Claudia Honisch master thesis*

6.15 was prepared from cyclohexylisocyanate (219 mg, 1.75 mmol), **3.32** (500 mg, 2.63 mmol) and triethylamine (2.25 eq., 400 mg, 3.94 mmol) according to general procedure. Purification by automated flash chromatography (PE/EtOAc 100:0-85:15 in 35 min) and removal of the solvent *in vacuo* afforded the product as a white solid (0.47 g, 85%). Mp: 149.5-152.3 °C. ^{1}H-NMR (400 MHz, $CDCl_3$): δ (ppm) 1.12-1.26 (m, 3H), 1.31-1.42 (m, 2H), 1.47 (s, 9H), 1.59-1.66 (m, 1H), 1.71-1.76 (m, 2H), 1.93-1.97 (m, 2H), 2.34 (s, 3H), 3.53-3.63 (m, 1H), 12.43 (br , 1H). ^{13}C-NMR (100 MHz, $CDCl_3$):

δ (ppm) 14.4, 24.9, 25.5, 28.0, 33.1, 49.1, 82.7, 151.0, 160.9, 167.6. HRMS (ESI) *m/z* (*M*+H)$^+$ calcd. for $C_{14}H_{26}N_3O_3S^+$: 316.1689, found: 316.1700. $C_{14}H_{25}N_3O_3S$ (315.43).

S-Methyl-(N-(tert-butoxycarbonyl))-(N'-(phenylcarbamoyl)thiourea) (6.16) *Claudia Honisch master thesis*

6.16 was prepared from phenylisocyanate (210 mg, 1.75 mmol), **3.32** (500 mg, 2.63 mmol) and triethylamine (400 mg, 3.9 mmol) according to general procedure. Purification by automated flash chromatography (PE/EtOAc 100:0-90:10 in 25 min) and removal of the solvent *in vacuo* afforded the product as a white solid (0.31 g, 57%). Mp: 126.3-129.6 °C. R_f= 0.66 (PE/EtOAc 3:1). ^{1}H-NMR (400 MHz, $CDCl_3$): *δ* (ppm) 1.50 (s, 9H), 2.40 (s, 3H), 7.08-7.12 (m, 1H), 7.31-7.35 (m, 2H), 7.42 (br s, 1H), 7.49-7.51 (m, 2H), 12.22 (br s, 1H). ^{13}C-NMR (100 MHz, $CDCl_3$): *δ* (ppm) 14.6, 28.0, 83.1, 119.4, 124.0, 129.1, 137.9, 151.0, 159.3, 169.2. HRMS (ESI) *m/z* (*M*+H)$^+$ calcd. for $C_{14}H_{20}N_3O_3S^+$: 310.1220, found: 310.1228. $C_{14}H_{19}N_3O_3S$ (309.38)

S-Methyl-(N-(tertbutoxycarbonyl))-(N'-benzylcarbamoyl)thiourea (6.17) *Claudia Honisch master thesis*

6.17 was prepared from benzylisocyanate (234 mg, 1.75 mmol), **3.32** (500 mg, 2.63 mmol) and triethylamine (400 mg, 3.94 mmol) according to general procedure. Purification by automated flash chromatography (PE/EtOAc 100:0-85:15 in 35 min) and removal of the solvent *in vacuo* afforded the product as a white solid (0.45 g, 80%). Mp: 103.8-106.6 °C. R_f= 0.77 (PE/EtOAc 3:1). ^{1}H-NMR (400MHz, $CDCl_3$): *δ* (ppm) 1.49 (s, 9H), 2.34 (s, 3H), 4.43 (d, 2H, *J* 6.09 Hz), 6.09 (br s, 1H), 7.27-7.37 (m, 5H), 12.38 (br s, 1H). ^{13}C-NMR (100 MHz, $CDCl_3$): *δ* (ppm) 14.5, 28.0, 44.2, 83.0, 127.56, 127.64, 128.8, 138.2, 151.0, 155.3, 168.5. HRMS (ESI) *m/z* (*M*+H)$^+$ calcd. for $C_{15}H_{22}N_3O_3S^+$: 324.1376, found: 324.1384. $C_{15}H_{21}N_3O_3S$ (323.41).

S-Methyl-(N-(tertbutoxycarbonyl))-(N'-(2-phenylethyl)carbamoyl)thiourea (6.18) *Claudia Honisch master thesis*

6.18 was prepared from phenethylisocyanate (258 mg, 1.75 mmol), **3.32** (500 mg, 2.63 mmol) and triethylamine (400 mg, 3.94 mmol) according to general procedure. . Purification by automated flash chromatography (PE/EtOAc 100:0-85:15 in 35 min) and removal of the solvent *in vacuo* afforded the product as a white solid (0.43 g, 73%). Mp: 101.8-103.7 °C. R_f= 0.73 (PE/EtOAc 3:1). ^{1}H-NMR (400 MHz, $CDCl_3$): *δ* (ppm) 1.49 (s, 9H), 2.29 (s, 3H), 2.86 (t, 2H, *J* 7.18 Hz) 3.47-3.52 (m, 2H), 7.17-7.34 (m, 5H), 12.32 (br s, 1H). ^{13}C-NMR (100 MHz, $CDCl_3$): *δ* (ppm) 14.4, 28.1, 35.9, 41.4, 82.8, 126.5, 128.6, 128.8, 138.8, 151.1, 161.7, 168.9. HRMS (ESI) *m/z* (*M*+H)$^+$ calcd. for $C_{16}H_{24}N_3O_3S^+$: 338.1533, found: 338.1546. $C_{16}H_{23}N_3O_3S$ (337.44).

General procedure for the synthesis of S-methylcarbamoyl thiourea derivatives (6.19-6.25) from carbonic acids

The respective carbon acid (1 eq) was dissolved in CH_2Cl_2 (2.5-4.5 mL) and cooled with an ice bath. DMF (25-45 µL) and oxalyl chloride (1.5 eq) were added under Ar-atmosphere. The reaction mixture was stirred for 10 min under cooling. The ice bath was removed and stirring was continued for another 15 min at room temperature. The solvent was carefully removed under reduced pressure (water bath temperature under 30 °C). The residue was dissolved in anhydrous acetone (2.5-4.5 mL) and added drop wise under cooling to an ice cold solution of sodium azide (2.4 eq) in H_2O (1-3 mL). The reaction mixture was stirred for 30 min under cooling. Brine (5-10 mL) was added and the acyl azide was extracted three times with CH_2Cl_2 (10 mL). The organic layers were combined and dried over Na_2SO_4. Molecular sieve was added and the solvent was partially removed under reduced pressure. The resulting yellow solution was stirred for 30 min under reflux conditions to afford the isocyanate. The solution was cooled to room temperature and **3.32** (1 eq) and triethylamine (5 eq) were added. The reaction mixture was stirred over night at room temperature. The molecular sieve was filtered off and the organic layer was washed three times with H_2O (10 mL) and three times with brine (10 mL). The organic layers were combined and dried over Na_2SO_4. The crude product was purified by either automated flash chromatography or column chromatography.

S-Methyl-(N-(tertbutoxycarbonyl))-(N'-[2-methyl 3-(4-methylphenyl)propyl]carbamoyl)thiourea (6.19)

6.19 was prepared from 3-methyl 4-(4-methylphenyl)butanoic acid (100 mg, 0.52 mmol, 1 eq), oxalyl chloride (99 mg, 0.75 mmol, 1.5 eq), sodium azide (85 mg, 1.30 mmol, 2.4 eq), **3.32** (100 mg, 0.52 mmol, 1 eq) and triethylamine (263 mg, 2.60 mmol, 5 eq) according to general procedure. Purification by automated flash chromatography (PE/EtOAc 100:0-85:15 in 20 min) and removal of the solvent *in vacuo* afforded the product as colourless oil (140 mg, 71%). R_f= 0.80 (PE/EtOAc 3:1). ^{1}H-NMR (400 MHz, $CDCl_3$): δ (ppm) 0.92 (d, 3H, *J* 6.5 Hz), 1.48 (s, 9H), 1.92-2.04 (m, 1H), 2.31-2.33 (m, 6H), 2.39-2.44 (m, 1H), 2.63-2.68 (m, 1H), 3.08-3.22(m, 2H), 7.04-7.10 (m, 4H), 12.36 (br s, 1H). ^{13}C-NMR (75 MHz, $CDCl_3$): δ (ppm) 14.3, 17.7, 21.0, 28.0, 35.7, 40.8, 46.0, 82.6, 128.9, 129.0, 135.5, 137.1, 151.2, 162.0, 167.2. HRMS (ESI) *m/z* $(M+H)^+$ calcd. for $C_{19}H_{30}N_3O_3S^+$: 380.2002, found: 380.2009. $C_{19}H_{29}N_3O_3S$ (379.52).

S-Methyl-(N-(tertbutoxycarbonyl))-[N'-(2-methyl 4-phenylbutyl)carbamoyl]thiourea (6.20)

6.20 was prepared from 3-methyl 5-phenyl pentanoic acid (150 mg, 0.78 mmol, 1 eq), oxalyl chloride (149 mg, 1.17 mmol, 1.5 eq), sodium azide (122 mg, 1.87 mmol, 2.4 eq), **3.32** (148 mg, 0.78 mmol, 1 eq) and triethylamine (395 mg, 3.90 mmol, 5 eq) according to general procedure. Purification by column chromatography (PE/EtOAc 3:1 isocratic) and removal of the solvent *in vacuo* afforded the product as colourless oil (220 mg, 74%). R_f= 0.66 (PE/EtOAc 3:1). ^{1}H-NMR (300 MHz, $CDCl_3$): δ (ppm) 1.01 (d, 3H, *J* 6.57 Hz), 1.43-1.51 (m, 10H), 1.62-1.78 (m, 2H), 2.35 (br s, 3H), 2.55-2.77 (m, 2H), 3.05-3.25(m, 2H), 7.15-7.31 (m, 5H), 12.40 (br s, 1H). ^{13}C-NMR (100 MHz,

$CDCl_3$): δ (ppm) 14.4, 17.7, 28.2, 33.3, 33.4, 36.3, 46.1, 82.7, 125.9, 128.46, 128.49, 142.5, 151.3, 162.2, 167.4. HRMS (ESI) *m/z* $(M+H)^+$ calcd. for $C_{19}H_{30}N_3O_3S^+$: 380.2002, found: 380.2025. $C_{19}H_{29}N_3O_3S$ (379.52).

S-Methyl-(N-(tertbutoxycarbonyl))-[N'-(2-cyclohexyl propyl)carbamoyl]thiourea (6.21)

6.21 was prepared from 3-cyclohexyl butanoic acid (150 mg, 0.88 mmol, 1 eq), oxalyl chloride (168 mg, 1.32 mmol, 1.5 eq), sodium azide (137 mg, 2.11 mmol, 2.4 eq), **3.32** (167 mg, 0.88 mmol, 1 eq) and triethylamine (446 mg, 4.41 mmol, 5 eq) according to general procedure. Purification by column chromatography (PE/EtOAc 3:1 isocratic) and removal of the solvent *in vacuo* afforded the product as colourless oil (210 mg, 67%). R_f= 0.81 (PE/EtOAc 3:1). ^{1}H-NMR (300 MHz, $CDCl_3$): δ (ppm) 0.89 (d, 3H, *J* 6.91 Hz), 0.97-1.30 (m, 6H), 1.48 (s, 9H), 1.62-1.76 (m, 6H), 2.37 (br s, 3H), 2.99-3.09 (m, 1H), 3.22-3.30 (m, 1H), 12.43 (br s, 1H). ^{13}C-NMR (100 MHz, $CDCl_3$): δ (ppm) 14.4, 14.5, 26.67, 26.74, 26.8, 28.1, 28.6, 30.9, 38.7, 40.6, 44.1, 82.6, 151.3, 162.2, 167.2. HRMS (ESI) *m/z* $(M+H)^+$ calcd. for $C_{17}H_{32}N_3O_3S^+$: 358.2159, found: 358.2199. $C_{17}H_{31}N_3O_3S$ (357.51).

S-Methyl-(N-(tertbutoxycarbonyl))-[N'-(2-(4-prop-2-yl phenyl) propyl)carbamoyl]thiourea (6.22)

6.22 was prepared from 3-(4-prop-2-yl phenyl) butanoic acid (150 mg, 0.73 mmol, 1 eq), oxalyl chloride (138 mg, 1.09 mmol, 1.5 eq), sodium azide (114 mg, 1.75 mmol, 2.4 eq), **3.32** (138 mg, 0.73 mmol, 1 eq) and triethylamine (368 mg, 3.64 mmol, 5 eq) according to general procedure. Purification by column chromatography (PE/EtOAc 3:1 isocratic) and removal of the solvent *in vacuo* afforded the product as colourless oil (220 mg, 77%). R_f= 0.74 (PE/EtOAc 3:1). ^{1}H-NMR (300 MHz, $CDCl_3$): δ (ppm) 1.24-1.30 (m, 9H), 1.48 (s, 9H), 2.29 (br s, 3H), 2.85-2.99 (m, 2H), 3.24-3.33 (m, 1H), 3.44-3.53 (m, 1H), 7.12-7.21 (m, 4H), 12.37 (br s, 1H). ^{13}C-NMR (100 MHz, $CDCl_3$): δ (ppm) 14.4, 19.4, 24.1, 28.15, 28.23, 33.8, 39.6, 47.1, 82.7, 126.8, 127.2, 141.5, 147.3, 151.2, 162.1, 167.5. HRMS (ESI) *m/z* $(M+H)^+$ calcd. for $C_{20}H_{32}N_3O_3S^+$: 394.2159, found: 394.2159. $C_{20}H_{31}N_3O_3S$ (393.55).

S-Methyl-(N-(tertbutoxycarbonyl))-[N'-(3-methyl 2-phenyl butyl)carbamoyl]thiourea (6.23)

6.23 was prepared from 4-methyl 3-phenyl pentanoic acid (150 mg, 0.78 mmol, 1 eq), oxalyl chloride (149 mg, 1.17 mmol, 1.5 eq), sodium azide (122 mg, 1.87 mmol, 2.4 eq), **3.32** (148 mg, 0.78 mmol, 1 eq) and triethylamine (395 mg, 3.90 mmol, 5 eq) according to general procedure. Purification by column chromatography (PE/EtOAc 3:1 isocratic) and removal of the solvent *in vacuo* afforded the product as colourless oil (130 mg, 44%). R_f= 0.81 (PE/EtOAc 3:1). ^{1}H-NMR (300 MHz, $CDCl_3$): δ (ppm) 0.75 (d, 3H, *J* 6.71 Hz), 1.02 (d, 3H, *J* 6.71 Hz), 1.48 (s, 9H), 1.85-1.97 (m, 1H), 2.24 (s, 3H), 2.50-2.58 (m, 1H), 3.25-3.37 (m, 1H), 3.79-3.88 (m, 1H), 7.10-7.35 (m, 5H), 12.36 (br s, 1H). ^{13}C-NMR (100 MHz, $CDCl_3$): δ (ppm) 14.4, 20.5, 20.9, 28.0, 31.5, 43.1, 52.6, 82.8, 126.7, 128.48, 128.54, 141.6, 151.0, 161.4, 167.7. HRMS (ESI) *m/z* $(M+H)^+$ calcd. for $C_{19}H_{30}N_3O_3S^+$: 380.2002, found: 380.2034. $C_{19}H_{29}N_3O_3S$ (379.52).

S-Methyl-(N-(tertbutoxycarbonyl))-[N'-(2-phenyl butyl)carbamoyl]thiourea (6.24)

6.24 was prepared from 3-phenyl pentanoic acid (150 mg, 0.84 mmol, 1 eq), oxalyl chloride (160 mg, 1.26 mmol, 1.5 eq), sodium azide (131 mg, 2.02 mmol, 2.4 eq), **3.32** (160 mg, 0.84 mmol, 1 eq) and triethylamine (426 mg, 4.21 mmol, 5 eq) according to general procedure. Purification by automated flash chromatography (PE/EtOAc 3:1 isocratic) and removal of the solvent *in vacuo* afforded the product as colourless oil (190 mg, 62%). R_f= 0.71 (PE/EtOAc 3:1). ^{1}H-NMR (300 MHz, $CDCl_3$): δ (ppm) 0.82 (t, 3H, *J* 7.37 Hz), 1.48-1.85 (m, 11H), 2.37 (br s, 3H), 2.66-2.76 (m, 1H), 3.25-3.33 (m, 1H), 3.56-3.65 (m, 1H), 7.15-7.36 (m, 5H), 12.53 (br s, 1H). ^{13}C-NMR (100 MHz, $CDCl_3$): δ (ppm) 12.0, 14.4, 26.8, 28.2, 45.7, 47.8, 82.7, 126.8, 128.0, 128.8, 142.6, 151.3, 162.0, 167.5. HRMS (ESI) *m/z* $(M+H)^+$ calcd. for $C_{18}H_{28}N_3O_3S^+$: 366.1846, found: 366.1895. $C_{18}H_{27}N_3O_3S$ (365.49).

S-Methyl-(N-(tertbutoxycarbonyl))-[N'-(3-cyclohexyl 2-methyl propyl)carbamoyl]thiourea (6.25)

6.25 was prepared from 4-cyclohexyl 3-methyl butanoic acid (150 mg, 0.76 mmol, 1 eq), oxalyl chloride (144 mg, 1.13 mmol, 1.5 eq), sodium azide (118 mg, 1.82 mmol, 2.4 eq), **3.32** (144 mg, 0.76 mmol, 1 eq) and triethylamine (383 mg, 3.78 mmol, 5 eq) according to general procedure. Purification by column chromatography (PE/EtOAc 3:1 isocratic) and removal of the solvent *in vacuo* afforded the product as colourless oil (110 mg, 38%). R_f= 0.72 (PE/EtOAc 3:1). ^{1}H-NMR (300 MHz, $CDCl_3$): δ (ppm) 0.79-0.95 (m, 5H), 0.99-1.06 (m, 1H), 1.14-1.34 (m, 5H), 1.49-1.83 (m, 16H), 2.68 (br s, 2H), 2.97-3.24 (m, 2H), 13.08 (br s, 1H). ^{13}C-NMR (75 MHz, $CDCl_3$): δ (ppm) 14.6, 17.9, 26.3, 26.4, 26.7, 28.0, 30.3, 32.9, 34.2, 34.8, 42.4, 46.6, 83.6, 150.9, 162.0, 168.2. HRMS (ESI) *m/z* $(M+H)^+$ calcd. for $C_{18}H_{34}N_3O_3S^+$: 372.2315, found: 372.2321. $C_{18}H_{33}N_3O_3S$ (371.54).

General procedure for the synthesis of the N^G-carbamoylated guanidines

The respective S-methylcarbamoyl thiourea derivative **6.13-6.25** or **3.33** (1 eq) and the amine **6.5**, **6.7**, **6.12** (1-1.5 eq) or 3-(1-trityl-1*H*-pyrazol-4-yl)prop-1-yl-amine (3 eq) were dissolved in anhydrous CH_2Cl_2 (5-25 mL). Triethylamine (2.25-5 eq) and $HgCl_2$ (2-2.2 eq) were added under Ar-atmosphere. The reaction mixture was stirred over night at room temperature. The resulting suspension was filtered through Celite® in order to remove the mercury salt and the crude product was purified by either automated flash chromatography or column chromatography. Removal of the solvent *in vacuo* afforded the Boc-protected products **6.26-6.46**, **6.68** and **6.69**. Subsequently, the deprotection was performed by stirring the intermediate in a mixture of CH_2Cl_2 and TFA over night at room temperature. The solvent was removed *in vacuo* and the product was purified by preparative HPLC.

4-Methyl-5-(3-(3-(propylcarbamoyl)guanidino)propyl)-2-aminothiazole bis(hydrotrifluoroacetate) (6.47) *Claudia Honisch master thesis*

6.47 was prepared from **6.13** (150 mg, 0.54 mmol, 1 eq), **6.5** (148 mg, 0.54 mmol, 1 eq), $HgCl_2$ (293 mg, 1.08 mmol, 2 eq) and triethylamine (164 mg, 1.62 mmol, 3 eq) dissolved in CH_2Cl_2 (25

mL) according to the general procedure. Purification by automated flash chromatography (PE/EtOAc 100:0-85:15 in 30 min) afforded the Boc-protected intermediate **6.26** as a glassy colourless solid (250 mg, 93%). 230 mg (0.46 mmol) of **6.26** were dissolved in a mixture of TFA (1 mL) and CH_2Cl_2 (5 mL) and stirred over night at room temperature. Removal of the solvent *in vacuo* and purification by preparative HPLC (column: Interchim, gradient: 0-30 min: MeCN/0.05% aq. TFA 15:85-37:63, t_R = 12.6 min) afforded the product as white fluffy solid (140 mg, 58%). Mp: 72.4-73.2 °C. R_f= 0.62 (CH_2Cl_2/ 1.75 N NH_3 in MeOH 9:1). IR (KBr): 602.13 660.12 697.18 726.78 761.84 797.25 844.40 1144.09 1197.67 1242.49 1269.25 1391.01 1439.56 1467.73 1545.20 1697.45 2882.67 2972.53 3122.82 3288.70 cm^{-1}. RP-HPLC (gradient 2, 220 nm): 99.23% (t_R =10.92 min, k = 2.8). ^{1}H-NMR (600 MHz, [D_6]DMSO, COSY, HSQC, HMBC, NOESY): δ (ppm) 0.85 (t, 3H, J 7.36 Hz), 1.42-1.48 (m, 2H), 1.72 (qui, 2H, *J* 7.23 Hz), 2.07 (s, 3H), 2.59 (t, 2H, *J* 7.47 Hz), 3.04-3.07 (m, 2H), 3.22-3.26 (m, 2H, interfering with the water signal), 7.49 (br s, 1H), 8.49 (br s, 2H), 8.87 (br s, 2H), 8.99 (br s, 1H), 10.22 (br s, 1H). ^{13}C-NMR (150 MHz, [D_6]DMSO, COSY, HSQC, HMBC, NOESY): δ (ppm) 11.1, 11.6, 22.0, 22.2, 28.9, 1C under solvent peak (38.7-40.3), 40.9, 116.3, 132.6, 153.7, 153.8, 167.6. HRMS (ESI) *m/z* (M+H)$^+$ calcd. for $C_{12}H_{23}N_6OS^+$: 299.1649, found: 299.1651. $C_{12}H_{22}N_6OS \cdot C_4H_2F_6O_4$ (298.16 + 228.05).

4-Methyl-5-(3-(3-(hexylcarbamoyl)guanidino)propyl)-2-aminothiazole bis(hydrotrifluoroacetate) (6.48) *Claudia Honisch master thesis*

6.48 was prepared from **6.14** (150 mg, 0.47 mmol, 1 eq), **6.5** (128 mg, 0.47 mmol, 1.5 eq), $HgCl_2$ (257 mg, 0.95 mmol, 2 eq) and triethylamine (144 mg, 1.42 mmol, 2.25 eq) dissolved in CH_2Cl_2 (25 mL) according to the general procedure. Purification by automated flash chromatography (PE/EtOAc 100:0-85:15 in 30 min) afforded the Boc-protected intermediate **6.27** as a glassy colourless solid (90 mg, 35%). 85 mg (0.16 mmol) of **6.27** were dissolved in a mixture of TFA (1 mL) and CH_2Cl_2 (10 mL) and stirred over night at room temperature. Removal of the solvent *in vacuo* and purification by preparative HPLC (column: Interchim, gradient: 0-30 min: MeCN/0.05% aq. TFA 24:76-46:54, t_R = 13.0 min) afforded the product as white hygroscopic solid (50 mg, 56%). R_f= 0.56 (CH_2Cl_2/ 1.75 N NH_3 in MeOH 9:1). RP-HPLC (220 nm, gradient 2): 99.1% (t_R =16.70 min, k = 4.8). ^{1}H-NMR (600 MHz, [D_6]DMSO, COSY, HSQC, HMBC, NOESY): δ (ppm) 0.84-0.86 (m, 3H), 1.24-1.28 (m, 6H), 1.39-1.43 (m, 2H), 1.71 (qui, 2H, *J* 7.27 Hz), 2.05 (s, 3H), 2.58 (t, 2H, *J* 7.44 Hz), 3.06-3.09 (m, 2H), 3.22-3.25 (m, 2H, interfering with the water signal), 6.57 (br s, 1H), 7.49 (br s, 1H), 8.50 (br s, 2H), 8.73 (br s,2H), 9.00 (br s, 1H), 10.39 (br s, 1H). ^{13}C-NMR (150 MHz, [D_6]DMSO, COSY, HSQC, HMBC, NOESY): δ (ppm) 11.8, 13.8, 21.98, 22.03, 25.8, 28.8, 29.0, 30.8, 2Cs under solvent peak (38.7-40.3), 116.3, 133.5, 153.7, 153.8, 167.4. HRMS (ESI) *m/z* (M+H)$^+$ calcd. for $C_{15}H_{29}N_6OS^+$: 341.2118, found: 341.2127. $C_{15}H_{28}N_6OS \cdot C_4H_2F_6O_4$ (340.49 + 228.05).

4-Methyl-5-(3-(3-(cyclohexylcarbamoyl)guanidino)propyl)-2-aminothiazole bis(hydrotrifluoroacetate) (6.49) *Claudia Honisch master thesis*

6.49 was prepared from **6.15** (150 mg, 0.47 mmol, 1 eq), **6.5** (129 mg, 0.47 mmol, 1.5 eq), $HgCl_2$ (258 mg, 0.95 mmol, 2 eq) and triethylamine (144 mg, 1.43 mmol, 2.25 eq) dissolved in CH_2Cl_2 (25 mL) according to the general procedure. Purification by automated flash chromatography

(PE/EtOAc 100:0-85:15 in 30 min) afforded the Boc-protected intermediate **6.28** as a glassy colourless solid (0.14 g, 55%). 140 mg (0.26 mmol) of **6.28** were dissolved in a mixture of TFA (1 mL) and CH_2Cl_2 (5 mL) and stirred over night at room temperature. Removal of the solvent *in vacuo* and purification by preparative HPLC (column: Interchim, gradient: 0-30 min: MeCN/0.05% aq. TFA 19:81-42:58, t_R = 13.9 min) afforded the product as white fluffy solid (99 mg, 67%). Mp: 69.6-71.8°C. R_f= 0.82 (CH_2Cl_2 / 1.75 N NH_3 in MeOH 9:1). FT-ATR: 723, 798, 839, 895, 1129, 1178, 1315, 1435, 1543, 1654, 2858, 2937, 3086, 3280 cm^{-1}. RP-HPLC (gradient 2, 220 nm): 99.10% (t_R = 14.55 min, k = 4.0). ^{1}H-NMR (600 MHz, [D_6]DMSO, COSY, HSQC, HMBC, NOESY): δ (ppm) 1.11-1.32 (m, 5H), 1.51-1.54 (m, 1H), 1.63-1.77 (m, 6H), 2.08 (s, 3H), 2.59 (t, 2H, *J* 7.51 Hz), 3.23 (q, 2H, *J* 6.25 Hz), 3.44-3.46 (m, 1H), 7.47 (br s, 1H), 8.47 (br s, 2H), 8.96 (br s, 1H), 9.12 (br s, 2H), 10.06 (br s, 1H). ^{13}C-NMR (150 MHz, [D_6]DMSO, COSY, HSQC, HMBC, NOESY): δ (ppm) 11.3, 21.9, 24.1, 24.9, 28.7, 32.0, 1C under solvent peak (38.7-40.3), 48.3, 116.3, 131.4, 152.8, 153.7, 167.9. HRMS (ESI) *m/z* $(M+H)^+$ calcd. for $C_{15}H_{27}N_6OS^+$: 339.1962, found: 339.1970. $C_{15}H_{26}N_6OS \cdot C_4H_2F_6O_4$ (338.47 + 228.05).

4-Methyl-5-(3-(3-(phenylcarbamoyl)guanidino)propyl)-2-aminothiazole bis(hydrotrifluoroacetate) (6.50) *Claudia Honisch master thesis*

6.50 was prepared from **6.16** (100 mg, 0.32 mmol, 1 eq), **6.5** (88 mg, 0.32 mmol, 1.5 eq), $HgCl_2$ (175 mg, 0.65 mmol, 2 eq) and triethylamine (98 mg, 0.97 mmol, 2.25 eq) dissolved in CH_2Cl_2 (25 mL) according to the general procedure. Purification by automated flash chromatography (PE/EtOAc 100:0-85:15 in 30 min) afforded the Boc-protected intermediate **6.29** as a glassy colourless solid (110 mg, 64%). 100 mg (0.19 mmol) of **6.29** were dissolved in a mixture of TFA (5 mL) and CH_2Cl_2 (1 mL) and stirred over night at room temperature. Removal of the solvent *in vacuo* and purification by preparative HPLC (column: Interchim, gradient: 0-30 min: MeCN/0.05% aq. TFA 19:81-42:58, t_R = 12.4 min) afforded the product as white hygroscopic solid (63 mg, 60%). R_f= 0.80 (CH_2Cl_2 / 1.75 N NH_3 in MeOH 9:1). FT-ATR: 693, 719, 753, 798, 835, 1126, 1178, 1316, 1446, 1498, 1551, 1640, 1595, 2363, 3094, 3276 cm^{-1}. RP-HPLC (gradient 2, 220 nm): 98.98% (t_R = 14.75 min, k = 4.09). ^{1}H-NMR (600 MHz, [D_6]DMSO, COSY, HSQC, HMBC, NOESY): δ (ppm) 1.75 (qui, 2H, *J* 7.21 Hz), 2.09 (s, 3H), 2.61 (t, 2H, *J* 7.50 Hz), 3.28 (q, 2H, *J* 6.47 Hz), 7.08-7.12 (m, 1H), 7.32-7.36 (m, 2H), 7.43-7.45 (m, 2H), 8.56 (br s, 2H), 8.93 (br s, 1H), 9.05 (br s, 2H), 10.47 (br s, 1H). ^{13}C-NMR (150 MHz, [D_6]DMSO, COSY, HSQC, HMBC, NOESY): δ (ppm) 11.4, 21.9, 28.7, 1C under solvent peak (38.7-40.3), 116.3, 119.6, 123.9, 129.0, 133.8, 137.5, 153.4 (2C), 167.8. HRMS (ESI) *m/z* $(M+H)^+$ calcd. for $C_{15}H_{21}N_6OS^+$: 333.1492, found: 333.1496. $C_{15}H_{20}N_6OS \cdot C_4H_2F_6O_4$ (332.43 + 228.05).

4-Methyl-5-(3-(3-((phenylmethyl)carbamoyl)guanidino)propyl)-2-aminothiazole bis(hydrotrifluoroacetate) (6.51) *Claudia Honisch master thesis*

6.51 was prepared from **6.17** (150 mg, 0.464 mmol, 1 eq), **6.5** (126 mg, 0.464 mmol, 1.5 eq), $HgCl_2$ (252 mg, 0.928 mmol, 2 eq) and triethylamine (141 mg, 1.392 mmol, 2.25 eq) dissolved in CH_2Cl_2 (25 mL) according to the general procedure. Purification by automated flash chromatography (PE/EtOAc 100:0-85:15 in 30 min) afforded the Boc-protected intermediate **6.30**

as a glassy colourless solid (170 mg, 67%). 90 mg (0.16 mmol) of **6.30** were dissolved in a mixture of TFA (1 mL) and CH_2Cl_2 (5 mL) and stirred for 6 h at room temperature. Removal of the solvent *in vacuo* and purification by preparative HPLC (column: Interchim, gradient: 0-30 min: MeCN/0.05% aq. TFA 19:81-42:58, t_R = 12.2 min) afforded the product as white hygroscopic solid (49 mg, 52%). R_f= 0.73 (CH_2Cl_2/ 1.75 N NH_3 in MeOH 9:1). FT-ATR: 723.1, 797.7, 834.9, 1129.4, 1177.8, 1252.4, 1431.3, 1543.1, 1640.0, 3090.0, 3276.3 cm^{-1}. RP-HPLC (gradient 2, 220 nm): 97.4% (t_R = 14.89 min, k =4.1). ^{1}H-NMR (600 MHz, [D_6]DMSO, COSY, HSQC, HMBC, NOESY): δ (ppm) 1.72 (qui, 2H, J 7.22 Hz), 2.07 (s, 3H), 2.58 (t, 2H, J 7.49 Hz), 3.23 (q, 2H, J 6.66 Hz), 4.30 (d, 2H, J 5.83 Hz), 7.25-7.28 (m, 3H), 7.32-7.35 (m, 2H), 7.98 (br s, 1H), 8.52 (br s, 2H), 9.01 (br s, 1H), 9.10 (br s, 2H), 10.35 (br s, 1H). ^{13}C-NMR (150 MHz, [D_6]DMSO, COSY, HSQC, HMBC, NOESY): δ (ppm) 11.3, 21.9, 28.7, 40.0, 42.7, 116.3, 127.1, 127.2, 128.4, 131.6, 138.6, 153.7, 153.8, 167.8. HRMS (ESI) *m/z* $(M+H)^+$ calcd. for $C_{16}H_{23}N_6OS^+$: 347.1649, found: 347.1653. $C_{16}H_{22}N_6OS \cdot C_4H_2F_6O_4$ (346.45 + 228.05).

4-Methyl-5-(3-(3-((2-phenylethyl)carbamoyl)guanidino)propyl)-2-aminothiazole bis(hydrotrifluoroacetate) (6.52) *Claudia Honisch master thesis*

6.52 was prepared from **6.18** (150 mg, 0.444 mmol, 1 eq), **6.5** (120 mg, 0.444 mmol, 1 eq), $HgCl_2$ (241 mg, 0.888 mmol, 2 eq) and triethylamine (135 mg, 1.332 mmol, 3 eq) dissolved in CH_2Cl_2 (25 mL) according to the general procedure. Purification by automated flash chromatography (PE/EtOAc 100:0-85:15 in 30 min) afforded the Boc-protected intermediate **6.31** as a glassy colourless solid (190 mg, 76%). 190 mg (0.34 mmol) of **6.31** were dissolved in a mixture of TFA (1 mL) and CH_2Cl_2 (5 mL) and stirred for 6 h at room temperature. Removal of the solvent *in vacuo* and purification by preparative HPLC (column: Interchim, gradient: 0-30 min: MeCN/0.05% aq. TFA 19:81-46:54, t_R = 13.2 min) afforded the product as white hygroscopic solid (11 mg, 53%). R_f= 0.89 (CH_2Cl_2/ 1.75 N NH_3 in MeOH 9:1). RP-HPLC (220 nm, gradient 2): 98.6% (t_R = 15.0 min, k = 4.2) ^{1}H-NMR (600 MHz, [D_6]DMSO, COSY, HSQC, HMBC, NOESY): δ (ppm) 1.71 (qui, 2H, J 7.19 Hz), 2.08 (s, 3H), 2.58-2.60 (m, 2H), 2.75 (t, 2H, J 7.24 Hz), 3.24 (br s, 2H), 3.32-3.33 (m, 2H), 7.19-7.22 (m, 3H), 7.28-7.30 (m, 2H), 7.60 (br s, 1H), 8.52 (br s, 2H), 9.04 (br , 3H), 10.29 (br s, 1H). ^{13}C-NMR (150 MHz, [D_6]DMSO, COSY, HSQC, HMBC, NOESY): δ (ppm) 11.5, 21.9, 28.8, 35.0, 40.0, 40.7, 116.3, 126.2, 128.4, 128.6, 131.7, 138.9, 153.6, 153.7, 167.7. HRMS (ESI) *m/z* $(M+H)^+$ calcd. for $C_{17}H_{25}N_6OS^+$: 361.1805, found: 361.1812. $C_{17}H_{24}N_6OS \cdot C_4H_2F_6O_4$ (360.48 + 228.05).

4-Methyl-5-(3-[3-([2-methyl 3-(4-methylphenyl)propyl]carbamoyl)guanidino]propyl)-2-aminothiazole bis(hydrotrifluoroacetate) (6.53)

6.53 was prepared from **6.19** (84 mg, 0.22 mmol, 1 eq), **6.5** (60 mg, 0.22 mmol, 1 eq), $HgCl_2$ (120 mg, 0.44 mmol, 2 eq) and triethylamine (67 mg, 0.66 mmol, 3 eq) dissolved in CH_2Cl_2 (5 mL) according to the general procedure. Purification by column chromatography (PE/EtOAc 3:1 - 1:1) afforded the Boc-protected intermediate **6.32** as a yellow oil (90 mg, 68%). 90 mg of **6.32** were dissolved in a mixture of TFA (1 mL) and CH_2Cl_2 (5 mL) and stirred over night at room temperature. Removal of the solvent *in vacuo* and purification by preparative HPLC (column: Kinetex, gradient: 0-30 min: MeCN/0.1% aq. TFA 0:100-65:35, t_R = 16.9 min) afforded the product

as white hygroscopic solid (30.1 mg, 32%). R_f= 0.73 (CH_2Cl_2 / 1.75 N NH_3 in MeOH 4:1). RP-HPLC (gradient 2, 220 nm): 97.9% (t_R = 20.21 min, k = 5.97). ^{1}H-NMR (600 MHz, [D_6]DMSO, COSY, HSQC, HMBC, NOESY): δ (ppm) 0.78 (d, 3H, J 6.69 Hz), 1.72 (qui, 2H, J 7.20 Hz), 1.82-1.88 (m, 1H), 2.07 (s, 3H), 2.25 (s, 3H),2.28-2.31 (m, 1H), 2.55-2.60 (m, 3H), 2.89-2.93 (m, 1H), 3.05-3.09 (m, 1H),3.23 (q, 2H, J 6.50 Hz), 7.03-7.07 (m, 4H), 7.53 (br s, 1H), 8.51 (br s, 2H), 8.99 (br s, 1H), 9.14 (br s, 2H), 10.49 (br s, 1H). ^{13}C-NMR (150 MHz, [D_6]DMSO, COSY, HSQC, HMBC, NOESY): δ (ppm) 11.3, 17.0, 20.6, 21.9, 28.8, 34.9, 2Cs under solvent peak (38.7-40.3), 44.6, 116.3, 128.76, 128.79, 131.6, 134.7, 137.0, 153.77, 153.78, 167.9. HRMS (ESI) *m/z* (M+H)$^+$ calcd. for $C_{20}H_{31}N_6OS^+$: 403.2275, found: 403.2277. $C_{20}H_{30}N_6OS \cdot C_4H_2F_6O_4$ (402.56 + 228.05).

4-Methyl-5-(3-[3-([2-methyl 4-phenylbutyl]carbamoyl)guanidino]propyl)-2-aminothiazole bis(hydrotrifluoroacetate) (6.54)

6.54 was prepared from **6.20** (90 mg, 0.24 mmol, 1 eq), **6.5** (64 mg, 0.24 mmol, 1 eq), $HgCl_2$ (129 mg, 0.47 mmol, 2 eq) and triethylamine (72 mg, 0.71 mmol, 3 eq) dissolved in CH_2Cl_2 (5 mL) according to the general procedure. Purification by column chromatography (PE/EtOAc 3:1 isocratic) afforded the Boc-protected intermediate **6.33** as a colourless oil (90 mg, 63%). 90 mg (0.15 mmol) of **6.33** were dissolved in a mixture of TFA (1 mL) and CH_2Cl_2 (5 mL) and stirred over night at room temperature. Removal of the solvent *in vacuo* and purification by preparative HPLC (column: Kinetex, gradient: 0-30 min: MeCN/0.1% aq. TFA 10:90-70:30, t_R = 18.22 min) afforded the product as white hygroscopic solid (30.0 mg, 32%). Mp: 61-68 °C. R_f= 0.35 (CH_2Cl_2 / 1% NH_3 in MeOH 9:1). RP-HPLC (gradient 2, 220 nm): 99.8% (t_R = 18.49 min, k = 5.38). ^{1}H-NMR (600 MHz, [D_6]DMSO, COSY, HSQC, HMBC, NOESY): δ (ppm) 0.89 (d, 3H, J 6.45 Hz), 1.33-1.39 (m, 1H), 1.56-1.63 (m, 2H), 1.71 (qui, 2H, J 7.21 Hz), 2.05 (s, 3H), 2.51-2.65 (m, 4H), 2.96-3.01 (m, 1H), 3.05-3.09 (m, 1H), 3.21-3.25 (m, 2H, interfering with the water signal), 7.14-7.19 (m, 3H), 7.24-7.26 (m, 2H), 7.51(br s, 1H), 8.49 (br s, 2H), 8.82 (br s, 2H), 8.98(br s, 1H), 10.32 (br s, 1H). ^{13}C-NMR (150 MHz, [D_6]DMSO, COSY, HSQC, HMBC, NOESY): δ (ppm) 11.7, 17.2, 22.0, 28.9, 32.4, 32.5, 35.6, 1C under solvent peak (38.7-40.3), 44.8, 116.3, 125.6, 128.20, 128.23, 132.9, 142.2, 153.7, 153.8, 167.5. HRMS (ESI) *m/z* (M+H)$^+$ calcd. for $C_{17}H_{25}N_6OS^+$: 403.2275, found: 403.2277. $C_{20}H_{30}N_6OS \cdot C_4H_2F_6O_4$ (402.56 + 228.05).

4-Methyl-5-(3-[3-([2-cyclohexylpropyl]carbamoyl)guanidino]propyl)-2-aminothiazole bis(hydrotrifluoroacetate) (6.55)

6.55 was prepared from **6.21** (90 mg, 0.25 mmol, 1 eq), **6.5** (68 mg, 0.25 mmol, 1 eq), $HgCl_2$ (137 mg, 0.50 mmol, 2 eq) and triethylamine (76 mg, 0.76 mmol, 3 eq) dissolved in CH_2Cl_2 (5 mL) according to the general procedure. Purification by column chromatography (PE/EtOAc 3:1 isocratic) afforded the Boc-protected intermediate **6.34** as a colourless oil (130 mg, 89%). 130 mg (0.22 mmol) of **6.34** were dissolved in a mixture of TFA (1 mL) and CH_2Cl_2 (5 mL) and stirred over night at room temperature. Removal of the solvent *in vacuo* and purification by preparative HPLC (column: Kinetex, gradient: 0-30 min: MeCN/0.1% aq. TFA 10:90-70:30, t_R = 18.8 min) afforded the product as white hygroscopic solid (80.0 mg, 59%). Mp: 51-57 °C. R_f= 0.34 (CH_2Cl_2 / 1.75 N NH_3 in MeOH 9:1). RP-HPLC (gradient 2, 220 nm): 99.0% (t_R = 18.61 min, k = 5.42). ^{1}H-NMR (600

MHz, [D_6]DMSO, COSY, HSQC, HMBC, NOESY): δ (ppm) 0.78 (d, 3H, *J* 6.8 Hz), 0.90-1.22 (m, 6H), 1.43-1.47 (m, 1H), 1.55-1.61 (m, 3H), 1.67-1.74 (m, 4H), 2.07 (s, 3H), 2.58-2.60 (m, 2H), 2.90-2.94 (m, 1H), 3.10-3.14 (m, 1H), 3.22-3.25 (m, 2H), 7.44 (br s, 1H), 8.49 (br s, 2H), 8.98-9.07 (m, 3H), 10.34 (br s, 1H),13.55 (br s, 1H). ^{13}C-NMR (150 MHz, [D_6]DMSO, COSY, HSQC, HMBC, NOESY): δ (ppm) 11.4, 14.0, 22.0, 26.06, 26.16, 26.23, 27.9, 28.8, 30.3, 37.8, 2Cs under solvent peak (38.7-40.3), 42.9, 116.3, 131.8, 153.70, 153.74, 167.8. HRMS (ESI) *m/z* (M+H)$^+$ calcd. for $C_{18}H_{33}N_6OS^+$: 381.2431, found: 381.2436. $C_{18}H_{32}N_6OS \cdot C_4H_2F_6O_4$ (380.56 + 228.05).

4-Methyl-5-(3-[3-([2-(4-prop-2-ylphenyl)propyl]carbamoyl)guanidino]propyl)-2-aminothiazole bis(hydrotrifluoroacetate) (6.56)

6.56 was prepared from **6.22** (90 mg, 0.23 mmol, 1 eq), **6.5** (62 mg, 0.23 mmol, 1 eq), $HgCl_2$ (124 mg, 0.46 mmol, 2 eq) and triethylamine (69 mg, 0.69 mmol, 3 eq) dissolved in CH_2Cl_2 (5 mL) according to the general procedure. Purification by column chromatography (PE/EtOAc 3:1 isocratic) afforded the Boc-protected intermediate **6.35** as a colourless oil (120 mg, 85%). 120 mg (0.19 mmol) of **6.35** were dissolved in a mixture of TFA (1 mL) and CH_2Cl_2 (5 mL) and stirred over night at room temperature. Removal of the solvent *in vacuo* and purification by preparative HPLC (column: Kinetex, gradient: 0-30 min: MeCN/0.1% aq. TFA 10:90-70:30, t_R = 19.1 min) afforded the product as white hygroscopic solid (80.0 mg, 64%). Mp: 59-64 °C. R_f= 0.34 (CH_2Cl_2 / 1.5 N NH_3 in MeOH 9:1). RP-HPLC (gradient 2, 220 nm): 96.3% (t_R = 19.33 min, k = 5.67). ^{1}H-NMR (600 MHz, [D_6]DMSO, COSY, HSQC, HMBC, NOESY): δ (ppm) 1.16-1.18 (m, 9H), 1.72 (qui, 2H, *J* 7.14 Hz), 2.08 (s, 3H), 2.58-2.61 (m, 2H), 2.82-2.89 (m, 2H), 3.22-3.25 (m, 4H), 7.14-7.18 (m, 4H), 7.38 (br s, 1H), 8.51 (br s, 2H), 9.01 (br s, 1H), 9.23 (br s, 2H), 10.36 (br s, 1H). ^{13}C-NMR (150 MHz, [D_6]DMSO, COSY, HSQC, HMBC, NOESY): δ (ppm) 11.2, 19.1, 21.9, 23.9, 28.7, 33.0, 38.6, 1C under solvent peak (38.7-40.3), 46.0, 116.3, 126.3, 127.0, 131.3, 141.5, 146.4, 153.68, 153.71, 168.0. HRMS (ESI) *m/z* (M+H)$^+$ calcd. for $C_{21}H_{33}N_6OS^+$: 417.2431, found: 417.2435. $C_{21}H_{32}N_6OS \cdot C_4H_2F_6O_4$ (416.59 + 228.05).

4-Methyl-5-(3-[3-([3-methyl 2-phenylbutyl]carbamoyl)guanidino]propyl)-2-aminothiazole bis(hydrotrifluoroacetate) (6.57)

6.57 was prepared from **6.23** (90 mg, 0.24 mmol, 1 eq), **6.5** (64 mg, 0.24 mmol, 1 eq), $HgCl_2$ (129 mg, 0.47 mmol, 2 eq) and triethylamine (72 mg, 0.71 mmol, 3 eq) dissolved in CH_2Cl_2 (5 mL) according to the general procedure. Purification by column chromatography (PE/EtOAc 3:1 isocratic) afforded the Boc-protected intermediate **6.36** as a colourless oil (110 mg, 77%). 110 mg (0.18 mmol) of **6.36** were dissolved in a mixture of TFA (1 mL) and CH_2Cl_2 (5 mL) and stirred over night at room temperature. The solvent was removed *in vacuo* and the residue was purified by preparative HPLC (column: Kinetex, gradient: 0-30 min: MeCN/0.1% aq. TFA 10:90-70:30, t_R = 17.9 min). The resulting product (80 mg) showed an insufficient purity and was purified a second time by preparative HPLC (column: Kinetex, gradient: 0-30 min: MeCN/0.1% aq. TFA 5:95-65:35, t_R = 20.2 min). Lyophilisation afforded the product as white hygroscopic solid (40.0 mg, 17%). Mp: 59-64 °C. R_f= 0.34 (CH_2Cl_2 / 1.5 N NH_3 in MeOH 9:1). RP-HPLC (gradient 2, 220 nm): 98.6% (t_R = 18.31 min, k = 5.31). ^{1}H-NMR (600 MHz, [D_6]DMSO, COSY, HSQC, HMBC, NOESY): δ (ppm) 0.66 (d,

3H, *J* 6.73 Hz), 0.91 (d, 3H, *J* 6.72 Hz), 1.69 (qui, 2H, *J* 7.17 Hz), 1.83-1.88 (m, 1H), 2.06 (s, 3H), 2.52-2.57 (m, 3H), 3.19-3.20 (m, 2H), 3.31-3.36 (m, 1H), 3.56-3.60 (m, 1H), 7.11-7.16 (m, 3H), 7.19-7.22 (m, 1H), 7.28-7.30 (m, 2H), 8.45 (br s, 2H), 8.93 (br s, 1H), 9.16 (br s, 2H), 10.08 (br s, 1H). ^{13}C-NMR (150 MHz, [D_6]DMSO, COSY, HSQC, HMBC, NOESY): δ (ppm) 11.3, 20.0, 20.7, 21.9, 28.7, 30.4, 1C under solvent peak (38.7-40.3), 42.0, 51.5, 116.3, 126.4, 128.1, 128.4, 131.3, 141.4, 153.51, 153.54, 167.9. HRMS (ESI) *m/z* (*M*+H)$^+$ calcd. for $C_{20}H_{31}N_6OS^+$: 403.2275, found: 403.2282. $C_{20}H_{30}N_6OS \cdot C_4H_2F_6O_4$ (402.56 + 228.05).

4-Methyl-5-(3-[3-([2-phenylbutyl]carbamoyl)guanidino]propyl)-2-aminothiazole bis(hydrotrifluoroacetate) (6.58)

6.58 was prepared from **6.24** (90 mg, 0.25 mmol, 1 eq), **6.5** (67 mg, 0.25 mmol, 1 eq), $HgCl_2$ (134 mg, 0.50 mmol, 2 eq) and triethylamine (75 mg, 0.74 mmol, 3 eq) dissolved in CH_2Cl_2 (5 mL) according to the general procedure. Purification by column chromatography (PE/EtOAc 3:1 isocratic) afforded the Boc-protected intermediate **6.37** as a colourless oil (110 mg, 76%). 110 mg (0.19 mmol) of **6.37** were dissolved in a mixture of TFA (1 mL) and CH_2Cl_2 (5 mL) and stirred over night at room temperature. Removal of the solvent *in vacuo* and purification by preparative HPLC (column: Kinetex, gradient: 0-30 min: MeCN/0.1% aq. TFA 10:90-70:30, t_R = 16.1 min) afforded the product as white hygroscopic solid (80.0 mg, 69%). Mp: 55-60 °C. R_f= 0.34 (CH_2Cl_2 / 1.5 N NH_3 in MeOH 9:1). RP-HPLC (gradient 2, 220 nm): 97.5% (t_R = 16.71 min, *k* = 4.76). ^{1}H-NMR (600 MHz, [D_6]DMSO, COSY, HSQC, HMBC, NOESY): δ (ppm) 0.71 (t, 3H, *J* 7.32 Hz), 1.46-1.54 (m, 1H), 1.64-1.73 (m, 3H), 2.06 (s, 3H), 2.56-2.58 (m, 2H), 2.62-2.67 (m, 1H), 3.20-3.29 (m, 3H), 3.34-3.38 (m, 1H), 7.18-7.21 (m, 3H), 7.28-7.31 (m, 3H), 8.50 (br s, 2H), 8.98 (br s, 1H), 9.08 (br s, 2H), 10.37 (br s, 1H). ^{13}C-NMR (150 MHz, [D_6]DMSO, COSY, HSQC, HMBC, NOESY): δ (ppm) 11.4, 11.7, 22.0, 25.8, 28.8, 1C under solvent peak (38.7-40.3), 44.6, 46.7, 116.3, 126.4, 127.7, 128.4, 132.0, 142.5, 153.67, 153.69, 167.8. HRMS (ESI) *m/z* (*M*+H)$^+$ calcd. for $C_{19}H_{29}N_6OS^+$: 389.2118, found: 389.2118. $C_{19}H_{28}N_6OS \cdot C_4H_2F_6O_4$ (388.53 + 228.05).

4-Methyl-5-(3-[3-([3-cyclohexyl 2-methylpropyl]carbamoyl)guanidino]propyl)-2-aminothiazole bis(hydrotrifluoroacetate) (6.59)

6.59 was prepared from **6.25** (80 mg, 0.22 mmol, 1 eq), **6.5** (59 mg, 0.22 mmol, 1 eq), $HgCl_2$ (117 mg, 0.43 mmol, 2 eq) and triethylamine (66 mg, 0.65 mmol, 3 eq) dissolved in CH_2Cl_2 (5 mL) according to the general procedure. Purification by column chromatography (PE/EtOAc 3:1 isocratic) afforded the Boc-protected intermediate **6.38** as a colourless oil (140 mg, 97%). 140 mg (0.23 mmol) of **6.38** were dissolved in a mixture of TFA (1 mL) and CH_2Cl_2 (5 mL) and stirred over night at room temperature. Removal of the solvent *in vacuo* and purification by preparative HPLC (column: Kinetex, gradient: 0-30 min: MeCN/0.1% aq. TFA 10:90-70:30, t_R = 19.9 min) afforded the product as white hygroscopic solid (110.0 mg, 75%). Mp: 61-66 °C. R_f= 0.34 (CH_2Cl_2 / 1 N NH_3 in MeOH 9:1). RP-HPLC (gradient 2, 220 nm): 99.7% (t_R = 20.10 min, *k* = 5.93). ^{1}H-NMR (600 MHz, [D_6]DMSO, COSY, HSQC, HMBC, NOESY): δ (ppm) 0.73-0.88 (m, 5H), 0.93-0.97 (m, 1H), 1.07-1.23 (m, 4H), 1.26-1.31 (m, 1H), 1.59-1.75 (m, 8H), 2.08 (s,3H), 2.58-2.61 (m, 2H), 2.84-2.89 (m, 1H), 3.02-3.06 (m, 1H), 3.23-3.26 (m, 2H), 7.47 (br s,1H), 8.51 (br s, 2H), 9.00-9.06 (m, 3H), 10.42 (br s,

1H). ^{13}C-NMR (150 MHz, [D_6]DMSO, COSY, HSQC, HMBC, NOESY): δ (ppm) 11.4, 17.7, 22.0, 25.7, 25.8, 26.2, 28.8, 29.6, 32.5, 33.5, 34.2, 1C under solvent peak (38.7-40.3), 41.7, 45.3, 116.3, 131.9, 153.77, 153.78, 167.8. HRMS (ESI) *m/z* (*M*+H)$^+$ calcd. for $C_{19}H_{35}N_6OS^+$: 395.2588, found: 395.2590. $C_{19}H_{34}N_6OS \cdot C_4H_2F_6O_4$ (394.58 + 228.05).

4-(3-(3-(Propylcarbamoyl)guanidino)phenyl)-2-aminothiazole bis(hydrotrifluoroacetate) (6.60)

6.60 was prepared from **6.13** (80 mg, 0.29 mmol, 1 eq), **6.7** (56 mg, 0.29 mmol, 1 eq), $HgCl_2$ (158 mg, 0.58 mmol, 2 eq) and triethylamine (88 mg, 0.87 mmol, 3 eq) dissolved in CH_2Cl_2 (5 mL) according to the general procedure. Purification by automated flash chromatography (PE/EtOAc 100:0-50:50 in 25 min) afforded the Boc-protected intermediate **6.39** as a yellow oil (70 mg, 57%). 70 mg (0.17 mmol) of **6.39** were dissolved in a mixture of TFA (2 mL) and CH_2Cl_2 (5 mL) and stirred over night at room temperature. Removal of the solvent *in vacuo* and purification by preparative HPLC (column: Kinetex, gradient: 0-30 min: MeCN/0.1% aq. TFA 15:85-45:55, t_R = 10.3 min) afforded the product as white hygroscopic solid (40.0 mg, 44%). R_f= 0.10 (PE/EtOAc 2:1). RP-HPLC (gradient 1, 220 nm): 99.2% (t_R = 13.87 min, *k* = 3.78). ^{1}H-NMR (600 MHz, [D_6]DMSO, COSY, HSQC, HMBC): δ (ppm) 0.86 (t, 3H, *J* 7.50 Hz), 1.43-1.49 (m, 2H), 3.06-3.10 (m, 2H), 7.15 (s, 1H), 7.23-7.24 (m, 1H), 7.49 (t, 1H, *J* 7.74 Hz), 7.60 (t, 1H, *J* 5.56 Hz), 7.72-7.73 (m, 1H), 7.78-7.80 (m, 1H), 8.62 (br s, 1H), 8.97 (br s, 1H), 10.15 (s,1H), 10.74 (s, 1H). ^{13}C-NMR (150 MHz, [D_6]DMSO, COSY, HSQC, HMBC): δ (ppm) 11.2, 22.2, 41.0, 103.0, 123.0, 124.81, 124.84, 130.1, 134.0, 135.5, 147.0, 153.5, 153.6, 168.7. HRMS (ESI) *m/z* (*M*+H)$^+$ calcd. for $C_{14}H_{19}N_6OS^+$: 319.1336, found: 319.1346. $C_{14}H_{18}N_6OS \cdot C_4H_2F_6O_4$ (318.40 + 228.05).

4-(3-(3-(Hexylcarbamoyl)guanidino)phenyl)-2-aminothiazole bis(hydrotrifluoroacetate) (6.61)

6.61 was prepared from **6.14** (90 mg, 0.28 mmol, 1 eq), **6.7** (54 mg, 0.28 mmol, 1 eq), $HgCl_2$ (154 mg, 0.57 mmol, 2 eq) and triethylamine (86 mg, 0.85 mmol, 3 eq) dissolved in CH_2Cl_2 (5 mL) according to the general procedure. Purification by automated flash chromatography (PE/EtOAc 100:0-55:45 in 25 min) afforded the Boc-protected intermediate **6.40** as a yellow solid (110 mg, 84%). 110 mg (0.24 mmol) of **6.40** were dissolved in a mixture of TFA (2 mL) and CH_2Cl_2 (5 mL) and stirred over night at room temperature. Removal of the solvent *in vacuo* and purification by preparative HPLC (column: Kinetex, gradient: 0-30 min: MeCN/0.1% aq. TFA 20:80-70:30, t_R = 13.4 min) afforded the product as white hygroscopic solid (60.0 mg, 43%). R_f= 0.10 (PE/EtOAc 2:1). RP-HPLC (gradient 1, 220 nm): 99.2% (t_R = 19.25 min, *k* = 5.64). ^{1}H-NMR (600 MHz, [D_6]DMSO, COSY, HSQC, HMBC): δ (ppm) 0.84-0.87 (m, 3H), 1.22-1.30 (m, 6H), 1.41-1.44 (m, 2H), 3.09-3.13 (m, 2H), 7.15 (s, 1H), 7.23-7.24 (m, 1H), 7.49 (t, 1H, *J* 7.93 Hz), 7.59 (t, 1H, *J* 5.50 Hz), 7.73 (m, 1H), 7.79 (d, 1H ,7.89 Hz), 8.65 (br s, 1H), 8.97 (br s, 1H), 10.26 (s, 1H), 10.80 (s, 1H). ^{13}C-NMR (150 MHz, [D_6]DMSO, COSY, HSQC, HMBC): δ (ppm) 13.9, 22.0, 25.9, 28.8, 30.9, 1C under solvent peak (38.7-40.3), 102.9, 122.9, 124.76, 124.80, 130.1, 134.0, 135.5, 147.0, 153.4, 153.6, 168.7. HRMS (ESI) *m/z* (*M*+H)$^+$ calcd. for $C_{17}H_{25}N_6OS^+$: 361.1805, found: 361.1813. $C_{17}H_{24}N_6OS \cdot C_4H_2F_6O_4$ (360.48 + 228.05).

4-(3-(3-(Cyclohexylcarbamoyl)guanidino)phenyl)-2-aminothiazole bis(hydrotrifluoroacetate) (6.62)

6.62 was prepared from **6.15** (90 mg, 0.29 mmol, 1 eq), **6.7** (55 mg, 0.29 mmol, 1 eq), $HgCl_2$ (155 mg, 0.57 mmol, 2 eq) and triethylamine (87 mg, 0.86 mmol, 3 eq) dissolved in CH_2Cl_2 (5 mL) according to the general procedure. Purification by automated flash chromatography (PE/EtOAc 100:0-50:50 in 25 min) afforded the Boc-protected intermediate **6.41** as a yellow oil (90 mg, 69%). 90 mg (0.20 mmol) of **6.41** were dissolved in a mixture of TFA (2 mL) and CH_2Cl_2 (5 mL) and stirred over night at room temperature. Removal of the solvent *in vacuo* and purification by preparative HPLC (column: Kinetex, gradient: 0-30 min: MeCN/0.1% aq. TFA 20:80-50:50, t_R = 11.8 min) afforded the product as white hygroscopic solid (70 mg, 61%). Mp: 80-84 °C. R_f= 0.05 (PE /EtOAc 2:1). RP-HPLC (gradient 2, 220 nm): 99.5% (t_R = 16.34 min, k = 4.6). ^{1}H-NMR (600 MHz, [D_6]DMSO, COSY, HSQC, HMBC): δ (ppm) 1.14-1.32 (m, 5H), 1.51-1.54 (m, 1H), 1.63-1.66 (m, 2H), 1.77-1.80 (m, 2H), 3.45-3.51 (m, 1H), 7.15 (s, 1H), 7.23-7.25 (m, 1H), 7.50 (t, 1H, *J* 7.91 Hz), 7.59 (d, 1H, *J* 7.58 Hz), 7.73 (m, 1H), 7.79-7.81 (m, 1H), 8.65 (br s, 1H), 8.96 (br s, 1H), 9.93 (s, 1H), 10.74 (s, 1H). ^{13}C-NMR (150 MHz, [D_6]DMSO, COSY, HSQC, HMBC): δ (ppm) 24.6, 25.4, 32.5, 48.9, 103.5, 123.6, 125.3, 125.5, 130.6, 134.4, 136.0, 147.4, 153.1, 154.1, 169.2. HRMS (ESI) *m/z* (M+H)$^+$ calcd. for $C_{17}H_{23}N_6OS^+$: 359.1649, found: 359.1649. $C_{17}H_{22}N_6OS \cdot C_4H_2F_6O_4$ (358.46 + 228.05).

4-(3-(3-(Phenylcarbamoyl)guanidino)phenyl)-2-aminothiazole bis(hydrotrifluoroacetate) (6.63)

6.63 was prepared from **6.16** (81 mg, 0.26 mmol, 1 eq), **6.7** (50 mg, 0.26 mmol, 1 eq), $HgCl_2$ (142 mg, 0.52 mmol, 2 eq) and triethylamine (79 mg, 0.78 mmol, 3 eq) dissolved in CH_2Cl_2 (5 mL) according to the general procedure. Purification by automated flash chromatography (PE/EtOAc 100:0-50:50 in 30 min) afforded the Boc-protected intermediate **6.42** as a yellow oil (30 mg, 25%). 30 mg (0.07 mmol) of **6.42** were dissolved in a mixture of TFA (2 mL) and CH_2Cl_2 (5 mL) and stirred over night at room temperature. Removal of the solvent *in vacuo* and purification by preparative HPLC (column: Kinetex, gradient: 0-30 min: MeCN/0.1% aq. TFA 15:85-70:30, t_R = 13.0 min) afforded the product as white hygroscopic solid (27 mg, 71%). R_f= 0.4 (CH_2Cl_2 / 1.75 N NH_3 in MeOH 9:1). RP-HPLC (gradient 1, 220 nm): 99.4% (t_R = 16.70 min, k = 4.76). ^{1}H-NMR (600 MHz, [D_6]DMSO, COSY, HSQC, HMBC): δ (ppm) 7.10-7.14 (m, 2H), 7.26-7.28 (m, 1H), 7.34-7.37 (m, 2H), 7.45-7.46 (m, 2H), 7.51 (t, 1H, J 7.84 Hz), 7.77-7.78 (m, 1H), 7.81-7.83 (m, 1H), 8.76-8.92 (m, 3H), 9.92 (s, 1H), 10.10 (br s, 1H), 10.70 (s, 1H). ^{13}C-NMR (150 MHz, [D_6]DMSO, COSY, HSQC, HMBC): δ (ppm) 102.9, 119.5, 122.9, 124.0, 124.6, 124.8, 129.1, 130.1, 134.0, 136.1, 137.3, 148.0, 151.1, 153.3, 168.5. HRMS (ESI) *m/z* (M+H)$^+$ calcd. for $C_{17}H_{17}N_6OS^+$: 353.1179, found: 353.1180. $C_{17}H_{16}N_6OS \cdot C_4H_2F_6O_4$ (352.41 + 228.05).

4-(3-(3-((Phenylmethyl)carbamoyl)guanidino)phenyl)-2-aminothiazole bis(hydrotrifluoroacetate) (6.64)

6.64 was prepared from **6.17** (85 mg, 0.26 mmol, 1 eq), **6.7** (50 mg, 0.26 mmol, 1 eq), $HgCl_2$ (142 mg, 0.52 mmol, 2 eq) and triethylamine (79 mg, 0.78 mmol, 3 eq) dissolved in CH_2Cl_2 (8 mL)

according to the general procedure. Purification by automated flash chromatography (PE/EtOAc 100:0-60:40 in 30 min) afforded the Boc-protected intermediate **6.43** as a yellow oil (110 mg, 90%). 100 mg (0.21 mmol) of **6.43** were dissolved in a mixture of TFA (1 mL) and CH_2Cl_2 (5 mL) and stirred for 12 h at room temperature. Removal of the solvent *in vacuo* and purification by preparative HPLC (column: Kinetex, gradient: 0-30 min: MeCN/0.1% aq. TFA 15:85-70:30, t_R = 13.1 min) afforded the product as white hygroscopic solid (90 mg, 70%). R_f= 0.1 (PE/EtOAc 2:1). RP-HPLC (gradient 1, 220 nm): 99.1% (t_R = 16.57 min, k = 4.71). ^{1}H-NMR (600 MHz, MeOD, COSY, HSQC, HMBC): δ (ppm) 4.41 (s, 2H), 7.25-7.28 (m, 1H), 7.32-7.35 (m, 4H), 7.40-7.41 (m, 1H), 7.60 (t, 1H, J 7.81 Hz), 7.71-7.72 (m, 1H), 7.75-7.77 (m, 1H). ^{13}C-NMR (150 MHz, MeOD, COSY, HSQC, HMBC): δ (ppm) 44.6, 104.7, 124.8, 127.1, 127.9, 128.5, 128.6, 129.7, 132.3, 133.3, 135.4, 139.4, 142.1, 155.3, 155.9, 172.6. HRMS (ESI) *m/z* (M+H)$^+$ calcd. for $C_{18}H_{19}N_6OS^+$: 367.1336, found: 367.1341. $C_{18}H_{18}N_6OS \cdot C_4H_2F_6O_4$ (366.44 + 228.05).

4-(3-(3-((2-Phenylethyl)carbamoyl)guanidino)phenyl)-2-aminothiazole bis(hydrotrifluoroacetate) (6.65)

6.65 was prepared from **6.18** (88 mg, 0.26 mmol, 1 eq), **6.7** (50 mg, 0.26 mmol, 1 eq), $HgCl_2$ (142 mg, 0.52 mmol, 2 eq) and triethylamine (79 mg, 0.78 mmol, 3 eq) dissolved in CH_2Cl_2 (5 mL) according to the general procedure. Purification by automated flash chromatography (PE/EtOAc 100:0-60:40 in 30 min) afforded the Boc-protected intermediate **6.44** as a yellow solid (80 mg, 63%). 80 mg (0.17 mmol) of **6.44** were dissolved in a mixture of TFA (2 mL) and CH_2Cl_2 (5 mL) and stirred over night at room temperature. Removal of the solvent *in vacuo* and purification by preparative HPLC (column: Kinetex, gradient: 0-30 min: MeCN/0.1% aq. TFA 15:85-70:30, t_R = 13.9 min) afforded the product as white hygroscopic solid (50 mg, 50%). R_f= 0.3 (CH_2Cl_2 / 1.75 N NH_3 in MeOH 9:1). RP-HPLC (gradient 1, 220 nm): 99.8% (t_R = 17.32 min, k = 4.97). ^{1}H-NMR (600 MHz, [D_6]DMSO, COSY, HSQC, HMBC): δ (ppm) 2.77 (t, 2H, J 7.16 Hz), 3.36-3.39 (m, 2H), 7.13 (s, 1H), 7.20-7.23 (m, 4H), 7.29-7.31 (m, 2H), 7.48 (t, 1H, J 7.95 Hz), 7.58 (t, 1H, J 5.59 Hz), 7.72-7.73 (m, 1H), 7.79-7.80 (m, 1H), 8.62 (br s, 1H), 8.96 (br s, 1H), 10.06 (s, 1H), 10.67 (s, 1H). ^{13}C-NMR (150 MHz, [D_6]DMSO, COSY, HSQC, HMBC): δ (ppm) 34.9, 40.7, 102.9, 122.9, 124.7, 124.8, 126.3, 128.4, 128.7, 130.1, 133.9, 135.9, 138.8, 147.6, 153.40, 153.44, 168.5. HRMS (ESI) *m/z* (M+H)$^+$ calcd. for $C_{19}H_{21}N_6OS^+$: 381.1492, found: 381.1493. $C_{19}H_{20}N_6OS \cdot C_4H_2F_6O_4$ (380.47 + 228.05).

6-(3-(Hexylcarbamoyl)guanidino)-2-amino-4,5,6,7-tetrahydrobenzo[d]thiazole bis(hydrotrifluoroacetate) (6.66)

6.66 was prepared from **6.14** (140 mg, 0.44 mmol, 1 eq), **6.12** (90 mg, 0.53 mmol, 1.2 eq), $HgCl_2$ (239 mg, 0.88 mmol, 2 eq) and triethylamine (134 mg, 1.32 mmol, 3 eq) dissolved in CH_2Cl_2 (11 mL) according to the general procedure. Purification by automated flash chromatography (CH_2Cl_2 /MeOH 100:0-85:15 in 30 min) afforded the Boc-protected intermediate **6.45** as a yellow solid (110 mg, 57%). 110 mg (0.25 mmol) of **6.45** were dissolved in a mixture of TFA (2 mL) and CH_2Cl_2 (5 mL) and stirred over night at room temperature. Removal of the solvent *in vacuo* and purification by preparative HPLC (column: Kinetex, gradient: 0-30 min: MeCN/0.1% aq. TFA 10:90-60:40, t_R = 12.0 min) afforded the product as white hygroscopic solid (46 mg, 33%). Mp: 121-

122 °C. R_f= 0.2 (CH_2Cl_2 / 1.7 N NH_3 in MeOH 9:1). RP-HPLC (gradient 1, 220 nm): 95.3% (t_R = 17.10 min, k = 4.90). ^{1}H-NMR (600 MHz, [D_6]DMSO, COSY, HSQC, HMBC): δ (ppm) 0.84-0.86 (m, 3H), 1.24-1.29(m, 6H), 1.39-1.42 (m, 2H), 1.83-1.97 (m, 2H), 2.51-2.60 (m, 3H), 2.86-2.89 (m, 1H), 3.06-3.09 (m, 2H), 4.04-4.05 (m, 1H), 7.50 (s, 1H), 8.67 (br s, 4H), 9.07 (s,1H), 10.17 (s, 1H). ^{13}C-NMR (150 MHz, [D_6]DMSO, COSY, HSQC, HMBC): δ (ppm) 14.3, 21.7, 22.5, 26.3, 26.8, 28.4, 29.3, 31.3, 1C under solvent peak (38.7-40.3), 46.9, 112.0, 136.5, 153.7, 154.2, 168.9. HRMS (ESI) *m/z* (M+H)$^+$ calcd. for $C_{15}H_{27}N_6OS^+$: 339.1962, found: 339.1962. $C_{15}H_{26}N_6OS \cdot C_4H_2F_6O_4$ (338.47 + 228.05).

6-(3-((Phenylmethyl)carbamoyl)guanidino)-2-amino-4,5,6,7-tetrahydrobenzo[d]thiazole bis(hydrotrifluoroacetate) (6.67)

6.67 was prepared from **6.17** (192 mg, 0.59 mmol, 1 eq), **6.12** (110 mg, 0.65 mmol, 1.1 eq), $HgCl_2$ (320 mg, 1.18 mmol, 2 eq) and triethylamine (180 mg, 1.77 mmol, 3 eq) dissolved in CH_2Cl_2 (16 mL) according to the general procedure. Purification by automated flash chromatography (CH_2Cl_2/MeOH 100:0-85:15 in 30 min) afforded the Boc-protected intermediate **6.46** as a yellow solid (80 mg, 34%). 80 mg (0.18 mmol) of **6.46** were dissolved in a mixture of TFA (2 mL) and CH_2Cl_2 (5 mL) and stirred over night at room temperature. Removal of the solvent *in vacuo* and purification by preparative HPLC (column: Kinetex, gradient: 0-30 min: MeCN/0.1% aq. TFA 15:85-60:40, t_R = 11.2 min) afforded the product as white solid (16 mg, 16%). Mp: 140-145 °C. R_f= 0.2 (CH_2Cl_2 / 1.7 N NH_3 in MeOH 9:1). RP-HPLC (gradient 1, 220 nm): 97.0% (t_R = 14.40 min, k = 3.97). ^{1}H-NMR (600 MHz, [D_6]DMSO, COSY, HSQC, HMBC): δ (ppm) 1.83-1.89 (m, 1H), 1.95-1.97 (m, 1H), 2.53-2.60 (m, 3H), 2.86-2.89 (m, 1H), 4.03-4.05 (m, 1H), 4.30 (d,2H, J 5.70 Hz), 7.24-7.28 (m, 3H), 7.32-7.34 (m, 2H), 8.02 (br s, 1H), 8.74 (br s, 4H), 9.07 (br s, 1H), 10.36 (br s, 1H). ^{13}C-NMR (150 MHz, [D_6]DMSO, COSY, HSQC, HMBC): δ (ppm) 21.2, 26.3, 27.9, 42.7, 46.4, 111.5, 127.1, 127.2, 128.4, 138.6, 140.2, 153.2, 153.8, 168.5. HRMS (ESI) *m/z* (M+H)$^+$ calcd. for $C_{16}H_{21}N_6OS^+$: 345.1492, found: 345.1485. $C_{16}H_{20}N_6OS \cdot C_4H_2F_6O_4$ (344.44 + 228.05).

1-(Amino[3-(2-aminothiazol-4-yl)phenylamino]methylene)-3-(6-[3-(amino[3-(2-aminothiazol-4-yl)phenylamino]methylene)ureido]hexyl)urea tetra(hydrotrifluoracetate) (6.70)

6.70 was prepared from **3.33** (130 mg, 0.24 mmol, 1 eq), **6.7** (136 mg, 0.71 mmol, 3 eq), $HgCl_2$ (143 mg, 0.53 mmol, 2.2 eq) and DIPEA (155 mg, 1.20 mmol, 5 eq) dissolved in CH_2Cl_2 (5 mL) according to the general procedure. Purification by automated flash chromatography (PE/EtOAc 80:20-20:80 in 30 min) afforded the Boc-protected intermediate **6.68** as a yellow foam (180 mg, 91%). 160 mg (0.19 mmol) of **6.68** were dissolved in a mixture of TFA (2 mL) and CH_2Cl_2 (5 mL) and stirred over night at room temperature. Removal of the solvent *in vacuo* and purification by preparative HPLC (column: Kinetex, gradient: 0-30 min: MeCN/0.1% aq. TFA 15:85-45:55, t_R = 13.4 min) afforded the product as white solid (140 mg, 67%). Mp: 128-133 °C. R_f= 0.1 (PE/EtOAc 2:1). RP-HPLC (gradient 1, 220 nm): 97.3% (t_R = 14.99 min, k = 4.17). ^{1}H-NMR (600 MHz, MeOD, COSY, HSQC, HMBC): δ (ppm) 1.38-1.41 (m, 2H), 1.56-1.58 (m, 2H), 3.24 (t, 2H, J 7.03 Hz), 7.35-7.41 (m, 1H), 7.60 (t,1H, J 7.95 Hz), 7.71 (m, 1H), 7.75-7.76 (m, 1H). ^{13}C-NMR (150 MHz, MeOD, COSY, HSQC, HMBC): δ (ppm) 27.4, 30.3, 40.7, 104.6, 124.7, 127.0, 127.9, 132.1, 133.2, 135.5, 142.0, 155.3, 155.9, 172.6. HRMS (ESI) *m/z* (M+H)$^+$ calcd. for $C_{28}H_{35}N_{12}O_2S_2^+$: 635.2442, found: 635.2443. $C_{28}H_{34}N_{12}O_2S_2 \cdot C_4H_2F_6O_4$ (634.78 + 228.05).

1-(Amino[3-(1*H*-pyrazol-4-yl)propylamino]methylene)-3-(6-[3-(amino[3-(1*H*-pyrazol-4-yl)propylamino]methylene)ureido]hexyl)urea tetra(hydrotrifluoracetate) (6.71)

6.71 was prepared from **3.33** (129 mg, 0.24 mmol, 1 eq), 3-(1-trityl-1*H*-pyrazol-4-yl)prop-1-yl-amine (260 mg, 0.71 mmol, 3 eq), $HgCl_2$ (143 mg, 0.53 mmol, 2.2 eq) and DIPEA (155 mg, 1.20 mmol, 5 eq) dissolved in CH_2Cl_2 (5 mL) according to the general procedure. Purification by automated flash chromatography (PE/EtOAc 100:0-70:30 in 20 min) afforded the Boc-protected intermediate **6.69** as a white foam (230 mg, 81%). 190 mg (0.16 mmol) of **6.69** were dissolved in a mixture of TFA (2 mL) and CH_2Cl_2 (10 mL) and stirred over night at room temperature. Removal of the solvent *in vacuo* and purification by preparative HPLC (column: Nucleodur, gradient: 0-30 min: MeCN/0.1% aq. TFA 10:90-55:45, t_R = 13.8 min) afforded the product as white solid (80 mg, 52%). Mp: 84-88 °C. R_f= 0.1 (CH_2Cl_2 / 1.7 N NH_3 in MeOH 9:1). RP-HPLC (gradient 2, 220 nm): 97.3% (t_R = 12.84 min, k = 3.43). ^{1}H-NMR (600 MHz, [D_6]DMSO, COSY, HSQC, HMBC): δ (ppm) 1.26 (br s, 4H), 1.41-1.43 (m, 4H), 1.76 (qui, 4H, J 7.25 Hz), 2.46 (t, 4H, J 7.60 Hz), 3.06-3.09 (m, 4H), 3.21-3.24 (m, 4H), 7.49 (s, 6H), 8.47 (br s, 4H), 9.00 (br s, 2H), 10.34 (br s, 2H). ^{13}C-NMR (150 MHz, [D_6]DMSO, COSY, HSQC, HMBC): δ (ppm) 20.5, 25.9, 28.9, 29.2, 1C under solvent peak (38.7-40.3), 40.4, 118.7, 132.2, 153.78, 153.82. HRMS (ESI) *m/z* (M+H)$^+$ calcd. for $C_{22}H_{39}N_{12}O_2^+$: 503.3313, found: 503.3309. $C_{22}H_{38}N_{12}O_2 \cdot C_4H_2F_6O_4$ (502.63 + 228.05).

Investigation of the chemical stability *Claudia Honisch Master Thesis*

The chemical stability of the compounds **6.49**, **6.50** and **6.52** as well as the acylguanidines UR-Bit22, UR-Bit23 and UR-Bit29 was investigated in PBS (pH = 7.4) at room temperature. The incubation was started by dilution of a 10 mM solution of the compound in aqueous HCl (20 mM) with PBS (pH 7.4), resulting in a 100 µM solution. After 0 h, 72 h and 7 days a 20 µL aliquot was added to 20 µL of a mixture of aqueous TFA solution (1%)/$H_2O_{millipore}$/MeCN (6:3:1, v:v:v). A sample (20 µL) was immediately analyzed by analytical HPLC. A system from Agilent Technologies, composed of a 1290 Infinity binary pump equipped with a degasser, a 1290 Infinity autosampler, a 1290 Infinity thermostated column compartment and a 1260 Infinity diode array was used. A Kinetex XB-C18 100A (100 x 3 mm, 2.6 µm, Phenomenex, Aschaffenburg, Germany) served as RP-column. Mixtures of CH_3CN (A) and 0.05% aq. TFA (B) were used as mobile phase. Helium degassing, 25 °C, a flow rate of 0.5 mL/min and a detection wavelength of 220 nm were used throughout. The following linear gradient was applied for the HPLC analysis: 0-15 min: A/B 5:95-35:65, 15-18 min: 35:65-95:5, 18-23 min: 95:5 (isocratic).

6.3.3 Pharmacological Methods

Radioligand competition binding assay on Sf9 insect cell membranes

Preparation of the membranes of Sf9 insect cells expressing the hH_2R-$G_{s\alpha S}$ fusion protein or co-expressing the hH_1R + RGS4, the hH_3R + $G_{i\alpha 2}$ + $\beta_1\gamma_2$ or hH_4R + $G_{i\alpha 2}$ + $\beta_1\gamma_2$ proteins was described elsewhere.[30]

Radioligand competition binding assays were performed as described previously with minor adjustments using the following radioligands: [^{3}H]mepyramine (Hartmann Analytic, Braunschweig, Germany; specific activity = 20 Ci/mmol; hH_1R: K_d = 4.5 nM, c_{final} = 5 nM), [^{3}H]UR-DE257[14] (hH_2R: specific activity = 32.89 Ci/mmol, K_d = 12.2 nM, c_{final} = 20 nM), [^{3}H]UR-PI294[31] (specific activity = 93.3 Ci/mmol; hH_3R: K_d = 1.1 nM, c_{final} = 2 nM; hH_4R: K_d = 5.1 nM, c_{final} = 5 nM) and [^{3}H]histamine (Hartmann Analytic, Braunschweig, Germany; specific activity = 25 Ci/mmol; hH_3R: K_d = 12.1 nM, c_{final} = 15 nM; hH_4R: K_d = 15.9 nM, c_{final} = 10 nM).

On the day of the experiment Sf9 membranes were thawed and sedimented by centrifugation at 13,000 rpm at 4 °C for 10 min. The membranes were resuspended in ice cold binding buffer (12.5 mM $MgCl_2$, 1mM EDTA and 75 mM Tris/HCl, pH 7.4; in the following referred to as BB) and adjusted to a protein concentration of 2-4 µg/µL. 80 µL BB containing 0.2% BSA and the respective radioligand, followed by 10 µL of the investigated ligands at various concentrations (dissolved in H_2O), were added to every well of a 96-well plate (PP microplates 96 well, Greiner Bio-One, Frickenhausen, Germany). Incubation was started by addition of the membrane suspension (10 µL). The plates were shaken for 60 min at room temperature in the dark. Subsequently, bound radioligand was separated from free radioligand by filtration through glass microfiber filters (Whatman GF/C, Maidstone, UK), treated with 0.3% polyethylenimine (PEI), using a 96-well Brandel harvester (Brandel Inc., Unterföhring, Germany). The punched out filter pieces were transferred into clear, flexible 96-well PET microplate (round bottom, 1450-401, Perkin Elmer, Rodgau, Germany). Each well was supplemented with 200 µL of scintillation cocktail (Rotiscint Eco plus, Roth, Karlsruhe, Germany) and incubated in the dark for at least 4 h. The radioactivity was measured with a MicroBeta2 1450 scintillation counter (Perkin Elmer, Rodgau, Germany).

Functional GTPγS assay on Sf9 insect cell membranes

GTPγS assays were performed as described previously[5] with minor modifications. [^{35}S]GTPγS (specific activity = 1000 Ci/mmol) was purchased from Hartmann Analytic (Braunschweig, Germany). Sf9 membranes were prepared in the same manner as for radioligand competition binding and the protein concentration was adjusted to 0.5-1.5 µg/µL.

Agonist mode: 80 µL of BB containing BSA (0.05% final), GDP (1 µM final) and [^{35}S]GTPγS (20 nCi final), followed by 10 µL of the investigated ligands at various concentrations (dissolved in H_2O) were added to every well of a 96-well plate (PP microplates 96 well, Greiner Bio-One, Frickenhausen, Germany). Incubation was started by addition of the membrane suspension (10 µL). The plates were shaken for 60 min at room temperature in the dark. Subsequently, bound radioligand was separated from free radioligand by filtration through glass microfiber filters

(Whatman GF/C, Maidstone, UK) using a 96-well Brandel harvester (Brandel Inc., Unterföhring, Germany).

Antagonist mode of the GTPγS assay was performed in the same way as the agonist mode, but in the presence of the agonist histamine (1 µM final).

Cell culture

The preparation of stably transfected HEK293T-hH_2R-βArr2[15,32] cells was described elsewhere.

Cells were cultivated at 37 °C in a water saturated atmosphere containing 5% CO_2. Dulbecco´s Modified Eagle Medium, containing 4.5 g/L glucose, 3.7 g/L $NaHCO_3$, 110 mg/L sodium pyruvate (DMEM, Sigma-Aldrich Munich, Germany) and supplemented with 0.584 g/L L-glutamine (L-glutamine solution, Sigma-Aldrich Munich, Germany), 1% (v/v) penicillin-streptomycin (P/S, 10,000 U/mL, Sigma-Aldrich Munich, Germany), 10% (v/v) fetal calf serum (FCS, Biochrom GmbH, Merck, Berlin, Germany) were used as a culture medium. Additionally, 400 µg/mL zeocin (InvivoGen, San Diego,USA) and 600 µg/mL G418 were added to the culture medium of HEK293T-hH_2R-βArr2 cells.

β-Arrestin2 recruitment assay

The β-Arrestin2 recruitment assays were performed as described previously for the H_1R using HEK293T-hH_2R-βArr2 cells, stably expressing the hH_2R-ElucC and βArr2-ElucNfusion constructs[32].

One day prior to the experiment, HEK293T-hH_2R-βArr2 cells were trypsinized and detached with DMEM medium (high glucose without phenol red (Sigma Aldrich, Munich, Germany) containing 1% (v/v) P/S and 5% (v/v) FCS. The cell suspension was adjusted to $1.1 \cdot 10^6$ cells/mL and 90 µl (100,000 cells/well) were seeded in every well of a sterile, luciferase assay compatible, F-bottom 96-well plate (Cellstar®, Greiner Bio-One, Kremsmünster, Österreich). The cells were cultivated at 37 °C overnight in a water saturated atmosphere containing 5% CO_2. The investigated ligands were added at increasing concentrations (10 µL), and the plate was incubated at 25 °C for 60 min under shaking. 50 µL of the medium were removed, and 50 µL of Bright-Glo reagent (Promega, Madison, USA) were added. Bioluminescence was immediately measured for 1 s per well using a GENios Pro microplate reader (Tecan, Salzburg, Austria).

Radioligand competition binding assay on homogenates from HEK293T cells expressing the hD_{2long}R or hD_3R

The preparation of the cells (HEK293T-CRE-Luc-hD_{2long}R and HEK293T-CRE-Luc-hD_3R cells), their cultivation, the preparation of the homogenates and radioligand competition binding assays were performed by Lisa Foster as a part of her ongoing dissertation.

Radioligand competition binding assays were performed as described for Sf9 cell membranes with some adjustments using the radioligand [^{3}H]N-methylspiperone (specific activity of 77

Ci/mmol, Novandi Chemistry AB, Södertälje, Sweden; $hD_{2long}R$: K_d = 0.014 nM, c_{final} = 0.05 nM; hD_3R: K_d = 0.026 nM, c_{final} = 0.05 nM).

Cell lines expressing the human $D_{2long}R$ and D_3R were grown in 150 mm dishes to 80-90% confluency. Cells were rinsed with ice-cold PBS^- and scraped from the dishes using a cell scraper in the presence of harvest buffer (10 mM Tris·HCl, 0.5 mM EDTA, 5.5 mM KCl, 140 mM NaCl; pH 7.4) supplemented with protease inhibitors. After centrifugation (500g, 5 min), the $D_{2long}R$ expressing cells were resuspended in homogenate buffer (50 mM Tris·HCl, 5 mM EDTA, 1.5 mM $CaCl_2$, 5 mM $MgCl_2$, 5 mM KCl, 120 mM NaCl; pH 7.4) and the D_3R expressing cells were resuspended in Tris-$MgSO_4$ buffer (10 mM Tris·HCl, 5 mM $MgSO_4$; pH 7.4) and stored at -80°C. After thawing, the cells were resuspended in homogenate buffer or Tris-$MgSO_4$ buffer respectively and homogenized using an Ultraturrax (5 times for 5 s on ice). The homogenate was centrifuged (50 000 *g*, 6 °C, 15 min), the pellet resuspended in binding buffer (50 mM Tris·HCl, pH, 7.4, containing 1mM EDTA, 5 mM $MgCl_2$, 100 µg/mL bacitracin;) and homogenized using a syringe and needle. The homogenate was stored in small aliquots at -80°C.

For radioligand binding, to 80 µL of the homogenate suspension, 10 µL of radioligand and 10 µL of the ligand at various concentrations (dissolved in binding buffer), were added to every well of a 96-well plate (PP microplates 96 well, Greiner Bio-One, Frickenhausen, Germany). Unspecific binding was determined using (+)-butaclamol at a final concentration of 2 µM, instead of the ligand. The plates were shaken for 60 min at room temperature in the dark. Subsequently, bound radioligand was separated from free radioligand by filtration through glass microfiber filters (Whatman GF/C, Maidstone, UK), treated with 0.3% polyethylenimine (PEI), using a 96-well Brandel harvester (Brandel Inc., Unterföhring, Germany). The punched out filter pieces were transferred into clear, flexible 96-well PET microplate (round bottom, 1450-401, Perkin Elmer, Rodgau, Germany). Each well was supplemented with 200 µL of scintillation cocktail (Rotiscint Eco plus, Roth, Karlsruhe, Germany) and incubated in the dark for at least 4 h. The radioactivity was measured with a MicroBeta2 1450 scintillation counter (Perkin Elmer, Rodgau, Germany).

6.3.4 Data analysis

Retention factors *k* were calculated according to $k = (t_R - t_0)/ t_0$ (t_0 = dead time).
Total binding data from radioligand competition binding experiments were plotted against log(concentration competitor) and analyzed by a four-parameter logistic equation (log(inhibitor) vs response – variable slope, GraphPad Prism Software 5.0, San Diego, CA), followed by normalization (100% = "top" of the four-parameter logistic fit, 0% = unspecifically bound radioligand/ fluorescent ligand determined in the presence of famotidine at 100 µM). Normalized data from competition binding experiments was again analyzed by a four-parameter logistic equation (log(inhibitor) vs response – variable slope, GraphPad Prism) and obtained pIC_{50} values were converted into pK_i values according to the Cheng-Prusoff equation[33].

Data of the GTPγS assay (agonist mode) were processed by plotting the corrected counts per minute (ccpm) against log(concentration). In most cases data analysis by bell-shaped fit was ambiguous due to lack of data points at high concentrations (>100 µM). The data points at high concentrations (≥10-100 µM), where the signal decreased again, were excluded in the analysis by a four parameter logistic equation (GraphPad Software). The concentration response curve was normalized (0% = water value (basal activity), 100% = "top" histamine equation) and again analyzed by a four-parameter logistic equation (log(agonist) vs. response – variable slope, GraphPad Prism).

Data from the GTPγS assay (antagonist mode) were processed by plotting the ccpm against log(concentration) and analysis by a four parameter logistic equation (GraphPad Prism), followed by normalization (100% = "top" of the four-parameter logistic fit, 0% = unspecifically bound [^{35}S]GTPγS (ccpm) determined in the presence of famotidine at 100 µM) and analysis by four-parameter logistic equation (log(inhibitor) vs response – variable slope, GraphPad Prism). pIC_{50} values were converted into pK_B values according to the Cheng-Prusoff equation[33].

Data of the beta-Arrestin2 recruitment assay (agonist mode) were processed by plotting the luminescence (RLU) against log(concentration). In all cases data analysis by bell-shaped fit was ambiguous due to lack of data points at high concentrations (>300 µM). The data points at high concentrations (≥10-100 µM), where the signal decreased again, were excluded in the analysis by a four parameter logistic equation (GraphPad Prism). The concentration response curve was normalized (0% = water value (basal activity), 100% = "top" histamine equation) and again analyzed by a four-parameter logistic equation (log(agonist) vs. response – variable slope, GraphPad Prism).

6.4 SUMMARY AND CONCLUSION

The bioisosteric replacement of the acylguanidine moiety in the monomeric N^G-acylated amino(methyl)thiazolylpropylguanidines by a carbamoylguanidine moiety resulted in ligands with retained or even improved hH_2R potency with pEC_{50} values of 6.3-7.76 (ligands **6.47**-**6.59**). A variety of aliphatic and aromatic residues were well tolerated. Compounds containing an amino(methyl)thiazolyl propyl moiety achieved up to 80 fold the potency of histamine and partial to full agonistic activities with more or less pronounced bell-shaped concentration-response curves. Additionally, the ligands **6.53**, **6.55**, **6.58** and **6.59** were investigated for dopamine receptor affinity ($hD_{2long}R$ and hD_3R). These ligands showed affinity to the $hD_{2long}R$ (pK_i: 6.28-6.58) and hD_3R (pK_i: 6.88-7.36). There was a clear preference for the hH_2R over the $hD_{2long}R$. But only ligand **6.59** showed a clear preference towards the hH_2R over the hD_3R and the ligands **6.53**, **6.55** and **6.58** bound non-selective to both receptors. Incorporation of the less flexible 2-amino-4,5,6,7-tetrahydrobenzothiazol-6-yl moiety, derived from pramipexole, resulted in partial (**6.67**, E_{max}: 0.53, pEC_{50}: 6.7) or in weak partial agonism (**6.66**, E_{max}: 0.16, pEC_{50}: 6.83) and bell-shaped concentration-response curves. Interestingly, these two ligands showed a decreased $hD_{2long}R$ and hD_3R affinity compared to pramipexole. Incorporation of an aminothiazolylphenyl moiety (compounds **6.60-6.65**) resulted in weak antagonism at the hH_2R (pK_b: 4.8-6.14). Replacement of the amino(methyl)thiazolepropyl moiety of UR-NK22 with either a (aminothiazolyl)phenyl (**6.70**) or a pyrazolylpropyl moiety (**6.71**) resulted in strongly decreased hH_2R affinity and antagonistic or partial agonistic activity.

All full or partial agonists identified in the GTPγS assay showed a lower potency and efficacy in the βArrestin2 recruitment assay. The ligands **6.53-6.59** also showed in the βArrestin2 recruitment assay more or less pronounced bell-shaped concentration-response curves. While in case of the GTPγS assay plausible explanations would be binding through multiple binding sites or direct interaction with the $G_{s\alpha S}$ subunit of the fusion protein, in the βArrestin2 recruitment assay also cytotoxicity could be the reason.

High affinity ligands like **6.48**, **6.51** and **6.55** were highly selective for hH_2R over the other subtypes (Figure 6.11). The investigation of the binding affinity of aminothiazole containing ligands like **6.55** to the $hD_{2long}R$ and the hD_3R showed that achieving selectivity over these dopamine receptors might be a challenge. Notwithstanding, the monomeric N^G-carbamoylated amino(methyl)thiazolyl propylguanidines represent a good alternative to monomeric acylguanidines and dimeric ligands with high stability against hydrolytic cleavage. However, according to the current state of knowledge this is just speculation.

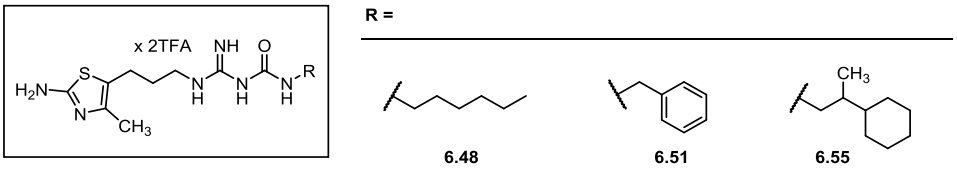

Figure 6.11. N^G-Carbamoylated 3-(2-amino-4-methylthiazol-5-yl)propylguanidines **6.48**, **6.51** and **6.55** as high potency H_2R agonists.

6.5 REFERENCES

1. Kraus, A.; Ghorai, P.; Birnkammer, T.; Schnell, D.; Elz, S.; Seifert, R.; Dove, S.; Bernhardt, G.; Buschauer, A. N-G-Acylated Aminothiazolylpropylguanidines as Potent and Selective Histamine H-2 Receptor Agonists. *ChemMedChem* **2009**, 4, 232-240.
2. Birnkammer, T.; Spickenreither, A.; Brunskole, I.; Lopuch, M.; Kagermeier, N.; Bernhardt, G.; Dove, S.; Seifert, R.; Elz, S.; Buschauer, A. The Bivalent Ligand Approach Leads to Highly Potent and Selective Acylguanidine-Type Histamine H-2 Receptor Agonists. *J. Med. Chem.* **2012**, 55, 1147-1160.
3. Ghorai, P.; Kraus, A.; Keller, M.; Gotte, C.; Igel, P.; Schneider, E.; Schnell, D.; Bernhardt, G.; Dove, S.; Zabel, M.; Elz, S.; Seifert, R.; Buschauer, A. Acylguanidines as bioisosteres of guanidines: NG-acylated imidazolylpropylguanidines, a new class of histamine H2 receptor agonists. *J. Med. Chem.* **2008**, 51, 7193-7204.
4. Ghorai, P.; Kraus, A.; Birnkammer, T.; Geyer, R.; Bernhardt, G.; Dove, S.; Seifert, R.; Elz, S.; Buschauer, A. Chiral NG-acylated hetarylpropylguanidine-type histamine H2 receptor agonists do not show significant stereoselectivity. *Bioorg. Med. Chem. Lett.* **2010**, 20, 3173-3176.
5. Kagermeier, N.; Werner, K.; Keller, M.; Baumeister, P.; Bernhardt, G.; Seifert, R.; Buschauer, A. Dimeric carbamoylguanidine-type histamine H receptor ligands: A new class of potent and selective agonists. *Bioorg. Med. Chem.* **2015**.
6. Brennauer, A.; Keller, M.; Freund, M.; Bernhardt, G.; Buschauer, A. Decomposition of 1-(ω-aminoalkanoyl)guanidines under alkaline conditions. *Tetrahedron Letters* **2007**, 48, 6996-6999.
7. Keller, M.; Kuhn, K. K.; Einsiedel, J.; Hubner, H.; Biselli, S.; Mollereau, C.; Wifling, D.; Svobodova, J.; Bernhardt, G.; Cabrele, C.; Vanderheyden, P. M.; Gmeiner, P.; Buschauer, A. Mimicking of Arginine by Functionalized N(omega)-Carbamoylated Arginine As a New Broadly Applicable Approach to Labeled Bioactive Peptides: High Affinity Angiotensin, Neuropeptide Y, Neuropeptide FF, and Neurotensin Receptor Ligands As Examples. *J. Med. Chem.* **2016**, 59, 1925-1945.
8. Keller, M.; Bernhardt, G.; Buschauer, A. [(3)H]UR-MK136: a highly potent and selective radioligand for neuropeptide Y Y(1) receptors. *ChemMedChem* **2011**, 6, 1566-1571.
9. Chen, J.; Collins, G. T.; Levant, B.; Woods, J.; Deschamps, J. R.; Wang, S. CJ-1639: A Potent and Highly Selective Dopamine D3 Receptor Full Agonist. *ACS Med. Chem. Lett.* **2011**, 2, 620-625.
10. Jones, D. F.; Oldham, K. Antisecretory guanidine derivatives and pharmaceutical compositions containing them. EP 0003640A2, 1979. Chem. Abstr. 92:94405.
11. Griss, G.; Schneider, C.; Hurnaus, R.; Kobinger, W.; Pichler, L.; Bauer, R.; Mierau, J. Tetrahydrobenzothiazolediamines. 1986. Chem. Abstr. 105:153056.
12. Kraus, A. Highly potent, selective acylguanidine-type histamine H2 receptor agonists: synthesis and structure-activity relationships. Dissertation, Universität Regensburg, Regensburg, 2007. https://epub.uni-regensburg.de/10699/.
13. Geyer, R.; Igel, P.; Kaske, M.; Elz, S.; Buschauer, A. Synthesis, SAR and selectivity of 2-acyl- and 2-cyano-1-hetarylalkyl-guanidines at the four histamine receptor subtypes: a bioisosteric approach. *MedChemComm* **2014**, 5, 72-81.
14. Baumeister, P.; Erdmann, D.; Biselli, S.; Kagermeier, N.; Elz, S.; Bernhardt, G.; Buschauer, A. [3H]UR-DE257: Development of a Tritium-Labeled Squaramide-Type Selective Histamine H2 Receptor Antagonist. *ChemMedChem* **2015**, 10, 83-93.
15. Felixberger, J. Luciferase complementation for the determination of arrestin recruitment: Investigations at histamine and NPY receptors. University of Regensburg, Regensburg, 2014. https://epub.uni-regensburg.de/31292/.
16. Birnkammer, T. Highly potent and selective acylguanidine-type histamine H2 receptor agonists: synthesis and structure-activity relationships of mono- and bivalent ligands. Dissertation, Universität Regensburg, Regensburg, 2011. https://epub.uni-regensburg.de/22237/.

17. Hornigold, D. C.; Mistry, R.; Raymond, P. D.; Blank, J. L.; Challiss, R. A. Evidence for cross-talk between M2 and M3 muscarinic acetylcholine receptors in the regulation of second messenger and extracellular signal-regulated kinase signalling pathways in Chinese hamster ovary cells. *Br. J. Pharmacol.* **2003**, 138, 1340-1350.
18. Chidiac, P.; Nouet, S.; Bouvier, M. Agonist-induced modulation of inverse agonist efficacy at the beta 2-adrenergic receptor. *Mol. Pharmacol.* **1996**, 50, 662-669.
19. Newman-Tancredi, A.; Cussac, D.; Marini, L.; Millan, M. J. Antibody capture assay reveals bell-shaped concentration-response isotherms for h5-HT(1A) receptor-mediated Galpha(i3) activation: conformational selection by high-efficacy agonists, and relationship to trafficking of receptor signaling. *Mol. Pharmacol.* **2002**, 62, 590-601.
20. Moriguchi, T.; Matsuura, H.; Itakura, Y.; Katsuki, H.; Saito, H.; Nishiyama, N. Allixin, a phytoalexin produced by garlic, and its analogues as novel exogenous substances with neurotrophic activity. *Life. Sci.* **1997**, 61, 1413-1420.
21. Zegarra-Moran, O.; Romio, L.; Folli, C.; Caci, E.; Becq, F.; Vierfond, J. M.; Mettey, Y.; Cabrini, G.; Fanen, P.; Galietta, L. J. Correction of G551D-CFTR transport defect in epithelial monolayers by genistein but not by CPX or MPB-07. *Br. J. Pharmacol.* **2002**, 137, 504-512.
22. Wreggett, K. A.; Wells, J. W. Cooperativity manifest in the binding properties of purified cardiac muscarinic receptors. *J. Biol. Chem.* **1995**, 270, 22488-22499.
23. Owen, S. C.; Doak, A. K.; Ganesh, A. N.; Nedyalkova, L.; McLaughlin, C. K.; Shoichet, B. K.; Shoichet, M. S. Colloidal drug formulations can explain "bell-shaped" concentration-response curves. *ACS Chem. Biol.* **2014**, 9, 777-784.
24. Chen, J.; Jiang, C.; Levant, B.; Li, X.; Zhao, T.; Wen, B.; Luo, R.; Sun, D.; Wang, S. Pramipexole derivatives as potent and selective dopamine D(3) receptor agonists with improved human microsomal stability. *ChemMedChem* **2014**, 9, 2653-2660.
25. Lober, S.; Hubner, H.; Gmeiner, P. Fused azaindole derivatives: molecular design, synthesis and in vitro pharmacology leading to the preferential dopamine D3 receptor agonist FAUC 725. *Bioorg. Med. Chem. Lett.* **2002**, 12, 2377-2380.
26. Schwalbe, T.; Kaindl, J.; Hubner, H.; Gmeiner, P. Potent haloperidol derivatives covalently binding to the dopamine D2 receptor. *Bioorg. Med. Chem.* **2017**, 25, 5084-5094.
27. Ran, K.; Gao, C.; Deng, H.; Lei, Q.; You, X.; Wang, N.; Shi, Y.; Liu, Z.; Wei, W.; Peng, C.; Xiong, L.; Xiao, K.; Yu, L. Identification of novel 2-aminothiazole conjugated nitrofuran as antitubercular and antibacterial agents. *Bioorg. Med. Chem. Lett.* **2016**, 26, 3669-3674.
28. Glennon, R. A.; Hong, S. S.; Bondarev, M.; Law, H.; Dukat, M.; Rakhi, S.; Power, P.; Fan, E.; Kinneau, D.; Kamboj, R.; Teitler, M.; Herrick-Davis, K.; Smith, C. Binding of O-alkyl derivatives of serotonin at human 5-HT1D beta receptors. *J. Med. Chem.* **1996**, 39, 314-322.
29. Patel, D. A.; Kumar, R.; Dwivedi, S. D. Process for preparation of pramipexole and intermediates thereof. 2008. Chem. Abstr. 148:426880.
30. Pop, N.; Igel, P.; Brennauer, A.; Cabrele, C.; Bernhardt, G. N.; Seifert, R.; Buschauer, A. Functional reconstitution of human neuropeptide Y (NPY) Y(2) and Y(4) receptors in Sf9 insect cells. *J. Recept. Signal. Transduct. Res.* **2011**, 31, 271-285.
31. Igel, P.; Schnell, D.; Bernhardt, G.; Seifert, R.; Buschauer, A. Tritium-labeled N(1)-[3-(1H-imidazol-4-yl)propyl]-N(2)-propionylguanidine ([(3)H]UR-PI294), a high-affinity histamine H(3) and H(4) receptor radioligand. *ChemMedChem* **2009**, 4, 225-231.
32. Lieb, S.; Littmann, T.; Plank, N.; Felixberger, J.; Tanaka, M.; Schafer, T.; Krief, S.; Elz, S.; Friedland, K.; Bernhardt, G.; Wegener, J.; Ozawa, T.; Buschauer, A. Label-free versus conventional cellular assays: Functional investigations on the human histamine H1 receptor. *Pharm. Res.* **2016**, 114, 13-26.
33. Cheng, Y.; Prusoff, W. H. Relationship between the inhibition constant (K1) and the concentration of inhibitor which causes 50 per cent inhibition (I50) of an enzymatic reaction. *Biochem. Pharmacol.* **1973**, 22, 3099-3108.

Chapter 7

SUMMARY

The H_2R, an aminergic GPCR, is one of four receptor subtypes (H_1R, H_2R, H_3R, H_4R) which mediate the action of the biogenic amine histamine. Activation of H_2R results e. g. in gastric acid secretion,[1,2] positive inotropic and chronotropic effects[3]. In humans, the H_2R is located on parietal cells in the stomach,[2] in the brain,[4,5] on neutrophiles and eosinophiles[6] as well as on smooth muscle cells[7]. However, the (patho-) physical role of the H_2R, especially in the brain, is still far from being understood. Therefore this work aimed at the development of selective high affinity molecular tools for the H_2R, including agonists, antagonists and radiolabeled as well as fluorescent H_2R ligands.

The number of high affinity tritiated radioligands for the H_2R is very limited. Guanidinothiazole containing ligands such as famotidine or ICI127032 represent a class of surmountable H_2R antagonists.[8,9] The combination of the 2-guanidino-4-[(2-aminoethyl)thiomethyl]thiazole structure derived from famotidine or the guanidino-4-(3-aminophenyl)thiazole structure derived from ICI127032 with a derivatized squaramide or a cyanoguanidine moiety ("urea equivalent") led to propionylated high affinity H_2R antagonists. N-[8-(2-[2-(2-guanidinothiazol-4-ylmethylthio)ethylamino]-3,4-dioxocyclobut-1-ene-1-ylamino)octyl]propionamide (**3.25**) showed a pK_i value of 7.65 at the hH_2R and selectivity over the other subtypes (no affinity at the hH_1R, hH_3R: pK_i value of 5.3 and hH_4R: pK_i value of 4.4). The radiolabled form [^{3}H]**3.25** bound in a saturable manner (K_d values of 15-22 nM) to membrane preparations of Sf9 cells and intact Hek cells both recombinantly expressing hH_2Rs. Although a part of [^{3}H]**3.25** bound in (pseudo)irreversible manner (plateau at 23%), the kinetic K_d value of 26 nM was comparable to that determined at equilibrium, and the radioligand ^{3}H]**3.25** was completely displacable by histamine, famotidine and ICI127032. However, the radioligand showed a radiochemical purity of only 87% and low stability in stock solution (radiochemical purity: <45% after 15 month). Nevertheless, [^{3}H]**3.25** can be a valuable molecular tool provided that purity and stability under storage conditions are improvable.

Aminopotentidine and it´s derivatives are reported as high affinity H_2R antagonists. Iodination in 3 position of the 4-aminobenzoic acid amide moiety results in an enormous gain in affinity (iodoaminopotentidine).[4,5] Aminopotentidine and its analogs with different substituents (e.g. iodine, bromine, chlorine, trifluoromethyl) in position 3, were prepared and propionylated. Within the series of propionylated derivatives the brominated ligand (**4.37**) and the iodinated ligand (**4.38**) showed the highest hH_2R affinities (pK_i values of 8.5 and 8.18) along with excellent selectivities over the hH_3R (6900- or 2500-fold). In general, for radiosynthesis an excess of precursor compared to radioactive labeling reagent is used. However, an adjustment of the reaction conditions for radiosynthesis might be challenging due to the necessary high excess of the "cold" labeling reagent propionic chloride and the low yields in the "cold" reaction. A test reaction under radiosynthesis conditions failed. To overcome this problem, a series of aminopotentidine derivatives containing a functionalized (propionylated, acetylated or methylated) aminomethyl substituent in 4-position of the aromatic ring was prepared. The dimethylated 3-bromo substituted ligand **4.50** showed the highest affinity within the series with a pK_i value of 7.54. The synthesis of radiolabeled **4.50** is accessible by dimethylation of **4.46** with [^{3}H]methyl iodide.

Fluorescent ligands have become an attractive alternative to radioligands for the investigation of ligand-receptor interactions. Besides advantages with respect to safety issues and waste disposal,

fluorescent ligands are a prerequisite for the application of a plethora of optical techniques (confocal microscopy, FRET,[10] FRAP,[11] TIRF,[12] high content imaging,[13] fluorescence polarization[14]). In order to expand the range of applications and avoid the high cellular autofluorescence, fluorescent ligands labeled with red-emitting fluorophores (emission wavelength > 600 nm) are required. Recently, a series of fluorescent ligands with a piperidinomethylphenoxypropylamino (potentidine) pharmacophore was reported.[15] The most promising ligands within this series were the squaramide-type ligands UR-DE229 and UR-DE56 which contained pyridinium or a cyanine fluorophore. Aiming at fluorescent high affinity H_2R antagonists with improved optical and physicochemical properties to gain access to a wide range of potential applications, the fluorescent labeled antagonists UR-DE229 (**5.12**) and UR-DE56 (**5.18**) were prepared and investigated in different assay systems (radioligand competition binding assay, GTPγS binding assay, flow cytometric binding assay and high content imaging). Furthermore, a small library of fluorescent ligands was synthesized for the exploration of the impact of length of the alkyl linker and the net charge of the fluorophores by coupling the positively charged pyrilium dye (Py-5) or differently charged cyanine dyes with amine precursors by linkers, differing in length (number of atoms). The highest affinities to the hH_2R (pK_i values > 7.0) in radioligand competition assays were obtained in case of the pyridinium labeled ligands **5.12-5.14** and the cyanine labeled ligands **5.16** (positively charged fluorophore, net charge: 2^+) and **5.18** (electroneutral fluorophore, net charge: 1^+). While the linker length (4-7 carbon atoms) had no significant influence on the hH_2R affinity in case of the pyridinium ligands, the cyanine ligands with a hexyl linker (**5.16** and **5.18**) showed an increased hH_2R affinity compared analogs, containing a butyl linker. Despite the low selectivity towards the hH_3R the investigated fluorescent ligands proved to be useful tools for binding studies using different techniques (flow cytometry, high content imaging and confocal microscopy), when genetically engineered cells, expressing the H_2R were used. Investigated ligands bound in a saturable manner to the hH_2R (flow cytometry and high content imaging) and the determined K_d values were in good agreement with the corresponding K_i values from radiolligand binding experiments. $K_{d\ (kin)}$ values calculated from kinetic experiments (flow cytometry or high content imaging) were consistent with the K_d values determined in saturation binding experiments even though they showed an incomplete dissociation (insurmountable antagonism). High content imaging and confocal microscopy showed that residual bound ligand was still located in the cell membrane. Nonetheless, the fluorescent ligands **5.14** and **5.18** also proved to be useful for the determination of binding affinities of unlabeled ligands in competition binding assays (flow cytometry and high content imaging).

N^G-acylated amino(methyl)thiazolepropylguanidines are reported as a class of potent and selective histamine H_2R agonists, but the acylguanidine group is prone to hydrolytic cleavage upon storage in aqueous solution[16,17]. A bioisosteric approach, replacing the N^G-acylguanidine structure with a N^G-carbamoylguanidine, led in many cases to more stable compounds.[17-19] For exploration of the structure-activity (H_2R) and the structure-selectivity relationships of this class of compounds, in addition to dimeric ligands, a series of carbamoylguanidines with various aminothiazole-based substructures, i.e., the 3-(2-amino-4-methylthiazol-5-yl)propyl moiety, a conformationally constrained (aminothiazolyl)phenyl and a 2-amino-4,5,6,7-tetrahydrobenzothiazol-6-yl portion were prepared. Compounds containing the conformationally constrained aminothiazolylphenyl moiety were antagonists with only a weak affinity to the hH_2R and compounds containing the less flexible 2-amino-4,5,6,7-tetrahydrobenzothiazol-6-yl moiety,

derived from pramipexole, showed partial (**6.67**, α: 0.53, pEC_{50} value: 6.7) or weak partial agonism (**6.66**, α: 0.16, pEC_{50} value: 6.83) and bell-shaped concentration-response curves. Amino(methyl)thiazolyl propyl containing compounds achieved up to 80-fold the potency of histamine (pEC_{50} values of 6.3-7.76) and partial to full agonistic activities with more or less pronounced bell-shaped concentration-response curves. A variety of aliphatic and aromatic residues was well tolerated and the agonistic N^G-carbamoylated guanidine-type ligands exhibited some functional bias towards G-protein activation. Additionally, representative ligands were investigated for dopamine receptor affinity ($hD_{2long}R$ and hD_3R). These ligands showed affinity to the $hD_{2long}R$ (pK_i value: 5.6-6.97) and hD_3R (pK_i value: 5.3-7.6).

In conclusion, this work afforded new radiolabeled and fluorescence labeled molecular tools for the hH_2R and showed that N^G-carbamoylated amino(methyl)thiazolepropylguanidines are G-Protein biased, high affinity hH_2R agonists with good longterm stability.

REFERENCES

1. Black, J. W.; Duncan, W. A.; Durant, C. J.; Ganellin, C. R.; Parsons, E. M. Definition and antagonism of histamine H 2 -receptors. *Nature* **1972**, 236, 385-390.
2. Domschke, W.; Domschke, S.; Classen, M.; Demling, L. Histamine and cyclic 3',5'-AMP in gastric acid secretion. *Nature* **1973**, 241, 454-455.
3. Reinhardt, D.; Schmidt, U.; Brodde, O. E.; Schumann, H. J. H1 - and H2-receptor mediated responses to histamine on contractility and cyclic AMP of atrial and papillary muscles from guinea-pig hearts. *Agents Actions* **1977**, 7, 1-12.
4. Traiffort, E.; Pollard, H.; Moreau, J.; Ruat, M.; Schwartz, J. C.; Martinez-Mir, M. I.; Palacios, J. M. Pharmacological characterization and autoradiographic localization of histamine H2 receptors in human brain identified with [125I]iodoaminopotentidine. *J. Neurochem.* **1992**, 59, 290-299.
5. Ruat, M.; Traiffort, E.; Bouthenet, M. L.; Schwartz, J. C.; Hirschfeld, J.; Buschauer, A.; Schunack, W. Reversible and Irreversible Labeling and Autoradiographic Localization of the Cerebral Histamine H-2-Receptor Using [I-125] Iodinated Probes. *P. Natl. Acad. Sci. USA* **1990**, 87, 1658-1662.
6. Reher, T. M.; Brunskole, I.; Neumann, D.; Seifert, R. Evidence for ligand-specific conformations of the histamine H(2)-receptor in human eosinophils and neutrophils. *Biochem. Pharmacol.* **2012**, 84, 1174-1185.
7. Mitznegg, P.; Schubert, E.; Fuchs, W. Relations between the effects of histamine, pheniramin and metiamide on spontaneous motility and the formation of cyclic AMP in the isolated rat uterus. *Naunyn Schmiedeberg´s Arch. Pharmacol.* **1975**, 287, 321-327.
8. Yellin, T. O.; Buck, S. H.; Gilman, D. J.; Jones, D. F.; Wardleworth, J. M. ICI 125,211: a new gastric antisecretory agent acting on histamine H2-receptors. *Life. Sci.* **1979**, 25, 2001-2009.
9. Black, J. W.; Leff, P.; Shankley, N. P. Further Analysis of Anomalous Pkb Values for Histamine H-2-Receptor Antagonists on the Mouse Isolated Stomach Assay. *Br. J. Pharmacol.* **1985**, 86, 581-587.
10. Lohse, M. J.; Nuber, S.; Hoffmann, C. Fluorescence/bioluminescence resonance energy transfer techniques to study G-protein-coupled receptor activation and signaling. *Pharmacol. Rev.* **2012**, 64, 299-336.
11. Deschout, H.; Raemdonck, K.; Demeester, J.; De Smedt, S. C.; Braeckmans, K. FRAP in pharmaceutical research: practical guidelines and applications in drug delivery. *Pharm. Res.* **2014**, 31, 255-270.
12. Fish, K. N. Total internal reflection fluorescence (TIRF) microscopy. *Current Protocols in Cytometry* **2009**, Chapter 12, Unit12 18.
13. Zanella, F.; Lorens, J. B.; Link, W. High content screening: seeing is believing. *Trends Biotechnol.* **2010**, 28, 237-245.
14. Jameson, D. M.; Ross, J. A. Fluorescence polarization/anisotropy in diagnostics and imaging. *Chem. Rev.* **2010**, 110, 2685-2708.
15. Baumeister, P.; Erdmann, D.; Biselli, S.; Kagermeier, N.; Elz, S.; Bernhardt, G.; Buschauer, A. [3H]UR-DE257: Development of a Tritium-Labeled Squaramide-Type Selective Histamine H2 Receptor Antagonist. *ChemMedChem* **2015**, 10, 83-93.
16. Brennauer, A.; Keller, M.; Freund, M.; Bernhardt, G.; Buschauer, A. Decomposition of 1-(ω-aminoalkanoyl)guanidines under alkaline conditions. *Tetrahedron Letters* **2007**, 48, 6996-6999.
17. Kagermeier, N.; Werner, K.; Keller, M.; Baumeister, P.; Bernhardt, G.; Seifert, R.; Buschauer, A. Dimeric carbamoylguanidine-type histamine H receptor ligands: A new class of potent and selective agonists. *Bioorg. Med. Chem.* **2015**.
18. Keller, M.; Kuhn, K. K.; Einsiedel, J.; Hubner, H.; Biselli, S.; Mollereau, C.; Wifling, D.; Svobodova, J.; Bernhardt, G.; Cabrele, C.; Vanderheyden, P. M.; Gmeiner, P.; Buschauer, A.

Mimicking of Arginine by Functionalized N(omega)-Carbamoylated Arginine As a New Broadly Applicable Approach to Labeled Bioactive Peptides: High Affinity Angiotensin, Neuropeptide Y, Neuropeptide FF, and Neurotensin Receptor Ligands As Examples. *J. Med. Chem.* **2016**, 59, 1925-1945.

19. Keller, M.; Bernhardt, G.; Buschauer, A. [(3)H]UR-MK136: a highly potent and selective radioligand for neuropeptide Y Y(1) receptors. *ChemMedChem* **2011**, 6, 1566-1571.

APPENDIX

NMR SPECTRA

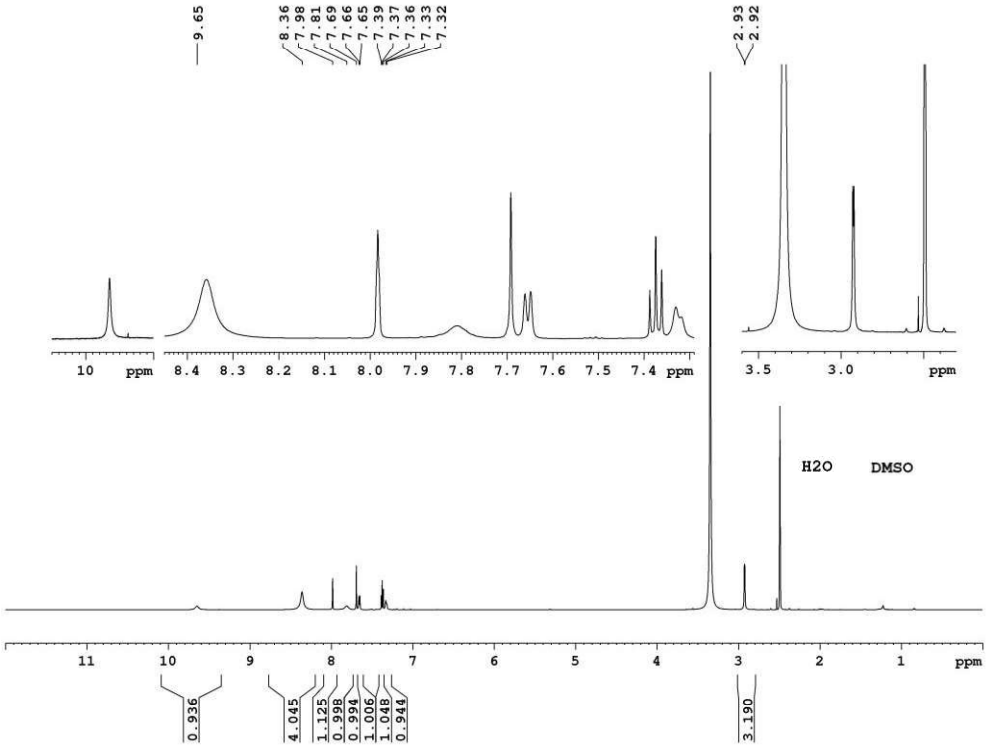

^{1}H-NMR spectrum (600 MHz, [D_6]DMSO) of **3.8**

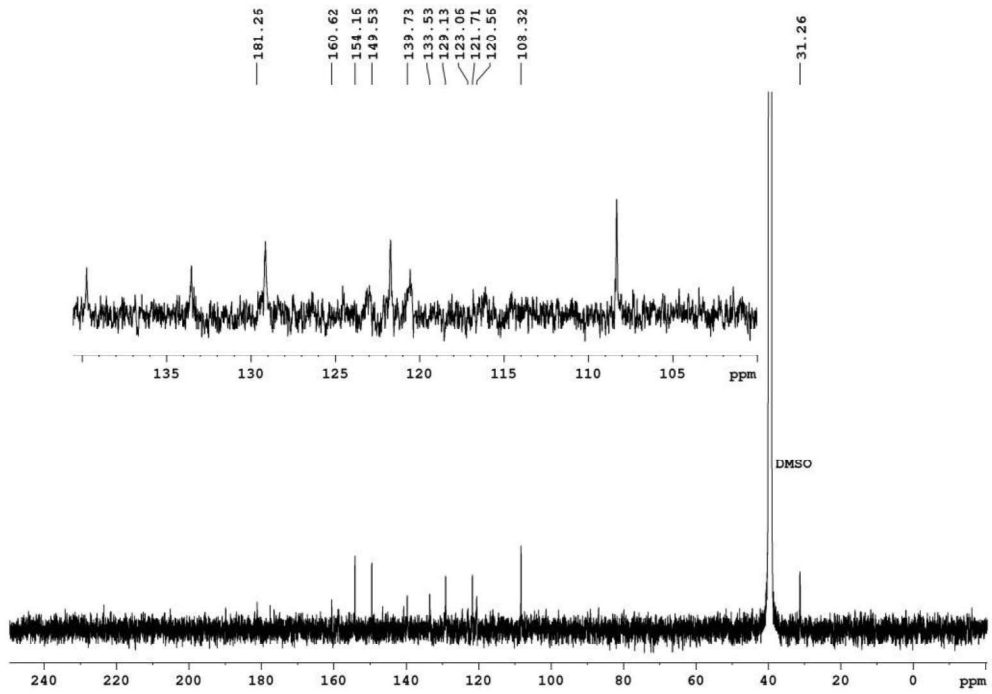

^{13}C-NMR spectrum (150 MHz, [D_6]DMSO) of **3.8**

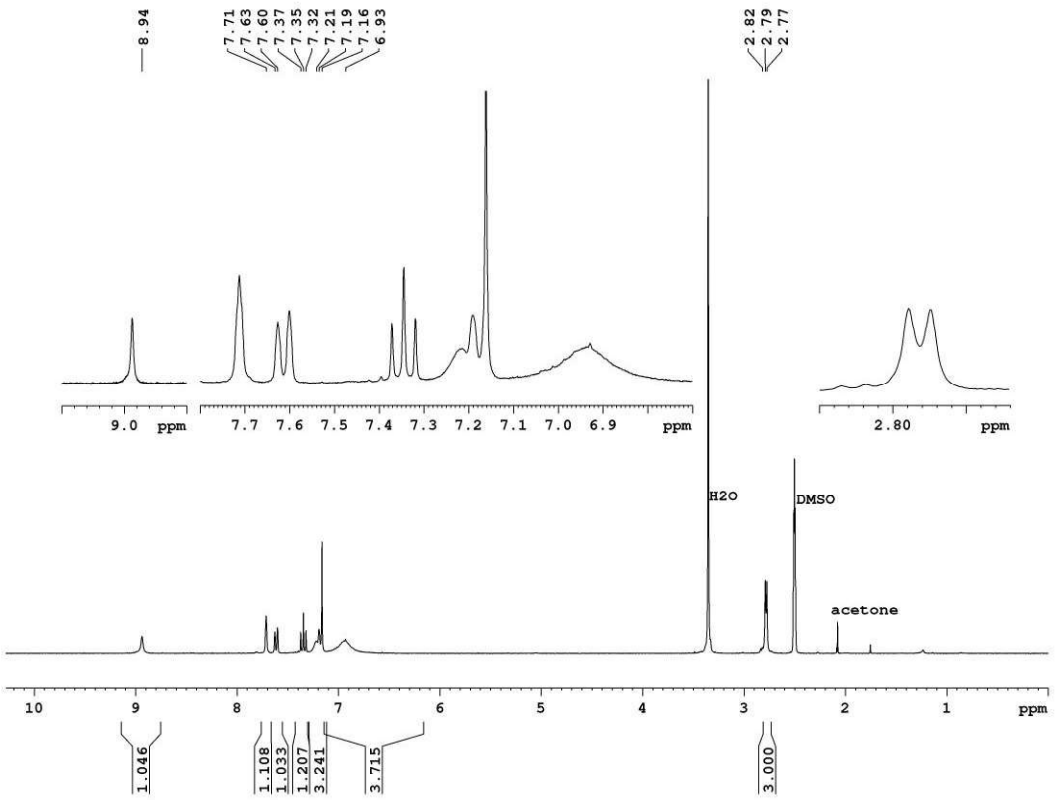

^{1}H-NMR spectrum (300 MHz, [D_6]DMSO) of **3.10**

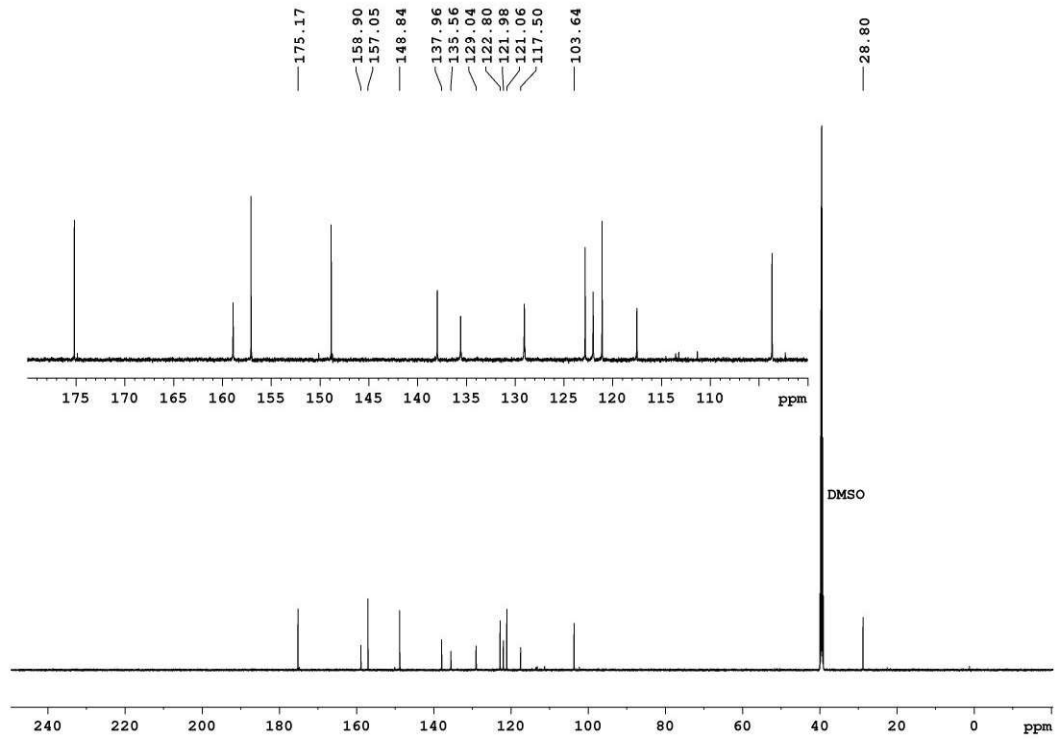

^{13}C-NMR spectrum (150 MHz, [D_6]DMSO) of **3.10**

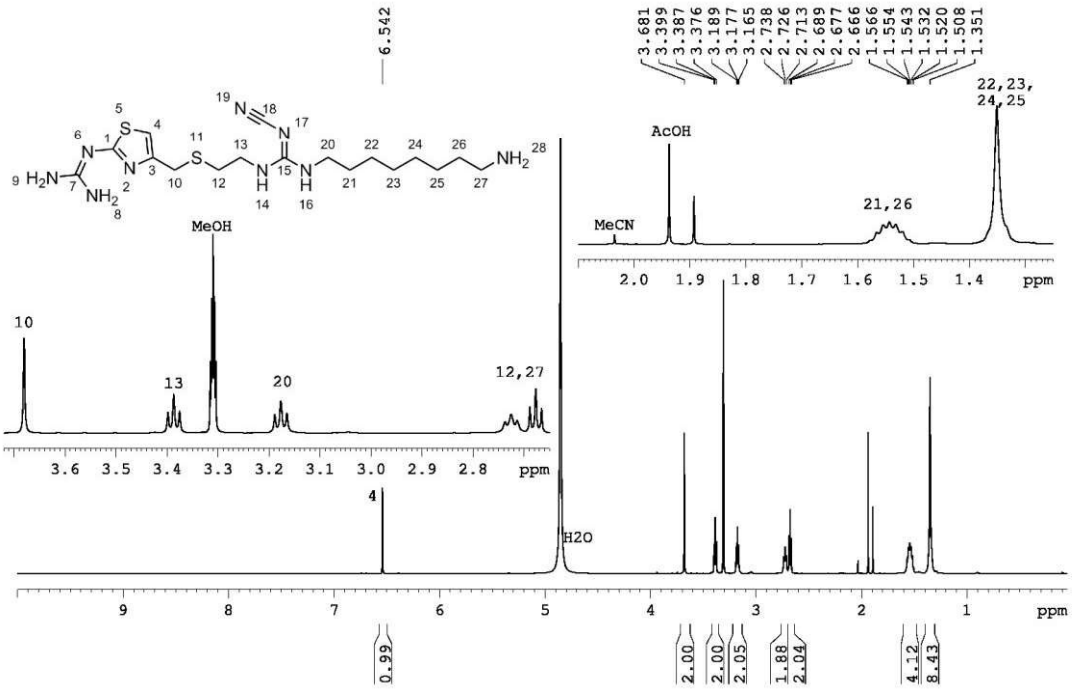

^{1}H-NMR spectrum (600 MHz, CD_3OD) of **3.12**

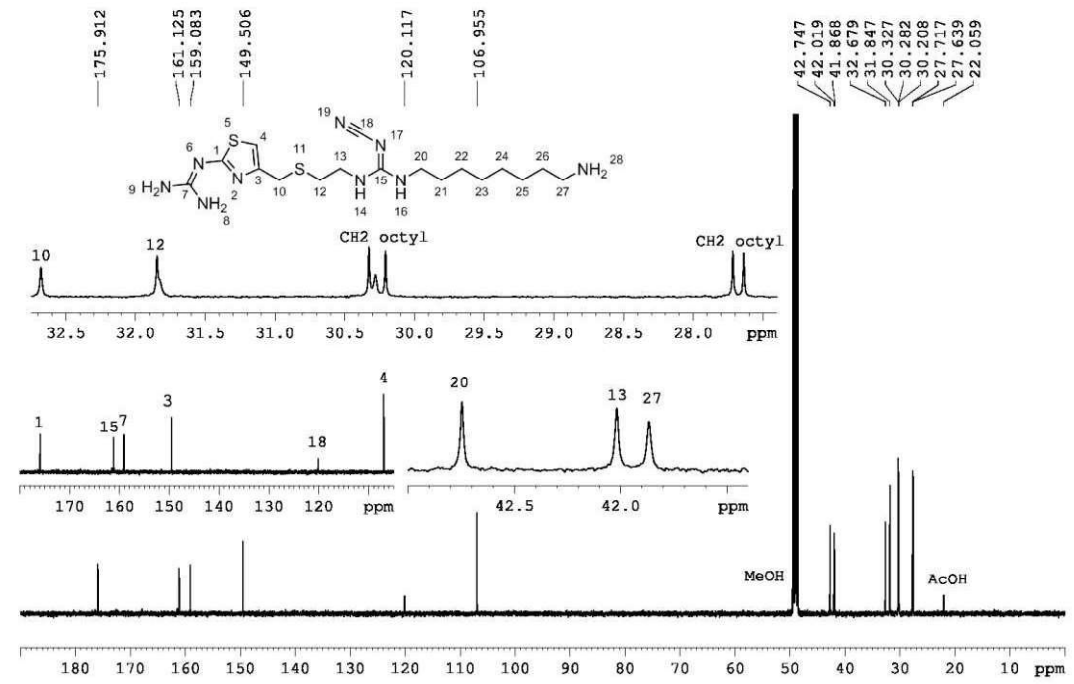

^{13}C-NMR spectrum (150 MHz, CD_3OD) of **3.12**

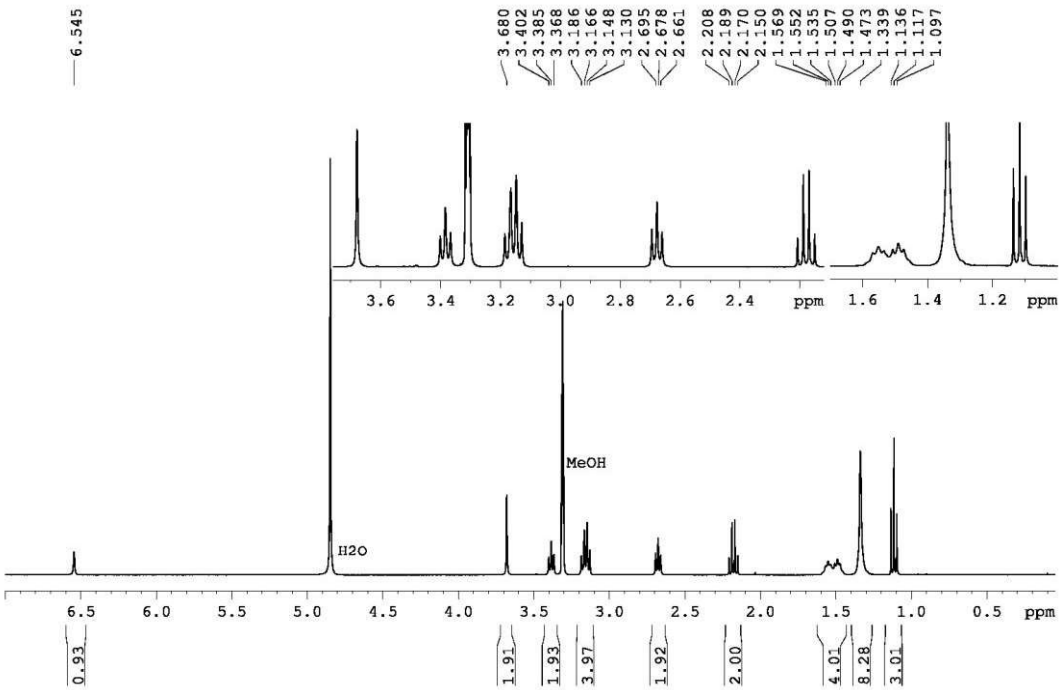

^{1}H-NMR spectrum (400 MHz, CD_3OD) of **3.13**

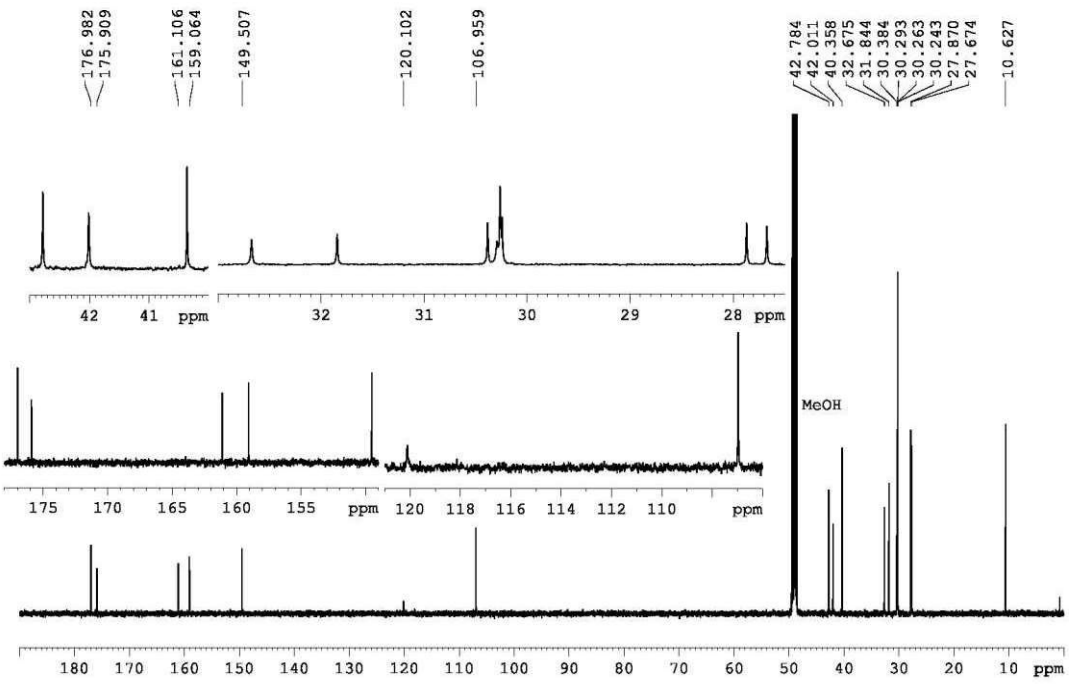

^{13}C-NMR spectrum (150 MHz, CD_3OD) of **3.13**

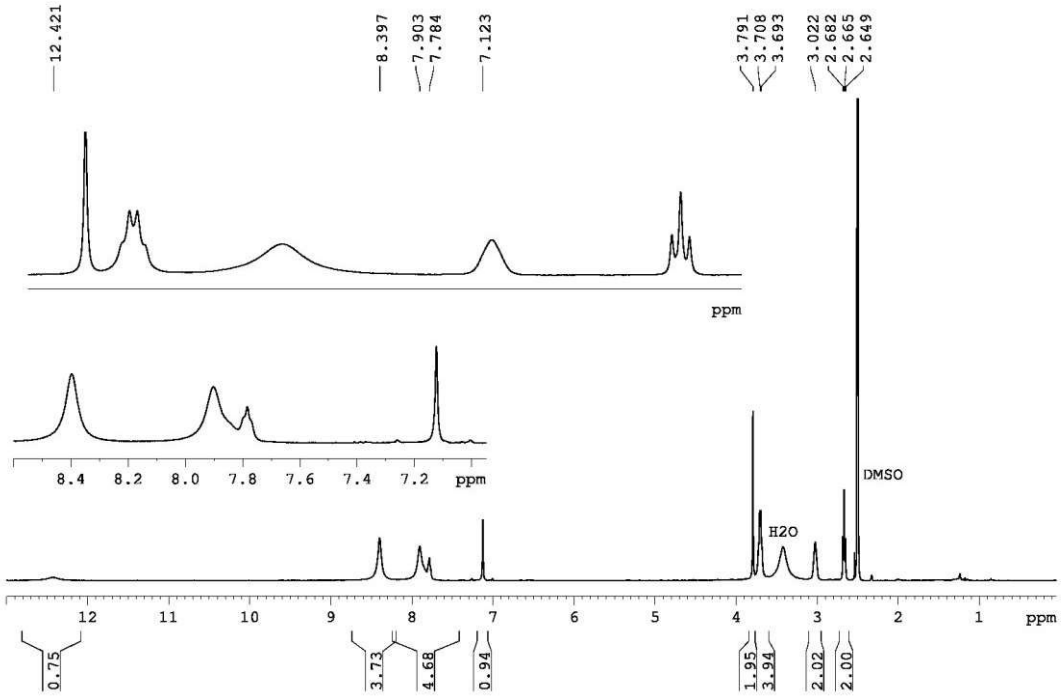

^{1}H-NMR spectrum (400 MHz, [D_6]-DMSO) of **3.21**

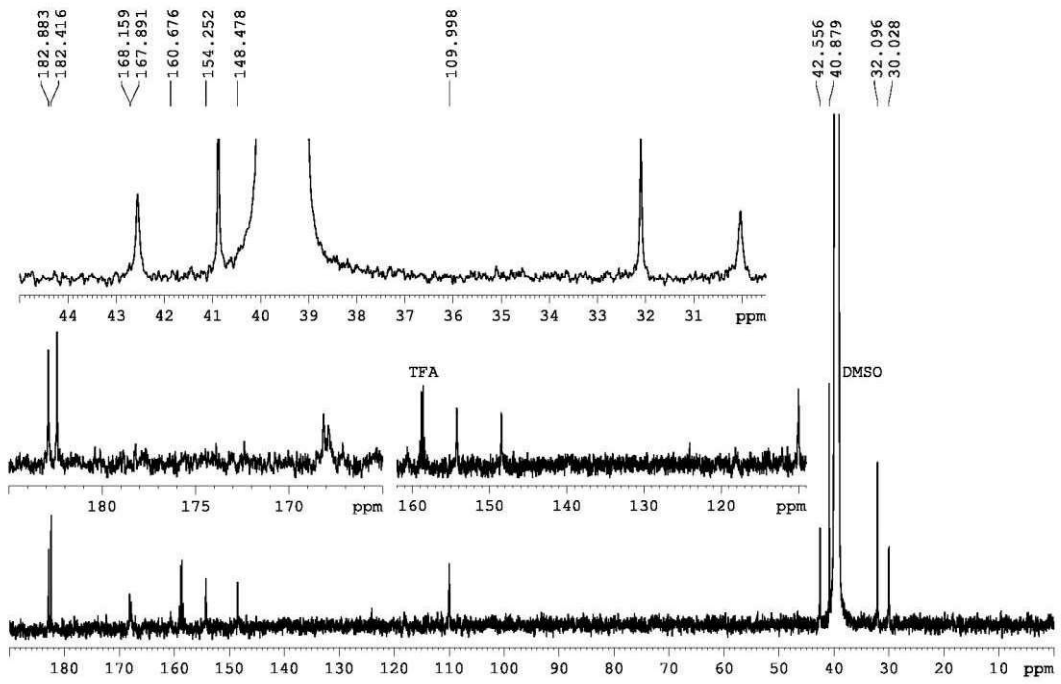

^{13}C-NMR spectrum (150 MHz, [D_6]-DMSO) of **3.21**

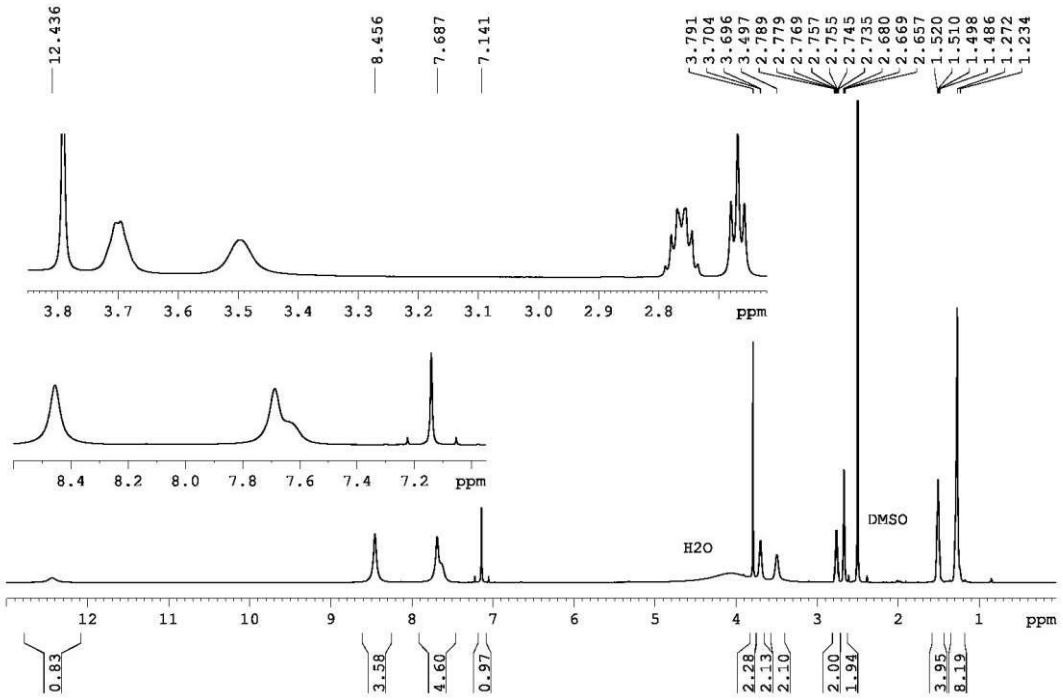

^{1}H-NMR spectrum (600 MHz, [D_6]-DMSO) of **3.22**

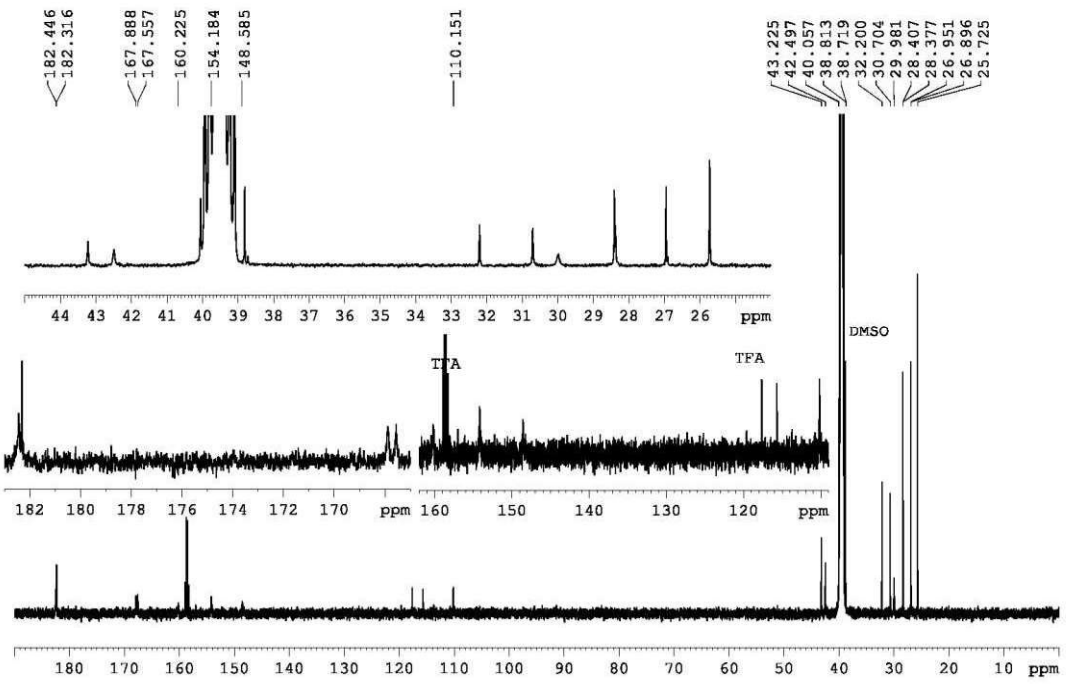

^{13}C-NMR spectrum (150 MHz, [D_6]-DMSO) of **3.22**

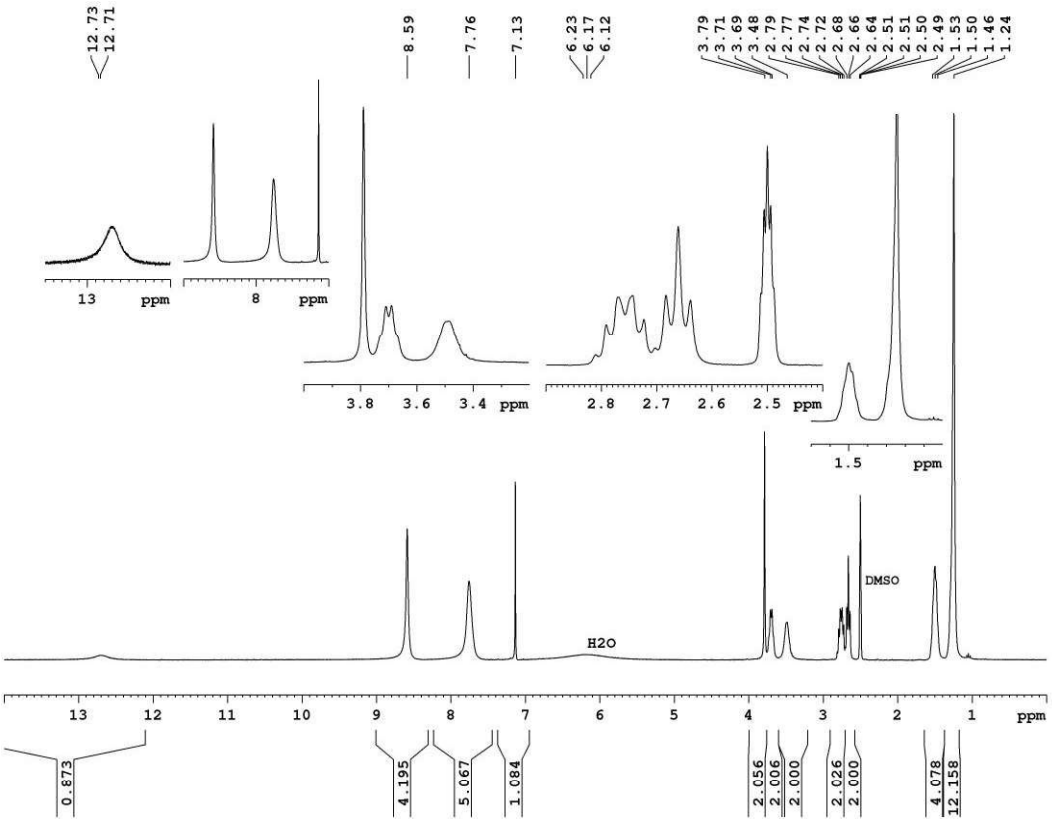

^{1}H-NMR spectrum (300 MHz, [D_6]-DMSO) of **3.23**

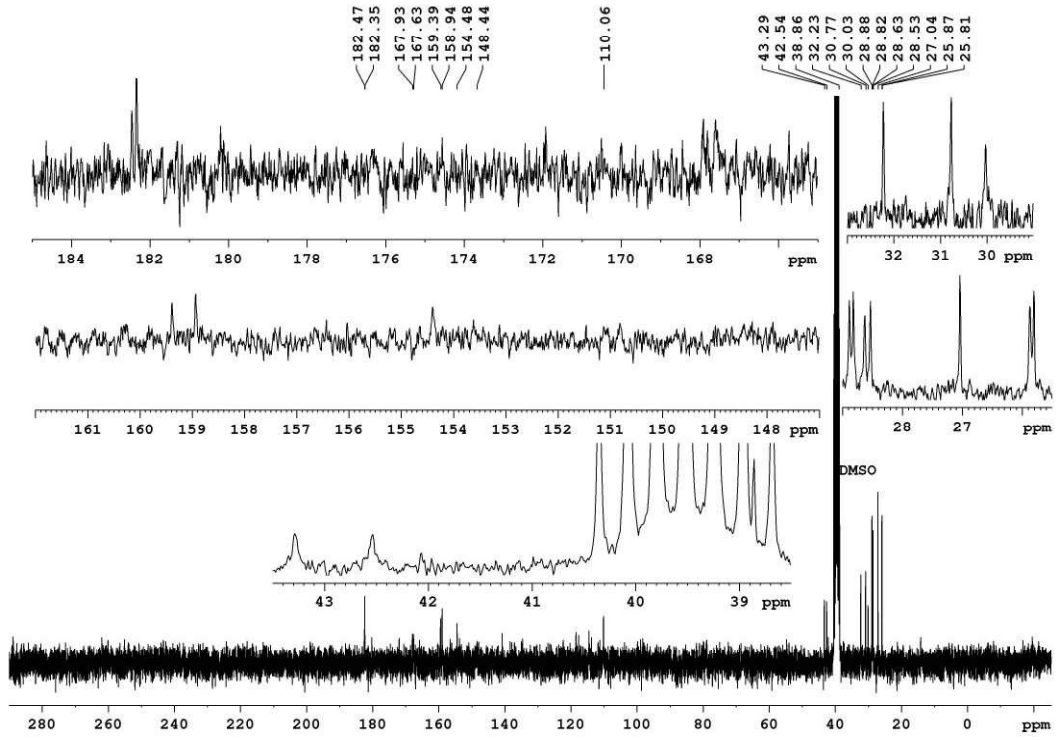

^{13}C-NMR spectrum (150 MHz, [D_6]-DMSO) of **3.23**

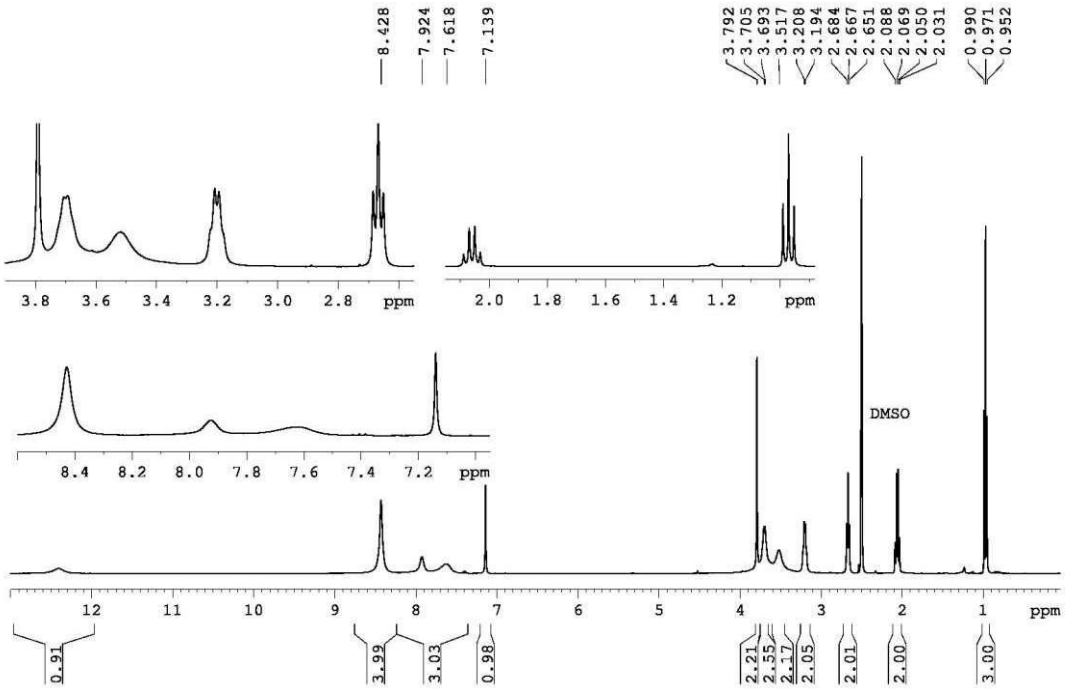

^{1}H-NMR spectrum (400 MHz, [D_6]-DMSO) of **3.24**

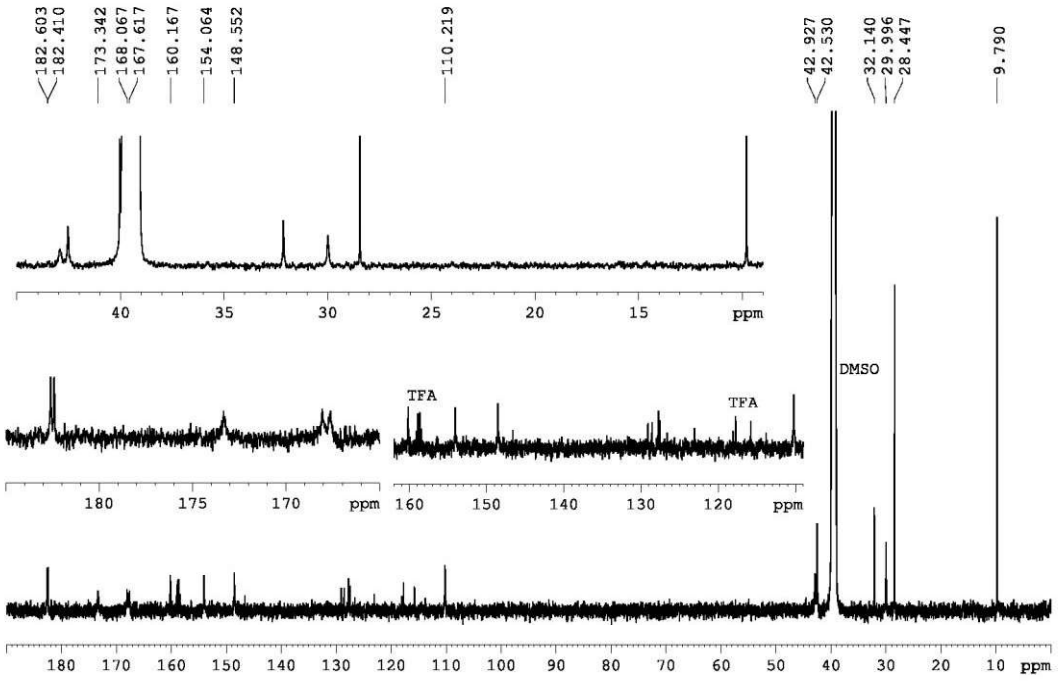

^{13}C-NMR spectrum (150 MHz, [D_6]-DMSO) of **3.24**

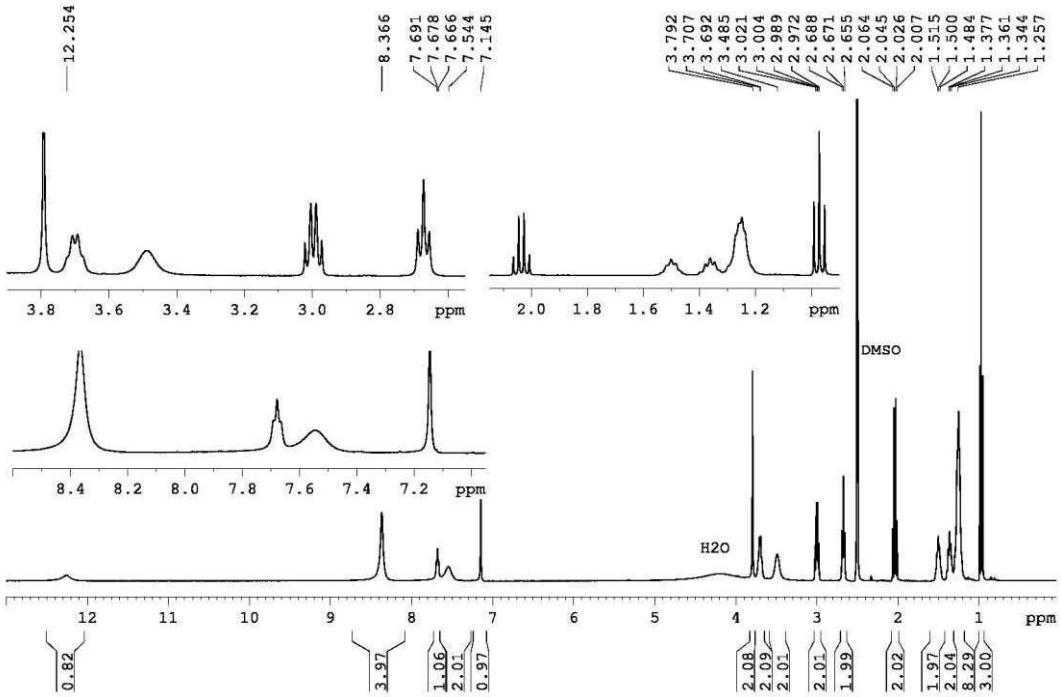

^{1}H-NMR spectrum (400 MHz, [D_6]-DMSO) of **3.25**

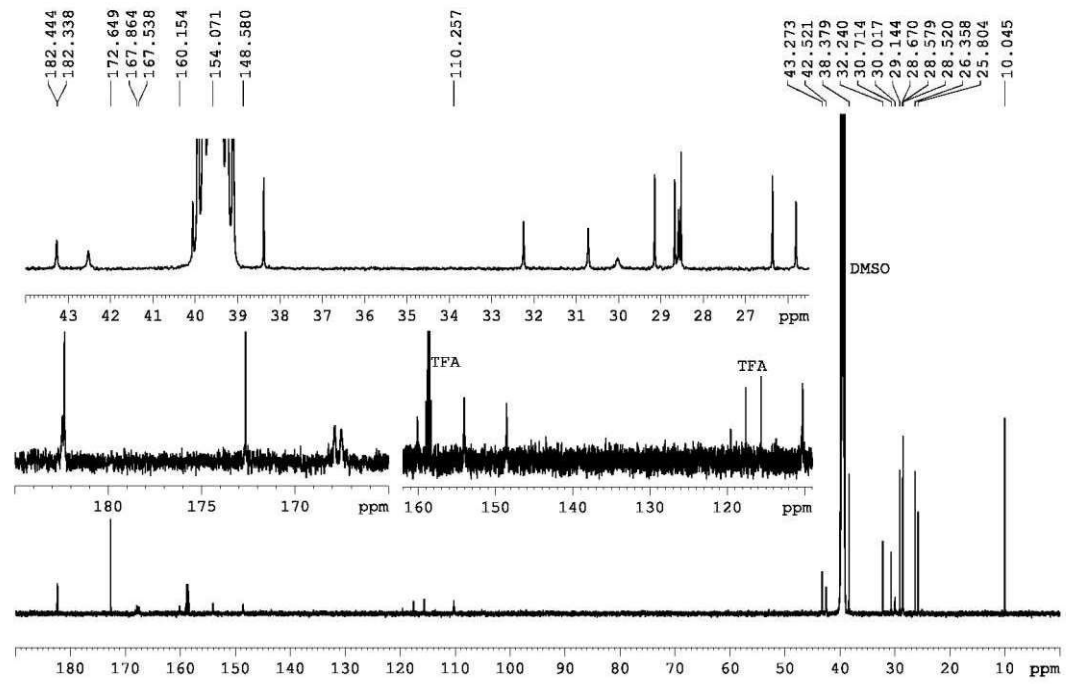

^{13}C-NMR spectrum (150 MHz, [D_6]-DMSO) of **3.25**

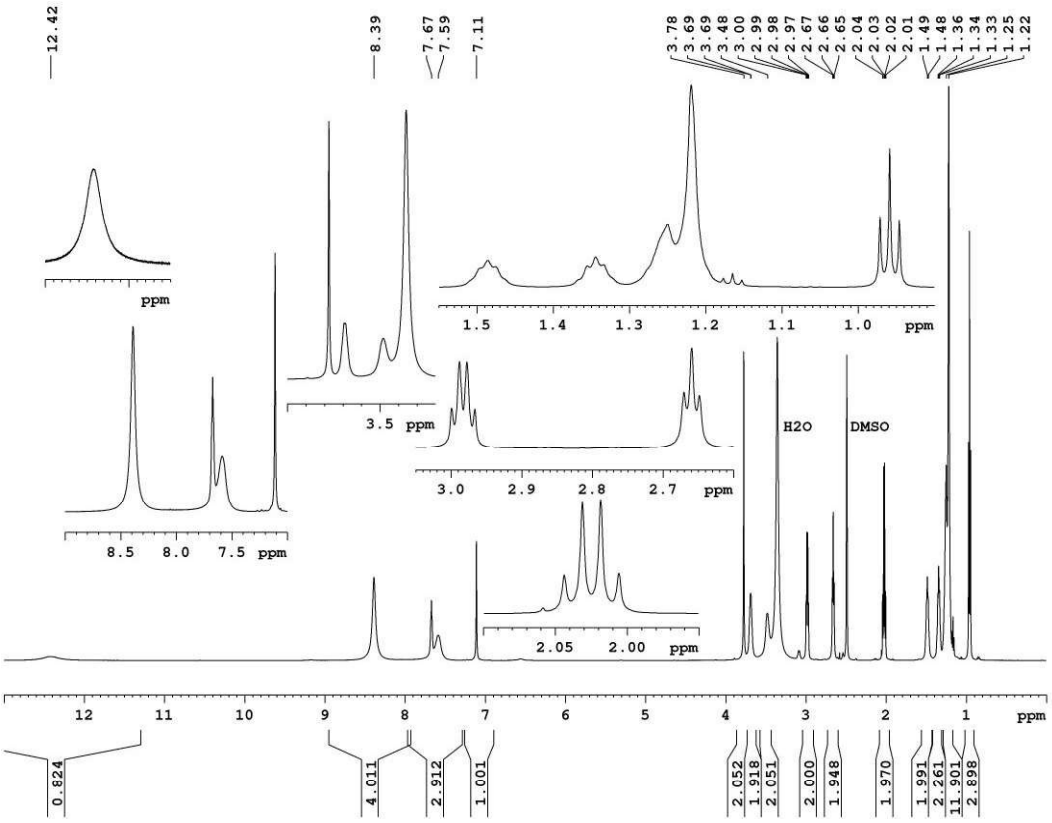

^{1}H-NMR spectrum (600 MHz, [D_6]-DMSO) of **3.26**

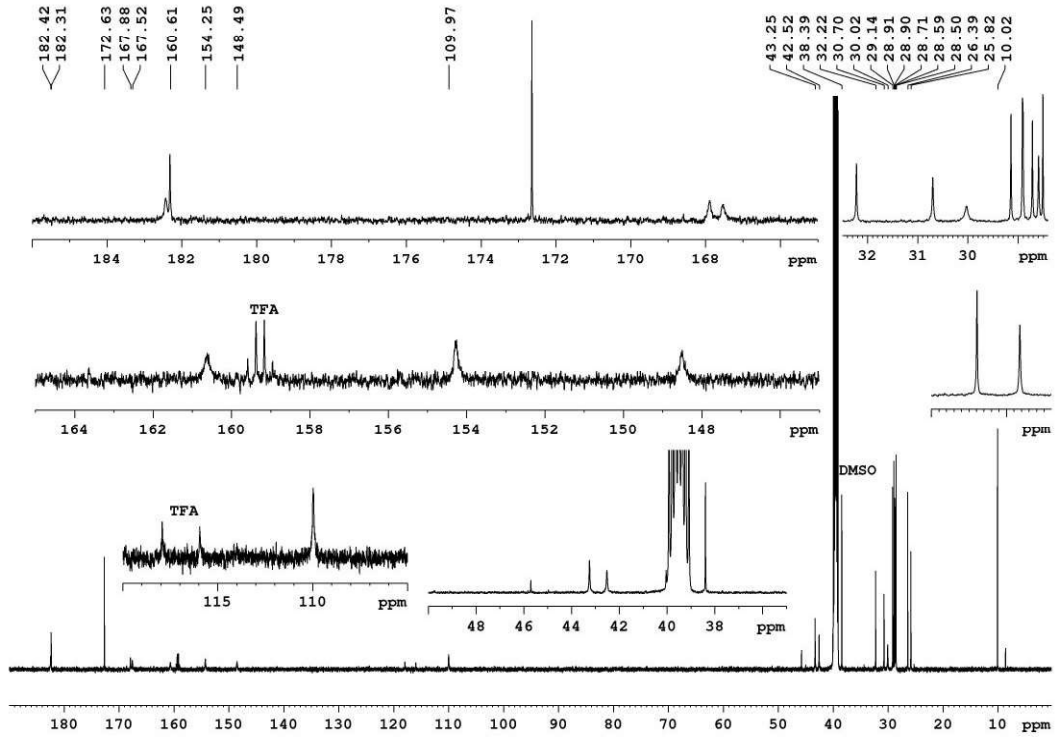

^{13}C-NMR spectrum (150 MHz, [D_6]-DMSO) of **3.26**

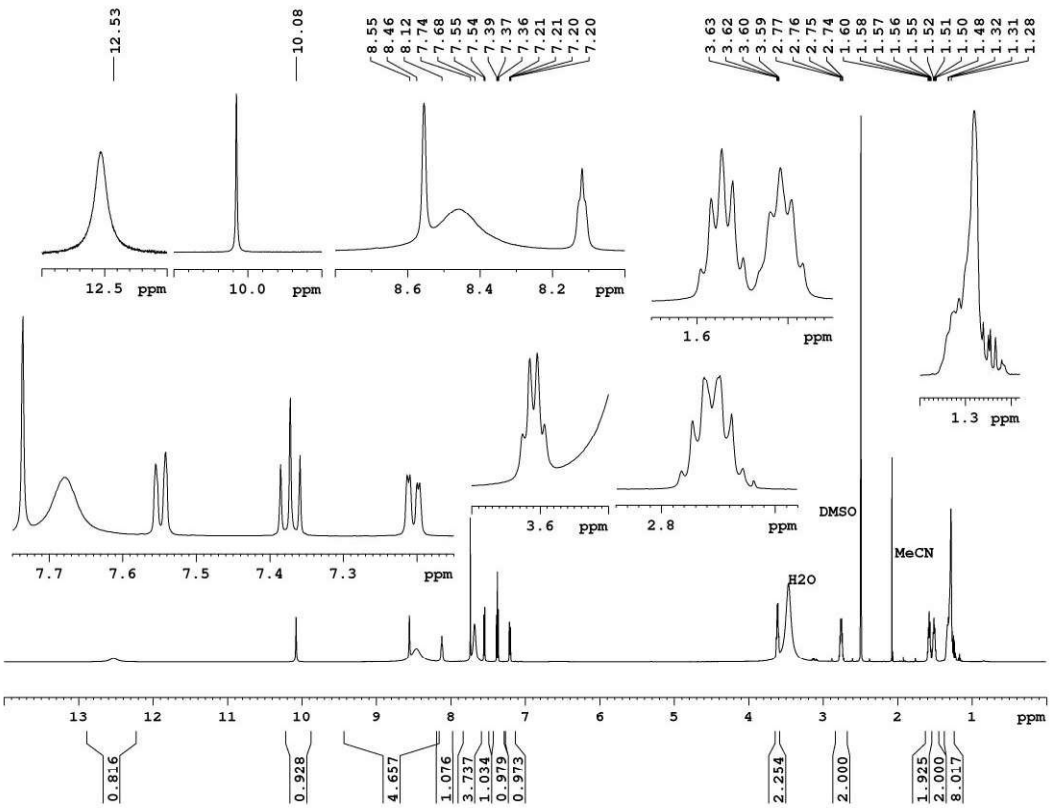

^{1}H-NMR spectrum (600 MHz, [D_6]-DMSO) of **3.29**

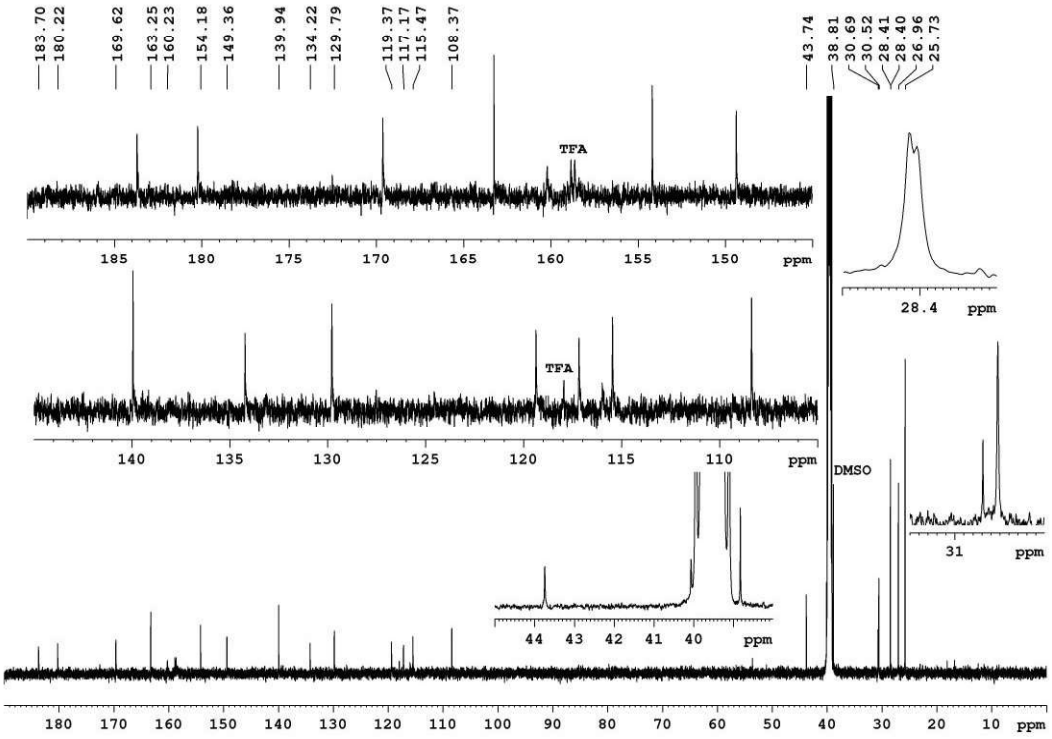

^{13}C-NMR spectrum (150 MHz, [D_6]-DMSO) of **3.29**

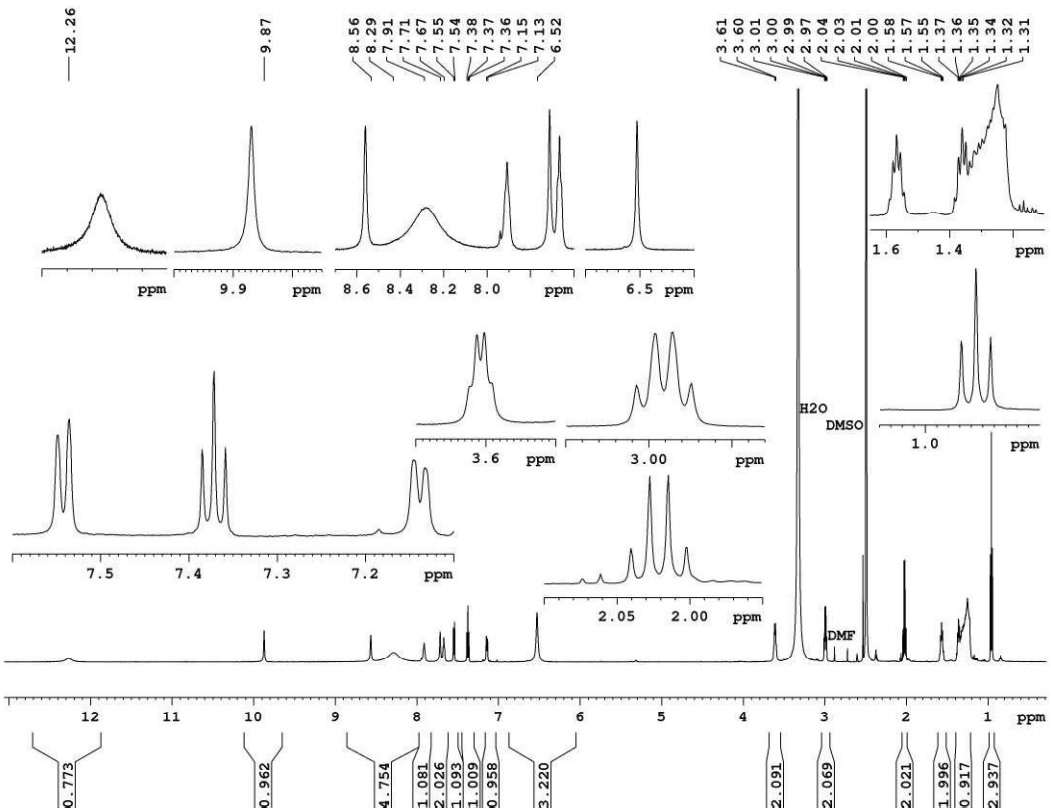

^{1}H-NMR spectrum (600 MHz, [D_6]-DMSO) of **3.30**

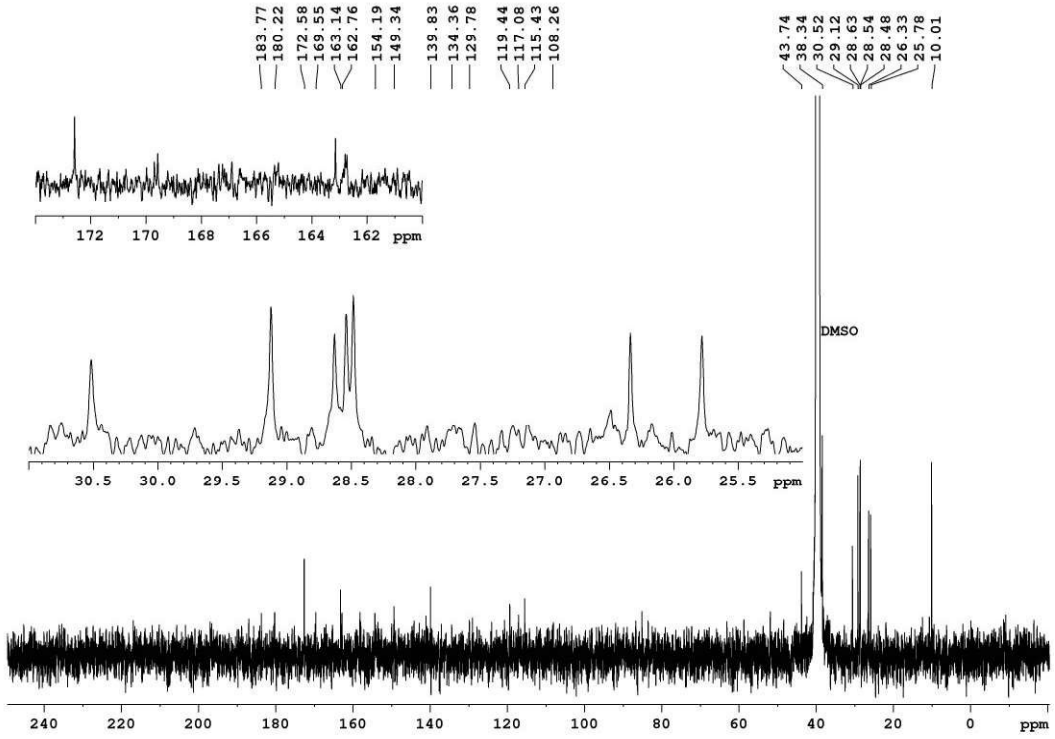

^{13}C-NMR spectrum (150 MHz, [D_6]-DMSO) of **3.30**

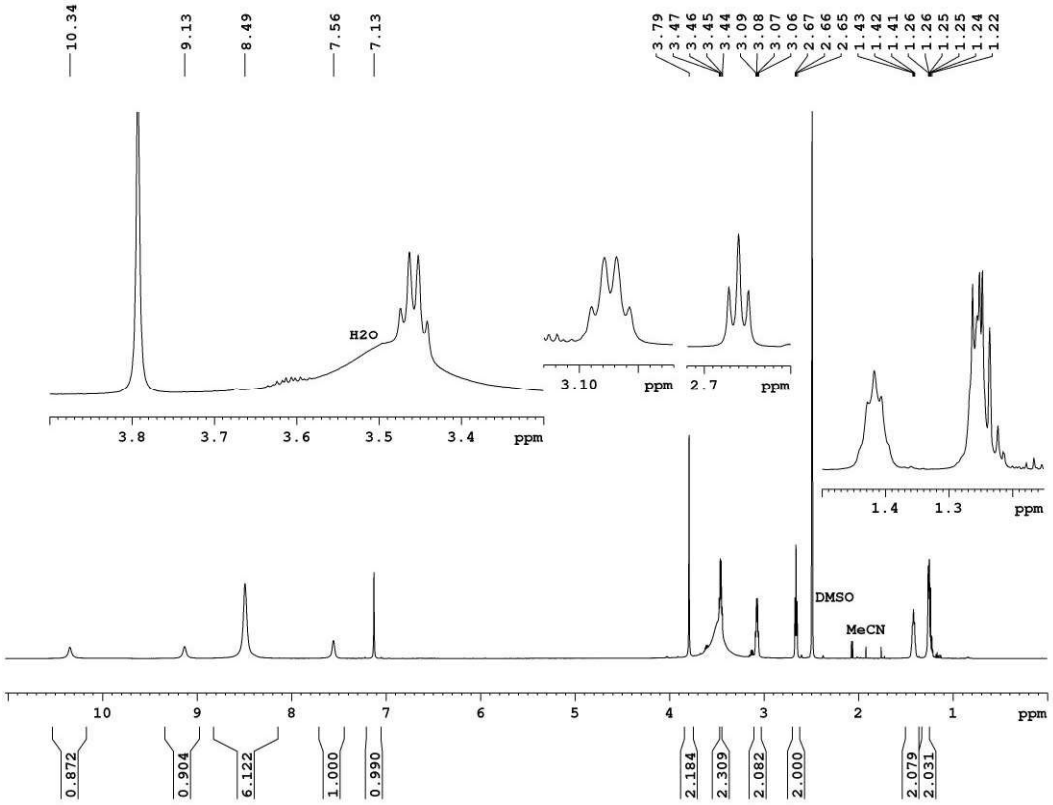

^{1}H-NMR spectrum (600 MHz, [D_6]-DMSO) of **3.34**

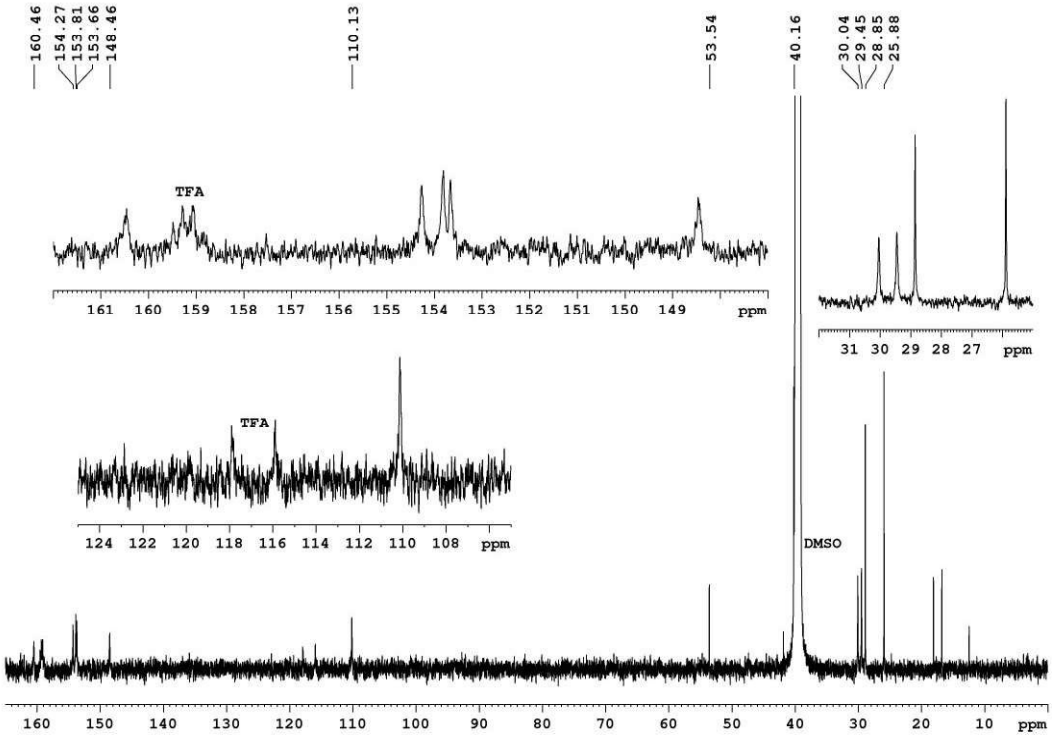

^{13}C-NMR spectrum (150 MHz, [D_6]-DMSO) of **3.34**

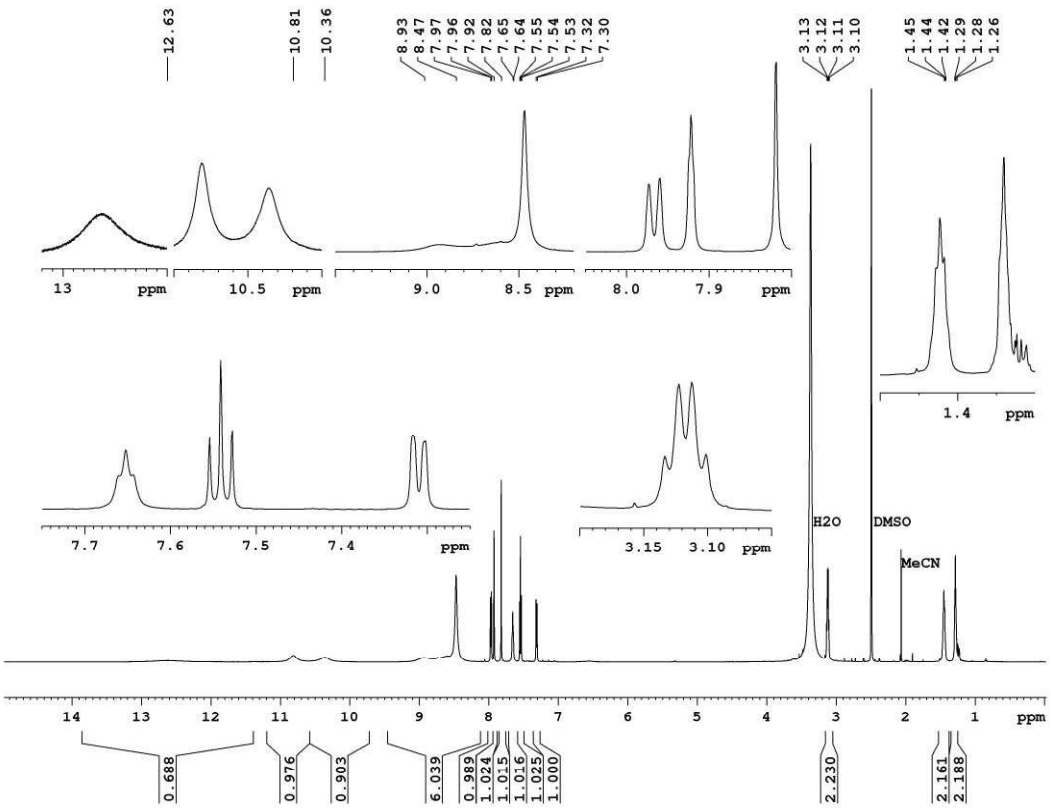

^{1}H-NMR spectrum (600 MHz, [D_6]-DMSO) of **3.35**

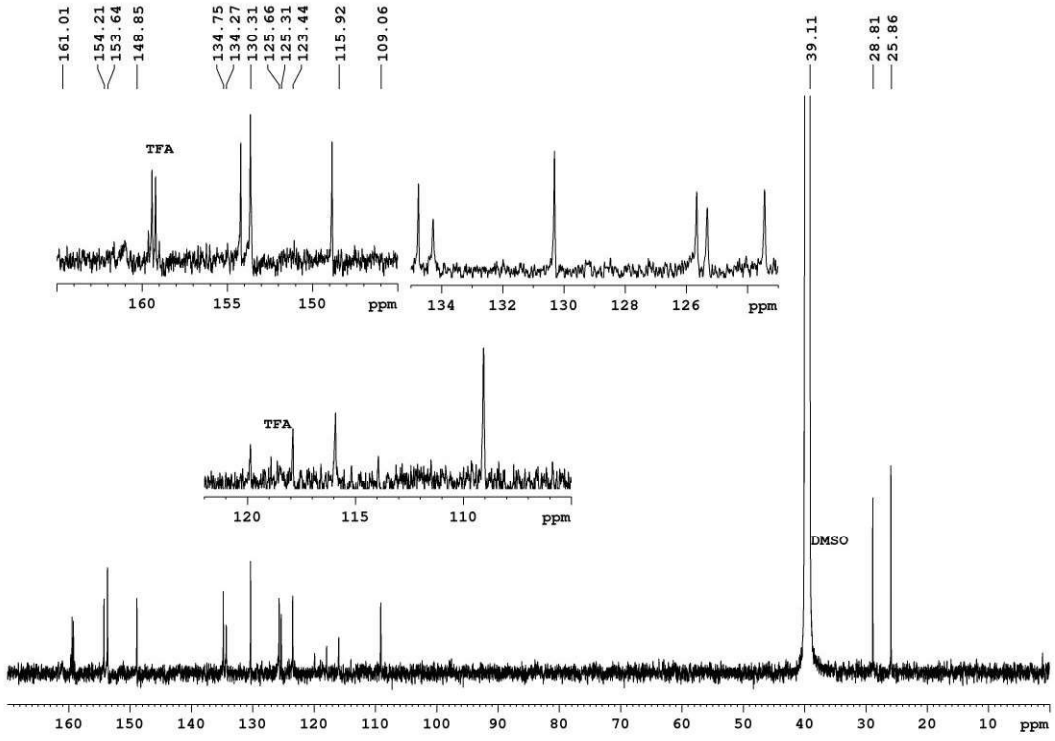

^{13}C-NMR spectrum (150 MHz, [D_6]-DMSO) of **3.35**

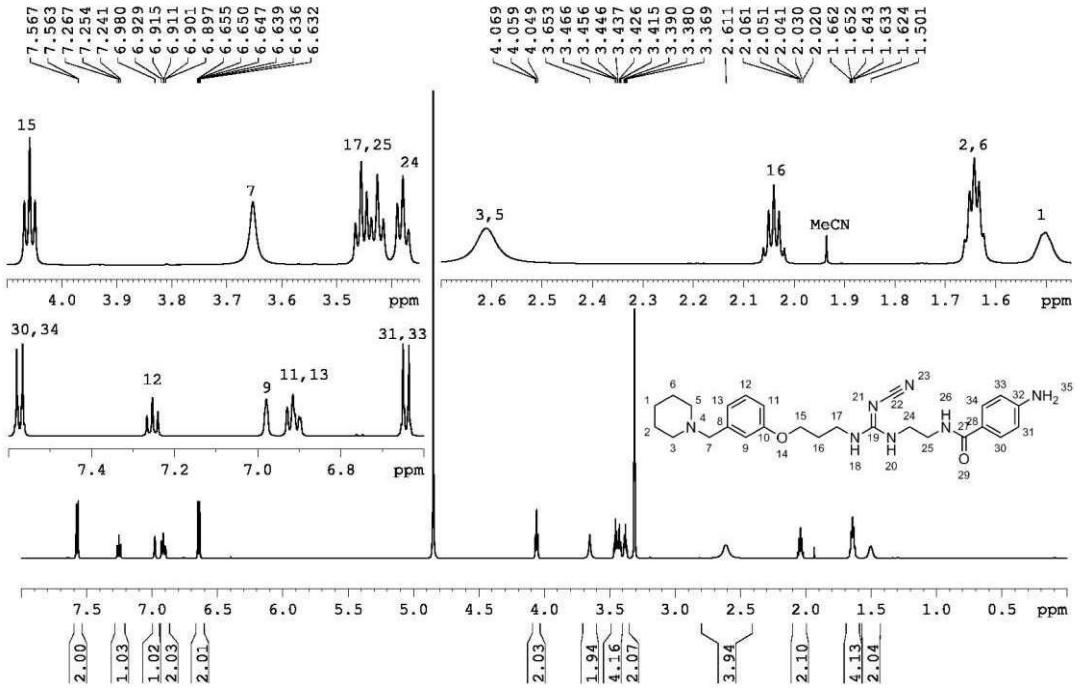

^{1}H-NMR spectrum (600 MHz, CD_3OD) of **4.30**

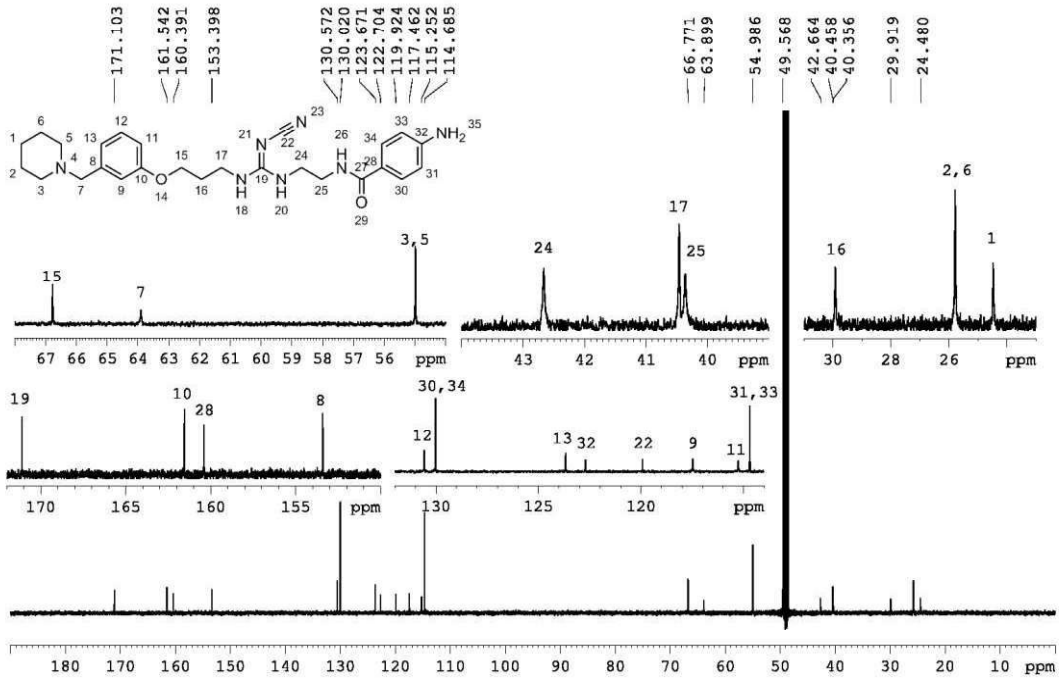

^{13}C-NMR spectrum (150 MHz, CD_3OD) of **4.30**

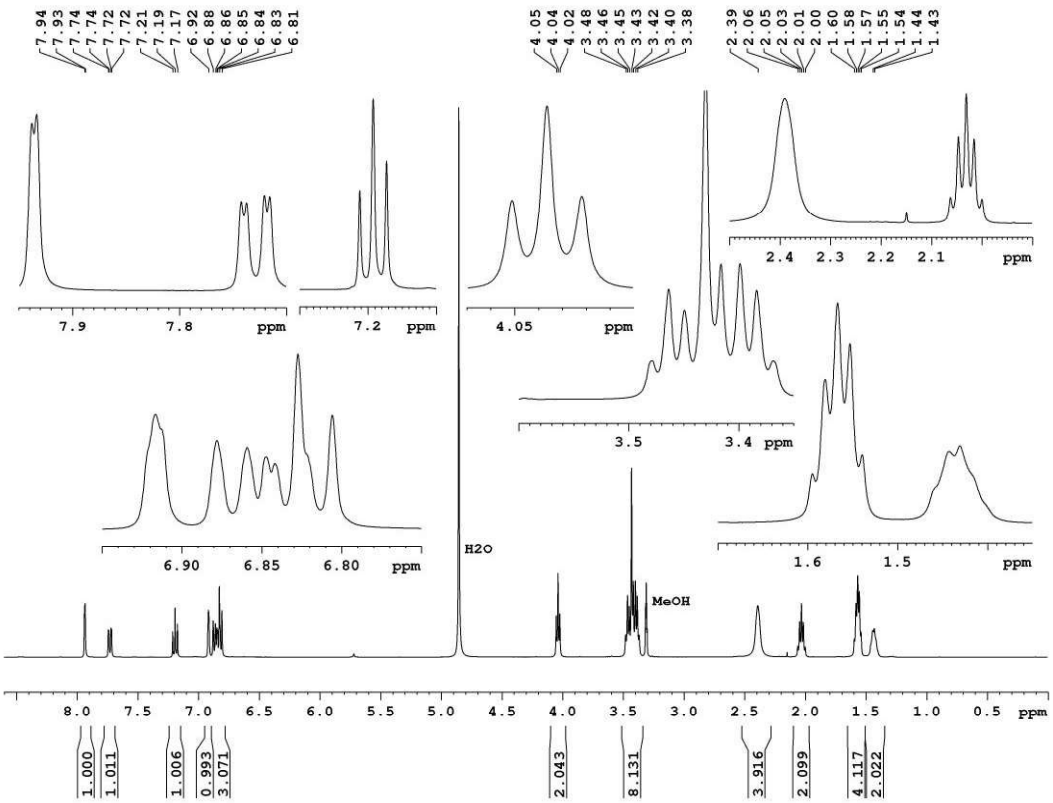

^{1}H-NMR spectrum (600 MHz, CD_3OD) of **4.31**

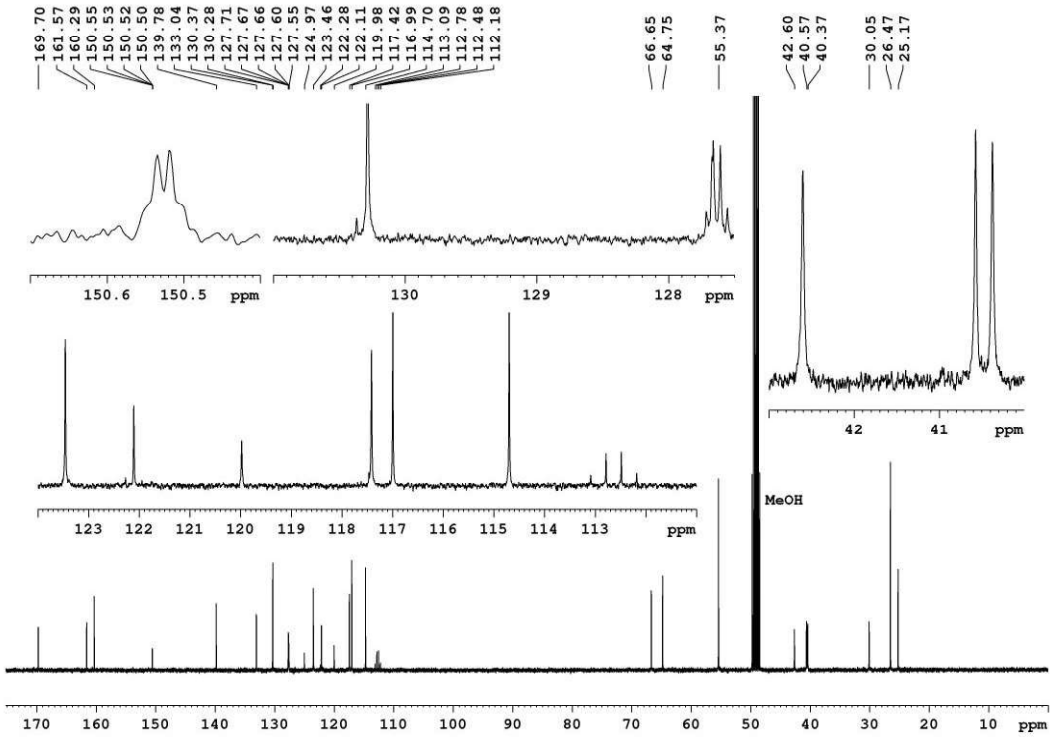

^{13}C-NMR spectrum (150 MHz, CD_3OD) of **4.31**

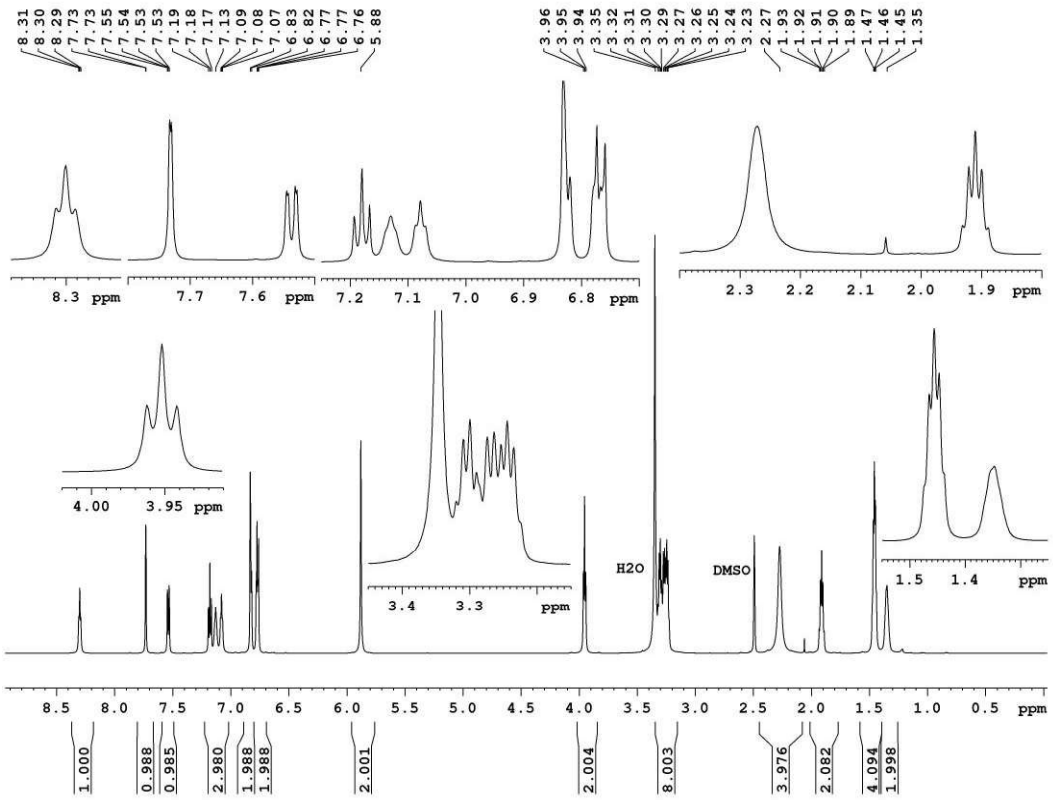

^{1}H-NMR spectrum (600 MHz, [D_6]DMSO) of **4.32**

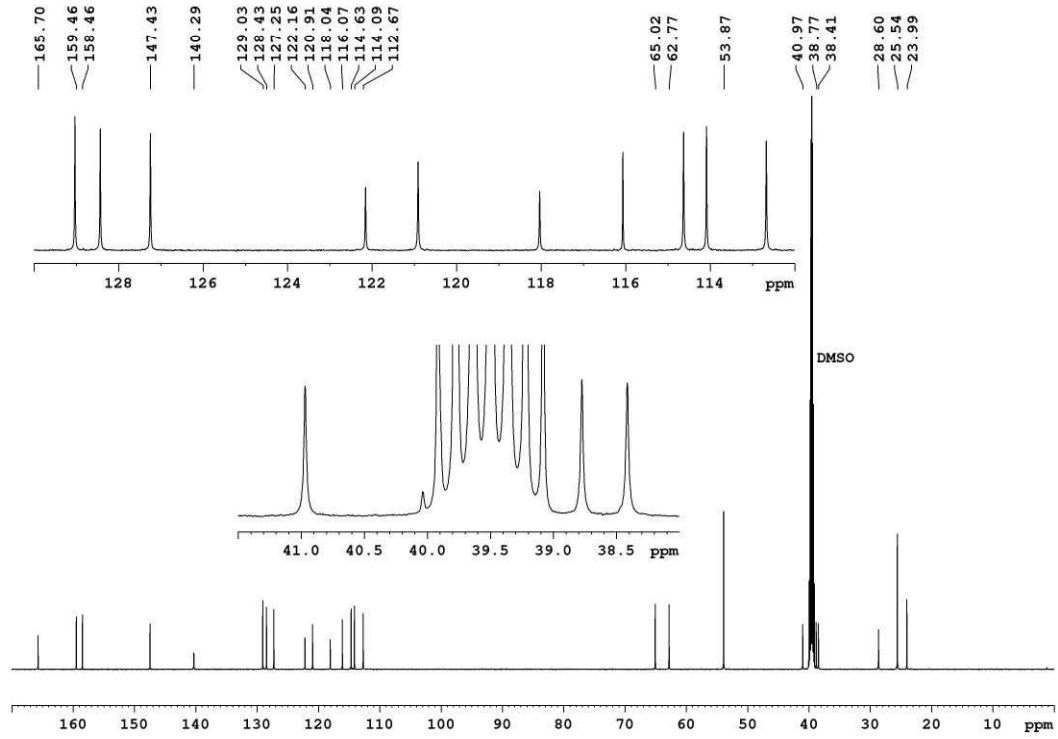

^{13}C-NMR spectrum (150 MHz, [D_6]DMSO) of **4.32**

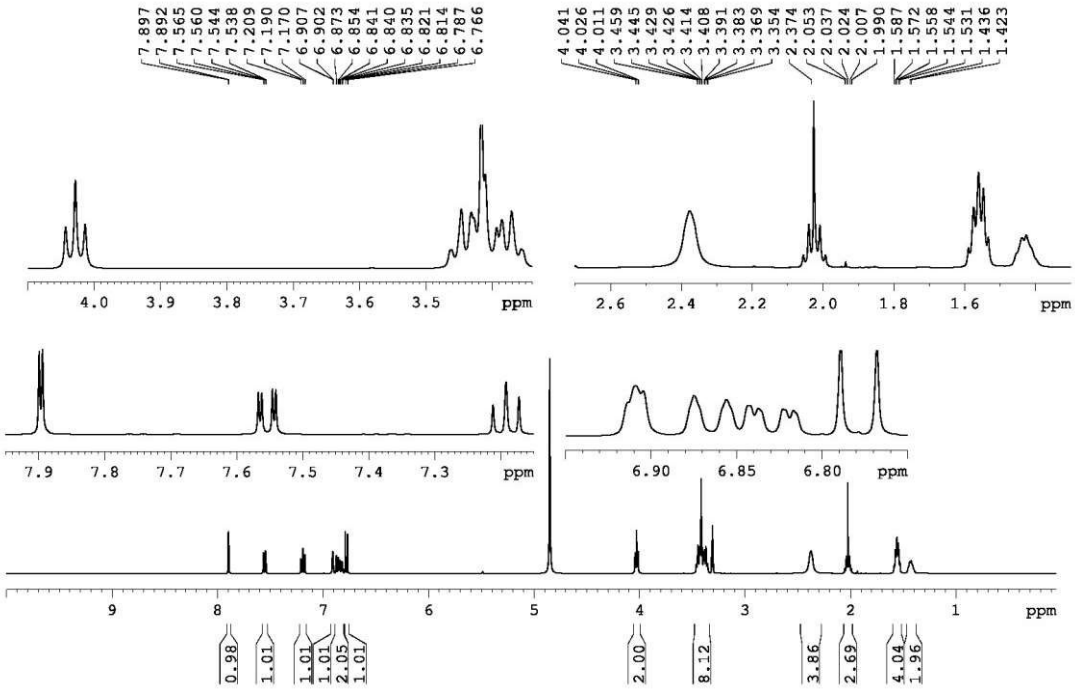

^{1}H-NMR spectrum (600 MHz, CD_3OD) of **4.33**

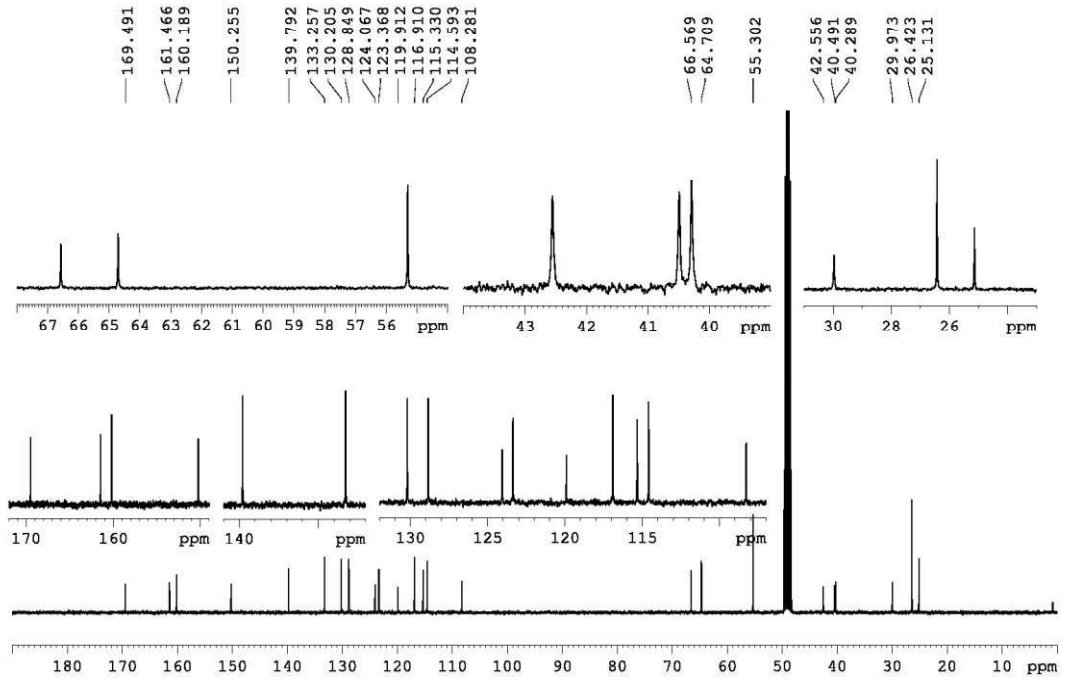

^{13}C-NMR spectrum (150 MHz, CD_3OD) of **4.33**

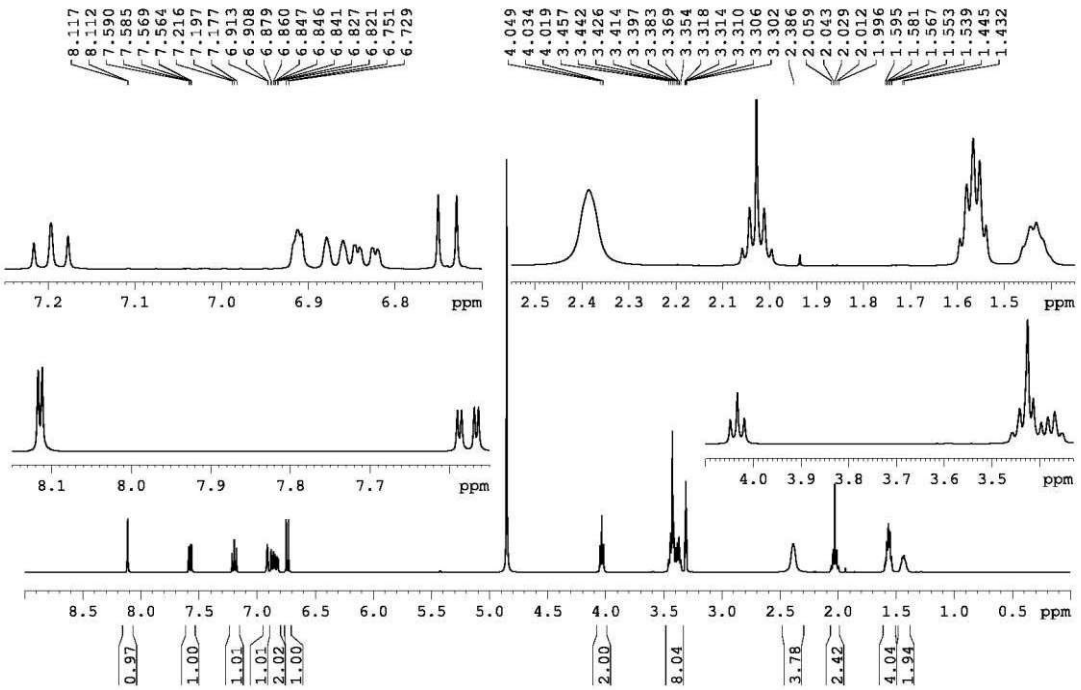

^{1}H-NMR spectrum (600 MHz, CD_3OD) of **4.34**

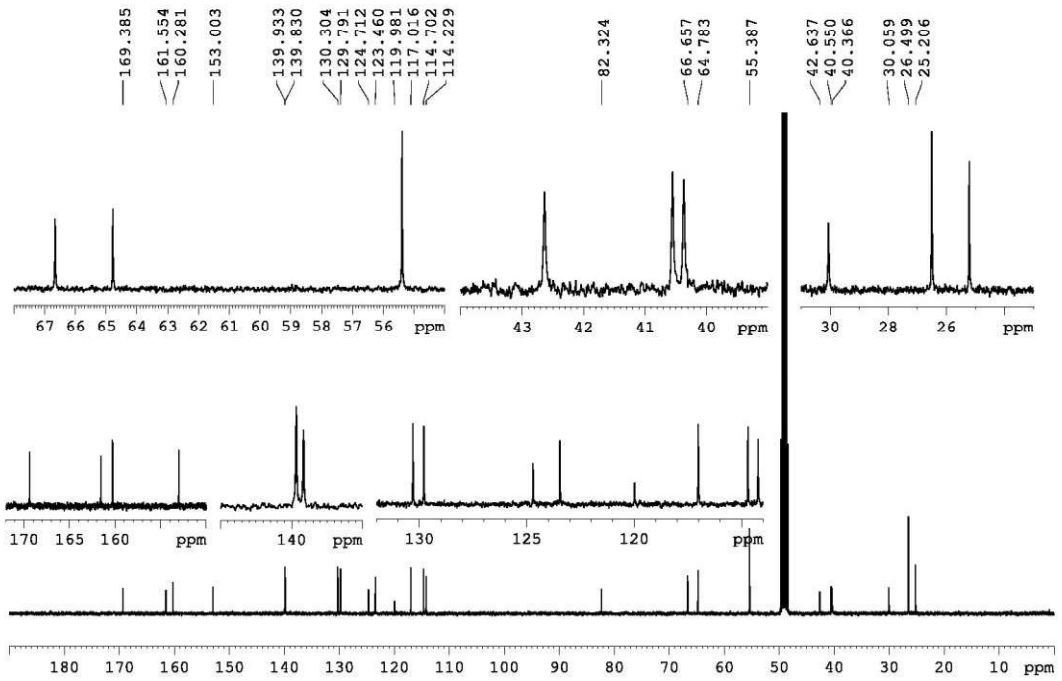

^{13}C-NMR spectrum (150 MHz, CD_3OD) of **4.34**

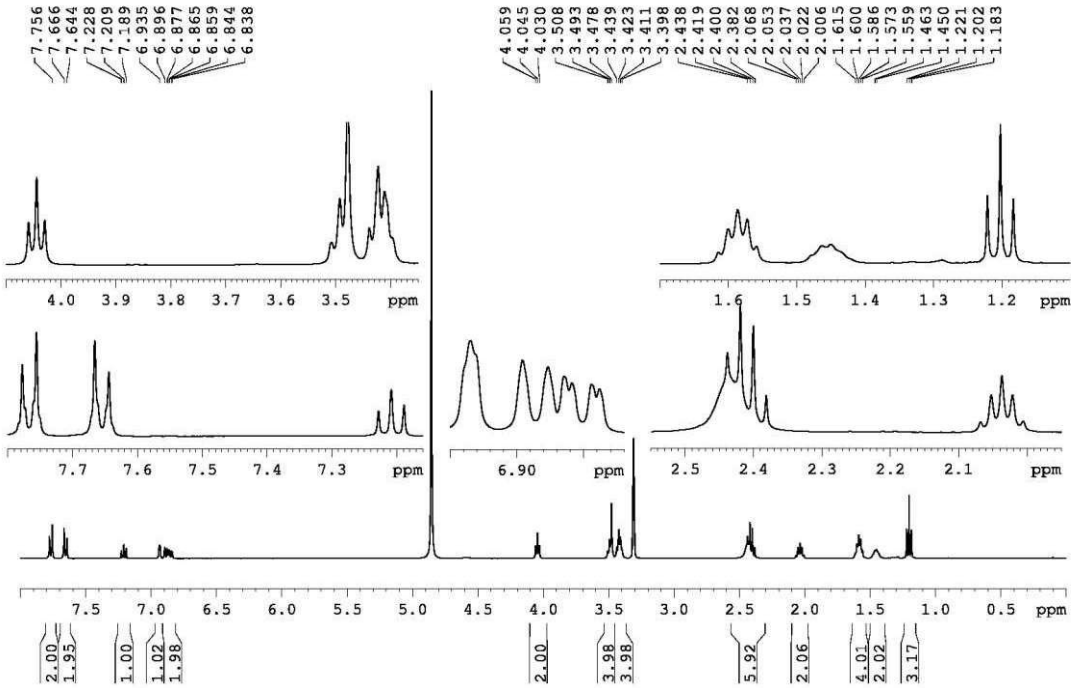

^{1}H-NMR spectrum (600 MHz, CD_3OD) of **4.35**

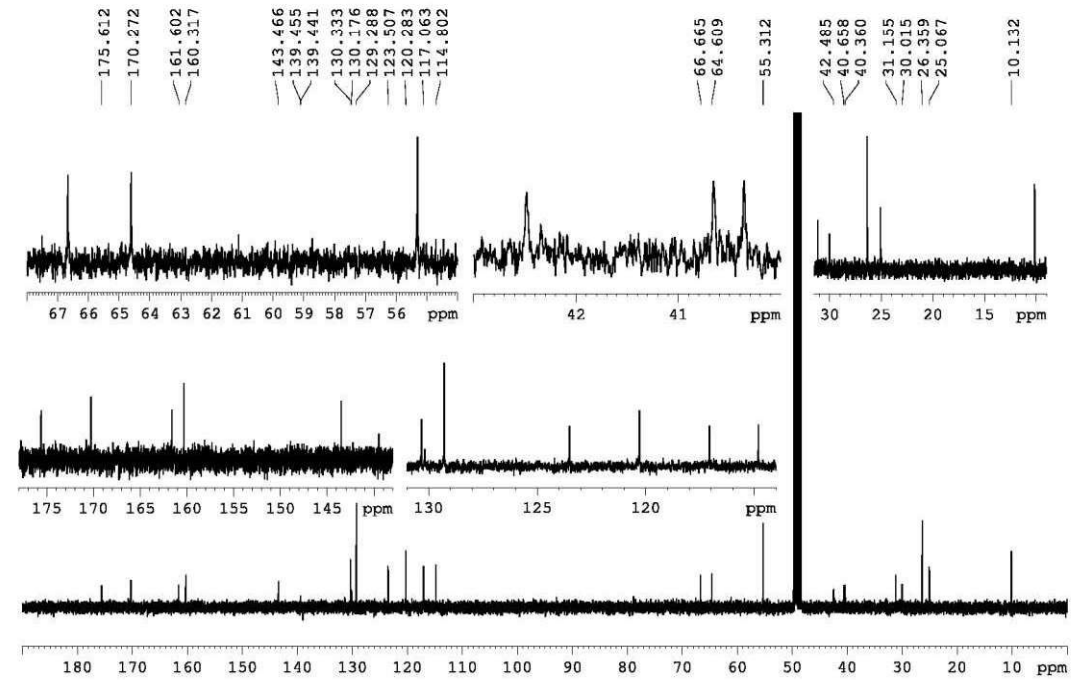

^{13}C-NMR spectrum (150 MHz, CD_3OD) of **4.35**

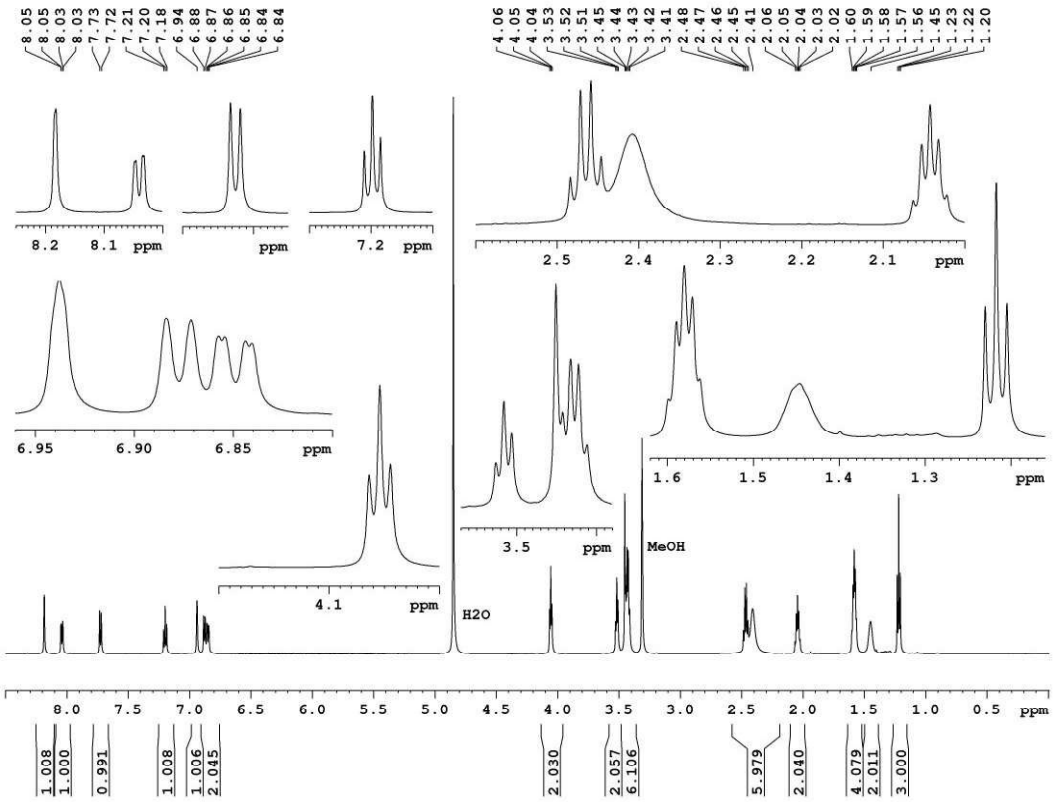

^{1}H-NMR spectrum (600 MHz, CD_3OD) of **4.36**

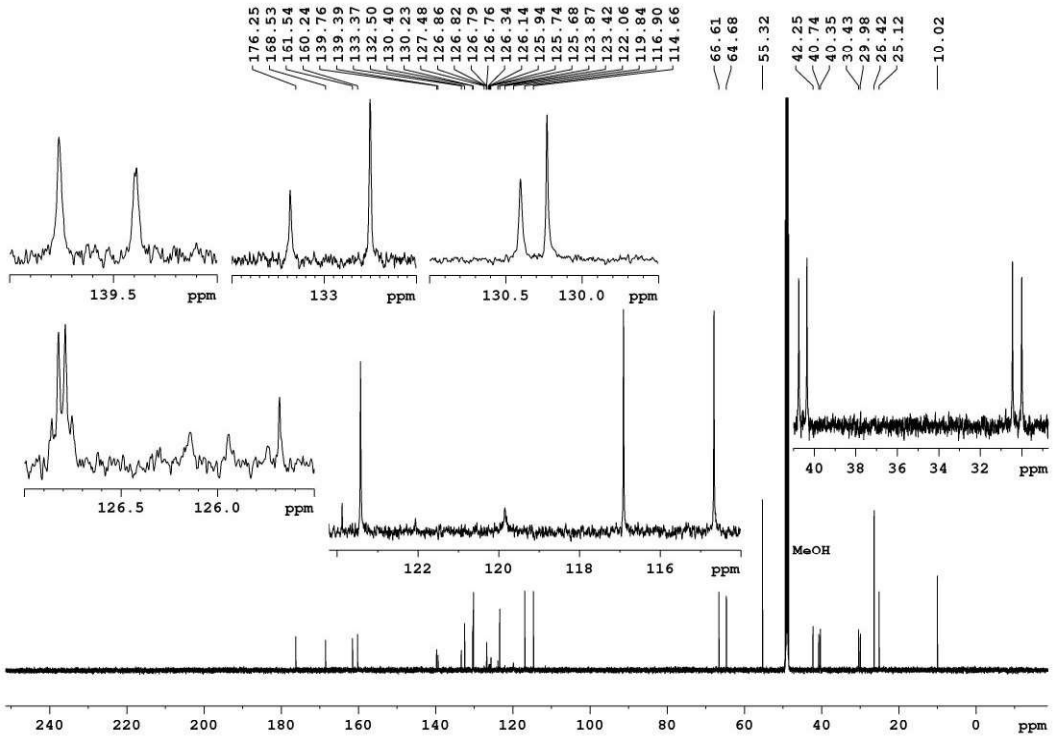

^{13}C-NMR spectrum (150 MHz, CD_3OD) of **4.36**

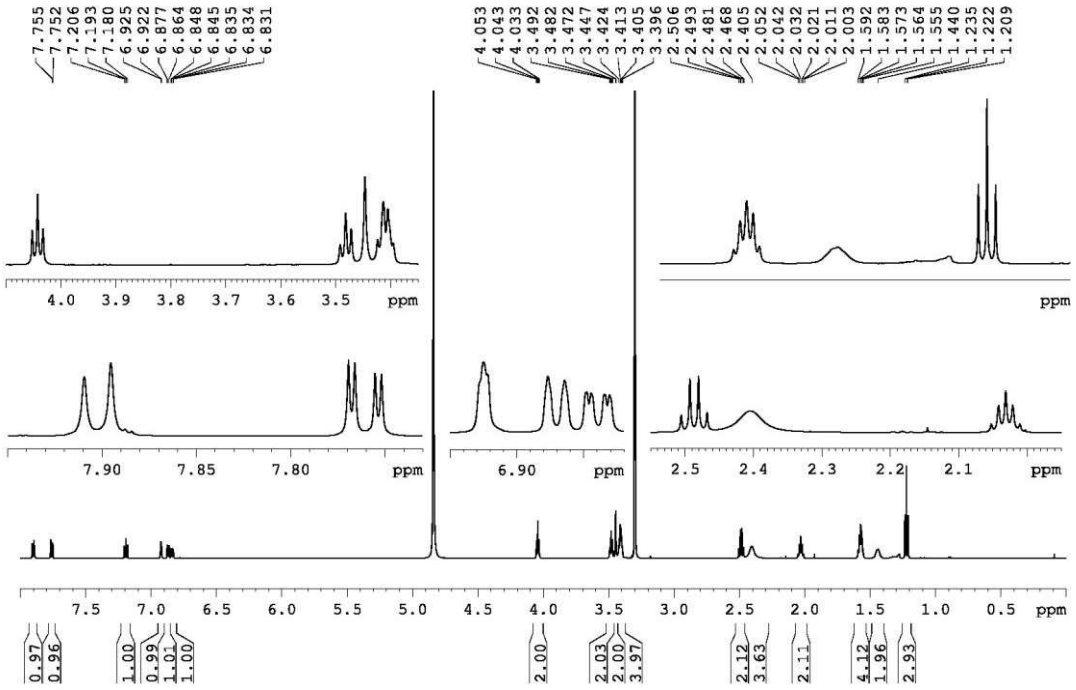

^{1}H-NMR spectrum (600 MHz, CD_3OD) of **4.37**

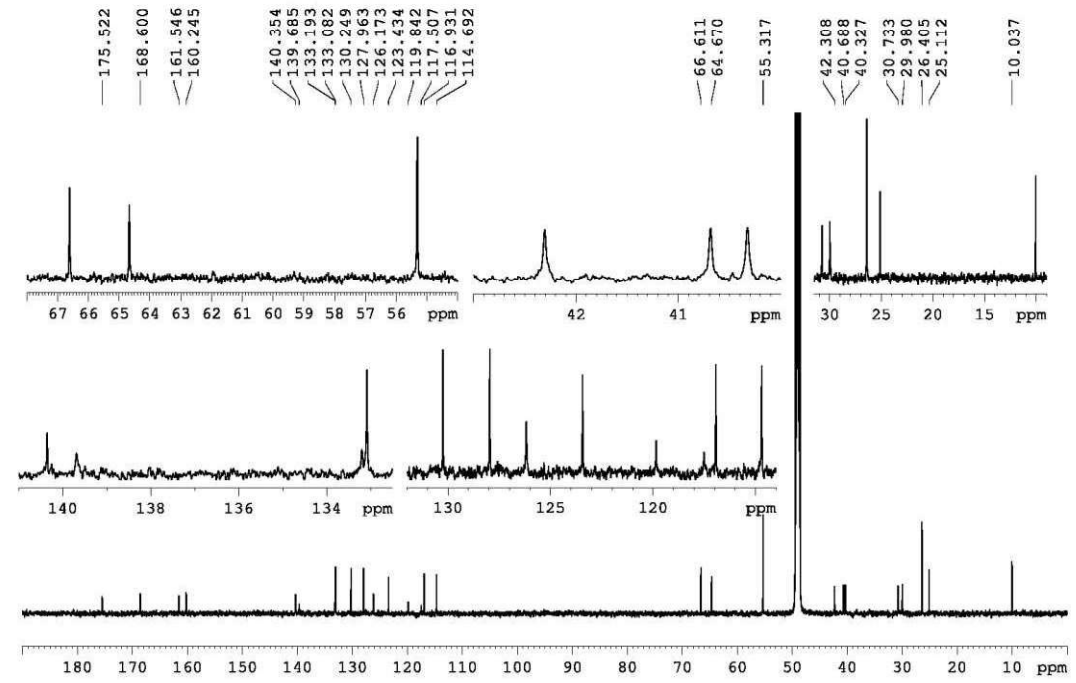

^{13}C-NMR spectrum (150 MHz, CD_3OD) of **4.37**

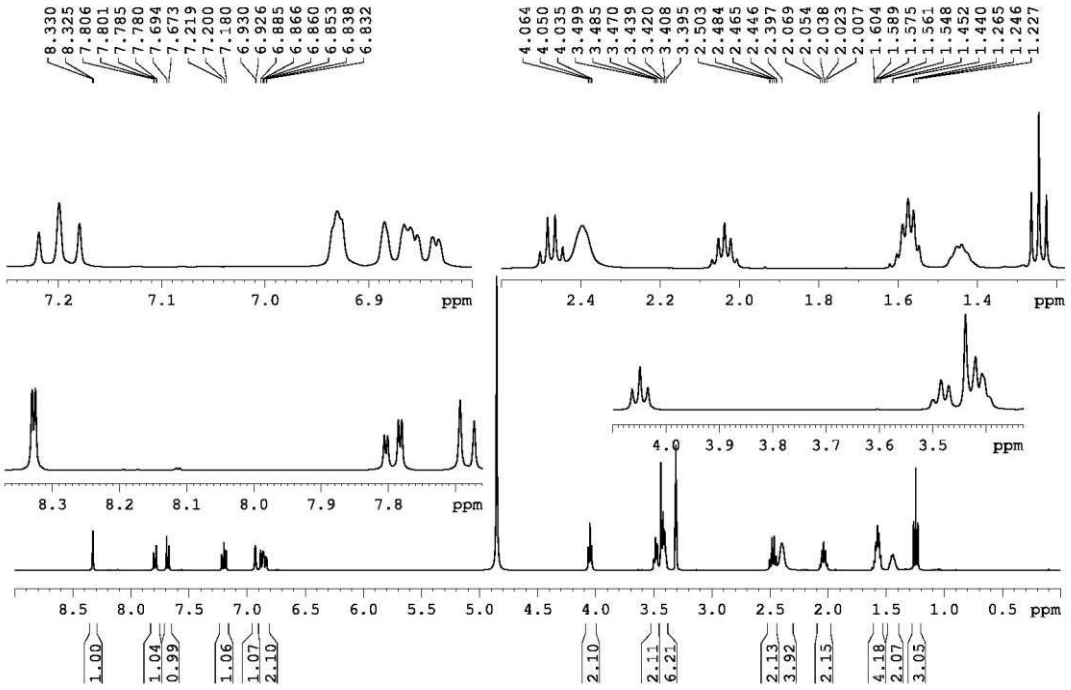

^{1}H-NMR spectrum (600 MHz, CD_3OD) of **4.38**

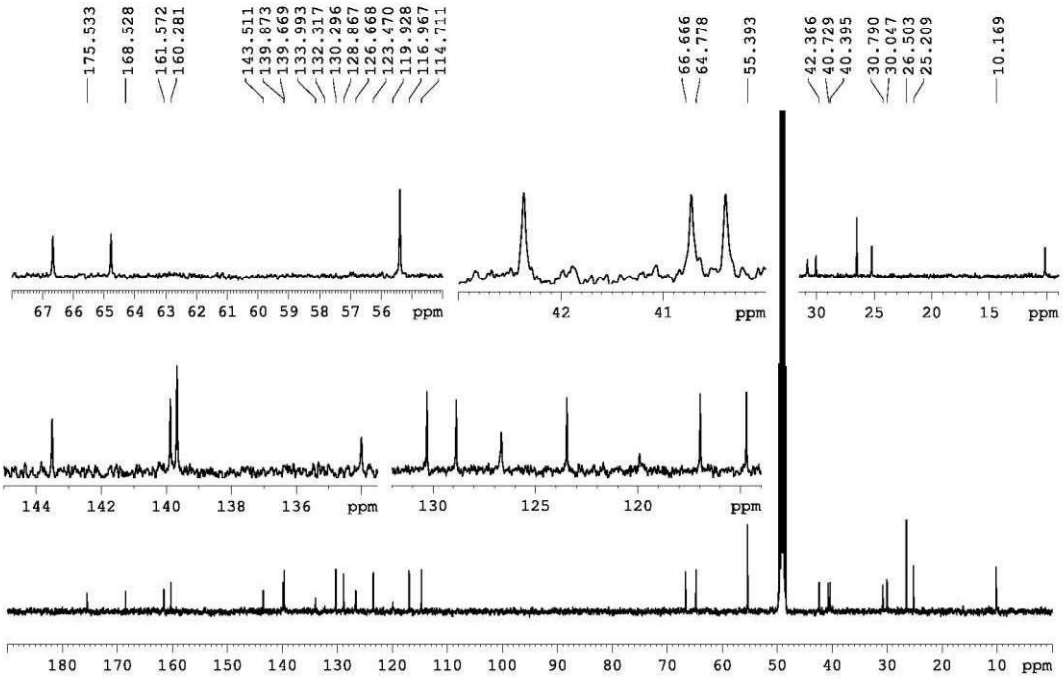

^{13}C-NMR spectrum (150 MHz, CD_3OD) of **4.38**

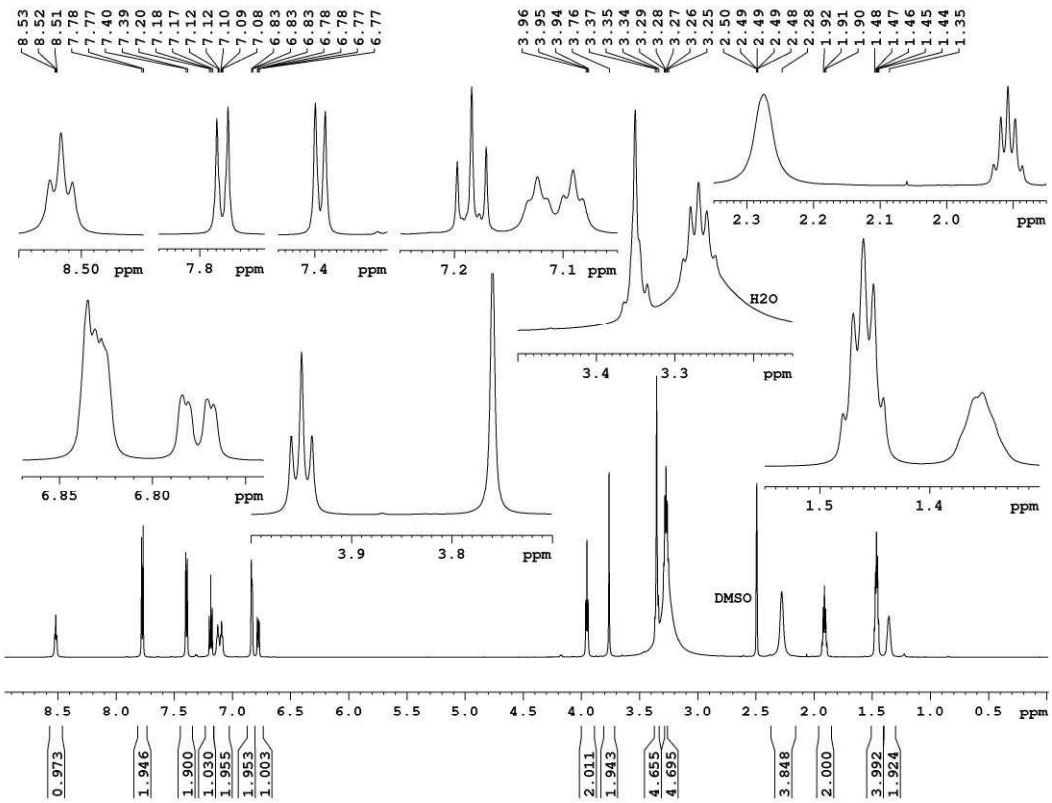

^{1}H-NMR spectrum (600 MHz, [D_6]DMSO) of **4.40**

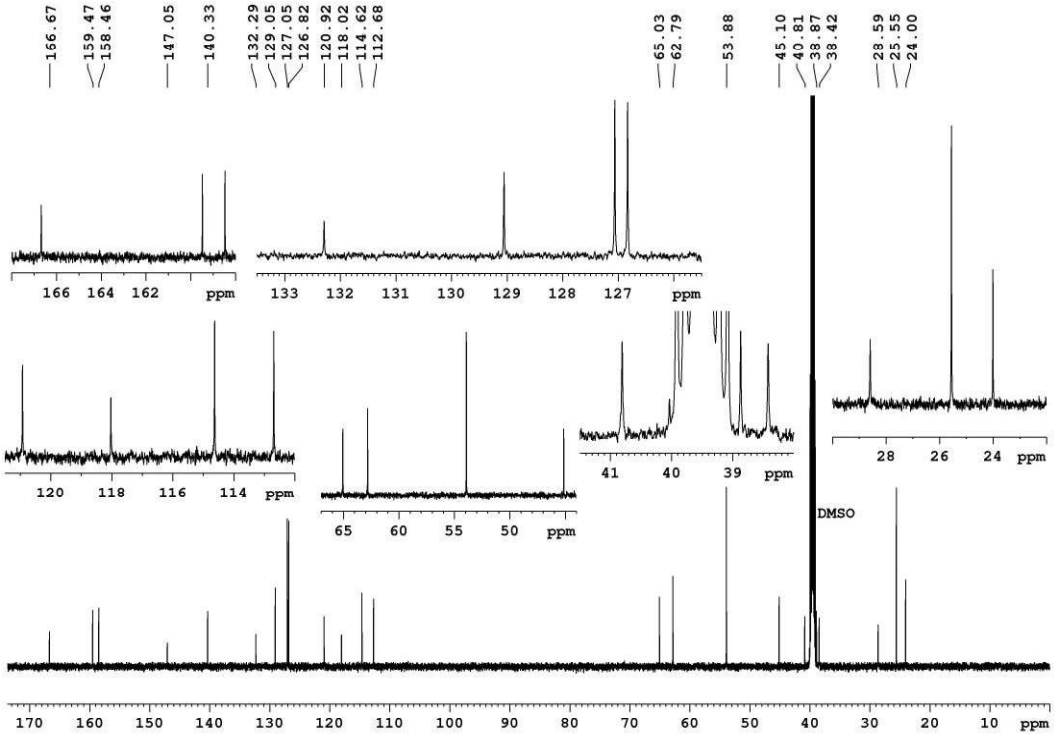

^{13}C-NMR spectrum (150 MHz, [D_6]DMSO) of **4.40**

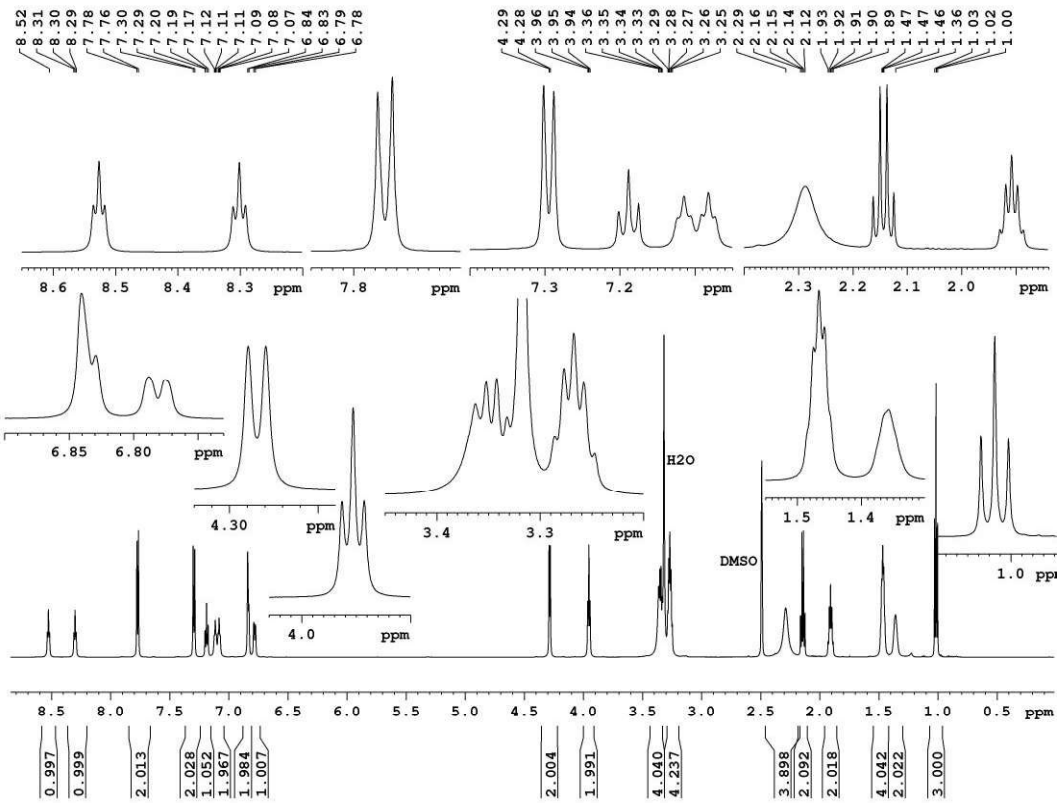

^{1}H-NMR spectrum (600 MHz, [D_6]DMSO) of **4.41**

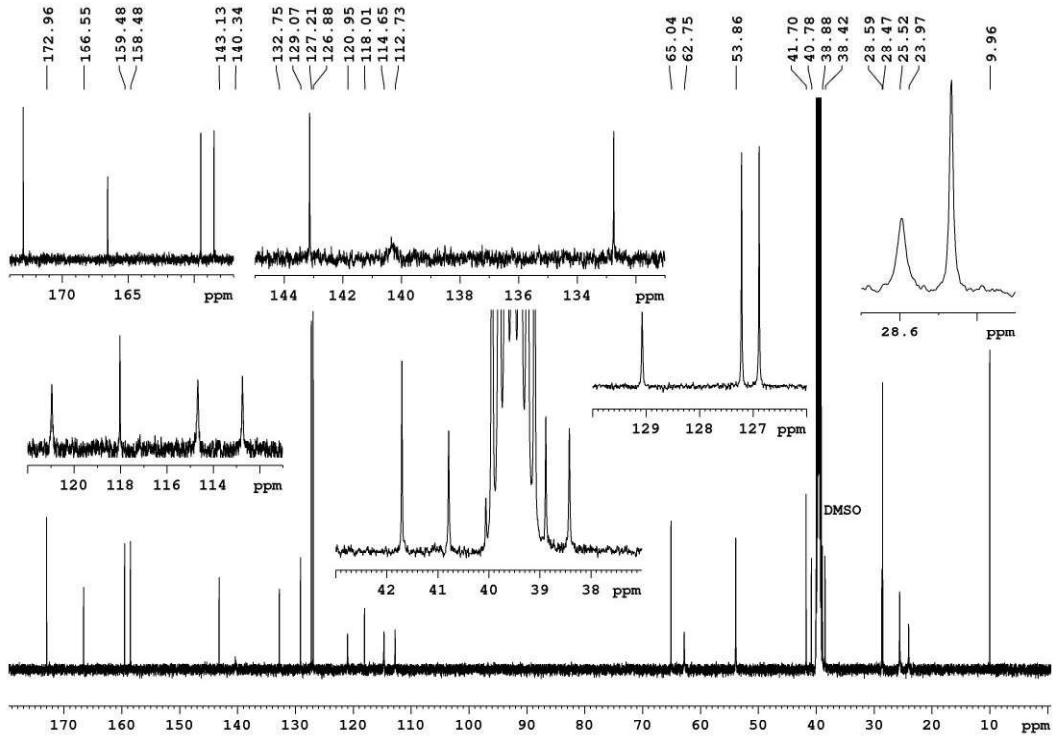

^{13}C-NMR spectrum (150 MHz, [D_6]DMSO) of **4.41**

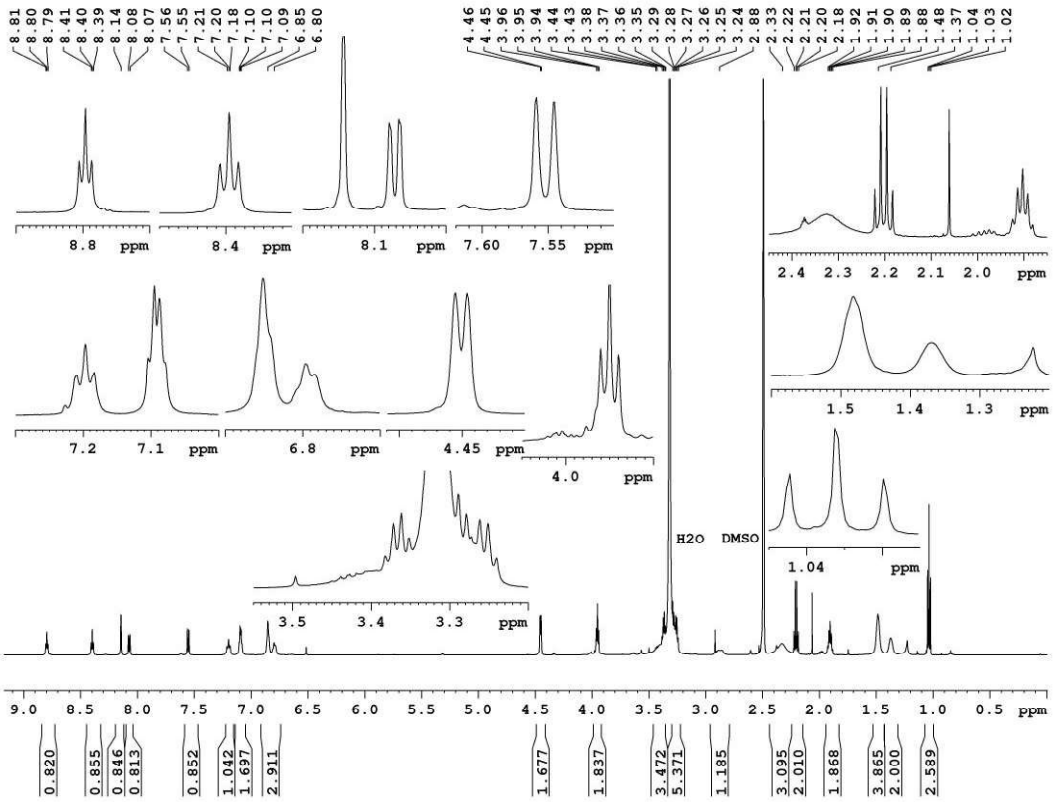

^{1}H-NMR spectrum (600 MHz, [D_6]DMSO) of **4.42**

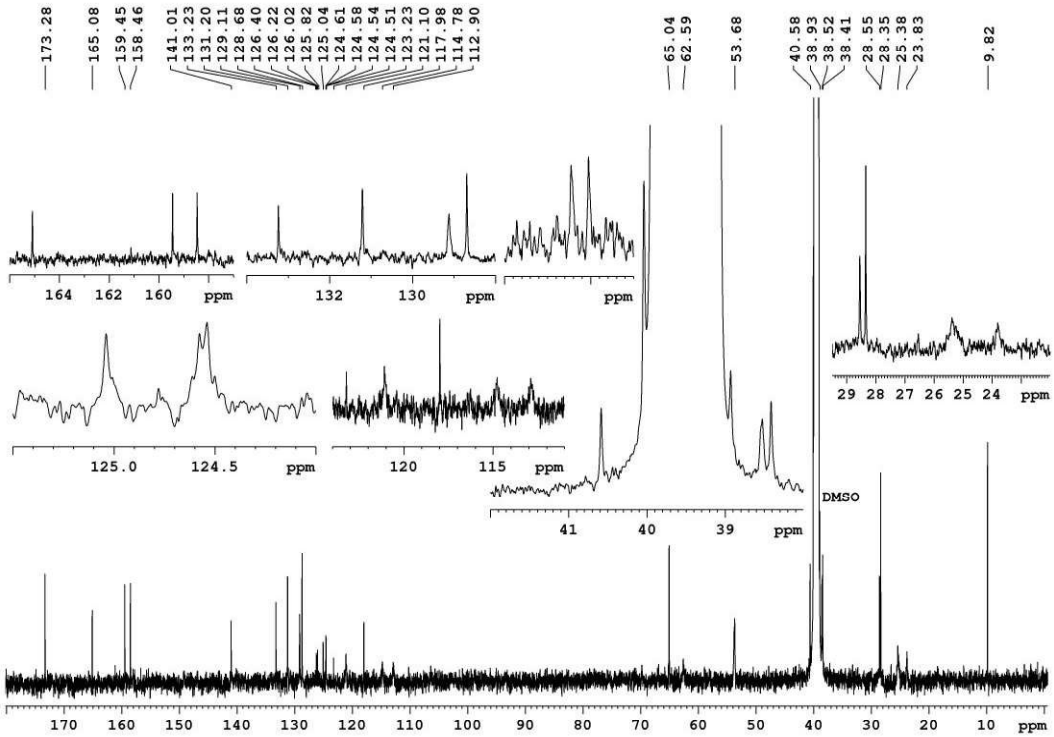

^{13}C-NMR spectrum (150 MHz, [D_6]DMSO) of **4.42**

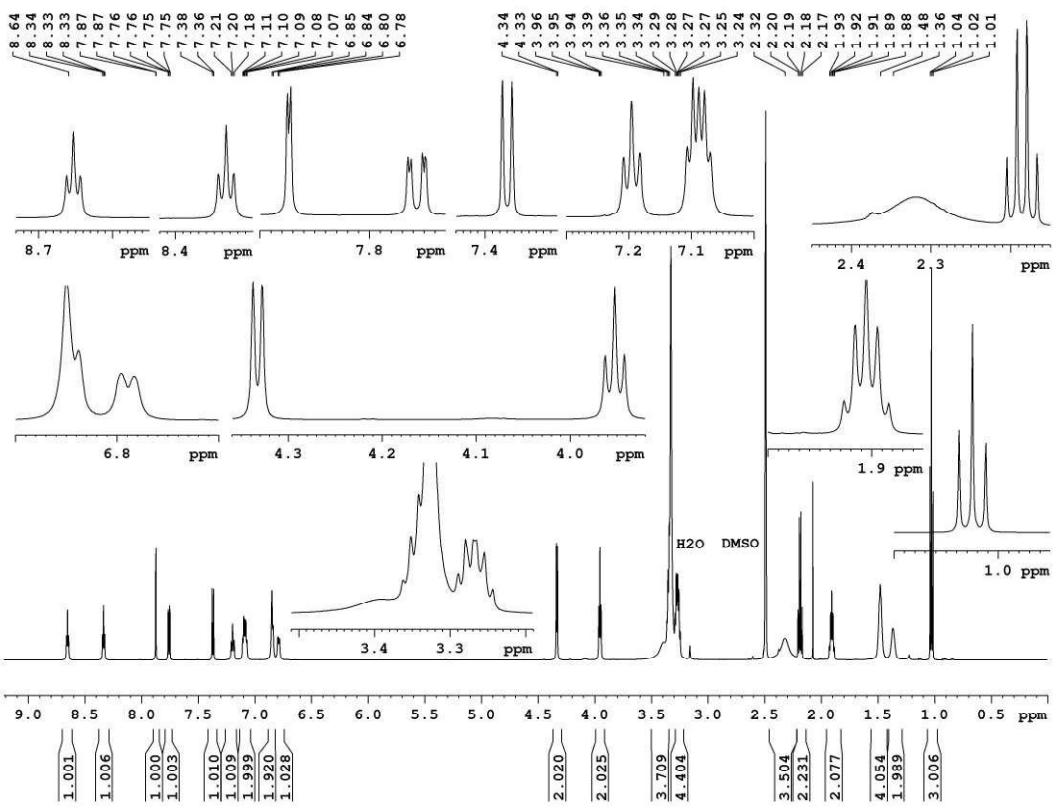

^{1}H-NMR spectrum (600 MHz, [D_6]DMSO) of **4.43**

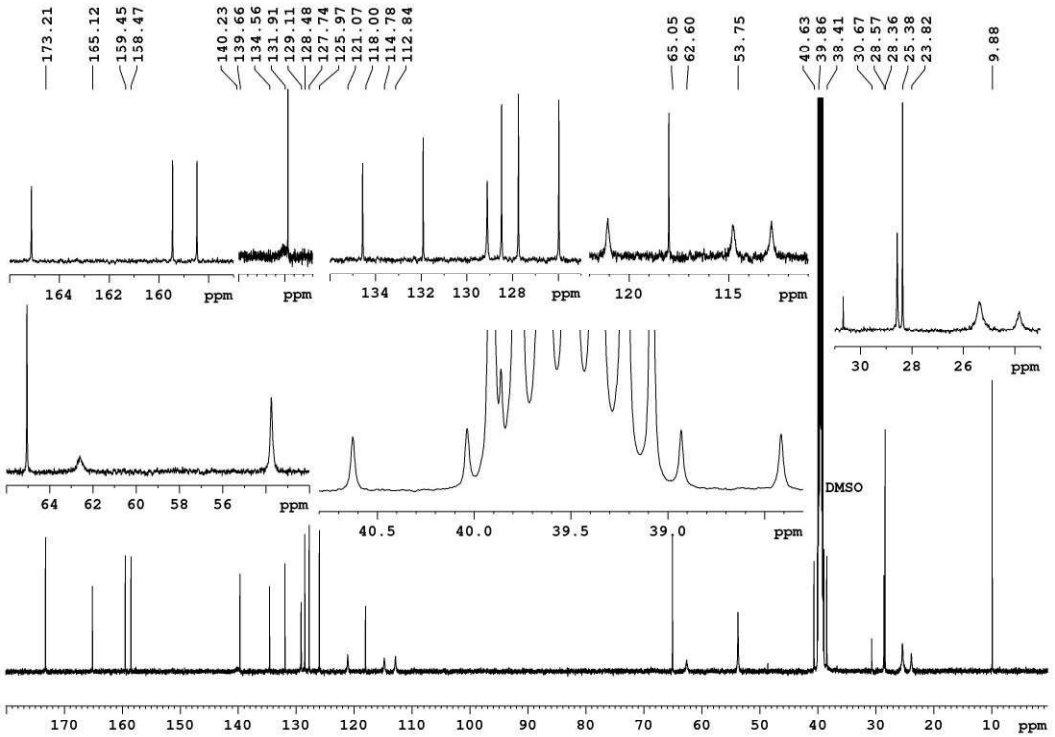

^{13}C-NMR spectrum (150 MHz, [D_6]DMSO) of **4.43**

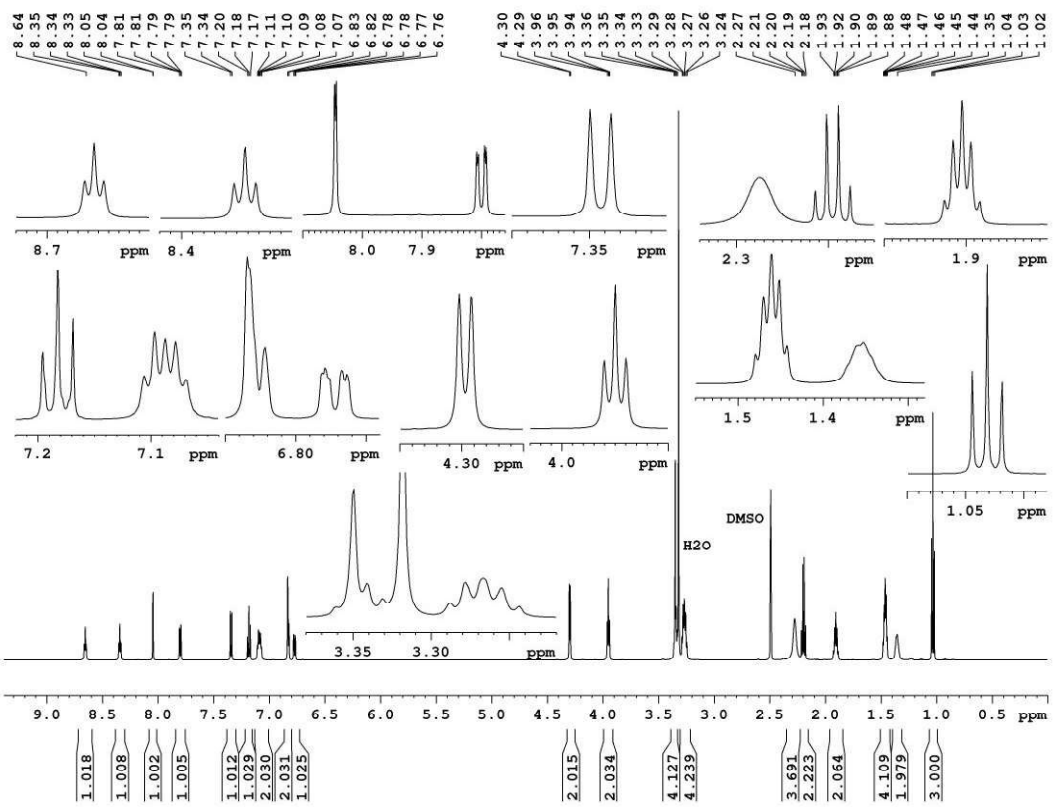

^{1}H-NMR spectrum (600 MHz, [D_6]DMSO) of **4.44**

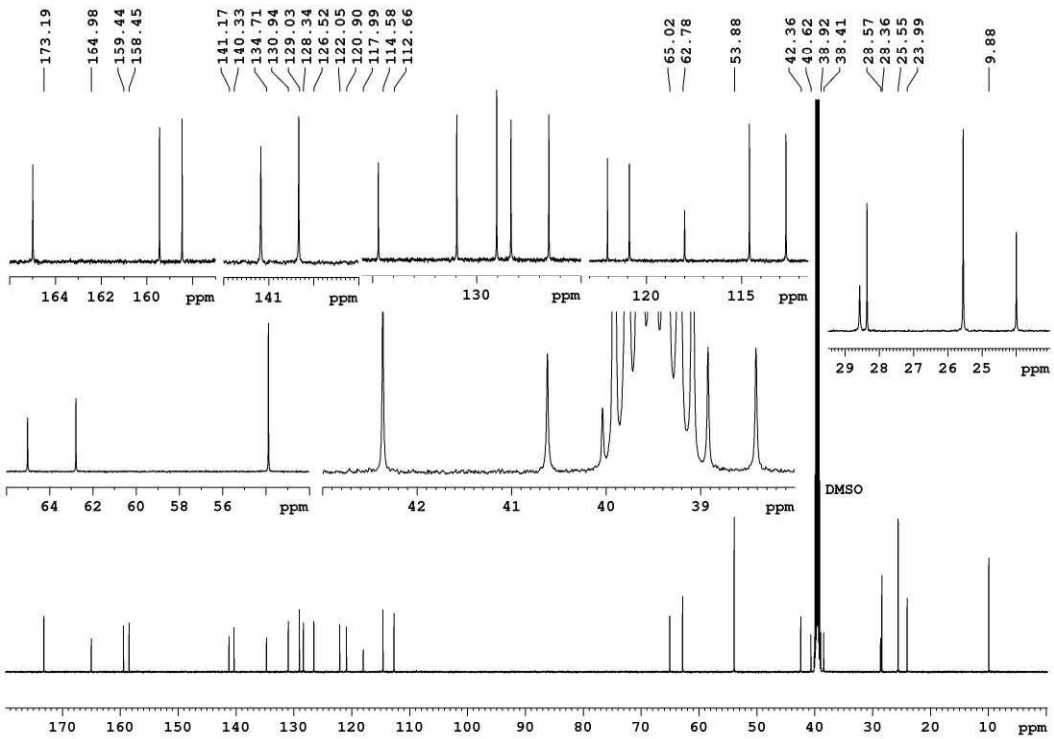

^{13}C-NMR spectrum (150 MHz, [D_6]DMSO) of **4.44**

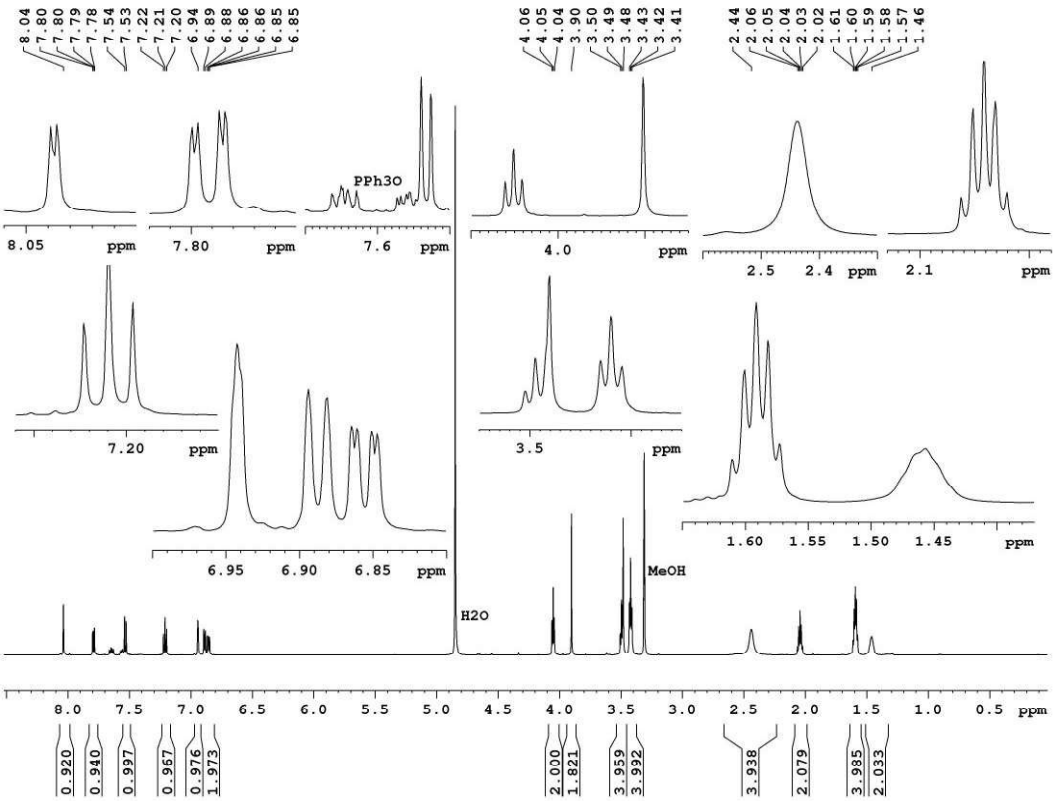

^{1}H-NMR spectrum (600 MHz, CD_3OD) of **4.46**

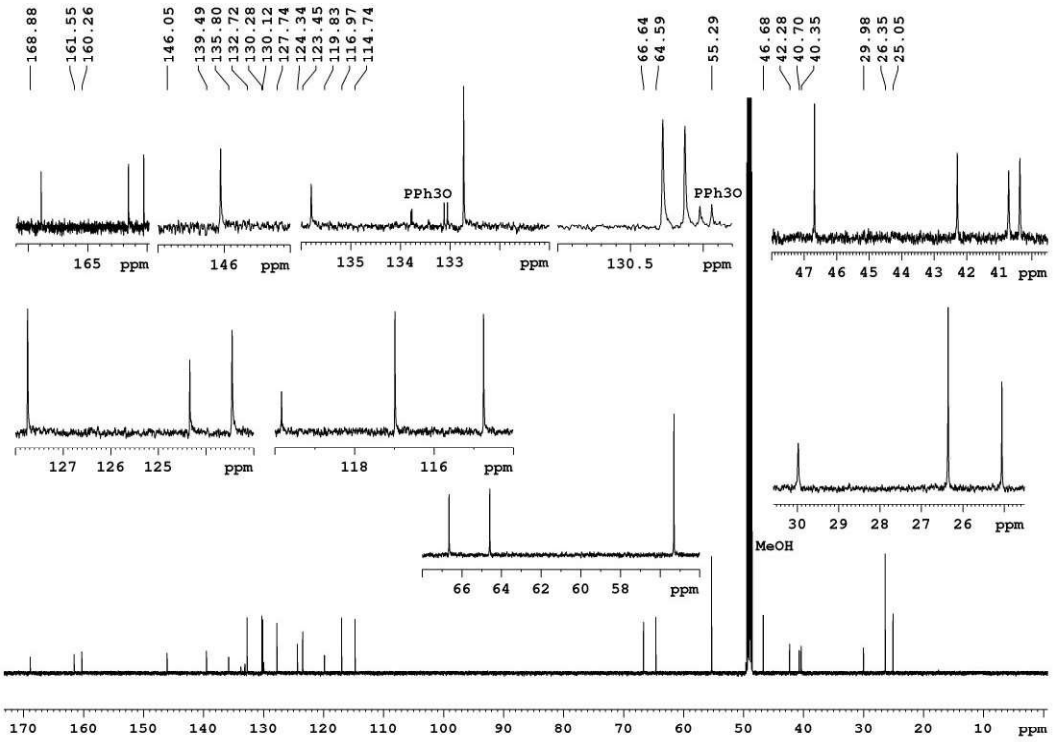

^{13}C-NMR spectrum (150 MHz, CD_3OD) of **4.46**

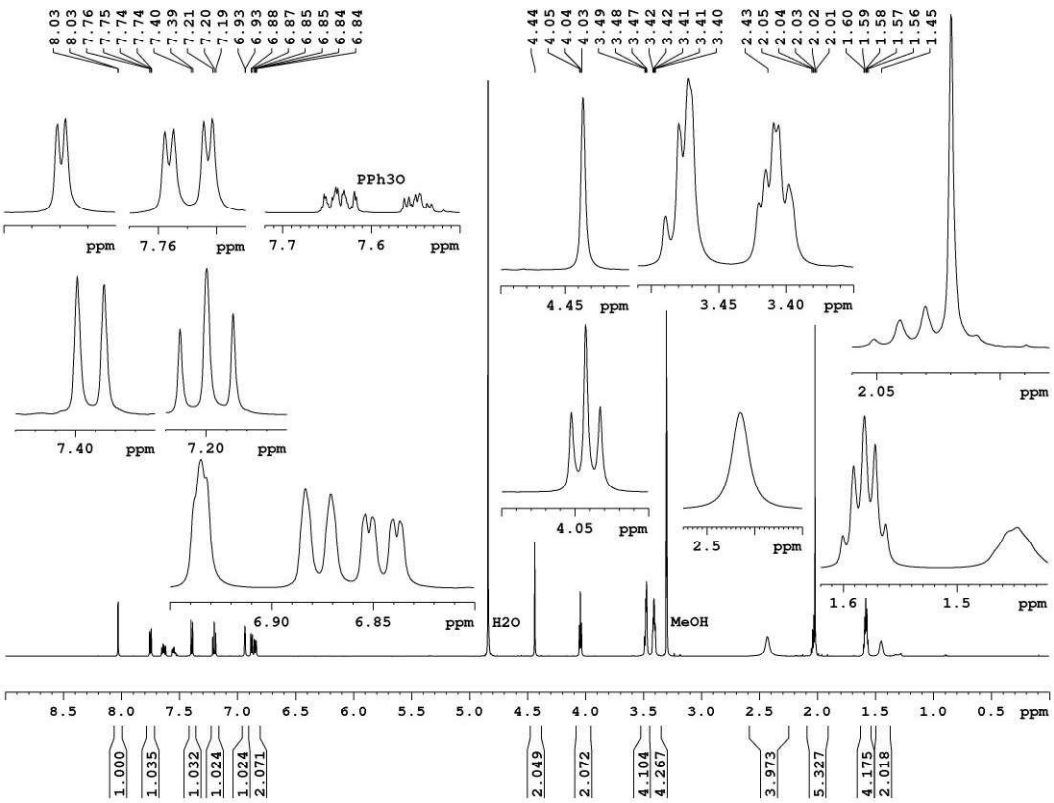

^{1}H-NMR spectrum (600 MHz, CD_3OD) of **4.47**

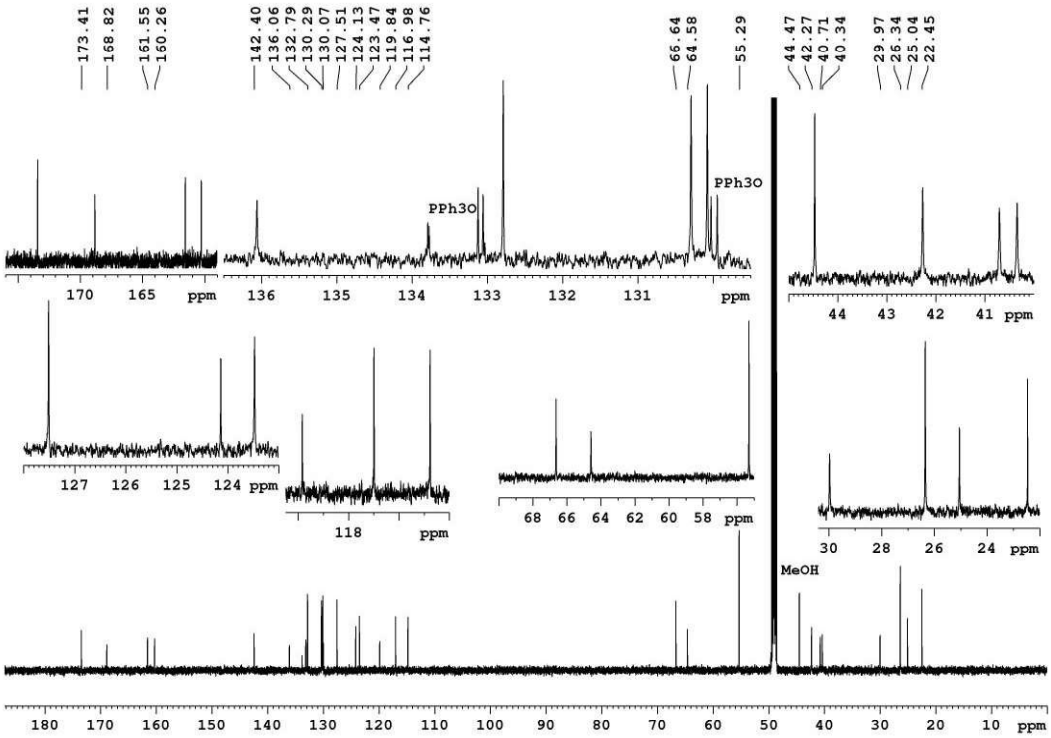

^{13}C-NMR spectrum (150 MHz, CD_3OD) of **4.47**

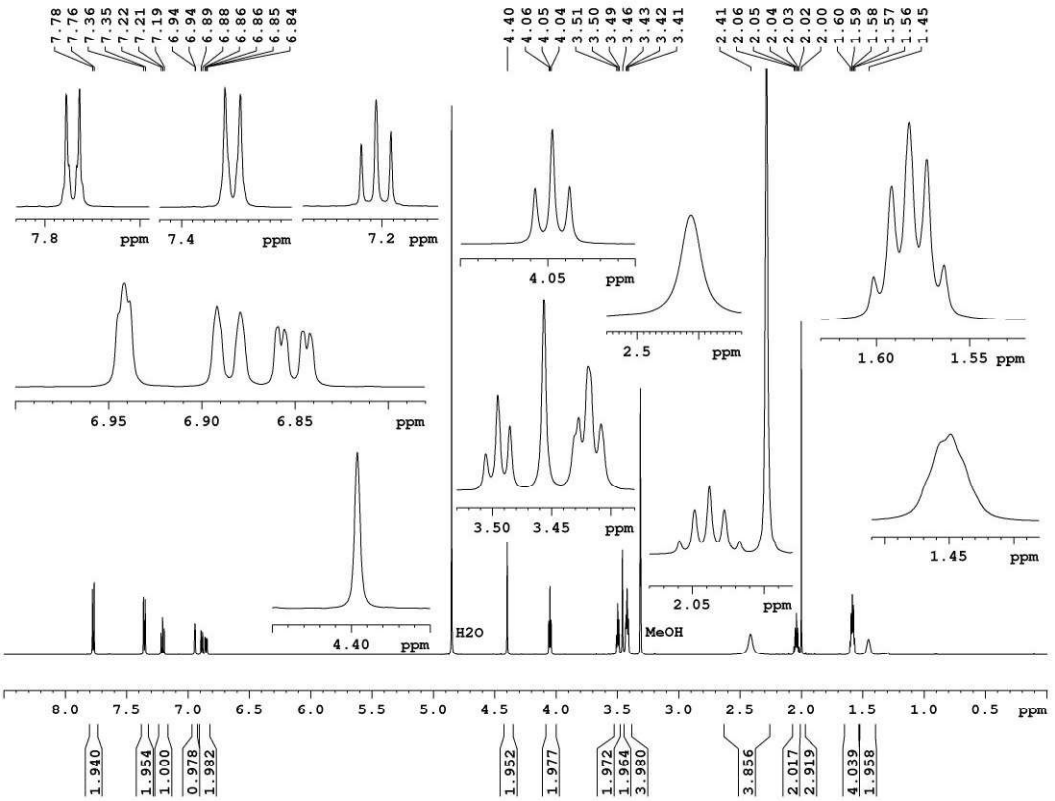

^{1}H-NMR spectrum (600 MHz, CD_3OD) of **4.48**

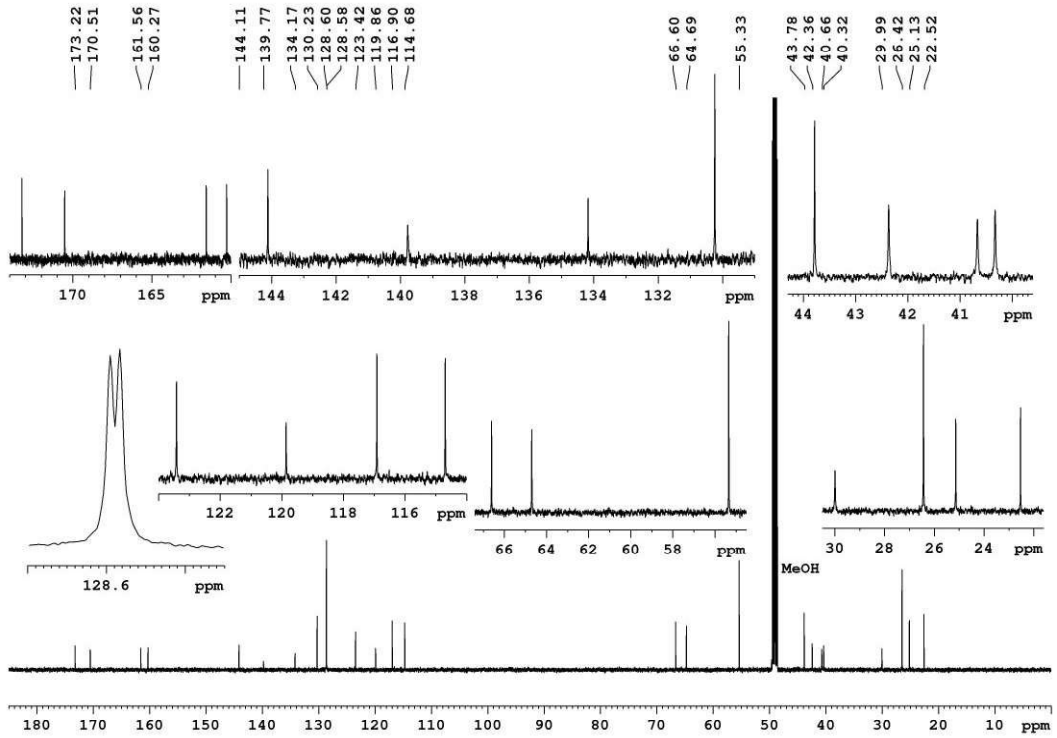

^{13}C-NMR spectrum (150 MHz, CD_3OD) of **4.48**

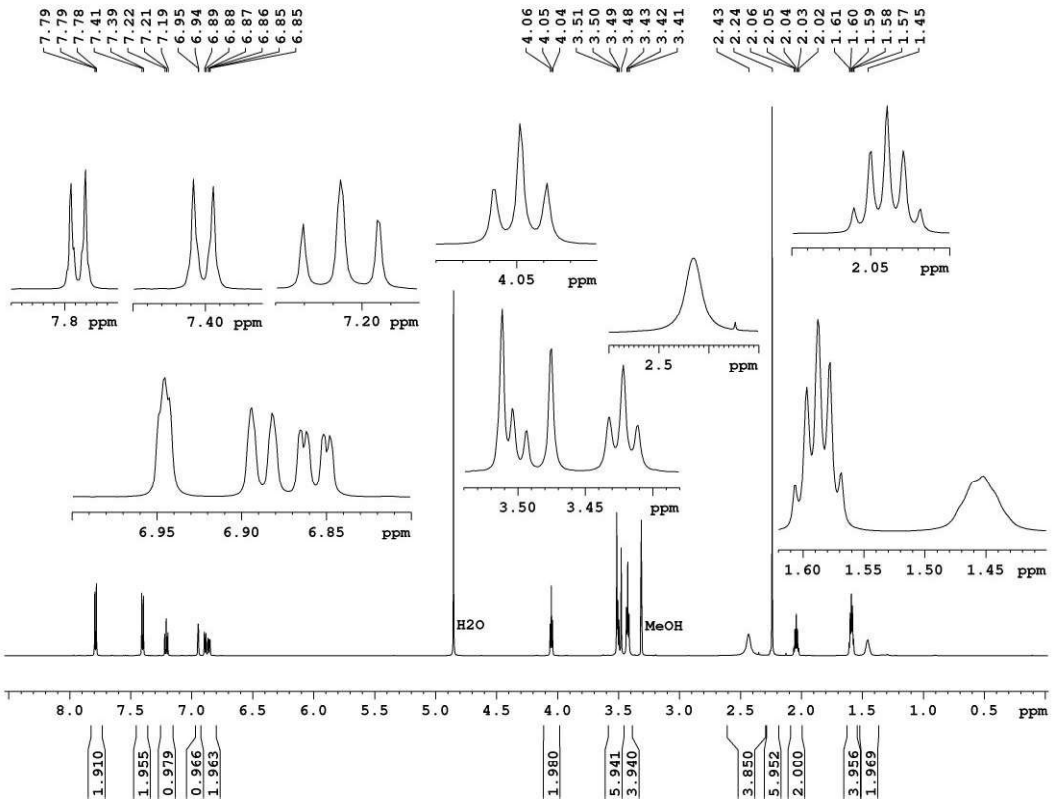

^{1}H-NMR spectrum (600 MHz, CD_3OD) of **4.49**

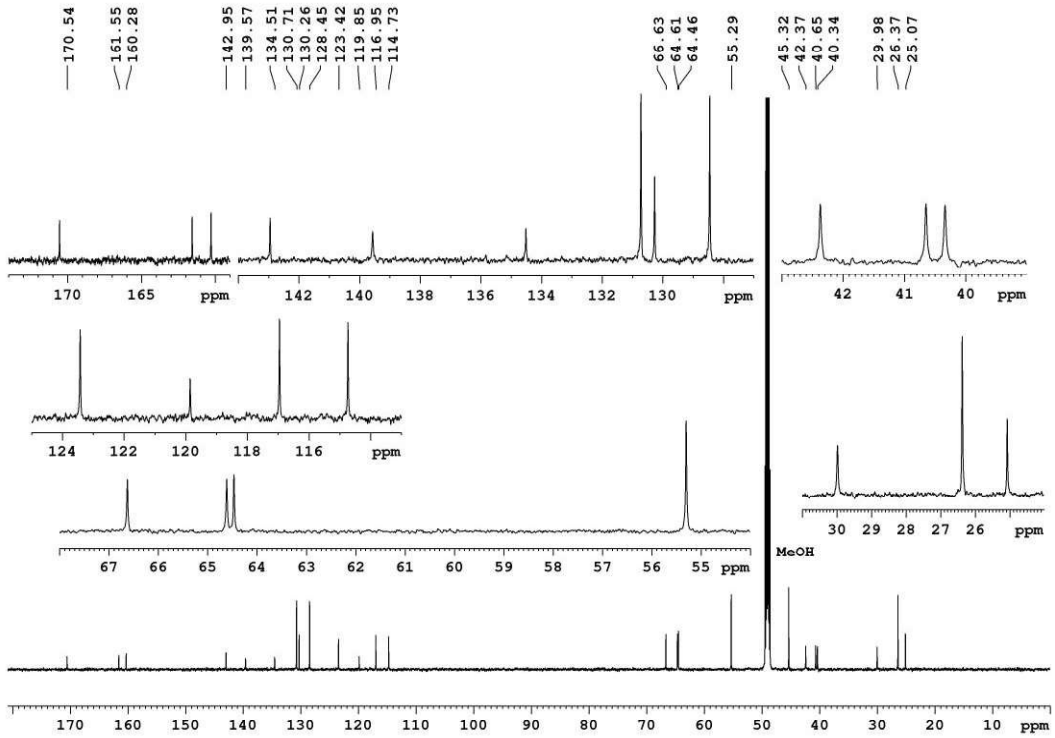

^{13}C-NMR spectrum (150 MHz, CD_3OD) of **4.49**

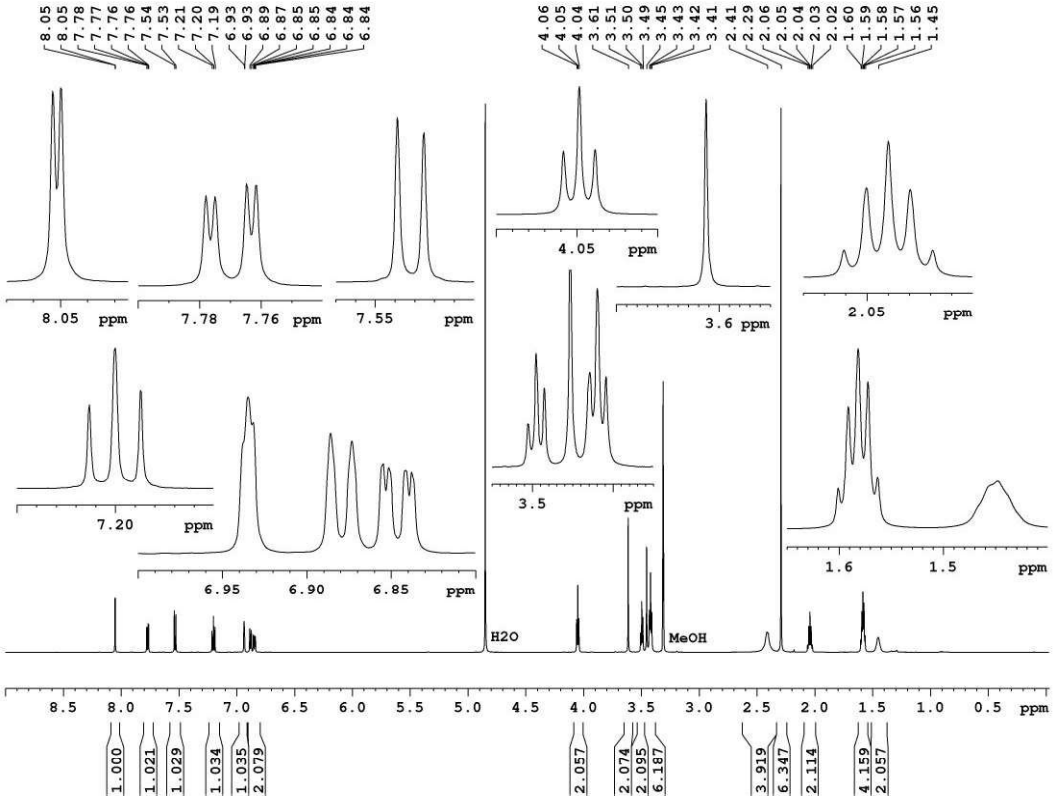

^{1}H-NMR spectrum (600 MHz, CD_3OD) of **4.50**

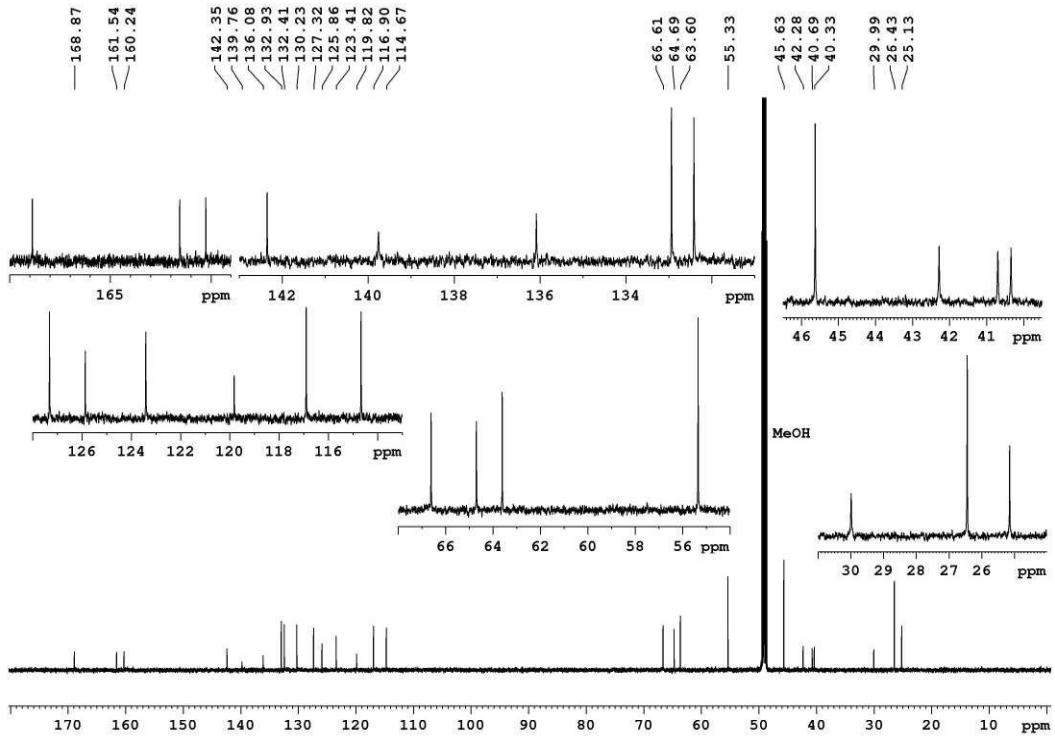

^{13}C-NMR spectrum (150 MHz, CD_3OD) of **4.50**

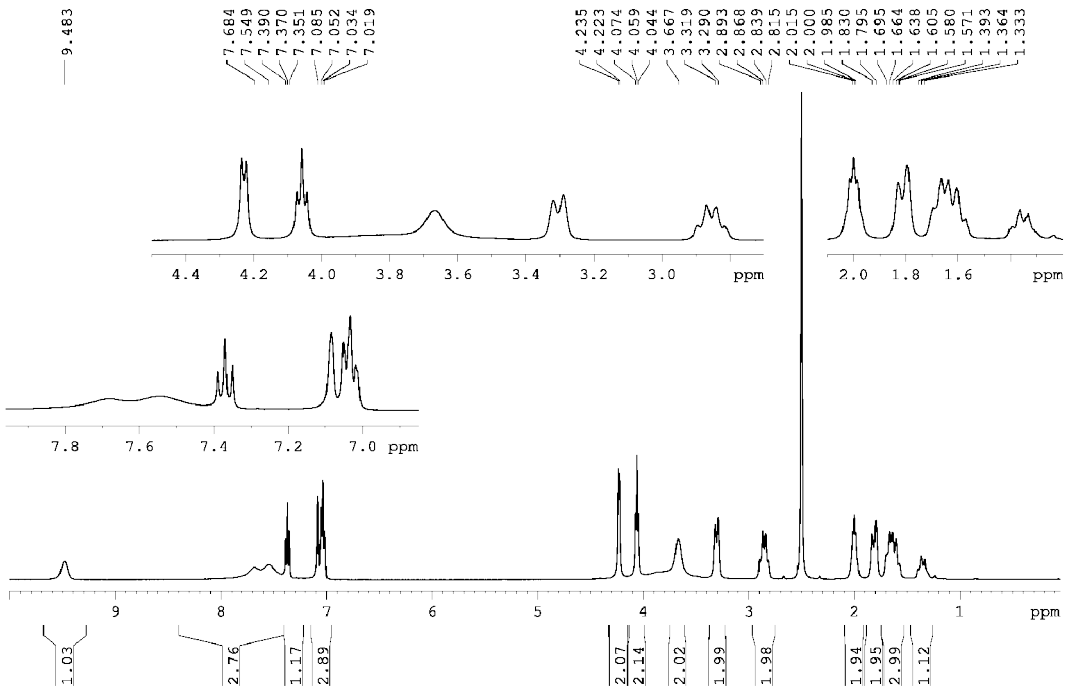

^{1}H-NMR spectrum (600 MHz, [D_6]-DMSO) of BMY 25368

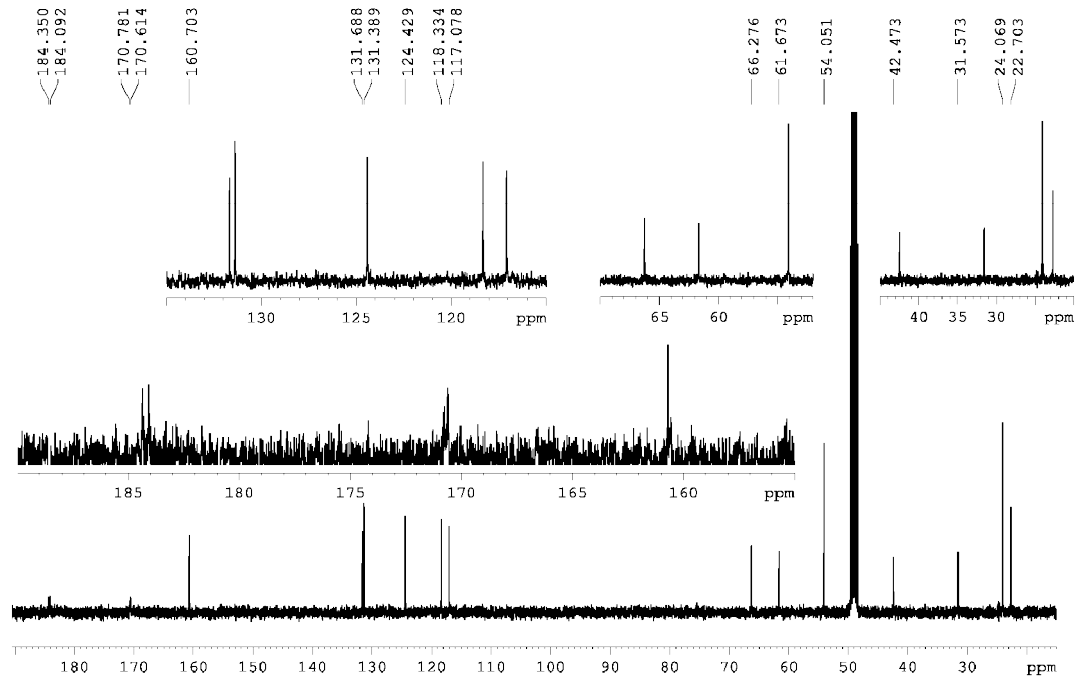

^{13}C-NMR spectrum (150 MHz, [D_6]-DMSO) of BMY 25368

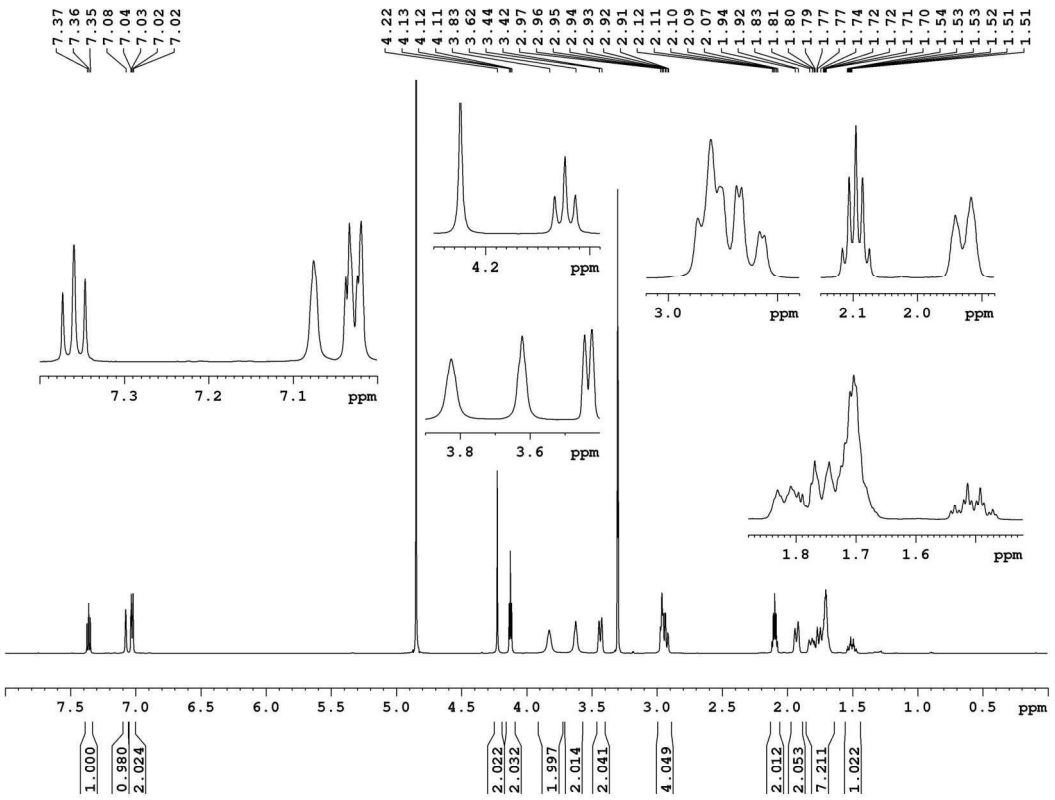

^{1}H-NMR spectrum (600 MHz, CD_3OD) of **5.9**

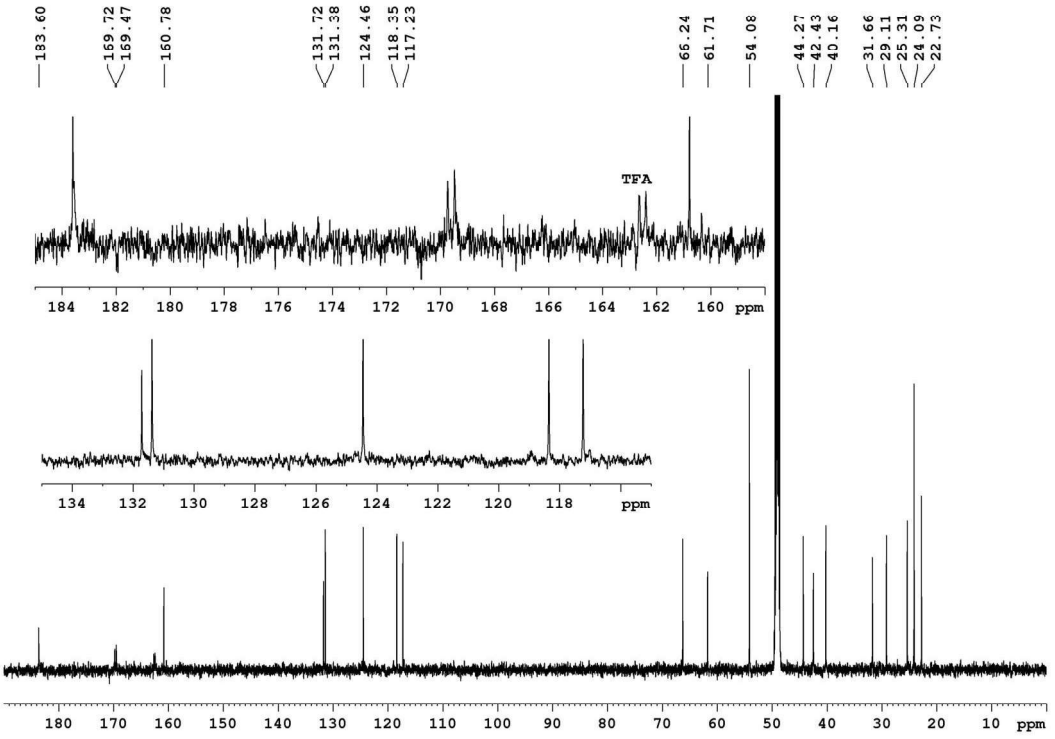

^{13}C-NMR spectrum (150 MHz, CD_3OD) of **5.9**

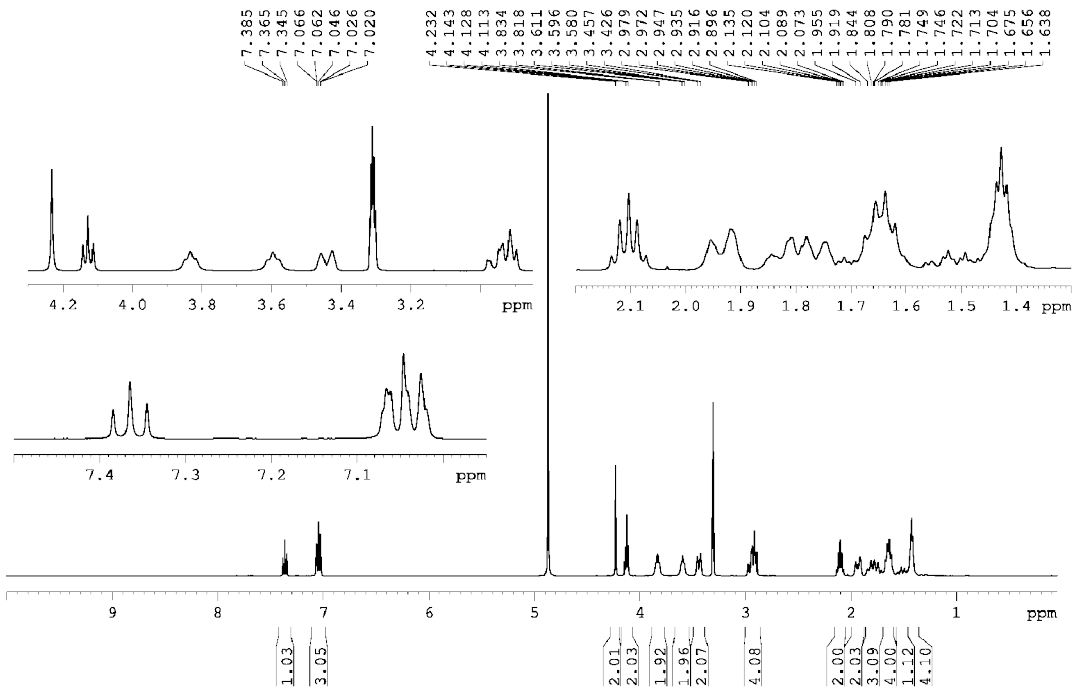

^{1}H-NMR spectrum (400 MHz, CD_3OD) of **5.10**

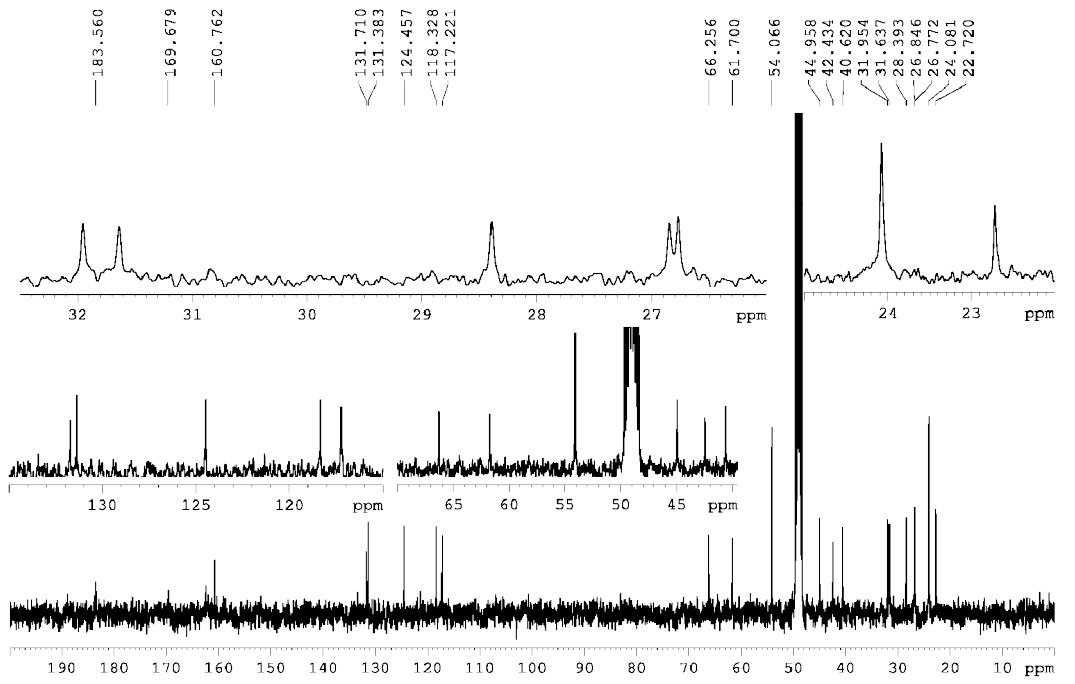

^{13}C-NMR spectrum (100 MHz, CD_3OD) of **5.10**

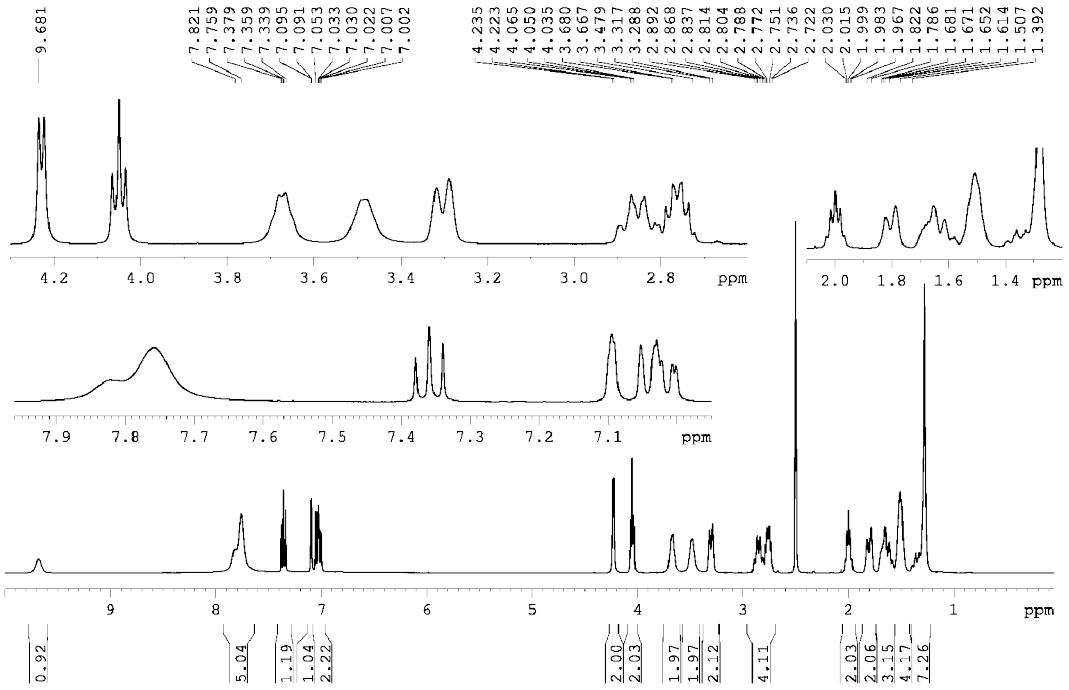

^{1}H-NMR spectrum (400 MHz, [D_6]DMSO) of **5.11**

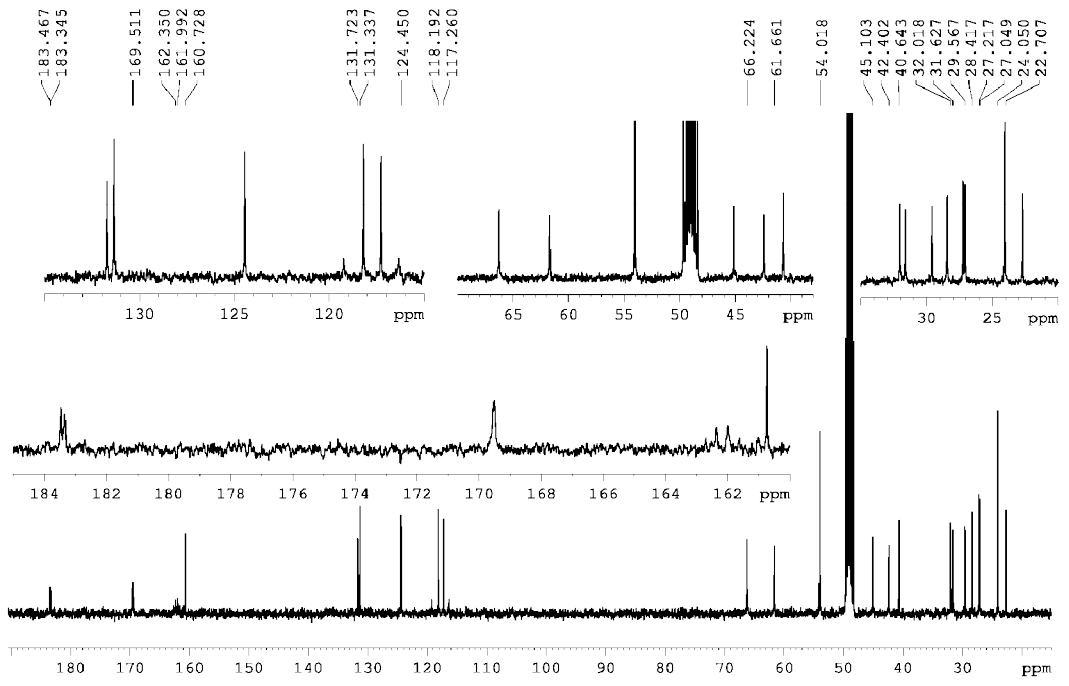

^{13}C-NMR spectrum (100 MHz, CD_3OD) of **5.11**

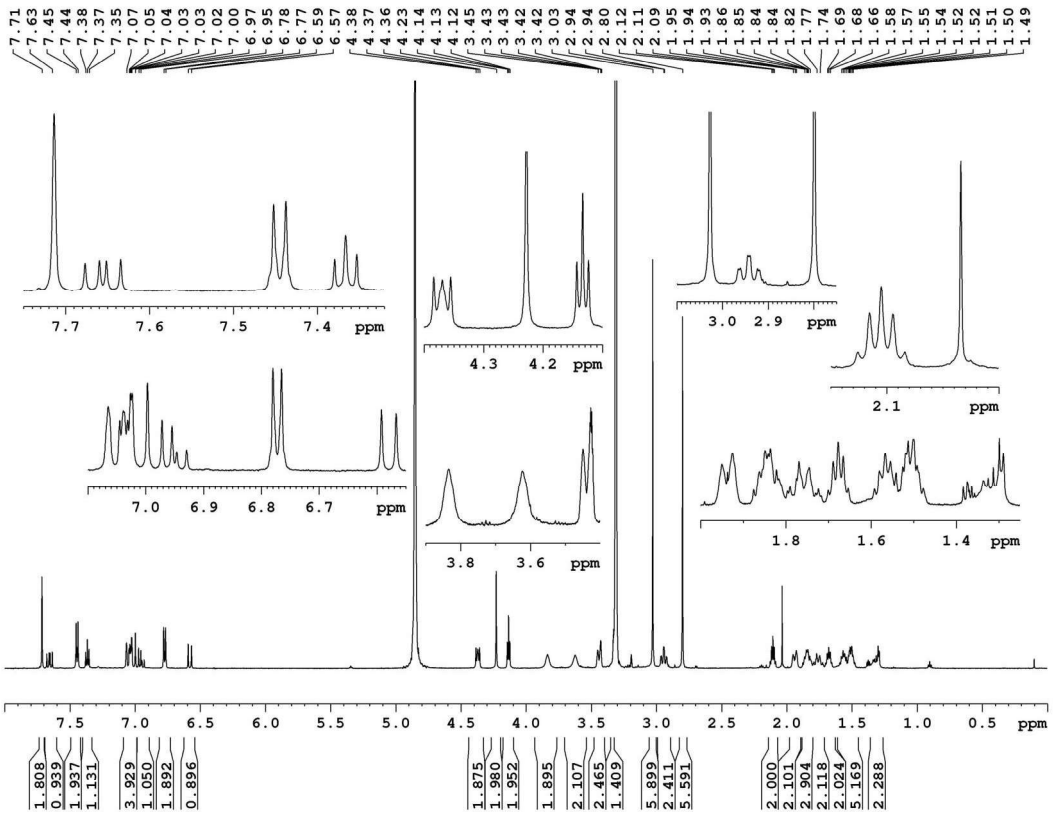

^{1}H-NMR spectrum (600 MHz, CD_3OD) of **5.13**

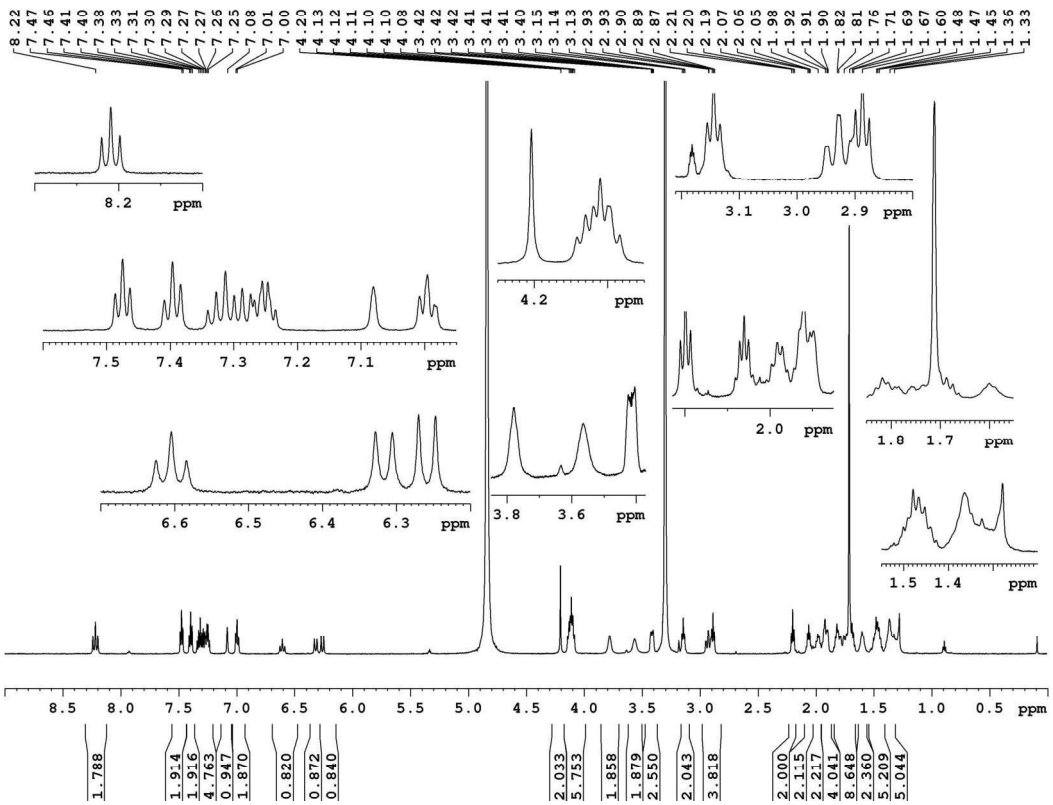

^{1}H-NMR spectrum (600 MHz, CD_3OD) of **5.18**

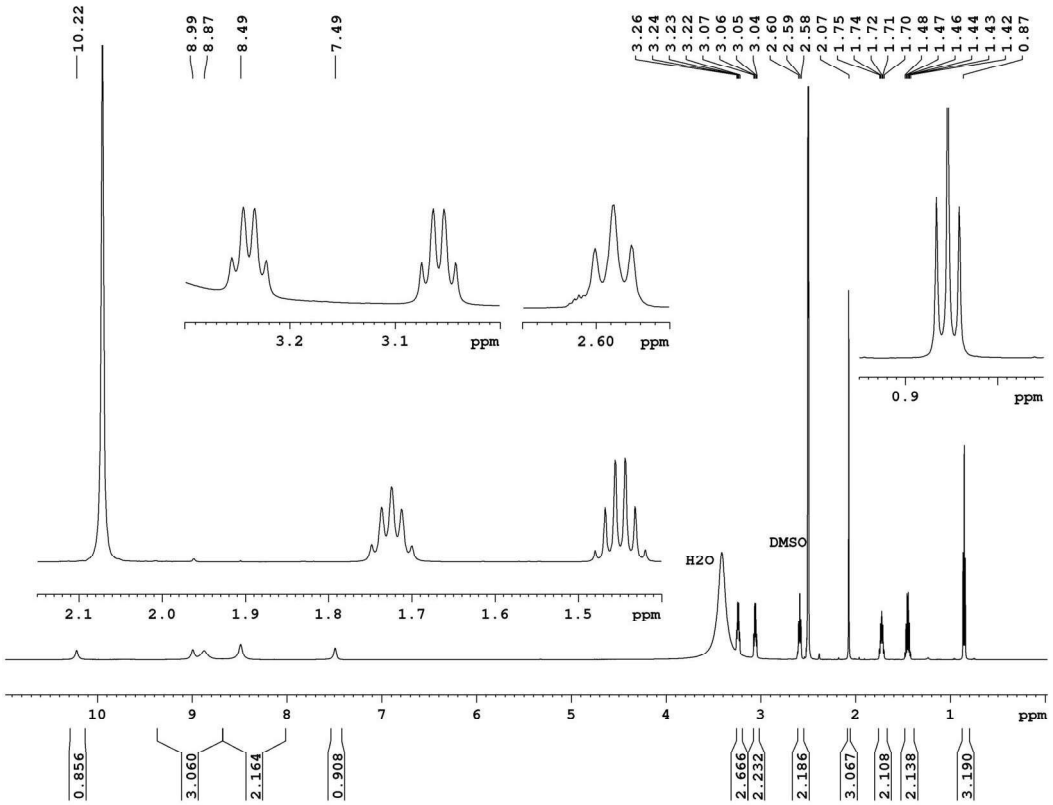

^{1}H-NMR spectrum (600 MHz, [D_6]-DMSO) of **6.47**

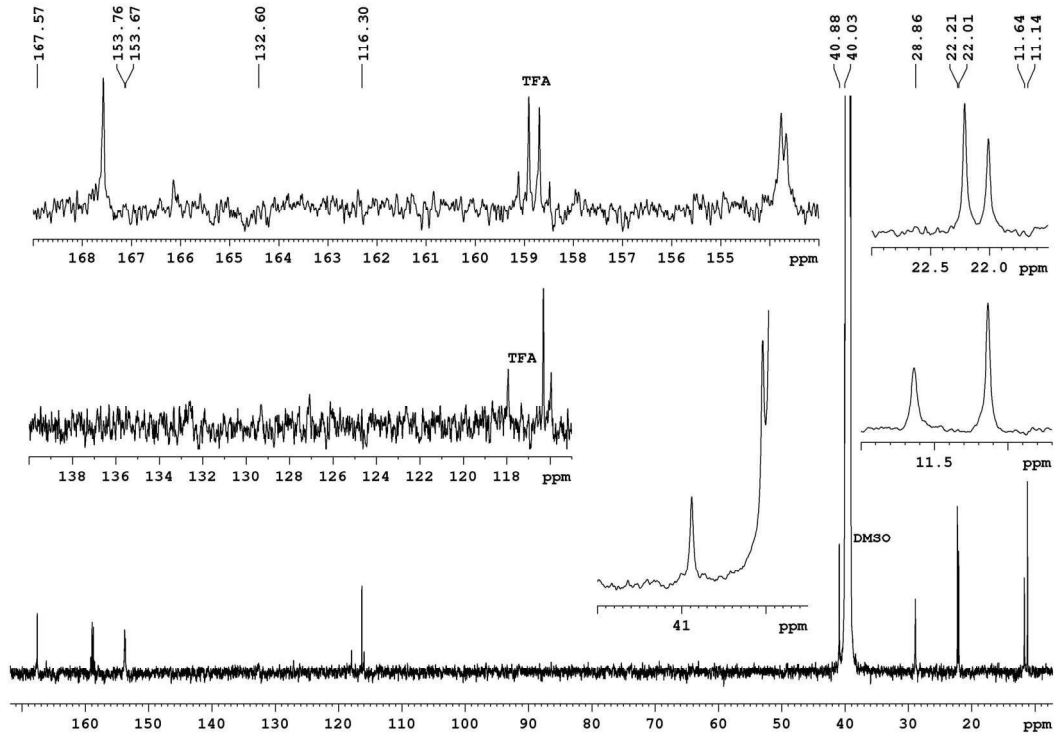

^{13}C-NMR spectrum (150 MHz, [D_6]-DMSO) of **6.47**

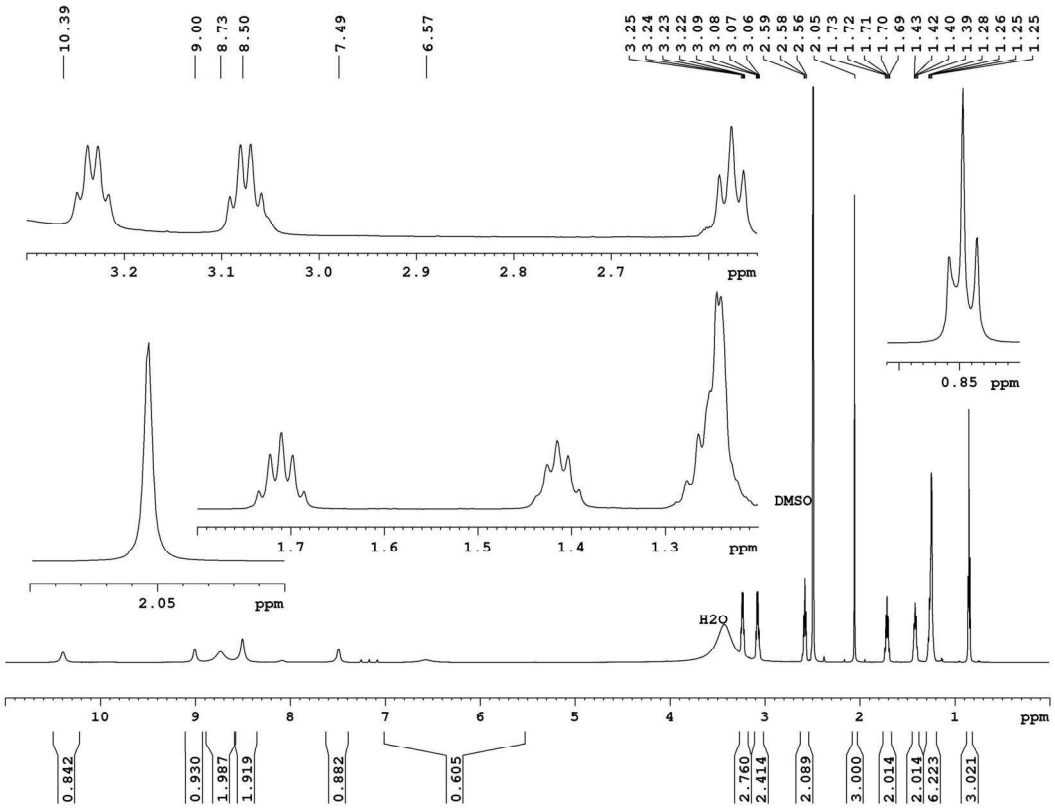

^{1}H-NMR spectrum (600 MHz, [D_6]-DMSO) of **6.48**

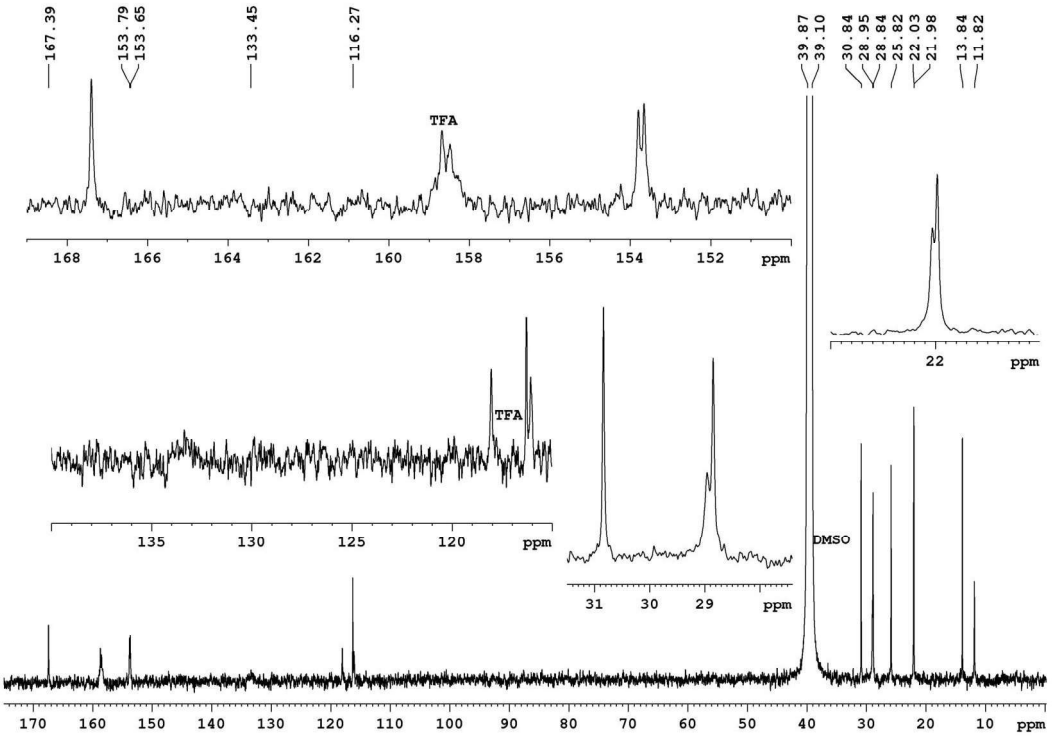

^{13}C-NMR spectrum (150 MHz, [D_6]-DMSO) of **6.48**

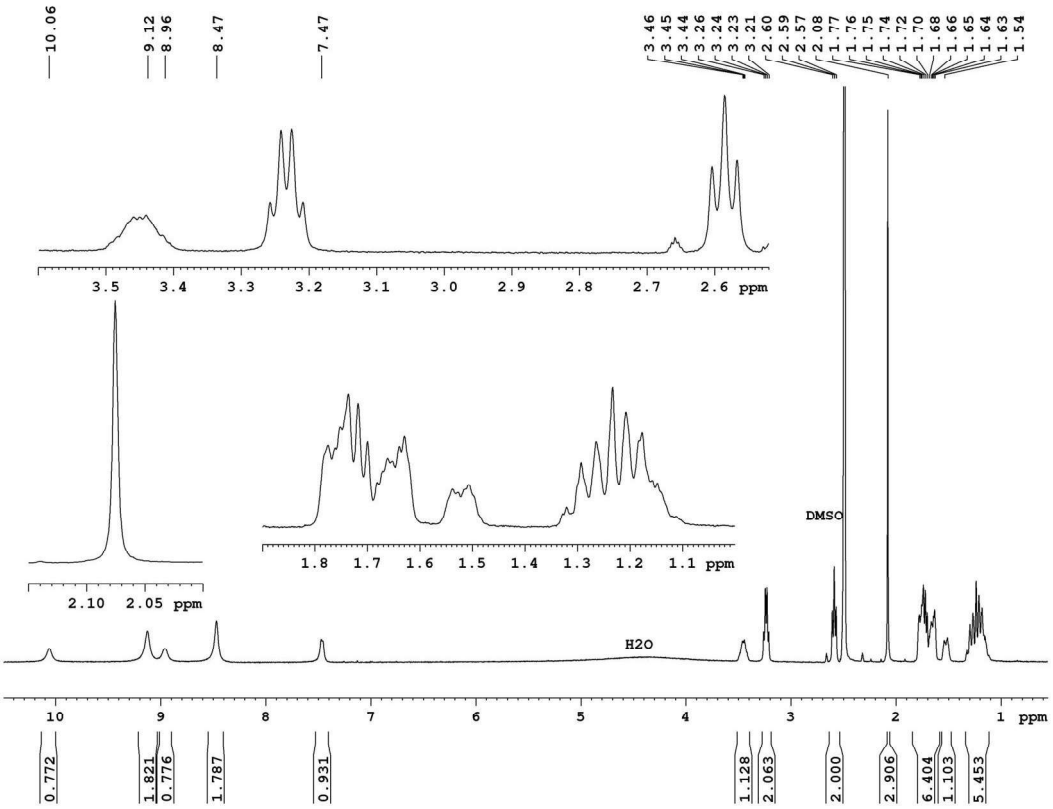

^{1}H-NMR spectrum (600 MHz, [D_6]-DMSO) of **6.49**

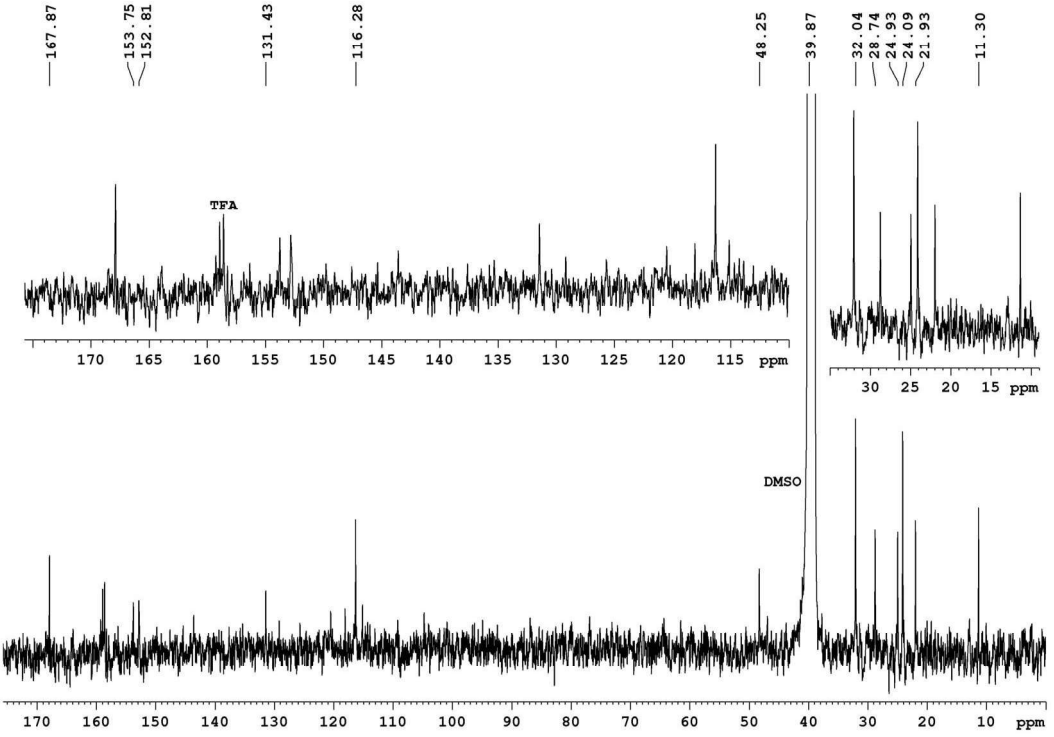

^{13}C-NMR spectrum (150 MHz, [D_6]-DMSO) of **6.49**

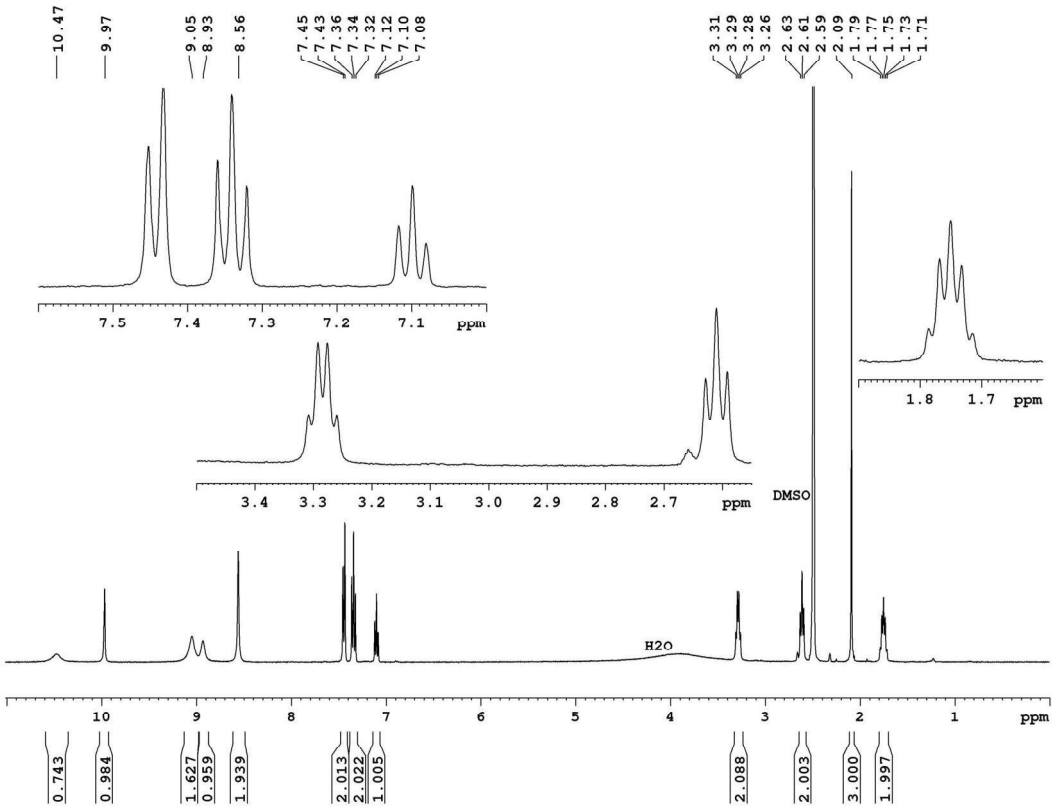

^{1}H-NMR spectrum (600 MHz, [D_6]-DMSO) of **6.50**

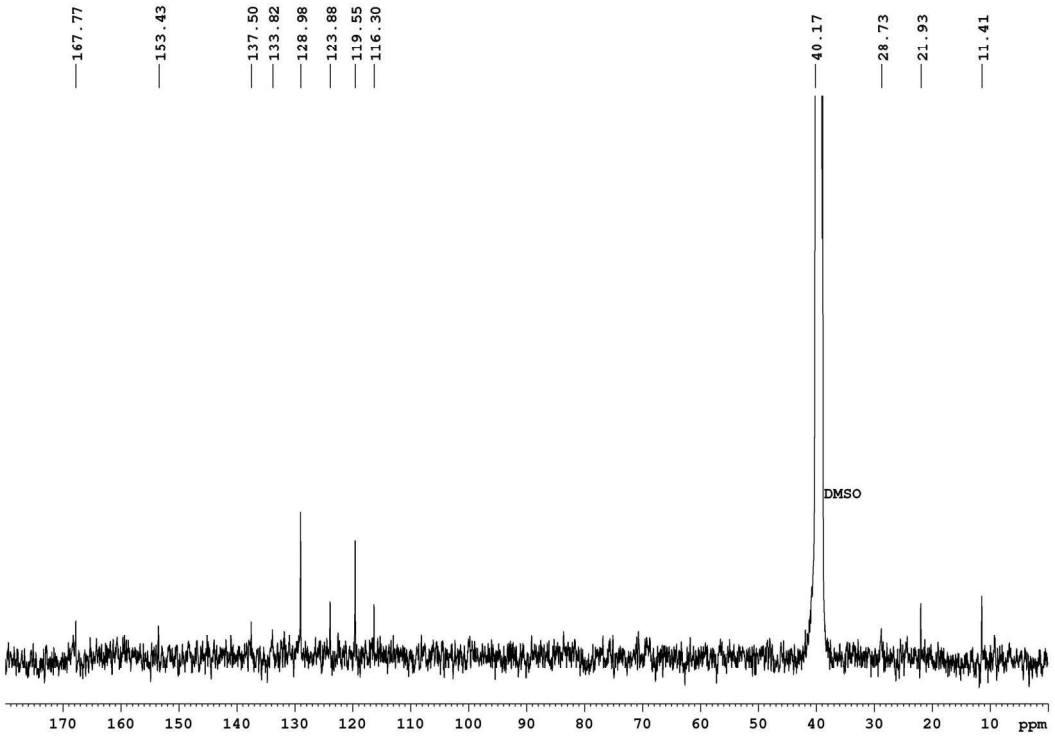

^{13}C-NMR spectrum (150 MHz, [D_6]-DMSO) of **6.50**

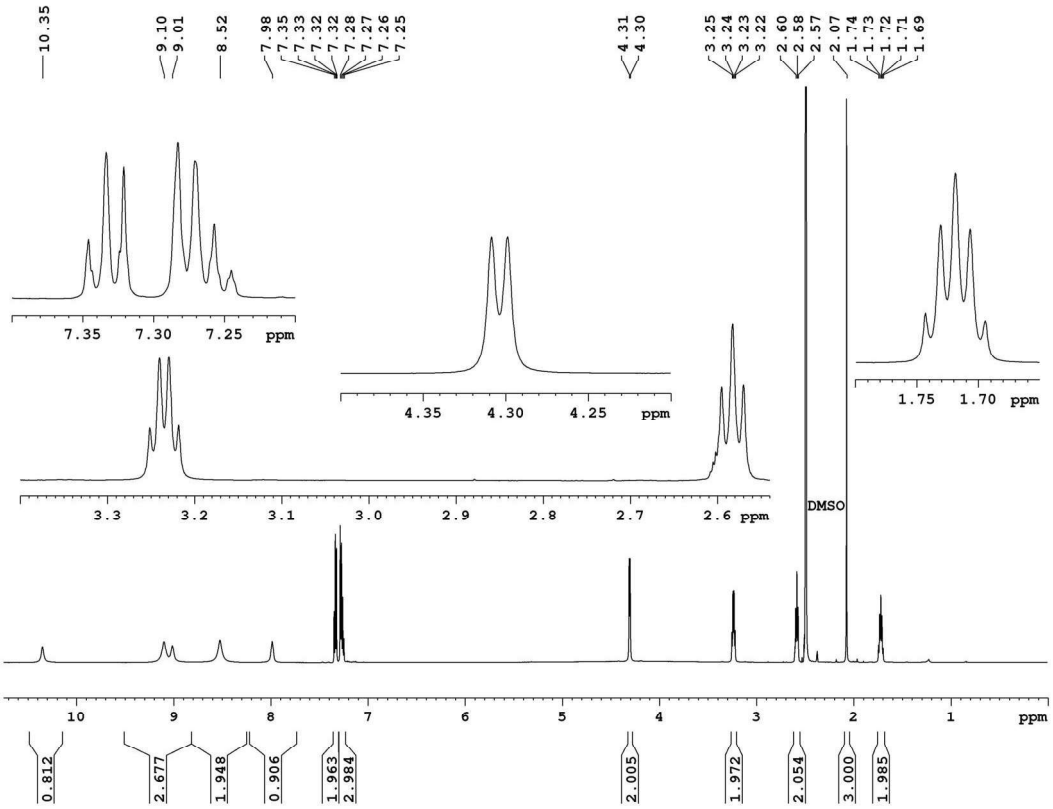

^{1}H-NMR spectrum (600 MHz, [D_6]-DMSO) of **6.51**

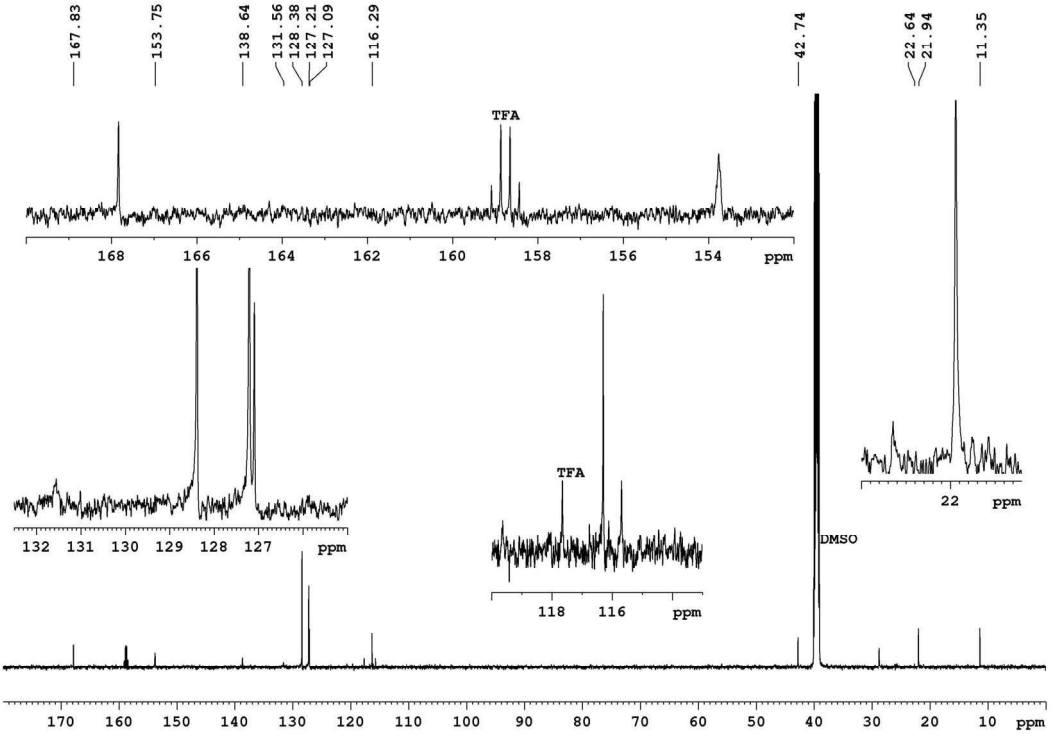

^{13}C-NMR spectrum (150 MHz, [D_6]-DMSO) of **6.51**

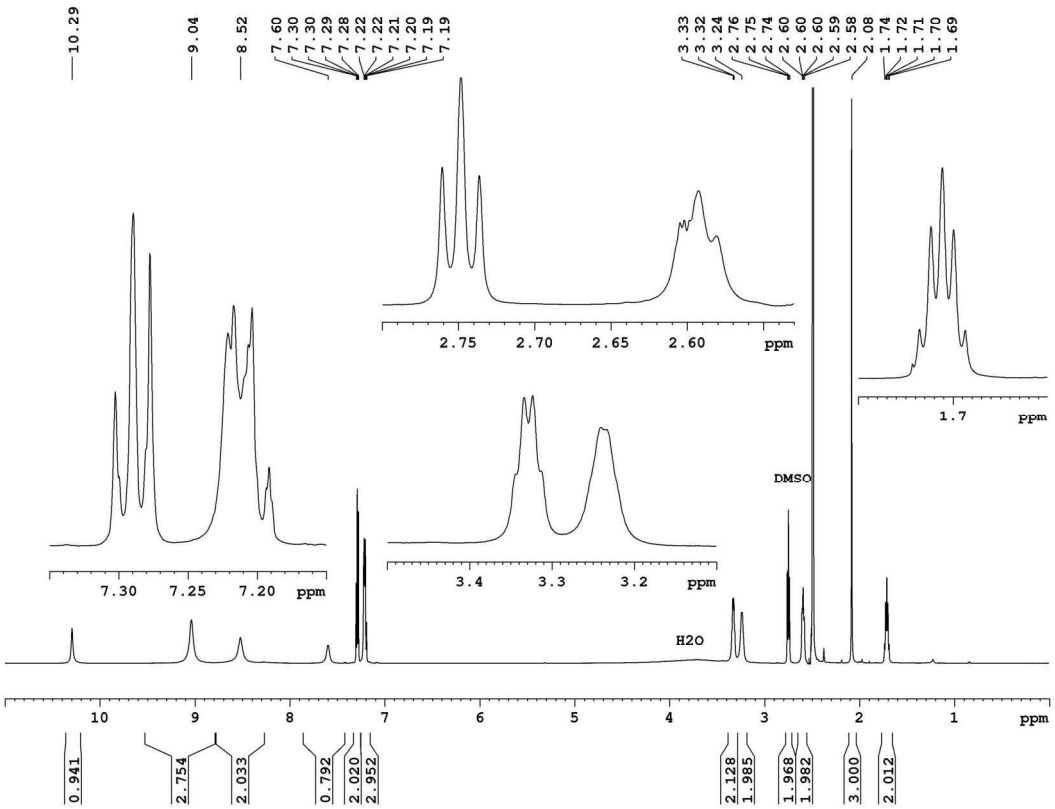

^{1}H-NMR spectrum (600 MHz, [D_6]-DMSO) of **6.52**

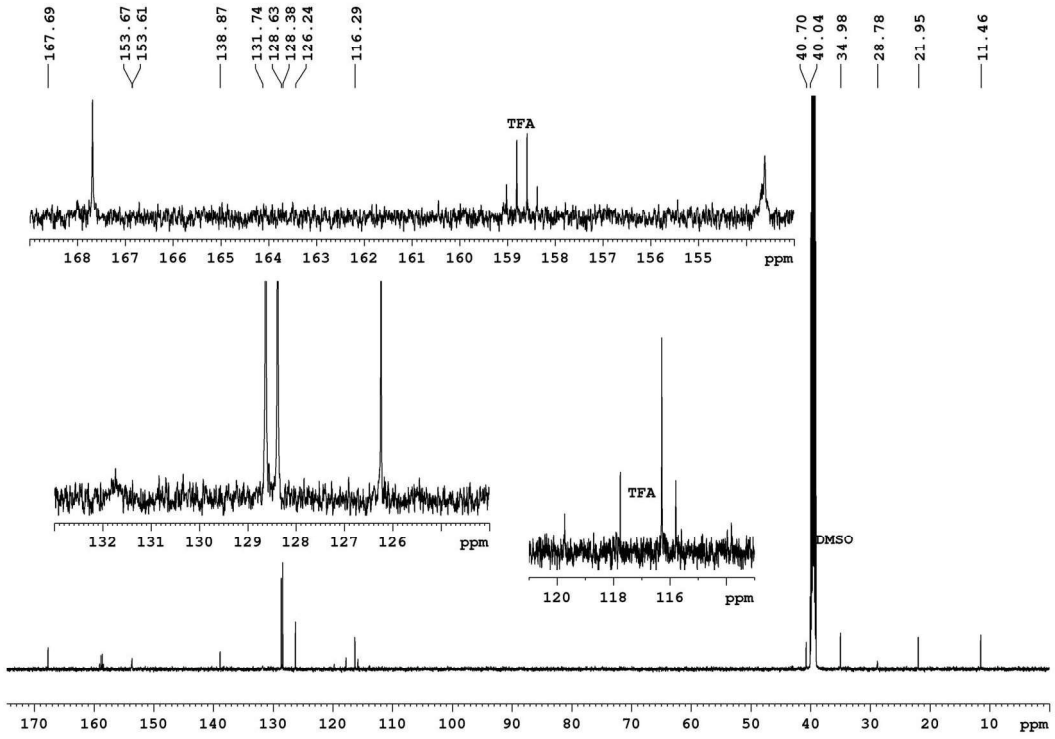

^{13}C-NMR spectrum (150 MHz, [D_6]-DMSO) of **6.52**

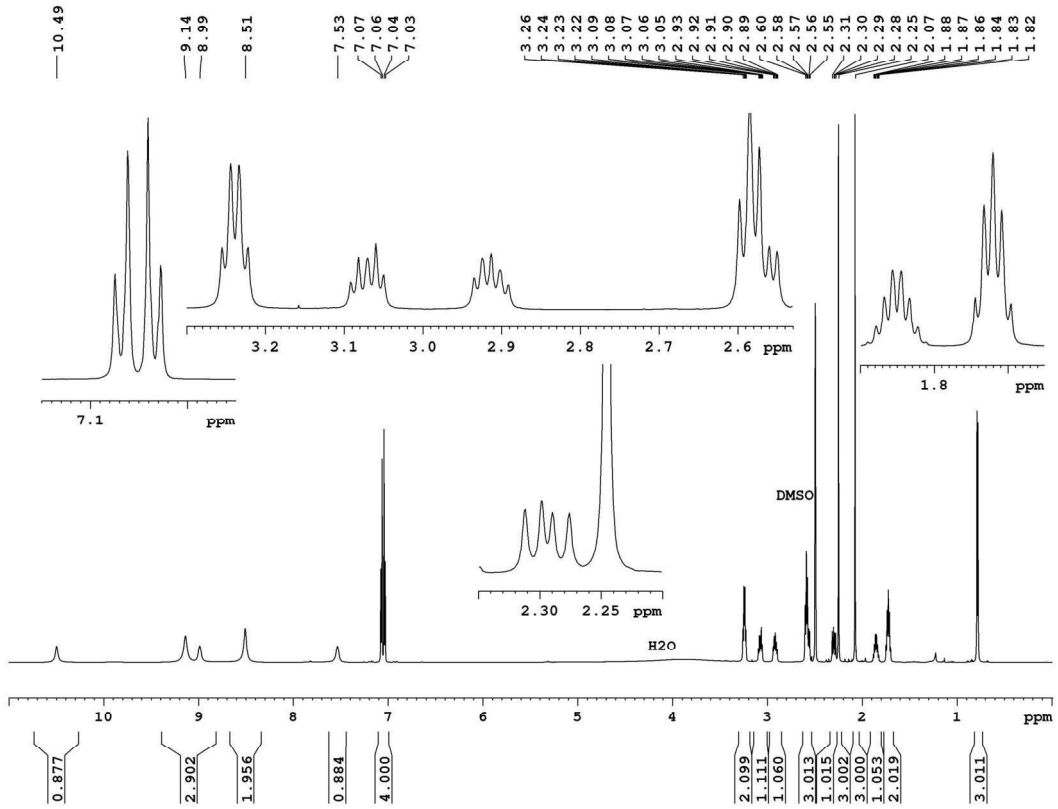

^{1}H-NMR spectrum (600 MHz, [D_6]-DMSO) of **6.53**

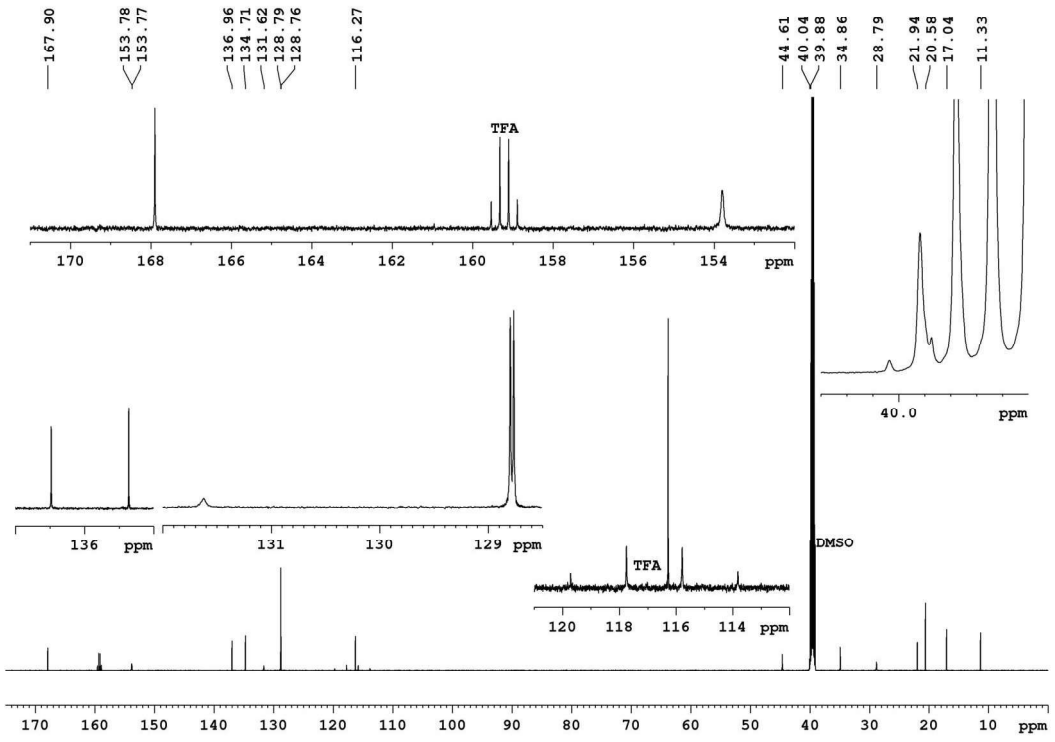

^{13}C-NMR spectrum (150 MHz, [D_6]-DMSO) of **6.53**

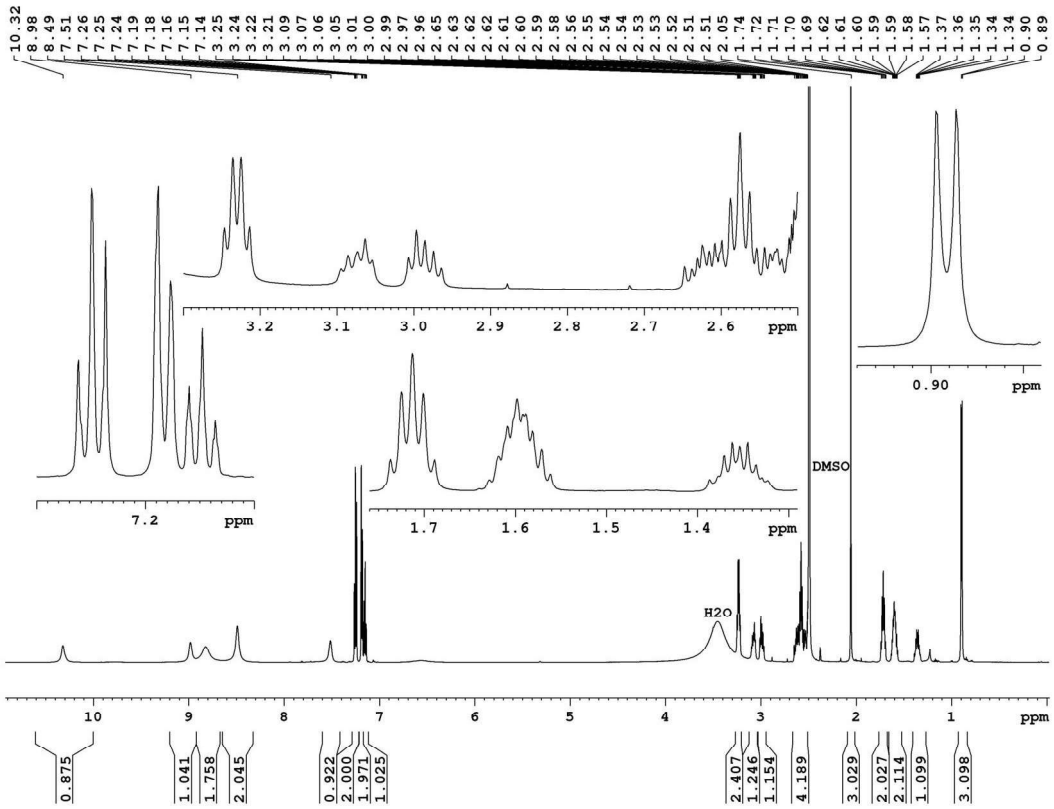

^{1}H-NMR spectrum (600 MHz, [D_6]-DMSO) of **6.54**

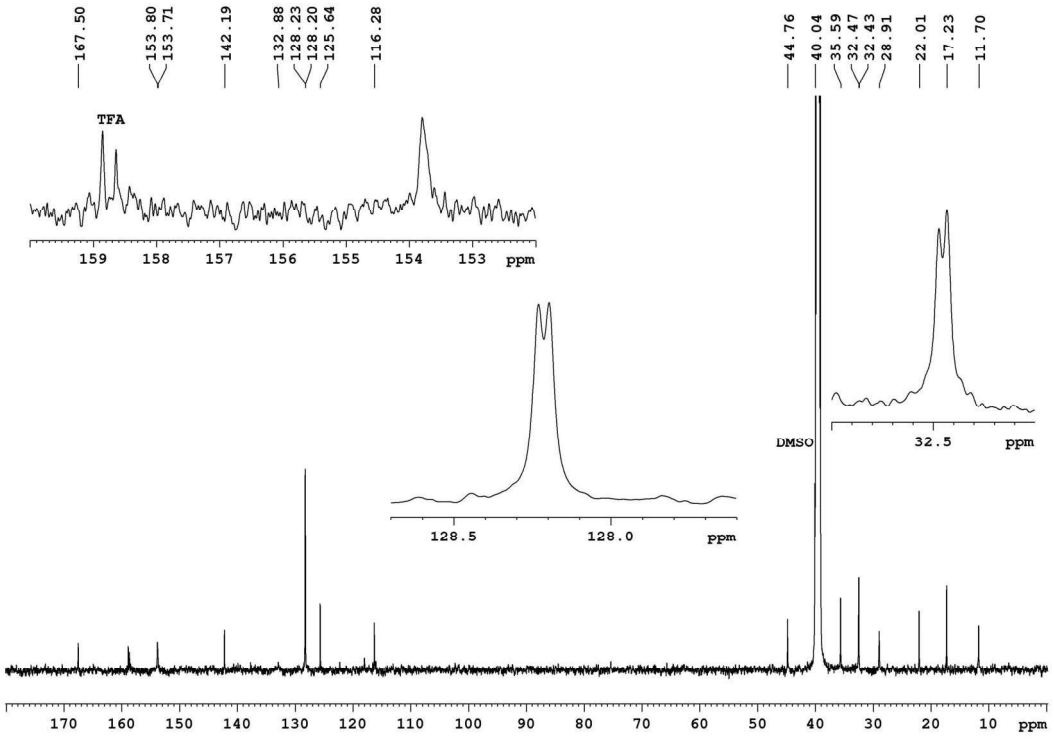

^{13}C-NMR spectrum (150 MHz, [D_6]-DMSO) of **6.54**

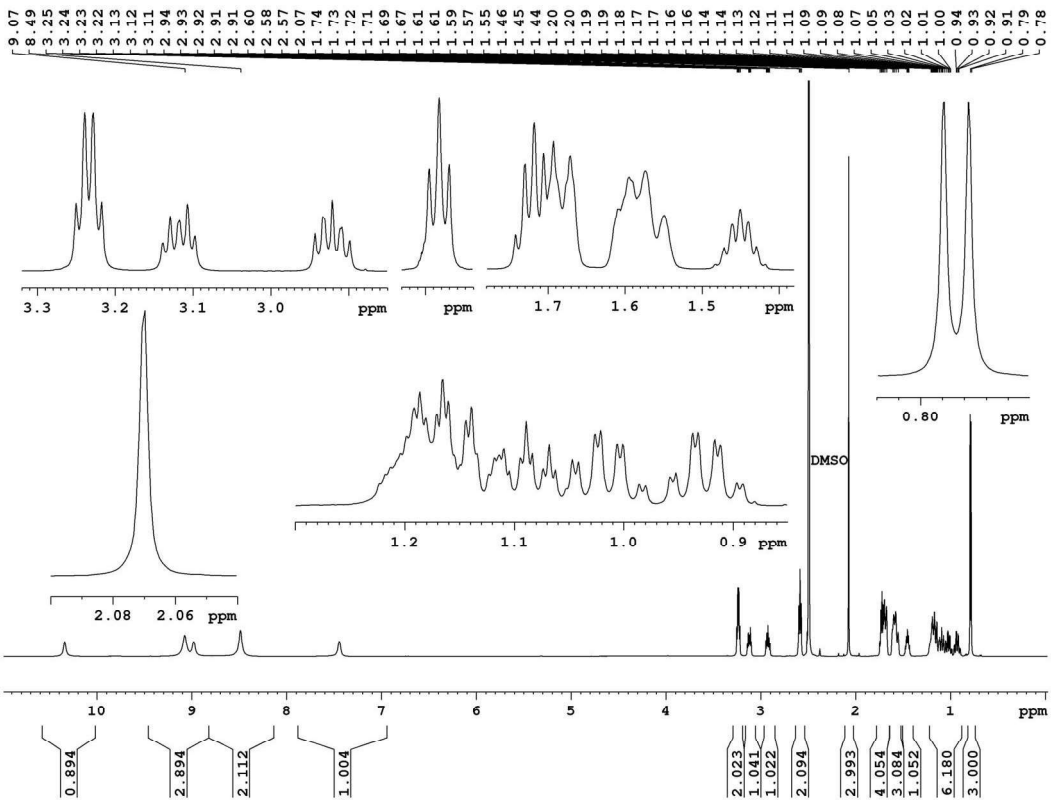

^{1}H-NMR spectrum (600 MHz, [D_6]-DMSO) of **6.55**

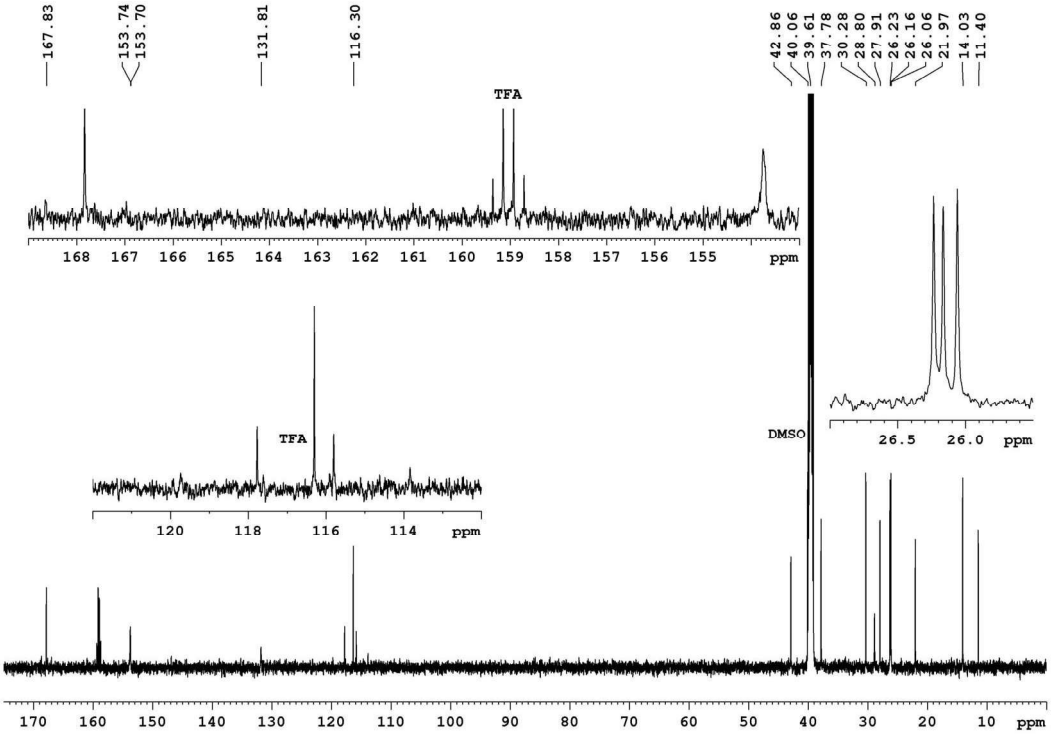

^{13}C-NMR spectrum (150 MHz, [D_6]-DMSO) of **6.55**

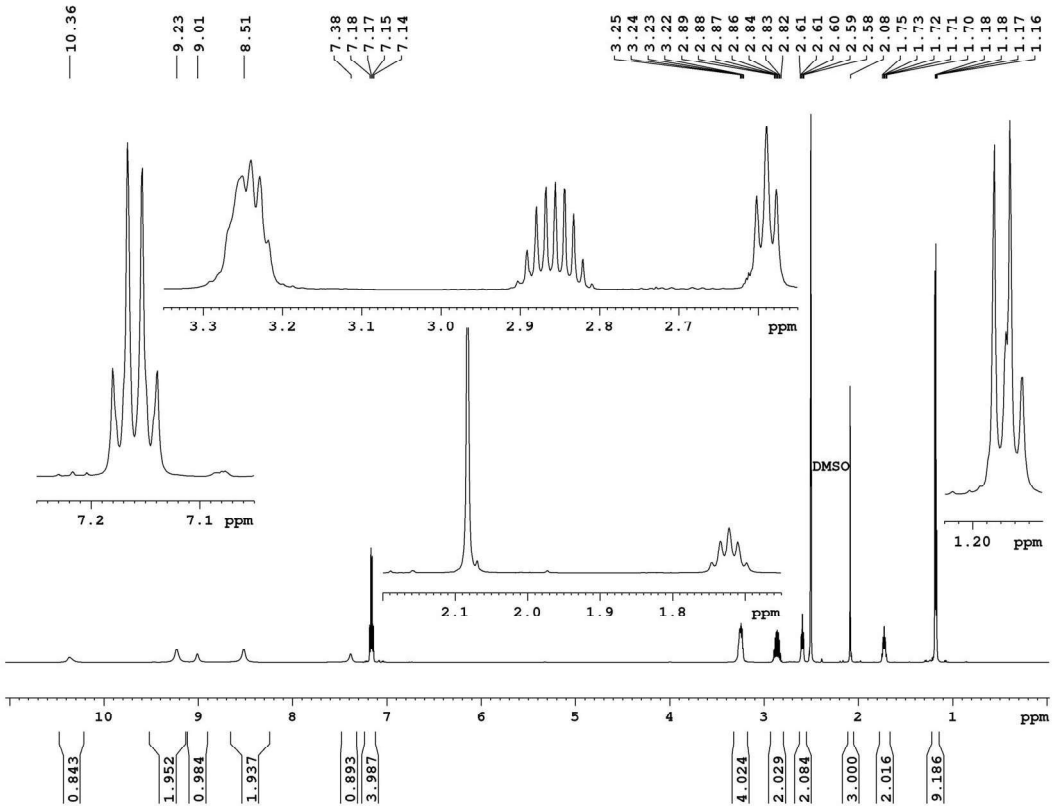

^{1}H-NMR spectrum (600 MHz, [D_6]-DMSO) of **6.56**

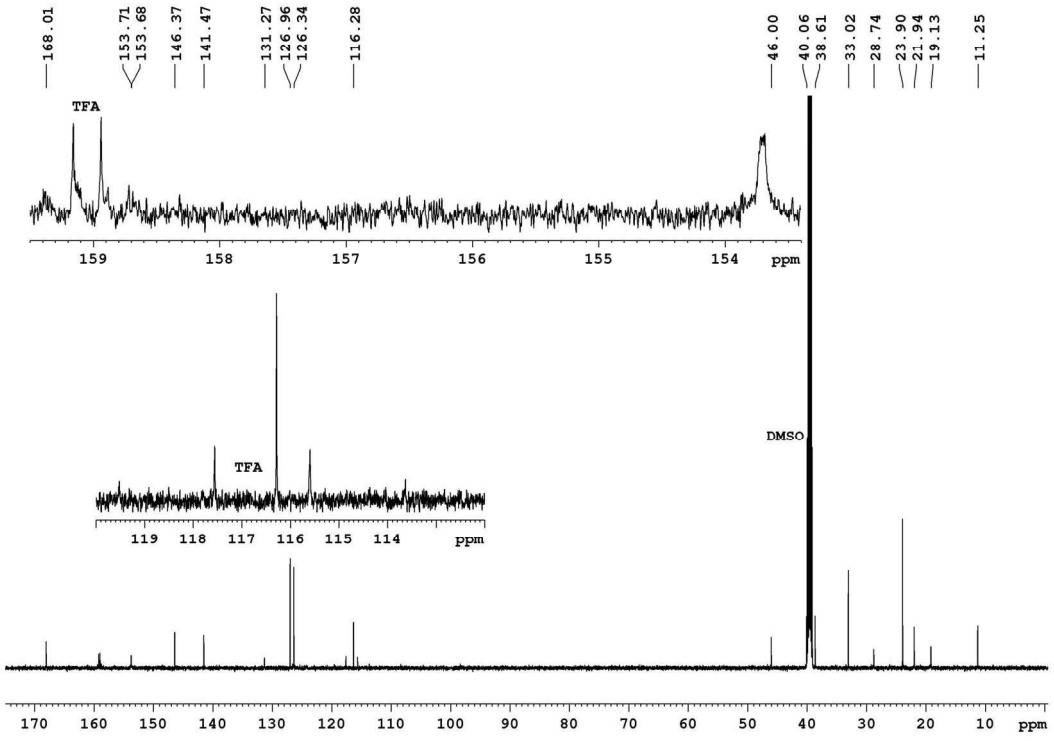

^{13}C-NMR spectrum (150 MHz, [D_6]-DMSO) of **6.56**

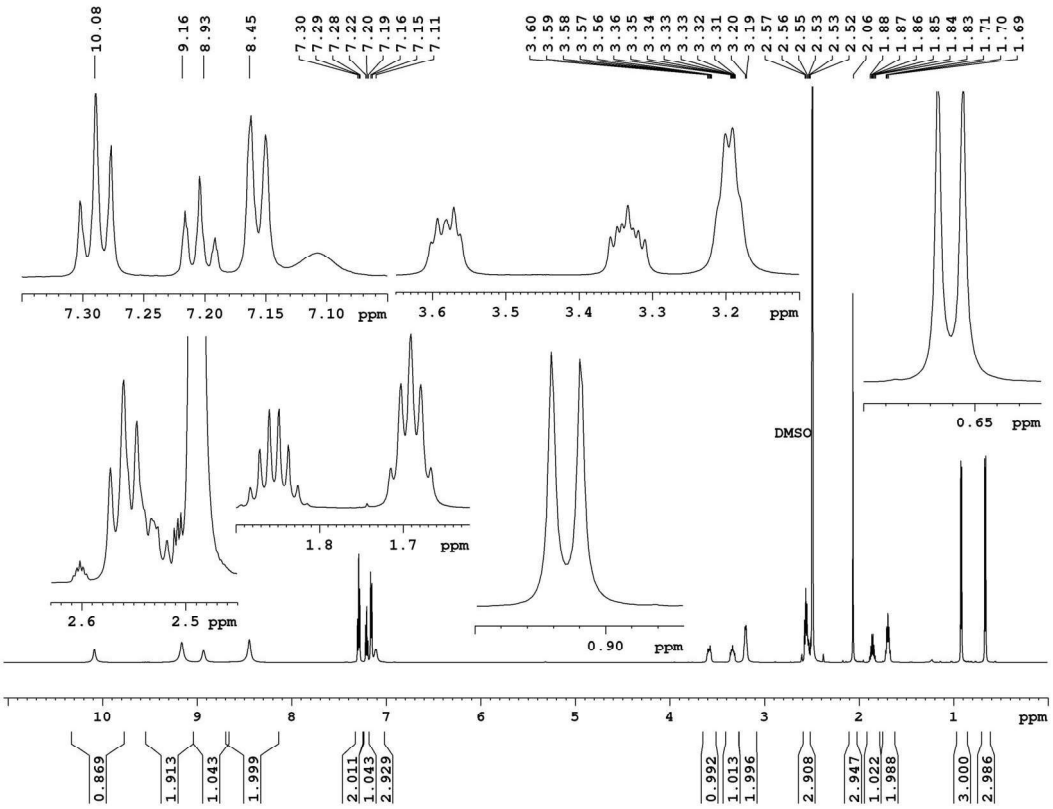

^{1}H-NMR spectrum (600 MHz, [D_6]-DMSO) of **6.57**

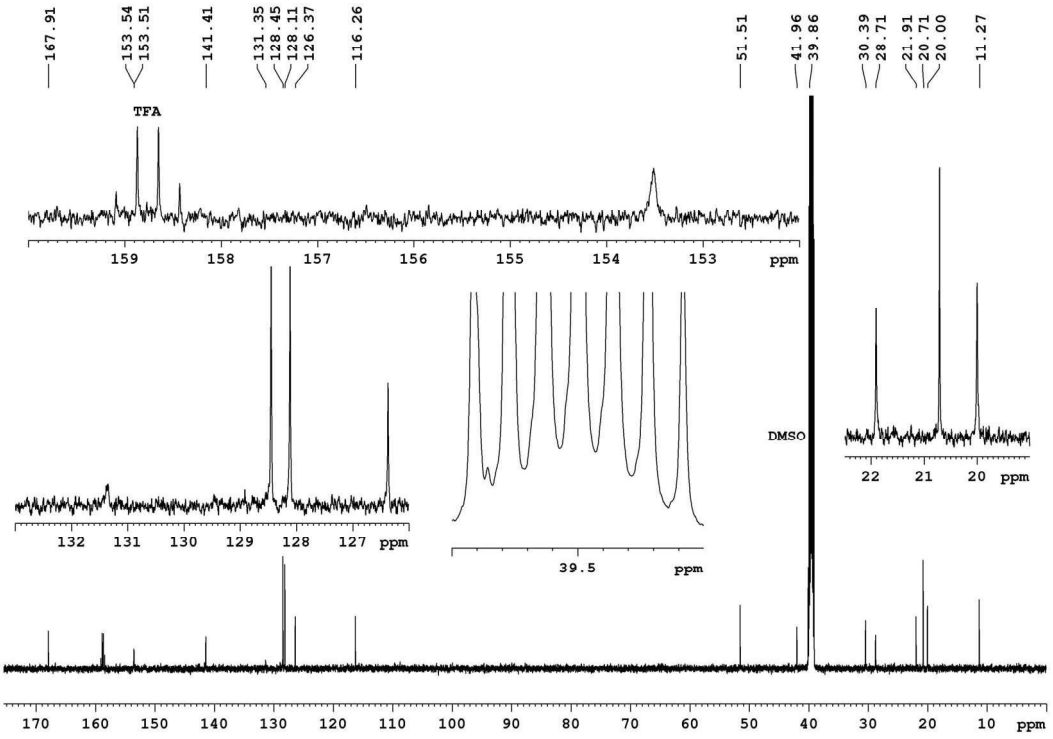

^{13}C-NMR spectrum (150 MHz, [D_6]-DMSO) of **6.57**

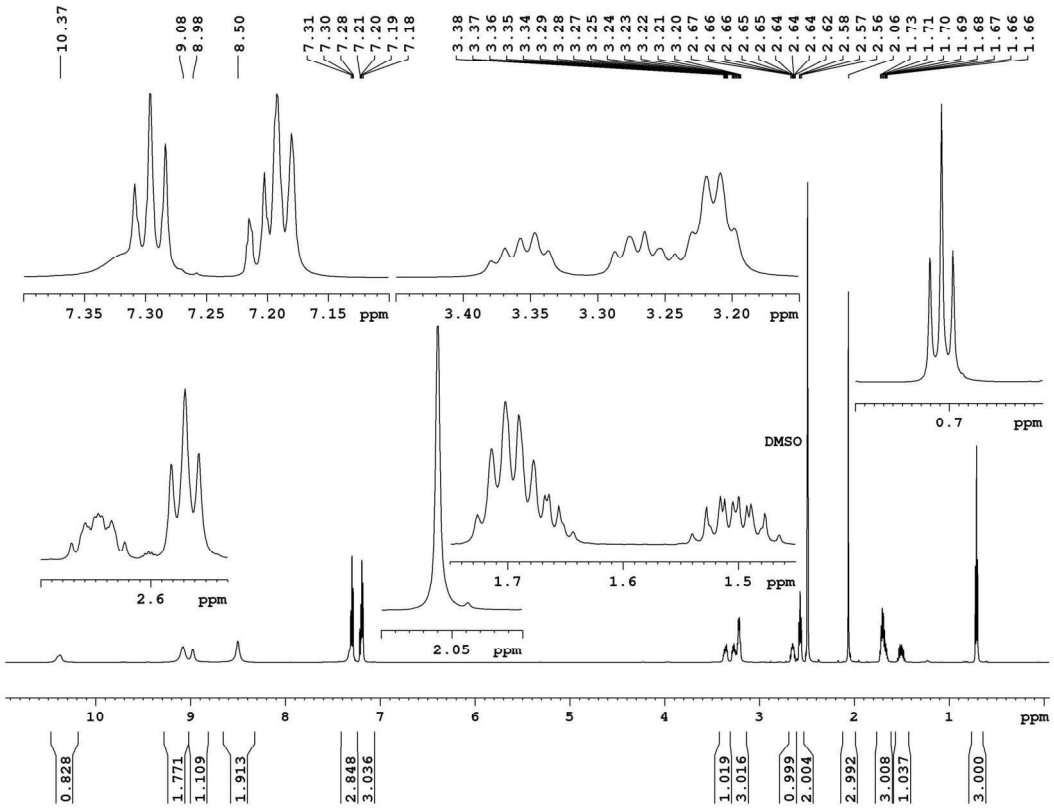

^{1}H-NMR spectrum (600 MHz, [D_6]-DMSO) of **6.58**

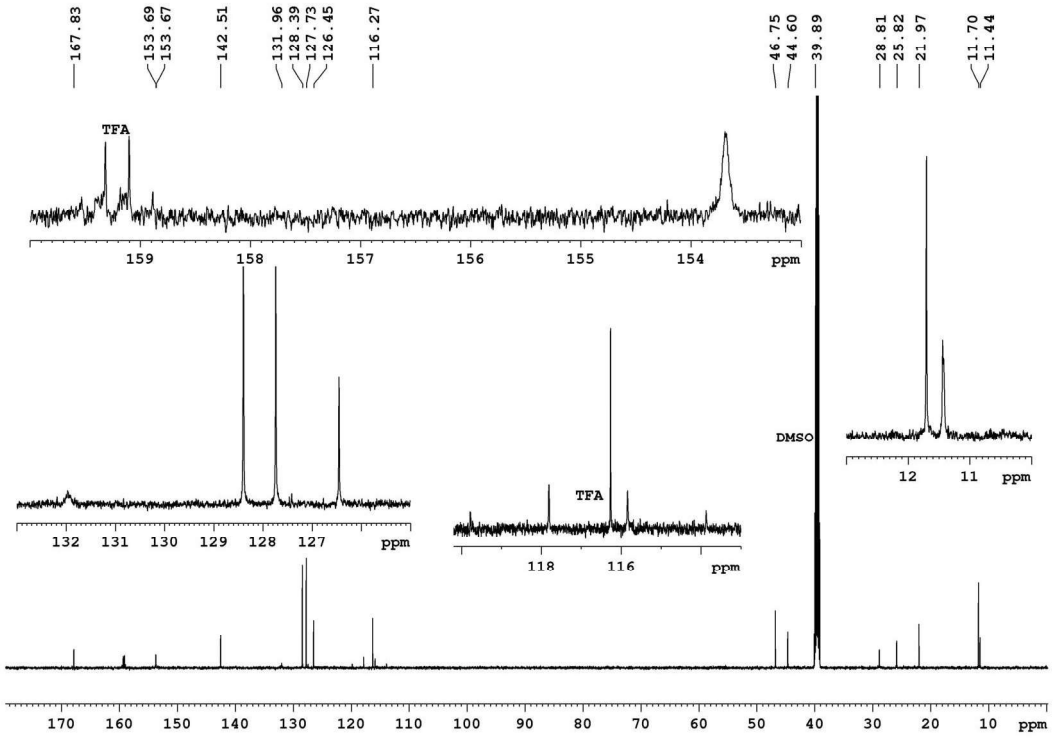

^{13}C-NMR spectrum (150 MHz, [D_6]-DMSO) of **6.58**

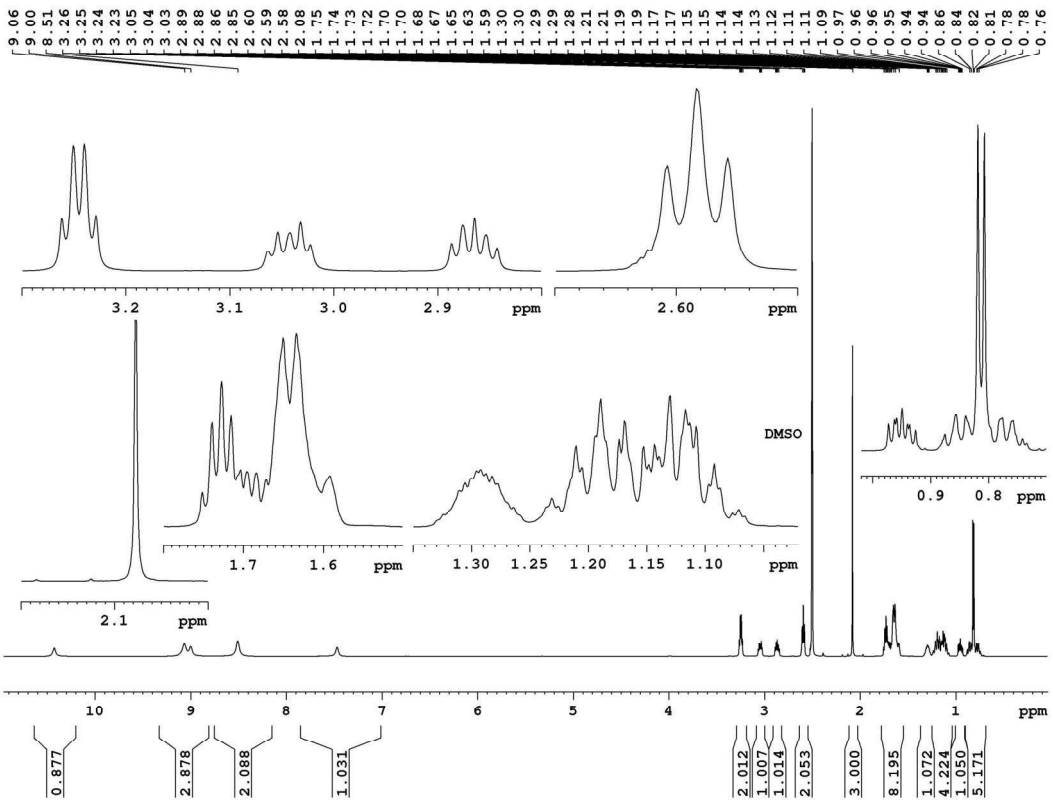

^{1}H-NMR spectrum (600 MHz, [D_6]-DMSO) of **6.59**

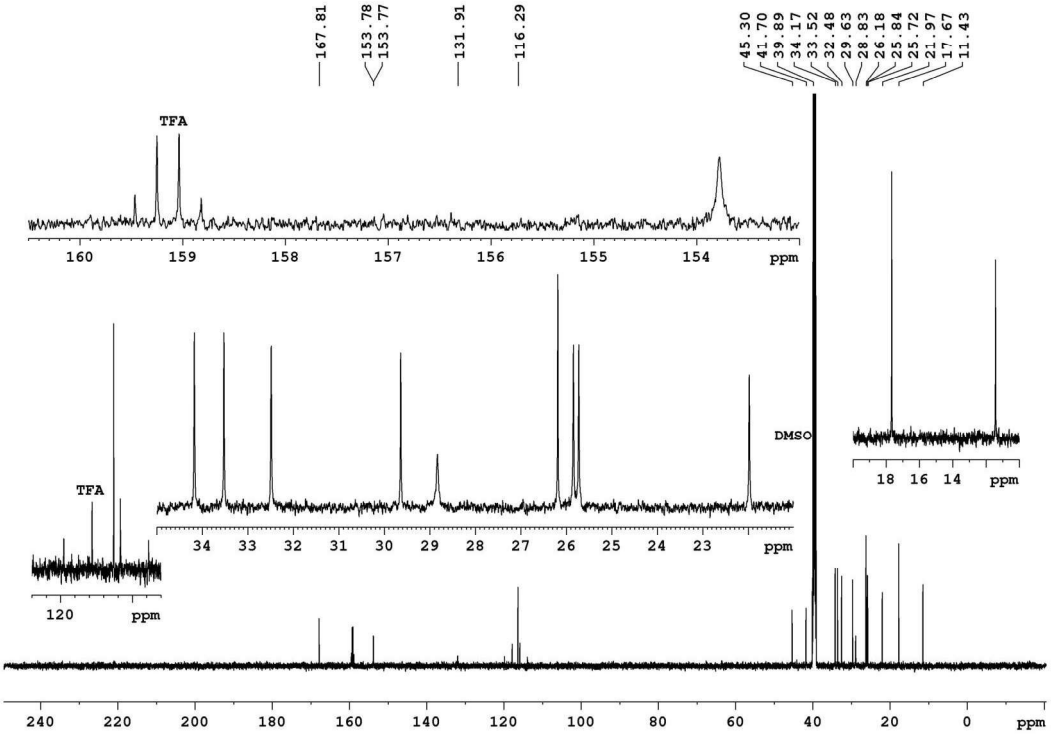

^{13}C-NMR spectrum (150 MHz, [D_6]-DMSO) of **6.59**

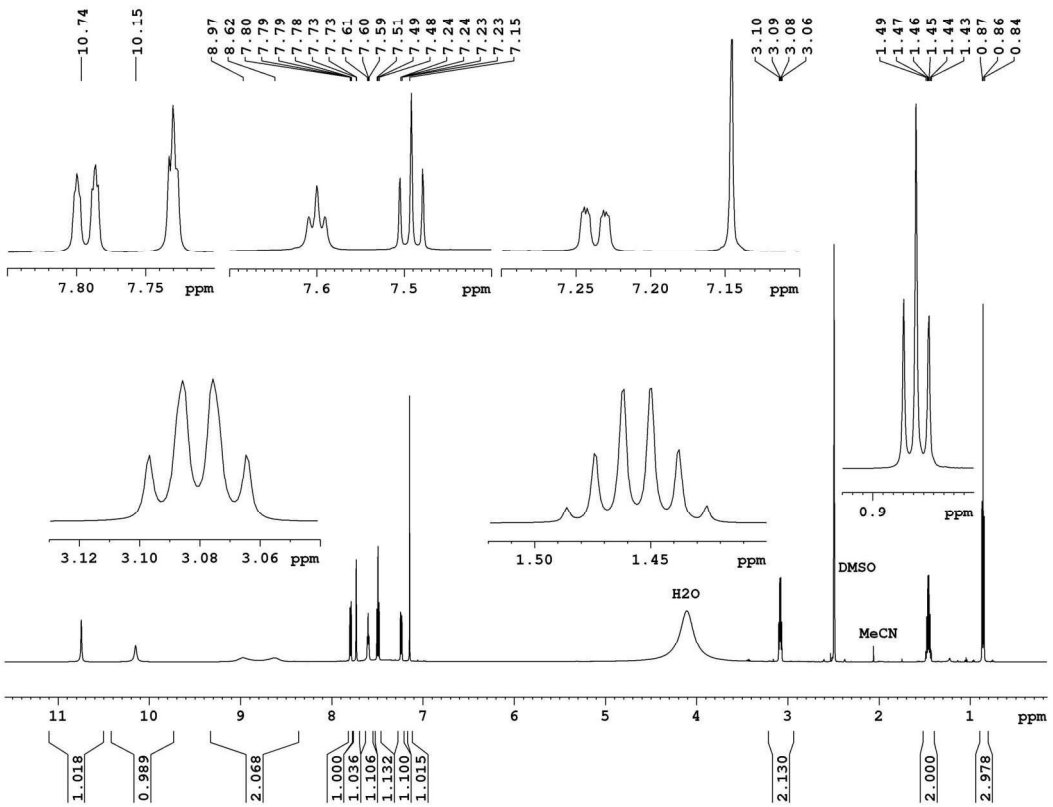

^{1}H-NMR spectrum (600 MHz, [D_6]-DMSO) of **6.60**

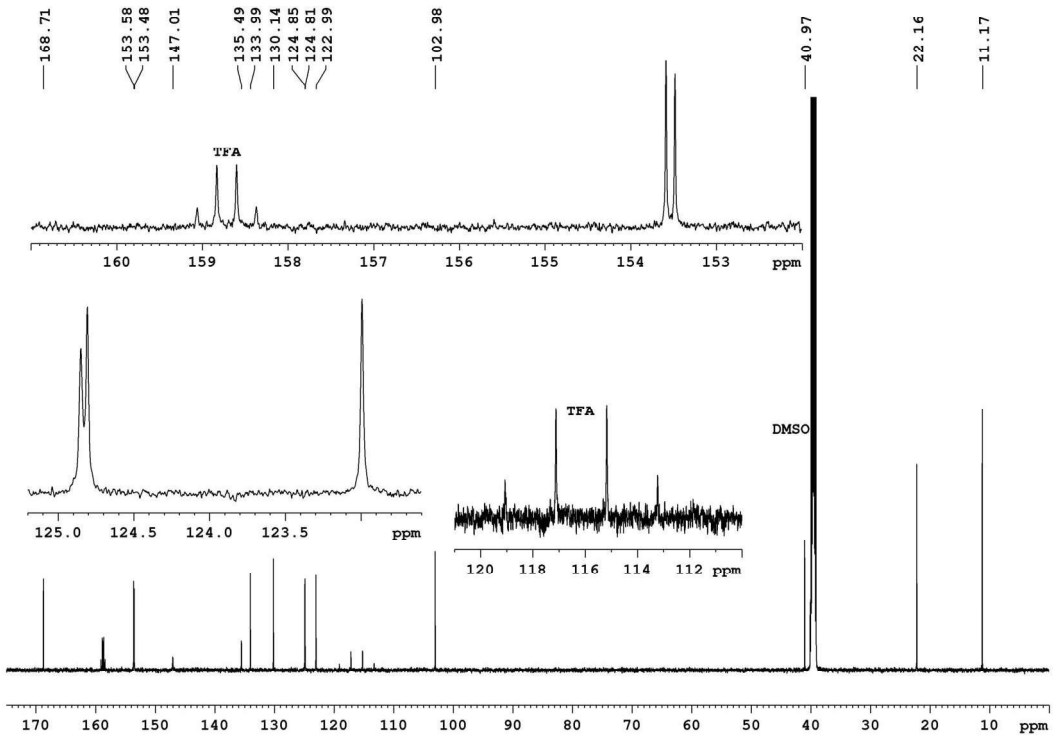

^{13}C-NMR spectrum (150 MHz, [D_6]-DMSO) of **6.60**

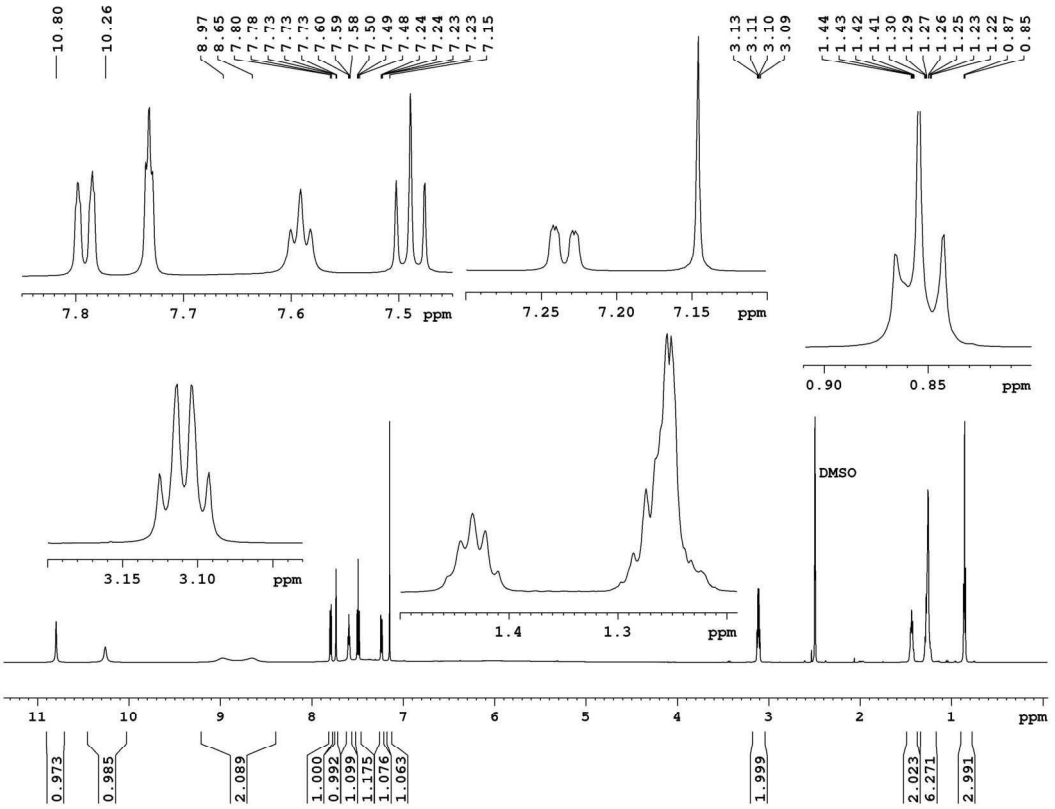

^{1}H-NMR spectrum (600 MHz, [D_6]-DMSO) of **6.61**

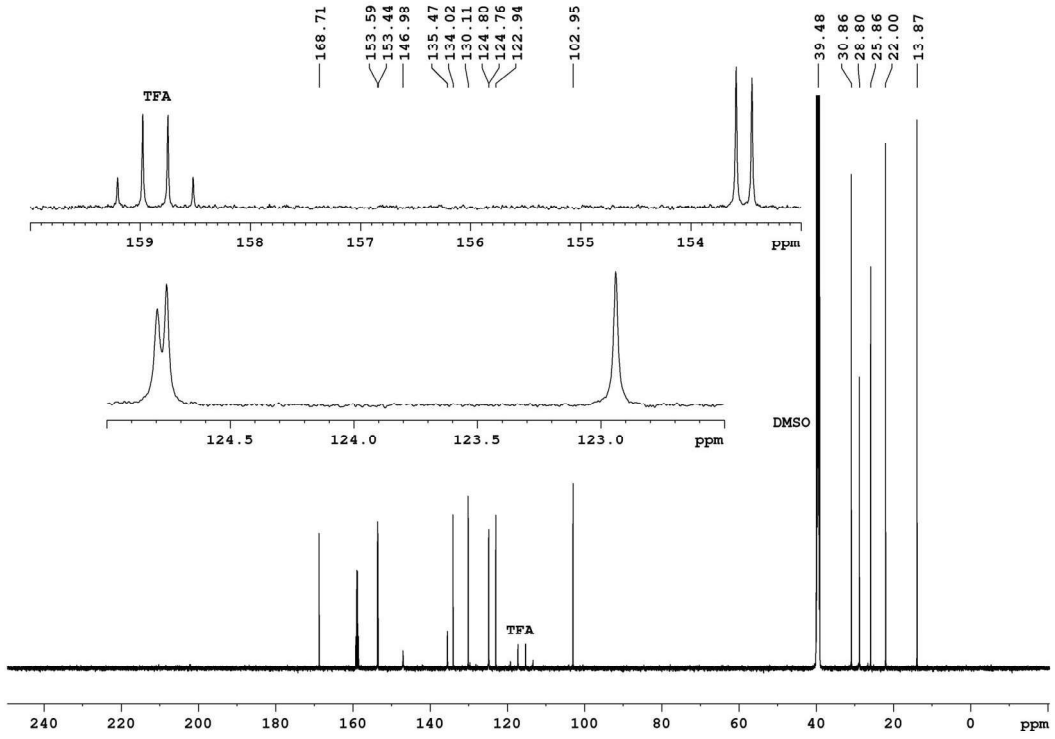

^{13}C-NMR spectrum (150 MHz, [D_6]-DMSO) of **6.61**

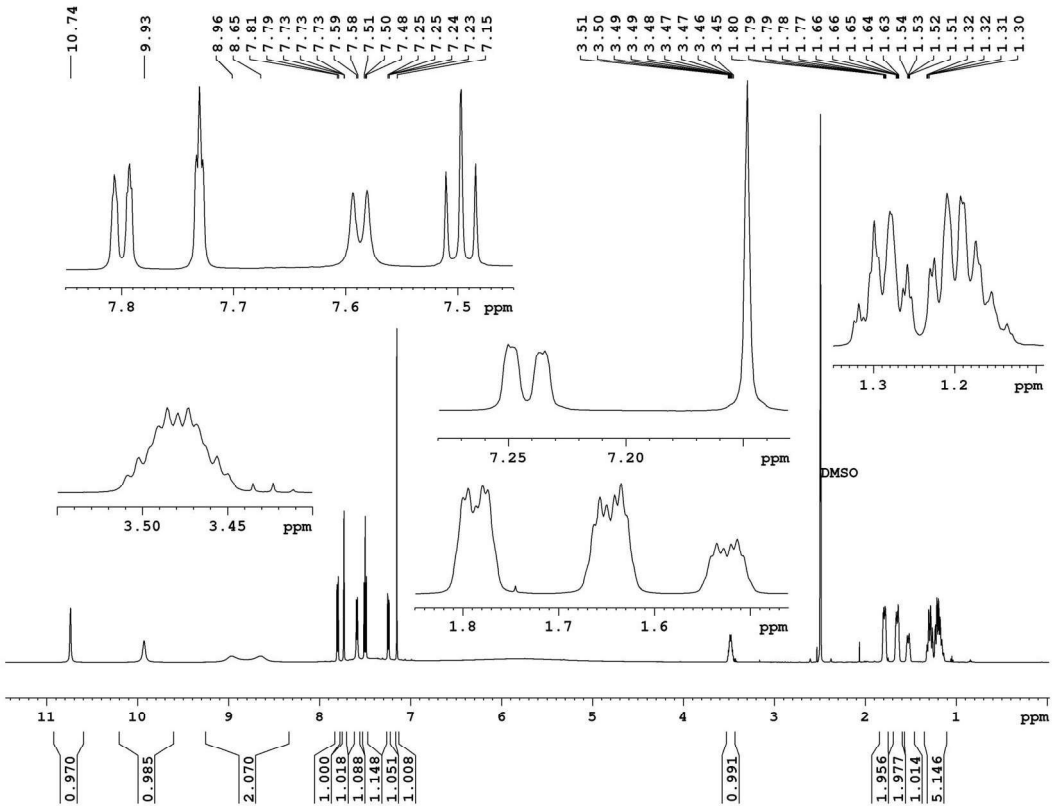

^{1}H-NMR spectrum (600 MHz, [D_6]-DMSO) of **6.62**

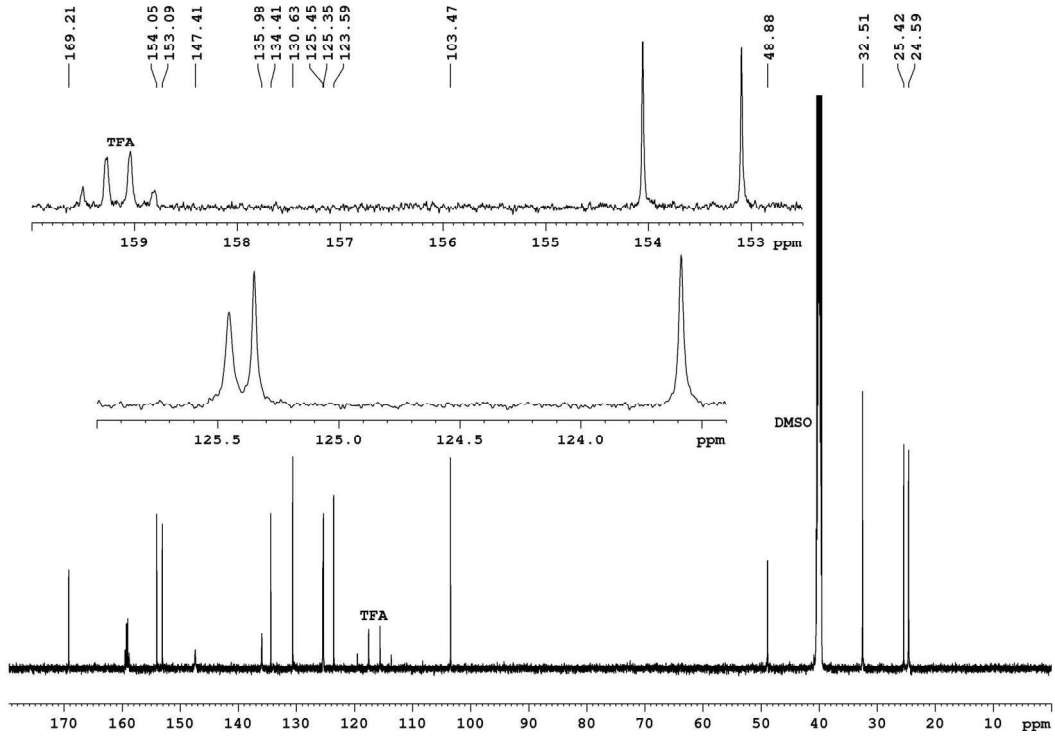

^{13}C-NMR spectrum (150 MHz, [D_6]-DMSO) of **6.62**

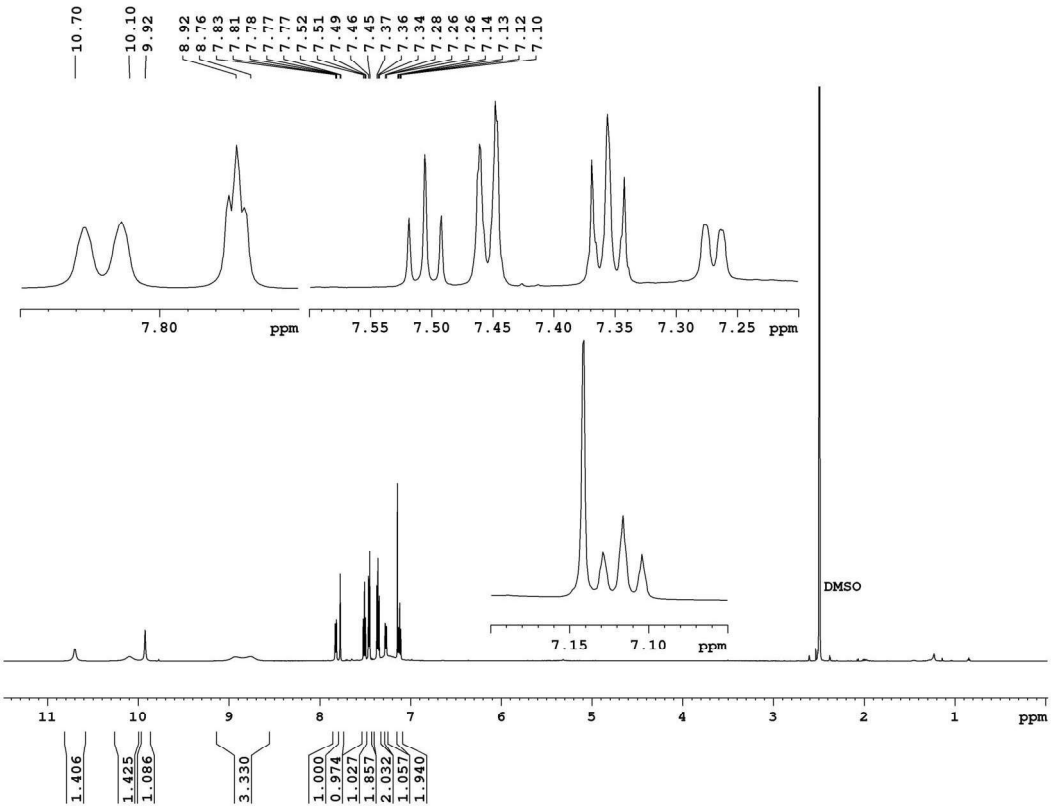

^{1}H-NMR spectrum (600 MHz, [D_6]-DMSO) of **6.63**

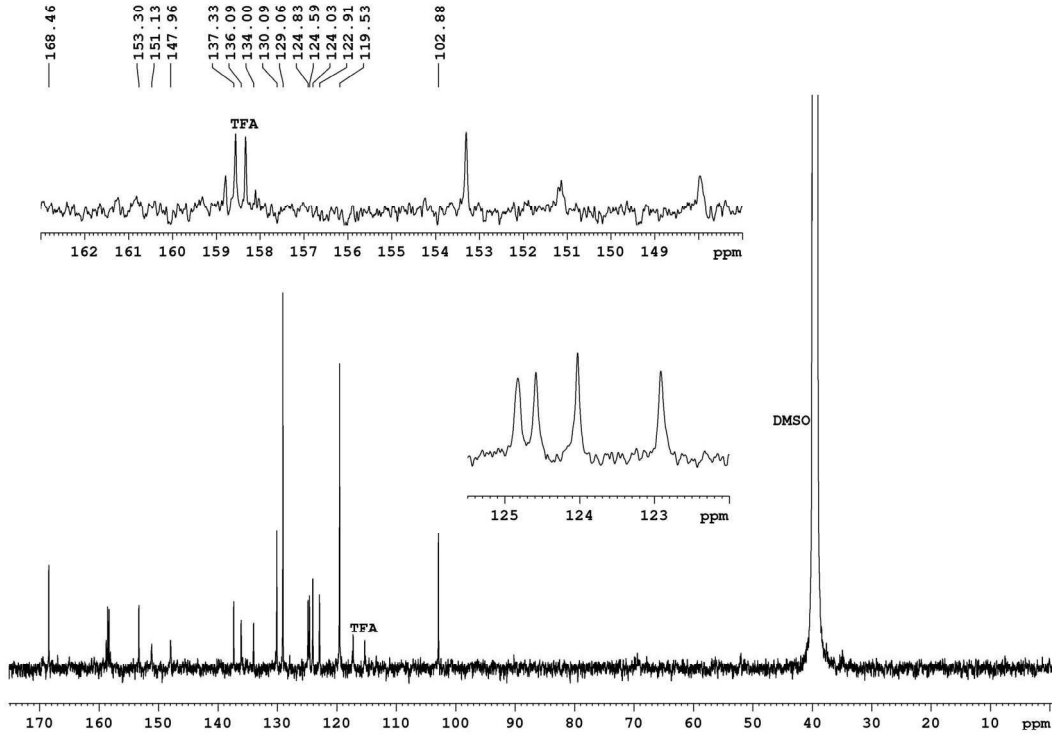

^{13}C-NMR spectrum (150 MHz, [D_6]-DMSO) of **6.63**

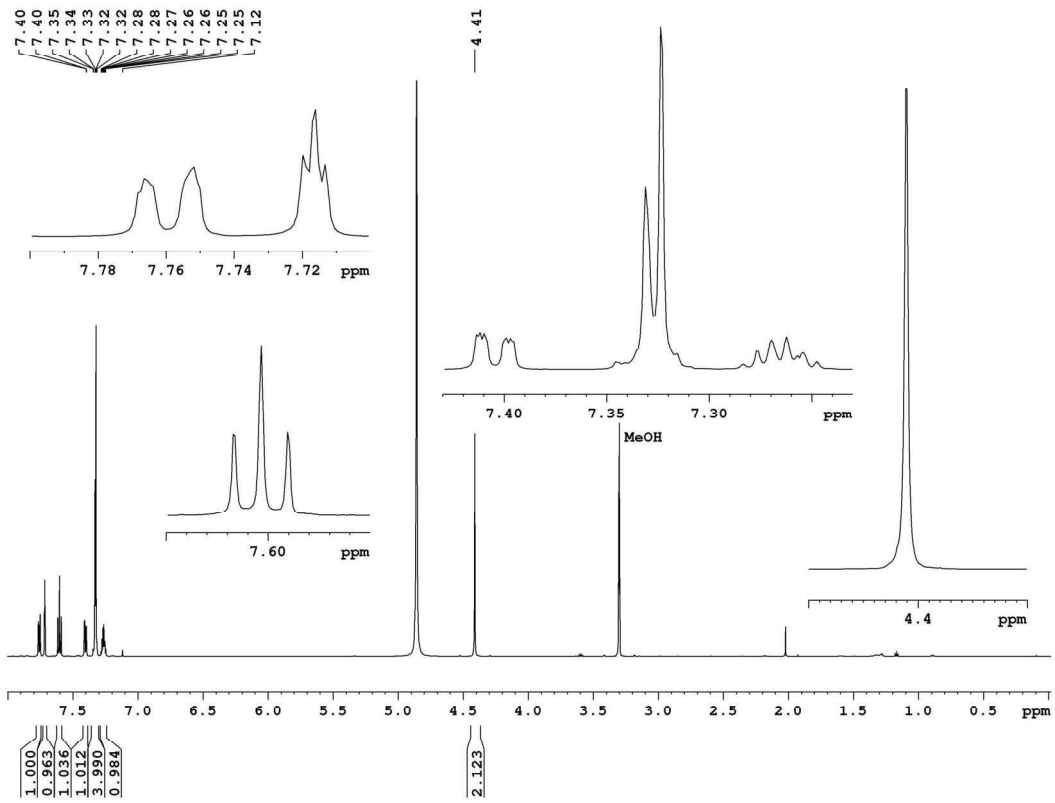

^{1}H-NMR spectrum (600 MHz, CD_3OD) of **6.64**

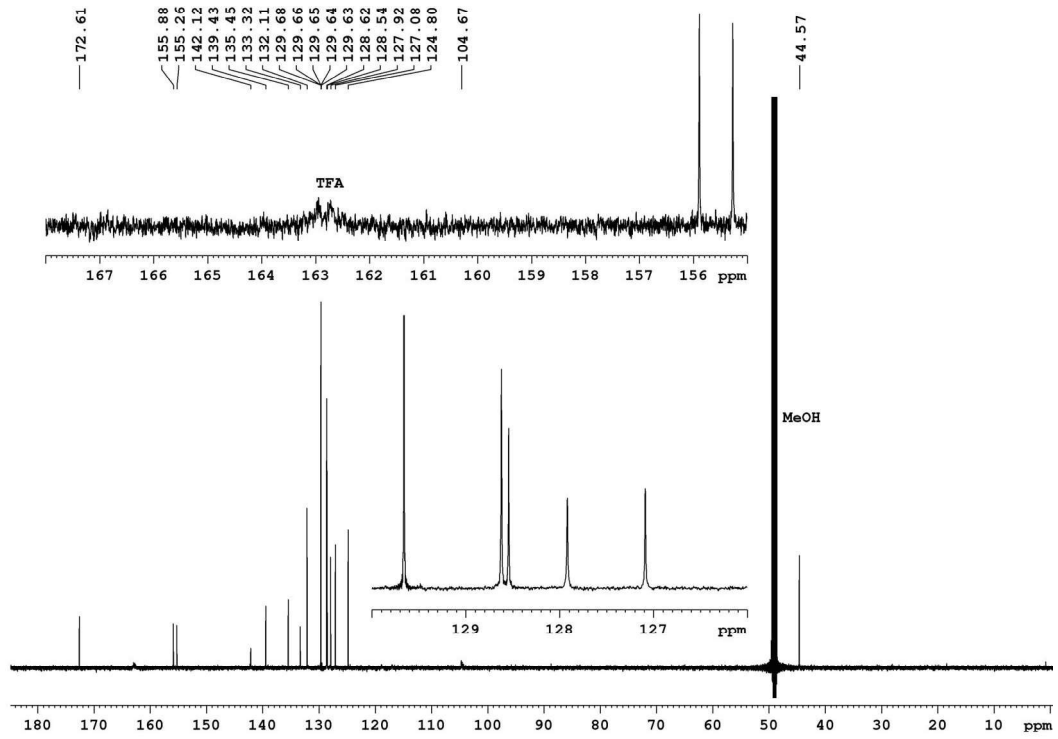

^{13}C-NMR spectrum (150 MHz, CD_3OD) of **6.64**

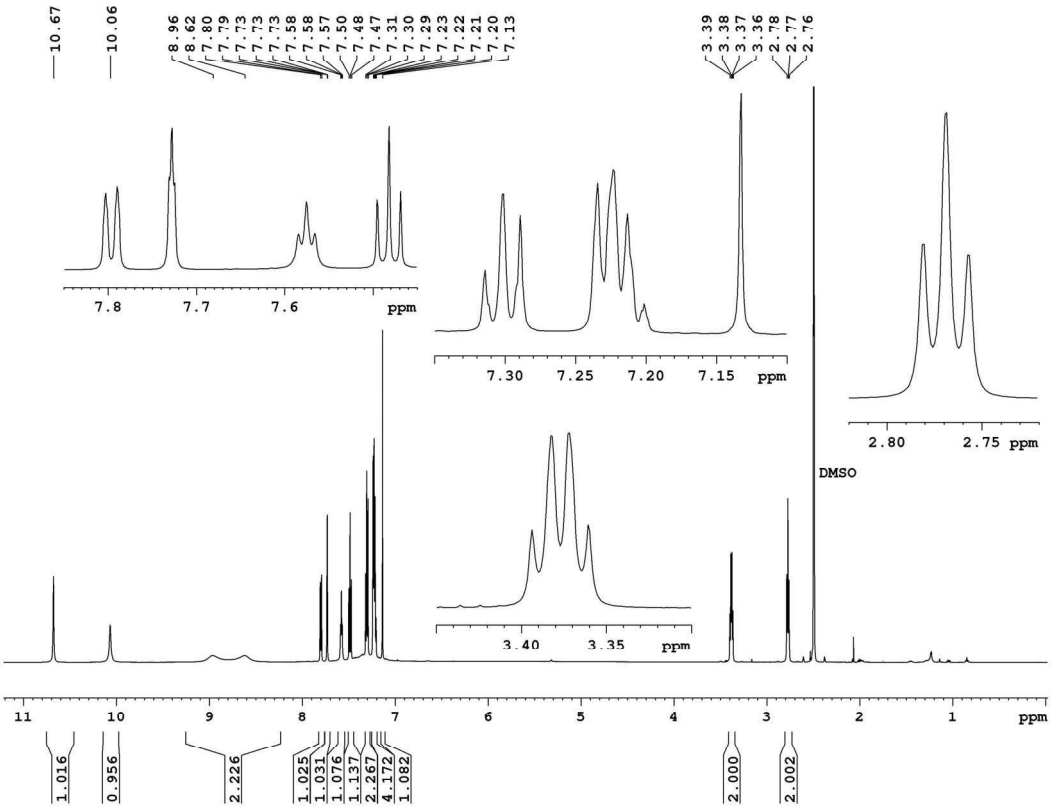

^{1}H-NMR spectrum (600 MHz, [D_6]-DMSO) of **6.65**

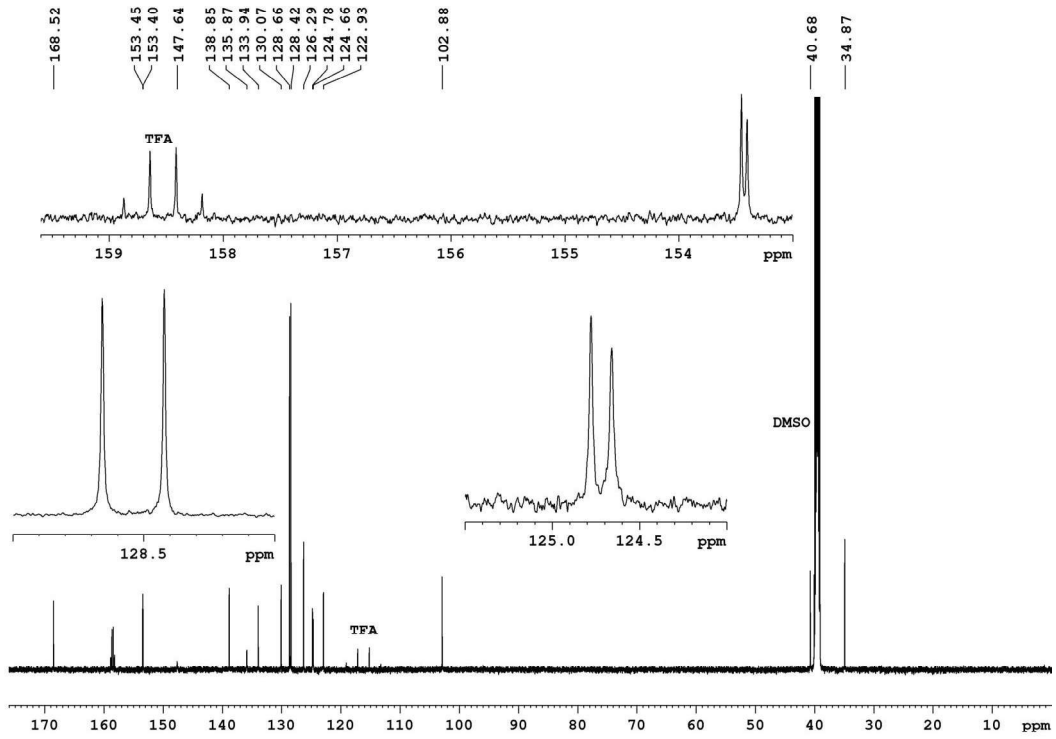

^{13}C-NMR spectrum (150 MHz, [D_6]-DMSO) of **6.65**

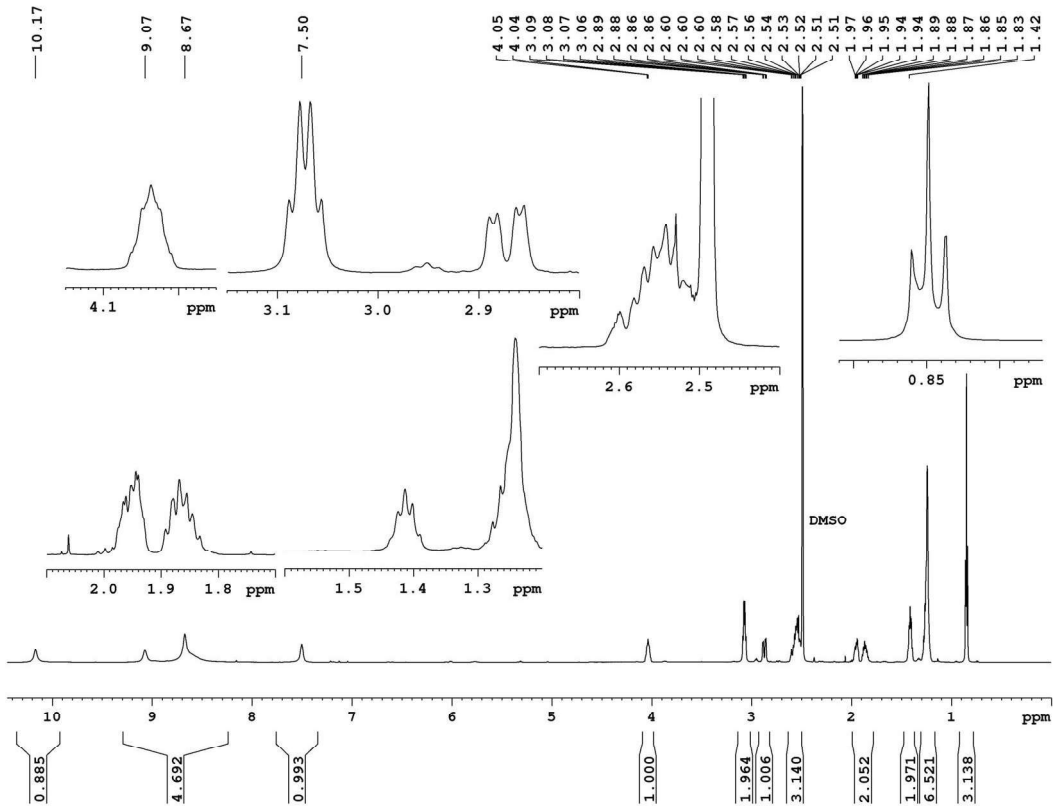

^{1}H-NMR spectrum (600 MHz, [D_6]-DMSO) of **6.66**

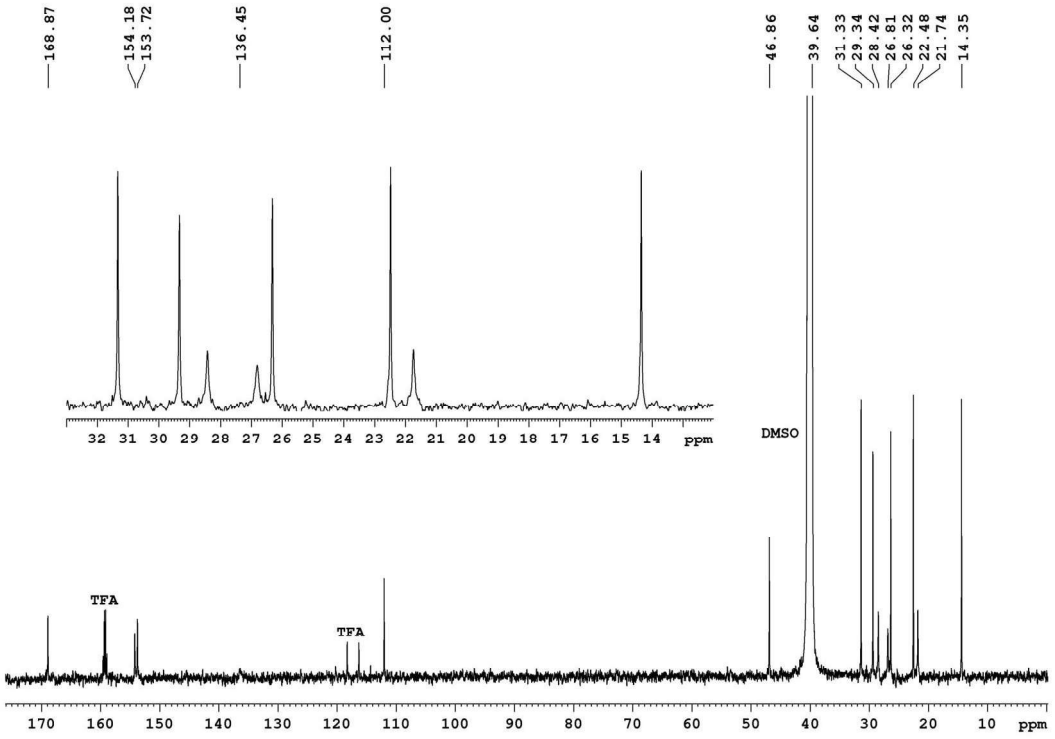

^{13}C-NMR spectrum (150 MHz, [D_6]-DMSO) of **6.66**

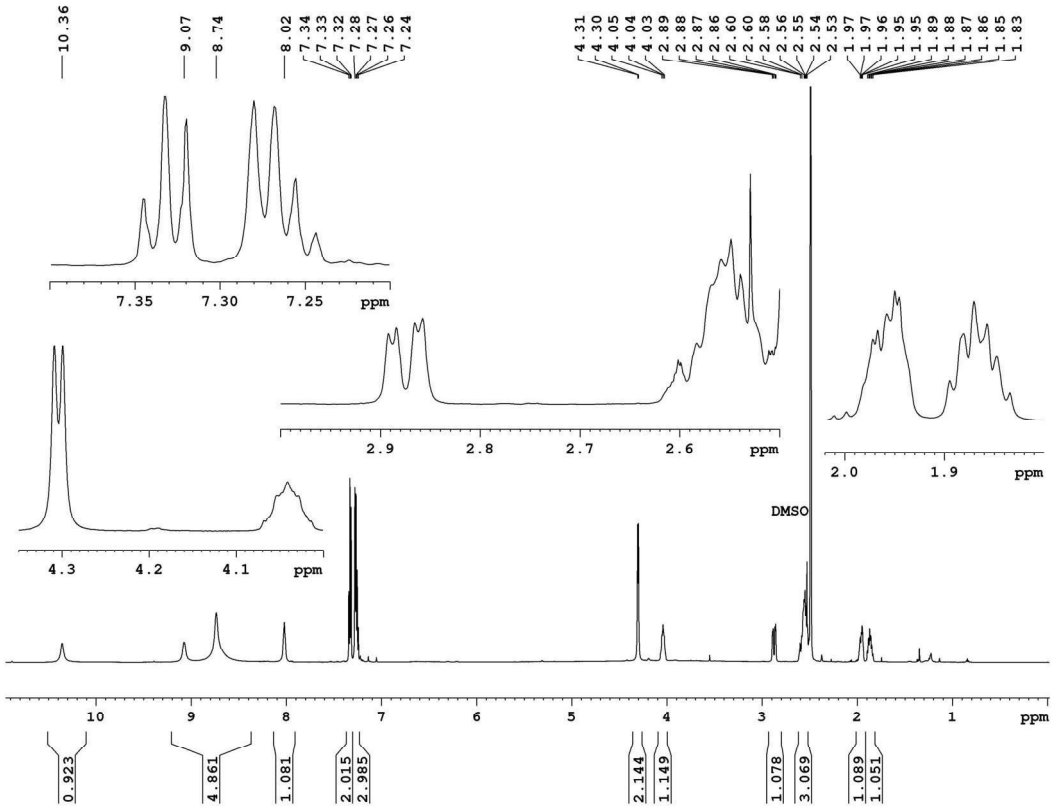

^{1}H-NMR spectrum (600 MHz, [D_6]-DMSO) of **6.67**

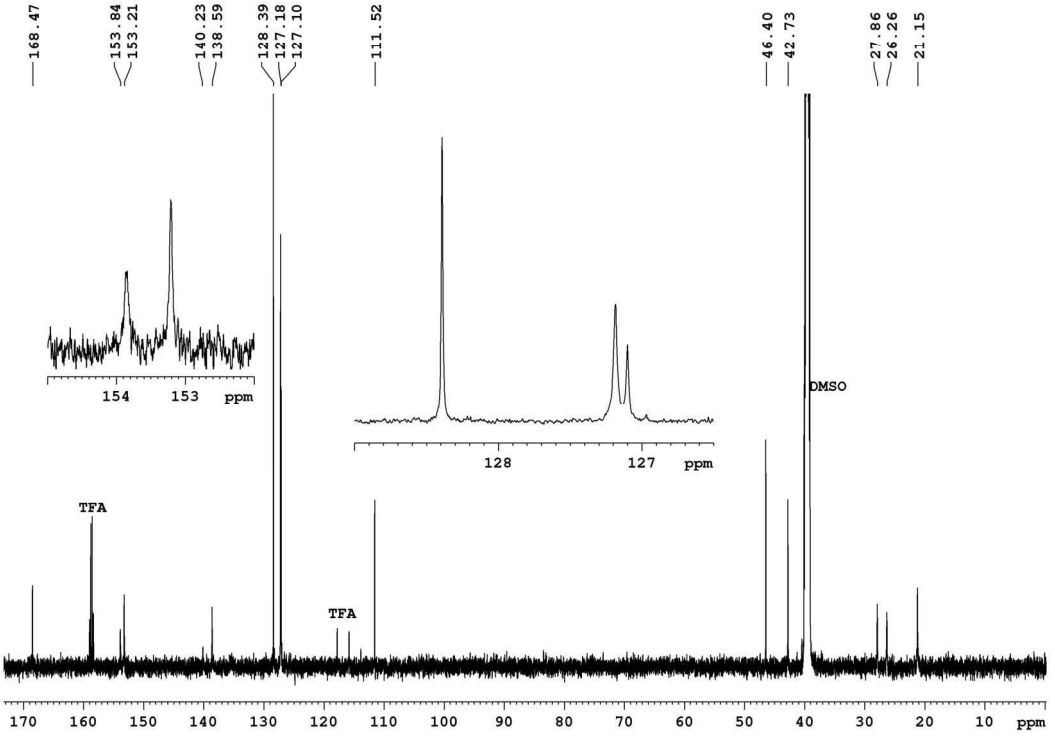

^{13}C-NMR spectrum (150 MHz, [D_6]-DMSO) of **6.67**

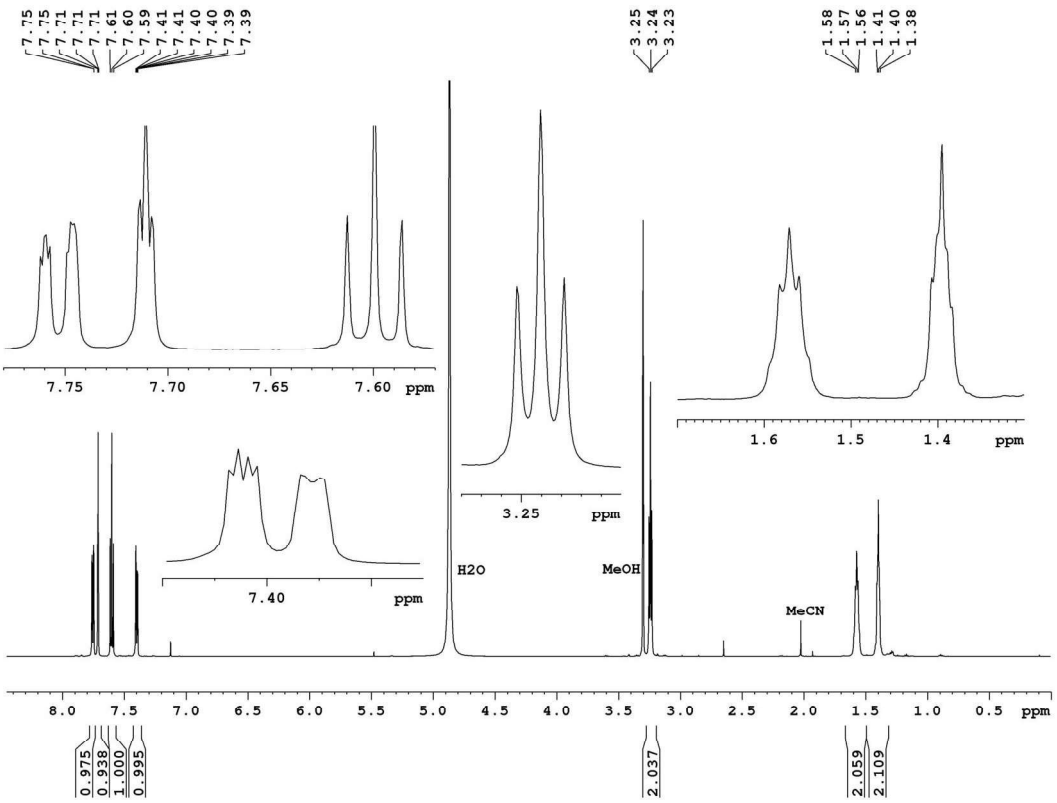

^{1}H-NMR spectrum (600 MHz, CD_3OD) of **6.70**

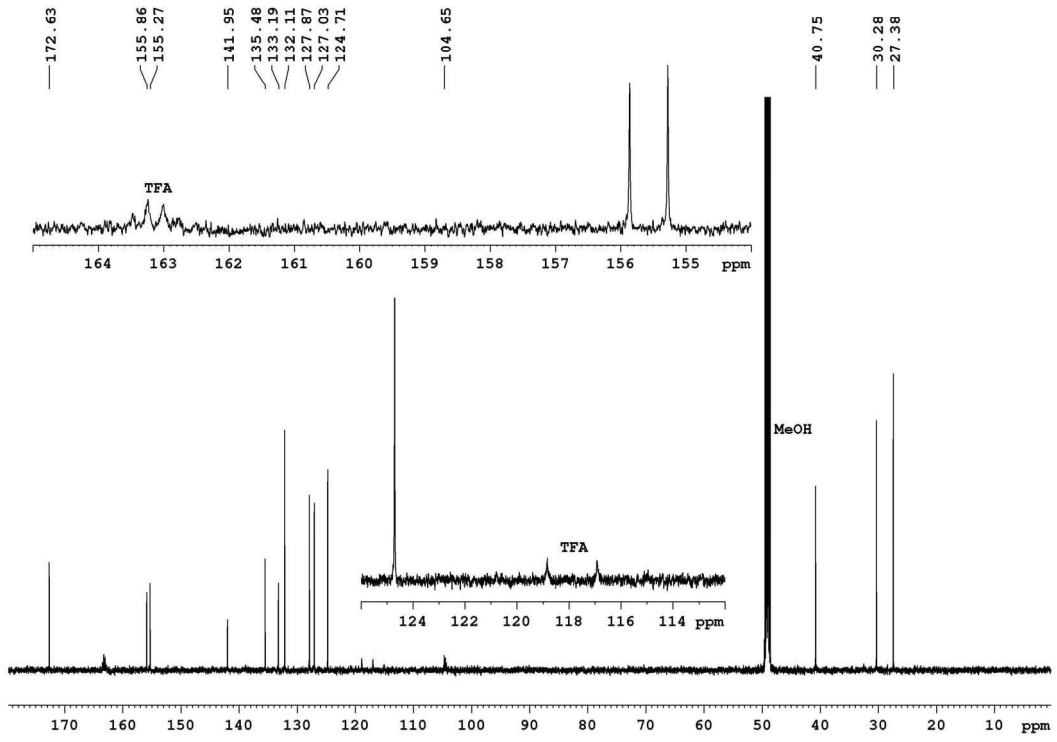

^{13}C-NMR spectrum (150 MHz, CD_3OD) of **6.70**

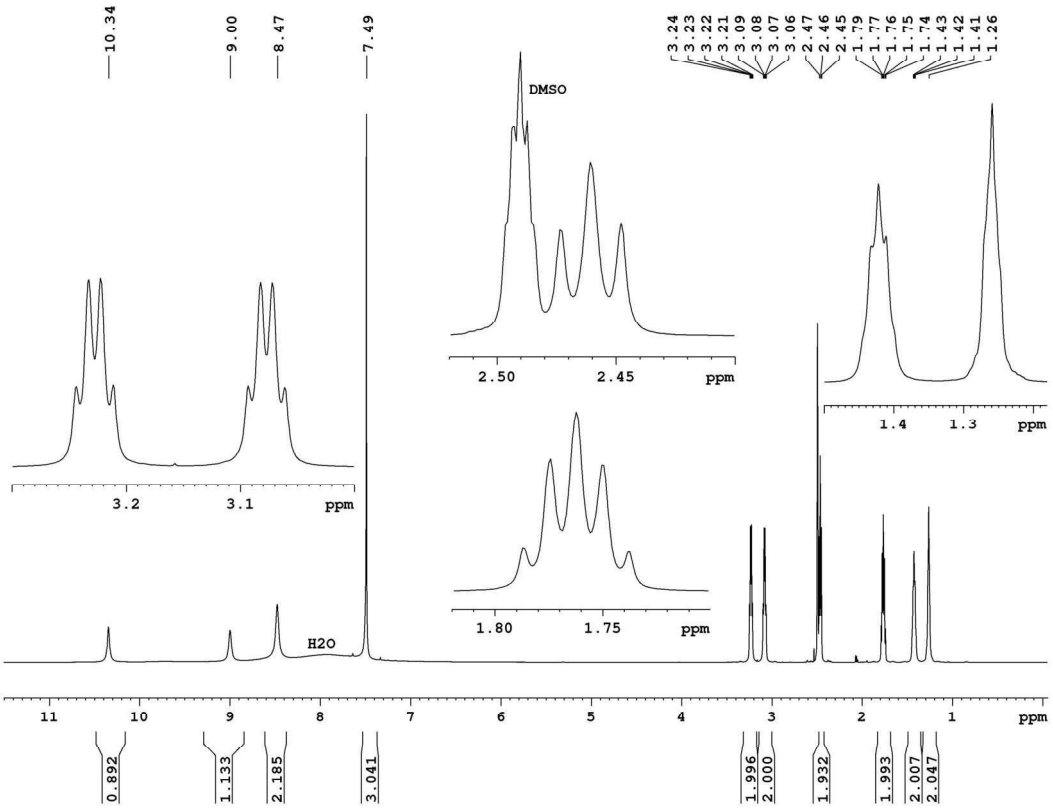

^{1}H-NMR spectrum (600 MHz, [D_6]-DMSO) of **6.71**

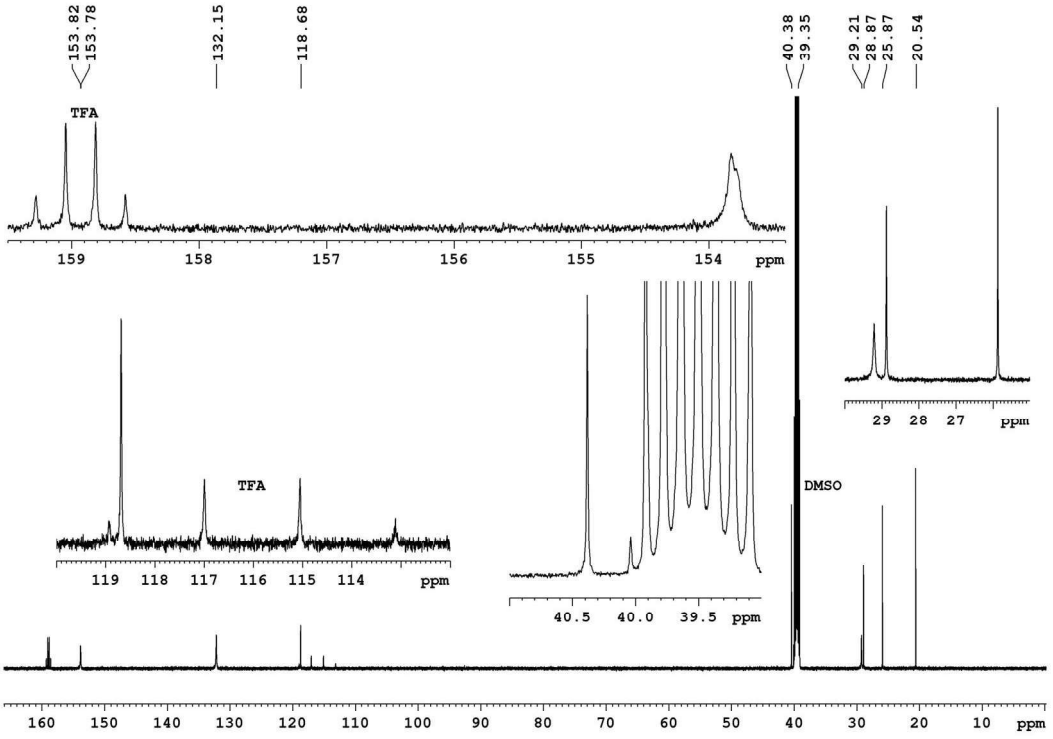

^{13}C-NMR spectrum (150 MHz, [D_6]-DMSO) of **6.71**

RP-HPLC CHROMATOGRAMS

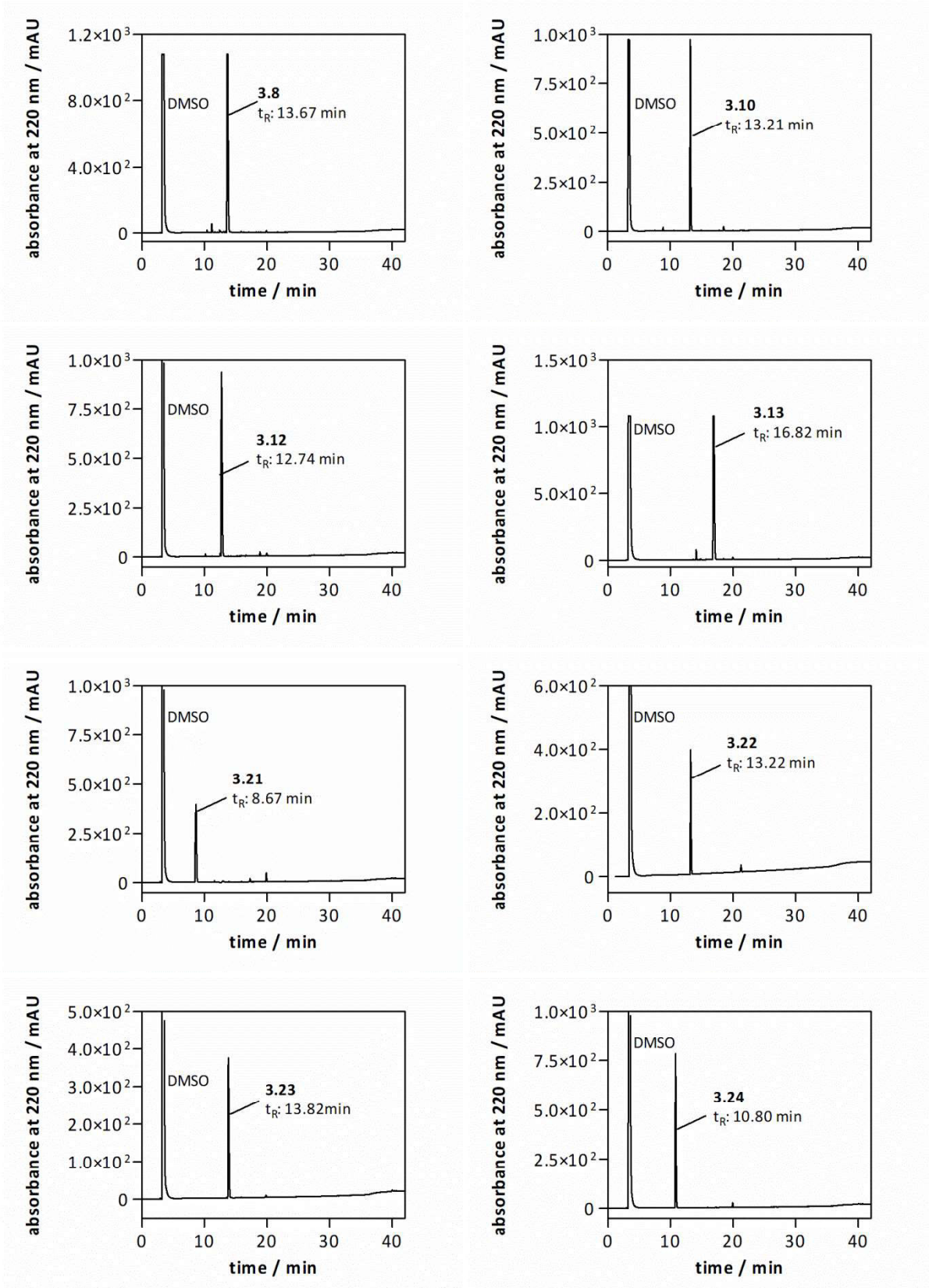

RP-HPLC analysis (purity control) of **3.8**, **3.10, 3.12**, **3.13**, **3.21**-**3.24**

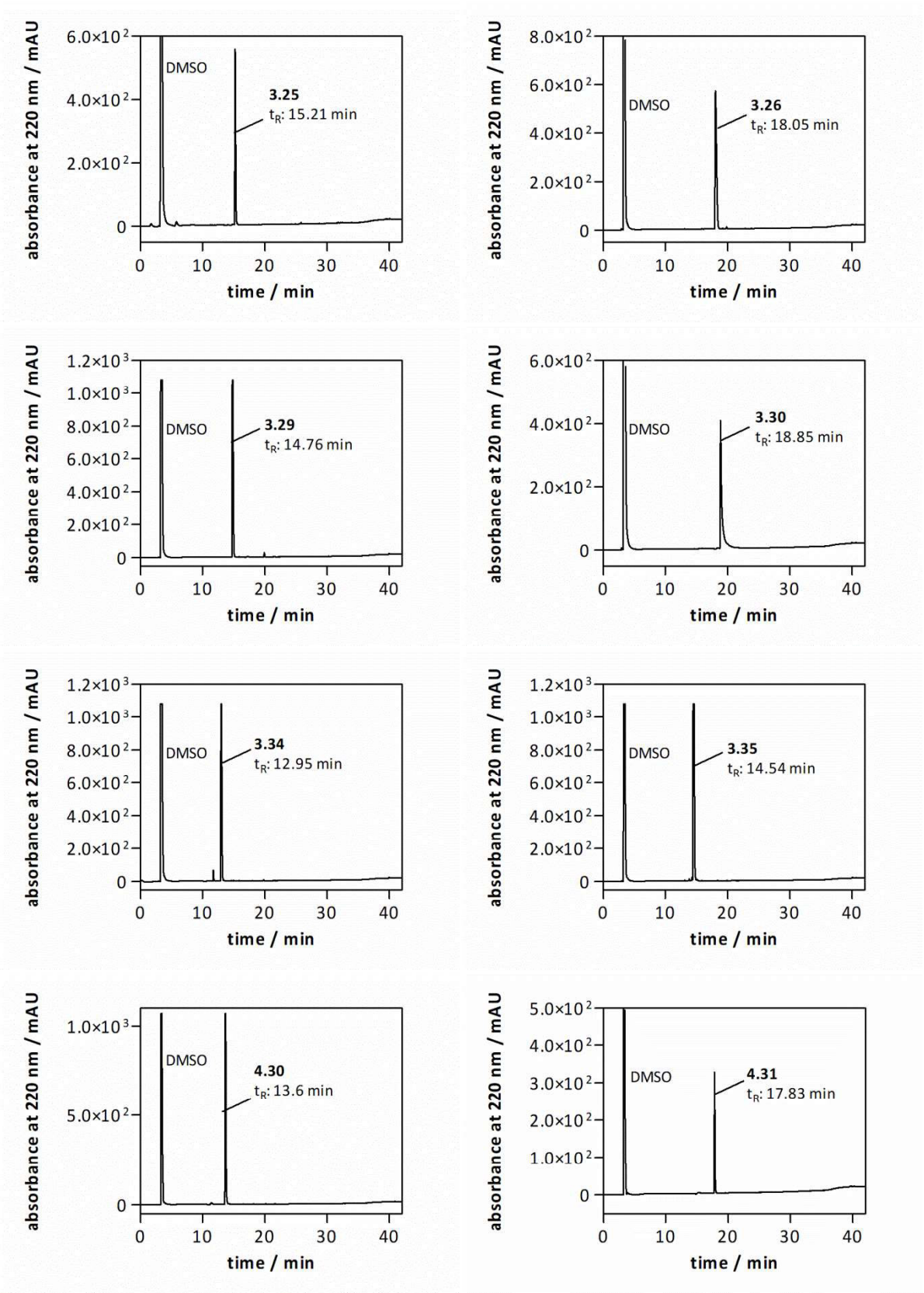

RP-HPLC analysis (purity control) of **3.25**, **3.26, 3.29**, **3.30**, **3.34**, **3.35**, **4.30**, **4.31**

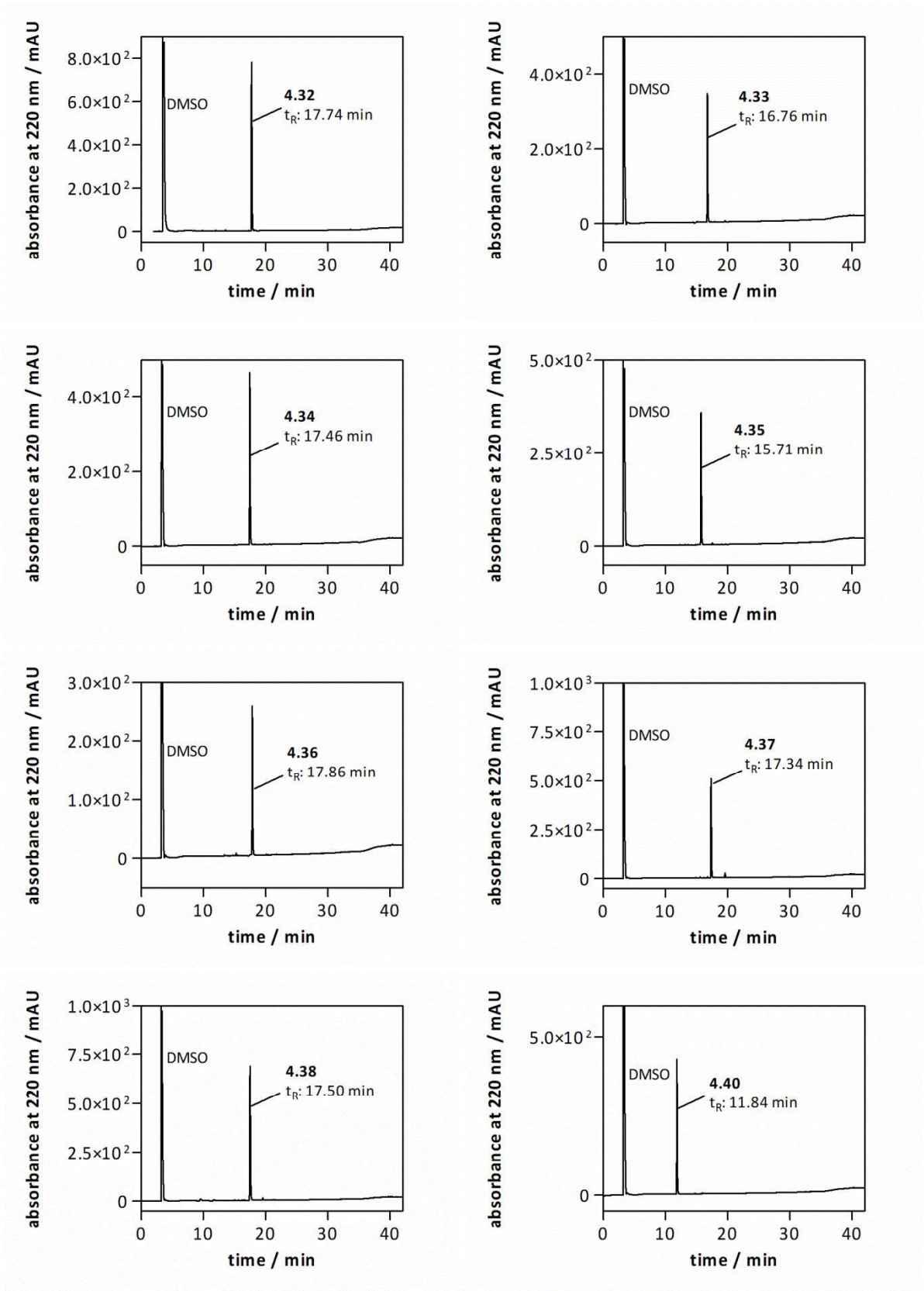

RP-HPLC analysis (purity control) of **4.32**-**4.38**, **4.40**

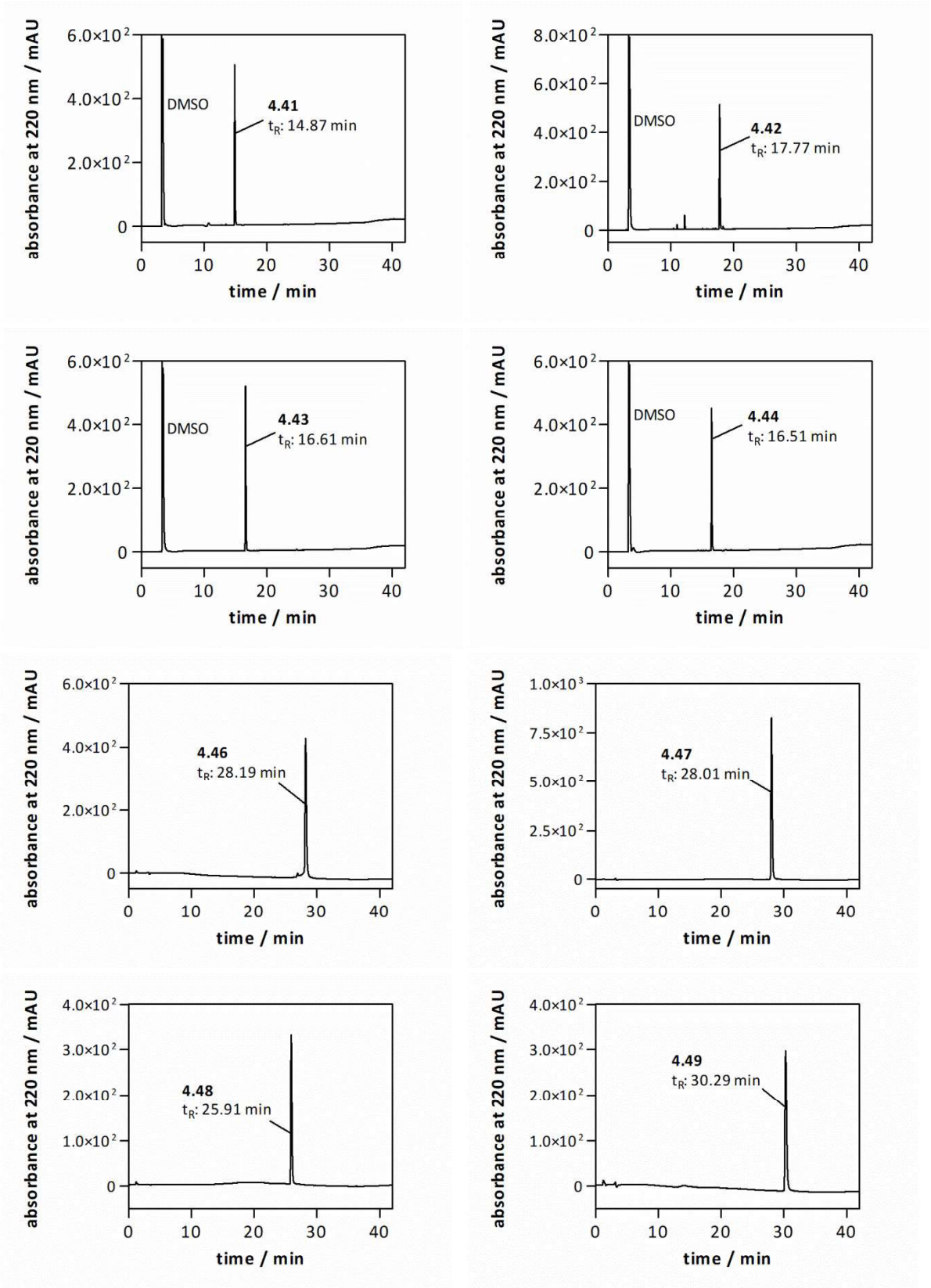

RP-HPLC analysis (purity control) of **4.41-4.44**, **4.46**-**4.49**

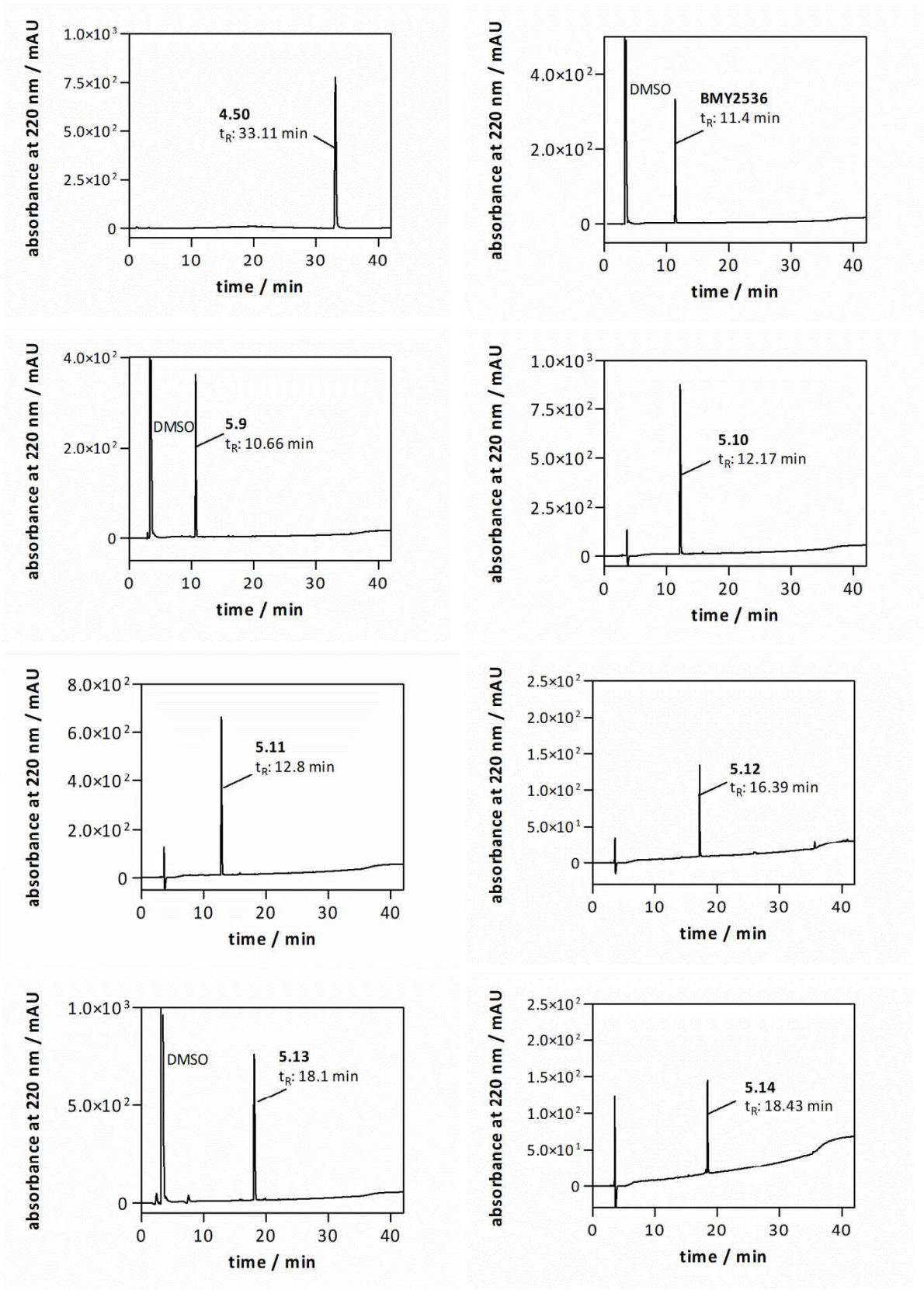

RP-HPLC analysis (purity control) of **4.50**, **BMY2536**, **5.9**-**5.14**

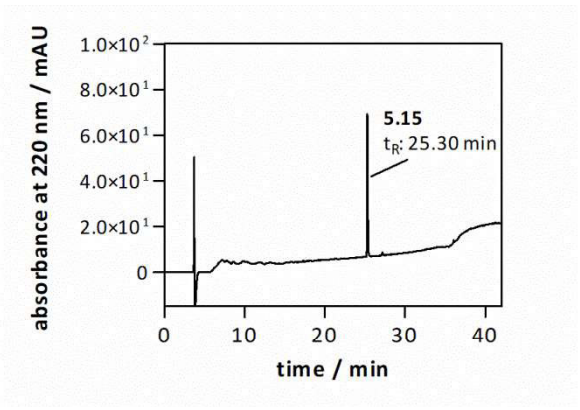

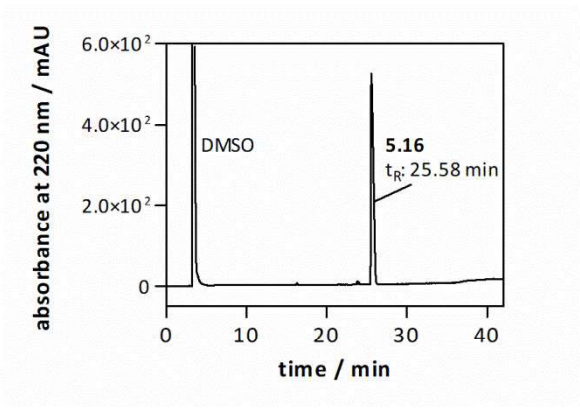

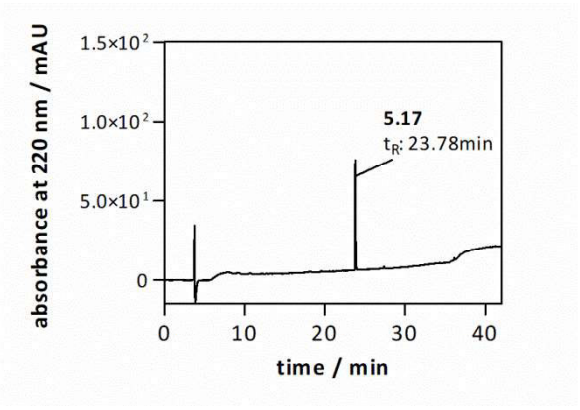

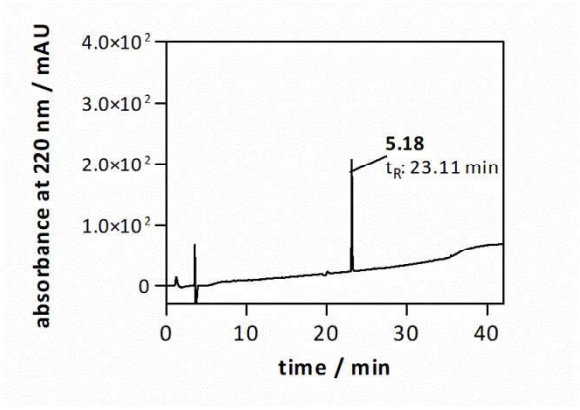

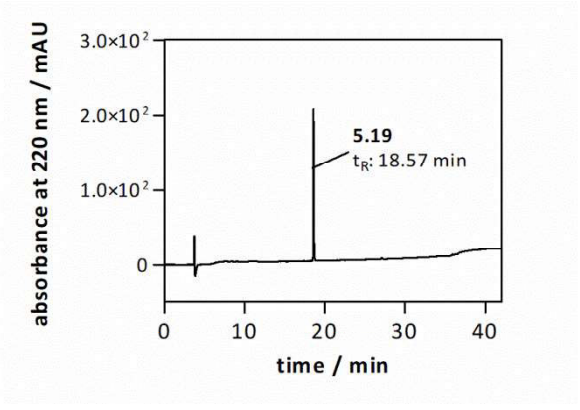

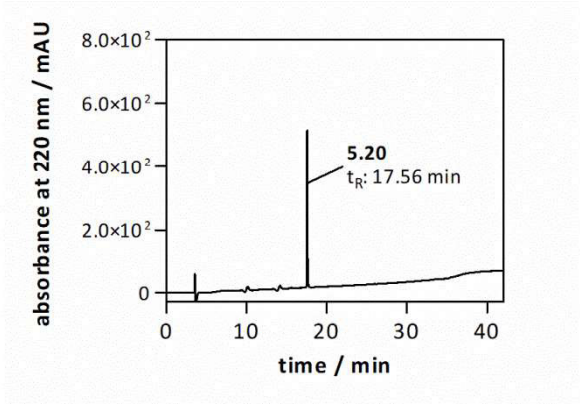

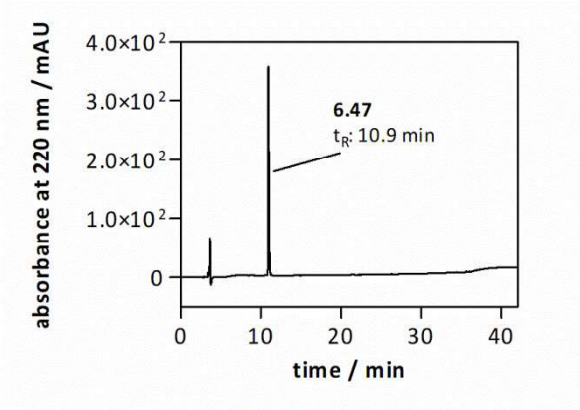

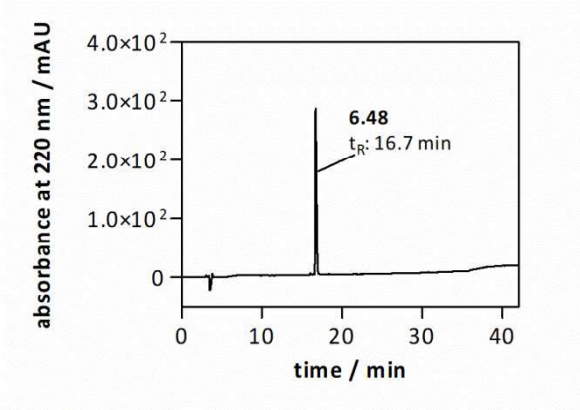

RP-HPLC analysis (purity control) of **5.15**-**5.20**, **6.47**, **6.48**

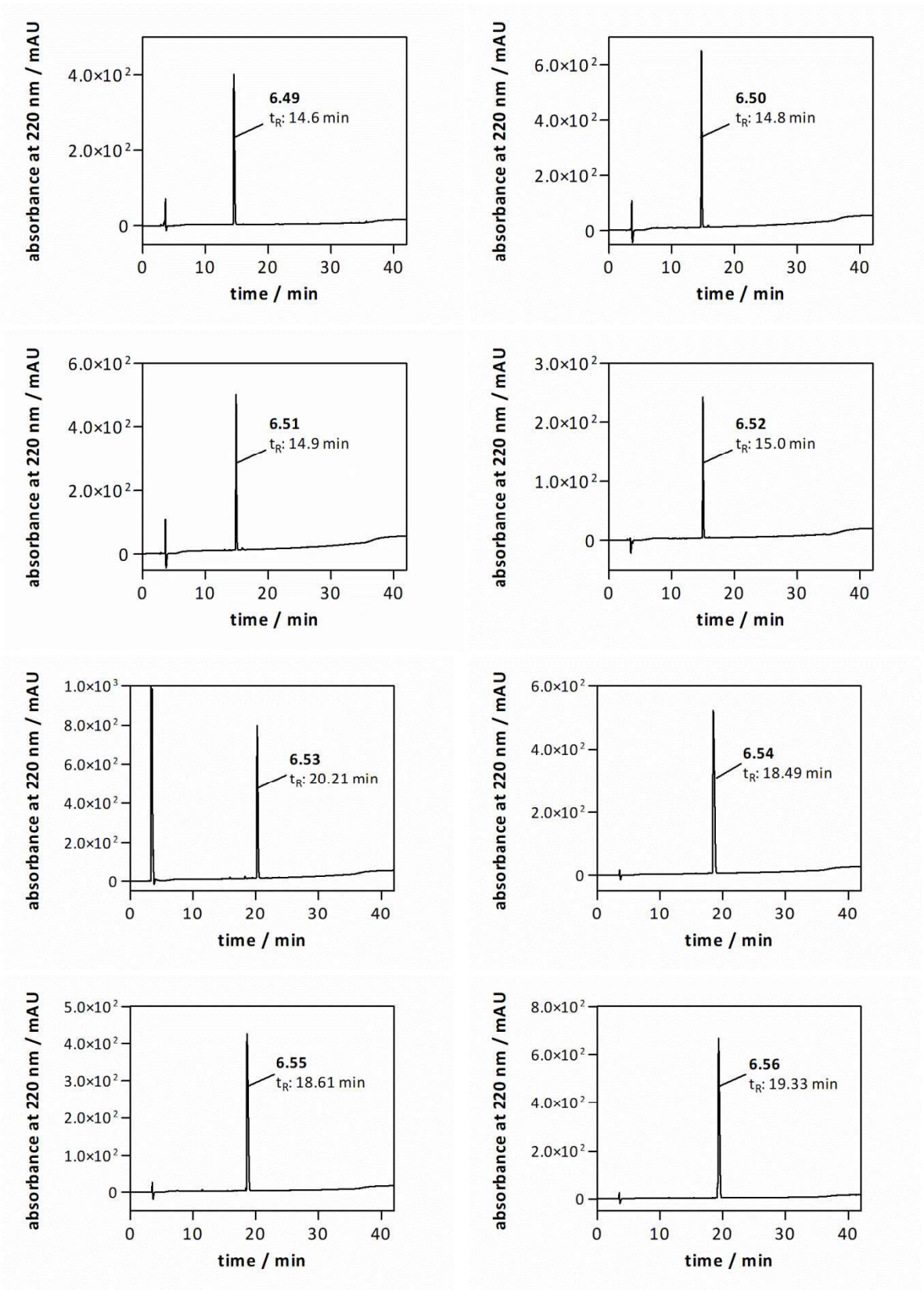

RP-HPLC analysis (purity control) of **6.49**-**6.56**

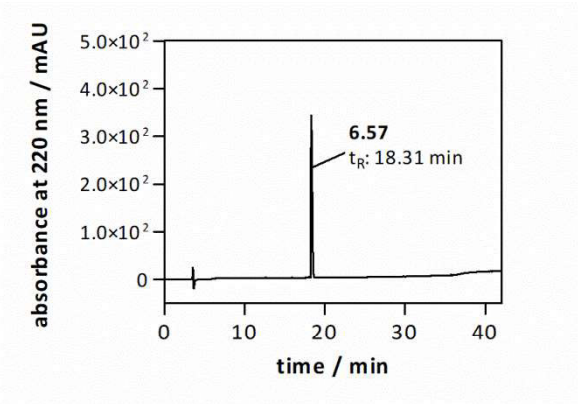

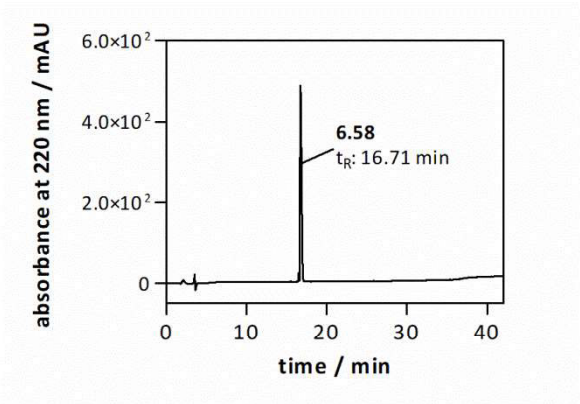

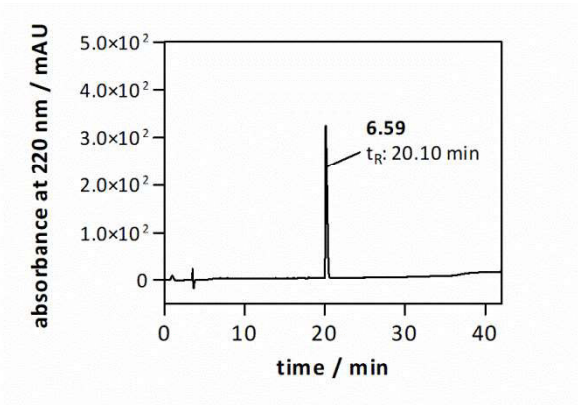

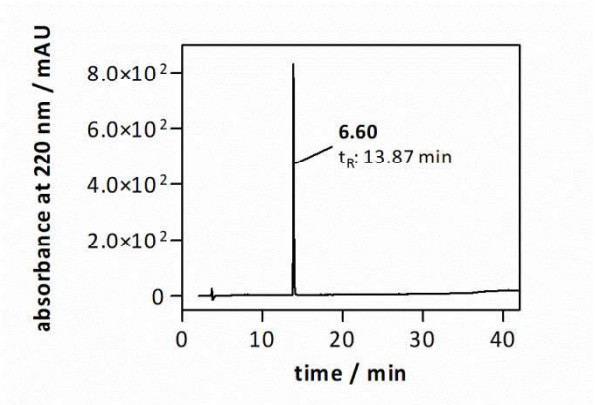

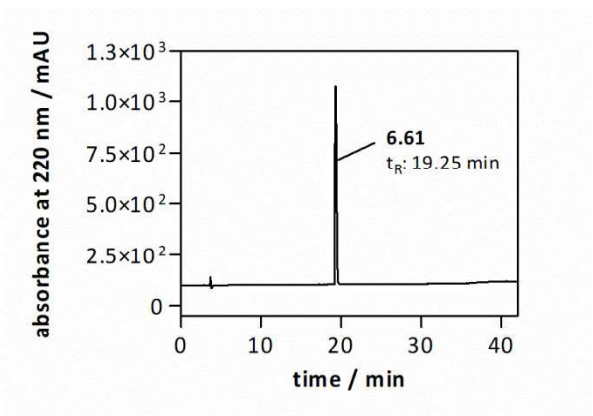

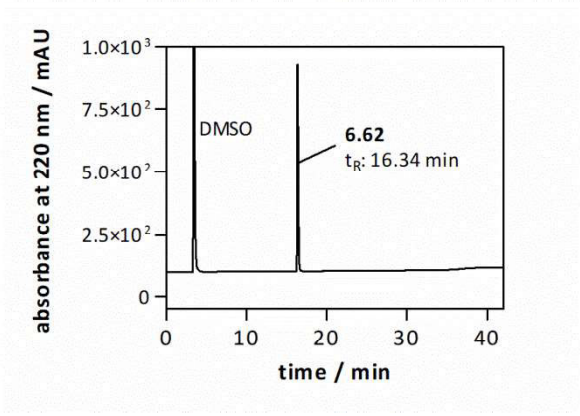

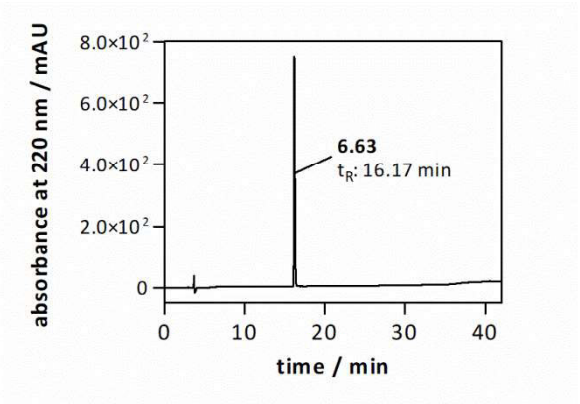

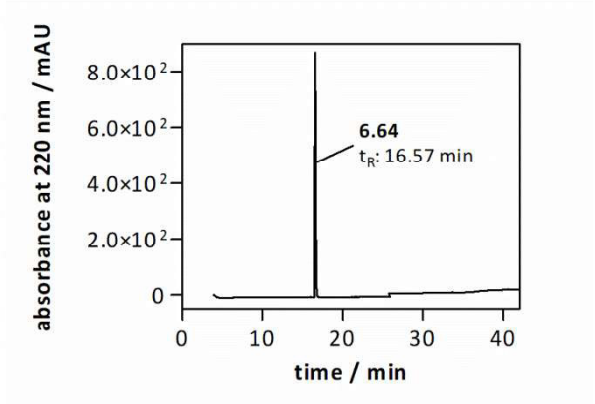

RP-HPLC analysis (purity control) of **6.57**-**6.64**

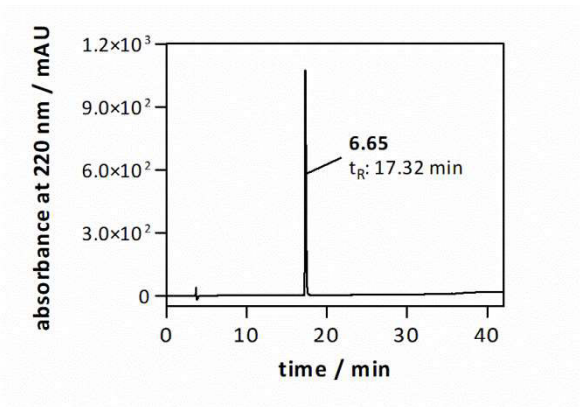

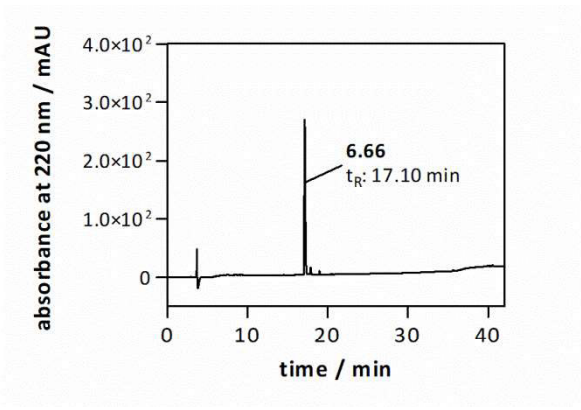

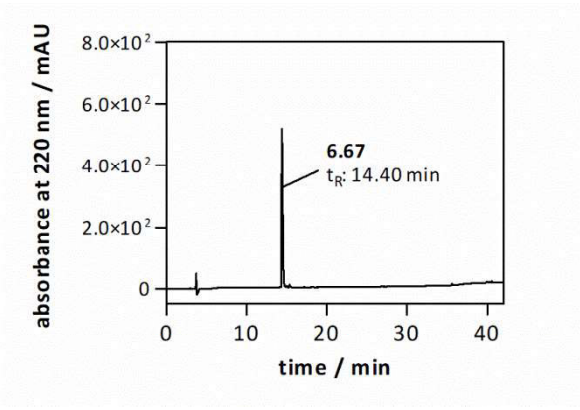

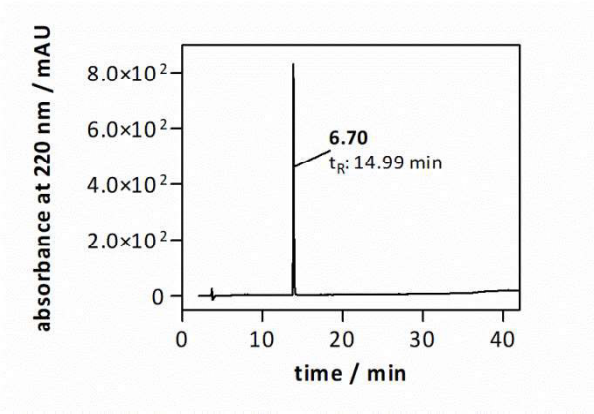

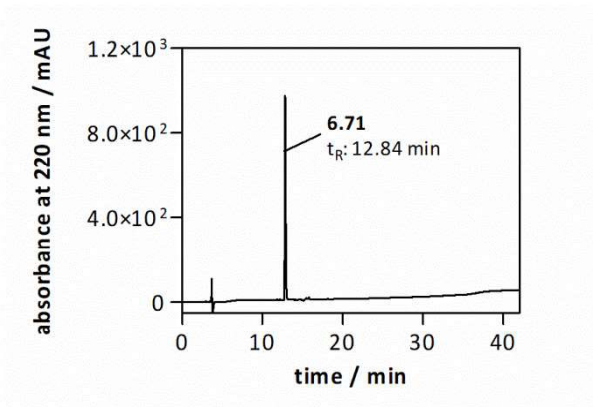

RP-HPLC analysis (purity control) of **6.65**-**6.67**, **6.70**, **6.71**

ABBREVIATIONS

AC	adenylyl cyclase
AcOH	acetic acid
AIBN	azobisisobutyronitrile
AML	acute myeloid leukemia
aq.	aqueous
Ar	aryl
B_{max}	maximum number of binding sites
Boc	*tert*-butoxycarbonyl
Bq	becquerel
br s	broad signal
BRET	bioluminescence resonance energy transfer
BSA	bovine serum albumin
c	concentration
cAMP	cyclic adenosine monophosphate
COSY	correlated spectroscopy
CNS	central nervous system
cpm	counts per million
d	doublet
δ	chemical shift
DAG	diacylglycerol
DCM	dichloromethane
DIPEA	*N,N*-diisopropylethylamine
DMAP	4-dimethylaminopyridine
DMEM	dulbecco´s modified eagle medium,
DMF	dimethylformamide
DMSO	dimethylsulfoxide
D_nR	Dopamine receptor subtypes, n = 1,2,3,4,5; human isoform: hD_nR
DPM	desintegrations per minute
EC_{50}	agonist concentration which induces 50% of the maximum response
EDTA	ethylenediaminetetraacetic acid
E_{max}	intrinsic activity
eq.	equivalent(s)
ESI	electrospray ionization
EtOAc	ethyl acetate
EtOH	ethanol
FCS	fetal calf serum
FP	fluorescence polarization
FRAP	fluorescence recovery after photobleaching
FRET	Förster resonance energy transfer
GDP	guanosine diphosphate
GEF	guanosine nucleotide exchange factor
GPCR	G-Protein coupled receptor
GRK	G-Protein coupled receptor kinase
GTP	guanosine triphosphate
hD_2R_{short}	short splice variant of the human dopamine D_2 receptor

H_nR	Histamine receptor subtypes, n = 1,2,3,4; isoforms: dog (cH_nR), guinea pig (gpH_nR), human (hH_nR), mouse (mH_nR), rat (rH_nR)
h	hour(s)
HBTU	2-(1*H*-benzotriazol-1-yl)-1,1,3,3-tetramethyluronium hexafluorophosphate
HEK293T	human embryonic kidney cells
HMBC	heteronuclear multiple bond correlation
HPLC	high-performance liquid chromatography
HRMS	high resolution mass spectrometry
HSQC	heteronuclear single quantum coherence
IC_{50}	inhibitor concentration which suppresses 50% of an agonist induced effect or displaces 50% of a labeled ligand from the binding site
IP_3	inositol trisphosphate
IR	infrared spectroscopy
k	retention factor
K_b	dissociation constant derived from a functional assay
K_d	dissociation constant derived from a saturation binding assay
K_i	dissociation constant derived from a competition binding assay
k_{obs}	observed association rate constant
k_{off}	dissociation rate constant
k_{on}	association rate constant
lit.	literature
m	multiplet
M	molar (mol/L)
MeCN	acetonitrile
MeOH	methanol
mol	mole(s)
mp	melting point
N^G	guanidine nitrogen
NMR	nuclear magnetic resonance
NOESY	nuclear Overhauser effect spectroscopy
ON	over night
PBS	phosphate buffered saline
PE	petroleum ether
PLC	phospholipase C
q	quartet
qui	quintet
R_f	relative to front
RP	reversed phase
RT	room temperature
s	(1) singlet or (2) second(s)
SEM	standard error of the mean
t	(1) triplet or (2) time
TBTU	2-(1H-Benzotriazole-1-yl)-1,1,3,3-tetramethylaminium tetrafluoroborate
TEA	triethyl amine
TFA	trifluoroacetic acid
THF	tetrahydrofuran

TIRF	total internal reflection fluorescence
TLC	thin layer chromatography
TM	transmembrane
t_R	retention time
Tris	tris(hydroxymethyl)aminomethane
UV	ultraviolet

Ich erkläre hiermit an Eides statt, dass ich die vorliegende Arbeit ohne unzulässige Hilfe Dritter und ohne Benutzung anderer als der angegebenen Hilfsmittel angefertigt habe; die aus anderen Quellen direkt oder indirekt übernommenen Daten und Konzepte sind unter Angabe des Literaturzitats gekennzeichnet.

Einige der experimentellen Arbeiten wurden in Zusammenarbeit mit anderen Personen durchgeführt. Entsprechende Vermerke finden sich in den entsprechenden Kapiteln. Eine detaillierte Auflistung aller Kooperationen enthält zudem der Abschnitt „Acknowledgements and declaration of collaborations“.

Weitere Personen waren an der inhaltlich-materiellen Erstellung der vorliegenden Arbeit nicht beteiligt. Insbesondere habe ich hierfür nicht die entgeltliche Hilfe eines Promotionsberaters oder anderer Personen in Anspruch genommen. Niemand hat von mir, weder unmittelbar noch mittelbar, geldwerte Leistungen für Arbeiten erhalten, die im Zusammenhang mit dem Inhalt der vorgelegten Dissertation stehen.

Sabrina Biselli